METHODS IN ENZYMOLOGY

Editors-in-Chief

JOHN N. ABELSON AND MELVIN I. SIMON

Division of Biology
California Institute of Technology
Pasadena, California, USA

Founding Editors

SIDNEY P. COLOWICK AND NATHAN O. KAPLAN

Academic Press is an imprint of Elsevier
525 B Street, Suite 1900, San Diego, CA 92101-4495, USA
30 Corporate Drive, Suite 400, Burlington, MA 01803, USA
32 Jamestown Road, London NW1 7BY, UK

First edition 2010

For information on all Academic Press publications
visit our website at elsevierdirect.com

ISBN: 978-0-12-381345-9
ISSN: 0076-6879

Printed and bound in United States of America
10 11 12 10 9 8 7 6 5 4 3 2 1

Contributors

Beatriz Alvarez
Laboratorio de Enzimología, Facultad de Ciencias, and Center for Free Radical and Biomedical Research, Facultad de Medicina, Universidad de la República, Montevideo, Uruguay

Angela Bachi
Biomolecular Mass Spectrometry Unit, Division of Genetics and Cell Biology, San Raffaele Scientific Institute, Milano, Italy

Erika Bechtold
Department of Chemistry, Wake Forest University, Winston-Salem, North Carolina, USA

Louise Benazzi
Institute for Biomedical Technologies, National Research Council, Viale Fratelli Cervi, Segrate-Milano, Italy

Aruni Bhatnagar
Diabetes and Obesity Center, University of Louisville, Louisville, Kentucky, USA

Alex Bokov
Department of Cellular & Structural Biology, and Department of Epidemiology & Biostatistics, The University of Texas Health Science Center at San Antonio, San Antonio, Texas, USA

Joseph R. Burgoyne
Cardiovascular Division, Department of Cardiology, King's College London, The Rayne Institute, St Thomas' Hospital, London, United Kingdom

Enrique Cadenas
Department of Pharmacology and Pharmaceutical Sciences, School of Pharmacy, University of Southern California, Los Angeles, California, USA

Jian Cai
Department of Pharmacology and Toxicology, University of Louisville, Louisville, Kentucky, USA

Sebastián Carballal
Laboratorio de Enzimología, Facultad de Ciencias, and Departamento de Bioquímica, and Center for Free Radical and Biomedical Research, Facultad de Medicina, Universidad de la República, Montevideo, Uruguay

Asish Chaudhuri
Barshop Institute for Longevity and Aging Studies, and Geriatric Research Education and Clinical Center, South Texas Veterans Health Care System, and Department of Biochemistry, The University of Texas Health Science Center at San Antonio, San Antonio, Texas, USA

Juan Chavez
Department of Chemistry, Oregon State University, Corvallis, Oregon, USA

Giovanni Chiappetta
Laboratoire Stress Oxydants et Cancer, DSV, IBITECS, CEA-Saclay, Gif-sur-Yvette, France

Simona G. Codreanu
Department of Biochemistry, Vanderbilt University School of Medicine, Nashville, Tennessee, USA

Lucia Coppo
Department of Neuroscience, Pharmacology Unit, University of Siena, Siena, Italy

Larry W. Daniel
Department of Biochemistry, Wake Forest University School of Medicine, Winston-Salem, North Carolina, USA

Antonella De Palma
Institute for Biomedical Technologies, National Research Council, Viale Fratelli Cervi, Segrate-Milano, Italy

Eric M. de Waal
Department of Biology, University of Texas at San Antonio, San Antonio, Texas, USA

Paolo Di Simplicio
Department of Neuroscience, Pharmacology Unit, University of Siena, Siena, Italy

Philip Eaton
Cardiovascular Division, Department of Cardiology, King's College London, The Rayne Institute, St Thomas' Hospital, London, United Kingdom

Lisa Elviri
Dipartimento di Chimica Generale ed Inorganica, Chimica Analitica, Chimica Fisica, Università di Parma, Parma, Italy

Leopold Flohé
Otto-von-Guericke-Universität, and MOLISA GmbH, Magdeburg, Germany

Cristina M. Furdui
Section on Molecular Medicine, Department of Internal Medicine, Wake Forest University School of Medicine, Medical Center Boulevard, Winston-Salem, North Carolina, USA

Jerome Garcia
Department of Pharmacology and Pharmaceutical Sciences, School of Pharmacy, University of Southern California, Los Angeles, California, USA

Pietro Ghezzi
Brighton and Sussex Medical School, Falmer, Brighton, United Kingdom

Emmanuel Godat
Laboratoire d'Etude du Métabolisme des Médicaments, DSV/iBiTec-S/SPI, and Laboratoire de Biologie Intégrative, DSV/iBiTec-S/SBIGeM, CEA/Saclay, Gif-sur-Yvette Cedex, France

Derick Han
Research Center for Liver Diseases, Keck School of Medicine, University of Southern California, Los Angeles, California, USA

Jean-François Heilier
Laboratoire d'Etude du Métabolisme des Médicaments, DSV/iBiTec-S/SPI, CEA/Saclay, Gif-sur-Yvette Cedex, France, and Université catholique de Louvain, Louvain Centre for Toxicology and Applied Pharmacology, Brussels, Belgium

Bradford G. Hill
Diabetes and Obesity Center, University of Louisville, Louisville, Kentucky, USA

Aeid Igbaria
Laboratoire Stress Oxydants et Cancer, DSV, IBITECS, CEA-Saclay, Gif-sur-Yvette, France

Lynnette C. Johnson
Department of Biochemistry, Wake Forest University School of Medicine, Winston-Salem, North Carolina, USA

Christophe Junot
Laboratoire d'Etude du Métabolisme des Médicaments, DSV/iBiTec-S/SPI, CEA/Saclay, Gif-sur-Yvette Cedex, France

S. Bruce King
Department of Chemistry, Wake Forest University, Winston-Salem, North Carolina, USA

Chananat Klomsiri
Department of Biochemistry, Wake Forest University School of Medicine, Winston-Salem, North Carolina, USA

Chitranshu Kumar
Laboratoire Stress Oxydants et Cancer, DSV, IBITECS, CEA-Saclay, Gif-sur-Yvette, France

Jean Labarre
Laboratoire de Biologie Intégrative, DSV/iBiTec-S/SBIGeM, CEA/Saclay, Gif-sur-Yvette Cedex, France

Daniel C. Liebler
Department of Biochemistry, Vanderbilt University School of Medicine, Nashville, Tennessee, USA

W. Todd Lowther
Department of Biochemistry, Wake Forest University School of Medicine, Winston-Salem, North Carolina, USA

Geoffrey Madalinski
Laboratoire d'Etude du Métabolisme des Médicaments, DSV/iBiTec-S/SPI, CEA/Saclay, Gif-sur-Yvette Cedex, France

Claudia S. Maier
Department of Chemistry, Oregon State University, Corvallis, Oregon, USA

Matilde Maiorino
Department of Biological Chemistry, University of Padova, Viale G. Colombo, Padova, Italy

Pierluigi Mauri
Institute for Biomedical Technologies, National Research Council, Viale Fratelli Cervi, Segrate-Milano, Italy

Kwan-Hoon Moon
Laboratory of Membrane Biochemistry and Biophysics, National Institute on Alcohol Abuse and Alcoholism, Bethesda, Maryland, USA

Ludovic Muller
Laboratoire d'Etude du Métabolisme des Médicaments, DSV/iBiTec-S/SPI, CEA/Saclay, Gif-sur-Yvette Cedex, France, and Laboratoire de Chimie Biologique Organique et Structurale, IPCM, UMR-CNRS, UPMC Paris Universitas, Paris Cedex, France

Sega Ndiaye
Biological Mass Spectrometry and Proteomics, USR CNRS/ESPCI ParisTech, Ecole Supérieure de Physique et de Chimie Industrielles, Paris Cedex, France

Kimberly J. Nelson
Department of Biochemistry, Wake Forest University School of Medicine, Winston-Salem, North Carolina, USA

Viviana I. Pérez
Department of Cellular & Structural Biology, and Barshop Institute for Longevity and Aging Studies, The University of Texas Health Science Center at San Antonio, San Antonio, Texas, USA

Anson Pierce
Department of Cellular & Structural Biology, and Barshop Institute for Longevity and Aging Studies, The University of Texas Health Science Center at San Antonio, and Geriatric Research Education and Clinical Center, South Texas Veterans Health Care System, San Antonio, Texas, USA

Leslie B. Poole
Department of Biochemistry, Wake Forest University School of Medicine, Winston-Salem, North Carolina, USA

Raffaella Priora
Department of Neuroscience, Pharmacology Unit, University of Siena, Siena, Italy

Rafael Radi
Departamento de Bioquímica, and Center for Free Radical and Biomedical Research, Facultad de Medicina, Universidad de la República, Montevideo, Uruguay

Kota V. Ramana
The Department of Biochemistry and Molecular Biology, University of Texas Medical Branch, Galveston, Texas, USA

Arlan Richardson
Department of Cellular & Structural Biology, and Department of Physiology, and Barshop Institute for Longevity and Aging Studies, The University of Texas Health Science Center at San Antonio, and Geriatric Research Education and Clinical Center, South Texas Veterans Health Care System, San Antonio, Texas, USA

LeAnn C. Rogers
Department of Biochemistry, Wake Forest University School of Medicine, Winston-Salem, North Carolina, USA

Seong-Eon Ryu
Center for Cellular Switch Protein Structure, Korea Research Institute of Bioscience and Biotechnology, Yusong, Taejon, and Department of Bio-engineering, College of Engineering, Hanyang University, Seongdong-gu, Seoul, South Korea

Sonia Salzano
Brighton and Sussex Medical School, Falmer, Brighton, United Kingdom

Harsh Sancheti
Department of Pharmacology and Pharmaceutical Sciences, School of Pharmacy, University of Southern California, Los Angeles, California, USA

Andrea Scaloni
Proteomics and Mass Spectrometry Laboratory, ISPAAM, National Research Council, Naples, Italy

Laura Soito
Department of Biochemistry, Wake Forest University School of Medicine, Winston-Salem, North Carolina, USA

Byoung-Joon Song
Laboratory of Membrane Biochemistry and Biophysics, National Institute on Alcohol Abuse and Alcoholism, Bethesda, Maryland, USA

Satish K. Srivastava
The Department of Biochemistry and Molecular Biology, University of Texas Medical Branch, Galveston, Texas, USA

Soo-Kyung Suh
Laboratory of Membrane Biochemistry and Biophysics, National Institute on Alcohol Abuse and Alcoholism, Bethesda, Maryland, USA, and National Center for Toxicological Research, National Institute of Food and Drug Safety Evaluation, Korea Food and Drug Administration, Seoul, Korea

Gianluca Tell
Department of Biomedical Sciences and Technologies, University of Udine, Udine, Italy

Michel B. Toledano
Laboratoire Stress Oxydants et Cancer, DSV, IBITECS, CEA-Saclay, Gif-sur-Yvette, France

Stefano Toppo
Department of Biological Chemistry, University of Padova, Viale G. Colombo, Padova, Italy

Federico Torta
Biomolecular Mass Spectrometry Unit, Division of Genetics and Cell Biology, San Raffaele Scientific Institute, Milano, Italy

Lucía Turell
Laboratorio de Enzimología, and Laboratorio de Fisicoquímica Biológica, Facultad de Ciencias, and Center for Free Radical and Biomedical Research, Facultad de Medicina, Universidad de la República, Montevideo, Uruguay

Fulvio Ursini
Department of Biological Chemistry, University of Padova, Viale G. Colombo, Padova, Italy

Joelle Vinh
Biological Mass Spectrometry and Proteomics, USR CNRS/ESPCI ParisTech, Ecole Supérieure de Physique et de Chimie Industrielles, Paris Cedex, France

Jing Wang
Department of Chemistry, Oregon State University, Corvallis, Oregon, USA

Walter F. Ward
Department of Physiology, and Barshop Institute for Longevity and Aging Studies, The University of Texas Health Science Center at San Antonio, San Antonio, Texas, USA

Jianyong Wu
Department of Chemistry, Oregon State University, Corvallis, Oregon, USA

Li-Peng Yap
Department of Pharmacology and Pharmaceutical Sciences, School of Pharmacy, University of Southern California, Los Angeles, California, USA

Maria D. Ybanez
Research Center for Liver Diseases, Keck School of Medicine, University of Southern California, Los Angeles, California, USA

Preface

Signaling by reactive oxygen- and nitrogen species, mainly non-radical species such as hydrogen peroxide, lipid peroxides, and peroxynitrite—which may be viewed as second messengers—has emerged as a major regulatory process of cell function. Signaling targets are redox-sensitive protein cysteines and the large pool of low-molecular thiols, mainly glutathione. These volumes of *Methods in Enzymology* on Thiols Redox Transitions in Cell Signaling address two large topics Chemistry and Biochemistry of Low Molecular Weight and Protein Thiols (Part A, Volume 473) and Cellular Localization and Signaling (Part B, Volume 474). Both volumes serve to bring together current methods and concepts in the field of cell signaling driven by thiol redox modifications by techniques such as fluorescence-based proteomics, mass spectrometry approaches, and fluorescence reporters.

The editors thank all the contributors, whose thorough and innovative work is the basis of these two *Methods in Enzymology* volumes. The editors give special thanks to Leopold Flohé for providing the introductory chapter "Changing paradigms in thiology: from antioxidant defense toward redox regulation, whose critical thinking educated us on the major concepts by which metabolic regulation and adaptation are transduced via thiol modifications.

Enrique Cadenas
Lester Packer
March 2010

Methods in Enzymology

Volume I. Preparation and Assay of Enzymes
Edited by Sidney P. Colowick and Nathan O. Kaplan

Volume II. Preparation and Assay of Enzymes
Edited by Sidney P. Colowick and Nathan O. Kaplan

Volume III. Preparation and Assay of Substrates
Edited by Sidney P. Colowick and Nathan O. Kaplan

Volume IV. Special Techniques for the Enzymologist
Edited by Sidney P. Colowick and Nathan O. Kaplan

Volume V. Preparation and Assay of Enzymes
Edited by Sidney P. Colowick and Nathan O. Kaplan

Volume VI. Preparation and Assay of Enzymes *(Continued)*
Preparation and Assay of Substrates
Special Techniques
Edited by Sidney P. Colowick and Nathan O. Kaplan

Volume VII. Cumulative Subject Index
Edited by Sidney P. Colowick and Nathan O. Kaplan

Volume VIII. Complex Carbohydrates
Edited by Elizabeth F. Neufeld and Victor Ginsburg

Volume IX. Carbohydrate Metabolism
Edited by Willis A. Wood

Volume X. Oxidation and Phosphorylation
Edited by Ronald W. Estabrook and Maynard E. Pullman

Volume XI. Enzyme Structure
Edited by C. H. W. Hirs

Volume XII. Nucleic Acids (Parts A and B)
Edited by Lawrence Grossman and Kivie Moldave

Volume XIII. Citric Acid Cycle
Edited by J. M. Lowenstein

Volume XIV. Lipids
Edited by J. M. Lowenstein

Volume XV. Steroids and Terpenoids
Edited by Raymond B. Clayton

VOLUME XXXV. Lipids (Part B)
Edited by JOHN M. LOWENSTEIN

VOLUME XXXVI. Hormone Action (Part A: Steroid Hormones)
Edited by BERT W. O'MALLEY AND JOEL G. HARDMAN

VOLUME XXXVII. Hormone Action (Part B: Peptide Hormones)
Edited by BERT W. O'MALLEY AND JOEL G. HARDMAN

VOLUME XXXVIII. Hormone Action (Part C: Cyclic Nucleotides)
Edited by JOEL G. HARDMAN AND BERT W. O'MALLEY

VOLUME XXXIX. Hormone Action (Part D: Isolated Cells, Tissues, and Organ Systems)
Edited by JOEL G. HARDMAN AND BERT W. O'MALLEY

VOLUME XL. Hormone Action (Part E: Nuclear Structure and Function)
Edited by BERT W. O'MALLEY AND JOEL G. HARDMAN

VOLUME XLI. Carbohydrate Metabolism (Part B)
Edited by W. A. WOOD

VOLUME XLII. Carbohydrate Metabolism (Part C)
Edited by W. A. WOOD

VOLUME XLIII. Antibiotics
Edited by JOHN H. HASH

VOLUME XLIV. Immobilized Enzymes
Edited by KLAUS MOSBACH

VOLUME XLV. Proteolytic Enzymes (Part B)
Edited by LASZLO LORAND

VOLUME XLVI. Affinity Labeling
Edited by WILLIAM B. JAKOBY AND MEIR WILCHEK

VOLUME XLVII. Enzyme Structure (Part E)
Edited by C. H. W. HIRS AND SERGE N. TIMASHEFF

VOLUME XLVIII. Enzyme Structure (Part F)
Edited by C. H. W. HIRS AND SERGE N. TIMASHEFF

VOLUME XLIX. Enzyme Structure (Part G)
Edited by C. H. W. HIRS AND SERGE N. TIMASHEFF

VOLUME L. Complex Carbohydrates (Part C)
Edited by VICTOR GINSBURG

VOLUME LI. Purine and Pyrimidine Nucleotide Metabolism
Edited by PATRICIA A. HOFFEE AND MARY ELLEN JONES

VOLUME LII. Biomembranes (Part C: Biological Oxidations)
Edited by SIDNEY FLEISCHER AND LESTER PACKER

VOLUME 71. Lipids (Part C)
Edited by JOHN M. LOWENSTEIN

VOLUME 72. Lipids (Part D)
Edited by JOHN M. LOWENSTEIN

VOLUME 73. Immunochemical Techniques (Part B)
Edited by JOHN J. LANGONE AND HELEN VAN VUNAKIS

VOLUME 74. Immunochemical Techniques (Part C)
Edited by JOHN J. LANGONE AND HELEN VAN VUNAKIS

VOLUME 75. Cumulative Subject Index Volumes XXXI, XXXII, XXXIV–LX
Edited by EDWARD A. DENNIS AND MARTHA G. DENNIS

VOLUME 76. Hemoglobins
Edited by ERALDO ANTONINI, LUIGI ROSSI-BERNARDI, AND EMILIA CHIANCONE

VOLUME 77. Detoxication and Drug Metabolism
Edited by WILLIAM B. JAKOBY

VOLUME 78. Interferons (Part A)
Edited by SIDNEY PESTKA

VOLUME 79. Interferons (Part B)
Edited by SIDNEY PESTKA

VOLUME 80. Proteolytic Enzymes (Part C)
Edited by LASZLO LORAND

VOLUME 81. Biomembranes (Part H: Visual Pigments and Purple Membranes, I)
Edited by LESTER PACKER

VOLUME 82. Structural and Contractile Proteins (Part A: Extracellular Matrix)
Edited by LEON W. CUNNINGHAM AND DIXIE W. FREDERIKSEN

VOLUME 83. Complex Carbohydrates (Part D)
Edited by VICTOR GINSBURG

VOLUME 84. Immunochemical Techniques (Part D: Selected Immunoassays)
Edited by JOHN J. LANGONE AND HELEN VAN VUNAKIS

VOLUME 85. Structural and Contractile Proteins (Part B: The Contractile Apparatus and the Cytoskeleton)
Edited by DIXIE W. FREDERIKSEN AND LEON W. CUNNINGHAM

VOLUME 86. Prostaglandins and Arachidonate Metabolites
Edited by WILLIAM E. M. LANDS AND WILLIAM L. SMITH

VOLUME 87. Enzyme Kinetics and Mechanism (Part C: Intermediates, Stereo-chemistry, and Rate Studies)
Edited by DANIEL L. PURICH

VOLUME 88. Biomembranes (Part I: Visual Pigments and Purple Membranes, II)
Edited by LESTER PACKER

VOLUME 105. Oxygen Radicals in Biological Systems
Edited by LESTER PACKER

VOLUME 106. Posttranslational Modifications (Part A)
Edited by FINN WOLD AND KIVIE MOLDAVE

VOLUME 107. Posttranslational Modifications (Part B)
Edited by FINN WOLD AND KIVIE MOLDAVE

VOLUME 108. Immunochemical Techniques (Part G: Separation and Characterization of Lymphoid Cells)
Edited by GIOVANNI DI SABATO, JOHN J. LANGONE, AND HELEN VAN VUNAKIS

VOLUME 109. Hormone Action (Part I: Peptide Hormones)
Edited by LUTZ BIRNBAUMER AND BERT W. O'MALLEY

VOLUME 110. Steroids and Isoprenoids (Part A)
Edited by JOHN H. LAW AND HANS C. RILLING

VOLUME 111. Steroids and Isoprenoids (Part B)
Edited by JOHN H. LAW AND HANS C. RILLING

VOLUME 112. Drug and Enzyme Targeting (Part A)
Edited by KENNETH J. WIDDER AND RALPH GREEN

VOLUME 113. Glutamate, Glutamine, Glutathione, and Related Compounds
Edited by ALTON MEISTER

VOLUME 114. Diffraction Methods for Biological Macromolecules (Part A)
Edited by HAROLD W. WYCKOFF, C. H. W. HIRS, AND SERGE N. TIMASHEFF

VOLUME 115. Diffraction Methods for Biological Macromolecules (Part B)
Edited by HAROLD W. WYCKOFF, C. H. W. HIRS, AND SERGE N. TIMASHEFF

VOLUME 116. Immunochemical Techniques
(Part H: Effectors and Mediators of Lymphoid Cell Functions)
Edited by GIOVANNI DI SABATO, JOHN J. LANGONE, AND HELEN VAN VUNAKIS

VOLUME 117. Enzyme Structure (Part J)
Edited by C. H. W. HIRS AND SERGE N. TIMASHEFF

VOLUME 118. Plant Molecular Biology
Edited by ARTHUR WEISSBACH AND HERBERT WEISSBACH

VOLUME 119. Interferons (Part C)
Edited by SIDNEY PESTKA

VOLUME 120. Cumulative Subject Index Volumes 81–94, 96–101

VOLUME 121. Immunochemical Techniques (Part I: Hybridoma Technology and Monoclonal Antibodies)
Edited by JOHN J. LANGONE AND HELEN VAN VUNAKIS

VOLUME 122. Vitamins and Coenzymes (Part G)
Edited by FRANK CHYTIL AND DONALD B. MCCORMICK

VOLUME 139. Cellular Regulators (Part A: Calcium- and Calmodulin-Binding Proteins)
Edited by ANTHONY R. MEANS AND P. MICHAEL CONN

VOLUME 140. Cumulative Subject Index Volumes 102–119, 121–134

VOLUME 141. Cellular Regulators (Part B: Calcium and Lipids)
Edited by P. MICHAEL CONN AND ANTHONY R. MEANS

VOLUME 142. Metabolism of Aromatic Amino Acids and Amines
Edited by SEYMOUR KAUFMAN

VOLUME 143. Sulfur and Sulfur Amino Acids
Edited by WILLIAM B. JAKOBY AND OWEN GRIFFITH

VOLUME 144. Structural and Contractile Proteins (Part D: Extracellular Matrix)
Edited by LEON W. CUNNINGHAM

VOLUME 145. Structural and Contractile Proteins (Part E: Extracellular Matrix)
Edited by LEON W. CUNNINGHAM

VOLUME 146. Peptide Growth Factors (Part A)
Edited by DAVID BARNES AND DAVID A. SIRBASKU

VOLUME 147. Peptide Growth Factors (Part B)
Edited by DAVID BARNES AND DAVID A. SIRBASKU

VOLUME 148. Plant Cell Membranes
Edited by LESTER PACKER AND ROLAND DOUCE

VOLUME 149. Drug and Enzyme Targeting (Part B)
Edited by RALPH GREEN AND KENNETH J. WIDDER

VOLUME 150. Immunochemical Techniques (Part K: *In Vitro* Models of B and T Cell Functions and Lymphoid Cell Receptors)
Edited by GIOVANNI DI SABATO

VOLUME 151. Molecular Genetics of Mammalian Cells
Edited by MICHAEL M. GOTTESMAN

VOLUME 152. Guide to Molecular Cloning Techniques
Edited by SHELBY L. BERGER AND ALAN R. KIMMEL

VOLUME 153. Recombinant DNA (Part D)
Edited by RAY WU AND LAWRENCE GROSSMAN

VOLUME 154. Recombinant DNA (Part E)
Edited by RAY WU AND LAWRENCE GROSSMAN

VOLUME 155. Recombinant DNA (Part F)
Edited by RAY WU

VOLUME 156. Biomembranes (Part P: ATP-Driven Pumps and Related Transport: The Na, K-Pump)
Edited by SIDNEY FLEISCHER AND BECCA FLEISCHER

VOLUME 157. Biomembranes (Part Q: ATP-Driven Pumps and Related Transport: Calcium, Proton, and Potassium Pumps)
Edited by SIDNEY FLEISCHER AND BECCA FLEISCHER

VOLUME 158. Metalloproteins (Part A)
Edited by JAMES F. RIORDAN AND BERT L. VALLEE

VOLUME 159. Initiation and Termination of Cyclic Nucleotide Action
Edited by JACKIE D. CORBIN AND ROGER A. JOHNSON

VOLUME 160. Biomass (Part A: Cellulose and Hemicellulose)
Edited by WILLIS A. WOOD AND SCOTT T. KELLOGG

VOLUME 161. Biomass (Part B: Lignin, Pectin, and Chitin)
Edited by WILLIS A. WOOD AND SCOTT T. KELLOGG

VOLUME 162. Immunochemical Techniques (Part L: Chemotaxis and Inflammation)
Edited by GIOVANNI DI SABATO

VOLUME 163. Immunochemical Techniques (Part M: Chemotaxis and Inflammation)
Edited by GIOVANNI DI SABATO

VOLUME 164. Ribosomes
Edited by HARRY F. NOLLER, JR., AND KIVIE MOLDAVE

VOLUME 165. Microbial Toxins: Tools for Enzymology
Edited by SIDNEY HARSHMAN

VOLUME 166. Branched-Chain Amino Acids
Edited by ROBERT HARRIS AND JOHN R. SOKATCH

VOLUME 167. Cyanobacteria
Edited by LESTER PACKER AND ALEXANDER N. GLAZER

VOLUME 168. Hormone Action (Part K: Neuroendocrine Peptides)
Edited by P. MICHAEL CONN

VOLUME 169. Platelets: Receptors, Adhesion, Secretion (Part A)
Edited by JACEK HAWIGER

VOLUME 170. Nucleosomes
Edited by PAUL M. WASSARMAN AND ROGER D. KORNBERG

VOLUME 171. Biomembranes (Part R: Transport Theory: Cells and Model Membranes)
Edited by SIDNEY FLEISCHER AND BECCA FLEISCHER

VOLUME 172. Biomembranes (Part S: Transport: Membrane Isolation and Characterization)
Edited by SIDNEY FLEISCHER AND BECCA FLEISCHER

VOLUME 173. Biomembranes [Part T: Cellular and Subcellular Transport: Eukaryotic (Nonepithelial) Cells]
Edited by SIDNEY FLEISCHER AND BECCA FLEISCHER

VOLUME 174. Biomembranes [Part U: Cellular and Subcellular Transport: Eukaryotic (Nonepithelial) Cells]
Edited by SIDNEY FLEISCHER AND BECCA FLEISCHER

VOLUME 175. Cumulative Subject Index Volumes 135–139, 141–167

VOLUME 176. Nuclear Magnetic Resonance (Part A: Spectral Techniques and Dynamics)
Edited by NORMAN J. OPPENHEIMER AND THOMAS L. JAMES

VOLUME 177. Nuclear Magnetic Resonance (Part B: Structure and Mechanism)
Edited by NORMAN J. OPPENHEIMER AND THOMAS L. JAMES

VOLUME 178. Antibodies, Antigens, and Molecular Mimicry
Edited by JOHN J. LANGONE

VOLUME 179. Complex Carbohydrates (Part F)
Edited by VICTOR GINSBURG

VOLUME 180. RNA Processing (Part A: General Methods)
Edited by JAMES E. DAHLBERG AND JOHN N. ABELSON

VOLUME 181. RNA Processing (Part B: Specific Methods)
Edited by JAMES E. DAHLBERG AND JOHN N. ABELSON

VOLUME 182. Guide to Protein Purification
Edited by MURRAY P. DEUTSCHER

VOLUME 183. Molecular Evolution: Computer Analysis of Protein and Nucleic Acid Sequences
Edited by RUSSELL F. DOOLITTLE

VOLUME 184. Avidin-Biotin Technology
Edited by MEIR WILCHEK AND EDWARD A. BAYER

VOLUME 185. Gene Expression Technology
Edited by DAVID V. GOEDDEL

VOLUME 186. Oxygen Radicals in Biological Systems (Part B: Oxygen Radicals and Antioxidants)
Edited by LESTER PACKER AND ALEXANDER N. GLAZER

VOLUME 187. Arachidonate Related Lipid Mediators
Edited by ROBERT C. MURPHY AND FRANK A. FITZPATRICK

VOLUME 188. Hydrocarbons and Methylotrophy
Edited by MARY E. LIDSTROM

VOLUME 189. Retinoids (Part A: Molecular and Metabolic Aspects)
Edited by LESTER PACKER

VOLUME 190. Retinoids (Part B: Cell Differentiation and Clinical Applications)
Edited by LESTER PACKER

VOLUME 191. Biomembranes (Part V: Cellular and Subcellular Transport: Epithelial Cells)
Edited by SIDNEY FLEISCHER AND BECCA FLEISCHER

VOLUME 192. Biomembranes (Part W: Cellular and Subcellular Transport: Epithelial Cells)
Edited by SIDNEY FLEISCHER AND BECCA FLEISCHER

VOLUME 193. Mass Spectrometry
Edited by JAMES A. MCCLOSKEY

VOLUME 194. Guide to Yeast Genetics and Molecular Biology
Edited by CHRISTINE GUTHRIE AND GERALD R. FINK

VOLUME 195. Adenylyl Cyclase, G Proteins, and Guanylyl Cyclase
Edited by ROGER A. JOHNSON AND JACKIE D. CORBIN

VOLUME 196. Molecular Motors and the Cytoskeleton
Edited by RICHARD B. VALLEE

VOLUME 197. Phospholipases
Edited by EDWARD A. DENNIS

VOLUME 198. Peptide Growth Factors (Part C)
Edited by DAVID BARNES, J. P. MATHER, AND GORDON H. SATO

VOLUME 199. Cumulative Subject Index Volumes 168–174, 176–194

VOLUME 200. Protein Phosphorylation (Part A: Protein Kinases: Assays, Purification, Antibodies, Functional Analysis, Cloning, and Expression)
Edited by TONY HUNTER AND BARTHOLOMEW M. SEFTON

VOLUME 201. Protein Phosphorylation (Part B: Analysis of Protein Phosphorylation, Protein Kinase Inhibitors, and Protein Phosphatases)
Edited by TONY HUNTER AND BARTHOLOMEW M. SEFTON

VOLUME 202. Molecular Design and Modeling: Concepts and Applications (Part A: Proteins, Peptides, and Enzymes)
Edited by JOHN J. LANGONE

VOLUME 203. Molecular Design and Modeling: Concepts and Applications (Part B: Antibodies and Antigens, Nucleic Acids, Polysaccharides, and Drugs)
Edited by JOHN J. LANGONE

VOLUME 204. Bacterial Genetic Systems
Edited by JEFFREY H. MILLER

VOLUME 205. Metallobiochemistry (Part B: Metallothionein and Related Molecules)
Edited by JAMES F. RIORDAN AND BERT L. VALLEE

VOLUME 206. Cytochrome P450
Edited by MICHAEL R. WATERMAN AND ERIC F. JOHNSON

VOLUME 207. Ion Channels
Edited by BERNARDO RUDY AND LINDA E. IVERSON

VOLUME 208. Protein–DNA Interactions
Edited by ROBERT T. SAUER

VOLUME 209. Phospholipid Biosynthesis
Edited by EDWARD A. DENNIS AND DENNIS E. VANCE

VOLUME 210. Numerical Computer Methods
Edited by LUDWIG BRAND AND MICHAEL L. JOHNSON

VOLUME 211. DNA Structures (Part A: Synthesis and Physical Analysis of DNA)
Edited by DAVID M. J. LILLEY AND JAMES E. DAHLBERG

VOLUME 212. DNA Structures (Part B: Chemical and Electrophoretic Analysis of DNA)
Edited by DAVID M. J. LILLEY AND JAMES E. DAHLBERG

VOLUME 213. Carotenoids (Part A: Chemistry, Separation, Quantitation, and Antioxidation)
Edited by LESTER PACKER

VOLUME 214. Carotenoids (Part B: Metabolism, Genetics, and Biosynthesis)
Edited by LESTER PACKER

VOLUME 215. Platelets: Receptors, Adhesion, Secretion (Part B)
Edited by JACEK J. HAWIGER

VOLUME 216. Recombinant DNA (Part G)
Edited by RAY WU

VOLUME 217. Recombinant DNA (Part H)
Edited by RAY WU

VOLUME 218. Recombinant DNA (Part I)
Edited by RAY WU

VOLUME 219. Reconstitution of Intracellular Transport
Edited by JAMES E. ROTHMAN

VOLUME 220. Membrane Fusion Techniques (Part A)
Edited by NEJAT DÜZGÜNEŞ

VOLUME 221. Membrane Fusion Techniques (Part B)
Edited by NEJAT DÜZGÜNEŞ

VOLUME 222. Proteolytic Enzymes in Coagulation, Fibrinolysis, and Complement Activation (Part A: Mammalian Blood Coagulation Factors and Inhibitors)
Edited by LASZLO LORAND AND KENNETH G. MANN

VOLUME 223. Proteolytic Enzymes in Coagulation, Fibrinolysis, and Complement Activation (Part B: Complement Activation, Fibrinolysis, and Nonmammalian Blood Coagulation Factors)
Edited by LASZLO LORAND AND KENNETH G. MANN

VOLUME 224. Molecular Evolution: Producing the Biochemical Data
Edited by ELIZABETH ANNE ZIMMER, THOMAS J. WHITE, REBECCA L. CANN, AND ALLAN C. WILSON

VOLUME 225. Guide to Techniques in Mouse Development
Edited by PAUL M. WASSARMAN AND MELVIN L. DEPAMPHILIS

VOLUME 226. Metallobiochemistry (Part C: Spectroscopic and Physical Methods for Probing Metal Ion Environments in Metalloenzymes and Metalloproteins)
Edited by JAMES F. RIORDAN AND BERT L. VALLEE

VOLUME 227. Metallobiochemistry (Part D: Physical and Spectroscopic Methods for Probing Metal Ion Environments in Metalloproteins)
Edited by JAMES F. RIORDAN AND BERT L. VALLEE

VOLUME 228. Aqueous Two-Phase Systems
Edited by HARRY WALTER AND GÖTE JOHANSSON

VOLUME 229. Cumulative Subject Index Volumes 195–198, 200–227

VOLUME 230. Guide to Techniques in Glycobiology
Edited by WILLIAM J. LENNARZ AND GERALD W. HART

VOLUME 231. Hemoglobins (Part B: Biochemical and Analytical Methods)
Edited by JOHANNES EVERSE, KIM D. VANDEGRIFF, AND ROBERT M. WINSLOW

VOLUME 232. Hemoglobins (Part C: Biophysical Methods)
Edited by JOHANNES EVERSE, KIM D. VANDEGRIFF, AND ROBERT M. WINSLOW

VOLUME 233. Oxygen Radicals in Biological Systems (Part C)
Edited by LESTER PACKER

VOLUME 234. Oxygen Radicals in Biological Systems (Part D)
Edited by LESTER PACKER

VOLUME 235. Bacterial Pathogenesis (Part A: Identification and Regulation of Virulence Factors)
Edited by VIRGINIA L. CLARK AND PATRIK M. BAVOIL

VOLUME 236. Bacterial Pathogenesis (Part B: Integration of Pathogenic Bacteria with Host Cells)
Edited by VIRGINIA L. CLARK AND PATRIK M. BAVOIL

VOLUME 237. Heterotrimeric G Proteins
Edited by RAVI IYENGAR

VOLUME 238. Heterotrimeric G-Protein Effectors
Edited by RAVI IYENGAR

VOLUME 239. Nuclear Magnetic Resonance (Part C)
Edited by THOMAS L. JAMES AND NORMAN J. OPPENHEIMER

VOLUME 240. Numerical Computer Methods (Part B)
Edited by MICHAEL L. JOHNSON AND LUDWIG BRAND

VOLUME 241. Retroviral Proteases
Edited by LAWRENCE C. KUO AND JULES A. SHAFER

VOLUME 242. Neoglycoconjugates (Part A)
Edited by Y. C. LEE AND REIKO T. LEE

VOLUME 243. Inorganic Microbial Sulfur Metabolism
Edited by HARRY D. PECK, JR., AND JEAN LEGALL

VOLUME 244. Proteolytic Enzymes: Serine and Cysteine Peptidases
Edited by ALAN J. BARRETT

VOLUME 245. Extracellular Matrix Components
Edited by E. RUOSLAHTI AND E. ENGVALL

VOLUME 246. Biochemical Spectroscopy
Edited by KENNETH SAUER

VOLUME 247. Neoglycoconjugates (Part B: Biomedical Applications)
Edited by Y. C. LEE AND REIKO T. LEE

VOLUME 248. Proteolytic Enzymes: Aspartic and Metallo Peptidases
Edited by ALAN J. BARRETT

VOLUME 249. Enzyme Kinetics and Mechanism (Part D: Developments in Enzyme Dynamics)
Edited by DANIEL L. PURICH

VOLUME 250. Lipid Modifications of Proteins
Edited by PATRICK J. CASEY AND JANICE E. BUSS

VOLUME 251. Biothiols (Part A: Monothiols and Dithiols, Protein Thiols, and Thiyl Radicals)
Edited by LESTER PACKER

VOLUME 252. Biothiols (Part B: Glutathione and Thioredoxin; Thiols in Signal Transduction and Gene Regulation)
Edited by LESTER PACKER

VOLUME 253. Adhesion of Microbial Pathogens
Edited by RON J. DOYLE AND ITZHAK OFEK

VOLUME 254. Oncogene Techniques
Edited by PETER K. VOGT AND INDER M. VERMA

VOLUME 255. Small GTPases and Their Regulators (Part A: Ras Family)
Edited by W. E. BALCH, CHANNING J. DER, AND ALAN HALL

VOLUME 274. RNA Polymerase and Associated Factors (Part B)
Edited by SANKAR ADHYA

VOLUME 275. Viral Polymerases and Related Proteins
Edited by LAWRENCE C. KUO, DAVID B. OLSEN, AND STEVEN S. CARROLL

VOLUME 276. Macromolecular Crystallography (Part A)
Edited by CHARLES W. CARTER, JR., AND ROBERT M. SWEET

VOLUME 277. Macromolecular Crystallography (Part B)
Edited by CHARLES W. CARTER, JR., AND ROBERT M. SWEET

VOLUME 278. Fluorescence Spectroscopy
Edited by LUDWIG BRAND AND MICHAEL L. JOHNSON

VOLUME 279. Vitamins and Coenzymes (Part I)
Edited by DONALD B. MCCORMICK, JOHN W. SUTTIE, AND CONRAD WAGNER

VOLUME 280. Vitamins and Coenzymes (Part J)
Edited by DONALD B. MCCORMICK, JOHN W. SUTTIE, AND CONRAD WAGNER

VOLUME 281. Vitamins and Coenzymes (Part K)
Edited by DONALD B. MCCORMICK, JOHN W. SUTTIE, AND CONRAD WAGNER

VOLUME 282. Vitamins and Coenzymes (Part L)
Edited by DONALD B. MCCORMICK, JOHN W. SUTTIE, AND CONRAD WAGNER

VOLUME 283. Cell Cycle Control
Edited by WILLIAM G. DUNPHY

VOLUME 284. Lipases (Part A: Biotechnology)
Edited by BYRON RUBIN AND EDWARD A. DENNIS

VOLUME 285. Cumulative Subject Index Volumes 263, 264, 266–284, 286–289

VOLUME 286. Lipases (Part B: Enzyme Characterization and Utilization)
Edited by BYRON RUBIN AND EDWARD A. DENNIS

VOLUME 287. Chemokines
Edited by RICHARD HORUK

VOLUME 288. Chemokine Receptors
Edited by RICHARD HORUK

VOLUME 289. Solid Phase Peptide Synthesis
Edited by GREGG B. FIELDS

VOLUME 290. Molecular Chaperones
Edited by GEORGE H. LORIMER AND THOMAS BALDWIN

VOLUME 291. Caged Compounds
Edited by GERARD MARRIOTT

VOLUME 292. ABC Transporters: Biochemical, Cellular, and Molecular Aspects
Edited by SURESH V. AMBUDKAR AND MICHAEL M. GOTTESMAN

VOLUME 311. Sphingolipid Metabolism and Cell Signaling (Part A)
Edited by ALFRED H. MERRILL, JR., AND YUSUF A. HANNUN

VOLUME 312. Sphingolipid Metabolism and Cell Signaling (Part B)
Edited by ALFRED H. MERRILL, JR., AND YUSUF A. HANNUN

VOLUME 313. Antisense Technology
(Part A: General Methods, Methods of Delivery, and RNA Studies)
Edited by M. IAN PHILLIPS

VOLUME 314. Antisense Technology (Part B: Applications)
Edited by M. IAN PHILLIPS

VOLUME 315. Vertebrate Phototransduction and the Visual Cycle (Part A)
Edited by KRZYSZTOF PALCZEWSKI

VOLUME 316. Vertebrate Phototransduction and the Visual Cycle (Part B)
Edited by KRZYSZTOF PALCZEWSKI

VOLUME 317. RNA–Ligand Interactions (Part A: Structural Biology Methods)
Edited by DANIEL W. CELANDER AND JOHN N. ABELSON

VOLUME 318. RNA–Ligand Interactions (Part B: Molecular Biology Methods)
Edited by DANIEL W. CELANDER AND JOHN N. ABELSON

VOLUME 319. Singlet Oxygen, UV-A, and Ozone
Edited by LESTER PACKER AND HELMUT SIES

VOLUME 320. Cumulative Subject Index Volumes 290–319

VOLUME 321. Numerical Computer Methods (Part C)
Edited by MICHAEL L. JOHNSON AND LUDWIG BRAND

VOLUME 322. Apoptosis
Edited by JOHN C. REED

VOLUME 323. Energetics of Biological Macromolecules (Part C)
Edited by MICHAEL L. JOHNSON AND GARY K. ACKERS

VOLUME 324. Branched-Chain Amino Acids (Part B)
Edited by ROBERT A. HARRIS AND JOHN R. SOKATCH

VOLUME 325. Regulators and Effectors of Small GTPases
(Part D: Rho Family)
Edited by W. E. BALCH, CHANNING J. DER, AND ALAN HALL

VOLUME 326. Applications of Chimeric Genes and Hybrid Proteins
(Part A: Gene Expression and Protein Purification)
Edited by JEREMY THORNER, SCOTT D. EMR, AND JOHN N. ABELSON

VOLUME 327. Applications of Chimeric Genes and Hybrid Proteins
(Part B: Cell Biology and Physiology)
Edited by JEREMY THORNER, SCOTT D. EMR, AND JOHN N. ABELSON

VOLUME 328. Applications of Chimeric Genes and Hybrid Proteins (Part C: Protein–Protein Interactions and Genomics)
Edited by JEREMY THORNER, SCOTT D. EMR, AND JOHN N. ABELSON

VOLUME 329. Regulators and Effectors of Small GTPases (Part E: GTPases Involved in Vesicular Traffic)
Edited by W. E. BALCH, CHANNING J. DER, AND ALAN HALL

VOLUME 330. Hyperthermophilic Enzymes (Part A)
Edited by MICHAEL W. W. ADAMS AND ROBERT M. KELLY

VOLUME 331. Hyperthermophilic Enzymes (Part B)
Edited by MICHAEL W. W. ADAMS AND ROBERT M. KELLY

VOLUME 332. Regulators and Effectors of Small GTPases (Part F: Ras Family I)
Edited by W. E. BALCH, CHANNING J. DER, AND ALAN HALL

VOLUME 333. Regulators and Effectors of Small GTPases (Part G: Ras Family II)
Edited by W. E. BALCH, CHANNING J. DER, AND ALAN HALL

VOLUME 334. Hyperthermophilic Enzymes (Part C)
Edited by MICHAEL W. W. ADAMS AND ROBERT M. KELLY

VOLUME 335. Flavonoids and Other Polyphenols
Edited by LESTER PACKER

VOLUME 336. Microbial Growth in Biofilms (Part A: Developmental and Molecular Biological Aspects)
Edited by RON J. DOYLE

VOLUME 337. Microbial Growth in Biofilms (Part B: Special Environments and Physicochemical Aspects)
Edited by RON J. DOYLE

VOLUME 338. Nuclear Magnetic Resonance of Biological Macromolecules (Part A)
Edited by THOMAS L. JAMES, VOLKER DÖTSCH, AND ULI SCHMITZ

VOLUME 339. Nuclear Magnetic Resonance of Biological Macromolecules (Part B)
Edited by THOMAS L. JAMES, VOLKER DÖTSCH, AND ULI SCHMITZ

VOLUME 340. Drug–Nucleic Acid Interactions
Edited by JONATHAN B. CHAIRES AND MICHAEL J. WARING

VOLUME 341. Ribonucleases (Part A)
Edited by ALLEN W. NICHOLSON

VOLUME 342. Ribonucleases (Part B)
Edited by ALLEN W. NICHOLSON

VOLUME 343. G Protein Pathways (Part A: Receptors)
Edited by RAVI IYENGAR AND JOHN D. HILDEBRANDT

VOLUME 344. G Protein Pathways (Part B: G Proteins and Their Regulators)
Edited by RAVI IYENGAR AND JOHN D. HILDEBRANDT

VOLUME 345. G Protein Pathways (Part C: Effector Mechanisms)
Edited by RAVI IYENGAR AND JOHN D. HILDEBRANDT

VOLUME 346. Gene Therapy Methods
Edited by M. IAN PHILLIPS

VOLUME 347. Protein Sensors and Reactive Oxygen Species (Part A: Selenoproteins and Thioredoxin)
Edited by HELMUT SIES AND LESTER PACKER

VOLUME 348. Protein Sensors and Reactive Oxygen Species (Part B: Thiol Enzymes and Proteins)
Edited by HELMUT SIES AND LESTER PACKER

VOLUME 349. Superoxide Dismutase
Edited by LESTER PACKER

VOLUME 350. Guide to Yeast Genetics and Molecular and Cell Biology (Part B)
Edited by CHRISTINE GUTHRIE AND GERALD R. FINK

VOLUME 351. Guide to Yeast Genetics and Molecular and Cell Biology (Part C)
Edited by CHRISTINE GUTHRIE AND GERALD R. FINK

VOLUME 352. Redox Cell Biology and Genetics (Part A)
Edited by CHANDAN K. SEN AND LESTER PACKER

VOLUME 353. Redox Cell Biology and Genetics (Part B)
Edited by CHANDAN K. SEN AND LESTER PACKER

VOLUME 354. Enzyme Kinetics and Mechanisms (Part F: Detection and Characterization of Enzyme Reaction Intermediates)
Edited by DANIEL L. PURICH

VOLUME 355. Cumulative Subject Index Volumes 321–354

VOLUME 356. Laser Capture Microscopy and Microdissection
Edited by P. MICHAEL CONN

VOLUME 357. Cytochrome P450, Part C
Edited by ERIC F. JOHNSON AND MICHAEL R. WATERMAN

VOLUME 358. Bacterial Pathogenesis (Part C: Identification, Regulation, and Function of Virulence Factors)
Edited by VIRGINIA L. CLARK AND PATRIK M. BAVOIL

VOLUME 359. Nitric Oxide (Part D)
Edited by ENRIQUE CADENAS AND LESTER PACKER

VOLUME 360. Biophotonics (Part A)
Edited by GERARD MARRIOTT AND IAN PARKER

VOLUME 361. Biophotonics (Part B)
Edited by GERARD MARRIOTT AND IAN PARKER

VOLUME 381. Oxygen Sensing
Edited by CHANDAN K. SEN AND GREGG L. SEMENZA

VOLUME 382. Quinones and Quinone Enzymes (Part B)
Edited by HELMUT SIES AND LESTER PACKER

VOLUME 383. Numerical Computer Methods (Part D)
Edited by LUDWIG BRAND AND MICHAEL L. JOHNSON

VOLUME 384. Numerical Computer Methods (Part E)
Edited by LUDWIG BRAND AND MICHAEL L. JOHNSON

VOLUME 385. Imaging in Biological Research (Part A)
Edited by P. MICHAEL CONN

VOLUME 386. Imaging in Biological Research (Part B)
Edited by P. MICHAEL CONN

VOLUME 387. Liposomes (Part D)
Edited by NEJAT DÜZGÜNEŞ

VOLUME 388. Protein Engineering
Edited by DAN E. ROBERTSON AND JOSEPH P. NOEL

VOLUME 389. Regulators of G-Protein Signaling (Part A)
Edited by DAVID P. SIDEROVSKI

VOLUME 390. Regulators of G-Protein Signaling (Part B)
Edited by DAVID P. SIDEROVSKI

VOLUME 391. Liposomes (Part E)
Edited by NEJAT DÜZGÜNEŞ

VOLUME 392. RNA Interference
Edited by ENGELKE ROSSI

VOLUME 393. Circadian Rhythms
Edited by MICHAEL W. YOUNG

VOLUME 394. Nuclear Magnetic Resonance of Biological Macromolecules (Part C)
Edited by THOMAS L. JAMES

VOLUME 395. Producing the Biochemical Data (Part B)
Edited by ELIZABETH A. ZIMMER AND ERIC H. ROALSON

VOLUME 396. Nitric Oxide (Part E)
Edited by LESTER PACKER AND ENRIQUE CADENAS

VOLUME 397. Environmental Microbiology
Edited by JARED R. LEADBETTER

VOLUME 398. Ubiquitin and Protein Degradation (Part A)
Edited by RAYMOND J. DESHAIES

VOLUME 399. Ubiquitin and Protein Degradation (Part B)
Edited by RAYMOND J. DESHAIES

VOLUME 400. Phase II Conjugation Enzymes and Transport Systems
Edited by HELMUT SIES AND LESTER PACKER

VOLUME 401. Glutathione Transferases and Gamma Glutamyl Transpeptidases
Edited by HELMUT SIES AND LESTER PACKER

VOLUME 402. Biological Mass Spectrometry
Edited by A. L. BURLINGAME

VOLUME 403. GTPases Regulating Membrane Targeting and Fusion
Edited by WILLIAM E. BALCH, CHANNING J. DER, AND ALAN HALL

VOLUME 404. GTPases Regulating Membrane Dynamics
Edited by WILLIAM E. BALCH, CHANNING J. DER, AND ALAN HALL

VOLUME 405. Mass Spectrometry: Modified Proteins and Glycoconjugates
Edited by A. L. BURLINGAME

VOLUME 406. Regulators and Effectors of Small GTPases: Rho Family
Edited by WILLIAM E. BALCH, CHANNING J. DER, AND ALAN HALL

VOLUME 407. Regulators and Effectors of Small GTPases: Ras Family
Edited by WILLIAM E. BALCH, CHANNING J. DER, AND ALAN HALL

VOLUME 408. DNA Repair (Part A)
Edited by JUDITH L. CAMPBELL AND PAUL MODRICH

VOLUME 409. DNA Repair (Part B)
Edited by JUDITH L. CAMPBELL AND PAUL MODRICH

VOLUME 410. DNA Microarrays (Part A: Array Platforms and Web-Bench Protocols)
Edited by ALAN KIMMEL AND BRIAN OLIVER

VOLUME 411. DNA Microarrays (Part B: Databases and Statistics)
Edited by ALAN KIMMEL AND BRIAN OLIVER

VOLUME 412. Amyloid, Prions, and Other Protein Aggregates (Part B)
Edited by INDU KHETERPAL AND RONALD WETZEL

VOLUME 413. Amyloid, Prions, and Other Protein Aggregates (Part C)
Edited by INDU KHETERPAL AND RONALD WETZEL

VOLUME 414. Measuring Biological Responses with Automated Microscopy
Edited by JAMES INGLESE

VOLUME 415. Glycobiology
Edited by MINORU FUKUDA

VOLUME 416. Glycomics
Edited by MINORU FUKUDA

VOLUME 417. Functional Glycomics
Edited by MINORU FUKUDA

VOLUME 418. Embryonic Stem Cells
Edited by IRINA KLIMANSKAYA AND ROBERT LANZA

VOLUME 419. Adult Stem Cells
Edited by IRINA KLIMANSKAYA AND ROBERT LANZA

VOLUME 420. Stem Cell Tools and Other Experimental Protocols
Edited by IRINA KLIMANSKAYA AND ROBERT LANZA

VOLUME 421. Advanced Bacterial Genetics: Use of Transposons and Phage for Genomic Engineering
Edited by KELLY T. HUGHES

VOLUME 422. Two-Component Signaling Systems, Part A
Edited by MELVIN I. SIMON, BRIAN R. CRANE, AND ALEXANDRINE CRANE

VOLUME 423. Two-Component Signaling Systems, Part B
Edited by MELVIN I. SIMON, BRIAN R. CRANE, AND ALEXANDRINE CRANE

VOLUME 424. RNA Editing
Edited by JONATHA M. GOTT

VOLUME 425. RNA Modification
Edited by JONATHA M. GOTT

VOLUME 426. Integrins
Edited by DAVID CHERESH

VOLUME 427. MicroRNA Methods
Edited by JOHN J. ROSSI

VOLUME 428. Osmosensing and Osmosignaling
Edited by HELMUT SIES AND DIETER HAUSSINGER

VOLUME 429. Translation Initiation: Extract Systems and Molecular Genetics
Edited by JON LORSCH

VOLUME 430. Translation Initiation: Reconstituted Systems and Biophysical Methods
Edited by JON LORSCH

VOLUME 431. Translation Initiation: Cell Biology, High-Throughput and Chemical-Based Approaches
Edited by JON LORSCH

VOLUME 432. Lipidomics and Bioactive Lipids: Mass-Spectrometry–Based Lipid Analysis
Edited by H. ALEX BROWN

VOLUME 433. Lipidomics and Bioactive Lipids: Specialized Analytical Methods and Lipids in Disease
Edited by H. ALEX BROWN

VOLUME 449. RNA Turnover in Eukaryotes: Analysis of Specialized and Quality Control RNA Decay Pathways
Edited by LYNNE E. MAQUAT AND MEGERDITCH KILEDJIAN

VOLUME 450. Fluorescence Spectroscopy
Edited by LUDWIG BRAND AND MICHAEL L. JOHNSON

VOLUME 451. Autophagy: Lower Eukaryotes and Non-Mammalian Systems (Part A)
Edited by DANIEL J. KLIONSKY

VOLUME 452. Autophagy in Mammalian Systems (Part B)
Edited by DANIEL J. KLIONSKY

VOLUME 453. Autophagy in Disease and Clinical Applications (Part C)
Edited by DANIEL J. KLIONSKY

VOLUME 454. Computer Methods (Part A)
Edited by MICHAEL L. JOHNSON AND LUDWIG BRAND

VOLUME 455. Biothermodynamics (Part A)
Edited by MICHAEL L. JOHNSON, JO M. HOLT, AND GARY K. ACKERS (RETIRED)

VOLUME 456. Mitochondrial Function, Part A: Mitochondrial Electron Transport Complexes and Reactive Oxygen Species
Edited by WILLIAM S. ALLISON AND IMMO E. SCHEFFLER

VOLUME 457. Mitochondrial Function, Part B: Mitochondrial Protein Kinases, Protein Phosphatases and Mitochondrial Diseases
Edited by WILLIAM S. ALLISON AND ANNE N. MURPHY

VOLUME 458. Complex Enzymes in Microbial Natural Product Biosynthesis, Part A: Overview Articles and Peptides
Edited by DAVID A. HOPWOOD

VOLUME 459. Complex Enzymes in Microbial Natural Product Biosynthesis, Part B: Polyketides, Aminocoumarins and Carbohydrates
Edited by DAVID A. HOPWOOD

VOLUME 460. Chemokines, Part A
Edited by TRACY M. HANDEL AND DAMON J. HAMEL

VOLUME 461. Chemokines, Part B
Edited by TRACY M. HANDEL AND DAMON J. HAMEL

VOLUME 462. Non-Natural Amino Acids
Edited by TOM W. MUIR AND JOHN N. ABELSON

VOLUME 463. Guide to Protein Purification, 2nd Edition
Edited by RICHARD R. BURGESS AND MURRAY P. DEUTSCHER

VOLUME 464. Liposomes, Part F
Edited by NEJAT DÜZGÜNEŞ

VOLUME 465. Liposomes, Part G
Edited by NEJAT DÜZGÜNEŞ

VOLUME 466. Biothermodynamics, Part B
Edited by MICHAEL L. JOHNSON, GARY K. ACKERS, AND JO M. HOLT

VOLUME 467. Computer Methods Part B
Edited by MICHAEL L. JOHNSON AND LUDWIG BRAND

VOLUME 468. Biophysical, Chemical, and Functional Probes of RNA Structure, Interactions and Folding: Part A
Edited by DANIEL HERSCHLAG

VOLUME 469. Biophysical, Chemical, and Functional Probes of RNA Structure, Interactions and Folding: Part B
Edited by DANIEL HERSCHLAG

VOLUME 470. Guide to Yeast Genetics: Functional Genomics, Proteomics, and Other Systems Analysis, 2nd Edition
Edited by GERALD FINK, JONATHAN WEISSMAN, AND CHRISTINE GUTHRIE

VOLUME 471. Two-Component Signaling Systems, Part C
Edited by MELVIN I. SIMON, BRIAN R. CRANE, AND ALEXANDRINE CRANE

VOLUME 472. Single Molecule Tools: Fluorescence Based Approaches, Part A
Edited by NILS WALTER

VOLUME 473. Thiol Redox Transitions in Cell Signaling, Part A Chemistry and Biochemistry of Low Molecular Weight and Protein Thiols
Edited by ENRIQUE CADENAS AND LESTER PACKER

CHAPTER ONE

Changing Paradigms in Thiology: From Antioxidant Defense Toward Redox Regulation

Leopold Flohé*,†

Contents

Abstract

The history of free radical biochemistry is briefly reviewed in respect to major trend shifts from the focus on radiation damage toward enzymology of radical production and removal and ultimately the role of radicals, hydroperoxides, and related fast reacting compounds in metabolic regulation. Selected aspects of the chemistry of radicals and hydroperoxides, the enzymology of peroxidases,

* Otto-von-Guericke-Universität, Magdeburg, Germany
† MOLISA GmbH, Magdeburg, Germany

Methods in Enzymology, Volume 473
ISSN 0076-6879, DOI: 10.1016/S0076-6879(10)73001-9

and the biochemistry of adaptive responses and regulatory phenomena are compiled and discussed under the perspective of how the fragments of knowledge can be merged to biologically meaningful concepts of regulation. It is concluded that (i) not radicals but H_2O_2, hydroperoxides, and peroxynitrite are the best candidates for oxidant signals, (ii) peroxidases of the GPx and Prx family or functionally equivalent proteins have the chance to specifically sense hydroperoxides and to transduce the oxidant signal, (iii) redox signaling proceeds via reactions known from thiol peroxidase and redoxin chemistry, (iv) proximal targets are proteins that are modified at SH groups, and (v) redoxins are documented signal transducers but also used as terminators. The importance of kinetics for forward signaling and for sensitivity modulation by competition is emphasized and ways to restore resting conditions are discussed. Research needs to validate emerging concepts are outlined.

1. Introduction

A PubMed search for terms in the title of this article yielded 11,148 publications on "Redox regulation" and 6637 for "Antioxidant defense" by mid-November 2009 with a weekly increment of about 50. For sure these lists are incomplete, since related terms like "Oxidative stress," depending on the retrieval path, yielded 71,724 or 241,995 hits. Confronted with such numbers, my conclusions were (i) my life expectancy does not suffice to read all this beautiful science; (ii) it is impossible to condense the total of 2080 reviews included in the above numbers into an introductory chapter of a book on "Thiol Redox Transitions in Cell Signaling"; (iii) it will be a challenge not to reiterate what has been published often enough; and (iv) I have to apologize in advance for being unable to quote thousands of important contributions to the field.

Somehow, an unconventional escape strategy was indicated. I reasoned that it might be as interesting as it is revealing for the readers of this volume, particularly for the younger ones, to learn from somebody who has had the chance to watch the field for over five decades to see how trends and fashions advanced or hampered oxidative stress research up to its frontiers. I did not try to comprehensively trace the history from the first mentioning of radicals in biology up to their implication in redox regulation, but rather focused on selected aspects and discoveries that paved the way to our present understanding of how metabolic regulation and adaptation might be achieved via thiol modification. What finally came out may be perceived by the reader as a biased patchwork or, more benevolently, as an impressionistic panorama painted in the technique of French pointillism.

2. Early Concepts, Misconceptions, Unsettled Battles, and Persistent Confusion

The first time I came across a thiol that regulated a process was in the 1960s of the last century. In my textbook of organic chemistry I could read that thiols, more specifically thiophenols, are being used to terminate radical-driven polymerization of olefins, thus regulating the polymer size, and because the radical chain reaction in these procedures is initiated by strong oxidants, for example, peroxides, the chain terminators were called antioxidants (Beyer, 1968). The term "antioxidant" was indeed coined by chemists in the late nineteenth century to describe compounds that inhibited all kind of oxidative processes, but over the years became well defined to describe compounds capable of scavenging radicals, thereby becoming less reactive radicals themselves. In biochemistry, the term "antioxidant" did hardly become popular but in the late 1940s (Matill, 1947) was often used in a poorly defined way as any kind of compound interfering with any kind of oxidative biological process.

In the mid-1950s, the interest in the concept of radical scavenging in biological systems was substantially enhanced by Rebecca Gershman's theory on the involvement of free radicals in radiation damage and oxygen poisoning (Gerschman *et al.*, 1954) and Denham Harman's free radical theory of aging (Harman, 1956). The memory of the atomic bombs that had been dropped on Hiroshima and Nagasaki was still fresh, the mutagenic and carcinogenic potential of irradiation had become obvious, free radicals were evidently the culprits, and synthesis and testing of antioxidants started to flourish, likely driven by the surrealistic dream to fight irradiation damage with antioxidant pills. The somewhat naive idea to copy the chemical process of radical scavenging *in vivo* by loading an organism with antioxidants for "chemoprevention" or therapy is reflected in a letter to Nature from 1962 (Charlesby *et al.*, 1962) stating:

> It is known that many biological systems can be protected in part against the effect of ionizing radiation by the presence of very small amounts of additives. It is often difficult to assess the mechanism of this protection due to the complex nature of the system. The effect of radiation on simple organic polymers can also be reduced by various additives. It is believed that this offers many analogies with protection in the more complex biological systems.

Seemingly, the concept worked out in particular cases (Ershoff and Steers, 1960a,b; Jensen and Mc, 1960). But it has meanwhile become clear that *in vivo* the "antioxidants" most commonly do not work as such, but as constituents of enzymes, as cofactors or precursors of substrates or even in more complicated ways. There is no compelling evidence

whatsoever that any macro- or micronutrient may directly scavenge endogenous free radicals *in vivo* to any relevant extent. However, reports on "the antioxidant potential of..." (some secondary plant metabolite or vitamin) keep filling up the journals, although this parameter is likely meaningless with respect to potential biological effects. Also, even in 2009, endogenous compounds such as glutathione and thioredoxin are often called "most important cellular antioxidants," which in chemical terms, is wrong, and in biochemical terms, misleading.

The radicals implicated in irradiation damage were thought to primarily result from radiolysis of water and to yield *inter alia* the hydroxyl radical $^{\bullet}OH$, which was also postulated by Haber and Weiss to result from iron-catalyzed decomposition of H_2O_2 (Haber and Weiss, 1932, 1934) and is widely believed to represent the strong oxidant in Fenton reactions (Fenton, 1876). The precise mechanism of the often quoted Haber–Weiss cycle kept the physicochemist busy for decades and even the ultimate oxidant of the Fenton broth is still being debated. In fact, already Bray and Gorin (1932) implicated a ferryl oxygen complex as the oxidant species in Fenton-like reactions, and Symons and Gutteridge (1998) summarized the state of the dispute as follows:

> ...although many workers show a strong tendency to favour the $^{\bullet}OH$ radical concept as a panacea, others content that they are *never* involved. And the battle continues.

Whatever the ultimate oxidant in Fenton-type reactions is, it is something very destructive, promiscuously attacking all kind of thiols, olefines, aromatic compounds, and aliphatic polyhydroxy compounds. Not surprisingly, therefore, free radical research remained the domain of pathologists and toxicologists for decades with focus on lipid peroxidation associated with biomembrane damage, protein alteration with loss of function, and DNA destruction resulting in mutations and ultimately carcinogenesis. In respect to redox regulation the "Fenton reactant" appears a bit too promiscuous. Instead, less reactive oxidants such as H_2O_2 without the support of catalytic iron or other hydroperoxides might have a much better chance to fulfill the specificity requirements for regulation.

Already in 1966, the interplay of hydroperoxides with thiols has been discussed as a molecular basis of the regulation of metabolic events, the first example being the response of the pentose phosphate shunt in red blood cells to changes of the GSH/GSSG ratio (Jacob and Jandl, 1966), for review of the early literature see Brigelius (1985). Since, it has become common to stress the importance of thiol/disulfide ratios or related redox potentials in metabolic regulation. However, can a ratio, an electrochemical potential or a Gibb's free energy really regulate? It may appear provocative but it is by no means unreasonable to question the relevance of electrochemical or thermodynamic calculations to biology. For instance, according to the Nernst

equation, the redox potential of the GSH/GSSG system depends on $[GSH]^2$, because two molecules are needed to yield one GSSG. However, the common text book equation

$$2GSH - 2e^- \rightarrow GSSG + 2H^+ \tag{1.1}$$

may be valid for the process that happens at a platinum electrode, but has no real correspondence in biochemical GSH oxidation. A ternary collision, for example, of 2 GSH with 1 H_2O_2 to form GSSG and 2 H_2O, which is the justification of the quadratic term in the Nernst equation, is a very unlikely event compared with the glutathione peroxidase (GPx) reaction, which is a sequence of bimolecular steps. Also, *in vivo* the backward reaction yielding H_2O_2 from GSSG and water has no chance to compete with enzymatic reduction of GSSG. In this particular case the Nernst equation yields a potential based on reactions that never take place in biology. Moreover, measurements of various thiol/disulfide redox couples in general revealed that they are far off any equilibrium (Jones, 2006). This cannot really surprise, since life is a metastable system in which most of the chemical processes require catalysis. The electrochemical potential of a redox couple just tell us if a reaction is possible, but not how fast the equilibrium is approached. In fact, it does not tell us if the reaction occurs at all. And this implies that kinetics have a greater impact on biological phenomena than any electrochemical or thermodynamic parameter. In our context, one can safely state that ratios or potentials cannot regulate anything, rather will a regulation be exerted by the reaction between a single redox-active mediator and its specific target, while the reversal has to take a different path, if a meaningful regulatory circuit is to be achieved. Unfortunately, this reasoning demands that one needs a good estimate on the rate constants for the switch-on and the switch-off reactions before a qualitatively established process can be rated as physiologically relevant.

The discovery of additional radicals in biosystems and the formation of secondary radicals and other aggressive oxidants finally created a complexity that apparently overwhelmed the largely biology-trained free radical researchers. The fierce discussions on which particular oxidant species is responsible for a particular damage, which had dominated the meetings in the 1960s and 1970s, just faded away. Instead a new terminology was created and slowly adopted: (i)''oxidative stress'' for a situation in which defense mechanisms cannot cope with oxidant processes (Sies, 1985), later often misused to describe any pathology that might be associated with oxidative reactions, (ii) ''ROS,'' which stands for reactive oxygen species, that is, all kind of oxygen-containing compounds with a certain oxidation potential, (iii) ''RNS'' for reactive nitrogen species, and (iv), as mentioned above, ''antioxidant'' in a sense that it no longer matched any chemical definition. The simplicity of these terms allows a successful promotion of

the field in the lay press but is absolutely inadequate for scientific communication. One is tempted to quote Albert Einstein: "Make everything as simple as possible, but not simpler."

3. The Discovery of "Natural" Free Radicals

The first landmark toward understanding free radical physiology was the discovery of superoxide dismutase (SOD) by McCord and Fridovich (1969). This enzyme efficiently dismutated two $^{\bullet}O_2^-$ radicals to H_2O_2 and molecular oxygen, O_2. SODs, containing either Cu and Zn, Mn or Fe, were apparently spread over the living domains from bacteria to mammals (Keele *et al.*, 1970; McCord and Fridovich, 1969; Yost and Fridovich, 1973), but there was no evidence for a physiological source or role of its substrate. The superoxide ion had been observed as by-product of xanthine oxidase (McCord and Fridovich, 1968); yet xanthine oxidase was considered a pathologically altered xanthine dehydrogenase which does not produce $^{\bullet}O_2^-$. Otherwise formation of this radical had been postulated as intermediate of the (nonphysiological) Haber–Weiss cycle and as by-product of autoxidation processes or microsomal drug metabolism (Richter *et al.*, 1977). Babior *et al.* (1973), equipped with SOD as an analytical tool, were the first to discover an important physiological source of $^{\bullet}O_2^-$, the white blood cell (PMN). As already evident from the title of their inseminating publication, they had the idea that the radical production by leukocytes fulfilled a biological purpose: killing the engulfed bacteria, a concept that, with some amendments, proved to be correct (Babior, 1999). For the first time, a radical appeared to do something good. Also for the first time, the radical was evidently produced on demand only, that is, in a strictly regulated way (Babior, 1999; Babior *et al.*, 1973). The source of $^{\bullet}O_2^-$ turned out to be an NADPH oxidase (now Nox2), a flavocytochrome enzyme that usually stays dormant and only starts working upon recruiting regulatory proteins, which in turn depends on receptor-mediated phosphorylation (Babior, 1999). This discovery provided the molecular basis for a long known phenomenon, the respiratory burst that accompanies phagocytosis (Baldridge and Gerard, 1933; Sbarra and Karnowsky, 1959). It further became clear that the NADPH oxidase, in a concerted action with SOD and myeloperoxidase (Klebanoff, 1967, 1974), produces the bactericidal cocktail that is indispensable for appropriate PMN function (Babior, 2004).

NADPH oxidase activity was soon discovered in macrophages (Lowrie and Aber, 1977), mesangial (Radeke *et al.*, 1990) and endothelial cells (Jones *et al.*, 1996), thyroid (Dupuy *et al.*, 1999), and other tissues, where it is associated with other congeners of the Nox family (Dröge, 2002). The wide tissue distribution of NADPH oxidases, of course, suggested

that their product $^{\bullet}O_2^-$ must have functions beyond being the starting material for the production of antimicrobial toxins.

Another important source of $^{\bullet}O_2^-$ proved to be the respiratory chain. Irritated by the high GPx content of mitochondria (Flohé and Schlegel, 1971), my group became interested in the substrate the enzyme had to remove there. In cooperation with Britton Chance we could indeed demonstrate that mitochondria can produce considerable amounts of H_2O_2 (Chance and Oshino, 1971; Loschen *et al.*, 1971). Since one of us, Gerriet Loschen, insisted that the mitochondrial H_2O_2 resulted from autoxidation of a cytochrome, which catalyzes one electron transitions, we reasoned that the primary reaction product should be $^{\bullet}O_2^-$ (Azzi *et al.*, 1974). The assumption that a cytochrome is the source of H_2O_2 turned out to be wrong—it was the ubisemiquinone (Nohl and Jordan, 1986), as originally proposed by Boveris *et al.* (1976), but the wrong hypothesis prompted us to search for $^{\bullet}O_2^-$ produced in inside/out submitochondrial particles which were freed from SOD, and this way it could be verified that $^{\bullet}O_2^-$ is the source of H_2O_2 that leaks out from mitochondria (Loschen *et al.*, 1974). The surprising finding was confirmed in the same year by Forman and Kennedy (1974) and by now—with some amendments (Muller *et al.*, 2004)—is widely accepted.

The physiological importance of mitochondrial $^{\bullet}O_2^-$ formation for long remained debated (Nohl *et al.*, 2003). It was hardly detected in undamaged intact mitochondria, unless the respiratory chain was poisoned by antimycin A or fueled with succinate only (Chance and Oshino, 1971; Loschen *et al.*, 1971; Loschen *et al.*, 1974). Certainly, early estimates that 5% of the total oxygen consumption by mammalian mitochondria goes regularly to $^{\bullet}O_2^-$ (Chance *et al.*, 1979) were a bit exaggerated. More recently, however, it has become evident that this radical production does not just reflect a construction failure of the respiratory chain, which becomes obvious upon mistreatment. As first documented by Hennet *et al.* (1993), tumor necrosis factor α, in a Ca^{2+}-dependent way, triggers a mitochondrial $^{\bullet}O_2^-$ formation that may well be responsible for its suicidal activity (Goossens *et al.*, 1995). Since, mitochondrial $^{\bullet}O_2^-$ formation is increasingly implicated in the regulation of important processes such as apoptosis. Moreover, the $^{\bullet}NO$ radical (see below) was shown to enhance mitochondrial $^{\bullet}O_2^-$ production and might be considered as kind of endogenous antimycin A (Poderoso *et al.*, 1996).

One of the biggest surprises in the field, indeed, was the discovery of Moncada's group that a long known, but unstable factor that regulates the vascular tone, the endothelium-derived relaxing factor EDRF, proved to be the gaseous nitroxyl radical $^{\bullet}NO$ (Palmer *et al.*, 1987). This radical, that previously had at best attracted the interest of toxicologists as constituent of combustion smoke, clearly exerted a physiological function. It was shown to bind to the heme iron of a guanylate cyclase and to thereby enhance the rate of cGMP production, which leads to vessel dilation and inhibition of

platelet aggregation (Ignarro, 1997; Moncada *et al.*, 1988). In retrospect, the novel link between $^{\bullet}$NO and blood pressure explained the pharmacological profile of nitro drugs (Gruetter *et al.*, 1979; Moncada *et al.*, 1991). The actual surprise, thus, was not the action of $^{\bullet}$NO, but the notion that it was formed endogenously from arginine (Moncada *et al.*, 1988) by specific enzymes, the NO synthases (Förstermann *et al.*, 1991, 1994).

Clearly, $^{\bullet}$NO itself is a surprisingly beneficial radical: It lowers blood pressure, prevents thrombosis, is neuroprotective (Calabrese *et al.*, 2007) and guarantees penile erection (Andersson, 2001). But its radical character also enhanced the complexity of free radical biochemistry. It was soon recognized that it reacts with $^{\bullet}O_2^-$ (Beckman *et al.*, 1990), the bimolecular rate constant of $1.9 \times 10^{10}\ M^{-1}s^{-1}$ being practically limited by diffusion (Nausser and Koppenol, 2002). Although this reaction breaks a free radical chain, the outcome is by no means harmless (Beckman and Koppenol, 1996). The resulting product, peroxynitrite, is a strong oxidant, among others for thiols (Quijano *et al.*, 1997; Radi *et al.*, 1991; Trujillo *et al.*, 2004, 2007). Further, $^{\bullet}$NO may add oxygen, thus forming NO_x with the potential to nitrate proteins at tyrosine residues. Tyrosine nitration may also be achieved by peroxynitrite, if catalyzed by transition metals (Spear *et al.*, 1997). Another set of $^{\bullet}$NO products are the nitrosothiols. Their *in vivo* formation is assumed to result from a direct reaction of $^{\bullet}$NO with a thiol, whereby an R–S–•N–OH radical is formed. The latter then reacts with molecular oxygen, which yields the nitroso thiol R–S–N=O and, again, $^{\bullet}O_2^-$ (Gow *et al.*, 1997).

Many of the secondary $^{\bullet}$NO products have been implicated in signal transduction (Spear *et al.*, 1997). For sure, however, NO_x and peroxynitrite have a considerable toxic potential and account for pathology, when $^{\bullet}$NO is excessively produced. In this respect, $^{\bullet}$NO resembles the other physiological radical $^{\bullet}O_2^-$: Both radicals fulfill essential physiological roles, but are detrimental when overproduced. Due to the interplay of $^{\bullet}O_2^-$ and $^{\bullet}$NO, their pathogenic potential is particularly unraveled when they are excessively produced simultaneously, as for example, in adult respiratory distress syndrome (Baldus *et al.*, 2001; Sittipunt *et al.*, 2001), reperfusion injury (Zweier *et al.*, 1995), or other inflammatory conditions. The excessive formation of $^{\bullet}O_2^-$ under these circumstances had been established already in the decade before (Granger *et al.*, 1981; McCord, 1974) and had prompted numerous pharmacological and clinical studies aiming at a therapeutic use of parenterally administered Cu/Zn SOD (for review of older literature see Flohé, 1988; Flohé *et al.*, 1985). In a well-controlled animal experimentation at least the therapeutic results were excellent but hard to explain with the knowledge available at that time. It had become clear that $^{\bullet}O_2^-$ itself was not the damaging "ROS" and was therefore considered to be the source of the real culprit $^{\bullet}$OH by sustaining a Haber–Weiss cycle catalyzed by a transition metal which, however, could never be identified

(Flohé *et al.*, 1985). More likely, the SOD effects in reperfusion and sepsis models can, in retrospect, be explained by prevention of peroxynitrite formation, as originally proposed by Beckman *et al.* (1990).

4. Love Affairs Between Hydroperoxides and Thiolates or Selenolates

As outlined above, the natural radicals, O_2^- and $^{\bullet}NO$, turned out not be the destructive ROS or RNS that cause tissue damage in oxidative stress. The abundance of SODs guarantees that O_2^- is almost instantly dismutated to O_2 and the seemingly less dangerous H_2O_2. In pathologic conditions, however, H_2O_2 is used to produce hypochloric acid and similarly reactive compounds via the heme peroxidases of leukocytes or $^{\bullet}OH$ by Fenton-like chemistry. In analogy, peroxynitrite, which by itself is more reactive than H_2O_2, is transformed into more aggressive species. Interestingly, no enzyme has so far been discovered that could detoxify $^{\bullet}OH$, $^{\bullet}OR$, singlet oxygen, hypochloric acid, or chlorine atoms. Evidently, nature was wise enough not to embark on this task, because it is simply impossible to compete with the diffusion-limited attack of such species on biomolecules. However, since the risky radical reactions are nevertheless used by higher organism in the defense against intruding pathogens, self-protection is mandatory and is essentially achieved by preventing radical formation from hydroperoxides and peroxynitrite. The enzymes involved work with sulfur or selenium catalysis and, in mammals, belong to two distinct protein families, the GPxs and the peroxiredoxins (Prxs). Both act on H_2O_2 and on peroxynitrite and, beyond, on a wide spectrum of alkyl hydroperoxides (ROOH) comprising the products of lipoxygenases. Studies on these enzymes have greatly advanced our understanding of sulfur and selenium biochemistry (Flohé, 2009; Flohé and Brigelius-Flohé, 2006; Flohé and Harris, 2007; Flohé and Ursini, 2008; Rhee *et al.*, 2005). Open questions remain, but what came out so far, is pivotal for the understanding of both, detoxification of hydroperoxides and use of the latter for redox regulation.

4.1. Glutathione peroxidases

The first GPx, now mostly called cytosolic GPx or GPx1, was discovered in 1957 by Gordon C. Mills as an enzyme that prevented the oxidative destruction of hemoglobin in red blood cells by catalyzing the reduction of H_2O_2 by GSH (Eq. (1.2)):

$$2GSH + H_2O_2 \rightarrow GSSG + 2H_2O \tag{1.2}$$

The enzyme was reported not to contain any heme, at that time believed to be the obligatory prosthetic group of a peroxidase (Mills, 1957). For more than a decade the novel nonheme peroxidase attracted little attention, until in 1973 selenium was identified as its catalytic entity (Flohé, 2009; Flohé *et al.*, 1973; Rotruck *et al.*, 1973).

In order to appreciate the role of this enzyme, it should be stressed that thiols do not react with hydroperoxides at all. Therefore, Eq. (1.2), if it is to describe a noncatalyzed reaction, is wrong. First of all, dissociation of the thiol is a prerequisite for thiol oxidation by ROOH. Second, the primary product is not a disulfide, as we are used to read in textbooks, but a sulfenic acid (Eq. (1.3)).

$$GS^- + H_2O_2 \rightarrow GSOH + HO^- \tag{1.3}$$

The latter dissociates with a pK_a below 5 (Claiborne *et al.*, 1993) and then forms the disulfide with another GSH molecule.

$$GSO^- + H^+ + GSH \rightarrow GSSG + H_2O \tag{1.4}$$

This, of course, implies that the spontaneous oxidation of a thiol by hydroperoxides depends on its pK_a (Flohé *et al.*, 1971), and the major cellular reductant GSH with a pK_a beyond 9 appears to be specifically designed to prevent its spontaneous oxidation (Dominici *et al.*, 2003). The thiolate form is also the one that enables thiol oxidation by molecular oxygen, which would yield $^{\bullet}O_2^-$ and thiyl radicals (Eq. (1.5)), which are neither needed nor wanted all over the organism.

$$GS^- + O_2 \rightarrow {}^{\bullet}O_2{}^- + GS^{\bullet} \tag{1.5}$$

Such products are more readily observed during autoxidation of cysteine and cysteamine, which have a comparatively low pK_a, and even more drastically with selenols, which are almost completely dissociated at physiological pH (Spallholz, 1994). The catalytic trick of a typical GPx is to bypass the less favored direct interaction of GSH or GS^- with the hydroperoxide. Instead, the enzyme is oxidized itself at its selenocysteine moiety in analogy to Eq. (1.3) (Eq. (1.6))

$$GPx - Se^- + H_2O_2 \rightarrow GPx - SeOH + OH^- \tag{1.6}$$

and this oxidation proceeds with a rate constant close to $10^8\ M^{-1}s^{-1}$ (Flohé *et al.*, 1971). If the selenocysteine residue is replaced by cysteine by

site-directed mutagenesis, this rate constant was reported to fall by 2–3 orders of magnitude (Maiorino *et al.*, 1995), but for the natural GPx from *Drosophila* still a homologous rate constant of $>10^6\ M^{-1}s^{-1}$ was obtained (Maiorino *et al.*, 2006). All these constants contrast markedly with those for the noncatalyzed process. Even when extrapolated to full deprotonation, the bimolecular rate constants for the oxidation of low-molecular weight thiols such as cysteine or cysteamine do not exceed 30 $M^{-1}s^{-1}$ (Winterbourn and Metodiewa, 1999). The discrepancy reveals that GPxs are brilliant inventions, in which the microenvironment of the catalytic chalcogen dramatically enhances its reactivity. How this is achieved, is still a matter of speculation. X-ray structures reveal that the active site is strictly conserved (Epp *et al.*, 1983; Koh *et al.*, 2007; Ladenstein and Wendel, 1976; Ren *et al.*, 1997) and site-directed mutagenesis studies underline the functional importance of conserved Trp, Asn, and Gln residues in the (seleno) cysteine environment (Maiorino *et al.*, 1995; Schlecker *et al.*, 2007; Tosatto *et al.*, 2008). The most recent revisions of the mechanism of (seleno)cysteine activation, yet likely not the last ones, have been presented by Tosatto *et al.* (2008) and Toppo *et al.* (2009).

In GPx-1-type enzymes, the ground state enzyme (GPx–Se^-) is then regenerated by two consecutive reactions with GSH (Eqs. (1.7) and (1.8)), which proceed with an apparent net forward rate constant around $10^5\ M^{-1}s^{-1}$. The pronounced specificity for GSH implies that the reactions according to Eqs. (1.7) and (1.8) take place within typical enzyme/substrate complexes (Aumann *et al.*, 1997), which here are disregarded for sake of simplicity. The first reductive step is analogous to Eq. (1.4), the second one analogous to a reversible thiol/disulfide exchange.

$$\mathrm{GPx-SeO^- + GSH \rightarrow GPx-Se-SG + OH^-} \tag{1.7}$$

$$\mathrm{GPx-Se-SG + GSH \leftrightarrow GPx-Se^- + GSSG + H^+} \tag{1.8}$$

The essence of the GPx catalysis is that it enables the reaction according to Eq. (1.2) without the need to generate the thiolate form of GSH. Further, the clearly deprotonated active site selenocysteine (or cysteine) is evidently embedded in the micro-architecture in a way that one-electron transitions are prevented. The resulting clean reduction of H_2O_2 to water contrasts sharply to peroxide reduction by heme peroxidases which, with the notable exception of catalase, tend to generate radical intermediates (Mason, 1986). In detail, the GPx reaction is much more complex than outlined in Eqs. (1.6)–(1.8) and differs between different types of GPx.

In Eqs. (1.6) and (1.7) the first catalytic intermediate is shown as a selenenic acid, R–SeOH or R–SeO^-, respectively. So far, however, this unstable intermediate could never be trapped. In fact, short term exposure of mammalian GPx4 to H_2O_2 yields a product that is smaller by 2 mass units

than the reduced enzyme, while a mass increment of 16, as expected for a selenenic form, is undetectable (Toppo *et al.*, 2009). This suggests that H_2O is eliminated fast from the selenenic form with formation of an Se–X bond that can be readily attacked by GSH. A straight forward idea would be formation of an intramolecular Se–S bond which could be split by GSH in analogy to Eq. (1.8). There is, however, no cysteine residue in reach of the active site selenium in GPx4. More likely, therefore, the selenenic oxidation state is conserved as an Se–N bond that can be cleaved by GSH, as proposed for the catalytic cycle of the GPx mimic ebselen (Sarma and Mugesh, 2008).

$$\mathrm{R-SeOH + R' - NH_2 \rightarrow R - Se - NH - R' + H_2O} \qquad (1.9)$$

In contrast, in GPxs having the selenocysteine replaced by cysteine (CysGPx) the oxidation state of the cysteine sulfenic acid is often conserved in form of an intramolecular disulfide (reviewed in Toppo *et al.*, 2009). However, the formation of an equivalent sulfenylamide bond, as has been detected in tyrosine phosphatase 1B (Salmeen *et al.*, 2003), cannot be excluded for CysGPxs either (Sarma and Mugesh, 2008).

Physiologically more important are the tremendous variations in substrate specificities in the GPx family. All members appear to be able to reduce simple organic hydroperoxides apart from H_2O_2. Mammalian GPx4 is special in acting fast on complex hydroperoxides of phospholipids, even if these are integrated in biomembranes. Due to this peculiarity GPx4 has since its discovery been appreciated for its ability to prevent lipid peroxidation. In fact it was originally called "PIP" for peroxidation inhibiting protein (Ursini *et al.*, 1982). Later, the preference of GPx4 for hydroperoxides of unsaturated fatty acids was recognized as the basis for its role in regulating lipoxygenases. All lipoxygenases require a certain level of hydroperoxide to become active and, in consequences can be silenced by GPx. Although this had first been documented for GPx1 by Lands and coworkers (Hemler and Lands, 1980), it was later demonstrated that under *in situ* conditions GPx4 is the key regulator of leukotriene synthesis by 5-lipoxygenase (Weitzel and Wendel, 1993). Most recently it became clear that in neuronal cells at least GPx4 is the only enzyme that can counteract apoptosis triggered by the12,15-lipoxygenase which oxidizes membrane-integrated lipids (Seiler *et al.*, 2008). Interestingly, the cytosolic form of GP4 is so far the only GPx that proved to be indispensable for embryonic development (Conrad, 2009), and it is tempting to speculate that 12,15-lipoxygenase-induced apoptosis is also involved in prenatal tissue remodeling and is fatally disturbed if not balanced by GPx4.

GPx4 is also unique in its broad thiol specificity. While GPx1, which gave name to the entire family, is indeed a highly specific *glutathione* peroxidase (Flohé *et al.*, 1971), GPx4 also accepts a variety of other thiols including those

in of proteins such as chromatin (Godeas *et al.*, 1996), fragments, or mimics of the sperm mitochondrion-associated cysteine-rich protein that are characterized by adjacent cysteines (Maiorino *et al.*, 2005), and finally GPx-4 itself (Ursini *et al.*, 1999). The latter reaction, in which the oxidized selenium in GPx4 specifically attacks a cysteine residue at the opposite site of another GPx4 molecule (Mauri *et al.*, 2003), is revealing in many respects: (i) It generates GPx4 polymers that upon cross-linking with other cysteine-rich proteins build up the keratin-like material of the mitochondrial capsule in mammalian spermatozoa and thus is indispensable for late sperm differentiation (Schneider *et al.*, 2009). (ii) It is the first example of a GPx reaction that does not aim at hydroperoxide detoxification but makes use of hydroperoxides for the synthesis of a complex protein structure. (iii) It is the first example of a GPx acting as a thiol-modifying agent (Eq. (1.10)).

$$\mathrm{GPx4-SeOH+GPx4'-SH \rightarrow GPx4-Se-S-GPx4'+H_2O} \tag{1.10}$$

It could be envisaged that such selenylation of a protein thiol, in another context, could also regulate the activity of the target protein. This has not yet been established for any of the selenocysteine-containing GPxs. However, a CysGPx of brewer's yeast, Orp1, was documented to form a disulfide-linked heterodimer with the transcription factor Yap1, which ultimately leads to transcriptional gene activation via oxidized Yap1 (Delaunay *et al.*, 2002) (Eqs. (1.11)–(1.13)).

$$\mathrm{Orp1-S^{36}H+H_2O_2 \rightarrow Orp1-S^{36}OH+H_2O} \tag{1.11}$$

$$\mathrm{Orp1-S^{36}OH+Yap1-S^{598}H \rightarrow Orp1\,S^{36}-S^{598}-Yap1+H_2O} \tag{1.12}$$

$$\mathrm{Orp1\,S^{36}-S^{598}-Yap1-S^{303}H \rightarrow Yap1-S_2+Orp1-S^{36}H} \tag{1.13}$$

In this reaction sequence, Eqs. (1.11) and (1.12) are analogous to Eqs. (1.6) and (1.10), while Eq. (1.13) is a thiol/disulfide exchange analogous to Eq. (1.8) which, in principle, is reversible. *In situ*, however, the reduction of the internal disulfide bond between Cys303 and Cy598 in the oxidized transcription factor requires thioredoxin. In short, Eqs. (1.11)–(1.13) demonstrate how a GPx can act as a sensor for H_2O_2 and how the oxidant signal is transduced and reversed.

The yeast H_2O_2 sensor Orp1 belongs to a subfamily of CysGPXs which predominate in bacteria, lower eukaryotes, insects, and plants and, in

functional terms, are thioredoxin peroxidases (Maiorino *et al.*, 2006). As first shown for a CysGPx from *Plasmodium falciparum*, the reduction of the oxidized GPx by thioredoxin may be three orders of magnitude faster than by GSH (Sztajer *et al.*, 2001). With regards to substrate specificity, as well as in respect to the mode of catalysis, they resemble another family of peroxidases, the two-cysteine peroxiredoxins (2-Cys Prxs; see below). A highly reactive cysteine in the position of the selenocysteine of typical GPxs reacts with the hydroperoxide and is therefore called the peroxidatic cysteine "C_P" (S^{36} in Eq. (1.11)). The resulting sulfenic acid then forms an internal disulfide bond with a so-called resolving cysteine "C_R" which is localized in a remote but flexible loop.

$$\mathrm{GPx(C_P{-}OH)C_R{-}SH} \rightarrow \mathrm{GPxS_2} + \mathrm{H_2O} \tag{1.14}$$

The formation of the disulfide form and associated conformational changes appear to be prerequisites for the interaction with typical disulfide reductant proteins such as thioredoxins or related "redoxins", that is, proteins with a CxxC motif (Maiorino *et al.*, 2006; Schlecker *et al.*, 2007) (Eq. (1.15))

$$\mathrm{GPxS_2} + \mathrm{Trx(SH)_2} \rightarrow \mathrm{GPx(SH)_2} + \mathrm{TrxS_2} \tag{1.15}$$

With the knowledge of the role of Orp1 in yeast, it would not surprise if related CysGPxs also find alternate protein reaction partners beyond thioredoxins. But even if this is not the case, with "redoxins" as substrates the GPxs definitely arrived in the scenario of redox regulation. In mammals, though, the link to redoxin-dependent regulation is less likely for GPxs than for Prxs.

4.2. Peroxiredoxins

Prxs were independently discovered several times. They were first seen in electron microscopy by Harris (1968) as ring-shaped structures associated with red cell membranes and called "torins." Starting in the late 1980s they showed up in immunology under bewildering names such as "MER5," "natural killer cell enhancing factor," "macrophage 23 kDA stress protein," or "calpromotin" (compiled and translated into topical nomenclature in Flohé and Harris (2007). In 1988 a Prx was discovered in Earl Stadtman's lab as the yeast antioxidant protein "TSA" (Kim *et al.*, 1988), in 1989 by the group of Bruce Ames in bacteria as alkylhydroperoxide reductase (Ahp) (Jacobson *et al.*, 1989), and in 1997 in trypanosomatids as tryparedoxin peroxidase (Nogoceke *et al.*, 1997). With the advance of fast sequencing technology it became evident in the 1990s that all these different proteins

are related and make up the huge family of Prxs, a term coined by Sue Goo Rhee in 1994 (Chae *et al.*, 1994b). The same year TSA, which initially was considered a radical-scavenging protein, was characterized as a peroxidase (Chae *et al.*, 1994a; Rhee *et al.*, 2005), as had before been shown for the AhpCs. Although only a vanishing proportion of the Prxs known by sequence have so far been functionally characterized, there are good reasons to assume that they all are peroxidases. They are now commonly divided into five subfamilies by sequence similarity (Knoops *et al.*, 2007) or into three groups by functional criteria: typical 2-Cys Prx, atypical 2-Cys Prx, and 1-Cys Prx (Poole, 2007). All 2-Cys Prxs appear to be reduced by redoxin-type proteins, be they thioredoxins, tryparedoxins, or the CxxC motifs of bacterial AhpF, while the reducing substrates of 1-Cys Prxs remain largely unclear (Poole, 2007). The hydroperoxide specificity of Prxs is as broad as that of GPxs, and some of them, for example, several tryparedoxin peroxidases (Budde *et al.*, 2003a), TPx from *Mycobacterium tuberculosis* (Jaeger *et al.*, 2004) and type II poplar Prx (Rouhier *et al.*, 2004), were shown to even share with GPx4 the ability to reduce complex hydroperoxy lipids. Prxs working with sulfur catalysis were initially assumed to be generally less efficient than the GPxs that take advantage or the more reactive selenocysteine (Hofmann *et al.*, 2002). More recently, however, rate constants for Prx oxidation by hydroperoxides $>10^7\ M^{-1}s^{-1}$ could be measured (Budde *et al.*, 2003a; Parsonage *et al.*, 2008). As first shown for AhpCs, Prxs also reduce peroxynitrite (Bryk *et al.*, 2000). As compiled by Trujillo *et al.* (2007), also the rate constants for peroxynitrite reduction by Prxs can be quite impressive, reaching values beyond $10^7\ M^{-1}s^{-1}$ for mycobacterial TPx (Jaeger *et al.*, 2004) and human Prx V (Dubuisson *et al.*, 2004) (Eq. (1.16)).

$$\mathrm{PrxC-S^- + ONOO^- \rightarrow PrxC_P{-}SO^- + NO_2^-} \tag{1.16}$$

At least human Prx V beets GPx1 (Briviba *et al.*, 1998) in peroxynitrite reduction and, considering the usually higher abundance of Prxs, it may be speculated that peroxynitrite reduction is indeed a domain of Prxs (Trujillo *et al.*, 2007). Again, it remains enigmatic how such fast rate constants are achieved, in particular, since the Prxs (with one exception of a selenoprotein so far) work with sulfur catalysis. An Arg residue is constantly seen coordinated to the sulfur of C_P and certainly forces the thiol into dissociation. In this respect it is supported by a serine or, less frequently, by a threonine which is hydrogen bridged to the sulfur (Flohé *et al.*, 2002; Poole, 2007). But still the rate constants are by 2–5 orders of magnitude higher for Prxs than for the oxidation of any fully dissociated low-molecular weight thiol by H_2O_2 or peroxynitrite (Trujillo *et al.*, 2007).

Apart from the construction of the active site, the overall catalytic mechanism of Pxs very much resembles that of CysGPxs with thioredoxin

peroxidase activity. The C_P is oxidized to a sulfenic acid in analogy to Eq. (1.11). This primary oxidation product, Prx–SOH, could be trapped by different reagents and verified by mass spectrometry, first by Leslie Poole and Holly Ellis in AhpC of *Salmonella typhimurium* (Ellis and Poole, 1997a,b; Poole and Ellis, 2002). The sulfenic acid form then forms a disulfide bridge with the C_R. In the atypical 2-Cys Prxs, like in the CysGPxs, the C_R is located in the same subunit (Eq. (1.14)), whereas in the typical 2-Cys Prxs the C_P reacts with a C_R of another subunit within a homodimer with head-to-tail-oriented subunits. This implies that there are two equivalent reaction centers in each dimer and ten in the common ring structures build up of five dimers (for review of Prx structures see Karplus and Hall, 2007).

The growing number of Prx structures in different functional states reveals major structural changes during Prx catalysis (Karplus and Hall, 2007). In the reduced enzymes, the C_P sulfur is often >10 Å away from C_R, which is much too far to form a disulfide bond, and the obligatory domain movement comprising helix unfolding requires time, which has at least three functional consequences: (i) If exposed to excess hydroperoxide, the sulfenic acid form may be overoxidized to an inactive sulfenic form (Eq. (1.17))

$$\mathrm{PrxC_P{-}O^- + H_2O_2 \rightarrow PrxC_P{-}O_2^- + H_2O} \qquad (1.17)$$

Whether and how fast this overoxidation occurs, depends on the nature of the hydroperoxide and, more pronouncedly, on the kind of Prx. It is less frequently observed in AhpC-type and other bacterial Prxs, but is a common phenomenon in 2-Cys Prxs of higher eukaryotes (Wood *et al.*, 2003). Interestingly, these organisms can repair the overoxidized Prx (Woo *et al.*, 2003) by a specific enzyme called sulfiredoxin that reduces the overoxidized C_P in an ATP-dependent reaction (Biteau *et al.*, 2003) (for review see Jönsson and Lowther, 2007). (ii) The sulfenic acid form may react with alternate protein thiols before its oxidized C_P reaches the C_R, and hence, a Prx, like mammalian GPx4 and the yeast GPx Orp1, can be considered a potential protein thiol-modifying agent. Such disulfide-linked heterodimers involving one Prx have repeatedly been reported (Hofmann *et al.*, 2002) and are also implicated in transcriptional gene activation, for example, in *Schizosaccharomyces pombe*, where the Prx Tpx1 becomes linked to a stress-activated kinase to activate the transcription factor Atf1 (Veal *et al.*, 2004). (iii) The sulfenic form appears not to be an ideal reaction partner for redoxins. It is readily reduced by nonphysiological, small thiols such as dithiothreitol but only in exceptional cases by a redoxin. TPx of *M. tuberculosis* and a mutant lacking C_R were reduced by thioredoxin B equally fast ($\sim 10^4\ M^{-1}s^{-1}$), but the mutant was overoxidized within minutes (Trujillo *et al.*, 2006). The observation reveals an important aspect of Prx catalysis: The oxidation equivalents of the labile sulfenic acid form are

conserved in a more stable disulfide bond that is reduced by redoxins, which are specialized for disulfide reduction.

Typically, disulfide formation appears required to complete the physiological catalytic cycle of 2-Cys Prx catalysis. Accordingly, C_R proved to be indispensable for reduction of 2-Cys Prxs by specific high MW substrates, as revealed by numerous mutagenesis studies (Poole, 2007). Also, structural analyses suggested that the conformational changes associated with disulfide formation in 2-Cys Prxs lead to sterical shielding of C_P and exposure of the C_R sulfur at the surface, where it can be attacked by the exposed cysteine of the redoxin's CxxC motif (Hofmann *et al.*, 2002; Karplus and Hall, 2007; Poole, 2007). The correctness of the thus inferred reaction sequence was verified for tryparedoxin peroxidase by mass spectrometry (Budde *et al.*, 2003b).

4.3. Other thiol peroxidases

Not too long ago, the creativity of bacteria surprised with two more families of peroxidases that work with thiol catalysis, the Ohr and OsmC proteins. The two families are evolutionary related, but do not reveal any sequence homology with the GPx- or Prx-type peroxidases (Dubbs and Mongkolsuk, 2007; Gutierrez and Devedjian, 1991; Mongkolsuk *et al.*, 1998). Their mechanism of action, however, is practically the same as that outlined above for 2-Cys Prxs. They are, therefore, sometimes classified as Prxs, which is misleading, since the term "peroxiredoxin" was explicitly coined by Sue Goo Rhee (personal communication) for a protein family defined by sequence homology and not by mechanism or specificity. The first representatives of these families were discovered as genes products conferring resistance against organic hydroperoxides in *Xanthomonas campestris* (Ohr) or high osmolarity in *Escherichia coli* (OsmC). Interestingly, the expression of *ohr* was only triggered by organic hydroperoxides and not by H_2O_2, while *osmC* did not respond to any kind of peroxide challenge (Atichartpongkul *et al.*, 2001). The peroxidase nature of OsmC, inferred from the sequence homology with Ohr, was nevertheless established in 2003 (Lesniak *et al.*, 2003). Apparently, the families, which are widespread in bacteria, are generally distinct in hydroperoxide specificity, the Ohrs acting preferentially on organic hydroperoxides, the OsmCs on both, H_2O_2 and ROOH (for review see Dubbs and Mongkolsuk, 2007).

4.4. Redoxins

The term "redoxin" is here used for proteins characterized by CxxC, UxxC, or CxxU motifs (U = selenocysteine). They comprise the thioredoxins with a CGPC motif, the glutaredoxins with CPYC, tryparedoxins and nucleoredoxin with CPPC, protein disulfide reductases with CGHC,

DsbA with CPHC, AhpFs with variable motifs in their N-terminal domains (CHNC, CQNC, or CTNC), and a variety of selenoproteins with poorly defined function. They all are presumed to be thiol(selenol):disulfide oxidoreductases and to play a key role in disulfide reshuffling. The redox potential varies considerably, which implies that, in principle, the direction of the thiol/disulfide exchange reaction can go both ways. Thioredoxins and tryparedoxins with their more negative potential (∼−270 and 250 mV, respectively) tend to reduce disulfide bonds, glutaredoxins with −200 to −233 mV usually still reduce disulfides, protein disulfide isomerase, and DsbA with the highest potential near −125 mV tend to catalyze disulfide bond formation and appear ideal for rearrangement of disulfide patterns in proteins (Jacob *et al.*, 2003). Predictions from motif structures or potentials, however, are risky, because evidently sterical features determine the substrate specificity of these enzymes (Kalinina *et al.*, 2008).

Thioredoxins are fairly pleiotropic oxidoreductases. Their spectrum of activities expanded from cofactor for ribonucleotide reduction (Holmgren, 1985;, Laurent *et al.*, 1964) to immune modulator (Gasdaska *et al.*, 1994; Tagaya *et al.*, 1988), cosubstrate of Prx- and GPx-type peroxidases, reductant for transcription factors such as NFκB (Hayashi *et al.*, 1993) or Yap1 (Delaunay *et al.*, 2000) and many more (Ahsan *et al.*, 2009; Fomenko *et al.*, 2008). The common denominator of their activities is the reduction of protein disulfides by means of their CGPC motif. The oxidized CGPC motif is reduced by thioredoxin reductases, which in vertebrates are selenoproteins (Birringer *et al.*, 2002; Tamura and Stadtman, 1996; Tamura *et al.*, 1995). Similarly, glutaredoxin was discovered as a cofactor of ribonucleotide reductase (Holmgren, 1976) and later classified as a broad spectrum disulfide reductase (Holmgren, 1989). The glutaredoxins, however, are specialized for mixed disulfides between proteins and glutathione or "glutathionylated" proteins. Also, the reduction of oxidized glutaredoxins does not require a specialized enzyme, they are themselves apparently designed to bind GSH in a strategic position for thiol disulfide exchange reactions (Herrero and Ros, 2002). Similarly, the tryparedoxins are directly reduced by a low-MW thiol, but poorly with GSH. They require the bis (glutathionyl) spermidine, called trypanothione (Gommel *et al.*, 1997), but their specificity toward protein disulfide substrates again is broad (Castro and Tomas, 2008; Irigoin *et al.*, 2008; Krauth-Siegel *et al.*, 2007).

Thus thioredoxins, tryparedoxins, and glutaredoxins are obviously designed to be a bit unspecific. In fact, their structures do not disclose any characteristic pocket to bind their high-MW disulfide substrates. However, this is not to state that they are mutually exchangeable in their biological functions. By own experience, just a few examples of pronounced redoxin specificity may be quoted: (i) In *M. tuberculosis* three thioredoxins, TrxA, B, and C are found; only TrxB and C are reduced by the mycobacterial thioredoxin reductase; TrxC reduces both the mycobacterial AhpC and

the TPx; while TrxB can only reduce the TPx (Jaeger *et al.*, 2004). (ii) The thioredoxin in *Trypanosoma brucei* is a poor substitute tryparedoxin in Prx and ribonucleotide reduction and, surprisingly, proved to be dispensable (Schmidt *et al.*, 2002). In contrast, suppression the cytosolic tryparedoxin expression leads to severe morpholocical alteration of the parasite (Comini *et al.*, 2007). While tryparedoxin reacts with a variety of structurally unrelated proteins (Krauth-Siegel *et al.*, 2007), its specificity for trypanothione is achieved by a characteristic charge distribution on the otherwise poorly structured surface (Hofmann *et al.*, 2001; Krumme *et al.*, 2003). Collectively, the redoxins are selective enough to consider them as regulators.

5. Toward Regulatory Circuits with Puzzle Stones from Redox Biochemistry

This prefinal chapter will not celebrate what has already been achieved in respect to redox regulation of signaling cascades. The progress in the field has regularly been updated in excellent reviews, some of the seemingly outdated ones (Brigelius, 1985; Dröge, 2002; Thannickal and Fanburg, 2000) still being invaluable sources when topical directions of research are to be delineated from often forgotten findings. It here may suffice to recall that the idea of redox regulation of metabolic events is not new at all, but has for long been competed out by more popular regulatory principles such as limited proteolysis and protein phosphorylation/dephosphorylation. It took almost three decades to understand how intimately the regulatory principles complement each other. This is quite surprising, since the first examples of redox-regulated enzymes from the 1960s were kinases and phosphatases (Eldjarn and Bremer, 1962; Nakashima *et al.*, 1969) and a potential link between the prototype of a phosphorylation-dependent cascade, insulin/glucagon-regulated glycogen metabolism (for an authentic retrospect see Fischer, 1997), and a related redox-sensitive protein phosphatase showed up already in the 1970s (Shimazu *et al.*, 1978). Also, it had not attracted much attention of protein kinase researchers that H_2O_2 had been discussed as a second messenger in insulin signaling in the 1970s (Czech *et al.*, 1974; May and de Haen, 1979). While the kinase/phosphatase field nevertheless flourished, the free radical and oxygen clubs kept being concerned about the risks of aerobic life and, accordingly, the first milestones toward understanding of redox regulation dealt with adaptive preconditioning to cope with oxidative stress, for example, induction of tolerance to oxygen toxicity by LPS as inflammatory stimulus in mammals (Frank *et al.*, 1978) or enzyme induction in bacteria via the *oxyR* regulon (Tartaglia *et al.*, 1989). The fields started to merge, when in the mid-1990s several exciting publications (Bae *et al.*, 1997; Lo and Cruz, 1995; Ohba *et al.*, 1994; Sundaresan *et al.*, 1995)

reported on the production of $^{\bullet}O_2^-/H_2O_2$ during physiological signaling by growth factors that were presumed to signal via phosphorylation only (Thannickal and Fanburg, 2000). Evidently, they also needed "ROS" for signaling, as is now generally accepted (Groeger *et al.*, 2009).

However, redox regulation, though now becoming fashionable, remains confusing. The phosphorylation cascades are being filled up with more and more details; they started to cross talk with each other, and are now being complicated by the complex chemistry of ROS, RNS, and thiol interactions. In order to save any newcomer from no longer seeing the woods for the trees, I will here try to deduce just some basic principles of redox regulation from the ever growing mass of data.

A regulatory circuit has to meet some minimum requirements: (1) It needs a switch to send a message and a switch-on signal that must not be misunderstood, (2) a transducer or a chain of transducers, (3) a target structure that produces a meaningful answer, (4) devices to restore starting situations, and (5) a possibility to adjust the sensitivity of the system. In the context of redox regulation, the initial switching-on molecule is most likely a strong oxidant, which as we have seen above, will not likely associate with its receptor in a reversible way, but will oxidize it. This means that the receptor, the switch, cannot be reset to the resting position just by removing the initial signal like taking the finger off an alarm button. Since similar events have to be taken into account in further downstream steps of the circuit, it is wise to consider that the measures to restore resting positions might not take the very same path backward at any step of the circuit. Finally, in biology we are not dealing with a static system where everything is nicely equilibrated, but with steady states of substrate fluxes that are determined by the catalytic capacities of enzymes, which often compete for common substrates. With these trivialities in mind, let us return to the minimized minireviews on thiol redox biochemistry above to work out which (bio)chemical entities make good candidates for elements of regulatory circuits.

5.1. Triggering signals

Pathogenic bacteria trigger the innate immune response via common surface structures known as PAMPs (pathogen-associated molecular patterns) or MAMPs (microbe-associated molecular patterns) in animals (Mogensen, 2009) as well as in plants (Jones and Dangl, 2006). This response comprises *inter alia* the activation of Nox-type enzymes, lipoxygenases and NO synthase induction, and in PMNs the phagocytosis-associated production of the bactericidal cocktail. As to the latter, we first may ask which of its ingredients might be suited for redox signaling. The most aggressive ones, $HOCl^-$, $^{\bullet}CL$, $^{\bullet}OH$, $RO^{\bullet}$, or $^1\Delta_gO_2$, are designed for destruction and would ruin the regulatory machinery. $^{\bullet}O_2^-$ is stable enough to be

considered for signaling. It is conceivable that it, like $^{\bullet}NO$, binds reversibly to a heme iron, but its only known "receptors," the SODs, dismutate it almost instantly to O_2 and H_2O_2. Many lipoxygenase products, the prostaglandins and the leukotrienes are signaling molecules par excellence, but this is a different story. Instead, the primary products of lipoxygenases, ROOH, like H_2O_2 or $ONNO^-$, could signal through redox-sensitive pathways. In short, the hottest candidates for redox signaling are hydroperoxides, be they derived from cell exposure to PAMPs or endogenous stimuli such as growth factors or hormones. This is not to say that a regulated response to the more brutal ROS or RNS is not possible. However, if tissue damage prevails, characteristic products of the ongoing disaster, for example, α,β-unsaturated aldehydes resulting from lipid peroxidation, may signal an alarm at neighboring, still viable cells via the Nrf2/Keap1 system (Zhang and Forman, 2009).

5.2. Hydroperoxide sensors

The structures most commonly discussed to sense a hydroperoxide are proteins with an exposed, dissociated, and hence, reactive SH group. The inhibition of a protein phosphatase was likely the first example of an H_2O_2-dependent regulation of a phosphorylation cascade (Shimazu *et al.*, 1978). Insulin signaling could in fact be mimicked by H_2O_2 (Heffetz *et al.*, 1990) and even better by peroxovanadate (Posner *et al.*, 1994), and these effects could be attributed to oxidative inhibition of the protein tyrosine phosphatase that dephosphorylates the activated insulin receptor (Posner *et al.*, 1994). Later, the inhibition of protein phosphatases by H_2O_2 or peroxovanadate became a common and useful trick to experimentally enhance the extent of protein phosphorylation in signaling cascades, already suggesting that not only the insulin pathway contains redox-sensitive phosphatases. Other hydroperoxide targets implicated in signaling are membrane associated protein tyrosine kinases (PTKs) that are activated by oxidation of cysteines in conserved MxxCW or CxxxxxxMxxCW motifs (Nakashima *et al.*, 2005). Particularly interesting hydroperoxide targets are cytosolic inhibitors of transcription factors such as IκBα and Keap1 that prevent the translocation of the transcription factors NFκB or Nrf2, respectively, into the nucleus. NFκB can only initiate gene transcription, after its inhibitor IκB has been phosphorylated, ubiquitinylated and proteasomally degraded, and this process is initiated or facilitated by oxidation of an SH group in IκB (Na and Surh, 2006). In case of the Nrf2/Keap1 system, Nrf2 is released from a multicomponent complex in the cytosol upon oxidation or alkylation of defined SH groups in Keap1 (Kensler *et al.*, 2007). An example of a transcription factor that by itself senses H_2O_2 is the bacterial OxyR (Dubbs and Mongkolsuk, 2007).

The outcome of protein thiol modification by hydroperoxides varies and the mechanisms are not entirely clear. A meanwhile common phenomenon is the glutathionylation of proteins, *inter alia* of the phosphatases (Klatt and Lamas, 2000). In PTKs the oxidation of defined SH groups has tentatively been postulated to stabilize the receptor aggregation that is required for autophosphorylation by intermolecular disulfide bridging (Nakashima *et al.*, 2005). Intramolecular disulfide bonds are implicated, for example, in Keap1 and OxyR. As common first step of these thiol oxidations the formation of a sulfenic acid in analogy to the initial reactions of CysGPxs and Prxs is often proposed (Eqs. (1.6), (1.11), and (1.16)), which could be followed by a reaction with GSH (Eq. (1.7)), another protein thiol (Eqs. (1.12) and (1.14)) or an amide (Eq. (1.9)). The problem we have with all these proposals is the lack of kinetic data or, if kinetic measurements were reported, the low rate constants. For thiol oxidation of a PTP by H_2O_2, for instance, the highest bimolecular rate constant ever measured was just 43 $M^{-1}s^{-1}$(Barrett *et al.*, 1999; Denu and Tanner, 1998; Sohn and Rudolph, 2003), which means that this kind of reaction has not the slightest chance to compete with a GPx or Prx that react with H_2O_2 4–6 orders of magnitude faster. Only for the direct oxidation of OxyR by H_2O_2 the rate constant ($\sim 10^5$ $M^{-1}s^{-1}$) (Aslund *et al.*, 1999) may be rated as competitive.

This consideration brings us to the provocative conclusion that most of the above discussed proteins with a "redox-active thiol" cannot possibly be the primary sensors for H_2O_2. Their thiol oxidation, if it is to occur physiologically, has to proceed with a rate constant of at least 10^4 $M^{-1}s^{-1}$. As the OxyR example reveals, a cysteine environment that enables efficient hydroperoxide sensing might have been developed also in proteins unrelated to peroxidases, yet till now we keep waiting for a second example. In contrast, evidence is accumulating that peroxidases are excellent candidates to fulfill the role of primary H_2O_2 sensors. The two best investigated examples have already been mentioned; the CysGPx Orp1 that senses H_2O_2 in *Saccharomyces cerevisiae* and ultimately oxidizes the transcription factor Yap1 (Delaunay *et al.*, 2000) and the 2-CysPrx that activates the stress kinase Sty1 as well as the transcription factor Pap1 in *S. pombe* (Morgan and Veal, 2007; Veal *et al.*, 2004). Similarly, bacterial Ohr may be suspected to be the sensor for ROOH, thereby regulating its own biosynthesis. The expression of *ohr* is repressed by the transcription factor OhrR in its reduced state. Derepression requires oxidation of specific cysteines in OhrR and, interestingly, this derepression happens upon exposure of alkylhydroperoxides (and not H_2O_2) which are the preferred substrates of Ohr (Dubbs and Mongkolsuk, 2007). In mammalian systems, Prx I (*alias* PAG or MSP23) binds to the src homology domain 3 of the c-Abl kinase and might well be the H_2O_2 sensor for the c-Abl-regulated cell cycle progression (Wen and Van Etten, 1997). Similarly Prx I binds to the oncogene

c-Myc (Mu *et al.*, 2002). Also for plants, hydroperoxide sensing by Prxs becomes increasingly clear, as reviewed by Dietz (2003, 2008).

The advantage of using a peroxidase as sensor instead of allowing a direct hydroperoxide/transcription factor interaction may be seen in lending specificity to the oxidant signal. Increases in hydroperoxide flux can thus be monitored, before the steady state of hydroperoxides reaches a level that might cause unspecific damage. In order to meet this task, peroxidases have not to acquire entirely novel abilities; they are anyway specialized for efficient scavenging of, and reaction with, hydroperoxides, and the sensing process is nothing else but the first step or the first two steps in peroxidase catalysis. As a result of the sensing process, the oxidation equivalents of the peroxide are temporarily "stored" in the enzyme waiting for the conventional reductant, as in the normal peroxidase function, or a redox-competent signaling protein that evolution has designed for specific interaction.

5.3. Signal transducers

Peroxidases may also be regarded as transducers if they themselves transduce the signal they sensed to target molecules. In these cases the peroxidase is both, sensor *and* transducer, as in the mentioned reactions of Orp1 with Yap1 (Eqs. (1.11)–(1.13)) or of the *S. pombe* Prx with Sty1 or Pap1 (see above).

Alternatively, the product of the normal peroxidatic reaction may act as a transducer. In a typical GPx reaction, this would be GSSG, and the latter can, in principle, glutathionylate SH groups in proteins by thiol/disulfide reshuffling (Eq. (1.18)) (Klatt and Lamas, 2000)

$$\text{Prot} - \text{SH} + \text{GSSG} \leftrightarrow \text{GSH} + \text{Prot} - \text{SSG} \tag{1.18}$$

Whether this possibility is amply used *in vivo* for the growing examples of protein glutathionylation is hard to decide. In mammals at least, the intracellular steady state of GSSG is not easily increased due to fast reduction by glutathione reductase plus export of GSSG. Also, thiol/disulfide exchange is not particularly fast. Collectively, these concerns justify the speculation that glutathionylation by GSSG is a rare event, if not catalyzed. Glutaredoxin had originally been implicated in this context, but turned out to rather reverse protein glutathionylation (Kalinina *et al.*, 2008).

A peroxidase product that unambiguously takes part in redox signaling as transducer is oxidized thioredoxin. The best documented example is Trx-regulated signaling by the apoptosis signal-regulating kinase (ASK) 1 in mammals. ASK1 activates c-Jun kinase and p38 MAP kinase and ultimately mediates TNFα-induced apoptosis. Reduced Trx tightly binds and inhibits ASK1, whereas oxidized Trx does not, as was first observed by Saitoh *et al.* (1998). This implies that the phosphorylation cascade is arrested by thioredoxin which under normal conditions is overwhelmingly reduced. If Trx

becomes oxidized due to TNFα-triggered $^{\bullet}O_2^-/H_2O_2$ formation or any other hydroperoxide challenge, the apoptotic machinery can proceed. Originally Trx was presumed to be the peroxide sensor in this context, which, however, can almost certainly be ruled out because of the comparatively low reactivity of redoxins with H_2O_2. Knowing that five of the six mammalian Prxs are thioredoxin peroxidases, it appears straight forward to consider a Prx as the H_2O_2 sensor and the Prx product, oxidized Trx, as a transducer in oxidant-driven apoptosis. Similarly, the mammalian CPPC protein nucleoredoxin has been reported to bind to Dv1 (*disheveled*) in the Wnt/β-catenin signaling pathway and to be released by H_2O_2 (Funato and Miki, 2007; Funato *et al.*, 2006). Like Trx, nucleoredoxin fulfills the structural criteria of a Prx substrate and, thus, could be an analogous transducer of β-catenin activation.

5.4. Targets

In most of the examples of redox-sensitive signaling cascades the ultimate targets are transcription factors. In bacteria it is commonly the redox state of the transcription factor itself that determines transcription. The gene products resulting from activation of OxyR and OhrR, AhpC and AhpF, or Ohr, respectively, are peroxidases that eliminate the sensed oxidant signal (Dubbs and Mongkolsuk, 2007). Also in yeast, the response to the oxidatively activated transcription factor comprises the expression of peroxidases and other protective enzymes (D'Autreaux and Toledano, 2007; Morgan and Veal, 2007; Veal *et al.*, 2004). Expectedly, the situation is more complex in higher plants (Dietz, 2003, 2008) and animals. The mammalian transcription factors reported to be redox-regulated such as AP-1, NFκB, p53, NFAT, HIF1, β-catenin, and Nrf2 determine a wide range of gene transcriptions. Accordingly, the exposure of human tissue culture to subtoxic concentrations of H_2O_2 (100 μM for 30 min) led a complex transcription pattern that did not clearly reflect a response to an oxidative stress, which corroborates the presumed role of H_2O_2 in regulating the expression the genes relevant to pathways unrelated to stress response (Desaint *et al.*, 2004). Further, the mammalian transcription factors themselves are not necessarily redox-modified, as in bacteria and yeast. Their activation is more often achieved by translocation into the nucleus after being released from redox-sensitive cytosolic complexes, as documented for the NFκB, Nrf2, and β-catenin.

5.5. Shut-off switches and restoration of starting conditions

Regulatory pathways that are activated by oxidation can be stopped at different levels and by different means: by removing the signaling oxidant, by reducing an oxidized transducer or obligatorily oxidized transcription

factor. Continuation of signaling is sometimes prevented by proteolytic destruction or oxidative inactivation of sensors or transducers despite persistence of the signaling molecules. With time delay, *de novo* synthesis of hydroperoxide or disulfide-reducing enzymes may dampen the oxidant activation of the cascades at various levels. Although "ROS"-dependent activation of signaling cascades has attracted much more attention than its equally important termination, examples of all theoretical switch-off possibilities can be given:

- In the simple bacterial systems, the transcription factors that are directly or indirectly oxidized by H_2O_2 or an ROOH lead to fast *de novo* synthesis of enzymes that remove the oxidant signal (AhpC/AhpF Ohr or other peroxidases), whereby a new homeostasis is established for adaptation to the changed environment (Dubbs and Mongkolsuk, 2007).
- In budding yeast, the internal disulfide bond in the active transcription factor Yap1 is reduced by thioredoxin (Delaunay *et al.*, 2000).
- Protein disulfide reduction by reduced redoxins appears to be the most common mechanism to stop oxidant signaling and may be implicated in all kind of organisms (Kalinina *et al.*, 2008), while oxidized Trx rather works as switch-on if the rate of thioredoxin reduction by thioredoxin reductases becomes limiting, at least locally. The same reasoning applies to glutaredoxin-dependent processes. However, due to the usually higher capacity of glutathione reductase, a shortage of GSH will require a more pronounced hydroperoxide flux.
- For activation of NFκB the inhibitory protein that keeps the transcription factors in the cytosol is completely degraded by the proteasome. What results is a "hit and run" mechanism: Downstream signaling proceeds, while any further signal meets an refractory upstream signaling machinery, until IκB has been resynthesized from scratch.
- Overoxidation of a Prx (Eq. (1.17)) that works as ROOH sensor would similarly render a cascade refractory to further oxidant signaling until the Prx is regenerated by sulfiredoxin. In parentheses, the often quoted "floodgate hypothesis" (Wood *et al.*, 2003) regards this oxidative Prx inactivation as a way to save H_2O_2 for signaling purposes. Physiological redox signaling, however, appears to occur at H_2O_2 levels far below the threshold of significant Prx inactivation. There are equally good reasons to speculate that Prx overoxidation is kind of "give-up signal." Evolutionary wisdom might have told the higher organisms that there is "a point of no return." If the flood of H_2O_2 has reached a level sufficient to generate sulfinic or sulfonic acids from protein thiols, the collateral damage is likely severe enough to leave the cells with only one reasonable consequence: programmed cell death.
- *De novo* synthesis of protective enzymes to restore resting conditions is evidently best achieved via the Nrf2/Keap1 system, which responds to

peroxide challenge as well as to damage signals (unsaturated aldehydes) and plant-derived micronutrients such as sulforaphane and polyphenolic "antioxidants" (they likely react *in situ* with the most abundant radical, the biradical O_2, and thereby generate $^{\bullet}O_2^-$ and H_2O_2). The list of proteins expressed due to activation of Nrf2 comprises, apart from phase II enzymes, γ-glutamyl cysteine synthetase, and glutathione synthetase for restoring GSH, glucose-6-phosphate dehydrogenase which fuels both, the glutathione and the thioredoxin system, glutathione reductase (Thimmulappa *et al.*, 2002), thioredoxin 1 and 2, thioredoxin reductase 1, GPx1 and GPx2 (Banning *et al.*, 2005; Brigelius-Flohé and Banning, 2006), Prx1, 2, and 4, and sulfiredoxin (Bae *et al.*, 2009; Kensler *et al.*, 2007; for a recent update see Müller *et al.*, 2010).

5.6. Signaling versus defense or modulation of redox signaling by competition

While in former times the thiol peroxidases were almost exclusively considered to protect organisms against oxidative stress (Flohé, 1985, 1989; Sies, 1985; Ursini *et al.*, 1982), it has now become fashionable to primarily regard them as key players in signaling (Bindoli *et al.*, 2008; Dayer *et al.*, 2008; Flohé and Brigelius-Flohé, 2006; Flohé and Harris, 2007; Forman *et al.*, 2010; Neumann *et al.*, 2009; Poole and Nelson, 2008).

Indeed, numerous studies on peroxidase knock-out, knock-down, or overexpression have shown that cytokine signaling, apoptosis or other stress responses are almost regularly affected, and often enough similar responses are obtained irrespective of the peroxidase thus investigated. In mammals the list of thiol peroxidases by now comprises eight GPxs and six Prxs, which in part are colocalized, and, despite advanced technologies, it will remain a challenge to work out which one is "just a peroxidase" or integrated into a regulatory circuit. A few spot lights may suffice to demonstrate that the two principles are not mutually exclusive.

There is no experimental evidence that GPx1 is part of a signaling cascade. GPx1, because of its abundance and catalytic efficiency, is considered the prototype of enzymes defending against hydroperoxide challenge. Accordingly, GPx1−/− mice did not display any phenotype, unless they were challenged with LPS, viral infection, or poisoned with redox cyclers (reviewed in Beck, 2006; Flohé and Brigelius-Flohé, 2006). However, overexpression of GPx1 in human tissue culture inhibited TNFα-induced NFκB activation (Kretz-Remy *et al.*, 1996), as was also observed in PrxII overexpressing cells (Kang *et al.*, 1998). Moreover, the attempts to create a supermouse resistant to all kind of oxidative stressors by systemic overexpression of GPx1 yielded a sick one: These mice became fat and developed insulin resistance, that is, all symptoms of type-II diabetes (McClung

et al., 2004). The lessons from these genetic experiments are: (i) The risks of aerobic life have been overestimated in the past but (ii) become relevant in bacterial of viral infections. (iii) Overexpression studies by themselves do not disclose whether or not enzymes are integral parts of regulatory circuits; in case of TNFα activation such a role may be rated as possible for PrxII, but unlikely for GPx1. (iv) Optimizing defense against peroxide challenge is a risky concept; the delicate physiological balance of hydroperoxide production and reduction must not be disturbed to an extent that redox signaling is inhibited or prevented. (v) GPx1, which is spread over the cytosol (and the mitochondrial matrix), can obviously compete for H_2O_2 that is built locally at surface-bound receptors and thereby pushes up the threshold for appropriate cytokine or hormone signaling.

Interleukin 1 also signals via NFκB activation but likely uses a lipoxygenase product as supportive oxidant signal. Accordingly, a large variation in GPx1 achieved by selenium restriction and resupplementation did only marginally affect IL1 signaling. In contrast, a fourfold overexpression of GPx4, which did not significantly contribute to the overall GPx activity when measured with H_2O_2 as substrate, completely abrogated IL1-induced NFκB activation (Brigelius-Flohé *et al.*, 1997). The most likely interpretation for this finding is again competition for the specific oxidant signal by GPx4, although other possibilities have not been excluded.

Similarly, in oxidant-driven apoptosis the roles of the peroxidases may differ in mechanism and vary with the type of oxidant involved. As outlined above for ASK1-mediated apoptosis, a direct H_2O_2 sensing and signal transduction by a Prx is not unlikely, whereas the inhibition of apoptosis by overexpressing GPxs (Flohé and Brigelius-Flohé, 2006) is probably due to competition for the oxidant signal. Certain lipoxygenase product as signaling oxidants are preferentially (or exclusively?) metabolized by GPx4. The particularly hard-to-metabolize ones are the products of 12,15-lipoxygenase, an enzyme implicated in oxidative remodeling of intracellular membranes since the 1970s (Rapoport *et al.*, 1979) and now also in apoptosis (Seiler *et al.*, 2008). If GPx4 in this context acts as a competing peroxidase (modulator) or sensor/transducer is unknown. Apoptotic signaling occurs at borderline toxic hydroperoxide concentration, and therefore regeneration of reduced GSH or Trx may become rate limiting. This implies that thresholds for signaling may also be adjusted by induction of pertinent enzymes.

6. Conclusions and Perspectives

The old concept that thiol peroxidases are pivotal to fight oxidative stress is still valid for conditions in which the organism is flooded with hydroperoxide, as in infection and fulminant inflammation. The

accumulated knowledge on hydroperoxide reduction by the various peroxidase families teaches that these enzymes are also optimum candidates for peroxide sensors and transducers of redox signals and anyway modulate metabolic pathways that depend on their substrates. The emerging evidence that most signaling cascades respond to, or depend on, oxidants suggested a new look on seemingly antique science, and the lateral thinking proved to be surprisingly rewarding. Basically, the concept of redox reactions complementing phosphorylation/dephosphorylation and proteolytic events for metabolic regulation has been established. The details, though, are far from clear.

A few major deficiencies that still lend to the field a swampy character may be listed. Only in exceptional cases do we know which redox-competent protein reacts with a specific partner and how the partner translates the contact into function. If we believe that we understand this venture qualitatively, then, the consequent problems appear on the horizon: Does the presumed event really happen? Is it possible under consideration of space and time? Are the kinetics in line with the time course of the macroscopic phenomenon addressed? For most of the questions, the answers are still in the clouds. The technologies to solve the problems are available: Structural analysis is improving at a speed that promises *in silico* feasibility studies for almost any kind of protein–protein interaction in the near future; mass spectrometry can meanwhile detect any kind of protein modification; fast kinetics are being measured for decades already; molecular genetics are guiding the way for identifying key players; *in vivo* imaging of redox events is emerging. However, combining kinetics with structural analysis and matching the result from clean systems with *in vivo* or *ex vivo* data demands logistics that are not easily established. The topical ''omics'' may tell us where it is rewarding to have a closer look but might disappoint when looking for clarity. The scenario will not become more transparent without exploiting the synergism of complementary technologies.

REFERENCES

Ahsan, M. K., Lekli, I., Ray, D., Yodoi, J., and Das, D. K. (2009). Redox regulation of cell survival by the thioredoxin superfamily: An implication of redox gene therapy in the heart. *Antioxid. Redox Signal.* **11,** 2741–2758.

Andersson, K. E. (2001). Pharmacology of penile erection. *Pharmacol. Rev.* **53,** 417–450.

Aslund, F., Zheng, M., Beckwith, J., and Storz, G. (1999). Regulation of the OxyR transcription factor by hydrogen peroxide and the cellular thiol–disulfide status. *Proc. Natl. Acad. Sci. USA* **96,** 6161–6165.

Atichartpongkul, S., Loprasert, S., Vattanaviboon, P., Whangsuk, W., Helmann, J. D., and Mongkolsuk, S. (2001). Bacterial Ohr and OsmC paralogues define two protein families with distinct functions and patterns of expression. *Microbiology* **147,** 1775–1782.

Aumann, K. D., Bedorf, N., Brigelius-Flohé, R., Schomburg, D., and Flohé, L. (1997). Glutathione peroxidase revisited—Simulation of the catalytic cycle by computer-assisted molecular modelling. *Biomed. Environ. Sci.* **10,** 136–155.

Azzi, A., Loschen, G., and Flohé, L. (1974). Structural and functional aspects of H_2O_2 formation in the mitochondrial membrane. Discussion. *In* "Glutathione," (L. Flohé, H. C. Benöhr, H. Sies, H. D. Waller, and A. Wendel, eds.), p. 244. Georg Thieme, Stuttgart.

Babior, B. M. (1999). NADPH oxidase: An update. *Blood* **93,** 1464–1476.

Babior, B. M. (2004). NADPH oxidase. *Curr. Opin. Immunol.* **16,** 42–47.

Babior, B. M., Kipnes, R. S., and Curnutte, J. T. (1973). Biological defense mechanisms. The production by leukocytes of superoxide, a potential bactericidal agent. *J. Clin. Invest.* **52,** 741–744.

Bae, Y. S., Kang, S. W., Seo, M. S., Baines, I. C., Tekle, E., Chock, P. B., and Rhee, S. G. (1997). Epidermal growth factor (EGF)-induced generation of hydrogen peroxide. Role in EGF receptor-mediated tyrosine phosphorylation. *J. Biol. Chem.* **272,** 217–221.

Bae, S. H., Woo, H. A., Sung, S. H., Lee, H. E., Lee, S. K., Kil, I. S., and Rhee, S. G. (2009). Induction of sulfiredoxin via an Nrf2-dependent pathway and hyperoxidation of peroxiredoxin III in the lungs of mice exposed to hyperoxia. *Antioxid. Redox Signal.* **11,** 937–948.

Baldridge, C. W., and Gerard, R. W. (1933). The extra respiration of phagocytosis. *Am. J. Physiol.* **103,** 235–236.

Baldus, S., Castro, L., Eiserich, J. P., and Freeman, B. A. (2001). Is *NO news bad news in acute respiratory distress syndrome? *Am. J. Respir. Crit. Care Med.* **163,** 308–310.

Banning, A., Deubel, S., Kluth, D., Zhou, Z., and Brigelius-Flohe, R. (2005). The GI-GPx gene is a target for Nrf2. *Mol. Cell. Biol.* **25,** 4914–4923.

Barrett, W. C., DeGnore, J. P., Konig, S., Fales, H. M., Keng, Y. F., Zhang, Z. Y., Yim, M. B., and Chock, P. B. (1999). Regulation of PTP1B via glutathionylation of the active site cysteine 215. *Biochemistry* **38,** 6699–6705.

Beck, M. A. (2006). Selenium and viral infections. *In* "Selenium: Its Molecular Biology and Role in Human Health," (D. L. Hatfield, M. J. Berry, and V. N. Gladyshev, eds.), pp. 287–298. Springer, New York.

Beckman, J. S., and Koppenol, W. H. (1996). Nitric oxide, superoxide, and peroxynitrite: The good, the bad, and ugly. *Am. J. Physiol.* **271,** C1424–C1437.

Beckman, J. S., Beckman, T. W., Chen, J., Marshall, P. A., and Freeman, B. A. (1990). Apparent hydroxyl radical production by peroxynitrite: Implications for endothelial injury from nitric oxide and superoxide. *Proc. Natl. Acad. Sci. USA* **87,** 1620–1624.

Beyer, H. (1968). Lehrbuch der organischen Chemie, 15./16. Auflage. S. Hirzel Verlag, Leipzig, pp. 54–55.

Bindoli, A., Fukuto, J. M., and Forman, H. J. (2008). Thiol chemistry in peroxidase catalysis and redox signaling. *Antioxid. Redox Signal.* **10,** 1549–1564.

Birringer, M., Pilawa, S., and Flohé, L. (2002). Trends in selenium biochemistry. *Nat. Prod. Rep.* **19,** 693–718.

Biteau, B., Labarre, J., and Toledano, M. B. (2003). ATP-dependent reduction of cysteine-sulphinic acid by *S. cerevisiae* sulphiredoxin. *Nature* **425,** 980–984.

Boveris, A., Cadenas, E., and Stoppani, A. O. (1976). Role of ubiquinone in the mitochondrial generation of hydrogen peroxide. *Biochem. J.* **156,** 435–444.

Bray, W. C., and Gorin, M. H. (1932). Ferryl ion, a compound of tetravalent iron. *J. Am. Chem. Soc.* **54,** 2124–2125.

Brigelius, R. (1985). Mixed disulfides: Biological functions and increase in oxidative stress. *In* "Oxidative Stress," (H. Sies, ed.), pp. 243–272. Academic Press, London.

Brigelius-Flohé, R., and Banning, A. (2006). Part of the series: From dietary antioxidants to regulators in cellular signaling and gene regulation. Sulforaphane and selenium, partners in adaptive response and prevention of cancer. *Free Radic. Res.* **40,** 775–787.

Brigelius-Flohé, R., Friedrichs, B., Maurer, S., Schultz, M., and Streicher, R. (1997). Interleukin-1-induced nuclear factor kappa B activation is inhibited by overexpression of phospholipid hydroperoxide glutathione peroxidase in a human endothelial cell line. *Biochem. J.* **328,** 199–203.

Briviba, K., Kissner, R., Koppenol, W. H., and Sies, H. (1998). Kinetic study of the reaction of glutathione peroxidase with peroxynitrite. *Chem. Res. Toxicol.* **11,** 1398–1401.

Bryk, R., Griffin, P., and Nathan, C. (2000). Peroxynitrite reductase activity of bacterial peroxiredoxins. *Nature* **407,** 211–215.

Budde, H., Flohé, L., Hecht, H. J., Hofmann, B., Stehr, M., Wissing, J., and Lünsdorf, H. (2003a). Kinetics and redox-sensitive oligomerisation reveal negative subunit cooperativity in tryparedoxin peroxidase of *Trypanosoma brucei brucei*. *Biol. Chem. Hoppe-Seyler* **384,** 619–633.

Budde, H., Flohe, L., Hofmann, B., and Nimtz, M. (2003b). Verification of the interaction of a tryparedoxin peroxidase with tryparedoxin by ESI-MS/MS. *Biol. Chem. Hoppe-Seyler* **384,** 1305–1309.

Calabrese, V., Mancuso, C., Calvani, M., Rizzarelli, E., Butterfield, D. A., and Stella, A. M. (2007). Nitric oxide in the central nervous system: Neuroprotection versus neurotoxicity. *Nat. Rev. Neurosci.* **8,** 766–775.

Castro, H., and Tomas, A. M. (2008). Peroxidases of trypanosomatids. *Antioxid. Redox Signal.* **10,** 1593–1606.

Chae, H. Z., Chung, S. J., and Rhee, S. G. (1994a). Thioredoxin-dependent peroxide reductase from yeast. *J. Biol. Chem.* **269,** 27670–27678.

Chae, H. Z., Robison, K., Poole, L. B., Church, G., Storz, G., and Rhee, S. G. (1994b). Cloning and sequencing of thiol-specific antioxidant from mammalian brain: Alkyl hydroperoxide reductase and thiol-specific antioxidant define a large family of antioxidant enzymes. *Proc. Natl. Acad. Sci. USA* **91,** 7017–7021.

Chance, B., and Oshino, N. (1971). Kinetics and mechanisms of catalase in peroxisomes of the mitochondrial fraction. *Biochem. J.* **122,** 225–233.

Chance, B., Sies, H., and Boveris, A. (1979). Hydroperoxide metabolism in mammalian organs. *Physiol. Rev.* **59,** 527–605.

Charlesby, A., Garratt, P. G., and Kopp, P. M. (1962). Radiation protection with sulphur and some sulphur-containing compounds. *Nature* **194,** 782.

Claiborne, A., Miller, H., Parsonage, D., and Ross, R. P. (1993). Protein-sulfenic acid stabilization and function in enzyme catalysis and gene regulation. *FASEB J.* **7,** 1483–1490.

Comini, M. A., Krauth-Siegel, R. L., and Flohé, L. (2007). Depletion of the thioredoxin homologue tryparedoxin impairs antioxidative defence in African trypanosomes. *Biochem. J.* **402,** 43–49.

Conrad, M. (2009). Transgenic mouse models for the vital selenoenzymes cytosolic thioredoxin reductase, mitochondrial thioredoxin reductase and glutathione peroxidase 4. *Biochim. Biophys. Acta* **1790,** 1575–1585.

Czech, M. P., Lawrence, J. C. Jr., and Lynn, W. S. (1974). Evidence for the involvement of sulfhydryl oxidation in the regulation of fat cell hexose transport by insulin. *Proc. Natl. Acad. Sci. USA* **71,** 4173–4177.

D'Autreaux, B., and Toledano, M. B. (2007). ROS as signalling molecules: Mechanisms that generate specificity in ROS homeostasis. *Nat. Rev. Mol. Cell Biol.* **8,** 813–824.

Dayer, R., Fischer, B. B., Eggen, R. I., and Lemaire, S. D. (2008). The peroxiredoxin and glutathione peroxidase families in *Chlamydomonas reinhardtii*. *Genetics* **179,** 41–57.

Delaunay, A., Isnard, A. D., and Toledano, M. B. (2000). H_2O_2 sensing through oxidation of the Yap1 transcription factor. *EMBO J.* **19,** 5157–5166.

Delaunay, A., Pflieger, D., Barrault, M. B., Vinh, J., and Toledano, M. B. (2002). A thiol peroxidase is an H_2O_2 receptor and redox-transducer in gene activation. *Cell* **111,** 471–481.

Denu, J. M., and Tanner, K. G. (1998). Specific and reversible inactivation of protein tyrosine phosphatases by hydrogen peroxide: Evidence for a sulfenic acid intermediate and implications for redox regulation. *Biochemistry* **37,** 5633–5642.

Desaint, S., Luriau, S., Aude, J. C., Rousselet, G., and Toledano, M. B. (2004). Mammalian antioxidant defenses are not inducible by H_2O_2. *J. Biol. Chem.* **279,** 31157–31163.

Dietz, K. J. (2003). Redox control, redox signaling, and redox homeostasis in plant cells. *Int. Rev. Cytol.* **228,** 141–193.

Dietz, K. J. (2008). Redox signal integration: From stimulus to networks and genes. *Physiol. Plant.* **133,** 459–468.

Dominici, S., Paolicchi, A., Lorenzini, E., Maellaro, E., Comporti, M., Pieri, L., Minotti, G., and Pompella, A. (2003). Gamma-glutamyltransferase-dependent prooxidant reactions: A factor in multiple processes. *Biofactors* **17,** 187–198.

Dröge, W. (2002). Free radicals in the physiological control of cell function. *Physiol. Rev.* **82,** 47–95.

Dubbs, J. M., and Mongkolsuk, S. (2007). Peroxiredoxins in bacterial antioxidant defense. *In* "Peroxiredoxin Systems. Subcellular Biochemistry," (L. Flohé and J. R. Harris, eds.), Vol. 44, pp. 143–193. Springer, New York.

Dubuisson, M., Vander Stricht, D., Clippe, A., Etienne, F., Nauser, T., Kissner, R., Koppenol, W. H., Rees, J. F., and Knoops, B. (2004). Human peroxiredoxin 5 is a peroxynitrite reductase. *FEBS Lett.* **571,** 161–165.

Dupuy, C., Ohayon, R., Valent, A., Noel-Hudson, M. S., Deme, D., and Virion, A. (1999). Purification of a novel flavoprotein involved in the thyroid NADPH oxidase. Cloning of the porcine and human cdnas. *J. Biol. Chem.* **274,** 37265–37269.

Eldjarn, L., and Bremer, J. (1962). The inhibitory effect at the hexokinase level of disulphides on glucose metabolism in human erythrocytes. *Biochem. J.* **84,** 286–291.

Ellis, H. R., and Poole, L. B. (1997a). Novel application of 7-chloro-4-nitrobenzo-2-oxa-1, 3-diazole to identify cysteine sulfenic acid in the AhpC component of alkyl hydroperoxide reductase. *Biochemistry* **36,** 15013–15018.

Ellis, H. R., and Poole, L. B. (1997b). Roles for the two cysteine residues of AhpC in catalysis of peroxide reduction by alkyl hydroperoxide reductase from *Salmonella typhimurium*. *Biochemistry* **36,** 13349–13356.

Epp, O., Ladenstein, R., and Wendel, A. (1983). The refined structure of the selenoenzyme glutathione peroxidase at 0.2-nm resolution. *Eur. J. Biochem.* **133,** 51–69.

Ershoff, B. H., and Steers, C. W. Jr. (1960a). Antioxidants and survival time of mice exposed to multiple sublethal doses of x-irradiation. *Proc. Soc. Exp. Biol. Med.* **104,** 274–276.

Ershoff, B. H., and Steers, C. W. J. (1960b). Bioflavonoids and survival time of mice exposed to multiple sublethal doses of x-irradiation. *Proc. Soc. Exp. Biol. Med.* **105,** 283–286.

Fenton, H. J. H. (1876). On a new reaction of tartaric acid. *Chem. News* **33,** 190.

Fischer, E. H. (1997). Cellular regulation by protein phosphorylation: A historical overview. *Biofactors* **6,** 367–374.

Flohé, L. (1985). The glutathione peroxidase reaction: Molecular basis of the antioxidant function of selenium in mammals. *Curr. Top. Cell. Regul.* **27,** 473–788.

Flohé, L. (1988). Superoxide dismutase for therapeutic use: Clinical experience, dead ends and hopes. *Mol. Cell. Biochem.* **84,** 123–131.

Flohé, L. (1989). The selenoprotein glutathione peroxidase. *In* "Glutathione: Chemical, Biochemical, and Medical Aspects—Part A," (R. P. D. Dolphin and O. Avramovic, eds.), pp. 643–731. Wiley, New York.

Flohé, L. (2009). The labour pains of biochemical selenology: The history of selenoprotein biosynthesis. *Biochim. Biophys. Acta* **1790,** 1389–1403.

Flohé, L., and Brigelius-Flohé, R. (2006). Selenoproteins of the glutathione system. *In* "Selenium: Its Molecular Biology and Role in Human Health," (D. Hatfield, M. S. Berry, and V. N. Gladyshev, eds.), pp. 161–172. Springer, Heidelberg/New York.

Flohé, L., and Harris, J. R. (2007). History of peroxiredoxins and topical perspectives. *In* "Peroxiredoxin Systems: Structure and Function," (L. Flohé and J. R. Harris, eds.), Vol. 44, pp. 1–25. Springer, New York.

Flohé, L., and Schlegel, W. (1971). Glutathione peroxidase. IV. Intracellular distribution of the glutathione peroxidase system in the rat liver. *Hoppe-Seyler's Z. Physiol. Chem.* **352,** 1401–1410.

Flohé, L., and Ursini, F. (2008). Peroxidase: A term of many meanings. *Antioxid. Redox Signal.* **10,** 1485–1490.

Flohé, L., Günzler, W., Jung, G., Schaich, E., and Schneider, F. (1971). Glutathione peroxidase. II. Substrate specificity and inhibitory effects of substrate analogues. *Hoppe-Seyler's Z. Physiol. Chem.* **352,** 159–169.

Flohé, L., Günzler, W. A., and Schock, H. H. (1973). Glutathione peroxidase: A selenoenzyme. *FEBS Lett.* **32,** 132–134.

Flohé, L., Giertz, H., and Beckmann, R. (1985). Free radical scavengers as anti-inflammatory drugs. *In* "Handbook of Inflammation," (I. L. Bonta, M. A. Bray, and M. J. Parnham, eds.), pp. 255–281. Elsevier, Amsterdam, The Netherlands.

Flohé, L., Budde, H., Bruns, K., Castro, H., Clos, J., Hofmann, B., Kansal-Kalavar, S., Krumme, D., Menge, U., Plank-Schumacher, K., Sztajer, H., Wissing, J., Wylegalla, C., and Hecht, H. J. (2002). Tryparedoxin peroxidase of Leishmania donovani: Molecular cloning, heterologous expression, specificity, and catalytic mechanism. *Arch. Biochem. Biophys.* **397,** 324–335.

Fomenko, D. E., Marino, S. M., and Gladyshev, V. N. (2008). Functional diversity of cysteine residues in proteins and unique features of catalytic redox-active cysteines in thiol oxidoreductases. *Mol. Cells* **26,** 228–235.

Forman, H. J., and Kennedy, J. A. (1974). Role of superoxide radical in mitochondrial dehydrogenase reactions. *Biochem. Biophys. Res. Commun.* **60,** 1044–1050.

Forman, H. J., Maiorino, M., and Ursini, F. (2010). Signaling functions of reactive oxygen species. *Biochemistry* **49,** 835–842.

Förstermann, U., Closs, E. I., Pollock, J. S., Nakane, M., Schwarz, P., Gath, I., and Kleinert, H. (1994). Nitric oxide synthase isozymes. Characterization, purification, molecular cloning, and functions. *Hypertension* **23,** 1121–1131.

Förstermann, U., Schmidt, H. H., Pollock, J. S., Sheng, H., Mitchell, J. A., Warner, T. D., Nakane, M., and Murad, F. (1991). Isoforms of nitric oxide synthase. Characterization and purification from different cell types. *Biochem. Pharmacol.* **42,** 1849–1857.

Frank, L., Yam, J., and Roberts, R. J. (1978). The role of endotoxin in protection of adult rats from oxygen-induced lung toxicity. *J. Clin. Invest.* **61,** 269–275.

Funato, Y., and Miki, H. (2007). Nucleoredoxin, a novel thioredoxin family member involved in cell growth and differentiation. *Antioxid. Redox Signal.* **9,** 1035–1057.

Funato, Y., Michiue, T., Asashima, M., and Miki, H. (2006). The thioredoxin-related redox-regulating protein nucleoredoxin inhibits Wnt-beta-catenin signalling through dishevelled. *Nat. Cell Biol.* **8,** 501–508.

Gasdaska, P. Y., Oblong, J. E., Cotgreave, I. A., and Powis, G. (1994). The predicted amino acid sequence of human thioredoxin is identical to that of the autocrine growth factor human adult T-cell derived factor (ADF): Thioredoxin mRNA is elevated in some human tumors. *Biochim. Biophys. Acta* **1218,** 292–296.

Gerschman, R., Gilbert, D. L., Nye, S. W., Dwyer, P., and Penn, W. O. (1954). Oxygen poisoning and x-irradiation: A mechanism in common. *Science* **119,** 623–626.

Godeas, C., Tramer, F., Micali, F., Roveri, A., Maiorino, M., Nisii, C., Sandri, G., and Panfili, E. (1996). Phospholipid hydroperoxide glutathione peroxidase (PHGPx) in rat testis nuclei is bound to chromatin. *Biochem. Mol. Med.* **59,** 118–124.

Gommel, D. U., Nogoceke, E., Morr, M., Kiess, M., Kalisz, H. M., and Flohé, L. (1997). Catalytic characteristics of tryparedoxin. *Eur. J. Biochem.* **248,** 913–918.

Goossens, V., Grooten, J., De Vos, K., and Fiers, W. (1995). Direct evidence for tumor necrosis factor-induced mitochondrial reactive oxygen intermediates and their involvement in cytotoxicity. *Proc. Natl. Acad. Sci. USA* **92,** 8115–8119.

Gow, A. J., Buerk, D. G., and Ischiropoulos, H. (1997). A novel reaction mechanism for the formation of *S*-nitrosothiol in vivo. *J. Biol. Chem.* **272,** 2841–2845.

Granger, D. N., Rutili, G., and McCord, J. M. (1981). Superoxide radicals in feline intestinal ischemia. *Gastroenterology* **81,** 22–29.

Groeger, G., Quiney, C., and Cotter, T. G. (2009). Hydrogen peroxide as a cell-survival signaling molecule. *Antioxid. Redox Signal.* **11,** 2655–2671.

Gruetter, C. A., Barry, B. K., McNamara, D. B., Gruetter, D. Y., Kadowitz, P. J., and Ignarro, L. (1979). Relaxation of bovine coronary artery and activation of coronary arterial guanylate cyclase by nitric oxide, nitroprusside and a carcinogenic nitrosoamine. *J. Cyclic Nucleotide Res.* **5,** 211–224.

Gutierrez, C., and Devedjian, J. C. (1991). Osmotic induction of gene OsmC expression in *Escherichia coli* K12. *J. Mol. Biol.* **220,** 959–973.

Haber, F., and Weiss, J. (1932). Über die Katalyse des Hydroperoxydes. *Naturwissenschaften* **51,** 948–950.

Haber, F., and Weiss, J. (1934). The catalytic decomposition of hydrogen peroxide by iron salts. *Proc. R. Soc. Lond. A Math. Phys. Sci.* **147,** 332–351.

Harman, D. (1956). Aging: A theory based on free radical and radiation chemistry. *J. Gerontol.* **11,** 298–300.

Harris, J. R. (1968). Release of a macromolecular protein component from human erythrocyte ghosts. *Biochim. Biophys. Acta* **150,** 534–537.

Hayashi, T., Ueno, Y., and Okamoto, T. (1993). Oxidoreductive regulation of nuclear factor kappa B. Involvement of a cellular reducing catalyst thioredoxin. *J. Biol. Chem.* **268,** 11380–11388.

Heffetz, D., Bushkin, I., Dror, R., and Zick, Y. (1990). The insulinomimetic agents H_2O_2 and vanadate stimulate protein tyrosine phosphorylation in intact cells. *J. Biol. Chem.* **265,** 2896–9202.

Hemler, M. E., and Lands, W. E. (1980). Evidence for a peroxide-initiated free radical mechanism of prostaglandin biosynthesis. *J. Biol. Chem.* **255,** 6253–6261.

Hennet, T., Richter, C., and Peterhans, E. (1993). Tumour necrosis factor-alpha induces superoxide anion generation in mitochondria of L929 cells. *Biochem. J.* **289**(Pt 2), 587–592.

Herrero, E., and Ros, J. (2002). Glutaredoxins and oxidative stress defense in yeast. *Methods Enzymol.* **348,** 136–146.

Hofmann, B., Budde, H., Bruns, K., Guerrero, S. A., Kalisz, H. M., Menge, U., Montemartini, M., Nogoceke, E., Steinert, P., Wissing, J. B., Flohé, L., and Hecht, H. J. (2001). Structures of tryparedoxins revealing interaction with trypanothione. *Biol. Chem. Hoppe-Seyler* **382,** 459–471.

Hofmann, B., Hecht, H. J., and Flohé, L. (2002). Peroxiredoxins. *Biol. Chem. Hoppe-Seyler* **383,** 347–364.

Holmgren, A. (1976). Hydrogen donor system for *Escherichia coli* ribonucleoside-diphosphate reductase dependent upon glutathione. *Proc. Natl. Acad. Sci. USA* **73,** 2275–2279.

Holmgren, A. (1985). Thioredoxin. *Annu. Rev. Biochem.* **54,** 237–271.

Holmgren, A. (1989). Thioredoxin and glutaredoxin systems. *J. Biol. Chem.* **264,** 13963–13966.

Ignarro, L. J. (1997). Activation and regulation of the nitric oxide-cyclic GMP signal transduction pathway by oxidative stress. *In* "Oxidative Stress and Signal Transduction," (H. J. Forman and E. Cadenas, eds.), pp. 3–31. Chapman & Hall, New York.

Irigoin, F., Cibils, L., Comini, M. A., Wilkinson, S. R., Flohe, L., and Radi, R. (2008). Insights into the redox biology of *Trypanosoma cruzi*: Trypanothione metabolism and oxidant detoxification. *Free Radic. Biol. Med.* **45,** 733–742.

Jacob, H. S., and Jandl, J. H. (1966). Effects of sulfhydryl inhibition on red blood cells. 3. Glutathione in the regulation of the hexose monophosphate pathway. *J. Biol. Chem.* **241,** 4243–4250.

Jacob, C., Giles, G. I., Giles, N. M., and Sies, H. (2003). Sulfur and selenium: The role of oxidation state in protein structure and function. *Angew. Chem. Int. Ed. Engl.* **42,** 4742–4758.

Jacobson, F. S., Morgan, R. W., Christman, M. F., and Ames, B. N. (1989). An alkyl hydroperoxide reductase from *Salmonella typhimurium* involved in the defense of DNA against oxidative damage. Purification and properties. *J. Biol. Chem.* **264,** 1488–1496.

Jaeger, T., Budde, H., Flohé, L., Menge, U., Singh, M., Trujillo, M., and Radi, R. (2004). Multiple thioredoxin-mediated routes to detoxify hydroperoxides in *Mycobacterium tuberculosis*. *Arch. Biochem. Biophys.* **423,** 182–191.

Jensen, L. S., and Mc, G. J. (1960). Influence of selenium, antioxidants and type of yeast on vitamin E deficiency in the adult chicken. *J. Nutr.* **72,** 23–28.

Jones, D. P. (2006). Redefining oxidative stress. *Antioxid. Redox Signal.* **8,** 1865–1879.

Jones, J. D., and Dangl, J. L. (2006). The plant immune system. *Nature* **444,** 323–329.

Jones, S. A., O'Donnell, V. B., Wood, J. D., Broughton, J. P., Hughes, E. J., and Jones, O. T. (1996). Expression of phagocyte NADPH oxidase components in human endothelial cells. *Am. J. Physiol.* **271,** H1626–H1634.

Jönsson, T. J., and Lowther, W. T. (2007). The peroxiredoxin repair proteins. *In* "Peroxiredoxin Systems," (L. Flohé and J. R. Harris, eds.), Subcellular Biochemistry, Vol. 44, pp. 115–141.

Kalinina, E. V., Chernov, N. N., and Saprin, A. N. (2008). Involvement of thio-, peroxi-, and glutaredoxins in cellular redox-dependent processes. *Biochemistry Mosc.* **73,** 1493–1510.

Kang, S. W., Chae, H. Z., Seo, M. S., Kim, K., Baines, I. C., and Rhee, S. G. (1998). Mammalian peroxiredoxin isoforms can reduce hydrogen peroxide generated in response to growth factors and tumor necrosis factor-alpha. *J. Biol. Chem.* **273,** 6297–6302.

Karplus, P. A., and Hall, A. (2007). Structural survey of the peroxiredoxins. *In* "Peroxyredoxin Systems. Subcellular Biochemistry," Vol. 44, pp. 41–60. Springer, New York.

Keele, B. B. Jr., McCord, J. M., and Fridovich, I. (1970). Superoxide dismutase from *Escherichia coli* B. A new manganese-containing enzyme. *J. Biol. Chem.* **245,** 6176–6181.

Kensler, T. W., Wakabayashi, N., and Biswal, S. (2007). Cell survival responses to environmental stresses via the Keap1-Nrf2-ARE pathway. *Annu. Rev. Pharmacol. Toxicol.* **47,** 89–116.

Kim, K., Kim, I. H., Lee, K. Y., Rhee, S. G., and Stadtman, E. R. (1988). The isolation and purification of a specific "protector" protein which inhibits enzyme inactivation by a thiol/Fe(III)/O_2 mixed-function oxidation system. *J. Biol. Chem.* **263,** 4704–4711.

Klatt, P., and Lamas, S. (2000). Regulation of protein function by S-glutathiolation in response to oxidative and nitrosative stress. *Eur. J. Biochem.* **267,** 4928–4944.

Klebanoff, S. J. (1967). Iodination of bacteria: A bactericidal mechanism. *J. Exp. Med.* **126,** 1063–1078.

Klebanoff, S. J. (1974). Role of the superoxide anion in the myeloperoxidase-mediated antimicrobial system. *J. Biol. Chem.* **249,** 3724–3728.

Knoops, B., Loumaye, E., and Van Der Eecken, V. (2007). Evolution of the peroxiredoxins. *In* "Peroxiredoxin Systems," (L. Flohé and J. R. Harris, eds.), Subcellular Biochemistry, Vol. 44, pp. 27–40. Springer, New York.

Koh, C. S., Didierjean, C., Navrot, N., Panjikar, S., Mulliert, G., Rouhier, N., Jacquot, J. P., Aubry, A., Shawkataly, O., and Corbier, C. (2007). Crystal structures of a poplar thioredoxin peroxidase that exhibits the structure of glutathione peroxidases: Insights into redox-driven conformational changes. *J. Mol. Biol.* **370,** 512–529.

Krauth-Siegel, L. R., Comini, M. A., and Schlecker, T. (2007). The trypanothione system. *In* "Peroxiredoxin Systems," (L. Flohé and J. R. Harris, eds.), Subcellular Biochemistry, Vol. 44, pp. 231–251. Springer, New York.

Kretz-Remy, C., Mehlen, P., Mirault, M. E., and Arrigo, A. P. (1996). Inhibition of I kappa B-alpha phosphorylation and degradation and subsequent NF-kappa B activation by glutathione peroxidase overexpression. *J. Cell. Biol.* **133,** 1083–1093.

Krumme, D., Budde, H., Hecht, H. J., Menge, U., Ohlenschlager, O., Ross, A., Wissing, J., Wray, V., and Flohé, L. (2003). NMR studies of the interaction of tryparedoxin with redox-inactive substrate homologues. *Biochemistry* **42,** 14720–14728.

Ladenstein, R., and Wendel, A. (1976). Crystallographic data of the selenoenzyme glutathione peroxidase. *J. Mol. Biol.* **104,** 877–882.

Laurent, T. C., Moore, E. C., and Reichard, P. (1964). Enzymatic synthesis of deoxyribonucleotides. IV. Isolation and characterization of thioredoxin, the hydrogen donor from *Escherichia coli* B. *J. Biol. Chem.* **239,** 3436–3444.

Lesniak, J., Barton, W. A., and Nikolov, D. B. (2003). Structural and functional features of the *Escherichia coli* hydroperoxide resistance protein OsmC. *Protein Sci.* **12,** 2838–2843.

Lo, Y. Y., and Cruz, T. F. (1995). Involvement of reactive oxygen species in cytokine and growth factor induction of c-fos expression in chondrocytes. *J. Biol. Chem.* **270,** 11727–11730.

Loschen, G., Flohé, L., and Chance, B. (1971). Respiratory chain linked H(2)O(2) production in pigeon heart mitochondria. *FEBS Lett.* **18,** 261–264.

Loschen, G., Azzi, A., Richter, C., and Flohé, L. (1974). Superoxide radicals as precursors of mitochondrial hydrogen peroxide. *FEBS Lett.* **42,** 68–72.

Lowrie, D. B., and Aber, V. R. (1977). Superoxide production by rabbit pulmonary alveolar macrophages. *Life Sci.* **21,** 1575–1584.

Maiorino, M., Aumann, K. D., Brigelius-Flohé, R., Doria, D., van den Heuvel, J., McCarthy, J., Roveri, A., Ursini, F., and Flohé, L. (1995). Probing the presumed catalytic triad of selenium-containing peroxidases by mutational analysis of phospholipid hydroperoxide glutathione peroxidase (PHGPx). *Biol. Chem. Hoppe-Seyler* **376,** 651–660.

Maiorino, M., Roveri, A., Benazzi, L., Bosello, V., Mauri, P., Toppo, S., Tosatto, S. C., and Ursini, F. (2005). Functional interaction of phospholipid hydroperoxide glutathione peroxidase with sperm mitochondrion-associated cysteine-rich protein discloses the adjacent cysteine motif as a new substrate of the selenoperoxidase. *J. Biol. Chem.* **280,** 38395–38402.

Maiorino, M., Ursini, F., Bosello, V., Toppo, S., Tosatto, S. C., Mauri, P., Becker, K., Roveri, A., Bulato, C., Benazzi, L., De Palma, A., and Flohe, L. (2007). The thioredoxin specificity of *Drosophila* GPx: A paradigm for a peroxiredoxin-like mechanism of many glutathione peroxidases. *J. Mol. Biol.* **365,** 1037–1046.

Mason, R. P. (1986). One- and two-electron oxidation of reduced glutathione by peroxidases. *Adv. Exp. Med. Biol.* **197,** 493–503.

Matill, H. A. (1947). Antioxidants. *Ann. Rev. Biochem.* **16,** 177–192.

Mauri, P., Benazzi, L., Flohé, L., Maiorino, M., Pietta, P. G., Pilawa, S., Roveri, A., and Ursini, F. (2003). Versatility of selenium catalysis in PHGPx unraveled by LC/ESI-MS/MS. *Biol. Chem. Hoppe-Seyler* **384,** 575–588.

May, J. M., and de Haen, C. (1979). Insulin-stimulated intracellular hydrogen peroxide production in rat epididymal fat cells. *J. Biol. Chem.* **254,** 2214–2220.

McClung, J. P., Roneker, C. A., Mu, W., Lisk, D. J., Langlais, P., Liu, F., and Lei, X. G. (2004). Development of insulin resistance and obesity in mice overexpressing cellular glutathione peroxidase. *Proc. Natl. Acad. Sci. USA* **101,** 8852–8857.

McCord, J. M. (1974). Free radicals and inflammation: Protection of synovial fluid by superoxide dismutase. *Science* **185,** 529–531.

McCord, J. M., and Fridovich, I. (1968). The reduction of cytochrome *c* by milk xanthine oxidase. *J. Biol. Chem.* **243,** 5753–5760.

McCord, J. M., and Fridovich, I. (1969). Superoxide dismutase. An enzymic function for erythrocuprein (hemocuprein). *J. Biol. Chem.* **244,** 6049–6055.

Mills, G. C. (1957). Hemoglobin catabolism I. Glutathione peroxidase, an erythrocyte enzyme which protects hemoglobin from oxidative breakdown. *J. Biol. Chem.* **229,** 189–197.

Mogensen, T. H. (2009). Pathogen recognition and inflammatory signaling in innate immune defenses. *Clin. Microbiol. Rev.* **22,** 240–273.

Moncada, S., Palmer, R. M., and Higgs, E. A. (1988). The discovery of nitric oxide as the endogenous nitrovasodilator. *Hypertension* **12,** 365–372.

Moncada, S., Palmer, R. M., and Higgs, E. A. (1991). Nitric oxide: Physiology, pathophysiology, and pharmacology. *Pharmacol. Rev.* **43,** 109–142.

Mongkolsuk, S., Praituan, W., Loprasert, S., Fuangthong, M., and Chamnongpol, S. (1998). Identification and characterization of a new organic hydroperoxide resistance (*ohr*) gene with a novel pattern of oxidative stress regulation from *Xanthomonas campestris* pv. *phaseoli*. *J. Bacteriol.* **180,** 2636–2643.

Morgan, B. A., and Veal, E. A. (2007). Functions of typical 2-Cys peroxiredoxins in yeast. *In* "Peroxiredoxin Systems. Subcellular Biochemistry," (L. Flohé and J. R. Harris, eds.), Vol. 44, pp. 253–265. Springer, New York.

Mu, Z. M., Yin, X. Y., and Prochownik, E. V. (2002). Pag, a putative tumor suppressor, interacts with the Myc Box II domain of c-Myc and selectively alters its biological function and target gene expression. *J. Biol. Chem.* **277,** 43175–43184.

Muller, F. L., Liu, Y., and Van Remmen, H. (2004). Complex III releases superoxide to both sides of the inner mitochondrial membrane. *J. Biol. Chem.* **279,** 49064–49073.

Müller, M., Banning, A., Brigelius-Flohé, R., and Kipp, A. (2010). Nrf2 target genes are induced under marginal selenium deficiency. *Genes Nutr.* (in press).

Na, H. K., and Surh, Y. J. (2006). Transcriptional regulation via cysteine thiol modification: A novel molecular strategy for chemoprevention and cytoprotection. *Mol. Carcinog.* **45,** 368–380.

Nakashima, K., Pontremoli, S., and Horecker, B. L. (1969). Activation of rabbit liver fructose diphosphatase by coenzyme A and acyl carrier protein. *Proc. Natl. Acad. Sci. USA* **64,** 947–951.

Nakashima, I., Takeda, K., Kawamoto, Y., Okuno, Y., Kato, M., and Suzuki, H. (2005). Redox control of catalytic activities of membrane-associated protein tyrosine kinases. *Arch. Biochem. Biophys.* **434,** 3–10.

Nausser, T., and Koppenol, W. H. (2002). The rate constant of the reaction of superoxide with nitrogen monoxide: Approaching the diffusion limit. *J. Phys. Chem. A* **106,** 4984–4986.

Neumann, C. A., Cao, J., and Manevich, Y. (2009). Peroxiredoxin 1 and its role in cell signaling. *Cell Cycle* **8,** 4072–4078.

Nogoceke, E., Gommel, D. U., Kiess, M., Kalisz, H. M., and Flohé, L. (1997). A unique cascade of oxidoreductases catalyses trypanothione-mediated peroxide metabolism in Crithidia fasciculata. *Biol. Chem. Hoppe-Seyler* **378,** 827–836.

Nohl, H., and Jordan, W. (1986). The mitochondrial site of superoxide formation. *Biochem. Biophys. Res. Commun.* **138,** 533–539.

Nohl, H., Kozlov, A. V., Gille, L., and Staniek, K. (2003). Cell respiration and formation of reactive oxygen species: Facts and artefacts. *Biochem. Soc. Trans.* **31,** 1308–1311.

Ohba, M., Shibanuma, M., Kuroki, T., and Nose, K. (1994). Production of hydrogen peroxide by transforming growth factor-beta 1 and its involvement in induction of egr-1 in mouse osteoblastic cells. *J. Cell. Biol.* **126,** 1079–1088.

Palmer, R. M., Ferrige, A. G., and Moncada, S. (1987). Nitric oxide release accounts for the biological activity of endothelium-derived relaxing factor. *Nature* **327,** 524–526.

Parsonage, D., Karplus, P. A., and Poole, L. B. (2008). Substrate specificity and redox potential of AhpC, a bacterial peroxiredoxin. *Proc. Natl. Acad. Sci. USA* **105,** 8209–8214.

Poderoso, J. J., Carreras, M. C., Lisdero, C., Riobo, N., Schopfer, F., and Boveris, A. (1996). Nitric oxide inhibits electron transfer and increases superoxide radical production in rat heart mitochondria and submitochondrial particles. *Arch. Biochem. Biophys.* **328,** 85–92.

Poole, L. B. (2007). The catalytic mechanism of peroxiredoxins. *In* "Peroxiredoxin Systems," (L. Flohé and J. R. Harris, eds.), Subcellular Biochemistry, Vol. 44, pp. 61–81. Springer, New York.

Poole, L. B., and Ellis, H. R. (2002). Identification of cysteine sulfenic acid in AhpC of alkyl hydroperoxide reductase. *Methods Enzymol.* **348,** 122–136.

Poole, L. B., and Nelson, K. J. (2008). Discovering mechanisms of signaling-mediated cysteine oxidation. *Curr. Opin. Chem. Biol.* **12,** 18–24.

Posner, B. I., Faure, R., Burgess, J. W., Bevan, A. P., Lachance, D., Zhang-Sun, G., Fantus, I. G., Ng, J. B., Hall, D. A., Lum, B. S., *et al.* (1994). Peroxovanadium compounds. A new class of potent phosphotyrosine phosphatase inhibitors which are insulin mimetics. *J. Biol. Chem.* **269,** 4596–4604.

Quijano, C., Alvarez, B., Gatti, R. M., Augusto, O., and Radi, R. (1997). Pathways of peroxynitrite oxidation of thiol groups. *Biochem. J.* **322**(Pt 1), 167–173.

Radeke, H. H., Meier, B., Topley, N., Floge, J., Habermehl, G. G., and Resch, K. (1990). Interleukin 1-alpha and tumor necrosis factor-alpha induce oxygen radical production in mesangial cells. *Kidney Int.* **37,** 767–775.

Radi, R., Beckman, J. S., Bush, K. M., and Freeman, B. A. (1991). Peroxynitrite oxidation of sulfhydryls. The cytotoxic potential of superoxide and nitric oxide. *J. Biol. Chem.* **266,** 4244–4250.

Rapoport, S. M., Schewe, T., Wiesner, R., Halangk, W., Ludwig, P., Janicke-Hohne, M., Tannert, C., Hiebsch, C., and Klatt, D. (1979). The lipoxygenase of reticulocytes. Purification, characterization and biological dynamics of the lipoxygenase; its identity with the respiratory inhibitors of the reticulocyte. *Eur. J. Biochem.* **96,** 545–561.

Ren, B., Huang, W., Akesson, B., and Ladenstein, R. (1997). The crystal structure of seleno-glutathione peroxidase from human plasma at 2.9 A resolution. *J. Mol. Biol.* **268,** 869–885.

Rhee, S. G., Chae, H. Z., and Kim, K. (2005). Peroxiredoxins: A historical overview and speculative preview of novel mechanisms and emerging concepts in cell signaling. *Free Radic. Biol. Med.* **38,** 1543–1552.

Richter, C., Azzi, A., Weser, U., and Wendel, A. (1977). Hepatic microsomal dealkylations. Inhibition by a tyrosine-copper (II) complex provided with superoxide dismutase activity. *J. Biol. Chem.* **252,** 5061–5066.

Rotruck, J. T., Pope, A. L., Ganther, H. E., Swanson, A. B., Hafeman, D. G., and Hoekstra, W. G. (1973). Selenium: Biochemical role as a component of glutathione peroxidase. *Science* **179,** 588–590.

Rouhier, N., Gelhaye, E., Corbier, C., and Jacquot, J. P. (2004). Active site mutagenesis and phospholipid hydroperoxide reductase activity of poplar type II peroxiredoxin. *Physiol. Plant.* **120,** 57–62.

Saitoh, M., Nishitoh, H., Fujii, M., Takeda, K., Tobiume, K., Sawada, Y., Kawabata, M., Miyazono, K., and Ichijo, H. (1998). Mammalian thioredoxin is a direct inhibitor of apoptosis signal-regulating kinase (ASK) 1. *EMBO J.* **17,** 2596–2606.

Salmeen, A., Andersen, J. N., Myers, M. P., Meng, T. C., Hinks, J. A., Tonks, N. K., and Barford, D. (2003). Redox regulation of protein tyrosine phosphatase 1B involves a sulphenyl-amide intermediate. *Nature* **423,** 769–773.

Sarma, B. K., and Mugesh, G. (2008). Antioxidant activity of the anti-inflammatory compound ebselen: A reversible cyclization pathway via selenenic and seleninic acid intermediates. *Chemistry* **14,** 10603–10614.

Sbarra, A. J., and Karnowsky, M. L. (1959). The biochemical basis of phagocytosis. I. Metabolic changes during the ingestion of particles by polymorphonuclear leukocytes. *J. Biol. Chem.* **234,** 1355–1362.

Schlecker, T., Comini, M. A., Melchers, J., Ruppert, T., and Krauth-Siegel, R. L. (2007). Catalytic mechanism of the glutathione peroxidase-type tryparedoxin peroxidase of *Trypanosoma brucei*. *Biochem. J.* **405,** 445–454.

Schmidt, A., Clayton, C. E., and Krauth-Siegel, R. L. (2002). Silencing of the thioredoxin gene in *Trypanosoma brucei brucei*. *Mol. Biochem. Parasitol.* **125,** 207–210.

Schneider, M., Forster, H., Boersma, A., Seiler, A., Wehnes, H., Sinowatz, F., Neumuller, C., Deutsch, M. J., Walch, A., Hrabe de Angelis, M., Wurst, W., Ursini, F., Roveri, A., Maleszewski, M., Maiorino, M., and Conrad, M. (2009). Mitochondrial glutathione peroxidase 4 disruption causes male infertility. *FASEB J.* **23,** 3233–3242.

Seiler, A., Schneider, M., Forster, H., Roth, S., Wirth, E. K., Culmsee, C., Plesnila, N., Kremmer, E., Radmark, O., Wurst, W., Bornkamm, G. W., Schweizer, U., and Conrad, M. (2008). Glutathione peroxidase 4 senses and translates oxidative stress into 12/15-lipoxygenase dependent- and AIF-mediated cell death. *Cell Metab.* **8,** 237–248.

Shimazu, T., Tokutake, S., and Usami, M. (1978). Inactivation of phosphorylase phosphatase by a factor from rabbit liver and its chemical characterization as glutathione disulfide. *J. Biol. Chem.* **253,** 7376–7382.

Sies, H. (1985). Oxidative Stress. Academic Press, New York.

Sittipunt, C., Steinberg, K. P., Ruzinski, J. T., Myles, C., Zhu, S., Goodman, R. B., Hudson, L. D., Matalon, S., and Martin, T. R. (2001). Nitric oxide and nitrotyrosine in the lungs of patients with acute respiratory distress syndrome. *Am. J. Respir. Crit. Care Med.* **163,** 503–510.

Sohn, J., and Rudolph, J. (2003). Catalytic and chemical competence of regulation of cdc25 phosphatase by oxidation/reduction. *Biochemistry* **42,** 10060–10070.

Spallholz, J. E. (1994). On the nature of selenium toxicity and carcinostatic activity. *Free Radic. Biol. Med.* **17,** 45–64.

Spear, N., Estévez, A. G., Radi, R., and Beckman, J. S. (1997). Peroxynitrite and cell signaling. *In* "Oxidative Stress and Signal Transduction," (H. J. Forman and E. Cadenas, eds.), pp. 32–51. Chapman & Hall, New York.

Sundaresan, M., Yu, Z. X., Ferrans, V. J., Irani, K., and Finkel, T. (1995). Requirement for generation of H_2O_2 for platelet-derived growth factor signal transduction. *Science* **270,** 296–299.

Symons, M. R. C., and Gutteridge, J. M. C. (1998). Free Radicals and Iron: Chemistry, Biology, and Medicine. pp. 40–59, Oxford University Press, New York.

Sztajer, H., Gamain, B., Aumann, K. D., Slomianny, C., Becker, K., Brigelius-Flohé, R., and Flohé, L. (2001). The putative glutathione peroxidase gene of *Plasmodium falciparum* codes for a thioredoxin peroxidase. *J. Biol. Chem.* **276,** 7397–7403.

Tagaya, Y., Okada, M., Sugie, K., Kasahara, T., Kondo, N., Hamuro, J., Matsushima, K., Dinarello, C. A., and Yodoi, J. (1988). IL-2 receptor(p55)/Tac-inducing factor. Purification and characterization of adult T cell leukemia-derived factor. *J. Immunol.* **140,** 2614–2620.

Tamura, T., and Stadtman, T. C. (1996). A new selenoprotein from human lung adenocarcinoma cells: Purification, properties, and thioredoxin reductase activity. *Proc. Natl. Acad. Sci. USA* **93,** 1006–1011.

Tamura, T., Gladyshev, V., Liu, S. Y., and Stadtman, T. C. (1995). The mutual sparing effects of selenium and vitamin E in animal nutrition may be further explained by the discovery that mammalian thioredoxin reductase is a selenoenzyme. *Biofactors* **5,** 99–102.

Tartaglia, L. A., Storz, G., and Ames, B. N. (1989). Identification and molecular analysis of oxyR-regulated promoters important for the bacterial adaptation to oxidative stress. *J. Mol. Biol.* **210,** 709–719.

Thannickal, V. J., and Fanburg, B. L. (2000). Reactive oxygen species in cell signaling. *Am. J. Physiol. Lung Cell Mol. Physiol.* **279,** L1005–L1028.

Thimmulappa, R. K., Mai, K. H., Srisuma, S., Kensler, T. W., Yamamoto, M., and Biswal, S. (2002). Identification of Nrf2-regulated genes induced by the chemopreventive agent sulforaphane by oligonucleotide microarray. *Cancer Res.* **62,** 5196–5203.

Toppo, S., Flohé, L., Ursini, F., Vanin, S., and Maiorino, M. (2009). Catalytic mechanisms and specificities of glutathione peroxidases: Variations of a basic scheme. *Biochim. Biophys. Acta* **1790,** 1486–1500.

Tosatto, S. C., Bosello, V., Fogolari, F., Mauri, P., Roveri, A., Toppo, S., Flohé, L., Ursini, F., and Maiorino, M. (2008). The catalytic site of glutathione peroxidases. *Antioxid. Redox Signal.* **10,** 1515–1526.

Trujillo, M., Budde, H., Pineyro, M. D., Stehr, M., Robello, C., Flohé, L., and Radi, R. (2004). *Trypanosoma brucei* and *Trypanosoma cruzi* tryparedoxin peroxidases catalytically detoxify peroxynitrite via oxidation of fast reacting thiols. *J. Biol. Chem.* **279,** 34175–34182.

Trujillo, M., Mauri, P., Benazzi, L., Comini, M., De Palma, A., Flohé, L., Radi, R., Stehr, M., Singh, M., Ursini, F., and Jaeger, T. (2006). The mycobacterial thioredoxin peroxidase can act as a one-cysteine peroxiredoxin. *J. Biol. Chem.* **281,** 20555–20566.

Trujillo, M., Ferrer-Sueta, G., Thomson, L., Flohé, L., and Radi, R. (2007). Kinetics of peroxiredoxins and their role in the decomposition of peroxynitrite. *In* "Peroxyredoxin Systems. Subcellular Biochemistry," (L. Flohé and J. R. Harris, eds.), Vol. 44, pp. 83–113. Springer, New York.

Ursini, F., Maiorino, M., Valente, M., Ferri, L., and Gregolin, C. (1982). Purification from pig liver of a protein which protects liposomes and biomembranes from peroxidative degradation and exhibits glutathione peroxidase activity on phosphatidylcholine hydroperoxides. *Biochim. Biophys. Acta* **710,** 197–211.

Ursini, F., Heim, S., Kiess, M., Maiorino, M., Roveri, A., Wissing, J., and Flohé, L. (1999). Dual function of the selenoprotein PHGPx during sperm maturation. *Science* **285,** 1393–1396.

Veal, E. A., Findlay, V. J., Day, A. M., Bozonet, S. M., Evans, J. M., Quinn, J., and Morgan, B. A. (2004). A 2-Cys peroxiredoxin regulates peroxide-induced oxidation and activation of a stress-activated MAP kinase. *Mol. Cell* **15,** 129–139.

Weitzel, F., and Wendel, A. (1993). Selenoenzymes regulate the activity of leukocyte 5-lipoxygenase via the peroxide tone. *J. Biol. Chem.* **268,** 6288–6292.

Wen, S. T., and Van Etten, R. A. (1997). The PAG gene product, a stress-induced protein with antioxidant properties, is an Abl SH3-binding protein and a physiological inhibitor of c-Abl tyrosine kinase activity. *Genes Dev.* **11,** 2456–2467.

Winterbourn, C. C., and Metodiewa, D. (1999). Reactivity of biologically important thiol compounds with superoxide and hydrogen peroxide. *Free Radic. Biol. Med.* **27,** 322–328.

Woo, H. A., Chae, H. Z., Hwang, S. C., Yang, K. S., Kang, S. W., Kim, K., and Rhee, S. G. (2003). Reversing the inactivation of peroxiredoxins caused by cysteine sulfinic acid formation. *Science* **300,** 653–656.

Wood, Z. A., Poole, L. B., and Karplus, P. A. (2003). Peroxiredoxin evolution and the regulation of hydrogen peroxide signaling. *Science* **300,** 650–653.

Yost, F. J. Jr., and Fridovich, I. (1973). An iron-containing superoxide dismutase from *Escherichia coli*. *J. Biol. Chem.* **248,** 4905–4908.

Zhang, H., and Forman, H. J. (2009). Signaling pathways involved in phase II gene induction by alpha, beta-unsaturated aldehydes. *Toxicol. Ind. Health* **25,** 269–278.

Zweier, J. L., Wang, P., Samouilov, A., and Kuppusamy, P. (1995). Enzyme-independent formation of nitric oxide in biological tissues. *Nat. Med.* **1,** 804–809.

CHAPTER TWO

Mass Spectrometry-Based Methods for the Determination of Sulfur and Related Metabolite Concentrations in Cell Extracts

Emmanuel Godat,[*,†] Geoffrey Madalinski,[*] Ludovic Muller,[*,‡] Jean-François Heilier,[*,§] Jean Labarre,[†] *and* Christophe Junot[*]

Contents

* Laboratoire d'Etude du Métabolisme des Médicaments, DSV/iBiTec-S/SPI, CEA/Saclay, Gif-sur-Yvette Cedex, France
† Laboratoire de Biologie Intégrative, DSV/iBiTec-S/SBIGeM, CEA/Saclay, Gif-sur-Yvette Cedex, France
‡ Laboratoire de Chimie Biologique Organique et Structurale, IPCM, UMR-CNRS, UPMC Paris Universitas, Paris Cedex, France
§ Université catholique de Louvain, Louvain Centre for Toxicology and Applied Pharmacology, Brussels, Belgium

Methods in Enzymology, Volume 473
ISSN 0076-6879, DOI: 10.1016/S0076-6879(10)73002-0

Abstract

The sulfur metabolic pathway plays a central role in cell metabolism. It provides the sulfur amino acids methionine and cysteine, which are essential for protein synthesis, homocysteine, which lies at a critical juncture of this pathway, *S*-adenosylmethionine, the universal methyl donor in the cell, and glutathione (GSH), which has many crucial functions including protection against oxidative stress and xenobiotics. The intracellular level of these metabolites, which are closely connected with other cellular metabolic pathways, is of major importance for cell physiology and health. Three mass spectrometry-based methods for the determination of sulfur metabolites and also related compounds linked to the glutathione biosynthesis pathway are presented and discussed. The first one enables absolute quantification of these metabolites in cell extracts. It is based on liquid chromatography–electrospray triple quadrupole mass spectrometry coupled to ^{15}N uniform metabolic labeling of the yeast *Saccharomyces cerevisiae*. The two other methods are global approaches to metabolite detection involving a high-resolution mass spectrometer, the LTQ-Orbitrap. Ions related to metabolites of interest are picked up from complex and information-rich metabolic fingerprints. By these means, it is possible to detect analytical information outside the initial scope of investigation.

1. Introduction

The sulfur metabolic pathway plays a central role in cell metabolism. The structure of this metabolism is largely conserved among living organisms with three conserved subpathways: the methyl cycle, the transsulfuration pathway, and the synthesis of glutathione (see Fig. 2.1). In this metabolism, the sulfur amino acids methionine and cysteine are essential for protein synthesis.

The methyl cycle is composed of homocysteine, methionine, *S*-adenosylmethionine (SAM), and *S*-adenosylhomocysteine (Fig. 2.1). SAM is the universal methyl donor for all methylations in the cell (lipids, RNA, DNA, some proteins). In addition, it is a precursor for the synthesis of a number of essential metabolites (e.g., polyamines, biotin, choline) and neurotransmitters (e.g., dopamine, serotonin). Depending on the organisms, cysteine and homocysteine can be converted in either direction through the transsulfuration pathway, which involves cystathionine as an intermediate (Fig. 2.1). In addition to its utilization for the synthesis of proteins, cysteine serves as a precursor for the synthesis of thiamine, of iron–sulfur clusters and glutathione.

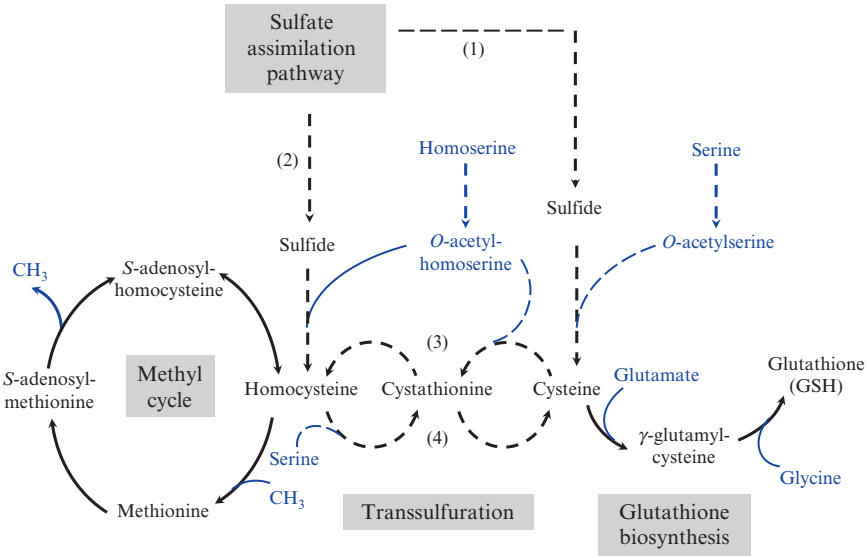

Figure 2.1 *The sulfur metabolite pathway*. Schematic representation of the core of sulfur metabolism. Plain arrows: pathway present in nearly all organisms. The sulfate assimilation (1) is present in bacteria, yeasts, protists, and plants. An alternative pathway is present in some yeast species (e.g., pathway (2) in *S. cerevisiae*). The transsulfuration pathway can be in either direction (e.g., direction (3) in bacteria, in plants and in the yeast *Schizosaccharomyces pombe*); direction (4) in mammals or both directions (*S. cerevisiae*, *Pseudomonas* species).

The glutathione (GSH) biosynthesis pathway (Fig. 2.1) is of primary importance for the cell regarding the multiple and essential functions of GSH. GSH exists in thiol-reduced (GSH) and disulfide-oxidized (GSSG) forms. GSH has several vital functions, including redox buffer, reduction of disulfide bonds, maintaining the thiol status of proteins, detoxification of electrophilic xenobiotics and heavy metals, scavenging free radicals, iron–sulfur cluster formation, and a reserve of cysteine. GSH is also required for the detoxification of methylglyoxal and formaldehyde, two metabolites produced as by-products of metabolism. In addition, GSH plays a role in other key cellular processes including apoptosis, cell proliferation, cytokine production, immune response, and signal transduction. GSH deficiency leads to oxidative stress, which plays an important role in many diseases and in aging. Decreased levels of cellular GSH are associated with several diseases including diabetes, cancer, liver diseases, Alzheimer's disease, Parkinson's disease, and cardiovascular risks (Wu *et al.*, 2004b). Homocysteine has adverse effects when its cellular concentration is elevated. For example in humans, high levels of homocysteine are an important risk factor for aging-related diseases, including Alzheimer's disease, osteoporosis, and vascular diseases (Maron and Loscalzo, 2009).

In all organisms, sulfur metabolism therefore has very important functions and strong metabolic constraints, as it provides the cell with optimal amounts of the essential metabolites SAM, methionine, cysteine, and glutathione. In consequence, this metabolism and the level of sulfur metabolites are tightly regulated in both prokaryotic and eukaryotic cells.

In bacteria, plants, and some eukaryotic microorganisms such as yeasts, a pathway for assimilating inorganic sulfate is also present (Fig. 2.1). The assimilation of inorganic sulfur is structurally connected to the serine or homoserine biosynthesis pathway as these amino acids are precursors respectively of *o*-acetylserine and *o*-acetylhomoserine, which provide the carbon backbone for the synthesis of cysteine and homocysteine. These amino acids are also required in the transsulfuration pathways that convert homocysteine to cysteine (and vice versa). The amino acids glutamate and glycine are also precursors for the synthesis of GSH. The sulfur pathway is thus highly connected to the metabolism of other amino acids. Consistent with these metabolic links, cross-regulations (or co-regulation) of multiple amino acid pathways have been evidenced in the yeast *Saccharomyces cerevisiae* (Natarajan *et al.*, 2001). Similar findings were also observed in the course of a study of cadmium toxicity in the yeast *S. cerevisiae* (Madalinski *et al.*, 2008). It is thus important for some studies to have analytical methods to quantify metabolite pools that are not restricted to sulfur metabolites alone.

2. Analytical Methods for the Determination of Sulfur and Amino Acid Metabolites

Sulfur metabolites are molecules containing either a free thiol function, as for example is the case for homocysteine, cysteine, glutathione, and its precursor the dipeptide γ-glutamyl-cysteine, or a blocked thiol function, as is the case for cystathionine and methionine. Metabolites containing free thiol groups are present at different redox states in biological media, either as reduced or oxidized (i.e., dimeric) forms. Other oxidized states are possible and metabolites may also be detected as sulfoxides, sulfonates, and sulfinic acids in biological extracts.

The detection and quantification of sulfur metabolites has to overcome three major analytical challenges. The first is to preserve the redox state of such metabolites for further biological interpretation of the results, the second is to detect both free and blocked thiol metabolites, and lastly, sulfur metabolites are highly polar and their retention on chromatographic columns may be problematic. Various analytical tools based on gas or liquid chromatography (LC) have been developed for the determination of sulfur metabolites.

Thiol derivatization with specific reagents coupled with reverse phase chromatography followed by ultraviolet (Raggi *et al.*, 1998), fluorimetric (Luo *et al.*, 1995; Parmentier *et al.*, 1998; Salazar *et al.*, 1999; Senft *et al.*, 2000; Yan and Huxtable, 1995), or mass spectrometric detection (Guan *et al.*, 2003; Hammermeister *et al.*, 2000) is a popular approach. Thiol labeling with bromobimanes can be used in LC methods for the quantitative determination of low-molecular-weight thiol molecules in biological extracts (Fahey and Newton, 1987). The reaction of bromobimanes with thiol metabolites converts the nonfluorescent derivatization agent into a water-soluble derivative. The specificity of this reagent is provided by its poor reactivity toward other nucleophiles (Kosower and Kosower, 1987). When coupled with fluorescent detection, such a method allows quantification of thiol metabolites at the picomole level (Fahey and Newton, 1987). However, because of the prior derivatization of sulfhydryl groups, these methods are limited to free thiol-containing compounds, thus preventing the concomitant analysis of both the reduced and oxidized glutathione, as well as compounds bearing a blocked thiol function such as methionine or cystathionine.

These drawbacks can be overcome by the use of LC coupled to electrochemical (Lakritz *et al.*, 1997) or mass spectrometric detection. Although gas chromatography–electron impact-mass spectrometry (GC–EI-MS) allows sensitive detection of sulfur metabolites such as cysteine, homocysteine, methionine, and cystathionine (Stabler *et al.*, 1987; White, 2003), this technique requires chemical derivatization procedures in order to enhance the volatility of compounds. Lastly, by using electrospray–tandem mass spectrometric (LC/MS–MS) detection, it is possible to detect both reduced and oxidized sulfur metabolites without any prior derivatization step, as reported for glutathione and glutathione disulfide in various biological extracts (Gucek *et al.*, 2002).

Electrospray MS-based techniques are of special interest because of their ability to cover different analytical needs such as qualitative or quantitative determination, structural characterization, and also metabolite profiling or targeted analysis of a few to many metabolites. This is mainly due to the sensitivity, specificity, and versatility of the different types of analyzers that are commercially available. Each of these analyzers has its own appropriate field of application. Triple quadrupole mass spectrometers operated in the selected reaction monitoring (SRM) MS^2-scanning mode are considered as reference instruments for quantification experiments, whereas ion traps, allowing rapid scanning over a large m/z ratio range and sequential MS^n experiments are well suited for metabolic profiling and structural elucidation. This is also the case for TOF and hybrid Q-TOF analyzers, thanks to their high acquisition rates and the possibility to perform accurate mass measurements (i.e., the capacity of a mass spectrometer to separate ions of adjacent but different m/z ratios).

Fourier transform-mass spectrometry (FT-MS) instruments, such as the Fourier Transform Ion Cyclotron and the recently released LTQ-Orbitrap mass spectrometers, provide accurate mass measurements with ppm and

even sub-ppm errors, high and ultrahigh resolving power, and MS^n capabilities. This is of special interest for global metabolite detection. Accurate mass measurements together with ultrahigh resolving power enable discrimination between isobaric ions and also indicate their elemental composition, which is useful for identification purposes.

The LTQ-Orbitrap® is a new type of hybrid mass spectrometer which consists of a linear ion trap coupled to an Orbitrap analyzer (Hardman and Makarov, 2003; Makarov, 2000). The linear ion trap is able to record its own full-scan mass spectra and sequential MS^n activation spectra from low-resolution precursor ion selection (mass window ≥ 0.3 u). Ions transitorily accumulated in the C-trap are injected into the Orbitrap analyzer (Hu *et al.*, 2005; Makarov *et al.*, 2006). Orbitrap devices achieve accurate mass measurements with errors below 3 ppm and resolving powers up to 100,000 ($m/\Delta m$ at m/z 1000, full width at half maximum).

We started to work on sulfur metabolites by developing an LC/ESI-MS/MS method based on hydrophilic interaction LC coupled to an ESI-triple quadrupole mass spectrometer operating in the SRM mode. When combined with uniform ^{15}N-metabolic labeling, this enabled absolute quantification of eight metabolites involved in the glutathione biosynthesis pathway (i.e., cysteine, homocysteine, methionine, γ-glutamyl-cysteine, cystathionine, reduced and oxidized forms of glutathione, and *S*-adenosylhomocysteine) (Lafaye *et al.*, 2005b). An alternative approach was then developed by directly introducing biological samples into the LTQ-Orbitrap mass spectrometer, allowing both targeted (i.e., focusing on few metabolites) and global metabolomics (i.e., coupling mass spectrometric detection with statistical and chemometric tools) approaches. Here, detection and further quantification are achieved in accurate mass measurements of ions contained in the mass spectra. When applied to the study of cadmium toxicity in the yeast *S. cerevisiae*, the latter method gave quantitative results similar to those of the initial LC/ESI-MS/MS (Madalinski *et al.*, 2008).

We report here on different MS-based methods for the detection and quantification of sulfur metabolites and also other metabolites closely connected to the glutathione biosynthesis pathway. All the procedures and analytical methods have been developed for the analysis of yeast cell extracts. However, their application to other cell types is possible. This will be discussed throughout this chapter.

3. Procedures

3.1. Cell growth and ^{15}N metabolic labeling

3.1.1. General considerations

Several issues have to be addressed for the quantification of metabolites in biological media. First, ion suppression effects caused by biological matrices have deleterious effects on the limits of quantification and on the precision

of analytical methods. Furthermore, the natural presence of metabolites in biological extracts complicates the construction of standard calibration curves. Lastly, because matrix effects are compound dependent, quantification requires an internal standard for each metabolite of interest. All these issues are addressed by developing a standardization procedure based on ^{15}N metabolic labeling of the yeast *S. cerevisiae* (Lafaye *et al.*, 2005b). Absolute quantification is achieved by mixing an aliquot of a labeled reference extract with the unlabeled biological sample before the LC/MS/MS analysis.

In principle, the ideal labeling of the reference extract would be with the stable isotope ^{34}S. This isotope is commercially available in its sulfate form enriched at 90%. It is more expensive than ^{15}N sources but the amount of sulfate required for growth (e.g., around 0.1 m*M* for microorganisms) is lower than that of nitrogen (around 3 m*M* for microorganisms). Using ^{34}S labeling, only sulfur compounds can be analyzed. However, in large-scale analyses, ^{15}N labeling is preferable, since a large number of metabolites contain at least one nitrogen atom. ^{15}N labeling is also relevant to the analysis of sulfur metabolites as most of them contain at least one nitrogen atom.

The ^{15}N-metabolite extract is prepared by *in vivo* labeling with an inorganic source of ^{15}N and extraction of the pool of labeled metabolites. [^{15}N]-ammonium, [^{15}N]-nitrate, and [^{15}N]-nitrite are commercially available. The cells used in the preparation of the reference extract must be grown in a minimum medium, deprived of ^{14}N-labeled compounds, but replaced by their corresponding ^{15}N-labeled forms in appropriate amounts. In order to obtain uniform labeling, cells must first be grown for at least 5–10 generations with [^{15}N]-nitrogen as the sole source of nitrogen. Depending on the cell type, it can be useful to freeze aliquots of this ^{15}N preculture. This precaution will avoid restarting the ^{15}N preculture and enrichment step if the ^{15}N labeling has to be repeated.

This approach is well adapted to bacteria (Sailer *et al.*, 1993), yeasts (Lafaye *et al.*, 2005b), algae, and plants (Engelsberger *et al.*, 2006). It can also be envisaged for organisms capable of consuming labeled microorganisms or plants, although in this case the time necessary to obtain efficient labeling may be long. For example, efficient ^{15}N metabolic labeling of rats has been successfully obtained by feeding the rats with a diet enriched in ^{15}N-labeled algae (Wu *et al.*, 2004a). Alternative to ^{15}N labeling, ^{13}C labeling can also be used if the analysis includes metabolites devoid of nitrogen (Birkemeyer *et al.*, 2005), but this type of labeling may be very expensive.

3.1.2. ^{15}N labeling of yeast

The *S. cerevisiae* strain S288c was grown in a minimum medium corresponding to YNB (yeast nitrogen base) medium minus ammonium sulfate (Difco). [^{15}N]-$(NH_4)_2SO_4$ was added to the medium at a final

concentration of 5 m*M*. In order to save ^{15}N, the concentration of [^{15}N]-$(NH_4)_2SO_4$ can be decreased to 3 m*M* without any growth problem.

Strain S288c is autotrophic for each amino acid and is therefore appropriate to obtain complete uniform labeling. An S288c strain colony grown on ^{14}N medium was inoculated and grown for at least seven generations in 50 mL of the ^{15}N medium. Such a ^{15}N preculture can be used to inoculate a large culture of approximately 1 L. It is important to prepare a large amount of ^{15}N metabolite extract to increase the number of analyses that can be performed with the ^{15}N reference extract (a given reference extract can be utilized several hundred times).

The culture was then treated with 50 μM cadmium for 3–4 h. This treatment has been shown to increase the pool of sulfur metabolites, leading to an elevated concentration of these ^{15}N sulfur metabolites in the reference extract (Lafaye *et al.*, 2005a,b). In this way, the volume of the culture can be limited to 1 L. If large volumes of culture can be processed, the cadmium treatment is not necessary. The ^{15}N-labeled metabolites were extracted as described below.

3.1.3. Culture conditions

For absolute quantification, the ^{15}N reference extract and the extracts to be analyzed must be prepared by the same methods and from similar cell types and culture media. In such conditions, the ''matrix effects'' can be considered to be the same in both ^{15}N and ^{14}N extracts. We used this method for metabolite quantification in *S. cerevisiae* extracts grown in different conditions (standard, H_2O_2, supplementation of different sulfur metabolites, treatment with cadmium (Lafaye *et al.*, 2005a), arsenite (Thorsen *et al.*, 2007), chromate (Pereira *et al.*, 2008), sulfur starvation, nitrogen starvation (not shown) or *S. cerevisiae* extracts from mutant strains. For each condition tested, a 25-mL culture was grown to a cellular concentration of 2–3 $\times$ 10^7 cells/mL in YNB minimum medium (with [^{14}N]-$(NH_4)_2SO_4$ as source of nitrogen). From this culture, at least 4 $\times$ 10^8 cells were collected for metabolite extraction (see below).

For relative quantification, the ^{15}N reference extract prepared from a given species (e.g., *S. cerevisiae*) can be used as an internal standard for extracts prepared from other organisms (e.g., bacteria or other yeast species or plants). In this case, the growth medium and the extraction method can be different from the ones used for the preparation of the ^{15}N reference extract.

3.2. Metabolite extraction

Metabolite extraction is highly dependent on cell type (i.e., mammalian cells, prokaryotic or eukaryotic cells) and also on the chemical structures of the metabolites to be detected. In some circumstances, metabolites are highly

unstable in biological media, requiring a quenching procedure in order to stop their enzymatic degradation. This is usually achieved by using cold water–organic mixtures during the collection step (Sellick *et al.*, 2009; Spura *et al.*, 2009), the leakage of intracellular metabolites being the major issue. Extraction procedures are performed by using cold organic solvents such as methanol, ethanol, or chloroform, or boiling ethanol or water (Canelas *et al.*, 2009; Villas-Boas *et al.*, 2005; Winder *et al.*, 2008). Metabolite extraction is especially a matter of concern for bacterial, fungal, and plant cells, due to the particular properties of their cell membranes, and readers are advised to refer to published extraction protocols, which should be as closely applicable as possible to the kind of cell studied and the field of application.

Typical extraction procedures for thiol-containing compounds are performed in 0.1 N hydrochloric acid (Gucek *et al.*, 2002; Noctor and Foyer, 1998), 200 m*M* phosphoric acid (Lenton *et al.*, 1999), or 10% perchloric acid (PCA) (Hammermeister *et al.*, 2000). Strong acid solvents are used to precipitate proteins and to preserve the redox state of thiol compounds. However, the use of such acid solutions may be prevented by the need to obtain a pH compatible with chromatographic column specifications. Furthermore, high concentrations of inorganic acids are not suitable for electrospray MS. As a consequence, we decided to use boiling water for protein precipitation. The pH of the extraction medium was optimized to obtain final pH values ranging from 2 to 3 in the cell extracts. For yeast cell extracts corresponding to 10^9 cells/mL, the use of 0.1% PCA (pH 2) appeared to be the best compromise between metabolite stability and LC/MS detection (Lafaye *et al.*, 2005b).

The protocol selected for yeast cell metabolite extraction was as follows. Cells were collected (typically $n = 10^9$) by centrifugation (4000 rpm at 4 °C), washed with cold water, boiled for 5 min in 0.1% PCA (pH 2), and centrifuged for 2 min at 4000 rpm. The supernatant containing the metabolites was collected and stored at −80 °C until further analysis.

4. Absolute LC–ESI-MS/MS Quantification of Thiol and Amino Acid Metabolites in Yeast Extracts

4.1. Sample preparation

Two kinds of samples have to be analyzed in the course of a typical experiment: biological samples and standard samples used for the calibration curve.

4.1.1. Biological samples

Aliquots of unlabeled and ^{15}N-labeled yeast extracts are mixed together (1/1, v/v) and 20 μL of the resulting sample (5×10^7 cells/mL) is injected into the chromatographic system. Working at high cell concentrations is

expected to improve the detection of analytes. Actually, decreased sensitivity is observed in these conditions because matrix-based ion suppression effects lead to an alteration of the ionization recoveries of analytes (Gangl *et al.*, 2001; Matuszewski *et al.*, 1998). It is thus recommended to carefully optimize the number of cells injected into the LC/MS system. This can be achieved by measuring the repeatability of the analytical method as a function of the number of injected cells (Lafaye *et al.*, 2005b). Matrix effects can also be evaluated by spiking selected metabolites in extracts from uniformly metabolically labeled cells and by comparing the resulting peak intensities observed for different cell concentrations with those obtained in pure solvent (Madalinski *et al.*, 2008).

For our application, a cell concentration of 5×10^7 cells/mL was found to provide suitable signal intensities for the metabolites of interest with limited clogging of the electrospray source.

4.1.2. Standard samples

Alanine, arginine, asparagine, aspartate, arginine, cysteine, glutamine, glutamate, glycine, histidine, isoleucine, leucine, methionine, phenylalanine, proline, serine, threonine, tyrosine, tryptophan, valine, γ-glutamyl-cysteine, reduced glutathione (GSH), oxidized glutathione (GSSG), *S*-adenosylhomocysteine, and cadmium were from Sigma-Aldrich (Saint Quentin Fallavier, France). *O*-acetylhomoserine was synthesized as previously described (Nagai and Falvain, 1971).

Our procedure for plotting standard calibration curves is as follows:

- Preparation of individual stock solutions at 1 mg/mL in 0.01 N HCl and at 2 mg/mL for cysteine and γ-glutamyl-cysteine.
- The stock solutions are mixed as indicated in Table 2.1 to obtain the first calibration point. Each metabolite concentration is adapted to the levels expected in cell extracts from preliminary experiments. Twelve calibration points are then obtained by further twofold serial dilutions.
- Each calibration point (20 μL) is mixed with 20 μL of the ^{15}N reference extract. The cell concentration of the latter (i.e., 10^8 cells/mL) is twice the number of cells used for sample preparation in order to keep the total cell concentration constant between samples and standard samples.

4.2. Liquid chromatography

Several approaches are available for the analysis of polar metabolites without derivatization, relying on ion exchange, hydrophilic interaction liquid chromatography (HILIC), and ion-pair chromatography. Ion exchange chromatography involves nonvolatile solvents with strong ionic strength requiring a desalting interface for further electrospray MS detection. Good chromatographic retention is obtained by using HILIC (Bajad *et al.*, 2006;

Table 2.1 Preparation of the first calibration point

Metabolite	Concentration in the first calibration point (μg/mL)
Alanine	100
Arginine	15
Asparagine	50
Aspartate	50
Cysteine	50
Glutamine	15
Glutamate	50
Glycine	100
Histidine	5
Isoleucine	15
Leucine	15
Lysine	15
Methionine	25
Phenylalanine	5
Proline	5
Serine	25
Threonine	25
Tryptophan	5
Tyrosine	5
Valine	15
Cystathionine	25
γ-Glutamyl-cysteine	50
Glutathione (reduced form)	25
Glutathione (oxidized form)	25
Homoserine + Threonine	15
Cystine	25
o-Acetylhomoserine	25
Methylthioadenosine	5
Transproline	15
S-adenosylhomocysteine	15
Homocysteine	25

Kiefer *et al.*, 2008; Lafaye *et al.*, 2005b; Strege *et al.*, 2000; Tolstikov and Fiehn, 2002). Bajad *et al.* have developed an HILIC–ESI-MS/MS-based method for the analysis of 141 metabolites and reported the quantification of 69 of them in *Escherichia coli* cell extracts. However, this method was not selective enough for the discrimination between isomers such as leucine and isoleucine.

The chromatographic retention and separation of the metabolites of interest may be improved by using ion pair-reverse phase chromatography. In this case, a hydrophobic counter ion is introduced in the mobile phase to form an ion pair with the analytes. Typical ion-pairing reagents are amines (Coulier *et al.*, 2006) and hydrophobic organic acids (Chaimbault *et al.*, 1999) for the analysis of acids and bases, respectively. The resulting ion pairs are neutral, hydrophobic, and well retained on reverse phase columns. The two main drawbacks of this approach are the limited volatility of the ion pair and/or the too strong affinity between the ion-pairing reagent and the analyte. This prevents the dissociation of the ion pair in the electrospray source and induces signal suppression effects (Apffel *et al.*, 1995). Perfluorinated carboxylic acids have been reported to provide optimal results for the analysis of basic metabolites (Chaimbault *et al.*, 1999; Gu *et al.*, 2007). Among the different kinds of perfluorinated acids, pentadecafluorooctanoic acid (PDFOA) provided optimal chromatographic retention and selectivities.

An HP1100 series LC system (Agilent Technologies, Massy, France) is used for sample introduction and separation. The chromatographic separation is performed on a BioSuite C_{18} column (2.1 × 150 mm, 3 μm) from Waters (Saint Quentin en Yvelines, France) equipped with an online prefilter (Interchim, Montluçon, France). The mobile phases are either (A) water containing PDFOA 5 m*M* or (B) acetonitrile. PDFOA and acetonitrile were from Sigma-Aldrich (Saint Quentin Fallavier, France). Water was deionized and filtered through a Millipore Milli-Q water purification system. Warning: PDFOA is a corrosive agent and precaution such as the use of gloves and goggles should be taken to avoid skin contact.

Gradient conditions were as follows: 0% B from 0 to 5 min, 0–100% B from 5 to 40 min, 100% B from 40 to 50 min, and 100% A from 50.1 to 60 min, at a flow rate of 300 μL/min. The temperature of the column is set at 30 °C, and the samples are stored at 4 °C in the autosampler. For optimal retention time stability, the column should be equilibrated overnight before analysis with 50% A at a low flow rate (e.g., 50 μL/min) and PDFOA should be added to the samples to be injected in order to improve the formation of the ion pair. Interfering peaks generated by PDFOA may be observed in chromatograms, limiting the detection of low levels of metabolites such as arginine, histidine, and lysine. If such artifacts are observed in blank samples, the experiment should be repeated with a new PDFOA batch. Typical retention times obtained with our chromatographic system are shown in Table 2.2.

4.3. Mass spectrometry

Electrospray mass spectrometric detection is performed by using a triple quadrupole instrument, the Quantum Ultra from ThermoFisher Scientifics (Courtaboeuf, France) operated in the positive ion mode. Capillary voltage is set at 4 kV and capillary temperature at 270 °C. The sheath gas pressure and

Table 2.2 Metabolite retention time and CID parameters

Metabolites	Retention time (min)	^{14}N metabolites		^{15}N metabolites		Elab (eV)
		$[MH]^+$	Transition pairs	$[MH]^+$	Transition pairs	
Alanine	2.8	90	90 → 55	91	91 → 55	20
Arginine	25.2	175	175 → 158	179	179 → 161	15
Asparagine	2.4	133	133 → 87	135	135 → 89	15
Aspartate	4.0	134	134 → 88	135	135 → 89	15
Cystathionine	6.8	223	223 → 134	225	225 → 135	17
Cysteine	2.7	122	122 → 105	123	123 → 105	15
Cystine	3.5	241	241 → 152	243	243 → 153	19
Glutamate	4.2	148	148 → 102	149	149 → 103	15
Glutamine	2.6	147	147 → 130	149	149 → 131	15
γ-Glu-Cys	8.1	251	251 → 122	253	253 → 123	17
Glycine	2.4	76	76 → 59	77	77 → 59	25
Glutathione (reduced form)	10.1	308	308 → 179	311	311 → 181	17
GSSG (oxidized form)	22.4	613	613 → 355	619	619 → 359	23
Histidine	24.2	156	156 → 110	159	159 → 113	17
Homocysteine	4.3	136	136 → 90	137	137 → 91	15
Homoserine + Threonine	2.7	120	120 → 74	121	121 → 75	15
Isoleucine	18.9	132	132 → 86	133	133 → 87	13
Leucine	20.6	132	132 → 86	133	133 → 87	13
Lysine	25.0	147	147 → 130	149	149 → 131	15
Methionine	11.7	150	150 → 133	151	151 → 105	16
methylthio-5′ adenosine	22.6	298	298 → 136	303	303 → 141	17
o-Acetylhomoserine	6.4	162	162 → 102	163	163 → 103	15
Phenylalanine	21.9	166	166 → 120	167	167 → 121	13
Proline	3.5	116	116 → 70	117	117 → 71	17
S-adenosylhomocysteine	25.1	385	385 → 136	391	391 → 141	18
Serine	2.4	106	106 → 60	107	107 → 61	15
Threonine	2.7	120	120 → 102	121	121 → 103	15
trans-Proline	2.4	132	132 → 68	133	133 → 69	15
Tryptophan	24.3	205	205 → 188	207	207 → 189	12
Tyrosine	14.8	182	182 → 136	183	183 → 137	15
Valine	11.6	118	118 → 72	119	119 → 73	12

the auxiliary gas pressure (both nitrogen) are set at 50 and 10 (arbitrary units). The mass resolution was fixed at 0.7 Th (as full width at half-maximum (FWHM) height, for a single charged ion) for both the first and third quadrupole mass analyzers. The collision gas (argon) pressure in the second quadrupole (RF only) is set at 1.5 mTorr. The dwell time and interchannel delay are fixed at 0.1 and 0.01 s, respectively. Cone voltage values, which have been optimized for each metabolite, are in the ranges from 20 to 30 V.

Metabolites are detected in the positive ionization mode using the SRM scanning mode. Collision energy values in the RF only quadrupole and transition pairs have to be optimized for each metabolite on reference compounds. The transition pairs of ^{15}N metabolites are calculated by taking into account the number of nitrogen atoms that are contained in both parent and product ions. Each product ion has to be carefully selected in order to avoid the occurrence of interference in the mass spectrometric detection (i.e., two transition pairs detected at the same retention time and having the same product ion). This is of special importance for this method because m/z values of ^{15}N-labeled and unlabeled metabolites may differ by only one or two units. This point is addressed in the following validation study. The SRM parameters (transition pairs and collision energies) for the 31 metabolites are shown in Table 2.2.

Furthermore, as many transition pairs have to be monitored by the mass spectrometer, it is necessary to optimize the detection parameters in order to achieve suitable chromatographic performances (i.e., more than 10 scans per chromatographic peak). To this end, the scan time has been set at 0.03 s and the SRM detection is performed according to two time segments, the first one corresponding to the first 8.5 min and the second the remaining part of the acquisition. Each time segment includes half of the transition pairs.

A typical LC/ESI-MS/MS chromatogram is shown in Fig. 2.2. By using a reverse phase column and PDFOA as ion-pairing reagent, most metabolites were retained and separated. Two distinct segments can be observed from Fig. 2.2: the first one contains peaks eluted from 2.5 to 5 min and corresponds to hydrophilic acid compounds, whereas the second corresponds to hydrophobic and basic compounds eluted from 5 to 30 min. This chromatographic method is able to discriminate between isomers such as leucine and isoleucine, but was unable to separate hydrophilic isomers like threonine and homoserine. Threonine was quantified by using a specific SRM transition corresponding to a loss of water, whereas no specific reaction was found for homoserine. As a consequence, the couple (homoserine + threonine) was quantified instead of homoserine alone.

4.4. Data processing

The areas of the signal corresponding to each SRM transition pair are obtained from the Quanbrowser® version 2.0 SR2 (Thermo-Fisher, Les Ulis, France), a software developed for quantification applications. Results

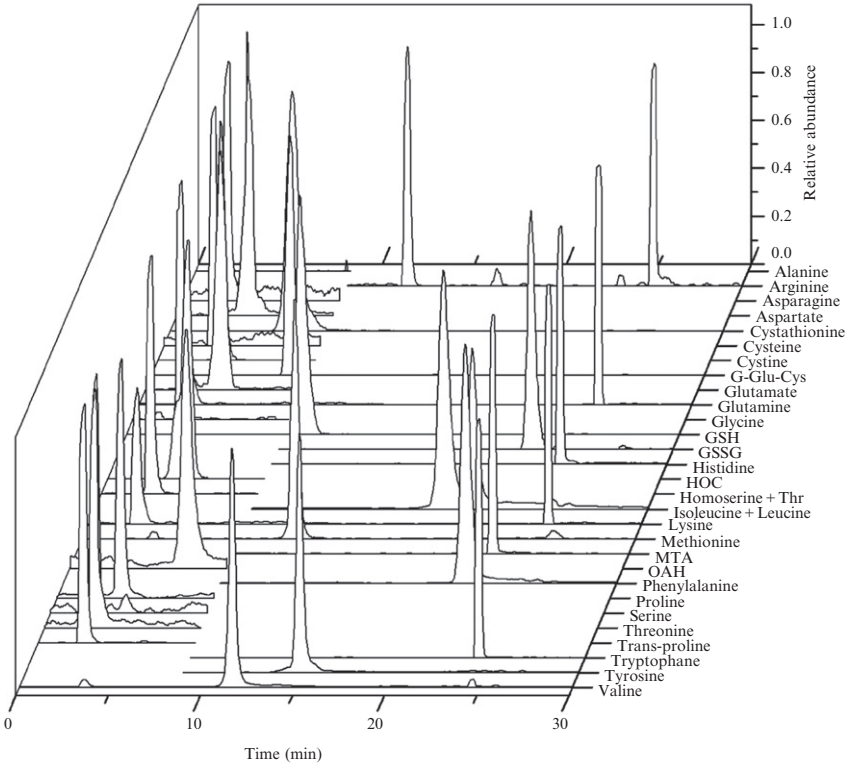

Figure 2.2 *LC/ESI-MS/MS chromatogram of a yeast cell extract (5.10^7 cells/mL).* **The chromatographic separation is performed on a BioSuite C_{18} column (2.1 × 150 mm, 3 μm) from Waters (Saint Quentin en Yvelines, France) equipped with an online prefilter (Interchim, Montluçon, France) and 20 μL of the extract are injected into the chromatographic system. The mobile phases are either A: water containing 5 m*M* pentadecafluorooctanoic acid (PDFOA) and B: acetonitrile. PDFOA and acetonitrile were from Sigma-Aldrich (Saint Quentin Fallavier, France). Gradient conditions were as follows: 0% B from 0 to 5 min, 0–100% B from 5 to 40 min, 100% B from 40 to 50 min, and 100% A from 50.1 to 60 min, at a flow rate of 300 μL/min.**

can be expressed as $^{14}N/^{15}N$ ratios for accurate quantification or as molarity units by using standard calibration curves for absolute quantification. Absolute concentrations in biological samples are obtained by comparing the $^{14}N/^{15}N$ ratios obtained for the samples with those of the calibration curves. Typical standard calibration curves, together with their equation and regression coefficients, are shown in Fig. 2.3.

Intracellular concentrations of metabolites are obtained as follows:

(i) The concentration (C) of a given metabolite expressed as ng/mL is obtained from its related calibration curve: $C = a \times R + b$, where R

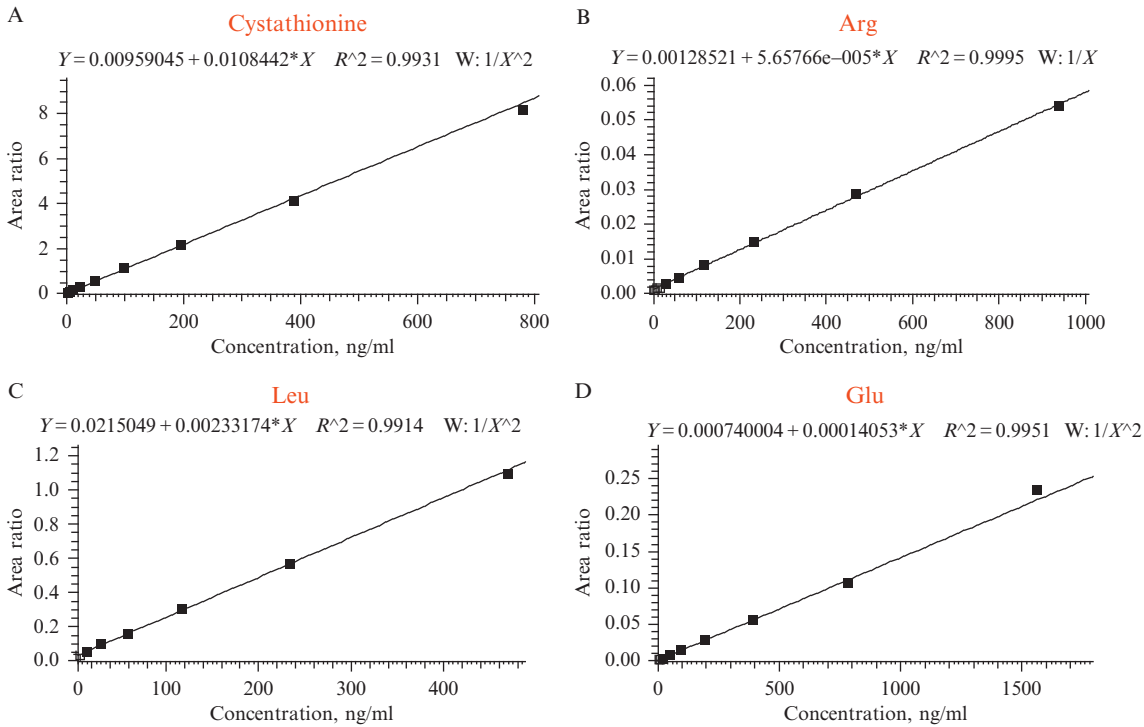

Figure 2.3 *Standard calibration curves obtained for four representative metabolites: cystathionine, arginine (Arg), leucine (Leu), and glutamate (Glu).* The reference yeast extract from cells grown on [^{15}N]-ammonium sulfate and treated by cadmium was spiked with increasing concentrations of a mixture containing reference ^{14}N metabolites.

corresponds to the $^{14}N/^{15}N$ ratio corresponding to a metabolite in a given biological sample.

(ii) Determine the injected quantity and then the quantity of metabolite present in 1 mL of solution.

(iii) The intracellular concentration expressed in mol/L is finally obtained by calculating the volume corresponding to the cell concentration of the sample. Assuming that yeast cells are spherical, the intracellular volume of 10^7 cells was calculated to be 4.5×10^{-7} L.

Typical concentrations of extracts from yeast cells cultured on minimal medium are shown in Table 2.3. Values are highly dependent on strains and culture conditions. Literature data were added for comparison.

4.5. Method validation

Bioanalytical method validation includes all the procedures required to demonstrate that a particular method for the quantitative determination of the concentration of an analyte in a given biological matrix is reliable for its intended application (Shah *et al.*, 2000). In this section, a methodology is proposed to validate analytical methods for quantitative metabolite profiling. It focuses on the evaluation of selectivity, stability, precision of the measurements, linearity, and determination of the limits of quantification.

4.5.1. Selectivity

Selectivity is challenging for analytical methods based on metabolic ^{15}N labeling of organisms because the natural occurrence of stable isotopes such as ^{13}C (1.09%), ^{15}N (0.40%), ^{18}O (0.20%), ^{33}S (0.76%), and ^{34}S (4.22%) in unlabeled metabolites could produce a significant signal at [M + 1] or [M + 2], which may interfere with the selective detection of ^{15}N-labeled metabolites containing only one or two nitrogen atoms. It must then be demonstrated that both ^{14}N and ^{15}N metabolites can be selectively detected when they are present in the same extract.

To evaluate the selectivity of the method, yeast cell extracts grown on a ^{14}N-containing culture medium were analyzed to evaluate the interfering presence of signals that could be attributed to ^{15}N metabolite. As expected, no interference was found for metabolites containing two and three nitrogen atoms. Conversely, interfering signals were observed for metabolites containing a single nitrogen atom and corresponding to the contribution of stable isotopes occurring in these molecules. Intensities of these signals were below 10% of the intensities of the related ^{14}N signals. This was the case for the signals corresponding to (Homoser + Thr): 5.7%, OAH: 5.1%, Tyr: 9.5%, Ile: 6.7%, Leu: 6%, and Phe: 9.4%. No interfering signals were observed for cysteine, cystine, and HOC because of their naturally low

Table 2.3 Intracellular concentrations of metabolites obtained from yeast cell extracts

Metabolites	Intracellular concentrations (m*M*)[a]	Data from Messenguy *et al.* (m*M*)[b]	Data from Kitamoto *et al.* (m*M*)[c]
Arginine	20.7	16.2	15.5
Aspartate	9.6	11.7	3.8
Glutamate	22.0	42.7	NA
Histidine	2.7	3.1	8.6
Isoleucine	0.3	1.2	2.1
Leucine	0.3	0.8	1.4
Lysine	4.2	10.1	10.4
Phenylalanine	0.2	0.6	0.3
Proline	1.1	NA	0.7
Serine	1.8	5.7	3.5
Threonine	2.0	5.2	NA
Tyrosine	0.09	0.5	1.4
Valine	0.8	5.5	5.5
Alanine	2.8		
Asparagine	1.0		
Glutamine	34.4		
Glycine	<1		
Homoserine + Threonine	2.3		
Tryptophan	0.2		
Homocysteine	<0.04		
Cystathionine	0.05		
Cysteine	<0.4		
γ-Glutamyl-cysteine	0.1		
Glutathione (reduced form)	1.3		
Glutathione (oxidized form)	0.1		
Methionine	0.1		
S-adenosylhomocysteine	0.03		
o-acetylhomoserine	2.9		
Methylthio-5′-adenosine	0.005		
Cystine	<0.02		

[a] These values were obtained from cell extracts of the yeast *S. cerevisiae* (see the protocol Section 3.1.3).
[b] Yeast cells (*S. cerevisiae*, stain S288c) were grown in a minimum medium containing 0.01 *M* $(NH_4)_2SO_4$ as nitrogen source, 3% glucose, vitamins, and mineral traces (Messenguy *et al.*, 1980).
[c] Yeast cells (*S. cerevisiae*, stain X2180-1A) were grown in YNBD medium (Kitamoto *et al.*, 1988).

levels in cell extracts. The symmetric analysis was performed on ^{15}N metabolically labeled yeast extracts and no signal corresponding to the MRM transition pairs of ^{14}N metabolites was detected in this extract.

In conclusion, these results demonstrate that ^{14}N and ^{15}N metabolites can be monitored without significant interference for further absolute quantification studies. They also confirm a high efficiency of ^{15}N labeling, close to 100% for all metabolites analyzed. Note that a ^{15}N-labeling efficiency of 95% may be sufficient.

4.5.2. Linearity of the calibration curves and limits of quantification

For absolute quantification purposes, standard calibration curves should be constructed in biological media and should have a minimum of five standard points, excluding blanks, and should cover the entire range of expected concentrations of the biological samples (Shah *et al.*, 2000). As shown in Table 2.4, each metabolite is normalized by its ^{15}N-related signal, except for alanine, cysteine, glycine, homocysteine, methionine, and transproline because their ^{15}N-related signals were not abundant enough to be taken into account. For these metabolites, a ^{15}N signal of similar structure and retention time was selected. The linearity of the calibration curves was optimized by selecting the most appropriate weighting indexes that give the best fit and minimize the relative errors in back-calculated values (i.e., the concentrations of the calibration points calculated with the equation of the calibration curve). All regression coefficients were in the range from 0.985 to 0.999.

The limit of quantification (LOQ) refers to the lowest concentration of the standard curve which can be measured with acceptable accuracy and precision (coefficients of variation, CV, below 20%) (Shah *et al.*, 2000). The accuracy of an analytical procedure expresses the closeness of agreement between a reference value and the value found, whereas precision, which is evaluated by calculating CVs, expresses the closeness of agreement between a series of measurements obtained from multiple sampling of the same homogeneous sample under the prescribed conditions.

Accuracy and precision are evaluated at each concentration level by using the back-calculated values obtained from five independent calibration curves. Back-calculated values should not deviate by more than $\pm 15\%$ from their theoretical values, and the CV should be below 15%. The lower and the upper limits of quantification (LLOQ and ULOQ, respectively) correspond to lowest and the highest calibration levels whose values do not deviate by more than 20 and 15% from their theoretical values, with CVs below 20 and 15%, respectively.

The LLOQ and ULOQ values for each metabolite are listed in Table 2.4. Of the 30 metabolites investigated, 18 had LLOQ values below 10 ng/mL and 9 of them between 10 and 50 ng/mL, whereas LLOQ values of cysteine and both alanine and glycine were 98 ng/mL and 195 ng/mL, respectively. Finally, the difference between LLOQ and ULOQ indicates the concentration range

Table 2.4 Linearity of the calibration curves and limits of quantification

Metabolites	Internal standard[a]	Weighting[b]	Retention time (min)	LLOQ[c] (ng/mL)	ULOQ[d] (ng/mL)
Alanine	^{15}N-Homo + Thr	$1/X^2$	2.8	195	3125
Arginine	^{15}N-Arg	$1/X$	25.2	29	1875
Asparagine	^{15}N-Asn	$1/X$	2.4	49	3125
Aspartate	^{15}N-Asp	$1/X^2$	4.0	49	6250
Cysteine	^{15}N-Homo + Thr	$1/X^2$	2.7	98	6250
Cystathionine	^{15}N-Cystathionine	$1/X^2$	6.8	3	3125
Cystine	^{15}N-Cystathionine	$1/X^2$	3.5	12	391
Glutathione (reduced form)	^{15}N-GSH	$1/X^2$	10.1	3	3125
GSSS (oxidized form)	^{15}N-Cystathionine	$1/X^2$	22.4	3	3125
γ-Glutamyl-cysteine	^{15}N-G-Glu-Cys	$1/X^2$	8.1	6	1563
Glutamine	^{15}N-Gln	$1/X^2$	2.6	2	1875
Glutamate	^{15}N-Glu	$1/X^2$	4.2	24	6250
Glycine	^{15}N-Homo + Thr	$1/X$	2.4	195	6250
Homocysteine	^{15}N-Homo + Thr	$1/X^2$	4.3	12	1563
Homoserine + Threonine	^{15}N-Homo + Thr	$1/X^2$	2.7	3	781
Histidine	^{15}N-His	$1/X$	24.2	10	625
Isoleucine	^{15}N-Ile	$1/X^2$	18.9	7	468
Leucine	^{15}N-Leu	$1/X^2$	20.6	15	937
Lysine	^{15}N-Lys	$1/X$	25.0	7	1875
Methionine	^{15}N-Cystathionine	$1/X^2$	11.7	12	781
Methylthioadenosine	^{15}N-MTA	$1/X^2$	22.6	1	625
o-acetylhomoserine	^{15}N-OAH	$1/X^2$	6.4	12	3125
Phenylalanine	^{15}N-Phe	$1/X^2$	21.9	5	625
Proline	^{15}N-Pro	$1/X^2$	3.5	5	313

S-adenosylhomocysteine	^{15}N-SAH	$1/X^2$	25.1	4	1875
Serine	^{15}N-Ser	$1/X^2$	2.4	6	1562
Threonine	^{15}N-Thr	$1/X^2$	2.7	12	3125
Transproline	^{15}N-Pro	$1/X^2$	2.4	2	59
Tryptophan	^{15}N-Trp	$1/X$	24.3	2	625
Tyrosine	^{15}N-Tyr	$1/X$	14.8	10	625
Valine	^{15}N-Val	$1/X^2$	11.6	4	1875

[a] Signals related to ^{14}N metabolites are normalized by their related ^{15}N signals, except when the latter are not abundant enough. In such a situation, another ^{15}N metabolite of chemical structure and chromatographic retention time similar to those of the ^{14}N metabolite to be quantified is then selected.

[b] The standard curve is linear and the selected weighting index minimizes the relative error in the back-calculated values.

[c] Lower limit of quantification (LLOQ) refers to as the lowest concentration value exhibiting acceptable accuracy (relative error below 20% in five-independent calibrations) and precision parameters (CV below 20% in five-independent calibration curves).

[d] Upper limit of quantification(ULOQ) refers to as the highest concentration value exhibiting acceptable accuracy (relative error below 15% in five-independent calibration curves) and precision (CV below 15% in five-independent calibration curves).

over which metabolites can be quantified in biological extracts. Large concentration ranges (i.e., from ng/mL to μg/mL) are enabled for sulfur metabolites such as GSH, GSSG, cystathionine, homocysteine, γ-Glu-Cys, MTA, and SAH, whereas they are of two orders of magnitude for most other metabolites.

4.5.3. Precision

Although precision studies are usually performed by calculating CVs for multiple injections of quality control (QC) samples (Shah *et al.*, 2000), it appears more convenient for us to evaluate precision on biological samples. Two levels of precision are considered: repeatability (i.e., intra-assay precision) and intermediate precision (i.e., inter-assay precision). Repeatability expresses the precision under the same operating conditions over a short time interval. It is typically assessed using five consecutive injections of the same sample. The study of intermediate precision evaluates the impact of factors like the day, the analyst, and the equipment on the performance of the method.

A typical example of a precision study is shown in Table 2.5: repeatability and intermediate precision of the analytical method were evaluated for cell extracts from yeast exposed or not to 50 μM $CdCl_2$. Intra-assay precision was determined by calculating CVs for six consecutive injections of the same samples. Intermediate precision was evaluated for both the day and the overall procedure of sample preparation effects. Interday precision was obtained by injecting the same two samples (i.e., one control and one Cd-exposed cell extract) on 6 different days, whereas the impact of sample preparation was investigated by performing five independent extractions of the two cultures corresponding to control and cadmium conditions. Except for *S*-adenosylhomocysteine, intra- and intermediate precision CVs were below 15%, indicating that the overall procedure is reliable.

4.5.4. Stability

Cell extracts were stored at −80 °C and maintained at 4 °C in the autosampler of the chromatographic system. The stability in experimental conditions is assessed by analyzing a QC sample corresponding to a calibration point. It is injected at least three times during the experimental process: at the beginning, the middle, and the end of the experiment, and it is checked that both areas of ^{15}N SRM transition pairs and $^{14}N/^{15}N$ ratios of analytes are constant throughout the LC/ESI-MS/MS acquisitions. We found that the metabolites of interest in cell extracts were stable in the experimental conditions for at least 72 h. Otherwise, aliquots of ^{15}N reference extracts are stored at −80 °C and used for a one-year period.

Table 2.5 Precision studies

	Intraday precision		Intermediate precision CV (%)			
	Repeatability CV (%)		Interday precision		Overall extraction process	
Metabolites	Control	Cd	Control	Cd	Control	Cd
Alanine	NA[a]	NA	NA	NA	NA	NA
Arginine	3.64	3.57	3.79	2.79	2.93	4.85
Asparagine	4.55	3.49	9.08	10.27	11.56	8.85
Aspartate	1.63	3.32	4.31	2.53	6.79	2.38
Cysteine	NA	NA	NA	NA	NA	NA
Cystathionine	3.03	2.17	3.58	1.84	12.62	8.91
Cystine	NA	NA	NA	NA	NA	NA
Glutamine	1.64	4.50	2.71	1.16	3.87	4.38
Glutamate	1.06	1.54	2.56	4.49	5.08	5.57
γ-Glutamyl-cysteine	9.73	3.01	7.54	4.50	15.40	7.82
Glycine	NA	NA	NA	NA	NA	NA
Glutathione (reduced form)	1.86	1.71	5.01	3.34	10.98	5.96
GSSS (oxidized form)	4.04	6.60	10.94	9.53	8.65	12.33
Histidine	0.81	0.74	1.97	1.34	5.17	4.06
Homocysteine	NA	NA	NA	NA	NA	NA
Homoserine + Threonine	3.28	1.49	1.23	2.08	6.03	4.30
Isoleucine	2.65	3.07	10.76	5.48	6.96	3.89
Leucine	3.06	3.02	14.70	4.54	4.49	2.15
Lysine	1.65	1.67	5.36	10.72	6.23	1.30
Methionine	4.62	5.55	6.03	12.23	12.40	10.33
Methylthioadenosine	2.37	2.98	9.94	1.84	6.69	5.85
o-Acetylhomoserine	0.89	1.15	1.83	1.91	5.15	4.33
Phenylalanine	2.45	1.82	2.90	2.43	5.54	5.30
Proline	2.11	1.25	1.70	2.04	3.88	3.38
S-adenosylhomocysteine	11.65	11.41	10.30	12.00	32.04	34.38
Serine	5.02	4.20	6.02	7.44	11.94	11.72
Threonine	5.09	7.97	10.01	2.69	9.03	3.26
Transproline	NA	NA	NA	NA	NA	NA
Tryptophan	1.31	2.58	3.04	3.55	6.42	6.03
Tyrosine	3.07	0.71	4.05	1.28	4.77	7.10
Valine	1.77	1.11	3.16	2.83	5.73	3.12

[a] NA: not available (metabolite not detected in these experimental conditions). The precision is expressed as coefficient of variation (CV) and is considered at two levels: repeatability (intra-assay) and intermediate precision (inter-assay precision and precision related to the overall extraction process). The repeatability is determined from six consecutive injections of either a control or cadmium-exposed yeast cell extract. The interday precision obtained by injecting the sample at 6 different days. The precision related to the overall extraction process is determined from five different extractions of the same preculture.

5. Qualitative and Quantitative Determination of Thiol and Amino Acid Metabolites in Yeast Extracts by Using an LTQ-Orbitrap Mass Spectrometer

5.1. Sample preparation

Cell extracts are diluted in 0.1% formic acid to a cell concentration of 1.6×10^8 cells/mL and are then mixed 1:1 (v/v) with ^{15}N-labeled yeast extracts, at the same cell concentration. The resulting sample is directly introduced into the analytical system: direct introduction into an LTQ-Orbitrap mass spectrometer by using flow injection analysis (FIA) or LC coupled with an LTQ-Orbitrap instrument.

5.2. Direct introduction

The analyses are carried out by using FIA at a flow rate of 30 μL/min by using a Surveyor LC system (ThermoFisher Scientifics, Courtaboeuf, France) and 20 μL samples are injected in the system for the acquisition of mass spectra. The mobile phase consists of a mixture of acetonitrile/water (1/1, v/v) with addition of formic acid (0.1% final concentration). Acquisitions are performed in the positive ion mode of electrospray ionization in the range from 75 to 1000 u at the maximum resolving power value 100,000 (FWHM: for a mass of 400 u). Each mass spectrum is the average of four scans. The electrospray voltage is set at 4 kV, the capillary voltage at 35 V, and the tube lens offset at 75 V. The sheath flow (both nitrogen) has been optimized at 16 (arbitrary units) and no auxiliary gas is used. The drying gas temperature is fixed at 275 °C. A typical mass spectrum of cell yeast extract is displayed in Fig. 2.4.

5.3. LC/MS

Global mass spectrometric detection requires the possibility to detect ions in both positive and negative modes of electrospray ionization. However, PDFOA generated interfering signals in the negative mode that hamper the recording of mass spectra. We then had to turn to an alternative chromatographic separation. We selected a pentafluorophenylpropyl bonded silica (HS-F5) column which has previously been reported to achieve efficient separations of polar metabolites such as amino acids, amines, nucleic bases, nucleosides, nucleotides, and organic acids (Yoshida *et al.*, 2007, 2009).

Chromatographic separation is performed on a Discovery® HS-F5 (2.1 × 250 mm, 5 μm) from Supelco Analytical (Interchim, Montluçon, France) by using a Surveyor LC system (ThermoFisher Scientifics,

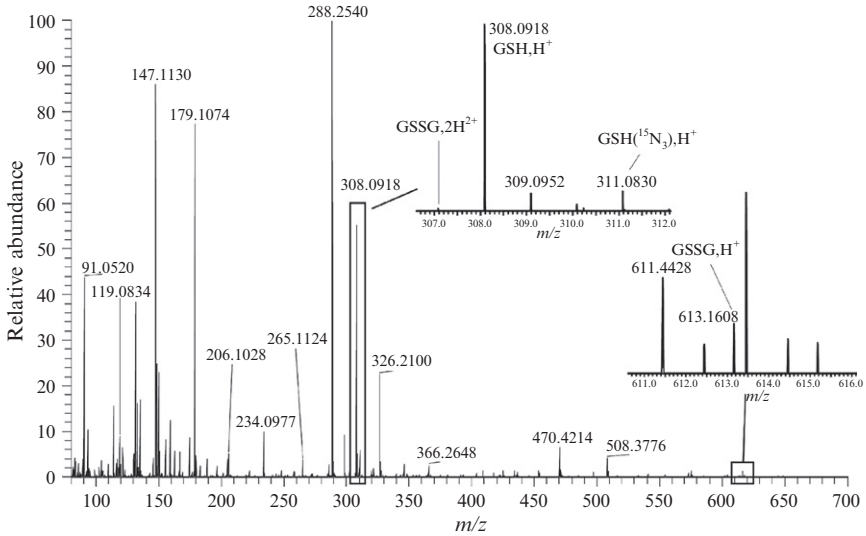

Figure 2.4 *Mass spectrum of a cadmium-exposed yeast extract (1.6.108 cells/mL) acquired by flow injection analysis in the positive ion mode of electrospray*. The analyses are carried out at a flow rate of 30 μL/min by using a Surveyor LC system (ThermoFisher Scientifics, Courtaboeuf, France) and 20 μL of samples are injected in the system for the acquisition of mass spectra. The mobile phase consists of a mixture of acetonitrile/water (1/1, v/v) with addition of formic acid (0.1% final concentration). Mass spectrometry detection is performed using an LTQ/Orbitrap hybrid mass spectrometer (ThermoFisher Scientifics, Courtaboeuf, France) fitted with an electrospray source operated in the positive ionization mode. The detection is achieved from 75 to 1000 u at the maximum resolving power (i.e., 100,000, FWHM for an ion at 400 u). Two insets show enlargement of the *m/z* ranges of 307–312 and 611–616, corresponding to ions related to reduced and oxidized glutathione, respectively.

Courtaboeuf, France). Before injection, samples are stored at 4 °C in the tray of the autosampler. Separations are carried out using the following gradient at 200 μL/min: 0–3 min, 0% B; 3–20 min, from 0 to 100% B; 20–25 min, 100% B; and 25–45 min, 0% B. Solvent A was water and solvent B was acetonitrile, both containing 0.1% formic acid. Column temperature is set at 30 °C.

Mass spectrometric detection is performed using an LTQ-Orbitrap hybrid mass spectrometer (ThermoFisher Scientifics, Courtaboeuf, France) fitted with an electrospray source operated in the positive ionization mode. The detection is achieved from 75 to 1000 u at the maximum resolving power (i.e., 100,000, FWHM for an ion at 400 u). The mass spectrometer is operated with capillary voltage at 4 kV and capillary temperature at 275 °C. The sheath gas pressure and the auxiliary gas pressure are set respectively at 45 and 10 (arbitrary units) with nitrogen gas. A typical LC/MS chromatogram of yeast cell extract is shown in Fig. 2.5.

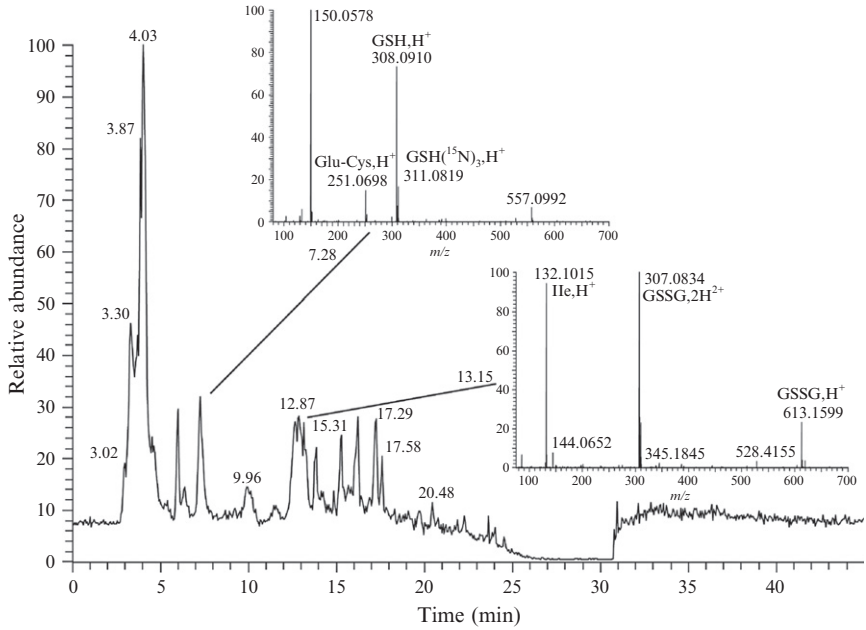

Figure 2.5 *LC/MS chromatogram of a yeast cell extract (1.6.10^8 cells/mL).* Chromatographic separations are performed on a Discovery® HS F5 (2.1 × 250 mm, 5 μm) from Supelco Analytical (Interchim, Montluçon, France). using the following gradient at 200 μL/min: 0–3 min, 0% B; 3–20 min, from 0 to 100% B; 20–25 min, 100% B; and 25–45, 0% B. Solvent A was water and solvent B was acetonitrile, both containing 0.1% formic acid. Column temperature is set at 30 °C and 20 μL is injected into the chromatographic system. Mass spectrometry detection is performed using an LTQ/Orbitrap hybrid mass spectrometer (ThermoFisher Scientifics, Courtaboeuf, France) fitted with an electrospray source operated in the positive ionization mode. The detection is achieved from 75 to 1000 u at the maximum resolving power (i.e., 100,000, FWHM for an ion at 400 u). Two insets show enlargement of the mass spectra recorded at 7 and 13 min, corresponding to ions related to reduced and oxidized glutathione, respectively.

5.4. Data processing

Spectra are recorded in RAW files and the data extraction from spectra is performed by using either the qualitative browser of the instrument software Xcalibur version 2.0 (ThermoFisher Scientifics, Les Ulis, France) or the peak detection software XCMS. The latter is a software dedicated to the analysis of series of chromatograms in the framework of metabolomics studies. It was initially developed at the Scripps Center for Mass Spectrometry (Smith *et al.*, 2006) and has subsequently been improved by other teams (Tautenhahn *et al.*, 2008). XCMS is a set of functions that have been included in an R library. Both library (XCMS) and platform (R) are free and regularly updated. XCMS

is an algorithm using mainly five functions (xcmsSet( ), group( ), rector( ), fillPeaks( ) and diffreport( )) that convert raw files (in netCDF or mzXML format) into a peak list (namely a retention time and a mass-to-charge ratio) reporting the peak area for each sample. Each function includes several parameters that should be optimized in the particular context of the analysis.

Peak detection is performed by the xcmsSet( ) function. It includes several peak picking methods such as Matched Filter as default method, which supports mass spectra recorded in both centroid and continuum modes, and also CentWave (Tautenhahn *et al.*, 2008), which supports only centroid data. These algorithms work with extracted ion chromatograms (EICs), and the width of the EIC is defined by the step parameter. Expected peak characteristics depending on chromatography performance, such as FWHM, as well as mass spectrometer characteristics, such as signal to noise (snthresh) or mass accuracy/precision (mzdiff), should also be defined in the peak picking step.

The peak matching step (group( )) makes clusters of signals across the samples. The main parameters of the peak matching step encompass (i) minfrac/minsamp, that is, the relative/absolute minimal number of samples exhibiting a particular signal, to compose a valid group and (ii) chromatographic (bw) and mass spectrometric (mzwid) tolerances in retention time and mass-to-charge ratio, respectively, for signals that are selected in the group.

The Retcor( ) function allows calculation of the corrected retention time of a valid group. The fillPeaks( ) function works on samples where peaks belonging to a validated group are not represented; it integrates the signal of the EIC in the region of the expected peaks. fillPeaks do not have any parameters. The diffreport( ) function generates the final peak list as a data matrix (*.tsv) (easily readable with Microsoft Excel®) that contains some basic statistical analyses.

All useful documents (tutorial and in-depth descriptions of functions and parameters) are available on the bioconductor website (http://www.bioconductor.org/packages/bioc/html/xcms.html) and on the XCMS website at the Scripps Center (http://masspec.scripps.edu/xcms/xcms.php). In addition, a user group was created a few years ago and its discussions are archived on Google groups (http://groups.google.com/group/xcms).

5.4.1. XCMS parameters for direct introduction MS

The parameters for the xcmsSet function have been optimized for the most reliable peak detection by using the Matched Filter algorithm, because our data are recorded in the continuum mode. They were set as follows: FWHM = 50, step = 0.01, steps = 2, mzdiff = 0.001, and snthresh = 3. The parameter values for the group function were bw = 50, minfrac = 0.3, mzwid = 0.01, max = 200, and sleep = 0. The resulting data matrix typically contains 2000 variables (i.e., m/z ratios) for a simple experimental design of six samples (i.e., $n = 3$ per group). The ions related to metabolites of interest and their areas in the samples are then picked up from the data matrix.

5.4.2. XCMS parameters for LC/ESI-MS

As for FIA spectra, LC/MS files are converted by using the file converter of the Xcalibur instrument software into netCDF files and the resulting data files are processed by using the XCMS package. When the Matched Filter algorithm is used, the parameter values for the xcmsSet function are as follows: FWHM = 25, step = 0.01, steps = 3, mzdiff = 0.01, and snthresh = 3. The values of the parameters for the group functions are bw = 5, minfrac = 0.3, mzwid = 0.01, max = 50, and sleep = 0. The resulting data matrix typically contains 2269 variables (i.e., retention time, m/z ratio couples) for a simple experimental design of six samples (i.e., $n = 3$ per group). In this case, a variable corresponds to an ion-retention time pair. The ions related to metabolites of interest and their areas in the samples are then picked up from the data matrix.

6. Discussion

MS-based methods enable the determination of sulfur metabolites in both their oxidized or reduced states without any derivatization step. They also make it possible concomitantly to evaluate other metabolites closely connected to the glutathione biosynthesis pathway. The aim of this paper is to provide the readers with different MS protocols for the detection and relative and absolute quantification of sulfur and related metabolites, thus illustrating the versatility of atmospheric pressure ionization MS instruments.

Absolute quantification was performed by using ion-pair chromatography, which provided good retention and appropriate chromatographic separation of the analytes, and a triple quadrupole instrument operated in the SRM detection mode. Limits of quantification in the range from 1 to 50 ng/mL were obtained for 31 metabolites. Absolute concentration can also be expressed in molarity units by taking into account the number of cells injected into the chromatographic system and their corresponding intracellular volume.

This method was initially developed for yeast cell extracts, but can be transposed to other cell types. Uniform metabolic labeling of microorganism or plant cells can be obtained for quantification purposes. For other kinds of cells, such as mammalian cells, which cannot be cultured in minimum media, it is possible to use the labeled yeast cell extracts whose preparation is described in this chapter. It should then be ensured that the biological samples do not generate additional matrix effects. This can be checked by spiking the ^{15}N yeast extract with either solvent or an aliquot of the sample. The ^{15}N metabolites should have similar peak areas or intensities in both situations.

Quantification with triple quadrupole instruments operated in the SRM mode suffers from two major drawbacks: development and validation are time-consuming and the inclusion of additional metabolites in the method is problematic because the validation process has to be started again. The use of global mass spectrometric detection using FT-MS instruments (i.e., LTQ-Orbitrap and FTICR devices) offers an attractive solution to these limitations (Zhang *et al.*, 2009), although it has not been demonstrated that the same level of sensitivity as that obtained with triple quadrupole mass spectrometers is generally achieved.

With FT-MS instruments, the protonated or deprotonated ions related to the metabolites of interest are picked up from mass spectra of biological samples and quantification is achieved by measuring the areas or intensities of their EICs. Very accurate mass measurements with sub-ppm errors and the high resolution achieved by using LTQ-Orbitrap mass spectrometers unambiguously discriminate isobaric ions, improving the number of metabolites to be detected when compared with low-resolution instruments. Furthermore, linear signal-concentration curves have been observed in biological extract conditions, indicating that such instruments are suitable for metabolite quantification (Madalinski *et al.*, 2008). The two protocols that are reported in this chapter enable detection and relative metabolite quantification in yeast extracts, and also in any other kind of biological media. Relative quantification of nitrogen-containing metabolites can be improved by adding labeled extracts to the biological extracts. When compared with the triple quadrupole mass spectrometer, FT-MS instruments make save time for optimization and method development. However, data treatment methods such as software for automatic peak detection have to be implemented in order to get the relevant analytical information. Optimization of software parameters is critical and time-consuming. The values reported in this chapter were optimal for our experimental conditions and should be carefully optimized for each set of analytical and biological conditions by evaluating the automatic recovery of selected standard compounds spiked in the biological medium of interest (Tautenhahn *et al.*, 2008).

Direct introduction of the biological sample into the LTQ-Orbitrap mass spectrometer is rapid but suffers from several drawbacks (Madalinski *et al.*, 2008). First, the sensitivity of the detection in biological media is altered by matrix effects, which can be attenuated by dilution or optimization of the cell concentration. Second, a metabolite does not produce a single m/z peak since adduct and product ions can be generated during the desolvation step following the atmospheric pressure ionization process. It is more difficult to highlight such signal redundancy in direct introduction MS than in LC/MS. For example, it is not possible to discriminate cysteine from the dipeptide γ-glutamyl-cysteine because the latter metabolite undergoes an in-source collision-induced dissociation process that generates some cysteine (Madalinski *et al.*, 2008). Identification of ions is achieved by

calculating elemental compositions thanks to accurate mass measurements. Databases are then consulted and the structure proposals are validated or not by further MS^n experiments. However, many metabolites are isomers or at least have similar accurate masses. In the latter case, the structural elucidation by using the LTQ-Orbitrap instrument is complicated by the selection of the precursor ion for further collision-induced dissociation (CID) that occurs at a low resolution in the LTQ cell, resulting in a mixture of isobaric ions undergoing the CID process. Thanks to the high resolving power, the Orbitrap analyzer allows discrimination between the origins of the fragmentation pattern. In some instances, it is also possible to distinguish between isomers with different CID spectra (Madalinski *et al.*, 2008).

Many of these issues may be addressed by using LC separation adapted to the retention of polar metabolites prior to mass spectrometric detection. For example, cysteine can be quantified in our two LC methods since its retention time is not the same as that of γ-glutamyl-cysteine (see Tables 2.2 and 2.6). Furthermore, metabolites such as cystine and *S*-adenosylhomocysteine that cannot be observed by using direct introduction are detected with the LC procedure, as shown in Table 2.6. Metabolite identification is also improved and facilitated by taking into account their retention time.

7. Summary

Three MS-based methods for the determination of sulfur metabolites and also related amino acids involved in the glutathione biosynthesis pathway have been presented and discussed. The first one enables absolute quantification of these metabolites in cell extracts. It is based on LC coupled to MS and ^{15}N uniform metabolic labeling of the yeast *S. cerevisiae*. The chromatographic separation involves PDFOA as an ion-pairing reagent. The mass spectrometer is a triple quadrupole instrument fitted with an electrospray source and the metabolites are detected using 54 SRM transitions over two time segments. Some strategies addressing method validation are proposed and, by using this assay, most metabolites of interest are quantified with limits of quantification ranging from 1 to 50 ng/mL.

The two other methods involve a high-resolution mass spectrometer, the LTQ-Orbitrap, which performs accurate mass measurements with ppm errors. Biological samples are introduced into the mass spectrometer either directly or after a chromatographic separation. Detection and quantification of the metabolites of interest are achieved by picking their accurate masses either manually or automatically from complex and information-rich metabolite fingerprints. By these means, several inspections of the data can be performed in order to get analytical information which may be outside the initial scope of the investigation.

Table 2.6 Detection of metabolites using the LTQ–Orbitrap mass spectrometer

		Direct introduction mass spectrometry			LC/MS			
Metabolites	[M + H]+	Detection in biological extracts	Isotopes observed	Identification	RT (min) from commercial sample	Detection in biological extracts	Isotopes observed	Identification
Alanine	90.0550	Yes	^{15}N	Identified	3.70	Yes	^{15}N	Identified[d]
Arginine	175.1190	Yes	^{15}N	Identified	3.74	Yes	^{15}N	Identified[d]
Asparagine	133.0608	Yes	^{15}N	To be confirmed[b]	3.20	Yes	^{15}N	Identified[d]
Aspartate	134.0448	Yes	^{15}N	To be confirmed[b]	3.25	Yes	^{15}N	Identified[d]
Cysteine	122.0270	Yes	^{15}N	To be confirmed[b]	3.46	Yes	$^{15}N,^{34}S$	Identified[d]
Cystathionine	223.0747	Yes	$^{15}N,^{34}S$	Identified	3.14	Yes	$^{15}N,^{34}S$	Identified[d]
Cystine	241.0311	No			3.06	Yes[a]	^{15}N	Identified[d]
GSH	308.0911	Yes	$^{15}N,^{34}S$	Identified	7.09	Yes	$^{15}N,^{34}S$	Identified[d]
GSSG	613.1593	Yes[a]	^{15}N	To be confirmed[c]	13.21	Yes	$^{15}N,^{34}S$	Identified[d]
Glu-Cys	251.0696	Yes	$^{15}N,^{34}S$	Identified	7.18	Yes	$^{15}N,^{34}S$	Identified[d]
Glutamine	147.0764	Yes	^{15}N	Identified	3.29	Yes	^{15}N	Identified[d]
Glutamate	148.0604	Yes	^{15}N	Identified	3.57	Yes	^{15}N	identified[d]
Glycine	76.0393	Yes[a]	^{15}N	To be confirmed[c]	3.16	Yes	^{15}N	Identified[d]
Homocysteine	136.0427	Yes[a]		To be confirmed[c]	4.71	Yes[a]		Identified[d]
Homoserine/ threonine	120.0655	Yes	^{15}N	Identified	3.31	Yes	^{15}N	Identified[d]
Histidine	156.0768	Yes	^{15}N	Identified	3.57	Yes	^{15}N	Identified[d]
Isoleucine	132.1019	Yes	^{15}N	Identified	12.74	Yes	^{15}N	Identified[d]
Leucine	132.1019				11.14	Yes	^{15}N	Identified[d]
Lysine	147.1128	Yes	^{15}N	Identified	3.31	Yes	^{15}N	Identified[d]
Methionine	150.0583	Yes	$^{15}N,^{34}S$	Identified	7.01	Yes	$^{15}N,^{34}S$	Identified[d]

(*continued*)

Table 2.6 (*continued*)

		Direct introduction mass spectrometry			LC/MS			
Metabolites	[M + H]+	Detection in biological extracts	Isotopes observed	Identification	RT (min) from commercial sample	Detection in biological extracts	Isotopes observed	Identification
5-methylthio adenosine	298.0968	Yes	$^{15}N,^{34}S$	Identified	16.40	Yes	$^{15}N,^{34}S$	Identified[d]
Phenylalanine	166.0863	Yes	^{15}N	To be confirmed[b]	15.34	Yes	^{15}N	Identified[d]
Proline	116.0706	Yes	^{15}N	To be confirmed[b]	3.91	Yes	^{15}N	Identified[d]
S-adenosylho-mocysteine	399.1445	No			13.98	Yes[a]	^{15}N	Identified[d]
Serine	106.0499	Yes[a]	^{15}N	Identified	3.16	Yes	^{15}N	Identified[d]
Threonine	120.0655	Yes	^{15}N	To be confirmed[b]	3.31	Yes	^{15}N	Identified[d]
Tryptophan	205.0972	Yes	^{15}N	To be confirmed[b]	17.18	Yes	^{15}N	Identified[d]
Tyrosine	182.0812	Yes[a]	^{15}N	Identified	13.83	Yes	^{15}N	identified[d]
Valine	118.0863	Yes	^{15}N	To be confirmed[b]	5.74	Yes	^{15}N	Identified[d]
Cysteinyl-Glycine	179.0485	Yes[a]	^{15}N	To be confirmed[b]	4.99	Yes	$^{15}N,^{34}S$	Identified[d]

[a] Detection in biological extract with low intensity.
[b] Identification on the basis of accurate mass measurement.
[c] No CID spectra due to low-signal intensity.
[d] Identification on the basis of accurate mass measurement and retention time of commercial product.

ACKNOWLEDGMENTS

This work was supported by the Commissariat à l'Energie Atomique and by a grant from the Agence Nationale pour la Recherche ("ModMatMet" program).

REFERENCES

Apffel, A., Fischer, S., Goldberg, G., Goodley, P. C., and Kuhlmann, F. E. (1995). Enhanced sensitivity for peptide mapping with electrospray liquid chromatography–mass spectrometry in the presence of signal suppression due to trifluoroacetic acid-containing mobile phases. *J. Chromatogr. A* **712,** 177–190.

Bajad, S. U., Lu, W. Y., Kimball, E. H., Yuan, J., Peterson, C., and Rabinowitz, J. D. (2006). Separation and quantitation of water soluble cellular metabolites by hydrophilic interaction chromatography–tandem mass spectrometry. *J. Chromatogr. A* **1125,** 76–88.

Birkemeyer, C., Luedemann, A., Wagner, C., Erban, A., and Kopka, J. (2005). Metabolome analysis: the potential of in vivo labeling with stable isotopes for metabolite profiling. *Trends Biotechnol.* **23,** 28–33.

Canelas, A. B., ten Pierick, A., Ras, C., Seifar, R. M., van Dam, J. C., van Gulik, W. M., and Heijnen, J. J. (2009). Quantitative evaluation of intracellular metabolite extraction techniques for yeast metabolomics. *Anal. Chem.* **81,** 7379–7389.

Chaimbault, P., Petritis, K., Elfakir, C., and Dreux, M. (1999). Determination of 20 underivatized proteinic amino acids by ion-pairing chromatography and pneumatically assisted electrospray mass spectrometry. *J. Chromatogr. A* **855,** 191–202.

Coulier, L., Bas, R., Jespersen, S., Verheij, E., van der Werf, M. J., and Hankemeier, T. (2006). Simultaneous quantitative analysis of metabolites using ion-pair liquid chromatography–electrospray ionization mass spectrometry. *Anal. Chem.* **78,** 6573–6582.

Engelsberger, W. R., Erban, A., Kopka, J., and Schulze, W. X. (2006). Metabolic labeling of plant cell cultures with K(15)NO3 as a tool for quantitative analysis of proteins and metabolites. *Plant Methods* **2,** 14.

Fahey, R. C., and Newton, G. L. (1987). Determination of low-molecular-weight thiols using monobromobimane fluorescent labeling and high-performance liquid chromatography. *Methods Enzymol.* **143,** 85–96.

Gangl, E. T., Annan, M. M., Spooner, N., and Vouros, P. (2001). Reduction of signal suppression effects in ESI-MS using a nanosplitting device. *Anal. Chem.* **73,** 5635–5644.

Gu, L., Jones, A. D., and Last, R. L. (2007). LC–MS/MS assay for protein amino acids and metabolically related compounds for large-scale screening of metabolic phenotypes. *Anal. Chem.* **79,** 8067–8075.

Guan, X., Hoffman, B., Dwivedi, C., and Matthees, D. P. (2003). A simultaneous liquid chromatography/mass spectrometric assay of glutathione, cysteine, homocysteine and their disulfides in biological samples. *J. Pharm. Biomed. Anal.* **31,** 251–261.

Gucek, M., Makuc, S., Mlakar, A., Bericnik-Vrbovsek, J., and Marsel, J. (2002). Determination of glutathione in spruce needles by liquid chromatography/tandem mass spectrometry. *Rapid Commun. Mass Spectrom.* **16,** 1186–1191.

Hammermeister, D. E., Serrano, J., Schmieder, P., and Kuehl, D. W. (2000). Characterization of dansylated glutathione, glutathione disulfide, cysteine and cystine by narrow bore liquid chromatography/electrospray ionization mass spectrometry. *Rapid Commun. Mass Spectrom.* **14,** 503–508.

Hardman, M., and Makarov, A. A. (2003). Interfacing the orbitrap mass analyzer to an electrospray ion source. *Anal. Chem.* **75,** 1699–1705.

Hu, Q., Noll, R. J., Li, H., Makarov, A., Hardman, M., and Graham, C. R. (2005). The Orbitrap: a new mass spectrometer. *J. Mass Spectrom.* **40,** 430–443.

Kiefer, P., Portais, J. C., and Vorholt, J. A. (2008). Quantitative metabolome analysis using liquid chromatography–high-resolution mass spectrometry. *Anal. Biochem.* **382,** 94–100.

Kitamoto, K., Yoshizawa, K., Ohsumi, Y., and Anraku, Y. (1988). Dynamic aspects of vacuolar and cytosolic amino acid pools of *Saccharomyces cerevisiae*. *J. Bacteriol.* **170,** 2683–2686.

Kosower, N. S., and Kosower, E. M. (1987). Thiol labeling with bromobimanes. *Methods Enzymol.* **143,** 76–84.

Lafaye, A., Junot, C., Pereira, Y., Lagniel, G., Tabet, J. C., Ezan, E., and Labarre, J. (2005a). Combined proteome and metabolite-profiling analyses reveal surprising insights into yeast sulfur metabolism. *J. Biol. Chem.* **280,** 24723–24730.

Lafaye, A., Labarre, J., Tabet, J. C., Ezan, E., and Junot, C. (2005b). Liquid chromatography–mass spectrometry and ^{15}N metabolic labeling for quantitative metabolic profiling. *Anal. Chem.* **77,** 2026–2033.

Lakritz, J., Plopper, C. G., and Buckpitt, A. R. (1997). Validated high-performance liquid chromatography–electrochemical method for determination of glutathione and glutathione disulfide in small tissue samples. *Anal. Biochem.* **247,** 63–68.

Lenton, K. J., Therriault, H., and Wagner, J. R. (1999). Analysis of glutathione and glutathione disulfide in whole cells and mitochondria by postcolumn derivatization high-performance liquid chromatography with ortho-phthalaldehyde. *Anal. Biochem.* **274,** 125–130.

Luo, J. L., Hammarqvist, F., Cotgreave, I. A., Lind, C., Andersson, K., and Wernerman, J. (1995). Determination of intracellular glutathione in human skeletal muscle by reversed-phase high-performance liquid chromatography. *J. Chromatogr. B* **670,** 29–36.

Madalinski, G., Godat, E., Alves, S., Lesage, D., Genin, E., Levi, P., Labarre, J., Tabet, J. C., Ezan, E., and Junot, C. (2008). Direct introduction of biological samples into a LTQ–Orbitrap hybrid mass spectrometer as a tool for fast metabolome analysis. *Anal. Chem.* **80,** 3291–3303.

Makarov, A. (2000). Electrostatic axially harmonic orbital trapping: a high-performance technique of mass analysis. *Anal. Chem.* **72,** 1156–1162.

Makarov, A., Denisov, E., Lange, O., and Horning, S. (2006). Dynamic range of mass accuracy in LTQ Orbitrap hybrid mass spectrometer. *J. Am. Soc. Mass Spectrom.* **17,** 977–982.

Maron, B. A., and Loscalzo, J. (2009). The treatment of hyperhomocysteinemia. *Annu. Rev. Med.* **60,** 39–54.

Matuszewski, B. K., Constanzer, M. L., and Chavez-Eng, C. M. (1998). Matrix effect in quantitative LC/MS/MS analyses of biological fluids: a method for determination of finasteride in human plasma at picogram per milliliter concentrations. *Anal. Chem.* **70,** 882–889.

Messenguy, F., Colin, D., and ten Have, J. P. (1980). Regulation of compartmentation of amino acid pools in *Saccharomyces cerevisiae* and its effects on metabolic control. *Eur. J. Biochem.* **108,** 439–447.

Nagai, S., and Flavin, M. (1971). Synthesis of *O*-acetylhomoserine. *Methods Enzymol.* **17,** 423–424.

Natarajan, K., Meyer, M. R., Jackson, B. M., Slade, D., Roberts, C., Hinnebusch, A. G., and Marton, M. J. (2001). Transcriptional profiling shows that Gcn4p is a master regulator of gene expression during amino acid starvation in yeast. *Mol. Cell. Biol.* **21,** 4347–4368.

Noctor, G., and Foyer, C. H. (1998). Simultaneous measurement of foliar glutathione, gamma-glutamylcysteine, and amino acids by high-performance liquid chromatography: comparison with two other assay methods for glutathione. *Anal. Biochem.* **264,** 98–110.

Parmentier, C., Leroy, P., Wellman, M., and Nicolas, A. (1998). Determination of cellular thiols and glutathione-related enzyme activities: versatility of high-performance liquid chromatography-spectrofluorimetric detection. *J. Chromatogr. B* **719,** 37–46.

Pereira, Y., Lagniel, G., Godat, E., Baudouin-Cornu, P., Junot, C., and Labarre, J. (2008). Chromate causes sulfur starvation in yeast. *Toxicol. Sci.* **106,** 400–412.

Raggi, M. A., Schiavone, P., Mandrioli, R., Bugamelli, F., Frabetti, F., and Marini, M. (1998). Spectrophotometric determination of thiols in human lymphocytes. *Pharmazie* **53,** 239–242.

Sailer, M., Helms, G. L., Henkel, T., Niemczura, W. P., Stiles, M. E., and Vederas, J. C. (1993). ^{15}N- and 13C-labeled media from Anabaena sp. for universal isotopic labeling of bacteriocins: NMR resonance assignments of leucocin A from Leuconostoc gelidum and nisin A from Lactococcus lactis. *Biochemistry* **32,** 310–318.

Salazar, J. F., Herbeth, B., Siest, G., and Leroy, P. (1999). Stability of blood homocysteine and other thiols: EDTA or acidic citrate? *Clin. Chem.* **45,** 2016–2019.

Sellick, C. A., Hansen, R., Maqsood, A. R., Dunn, W. B., Stephens, G. M., Goodacre, R., and Dickson, A. J. (2009). Effective quenching processes for physiologically valid metabolite profiling of suspension cultured Mammalian cells. *Anal. Chem.* **81,** 174–183.

Senft, A. P., Dalton, T. P., and Shertzer, H. G. (2000). Determining glutathione and glutathione disulfide using the fluorescence probe o-phthalaldehyde. *Anal. Biochem.* **280,** 80–86.

Shah, V. P., Midha, K. K., Findlay, J. W., Hill, H. M., Hulse, J. D., McGilveray, I. J., McKay, G., Miller, K. J., Patnaik, R. N., Powell, M. L., Tonelli, A., Viswanathan, C. T., *et al.* (2000). Bioanalytical method validation—a revisit with a decade of progress. *Pharm. Res.* **17,** 1551–1557.

Smith, C. A., Want, E. J., O'Maille, G., Abagyan, R., and Siuzdak, G. (2006). XCMS: processing mass spectrometry data for metabolite profiling using nonlinear peak alignment, matching, and identification. *Anal. Chem.* **78,** 779–787.

Spura, J., Reimer, L. C., Wieloch, P., Schreiber, K., Buchinger, S., and Schomburg, D. (2009). A method for enzyme quenching in microbial metabolome analysis successfully applied to gram-positive and gram-negative bacteria and yeast. *Anal. Biochem.* **394,** 192–201.

Stabler, S. P., Marcell, P. D., Podell, E. R., and Allen, R. H. (1987). Quantitation of total homocysteine, total cysteine, and methionine in normal serum and urine using capillary gas chromatography–mass spectrometry. *Anal. Biochem.* **162,** 185–196.

Strege, M. A., Stevenson, S., and Lawrence, S. M. (2000). Mixed-mode anion-cation exchange/hydrophilic interaction liquid chromatography–electrospray mass spectrometry as an alternative to reversed phase for small molecule drug discovery. *Anal. Chem.* **72,** 4629–4633.

Tautenhahn, R., Bottcher, C., and Neumann, S. (2008). Highly sensitive feature detection for high resolution LC/MS. *BMC Bioinf.* **9,** 504.

Thorsen, M., Lagniel, G., Kristiansson, E., Junot, C., Nerman, O., Labarre, J., and Tamas, M. J. (2007). Quantitative transcriptome, proteome, and sulfur metabolite profiling of the *Saccharomyces cerevisiae* response to arsenite. *Physiol. Genomics* **30,** 35–43.

Tolstikov, V. V., and Fiehn, O. (2002). Analysis of highly polar compounds of plant origin: combination of hydrophilic interaction chromatography and electrospray ion trap mass spectrometry. *Anal. Biochem.* **301,** 298–307.

Villas-Boas, S. G., Hojer-Pedersen, J., Akesson, M., Smedsgaard, J., and Nielsen, J. (2005). Global metabolite analysis of yeast: evaluation of sample preparation methods. *Yeast* **22,** 1155–1169.

White, R. H. (2003). The biosynthesis of cysteine and homocysteine in *Methanococcus jannaschii*. *Biochim. Biophys. Acta* **1624,** 46–53.

Winder, C. L., Dunn, W. B., Schuler, S., Broadhurst, D., Jarvis, R., Stephens, G. M., and Goodacre, R. (2008). Global metabolic profiling of *Escherichia coli* cultures: an evaluation of methods for quenching and extraction of intracellular metabolites. *Anal. Chem.* **80,** 2939–2948.

Wu, C. C., MacCoss, M. J., Howell, K. E., Matthews, D. E., and Yates, J. R. III (2004a). Metabolic labeling of mammalian organisms with stable isotopes for quantitative proteomic analysis. *Anal. Chem.* **76,** 4951–4959.

Wu, G., Fang, Y. Z., Yang, S., Lupton, J. R., and Turner, N. D. (2004b). Glutathione metabolism and its implications for health. *J. Nutr.* **134,** 489–492.

Yan, C. C., and Huxtable, R. J. (1995). Fluorimetric determination of monobromobimane and o-phthalaldehyde adducts of gamma-glutamylcysteine and glutathione: application to assay of gamma-glutamylcysteinyl synthetase activity and glutathione concentration in liver. *J. Chromatogr. B* **672,** 217–224.

Yoshida, H., Mizukoshi, T., Hirayama, K., and Miyano, H. (2007). Comprehensive analytical method for the determination of hydrophilic metabolites by high-performance liquid chromatography and mass spectrometry. *J. Agric. Food Chem.* **55,** 551–560.

Yoshida, H., Yamazaki, J., Ozawa, S., Mizukoshi, T., and Miyano, H. (2009). Advantage of LC–MS metabolomics methodology targeting hydrophilic compounds in the studies of fermented food samples. *J. Agric. Food Chem.* **57,** 1119–1126.

Zhang, N. R., Yu, S., Tiller, P., Yeh, S., Mahan, E., and Emary, W. B. (2009). Quantitation of small molecules using high-resolution accurate mass spectrometers—a different approach for analysis of biological samples. *Rapid Commun. Mass Spectrom.* **23,** 1085–1094.

CHAPTER THREE

Use of Dimedone-Based Chemical Probes for Sulfenic Acid Detection: Evaluation of Conditions Affecting Probe Incorporation into Redox-Sensitive Proteins

Chananat Klomsiri,* Kimberly J. Nelson,* Erika Bechtold,† Laura Soito,* Lynnette C. Johnson,* W. Todd Lowther,* Seong-Eon Ryu,‡,§ S. Bruce King,† Cristina M. Furdui,¶ *and* Leslie B. Poole*

Contents

* Department of Biochemistry, Wake Forest University School of Medicine, Winston-Salem, North Carolina, USA
† Department of Chemistry, Wake Forest University, Winston-Salem, North Carolina, USA
‡ Center for Cellular Switch Protein Structure, Korea Research Institute of Bioscience and Biotechnology, Yusong, Taejon, South Korea
§ Department of Bio-engineering, College of Engineering, Hanyang University, Seongdong-gu, Seoul, South Korea
¶ Section on Molecular Medicine, Department of Internal Medicine, Wake Forest University School of Medicine, Medical Center Boulevard, Winston-Salem, North Carolina, USA

Methods in Enzymology, Volume 473
ISSN 0076-6879, DOI: 10.1016/S0076-6879(10)73003-2

Abstract

Sulfenic acids, formed as transient intermediates during the reaction of cysteine residues with peroxides, play significant roles in enzyme catalysis and regulation, and are also involved in the redox regulation of transcription factors and other signaling proteins. Therefore, interest in the identification of protein sulfenic acids has grown substantially in the past few years. Dimedone, which specifically traps sulfenic acids, has provided the basis for the synthesis of a novel group of compounds that derivatize 1,3-cyclohexadione, a dimedone analogue, with reporter tags such as biotin for affinity capture and fluorescent labels for visual detection. These reagents allow identification of the cysteine sites and proteins that are sensitive to oxidation and permit identification of the cellular conditions under which such oxidations occur. We have shown that these compounds are reactive and specific toward sulfenic acids and that the labeled proteins can be detected at high sensitivity using gel analysis or mass spectrometry. Here, we further characterize these reagents, showing that the DCP-Bio1 incorporation rates into three sulfenic acid containing proteins, papaya papain, *Escherichia coli* fRMsr, and the *Salmonella typhimurium* peroxiredoxin AhpC, are significantly different and, in the case of fRMsr, are unaffected by changes in buffer pH from 5.5 and 8.0. We also provide protocols to label protein sulfenic acids in cellular proteins, either by *in situ* labeling of intact cells or by labeling at the time of lysis. We show that the addition of alkylating reagents and catalase to the lysis buffer is critical in preventing the formation of sulfenic acid subsequent to cell lysis. Data presented herein also indicate that the need to standardize, as much as possible, the protein and reagent concentrations during labeling. Finally, we introduce several new test or control proteins that can be used to evaluate labeling procedures and efficiencies.

1. Introduction

Cysteine sulfenic acids in proteins are formed upon reaction of an activated cysteinyl residue with oxidants such as hydrogen peroxide, hydroperoxides, hypochlorous acids, or peroxynitrite (Poole *et al.*, 2004; Reddie and Carroll, 2008). This chemistry occurs, and can be important for modulating biological outcomes (Michalek *et al.*, 2007; Oshikawa *et al.*, 2010), during many receptor-mediated cell signaling processes and as a consequence of oxidative injury occurring due to environmental insults or pathogenic processes (Poole *et al.*, 2004). Thus, development of comprehensive (or even partial) lists of *bona fide* oxidation-sensitive sites in proteins, as well as cellular conditions under which such oxidation sites are engaged, will be critical to better inform biochemical and cellular studies on the consequences of oxidation at specific sites in target proteins and to enhance our understanding of the features characteristic of oxidation-sensitive cysteine sites (Salsbury *et al.*,

2008). At the protein level, the sulfenic acid moiety may be generated as a catalytic or regulatory species or may be the result of an adventitious oxidation with or without structural and/or functional consequences. The development of chemical tools to identify oxidation sites is an important first step toward determining the role that these oxidation events play in modulating protein activity, and ultimately, cellular processes.

Several chemical approaches have been used to evaluate sulfenic acid formation in pure proteins (Allison, 1976; Poole and Ellis, 2002; Turell *et al.*, 2008); the most promising approach for directly and irreversibly modifying sulfenic acids within proteins for proteomics-level analyses has been through use of 5,5-dimethyl-1,3-cyclohexanedione (dimedone), an alkylating agent specific for cysteine sulfenic acid (Allison, 1976; Poole *et al.*, 2005, 2007) or analogues thereof to chemically trap such species (Fig. 3.1) (Poole and Nelson, 2008). This strategy provides new, powerful tools to investigate sulfenic acid formation in proteins. A series of reporter-linked or -linkable, sulfenic acid-directed labeling reagents have been generated by our group and others based upon dimedone or 1,3-cyclohexadione (Fig. 3.1), the latter of which lacks the two methyl groups attached to the ring of dimedone (Poole *et al.*, 2005, 2007; Charles *et al.*, 2007; Leonard *et al.*, 2009; Reddie *et al.*, 2008). Reagents that incorporate a biotin affinity tag or fluorescent groups into a 1,3-cyclohexadione moiety via a linker (Poole *et al.*, 2005, 2007) were used in this work and are shown in Fig. 3.2.

Reactivity of these reagents with protein sulfenic acids is determined in part by the accessibility and stability of the sulfenic acid species at each site. Moreover, within cells, "stability" of the sulfenic acid modification is significantly influenced by the local environment of the oxidized cysteine,

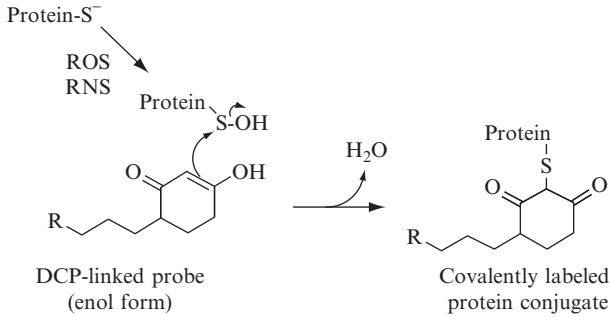

Figure 3.1 Reaction scheme for labeling protein sulfenic acids with DCP-linked probes. Protein thiolates (R–S–), which are susceptible to oxidation by reactive oxygen and nitrogen species (ROS and RNS, respectively) generate sulfenic acids (R–SOH), which can then be labeled by the probes that are synthesized using the reactive 1,3-cyclohexadione core of dimedone.

its tendency to react with other oxidants to form further oxidized cysteinyl moieties (i.e., sulfinic or sulfonic acids), and its accessibility to other thiol groups (i.e., cysteine or glutathione) that can react to form a disulfide bond. Thus, rapid "trapping" of sulfenic acids in proteins with alkylating chemical probes is of great advantage for detecting and identifying these species, even though only substoichiometric amounts of label would ever likely be incorporated into given proteins due to the generally transient nature of the modification. Reliable quantitative measurements based on the extent of probe incorporated are likely to be difficult to achieve, though large variations in oxidation for individual cellular proteins may be observable across samples within the same experimental set.

Evaluation of the reactivity of one of the most useful sulfenic acid probes, DCP-Bio1, toward pure proteins is the subject of the first part of this chapter. The second part provides protocols for labeling oxidized proteins within the cell and introduces several new tests or control proteins for evaluating labeling procedures and efficiencies. An accompanying chapter (Nelson *et al.*, 2010) addresses the use of various approaches for detecting and identifying oxidized proteins and specific sites of oxidation once probes have been incorporated.

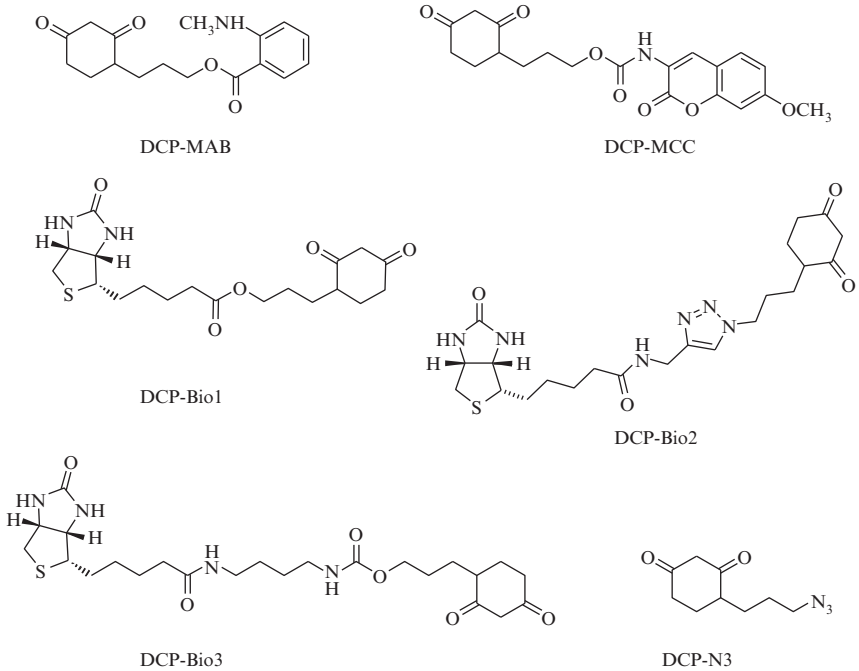

Figure 3.2 (*Continued*)

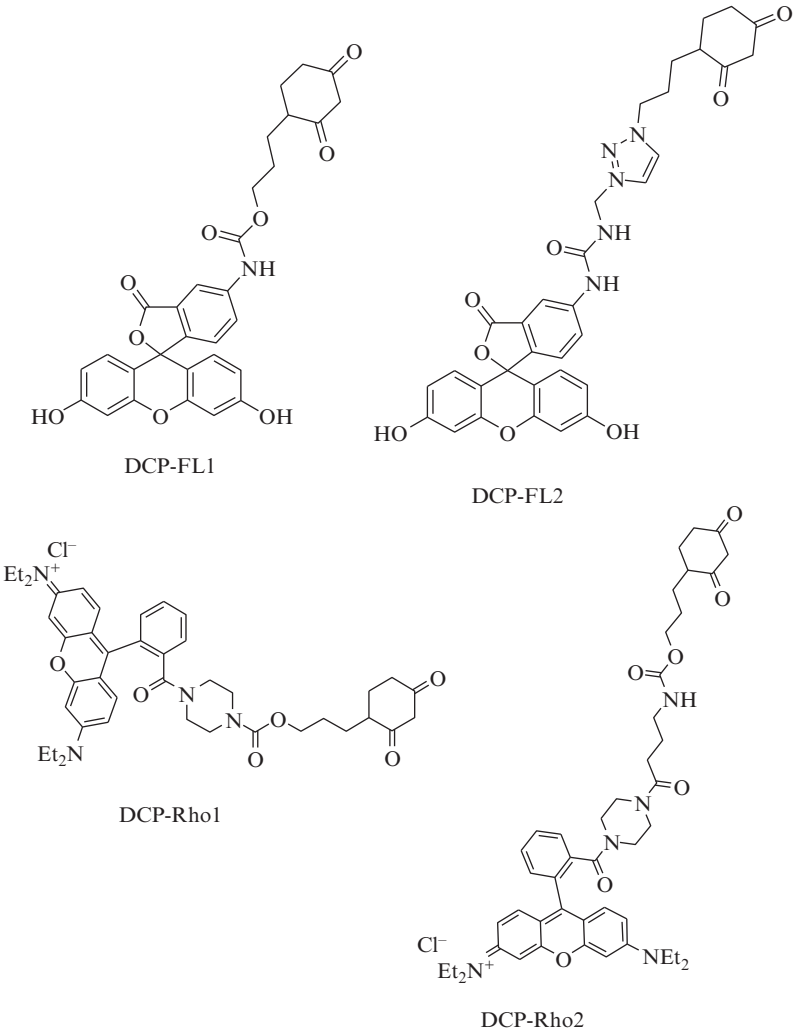

Figure 3.2 Structures and shortened names for the DCP-linked, sulfenic acid-reactive probes used in the present work.

2. Materials

2.1. Solutions

1. 100 m*M* Diethylene triamine pentaacetic acid (DTPA) in 1 *M* sodium hydroxide

2. Potassium phosphate buffers (5, 25, and 50 m*M*), pH 7.0, 100 μM DTPA
3. 50 m*M* Tris–HCl, pH 8.0, 100 μM DTPA
4. 50 m*M* 2-(*N*-morpholino)ethanesulfonic acid (MES), pH 5.3, 100 μM DTPA
5. 100 m*M* Methionine sulfoxide (racemic mixture) in 5 m*M* potassium phosphate, pH 7.0, 100 μM DTPA
6. 30% (~10 *M*) Hydrogen peroxide (H_2O_2)
7. 100 m*M* 1,4-Dithio-DL-threitol (DTT), 154.2 g/mol
8. Cell lysis buffer: 50 m*M* Tris base, pH 7.5 containing 100 m*M* sodium chloride, 100 μM DTPA, 20 m*M* β-glycerophosphate, 0.1% sodium dodecyl sulfate, 0.5% sodium deoxycholate, 0.5% NP-40, and 0.5% Triton-X-100
9. Phosphate-buffered saline (PBS); 100 m*M* sodium phosphate, 150 m*M* sodium chloride, pH 7.2
10. Sinapinic acid (20 mg) in 0.3% trifluoroacetic acid, 50% acetonitrile. Since this is a saturated solution, centrifuge prior to using.

2.2. Chemical modification agents

1. *N*-Ethylmaleimide (NEM), 125.13 g/mol
2. Iodoacetamide (IAAm), 184.96 g/mol
3. 3-(2,4-Dioxocyclohexyl)propyl 2-(methylamino)benzoate (DCP-MAB), 303.35 g/mol (Poole *et al.*, 2005)
4. 3-(2,4-Dioxocyclohexyl)propyl 7-methoxy-2-oxo-2H-chromen-3-ylcarbamate (DCP-MCC), 387.38 g/mol (Poole *et al.*, 2005)
5. Fluoresceinamine-5′-*N*-[3-(2,4-dioxocyclohexyl)propyl)]carbamate (DCP-FL1), 543.5 g/mol (Poole *et al.*, 2007)
6. Fluoresceinamine-5′-*N*-[3-((1-(3-(2,4-dioxocyclohexyl)propyl)-1*H*-1,2,3-triazol-4-yl)methyl]-urea (DCP-FL2), 623.6 g/mol (Poole *et al.*, 2007)
7. (DCP-Bio1), 396.5 g/mol (Poole *et al.*, 2007)
8. 5-((3a*R*,6*S*,6a*S*)-hexahydro-2-oxo-1*H*-thieno[3,4-*d*]imidazol-6-yl)-*N*-((1-(3-(2,4-dioxocyclohexyl)propyl)-1*H*-1,2,3-triazol-4-yl)methyl)pentanamide (DCP-Bio2), 476.6 g/mol (Poole *et al.*, 2007)
9. 3-(2,4-Dioxocyclohexyl)propyl 4-(5-((3a*R*,6*S*,6a*S*)-hexahydro-2-oxo-1*H*-thieno[3,4-*d*]imidazol-6-yl)pentanamido)butylcarbamate (DCP-Bio3), 510.7 g/mol (Poole *et al.*, 2007)
10. Rhodamine B [4-[3-(2,4-dioxocyclohexyl)propyl]carbamate]piperazine amide (DCP-Rho1), 707.9 g/mol (Poole *et al.*, 2007)
11. Rhodamine B 3-(2,4-dioxocyclohexyl)propyl 4-oxo-4-(piperazin-1-yl)butylcarbamate (DCP-Rho2), 793.0 g/mol (Poole *et al.*, 2007)

12. 4-(3-Azidopropyl)cyclohexane-1,3-dione, (DCP-N3), 195.1 g/mol, generated by deprotection of 3-ethoxy-6-(3-azidopropyl)-cyclohex-2-enone (Poole *et al.*, 2007) by treatment with 3 *M* HCl

2.3. Proteins

1. Catalase (2000 units/ml, Sigma) in 50 m*M* Tris–HCl, pH 7.5, 100 μM DTPA.
2. *Salmonella typhimurium* of AhpC C165S mutant, purified as described previously (Nelson *et al.*, 2008; Poole and Ellis, 1996) and stored at −20 °C in 5 m*M* DTT. Prior to conducting experiments, DTT is removed using a Bio-Gel P6 spin column equilibrated in 25 m*M* potassium phosphate, pH 7.0, 100 μM DTPA.
3. *Escherichia coli R*-specific free methionine sulfoxide reductase (fRMsr) C84, 94S mutant, purified as described previously (Lin *et al.*, 2007), and stored at −80 °C in 5 m*M* DTT. Prior to conducting experiments, DTT is removed using a Bio-Gel P6 spin column equilibrated in 5 m*M* potassium phosphate, pH 7.0, 100 μM DTPA.
4. *E. coli* OxyR, "C4A-RD" with C208S mutation and C-terminal His-tag, expressed and purified as described in Section 3 and stored at −80 °C in 5 m*M* DTT. Prior to conducting experiments, DTT is removed using a Bio-Gel P6 spin column equilibrated in 50 m*M* Tris–HCl, pH 8.0, 100 μM DTPA.

3. Methods

3.1. Characterization of "DCP"-linked compounds

3.1.1. Specificity of DCP-linked probes for cysteine sulfenic acid

The first two fluorophore-linked probes generated from 1,3-cyclohexadione had in common the sulfenic acid-reactive 3-(2,4-dioxocyclohexyl) propyl (DCP) group to which the fluorophores were attached (Poole *et al.*, 2005). As all subsequent reagents also possess this reactive "core," we used the "DCP" abbreviation followed by the reporter designation to nickname all subsequent reagents (Poole *et al.*, 2007) (Fig. 3.2). All compounds were tested for their dimedone-like chemical properties using the sulfenic acid-containing C165S mutant of the bacterial peroxiredoxin AhpC (Ellis and Poole, 1997; Poole and Ellis, 2002) and measuring adduct formation by electrospray ionization mass spectrometry (ESI-MS). Using this approach, all compounds demonstrated reactivity with sulfenic acid similar to dimedone and gave distinct adducts with AhpC by mass spectrometry (Poole *et al.*, 2005, 2007). This result indicates that the addition of the hydrocarbon

chain and reporter group, and the lack of the dimethyl group present in dimedone, do not interfere with sulfenic acid reactivity. To confirm the specificity of these reagents and dimedone toward only the sulfenic acid forms of Cys, control reactions were conducted and demonstrated that the thiol, disulfide, or hyperoxidized forms of AhpC (wild type or C165S) did not react with the original two compounds (DCP-MAB and DCP-MCC) and dimedone, based on the lack of ESI-MS-detectable adduct formation (Poole *et al.*, 2005). To test for general cross-reactivity of these reagents with other oxidized sulfur-containing functional groups, we tested the reactivity of dimedone, as a model reagent, with one *S*-nitrosothiol and two sulfoxides. Dimedone did not react with *S*-nitrosoglutathione (GSNO) over 1 h at room temperature as judged by absorbance spectroscopy. In addition, nuclear magnetic resonance (NMR), spectroscopic, and chemical isolation experiments showed that dimedone does not react with aqueous solutions of either dimethyl sulfoxide or methionine sulfoxide. Although dimedone is known to react with both aldehydes and amines (Benitez and Allison, 1974; Halpern and James, 1964; Vogel, 2005), control reactions demonstrated that these reactivities are only exhibited under very basic or organic solvent conditions (Poole *et al.*, 2005). The failure of these same compounds to react with either reduced or oxidized wild type or reduced or hyperoxidized (sulfinic or sulfonic acids) C165S AhpC proteins also indicate that these compounds do not react with protein amine groups under these conditions. In addition, a C165S adduct with hydroxynonenal was unreactive with DCP-FL1. Taken together, these results demonstrate the specificity of the reaction of these compounds for sulfenic acids in proteins in aqueous buffers.

3.1.2. Measuring rates of DCP-linked probe incorporation into pure proteins

Reactivity of protein sulfenic acids toward dimedone-based chemical probes is a complex function of the accessibility, electrostatic microenvironment, and stability of the sulfenic acid species within each protein; the specific nature of the probe will undoubtedly influence the reaction rate as well. To measure the rate of reaction, the sulfenic acid (or potentially sulfenamide) form of pure proteins can be generated, incubated with the reagent of interest for varying times, and then rapidly exchanged via a Bio-Gel P6 spin column into ammonium bicarbonate for analysis by ESI-time of flight (TOF) or matrix-assisted laser desorption/ionization-time of flight (MALDI-TOF) MS. Changes in intensity of peaks corresponding to the various mass components observed can then be fit to an appropriate kinetic model to evaluate rates of alkylation by the reagent; this is best accomplished in cases where hyperoxidation of the sulfenic acid is relatively slow compared with alkylation.

Three proteins known to form regulatory or catalytic sulfenic acids were investigated to address probe reactivity using DCP-Bio1 (Fig. 3.2). The first two proteins, alkyl hydroperoxide reductase C component (AhpC) and a methionine sulfoxide reductase protein (fRMsr), are oxidative defense enzymes known to form a sulfenic acid intermediate at the active site Cys during the course of turnover with their respective substrates, hydroperoxides or *R*-methionine sulfoxide. For each protein, all Cys other than the peroxide-sensitive Cys were removed by mutagenesis (C165S mutant of AhpC, with Cys46 remaining, and C84,94S mutant of fRMsr, with Cys118 remaining) (Ellis and Poole, 1997; Lin *et al.*, 2007) in order to stabilize the active site sulfenic acid, at least with respect to disulfide bond formation which is normally the next step of the mechanism. Papain is a cysteine protease with a low pK_a Cys at the active site that is sensitive to oxidation by hydrogen peroxide, reversibly blocking its protease activity (Allison, 1976).

To assess sulfenic acid alkylation rates, proteins are first incubated with 10 m*M* DTT for 30 min at room temperature, then excess DTT is removed using a Bio-Gel P6 spin column preequilibrated in 25 m*M* potassium phosphate, pH 7.0, and 100 μM DTPA (DTPA is a metal chelator). At this point, stable sulfenic acid forms of the protein to be assayed can be generated in advance of the alkylation reaction, or the protein oxidation reaction can be conducted in the presence of the DCP-Bio1 to help promote alkylation and avoid hyperoxidation in the presence of excess oxidant or air. For the experiments to assess alkylation rates, the sulfenic acid form of fRMsr was prepared in advance by incubation with a 100-fold excess of methionine sulfoxide for 2 min and removal of the excess amino acid using a Bio-Gel P6 column, and then DCP-Bio1 was added. Because papain and C165S AhpC are somewhat prone to hyperoxidation under aerobic conditions, as noted during the MS analyses, these proteins were oxidized by one (AhpC) or two (papain) equivalents of hydrogen peroxide after the addition of DCP-Bio1. The reaction was allowed to proceed at pH 7.0 and, at various times, a portion of the reaction mixture was rapidly exchanged into 50 m*M* ammonium bicarbonate using a Bio-Gel P6 spin column and analyzed by MS (Table 3.1).

The rates of probe incorporation into the three proteins are very different, as shown in Table 3.1, with papain (1.65 min^{-1}) being faster than either fRMsr (0.13 min^{-1}) or AhpC (0.003 min^{-1}). These data suggest that the sulfenic acid intermediate in papain is more accessible and/or reactive than in C84, 94S fRMsr, and C165S AhpC. The results for AhpC are consistent with previous studies showing that alkylation of AhpC by IAAm is very slow, presumably due to relative inaccessibility of Cys46 at the active site (Nelson *et al.*, 2008).

Table 3.1 Rates of DCP-Bio1 incorporation into pure proteins at pH 7.0 and 25 °C[a]

Proteins	Rate (min^{-1})
Papain	1.65 ± 0.22
fRMsr	0.13 ± 0.014
AhpC	0.003 ± 0.0004

[a] For AhpC and papain, 50 μM of prereduced protein was incubated in the presence of 1 m*M* DCP-Bio1, 25 m*M* potassium phosphate, pH 7.0, 100 μM DTPA with one (AhpC) or two (papain) equivalents of hydrogen peroxide. fRMsr was oxidized with a 100-fold excess of methionine sulfoxide; excess methionine sulfoxide was removed using a Bio-Gel P6 column, and the protein was diluted into a solution containing 2 m*M* DCP-Bio1 to give final concentrations of 50 μM fRMsr and 1 m*M* DCP-Bio1 in 5 m*M* potassium phosphate buffer, pH 7.0. At each timepoint, the reaction was quenched by rapidly removing compound using a Bio-Gel P6 spin column equilibrated in 50 m*M* ammonium bicarbonate. For AhpC and papain, 50% acetonitrile and 1% formic acid were added to each sample followed by direct infusion into an ESI-TOF MS. fRMsr was measured by MALDI-TOF MS using sinapinic acid as the matrix. The time-dependent appearance of alkylated protein by MS analysis was fit to a single exponential equation to obtain first-order rates. Alternatively, both the oxidation and alkylation rates for papain could be evaluated using KinTekSim and the kinetic model A → B → C, where A is the R–SH form, B the R–SOH form, and C the biotinylated form of papain (Poole *et al.*, 2007).

3.1.3. Effects of pH on probe incorporation into pure proteins

Variation of buffer pH may affect the rate at which oxidized proteins are alkylated with the DCP-linked probes either due to a change in the inherent rate at which the probe reacts with sulfenic acids or due to a change in accessibility and/or microenvironment of the target sulfenic acid. To assess the effect of pH changes on reactivity of the sulfenic acid in fRMsr, oxidized protein was prepared as described above, then diluted 1:1 into buffers containing various concentrations of DCP-Bio1 to obtain final pH values of 5.5 and 8.0. First-order reaction rates from three independent experiments were obtained for each buffer and reagent concentration. Results with oxidized fRMsr indicated that the labeling rate for this protein is constant between pH 5.5 and 8.0 (an equivalent rate was also observed at pH 7, Table 3.1), with an overall second-order reaction rate of 0.12 ± 0.012 mM^{-1} min^{-1} (Fig. 3.3). These data suggest that there is no effect of pH between 5.5 and 8 on the inherent reactivity of DCP-Bio1 toward sulfenic acids.

3.2. Protocols for labeling cysteine sulfenic acids within cellular proteins

3.2.1. Choice of approaches for labeling cysteine sulfenic acids within cellular proteins

We have synthesized a range of sulfenic acid-directed compounds and the choice of compound will depend on the types of experiments that are planned. The biotin-linked compounds (DCP-Bio1, DCP-Bio2, and

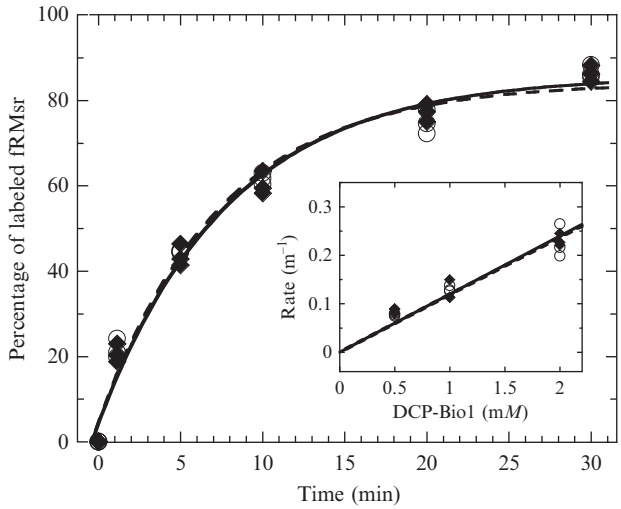

Figure 3.3 Effects of pH on incorporation of biotinylated probe into oxidized fMsr. Oxidized fRMsr (prepared by incubation with excess methionine sulfoxide in 5 m*M* potassium phosphate buffer, pH 7.0, as described in the text) was diluted 1:1 into either 50 m*M* MES, 100 m*M* DTPA, pH 5.3 or 50 m*M* Tris–HCl, 100 m*M* DTPA, pH 8.0, to a final concentration of 50 μM fRMsr, 0.5–2 m*M* DCP-Bio1, and a final pH of 5.5 (closed diamonds) or 8.0 (open circles). At the given incubation time, a sample of the reaction mixture was applied to a Bio-Gel P6 spin column to remove small molecules and exchange the protein into 50 m*M* ammonium bicarbonate, and then analyzed using MALDI-TOF MS using sinapinic acid as the matrix. Shown is the primary plot of the data obtained with 1 m*M* DCP-Bio, fit to a single exponential equation, yielding a first-order rate of 0.13 ± 0.014 min^{-1}. Using the secondary plot (inset), the second-order rates at both pH values were indistinguishable, at 0.12 ± 0.012 mM^{-1} min^{-1}. Each point represents a single replicate.

DCP-Bio3) are particularly powerful as they provide a means to affinity capture labeled proteins prior to analysis. DCP-Bio1 has been the most widely used among these reagents. We have also developed a series of compounds linked to fluorescent groups including methoxycoumarin (DCP-MCC), isatoic acid (DCP-MAB), fluorescein (DCP-FL1, DCP-FL2), and rhodamine (DCP-Rho1, DCP-Rho2). Finally, we have also generated an azide-linked reagent (DCP-N3) that can, after labeling, be further derivatized to any reporter group containing an alkyne or phosphine using either click chemistry or Staudinger ligation techniques, respectively (Reddie and Carroll, 2008).

With purified proteins, trapping of sulfenic acids can be conducted with reagent already present at the time of oxidant addition (AhpC and papain, above; Conway *et al.*, 2004), or with pretreatment of the protein prior to reagent addition, relying on generation of a relatively stable sulfenic acid

(fRMsr, above). Similarly, oxidized proteins can be cumulatively trapped over time within living cells or sampled at various times after treatment using lysis buffer containing the chemical probe. Neither approach is ideal; trapping of sulfenic acids at the time of cell lysis is dependent on the time chosen between stimulation and lysis and may cause certain sulfenic acids to be missed due to the transient nature of this species in many proteins. In contrast, trapping of sulfenic acids (e.g., by dimedone addition) within intact cells during the progression of signal transduction processes can and does alter the course and output of signaling pathways (Michalek *et al.*, 2007), and therefore does not reflect oxidation patterns of proteins during the normal course of signaling. Extent of labeling of given proteins using this latter approach may also reflect more of an accumulation of the product over time due to rapid redox cycling rather than serving as a readout of the amount of a given sulfenic acid form present at any one time in the intact cell. Because we are most interested in obtaining a "snapshot" of protein oxidation that reflects a given point in time after cell stimulation, we typically trap sulfenic acids during cell lysis. As there are situations where *in situ* labeling is more desirable, we provide below brief protocols for both approaches.

3.2.2. Protocol for "*in situ*" labeling of sulfenic acid-containing proteins in live cells

Cell permeability of the labeling reagent, which is observed with DCP-Bio1, DCP-Rho1, DCP-Rho2, and DCP-N3, allows for alkylation of protein sulfenic acids *in situ* prior to disruption of cells. Although one might expect the ester linkage of DCP-Bio1 to be subject to hydrolysis by nonspecific esterases in cells, our findings to date suggest that this reagent is resistant to such cleavage.

Briefly, cells of interest are grown in the appropriate media to 60–90% confluence in 100-mm dishes. The cells are then switched to media containing 100 μM DCP-Bio1 for a total of 30 or 60 min, and treated or not with the stimulant of interest during the course of this incubation. Following labeling, PBS is used to wash the cells three times to remove the excess DCP-Bio1 (or other reagent) and the stimulant. For further biochemical analyses, the cell lysates containing biotinylated proteins are analyzed using one of the methods described in the following chapter (Nelson *et al.*, 2010).

3.2.3. Protocol for labeling sulfenic acid-containing cellular proteins at time of lysis

Because cell lysates are exposed to oxidative stress as a result of lysis and exposure to atmospheric oxygen, the lysis buffer described here has been developed to minimize protein oxidation after cell disruption. Following treatment of cells with the stimulant of interest for the desired time, cells are washed with PBS to remove excess media and serum proteins, and

immediately scraped from the plate into lysis buffer containing DTPA, protease and phosphatase inhibitors, 1 m*M* DCP-Bio1, 200 units/ml catalase, 10 m*M* NEM, and 10 m*M* IAAm (note that phosphatase inhibitors may in some cases protect protein tyrosine phosphatases with oxidized Cys residues from being labeled by the probe). Typically, samples are incubated on ice for 1 h to let the reagent react with sulfenic acids then frozen at −80 °C to preserve the samples prior to analysis. We have found that sonication increases the amount of label incorporated into proteins, but may promote the adventitious oxidation that we are trying to avoid. In order to further protect against postlysis cysteine oxidation, we include catalase (which removes hydrogen peroxide) and DTPA (which complexes metals and prevents hydrogen peroxide generation through the Fenton reaction) to the lysis buffer containing the labeling agent. The NEM and IAAm are added to block free thiols and help prevent the formation of sulfenic acids after cell lysis. Previous studies have shown that individual Cys residues may be preferentially alkylated by either IAAm or NEM (Dennehy, 2006); therefore, we include both reagents. *Note*: for downstream MS analysis, it may be desirable to minimize the potential modifications and to only use one of the alkylating agents. Biotinylated proteins can be analyzed using methods shown in Figs. 3.4 and 3.5 and described in the accompanying chapter (Nelson *et al.*, 2010). As expected, excluding alkylating agents from the lysis buffer appears to cause an increase in nonspecific labeling of cellular proteins (Fig. 3.4), and this effect is further exacerbated if catalase is also excluded (not shown).

3.2.4. Effects of variables such as protein concentration and reagent concentration on extent of probe incorporation into cellular proteins

In addition to changes in lysis buffer components, the amount and/or concentration of cellular protein and the concentration of chemical trapping agent also affect the degree to which sulfenic acids are labeled. We have observed that the extent of DCP-Bio1 incorporation is affected by the protein concentration of the samples; as the protein concentration decreases, a higher percentage of cellular proteins are labeled by DCP-Bio1. This effect appears to be independent of stimulation with a cellular cytokine known to release intracellular reactive oxygen species, tumor necrosis factor α (Fig. 3.5A). The amount of label incorporation is also increased with increasing concentration of the DCP-Bio1 reagent, due at least in part to the better ability of the reagent to successfully outcompete other fates for the sulfenic acids (Fig. 3.5B). The presence of several strong bands in the samples, even in the absence of DCP-Bio1 (Fig. 3.5B), demonstrates the importance of including a "no reagent" control to identify protein bands that are present in the sample due to endogenous biotinylation. Together, these findings indicate that the optimal reagent

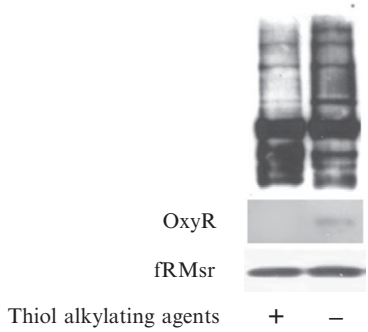

Figure 3.4 Addition of thiol alkylating agents helps block postlysis protein oxidation during incubation of cellular proteins with DCP-Bio1 in lysis buffer. For these experiments, HEK293 cells were grown in complete DMEM low glucose medium supplemented with 10% fetal bovine serum. Cells from each 100-mm plate were scraped into 1 ml PBS and transferred to microtubes. Cells were spun down and lysed with lysis buffer containing 0.1% SDS and protease and phosphatase inhibitors, as well as 1 m*M* DCP-Bio1 and 200 units/ml catalase. Thiol alkylating agents (10 m*M* NEM and 10 m*M* IAAm) were included or not as indicated. After incubation of the mixture on ice for 1 h, biotinylated proteins were captured using Streptavidin agarose resin. Mutant fRMsr was biotinylated with biotin maleimide (see Nelson *et al.*, 2010, for detailed protocol) and 1 μg fRMsr/500 μg of cell lysate was added to each sample prior to affinity capture for use as a procedural and loading control. Prereduced OxyR (mutated to contain only the peroxide-sensitive Cys) was included in the lysis buffer and used as a sensor of postlysis cysteine oxidation. The presence of biotinylated OxyR in the avidin-enriched material was visualized by Western blot using an antibody that recognizes the His tag.

concentration and cell number will have to be determined for each system and carefully matched in all experiments in order to obtain reproducible results.

3.2.5. OxyR as a reporter of postlysis cysteine oxidation

E. coli OxyR is a transcription factor which is directly activated by H_2O_2 through the oxidation of the reactive Cys residue, Cys199. In wild-type protein, the oxidation results in the formation of a sulfenic acid at Cys199 which subsequently reacts with Cys208 to form a disulfide bond (Choi *et al.*, 2001; Zheng *et al.*, 1998). A truncated construct of the C-terminal regulatory domain of OxyR lacking C208 as well as other nonperoxide sensitive cysteinyl residues, designated C4A-RD C208S OxyR, was previously generated (Choi *et al.*, 2001). Beginning with the pET21a-derived expression vector for this protein construct, we used the QuikChange XL Site-Directed Mutagenesis Kit (Stratagene) to remove the stop codon and express the protein with a C-terminal His tag.

The His-tagged C4A-RD C208S OxyR construct was expressed in *E. coli* strain B834 (DE3) using autoinduction medium PASM-5052

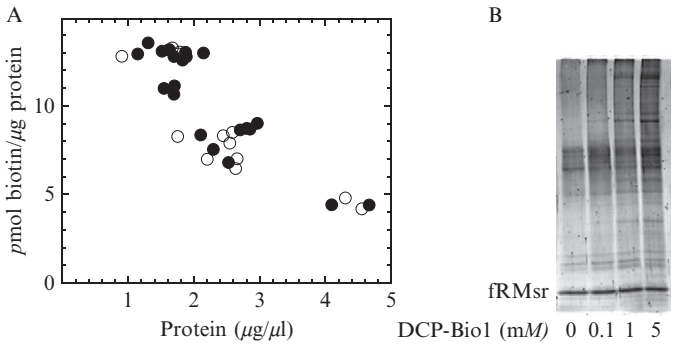

Figure 3.5 Effects of protein and reagent (DCP-Bio1) concentration on incorporation of biotin into cellular proteins. HEK293 cells were cultured and harvested as described in the text. After labeling with 1 m*M* DCP-Bio1, free probe was removed from the samples using a Bio-Gel P6 spin column and prepared for analyses as described in greater detail in the following chapter (Nelson *et al.*, 2010). In panel A, tumor necrosis factor alpha treated (closed circles) and untreated (open circles) samples were assessed for total biotin incorporation into proteins using the FluoReporter biotin incorporation assay kit from Invitrogen. For panel B, prebiotinylated fRMsr mutant was added to the starting protein concentrations prior to affinity capture for use as a procedural and loading control. Biotinylated proteins were captured using streptavidin-agarose, and extensively washed with 1% SDS, 4 *M* urea in PBS, 1 *M* NaCl, 100 m*M* ammonium bicarbonate, and deionized H_2O. The samples were eluted with 2% SDS in 50 m*M* Tris, pH 8.0, analyzed by SDS-PAGE, and stained with SYPRO Ruby.

overnight at 37 °C. Following centrifugation at 5000×*g* for 15 min, the washed cell pellets were resuspended in ~100 ml 50 m*M* sodium phosphate, pH 7.0, containing 10 m*M* 2-mercaptoethanol, and lysed with a pneumatic cell homogenizer (Avestin EmulsiFlex-C5). After centrifugation at 20,000×*g*, streptomycin sulfate (1%, w/v) was added to the supernatant, with stirring, for 15 min prior to centrifugation. The supernatant was filtered and bound to a Ni-NTA Superflow (Qiagen) column. The His-tagged C4A-RD C208S OxyR was eluted by gradually increasing the imidazole concentration to 250 m*M*. The eluted protein was concentrated and loaded onto a gel filtration (Superose 12 PG) column equilibrated with 50 m*M* Tris–HCl, pH 8.0, containing 100 m*M* NaCl, 100 μ*M* DTPA, and 2 m*M* DTT. The pure protein was concentrated to ~10 mg/ml based on an ε_{280} of 14,440 M^{-1} cm^{-1} and molecular weight of 26,470 Da (ε_{280} and molecular weight of His-tagged C4A-RD C208S OxyR were calculated using http://ca.expasy.org/tools/protparam.html) and stored at −80 °C.

Attempts to determine a rate for DCP-Bio1 incorporation into the OxyR construct as reported for the other three test proteins (Table 3.1) were inconclusive due to the high rate of hyperoxidation of this protein in the presence of oxygen or a second molecule of H_2O_2. With OxyR at

neutral pH, no further incorporation of DCP-Bio1 labeling is observed after 5 min and sulfinic and sulfonic acids can be observed within 2 min of the addition of 1.2 equivalents of H_2O_2. While this does not interfere with the ability to use OxyR as an effective sensor of adventitious oxidation occurring during lysis, it complicates the kinetic analyses.

As shown in Fig. 3.4, OxyR can be used as a "negative" control to monitor the amount of postlysis Cys oxidation. For this purpose, add reduced OxyR to the lysis buffer prior to harvesting the cells. The extent of undesired OxyR oxidation can be monitored by probing the OxyR content in the biotin pulldown using an antibody to the His-tag (Fig. 3.4). Using this technique, we confirmed that excluding thiol alkylating agents NEM and IAAm from the lysis buffer causes an increase in postlysis labeling (Fig. 3.4) since reduced OxyR becomes labeled under this experimental condition.

4. Summary

The development of a series of tagged sulfenic acid-directed compounds paves the way to determine the sites and proteins that are sensitive to cysteine oxidation in the cell as well as the cellular conditions under which such oxidations occur. We have shown that these compounds are reactive and specific. The rates with which DCP-Bio1 reacts toward sulfenic acids are significantly different for each of three pure proteins, papain, the C84, 94S mutant of fRMsr, and the C165S mutant of AhpC (Table 3.1), suggesting that the reaction of our DCP-linked probes is highly dependent on the accessibility and stability of sulfenic acid intermediates within their protein microenvironment. Interestingly, there was no difference in the rates of probe incorporation into fRMsr between pH 5.5 and 8.0. We have also provided protocols to label sulfenic acid modifications in cellular proteins; either *in situ* labeling of intact cells or labeling at the time of lysis can be conducted. We have investigated components of the lysis buffer and highly recommend the addition of alkylating reagents and catalase to prevent the formation of sulfenic acid subsequent to cell lysis. Data presented herein also indicate that the extent of labeling is highly dependent on protein concentration in the sample and highlight the need to standardize as much as possible the protein and reagent concentrations during labeling, especially when these reagents are applied to monitor temporal changes of oxidation or in comparative studies.

ACKNOWLEDGMENTS

This work was supported by NIH grants R21 CA112145 and R33 CA126659 to LBP and by an Established Investigator Grant to LBP from the American Heart Association. An NIH fellowship award to KJN (F32 GM074537) is also acknowledged.

REFERENCES

Allison, W. S. (1976). Formation and reactions of sulfenic acids in proteins. *Acc. Chem. Res.* **9,** 293–299.

Benitez, L. V., and Allison, W. S. (1974). The inactivation of the acyl phosphatase activity catalyzed by the sulfenic acid form of glyceraldehyde 3-phosphate dehydrogenase by dimedone and olefins. *J. Biol. Chem.* **249,** 6234–6243.

Charles, R. L., Schröder, E., May, G., Free, P., Gaffney, P. R., Wait, R., Begum, S., Heads, R. J., and Eaton, P. (2007). Protein sulfenation as a redox sensor: Proteomics studies using a novel biotinylated dimedone analogue. *Mol. Cell Proteomics* **6,** 1473–1484.

Choi, H., Kim, S., Mukhopadhyay, P., Cho, S., Woo, J., Storz, G., and Ryu, S. (2001). Structural basis of the redox switch in the OxyR transcription factor. *Cell* **105,** 103–113.

Conway, M. E., Poole, L. B., and Hutson, S. M. (2004). Roles for cysteine residues in the regulatory CXXC motif of human mitochondrial branched chain aminotransferase enzyme. *Biochemistry* **43,** 7356–7364.

Dennehy, M. K., Richards, K. A., Wernke, G. R., Shyr, Y., and Liebler, D. C. (2006). Cytosolic and nuclear protein targets of thiol-reactive electrophiles. *Chem. Res. Toxicol.* **19,** 20–29.

Ellis, H. R., and Poole, L. B. (1997). Roles for the two cysteine residues of AhpC in catalysis of peroxide reduction by alkyl hydroperoxide reductase from *Salmonella typhimurium*. *Biochemistry* **36,** 13349–13356.

Halpern, B., and James, L. B. (1964). Dimedone (5, 5-dimethylcyclohexane-1,3-dione) as a protecting agent for amino groups in peptide synthesis. *Aust. J. Chem.* **17,** 1282–1287.

Leonard, S. E., Reddie, K. G., and Carroll, K. S. (2009). Mining the thiol proteome for sulfenic acid modifications reveals new targets for oxidation in cells. *ACS Chem. Biol.* **4,** 783–799.

Lin, Z., Johnson, L. C., Weissbach, H., Brot, N., Lively, M. O., and Lowther, W. T. (2007). Free methionine-(R)-sulfoxide reductase from *Escherichia coli* reveals a new GAF domain function. *Proc. Natl. Acad. Sci. USA* **104,** 9597–9602.

Michalek, R. D., Nelson, K. J., Holbrook, B. C., Yi, J. S., Stridiron, D., Daniel, L. W., Fetrow, J. S., King, S. B., Poole, L. B., and Grayson, J. M. (2007). The requirement of reversible cysteine sulfenic acid formation for T cell activation and function. *J. Immunol.* **179,** 6456–6467.

Nelson, K. J., Parsonage, D., Hall, A., Karplus, P. A., and Poole, L. B. (2008). Cysteine pK_a values for the bacterial peroxiredoxin AhpC. *Biochemistry* **47,** 12860–12868.

Nelson, K. J., Klomsiri, C., Codreanu, S. G., Soito, L., Liebler, D. C., Rogers, L. A. C., Daniel, L. W., and Poole, L. B. (2010). Use of dimedone-based chemical probes for sulfenic acid detection: methods to visualize and identify labeled proteins. *Methods Enzymol.* **472,** 95–115.

Oshikawa, J., Urao, N., Kim, H. W., Kaplan, N., Razvi, M., McKinney, R., Poole, L. B., Fukai, T., and Ushio-Fukai, M. (2010). Extracellular SOD-derived H_2O_2 promotes VEGF signaling in caveolae/lipid rafts and post-ischemic angiogenesis in mice. *PLoS One* (in press).

Poole, L. B., and Ellis, H. R. (1996). Flavin-dependent alkyl hydroperoxide reductase from *Salmonella typhimurium*. 1. Purification and enzymatic activities of overexpressed AhpF and AhpC proteins. *Biochemistry* **35,** 56–64.

Poole, L. B., and Ellis, H. R. (2002). Identification of cysteine sulfenic acid in AhpC of alkyl hydroperoxide reductase. *Methods Enzymol.* **348,** 122–136.

Poole, L. B., and Nelson, K. J. (2008). Discovering mechanisms of signaling-mediated cysteine oxidation. *Curr. Opin. Chem. Biol.* **12,** 18–24.

Poole, L. B., Karplus, P. A., and Claiborne, A. (2004). Protein sulfenic acids in redox signaling. *Annu. Rev. Pharmacol. Toxicol.* **44,** 325–347.

Poole, L. B., Zeng, B. B., Knaggs, S. A., Yakubu, M., and King, S. B. (2005). Synthesis of chemical probes to map sulfenic acid modifications on proteins. *Bioconjug. Chem.* **16,** 1624–1628.

Poole, L. B., Klomsiri, C., Knaggs, S. A., Furdui, C. M., Nelson, K. J., Thomas, M. J., Fetrow, J. S., Daniel, L. W., and King, S. B. (2007). Fluorescent and affinity-based tools to detect cysteine sulfenic acid formation in proteins. *Bioconjug. Chem.* **18,** 2004–2017.

Reddie, K. G., and Carroll, K. S. (2008). Expanding the functional diversity of proteins through cysteine oxidation. *Curr. Opin. Chem. Biol.* **12,** 746–754.

Reddie, K. G., Seo, Y. H., Muse Iii, W. B., Leonard, S. E., and Carroll, K. S. (2008). A chemical approach for detecting sulfenic acid-modified proteins in living cells. *Mol. Biosyst.* **4,** 521–531.

Salsbury, F. R., Jr., Knutson, S. T., Poole, L. B., and Fetrow, J. S. (2008). Functional site profiling and electrostatic analysis of cysteines modifiable to cysteine sulfenic acid. *Protein Sci.* **17,** 299–312.

Turell, L., Botti, H., Carballal, S., Ferrer-Sueta, G., Souza, J. M., Duran, R., Freeman, B. A., Radi, R., and Alvarez, B. (2008). Reactivity of sulfenic acid in human serum albumin. *Biochemistry* **47,** 358–367.

Vogel, A. I. (2005). Investigation and characterisation of organic compounds. *In* "Vogel's Textbook of Practical Organic Chemistry," (B. S. Furniss, ed.), pp. 1259–1260. Pearson, Singapore.

Zheng, M., Aslund, F., and Storz, G. (1998). Activation of the OxyR transcription factor by reversible disulfide bond formation. *Science* **279,** 1718–1721.

CHAPTER FOUR

Use of Dimedone-Based Chemical Probes for Sulfenic Acid Detection: Methods to Visualize and Identify Labeled Proteins

Kimberly J. Nelson,* Chananat Klomsiri,* Simona G. Codreanu,† Laura Soito,* Daniel C. Liebler,† LeAnn C. Rogers,* Larry W. Daniel,* *and* Leslie B. Poole*

Contents

* Department of Biochemistry, Wake Forest University School of Medicine, Winston-Salem, North Carolina, USA
† Department of Biochemistry, Vanderbilt University School of Medicine, Nashville, Tennessee, USA

Methods in Enzymology, Volume 473
ISSN 0076-6879, DOI: 10.1016/S0076-6879(10)73004-4

Abstract

Reversible thiol modification is a major component of the modulation of cell-signaling pathways by reactive oxygen species. Hydrogen peroxide, peroxynitrite, or lipid hydroperoxides are all able to oxidize cysteines to form cysteine sulfenic acids; this reactive intermediate can be directly reduced to thiol by cellular reductants such as thioredoxin or further participate in disulfide bond formation with glutathione or cysteine residues in the same or another protein. To identify the direct protein targets of cysteine modification and the conditions under which they are oxidized, a series of dimedone-based reagents linked to affinity or fluorescent tags have been developed that specifically alkylate and trap cysteine sulfenic acids. In this chapter, we provide detailed methods using one of our biotin-tagged reagents, DCP-Bio1, to identify and monitor proteins that are oxidized *in vitro* and *in vivo*. Using streptavidin-linked agarose beads, this biotin-linked reagent can be used to affinity capture labeled proteins. Stringent washing of the beads prior to elution minimizes the contamination of the enriched material with unlabeled proteins through coimmunoprecipitation or nonspecific binding. In particular, we suggest including DTT in one of the washes to remove proteins covalently linked to biotinylated proteins through a disulfide bond, except in cases where these linked proteins are of interest. We also provide methods for targeted approaches monitoring cysteine oxidation in individual proteins, global approaches to follow total cysteine oxidation in the cell, and guidelines for proteomic analyses to identify novel proteins with redox sensitive cysteines.

1. Introduction

It is increasingly clear that reversible thiol modification is a major component of the modulation of cell-signaling pathways by reactive oxygen species (ROS). Superoxide anions result from the partial reduction of oxygen by the mitochondrial electron transport chain (Jones, 2006) and are subsequently converted to H_2O_2 either nonenzymatically or by superoxide dismutase. ROS are also generated by activated forms of the enzymes NADPH oxidase, xanthine oxidase, cyclooxygenase, and lipoxygenase (Schneider *et al.*, 2007; Thomas *et al.*, 2008). In general, the initial product of cysteine oxidation by H_2O_2, peroxynitrite, or lipid hydroperoxides is cysteine sulfenic acid, suggesting a pivotal importance for this modification in the response of proteins to ROS. Sulfenic acid-modified proteins can be directly reduced to thiol by cellular reductants or further participate in disulfide bond formation with glutathione or cysteine residues in the same or another protein.

Most evidence of catalytic or regulatory sulfenic acid formation has come from individual studies of purified proteins including peroxiredoxins,

organic hydroperoxide resistance protein (Ohr), NADH peroxidase, and methionine sulfoxide reductase (Claiborne *et al.*, 1999; Poole *et al.*, 2004). The redox status of cysteine has been shown to regulate cellular metabolism through oxidation of glyceraldehyde-3-phosphate dehydrogenase (GAPDH) (Cotgreave *et al.*, 2002; Schmalhausen *et al.*, 1999) and MetE (Hondorp and Matthews, 2004), and to regulate the molecular chaperone activity of HSP33 (Jakob *et al.*, 1999) and the activity of protein tyrosine phosphatases including PTP1B and PTEN (Tonks, 2005). Oxidative cysteine modifications have also been shown to control transcriptional regulation by OxyR (Zheng *et al.*, 1998), OhrR (Fuangthong and Helmann, 2002; Hong *et al.*, 2005; Panmanee *et al.*, 2006), RsrA (Kang *et al.*, 1999), Yap1p (Kuge *et al.*, 2001), and p53 (Rainwater *et al.*, 1995).

Because cysteine sulfenic acid is unstable in many proteins, studies have been limited by the ability to monitor and identify proteins and sites that have redox-regulated cysteines. To fill this gap, our labs and other groups have developed a series of reagents, based on dimedone, that specifically alkylate and, therefore, trap cysteine sulfenic acids; these chemical probes are or can be linked to affinity or fluorescent tags (Fig. 4.1) (Leonard *et al.*, 2009; Poole and Nelson, 2008; Poole *et al.*, 2007; Reddie *et al.*, 2008). These reagents are designed to enable enrichment and sensitive detection of proteins or peptides bearing sulfenic acid modifications. Though sulfenic acids likely represent a dynamic and transient oxidation product, their unique chemistry allows them to be captured by dimedone-based labeling reagents before progression to a potentially more complex array of disulfide-bonded or oxidized products. Even rapid "trapping" of sulfenic acids in proteins is still likely to yield substoichiometric amounts of label incorporated into given proteins due to the generally transient nature of the modification. Reliable quantification based on extent of probe incorporation is likely to be difficult

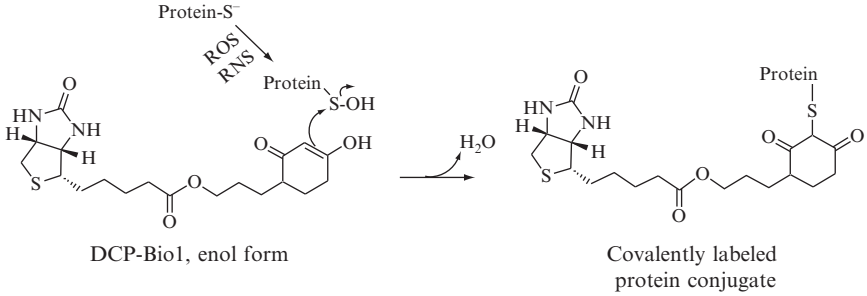

Figure 4.1 Reaction of DCP-Bio1 with cysteine sulfenic acid. The sulfenic acid-reactive reagent designated DCP-Bio1 [3-(2,4-dioxocyclohexyl)propyl 5-((3a*R*,6*S*,6a*S*)-hexahydro-2-oxo-1*H*-thieno[3,4-*d*]imidazol-6-yl)pentanoate] is shown in its enol form, reacting with a protein sulfenic acid to generate a stable, alkylated form of the protein (Poole *et al.*, 2007).

to achieve, though large time-dependent responses in oxidation for individual cellular proteins may be observed across samples within the same experimental set. Despite these challenges, these probes and techniques represent an important step forward in identifying cysteine residues that are oxidized in cells in response to a particular stimulant. As with phosphorylation sites, all oxidation sites are not expected to have the same role (or for that matter any role) in modulating protein function. Not only may cysteine oxidation be stimulatory, inhibitory, or inconsequential to the activity, stability, or localization of a given protein, but sulfenic acids also have the capacity to go on to form multiple products depending on cellular context that may themselves have different functional effects (Poole and Nelson, 2008). The true biochemical evaluation of these sites must ultimately involve both mapping the specific residue being oxidized and evaluating the effect of these oxidations on protein function.

We report here some of the potential applications of these sulfenic acid-specific reagents and provide protocols for visualizing and identifying labeled proteins. The previous chapter in this volume provides detailed protocols and controls for labeling both pure and cellular proteins with these probes (Klomsiri *et al.*, 2010). Although we have developed and used a variety of probes containing fluorescent groups such as rhodamine and fluorescein (Klomsiri *et al.*, 2010; Poole *et al.*, 2007), we have found that biotin-linked reagents are particularly powerful tools because they allow for affinity capture of the labeled proteins and/or peptides. In this chapter, we provide detailed methods using one of our biotin-tagged reagents, DCP-Bio1 (Fig. 4.1) to identify and monitor proteins that are oxidized *in vitro* and *in vivo*. We also provide methods to monitor global changes in cysteine sulfenic acid formation.

2. Biotin-Based Affinity Capture to Identify Proteins Containing Cysteine Sulfenic Acids

The greatest advantage of the biotin-conjugated, sulfenic acid-directed reagents is the ability to use affinity methods to capture the labeled proteins. Because the captured material will be used in many cases to identify labeled proteins and determine the extent of protein labeling, it is very important to ensure that essentially all proteins in the affinity-enriched material contain the biotin modification and are not simply coprecipitating with the labeled proteins. Thus, we have developed a protocol to stringently wash the streptavidin beads prior to elution. In particular, including DTT in one of the washes ensures that unlabeled proteins covalently linked to biotinylated proteins through a disulfide bond will not be included in the eluted material.

2.1. Materials

2.1.1. Solutions

1. 500 m*M* biotin maleimide in dimethyl sulfoxide (DMSO)
2. 100 m*M* 1,4-dithio-DL-threitol (DTT) in dH_2O
3. 100 m*M* diethylene triamine pentaacetic acid (DTPA) in 1 *M* sodium hydroxide
4. 25 m*M* potassium phosphate, pH 7.0, 100 μM DTPA
5. Empty spin columns with ~1.2-ml bed volume (e.g., Bio-Spin Chromatography columns from Bio-Rad)
6. Bio-Gel P6 desalting resin (Bio-Rad); 1 ml resin is loaded into empty spin column and equilibrated with 3 column volumes (CV) of buffer
7. Spin column with screw cap and column plug – 500-μl bed volume (e.g., Pierce Spin Columns – screw cap with Luer-Lok adaptors)
8. Streptavidin beads (e.g., Pierce High Capacity Streptavidin–Agarose Resin)
9. Sepharose CL-4B (or other resin similar to the streptavidin support material)
10. Phosphate-buffered saline (PBS): 100 m*M* sodium phosphate, 150 m*M* sodium chloride, pH 7.2
11. 8 *M* urea in PBS
12. Wash solution 1: 1% SDS in dH_2O
13. Wash solution 2: 4 *M* urea in PBS
14. Wash solution 3: 1 *M* NaCl in dH_2O
15. Wash solution 4: 100 μM ammonium bicarbonate with 10 m*M* DTT
16. Wash solution 5: 100 μM ammonium bicarbonate
17. Deionized H_2O (dH_2O)
18. Elution buffer for 1D gel electrophoresis: 2% SDS, 50 m*M* Tris–HCl, 1 m*M* EDTA, pH 8.0
19. Elution buffer for 2D gel electrophoresis: 8 *M* urea, 2% CHAPS

2.1.2. Proteins

1. Protein samples labeled with biotin-linked reagent specific for sulfenic acid (e.g., DCP-Bio1) (Poole *et al.*, 2007); see accompanying chapter for suggested labeling protocols (Klomsiri *et al.*, 2010).
2. *Salmonella typhimurium* AhpC C165S mutant, purified as described previously (Nelson *et al.*, 2008; Poole and Ellis, 1996) and stored at –20 °C in 5 m*M* DTT. Prior to conducting experiments, DTT is removed using a Bio-Gel P6 spin column equilibrated in 25 m*M* potassium phosphate, pH 7.0, 100 μM DTPA. Alternatively, any other pure protein containing at least one cysteine residue can be used.

2.2. Methods

2.2.1. Use of biotinylated AhpC as a procedural control for affinity capture of biotinylated samples

To ensure that changes to biotinylation levels between a set of samples is due to physiological changes and not variation in the efficiency of the affinity capture and elution procedure, we add a biotinylated control protein to each sample before affinity capture. We typically use a biotinylated version of the C165S mutant of *S. typhimurium* AhpC because large amounts of this recombinant protein can be purified in *Escherichia coli* and because the presence of only one cysteine allows for stoichiometric labeling. This protein is stored in 5 m*M* DTT, which is removed using a desalting column (i.e., PD10 or Bio-Gel P6). To do this, spin columns (1.2-ml bed volume) containing ~1 ml Bio-Gel P6 Resin are equilibrated with 25 m*M* potassium phosphate, 100 μM DTPA, pH 7.0, centrifuged for 25 min at 1000×*g*, and moved to clean, labeled microfuge tubes. Samples are applied to the top, the column is centrifuged for 2 min at 1000×*g*, then the material from the flow-through is supplemented with biotin maleimide from a 200 m*M* stock to a final concentration of 10 m*M* (DMSO concentration in final solution should be no more than 2%) and incubated at room temperature overnight. Excess biotin maleimide is removed using a second desalting column equilibrated in 25 m*M* potassium phosphate with 100 μM DTPA, pH 7.0, and the concentration of C165S AhpC is determined based upon absorbance at 280 nm ($\varepsilon = 24{,}300\ \mathrm{M}^{-1}\ \mathrm{cm}^{-1}$). Using this procedure, C165S AhpC was fully labeled with biotin maleimide based upon matrix-assisted laser desorption/ionization time of flight (MALDI-TOF) mass spectrometry (MS) analysis.

Any pure protein can be used for this purpose as long as it contains at least one Cys residue and is not present in the sample to be analyzed. For proteins not stored in DTT, 10 m*M* DTT should first be added and incubated for 30 min at room temperature prior to the first desalting column and alkylation with biotin maleimide.

2.2.2. Sample preparation to remove unreacted DCP-Bio1 and to add control protein

Cell lysates are labeled with DCP-Bio1 (Poole *et al.*, 2007) according to the protocol described in the preceding chapter (Klomsiri *et al.*, 2010). In order to prevent further biotinylation of proteins due to nonphysiological oxidation and to prevent free DCP-Bio1 from competing with biotinylated protein for binding to the streptavidin binding sites on the resin, proteins in the cell lysate are separated from small molecules immediately upon thawing. Columns containing ~1 ml Bio-Gel P6 resin are equilibrated with 2 CV PBS and 2 CV 2 *M* urea in PBS, pH 7.2. Columns are centrifuged for 2 min at 1000×*g* and moved to clean, labeled microfuge

tubes. Cell lysates are applied to the top of each 1-ml column (if samples are more than 0.2 ml, multiple columns are used). Samples are centrifuged for 2 min at 1000×*g* and the flow-through material contains the small molecule-free protein. Protein concentrations of each sample are measured using an appropriate assay, such as the BCA Protein Assay (Pierce) or the DC Protein Assay (Bio-Rad). Samples are diluted to 1 mg/ml with urea to a final concentration of 2 *M*, and biotinylated C165S AhpC (1 μg/500 μg of cell lysate) is added as a procedural control (prepared as described above).

2.2.3. Capture of biotinylated proteins with stringent washing to prevent coprecipitation of unlabeled proteins

For each sample, one spin column (0.5-ml bed volume with screw cap lid) is prepared with nonliganded support beads (i.e., cross-linked agarose, e.g., Sepharose CL-4B) to remove proteins with a tendency to bind nonspecifically to such beads; a second column with streptavidin–agarose beads is also prepared. The binding capacity of the streptavidin beads is used to determine the resin volume needed for the amount of protein being enriched. For Sepharose CL-4B (Sigma) and High Capacity Streptavidin–Agarose Resin (Pierce), 80 μl of resin is used for a typical sample containing 400 μg cell lysate. For HEK293 cells, 400 μg cellular protein can typically be obtained from two 75% confluent, 100-mm dishes harvested with 150 μl lysis buffer per plate. Both columns are equilibrated with 20 CV 2 *M* urea in PBS, pH 7.2. Immediately prior to adding sample, columns are placed in 1.5-ml microfuge tubes, then centrifuged for 2 min at 1000×*g*.

To remove proteins that might bind nonspecifically to the beads, prepared cell lysates are added to the plugged columns containing Sepharose CL-4B beads, the tops are closed with a screw cap lid, columns are sealed into a clean microfuge tube with Parafilm to prevent leaks, and the samples are incubated for 2 h at 4 °C with constant rotation. Parafilm and plugs are removed and columns are returned to the tubes, then centrifuged for 1000×*g* for 2 min. The flow-through from these columns is transferred to plugged columns containing streptavidin–agarose beads, capped, and sealed into microfuge tubes, and rotated for ~16 h at 4 °C. Column assemblies are centrifuged at 1000×*g* for 2 min to remove unbound proteins.

Beads bound to the biotinylated proteins are washed twice with 4 CV 1% SDS, twice with 4 CV 4 *M* urea, and twice with 4 CV 1 *M* NaCl. For each of these solutions, the first wash is incubated with constant rotation for 30 min at 4 °C and the second wash is applied for 1 min at room temperature prior to centrifugation. These are followed by additional successive washes at room temperature, once with 4 CV 10 m*M* DTT in 100 μ*M* ammonium bicarbonate for 5 min, once with 100 μ*M* ammonium bicarbonate without DTT, and twice with 4 CV dH_2O. For each wash, the beads are resuspended in the wash solution, rotated for the indicated amount of time, centrifuged at

1000×*g* for 2 min, and the supernatant is discarded. The last dH_2O wash is used to remove any resin from the lid of the column.

2.2.4. Elution conditions depend on the downstream application

Although streptavidin has a high affinity for biotin, various elution conditions can be used (Fig. 4.2) and should be selected based upon the intended downstream application. We recommend use of an SDS-containing sample buffer for 1D gel electrophoresis. First, the bottom of the column is stoppered, 2.5 CV of 2% SDS in 50 m*M* Tris–HCl, 1 m*M* EDTA pH 8.0 is added, the cap is replaced loosely to prevent leakage due to pressure build up, the column is placed inside a clean microfuge tube to collect any sample that might leak, and the whole assembly is heated to 90 °C for 10 min (Fig. 4.2 A). For 2D gel electrophoresis, we recommend adding 2.5 CV of 8 *M* urea, 2% CHAPS, and 50 m*M* DTT to the plugged and loosely capped column and heating for 20 min at 37 °C, shaking periodically. If the presence of SDS or urea is problematic for downstream applications (e.g., for MS experiments), alternate elution conditions include incubation with 100 m*M* glycine, pH 2.8 for 10 min at room temperature (Fig. 4.2 A) or proteolytic digestion of the sample while still bound to the streptavidin

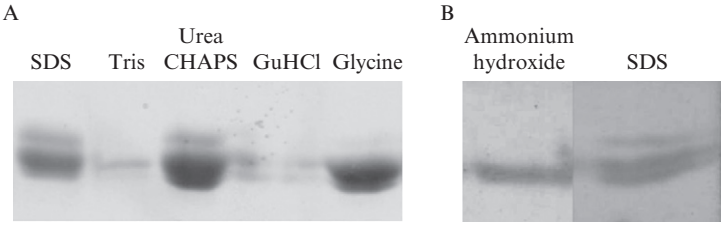

Figure 4.2 Use of various elution conditions to recover biotinylated proteins from streptavidin beads. A. Biotinylated AhpC (180 μg) was incubated with 80 μl streptavidin beads in 250 μl total volume of 2 *M* urea in PBS, pH 7.2 and incubated for 1.5 h at 24 °C. Beads were washed 3 × 0.5 ml 2 *M* urea in PBS, pH 7.2 and aliquotted into five different tubes prior to centrifugation for 2 min at 1000×*g* and removal of the supernatant. Elution solutions (10 μl) were added to each tube and incubated at the appropriate temperature for 10 min. Elution conditions were: 2% SDS in 50 m*M* Tris–HCl, 1 m*M* EDTA, pH 8.0 (90 °C); 50 m*M* Tris–HCl, 1 m*M* EDTA, pH 8.0 (90 °C); 8 *M* urea with 2% CHAPS (37 °C); 8 *M* guanidine hydrochloride (GuHCl) (37 °C); and 100 m*M* glycine, pH 2.8 (24 °C). The amount of AhpC protein in 2 μl of the eluted fraction was visualized by Coomassie Blue stain after SDS–PAGE. B. Sulfenic acid-containing C165S AhpC labeled with DCP-Bio1 was incubated with monoavidin beads overnight, washed three times with PBS buffer, and aliquotted into separate tubes. Samples were either incubated with 2.25 *M* ammonium hydroxide for 16 h at 24 °C or boiled in SDS sample buffer containing β-mercaptoethanol for 10 min, and AhpC in the eluant was visualized as in (A).

beads. Because DCP-Bio1 contains an ester linkage, labeled proteins containing the DCP functional group can be cleaved from the biotin moiety by incubation with 2.25 *M* ammonium hydroxide for ~16 h at 24 °C (Fig. 4.2 B). For all elution conditions, the spin column is centrifuged at 1000 × *g* for 3 min and the flow-through is retained.

3. Detection Methods to Identify Oxidized Proteins and Cysteines

Potential uses for sulfenic acid-specific trapping agents include monitoring of cysteine oxidation of a particular protein under various conditions (targeted approaches), following cysteine oxidation of total cellular proteins in response to various stimuli (global approaches), and identifying novel proteins with redox sensitive cysteine residues (proteomic approaches). In this section, we provide protocols suitable for all of these approaches. Although we briefly touch on techniques including Western blots, immunoprecipitation (IP), and MS analysis, detailed protocols for these are only given for the proteins studied herein, and we focus on how these techniques can be adapted to identify and monitor proteins labeled with DCP-Bio1 and related compounds.

3.1. Targeted approaches: Western blot of affinity-enriched proteins to analyze proteins of interest

3.1.1. Materials

1. DCP-Bio1-labeled samples after affinity capture of biotinylated proteins
2. Materials for 1D gel electrophoresis and transfer to nitrocellulose (or PVDF) membrane
3. TBST buffer: 50 m*M* Tris–HCl, 150 m*M* NaCl, 0.1% (v/v) Tween-20, pH 7.5
4. 5% (w/v) dried milk in TBST (alternate blocking and binding buffer may be preferred for individual antibodies; commonly used buffers include 1–5% bovine serum albumin (BSA) or 1–10% fetal bovine serum (FBS)
5. Primary antibody to protein of interest
6. Secondary antibody conjugated to horseradish peroxidase (HRP) (other conjugates such as alkaline phosphatase or fluorescein may also be used)
7. Chemiluminescence detection kit (such as Western Lightning® Plus–ECL, Enhanced Chemiluminescence Substrate form Perkin Elmer or Pico, Dura, or Femto Chemiluminescence kits from Pierce)

3.1.2. Methods

Western blots are performed on equal volumes of biotinylated, affinity-enriched samples according to the established protocol for each antibody and target protein. Although different proteins and samples will require optimization of conditions, we have found that the amount of affinity-captured material from 40 μg starting lysate is typically sufficient for visualization using the Dura chemiluminescence kit from Pierce.

Time-dependent changes in protein sulfenic acid levels in HEK293 cells, analyzed by Western blot analyses of the affinity-captured material, show that phosphatases (PTEN and SHP-2), kinases (protein kinase C, PKC-β1), chaperones (heat shock protein, HSP70), and glycolytic enzymes (GAPDH) are all transiently oxidized and labeled by DCP-Bio1 in tumor necrosis factor-α (TNFα) treated cells (Fig. 4.3). Some of the proteins we observe, such as GAPDH, are known to form a stabilized sulfenic acid, and others (PTEN, SHP-2, and HSP70) are known to be redox regulated, though not specifically through sulfenic acid formation. The signaling phosphatases PTEN (Kwon *et al.*, 2004; Lee *et al.*, 2002) and SHP-2 (Chen *et al.*, 2006; Kwon *et al.*, 2005; Meng *et al.*, 2002) are known to be oxidation sensitive, with the former yielding an intrasubunit disulfide bond between the active site Cys (Cys124) and Cys71; sulfenic acid formation has been postulated based on other protein tyrosine phosphatases (Tonks, 2005), but not fully demonstrated in each case. In the case of HSP70, protein S-glutathionylation in retinal pigment epithelium has been shown to convert this protein to an active chaperone (Hoppe *et al.*, 2004).

We note from our blots (Fig. 4.3) that patterns of oxidation differ between proteins in the same experimental samples, suggesting distinct influences on oxidation status of various proteins after cell stimulation. Because each protein exhibits a different profile (Fig. 4.3), we typically select a range of times between 1 min and 1 h after TNFα stimulation to maximize the chance of observing the transient intermediate on a particular protein.

3.2. Targeted approaches: Immunoprecipitation of protein of interest followed by Western blot to detect biotin

3.2.1. Materials

1. DCP-Bio1-labeled samples prior to affinity enrichment
2. Primary antibody to protein of interest (suitable for IP)
3. Secondary antibody complexed to agarose or magnetic beads
4. 2 *M* urea in PBS
5. Elution buffer for 1D gel electrophoresis: 2% SDS, 50 m*M* Tris–HCl, 1 m*M* EDTA, pH 8.0
6. Materials for 1D gel electrophoresis and transfer to nitrocellulose (or PVDF) membrane

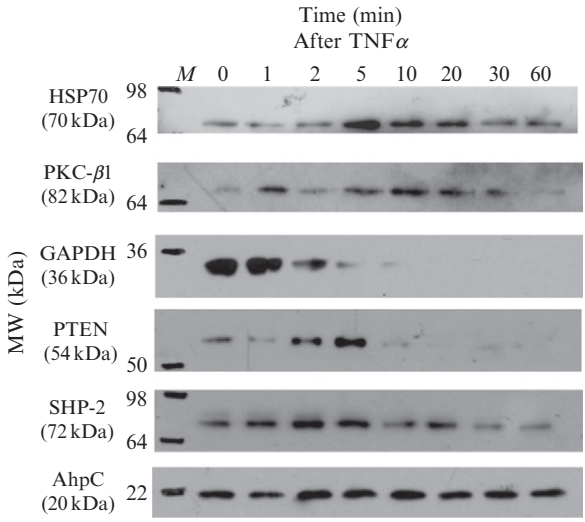

Figure 4.3 Time course of sulfenic acid formation in individual proteins monitored by Western blot analysis. HEK293 cells were stimulated with TNFα for the indicated amount of time, cells were washed with PBS, and sulfenic acids were trapped by the addition of lysis buffer containing 1 m*M* DCP-Bio1, 10 m*M* *N*-ethylmaleimide, 10 m*M* iodoacetamide, 200 U/ml catalase, 100 m*M* NaCl, 100 μM DTPA, 20 m*M* β-glycerophosphate, 1 m*M* sodium vanadate, 50 m*M* sodium fluoride, 1 m*M* PMSF, 0.01 mg/ml aprotinin, 0.01 mg/ml leupeptin, 0.1% sodium dodecyl sulfate, 0.5% sodium deoxycholate, 0.5% NP-40, and 0.5% Triton-X-100 in 50 m*M* Tris–HCl, pH 7.5, incubated on ice for 1 h, and stored at −80 °C. Biotinylated proteins were affinity captured according to the protocol described in methods, then separated by SDS–PAGE and transferred to a nitrocellulose membrane. The extent of cysteine oxidation on individual proteins was evaluated using protein-specific antibodies. Biotin-labeled AhpC was added based on protein concentrations prior to affinity capture and used as a procedural control for the biotin-based affinity capture, elution and gel loading steps. Antibodies to HSP70, PKC-β1, and GAPDH were from Santa Cruz; antibodies to PTEN and SHP-2 were from Cell Signaling, and the AhpC antibody was purified from rabbit serum.

7. Antibiotin antibody and HRP-conjugated secondary antibody (or streptavidin–HRP conjugate)
8. 5% (w/v) dried milk in TBST
9. 1% BSA in TBST

3.2.2. Methods

The previous section described performing a Western blot on the affinity-captured biotinylated samples to look for the target protein; an alternate and complementary approach is to immunoprecipitate the target protein, then probe the samples for biotin. Use of both techniques gives the strongest evidence that a given protein is indeed labeled by the biotinylated reagent as long as proper controls in the absence of reagent are included.

IP is performed according to established protocols specific to the protein of interest. After beads have been incubated with the protein samples, they are washed with PBS or more stringent conditions (if possible), then eluted with SDS sample buffer. Biotin blots are then performed on the eluted, electrophoresed samples using either HRP-conjugated streptavidin or antibiotin antibodies. In our hands, antibiotin antibodies perform somewhat better. In order to avoid coelution of the antibody proteins, antibodies may be cross-linked to the beads prior to IP. Otherwise, a control for the antibody without lysate should be included as we have observed biotinylation of the antibody subunits and these can mask detection of the target protein if of similar size.

Using this approach, we were able to clearly demonstrate the presence of biotinylated proteins at the correct molecular weight in the IPs of PTEN and SHP-2 proteins (Fig. 4.4), confirming the data using the affinity-captured material that identified these two proteins as sulfenic acid-containing proteins. For IP experiments shown in Fig. 4.4, TNFα-treated HEK293 lysates were preincubated with 20 μl Dynabeads-Protein A magnetic beads preequilibrated in PBS and then incubated overnight at 4 °C with 0.5 μl of either anti-PTEN or anti-SHP-2 antibody (Cell Signaling) and 20 μl Dynabeads-Protein A magnetic beads. The supernatant was then removed and the beads were washed three times with PBS buffer. Immunoprecipitated proteins were eluted with 35 μl SDS–PAGE-loading buffer and biotinylated proteins were visualized using Streptavidin–HRP.

3.3. Controls for endogenous biotinylation

The biotin affinity capture and detection procedures described herein (with the exception of MS analysis) cannot distinguish between proteins labeled with a biotinylated chemical reagent and those that are endogenously biotinylated on lysine. To test for endogenous biotinylation, it is important to include a sample that has not been labeled with the biotin compound as a control in all experiments (Fig. 4.4).

3.4. Global approaches: Identification of overall sulfenic acid levels for cellular proteins in response to stimuli

In order to estimate the relative of abundance proteins containing sulfenic acid in the cellular proteome under various conditions, we have used both biotinylated and fluorescent reagents. In addition to the affinity-based methods employed above, global biotin incorporation can be visualized using gel-based techniques such as total protein staining of gels following affinity capture of biotinylated proteins (Fig. 4.5 A) and antibiotin Western blots using either a streptavidin–HRP conjugate or an antibiotin antibody (Fig. 4.5 B). We have also labeled lysates with DCP-FL1, a dimedone analogue containing a fluorescein moiety (as well as other fluorescent compounds including DCP-FL2, DCP-Rho1, and DCP-Rho2) and have visualized sulfenic acid-modified

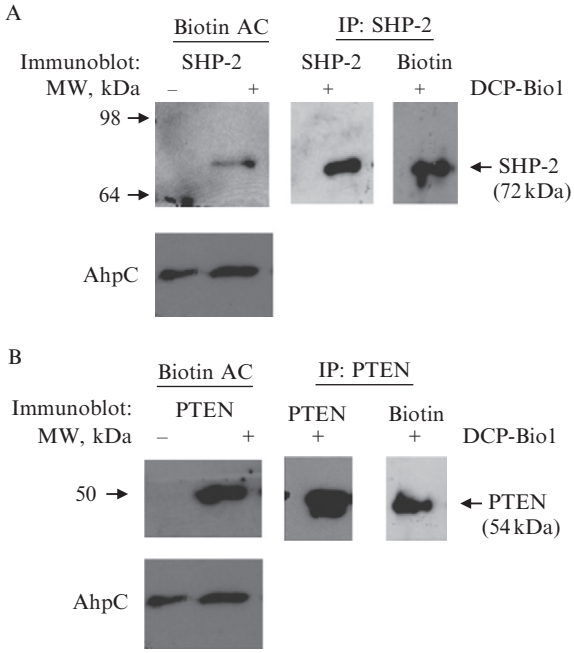

Figure 4.4 SHP-2 (A) and PTEN (B) labeling is established by immunoblots to SHP-2 and PTEN after biotin affinity capture (biotin AC) and by visualizing biotinylated proteins after immunoprecipitation (IP) of SHP-2 and PTEN, but these proteins are not endogenously biotinylated. HEK293 cells were grown in DMEM media containing 10% FBS and exchanged into serum-free DMEM media for 30 min prior to the addition of the 5 m*M* DCP-Bio1-containing lysis buffer and incubation (see Fig. 4.3). Cell lysates were centrifuged at 14,000×*g* for 10 min, and the protein concentration in each supernatant was determined using the BCA protein assay. For immunoprecipitation, lysates (175 μg of protein each) were preincubated for 1 h at 4 °C with 20 μl Dynabeads-Protein A magnetic beads preequilibrated in PBS (but lacking antibody) to remove nonspecifically associating proteins, then supernatants were transferred to tubes containing 0.5 μl of either anti-PTEN or anti-SHP-2 antibody (Cell Signaling) and a fresh aliquot (20 μl) of magnetic beads and incubated overnight at 4 °C. Supernatants were then removed and the beads were washed three times with PBS buffer. Immunoprecipitated proteins were eluted with 35 μl SDS sample buffer. Affinity capture of biotinylated proteins was conducted according to the protocol described in methods. Proteins (10 μl per sample) were separated by SDS–PAGE in 10% polyacrylamide gels, transferred to nitrocellulose membrane, and blocked with 5% milk. For immunoblotting, membranes were incubated for 2 h at 24 °C with a 1:10,000 dilution of streptavidin–HRP or for 16 h at 4 °C with a 1:1000 dilution of either anti-SHP-2 (A, Cell Signaling) or anti-PTEN antibodies (B, Cell Signaling), then visualized with Pico chemiluminescent substrate (Pierce).

proteins both in 1D (not shown) and 2D gels using a fluorescence imager (Fig. 4.5 C). Finally, we have used a FluoReporter biotin incorporation assay to evaluate total biotin incorporation into cellular proteins (Fig. 4.5 D).

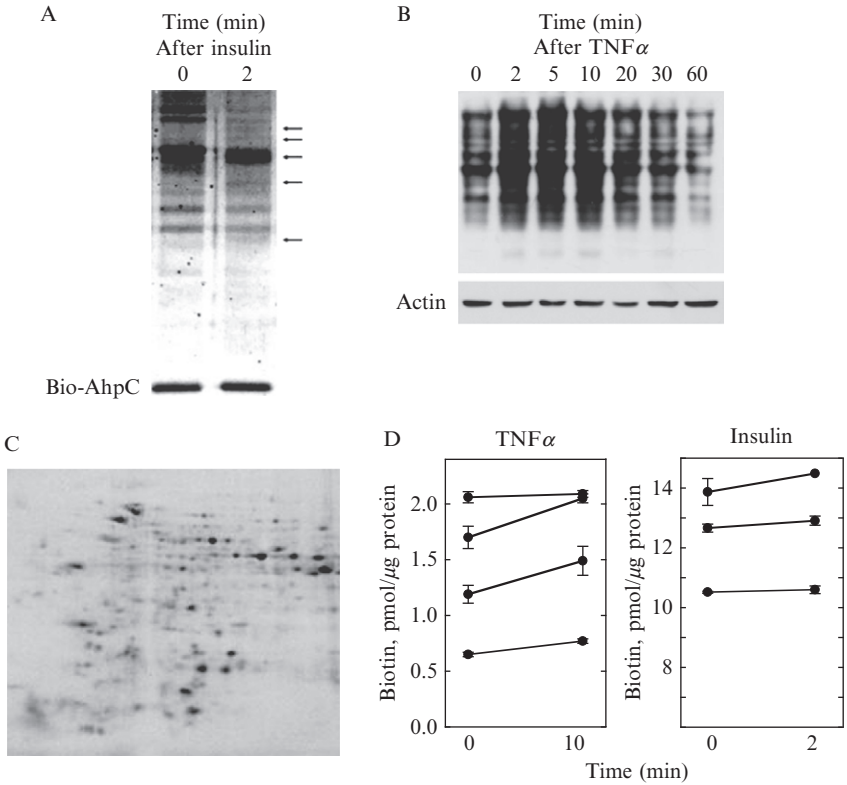

Figure 4.5 Techniques to monitor global sulfenic acid formation. (A) To visualize protein bands in samples after affinity capture of biotinylated proteins, HEK293 cells were treated (or not) with 100 n*M* insulin for 2 min, then sulfenic acids were trapped with 1 m*M* DCP-Bio1 in lysis buffer as in Fig. 4.3. Streptavidin–agarose beads were used to capture biotinylated proteins from lysates, then extensively washed with 1% SDS, 4*M* urea in PBS, 1 *M* NaCl, 100 μM ammonium bicarbonate and dH_2O. Proteins were eluted with 2% SDS in 50 m*M* Tris–HCl, pH 8.0, 1 m*M* EDTA, separated by SDS–PAGE, and stained with SYPRO Ruby (Pierce). Proteins showing increased sulfenic acid labeling in response to insulin are marked with arrows. (B) To blot for biotin after separation of total protein samples on gels, HEK293 cells were treated (or not) with TNFα for the indicated amount of time, then sulfenic acids were trapped with 1 m*M* DCP-Bio1 in lysis buffer. Unreacted DCP-Bio1 was removed using a Bio-Gel P6 spin column and 20 μg of protein from each sample was separated on a 10% SDS-PAGE followed by transfer to nitrocellulose. Membranes were blocked overnight with 5% milk, incubated with a 1:1000 dilution of antibiotin, HRP-conjugated antibody (Cell Signaling) for 2 h at 24 °C, and visualized with Pico chemiluminescence kit. As a loading control, 10 μg of each sample was probed for actin using an anti-actin antibody (Cell Signaling). (C) For protein analyses using 2D gels, HEK293 cells were treated with TNFα or insulin and labeled with 1 m*M* DCP-FL1. Proteins were precipitated with cold acetone, washed with 10% TCA and 1:1 ether:ethanol, and then resolubilized in 8 *M* urea, 2% CHAPS, 50 m*M* DTT, and 0.2% ampholytes. Proteins were separated by 2D electrophoresis using pH 3–10 IPG strips (BioRad), followed by 4–20% Criterion

For gel-based analyses of proteins labeled with fluorescent analogues, it is often preferable to first remove excess reagent either by passing lysates through a Bio-Gel P6 spin column, or by precipitating proteins and washing the pellets before resuspension into sample buffer. After electrophoresis, gels can be fixed with 10% acetic acid, 40% methanol and washed at least three times with water prior to visualization. For fluorophores such as fluorescein which are less fluorescent at low pH, fixed gels are washed two times for 15 min each with 40 m*M* ammonium bicarbonate, pH 8.0.

For separation of either biotinylated or fluorescently labeled proteins by 2D electrophoresis, it is important to ensure that samples not contain any excess reagents or salts as either of these may interfere with isoelectric focusing. Therefore, samples (up to 200 μl) are precipitated with 1 ml cold acetone, incubated on ice for 10 min and centrifuged at 14,000×*g* for 10 min at 4 °C. Supernatants are removed, the pellets are washed with 0.5 ml 10% trichloroacetic acid, then samples are centrifuged again and washed one more time with 200 μl of 1:1 ether:ethanol. Liquid is removed and pellets are allowed to air dry prior to the addition of an appropriate buffer for isoelectric focusing (e.g., 8 *M* urea 2% CHAPS). Sample resuspension is allowed to proceed at 37 °C for 20–60 min with occasional tapping. Protein content is measured, then ampholytes and DTT (10 μl of a freshly prepared 1 *M* stock per 200 μl final volume) are added to the samples just prior to their application onto isoelectric focusing strips. For 2D gels of affinity-captured, biotinylated samples, we typically use samples derived from 0.4 to 1 mg of starting lysate.

We have used the FluoReporter® biotin assay kit from Invitrogen to evaluate biotin incorporation into total protein, an assay which measures the increase in fluorescence as biotin displaces quencher dye from the biotin binding sites on their Biotective™ Green reagent. For this and all assays designed to measure biotin, unreacted DCP-Bio1 and other small molecules must first be removed using a Bio-Gel P6 spin column and the samples exchanged into PBS or another buffer compatible with the assay of interest. Following the directions in the kit, cell lysates (~10–25 μg total protein in 50-μl volume) are digested with a protease to disrupt protein structure and allow protein-bound biotin to access the binding sites on the dye (Fig. 4.5 D).

gel (BioRad), and fluorescein labeled proteins were visualized on a Amersham STORM 840 fluorescence imager. (D) A FluoReporter biotin quantitation assay kit (Invitrogen) was used to quantify the amount of biotin incorporation into HEK293 cells before and after stimulation with TNFα for 10 min. Briefly, cell lysates (~10–25 μg) were digested with *Streptomyces griseus* Protease type XIV overnight at 37 °C and diluted in PBS until each sample contained 1–2 μg total protein. After incubation for 5 min at room temperature in the dark with an equal volume of Biotective Green reagent, fluorescence was measured on a Tecan Safire 2 fluorescence plate reader using λ_{ex} = 485 nm and λ_{em} = 530 nm.

The FluoReporter assay is able to detect between 4 and 80 pmol of biotin per 50-μl sample, and the digestion mixture will most likely need to be diluted for samples to be in the correct range; for our experiments, 1–2 μg total protein per sample was a good starting amount. A standard curve is generated using a small molecule biotin provided in the kit; the standard curve should include 2–3 replicates of a zero and a minimum of four other biotin concentrations. Analysis of a biotinylated protein used as a positive control is also recommended in order to confirm that proteolysis is sufficient to yield assay-accessible biotin. Each sample is incubated with 50 μl of Biotective Green reagent in a 96-well plate for 5 min at room temperature in the dark. Sample fluorescence is measured on a fluorescence plate reader using $\lambda_{ex} = 485$ nm and $\lambda_{em} = 530$ nm.

For all of these assays, it is important to gauge the endogenous levels of biotinylation on lysine. Studies in our laboratory to date indicate that these levels are very low when compared with the amount of DCP-Bio1 incorporation, but some prominent bands are present even when no biotin is added (see Fig. 3.5B in the preceding chapter, Klomsiri *et al.*, 2010).

3.5. Global approaches: Identification of oxidized proteins by mass spectrometry after biotin affinity capture

Biotinylated samples can be used for proteomic level analyses in order to identify unknown proteins with peroxide-sensitive cysteines. In order to minimize false positives and to simplify analysis, we suggest performing affinity capture along with stringent washing procedures on such biotinylated samples. For these types of studies, the affinity-captured material is generally separated by 1D or 2D electrophoresis followed by in-gel proteolysis and standard MS analyses to identify the proteins (Shevchenko *et al.*, 2006) Table 4.1 lists a selection of proteins that we have identified from lysates, derived from TNFα-treated HEK-293 cells, using biotin-based affinity capture, separation by either 1D or 2D gel electrophoresis, in-gel proteolytic digestion, and MS analysis.

3.6. Identification of oxidized cysteine by MS–MS analysis

Although stringent washing of the streptavidin beads may help minimize the identification of false positives, the ultimate proof that a protein truly contains an oxidized cysteine comes from the direct identification of the oxidized cysteine. For this purpose, affinity capture of biotinylated peptides can be performed after proteolytic digestion of the cellular proteins (Dennehy *et al.*, 2006; Shin *et al.*, 2007). Alternatively, biotinylated proteins can first be enriched by affinity purification, then digested and further enriched for biotinylated peptides using a second affinity capture step. We have used the first type of experiment to identify the labeled cysteine residue in peroxiredoxin VI using a DCP-Bio1-treated lysate of HEK-293 cells

Table 4.1 Cysteine sulfenic acid-modified proteins identified in TNFα treated HEK293 cells

Protein name	Function	Affinity capture, gel & MS[a]	Affinity capture, gel & WB	Cysteine i.d [b]
Actin[d]	Cell structure & motility	X	X	C10
Tubulin B[d]	Microtubule protein	X	X	
Heat shock protein 70 (HSP70)[d]	Chaperone	X	X	C17
PrxI[c]	Peroxidase		X	
PrxII[c]	Peroxidase	X	X	
PrxIII[c]	Peroxidase		X	
PrxIV[c]	Peroxidase		X	
α-Enolase[d]	Glycolytic enzyme		X	
Glyceraldehyde-3-P dehydrogenase (GAPDH)[c]	Glycolytic enzyme	X	X	C151/155
Protein kinase C (PKC-β1)[d]	Signaling kinase		X	
Protein and lipid phosphatase (PTEN)[d]	Signaling phosphatase		X	
SH2 homology protein 2 (SHP-2)[c]	Signaling phosphatase		X	

[a] Gels were stained with Coomassie Blue dye, and protein spots of interest were excised, washed three times with 50% acetonitrile, dried, washed twice, successively, with 200 μl ammonium bicarbonate and 100% acetonitrile, dried, and digested with 0.1 mg/ml trypsin in 50 m*M* ammonium bicarbonate for 16 h at 37 °C. Peptides in the supernatant were combined with peptides eluted with 50% acetonitrile and spotted using a matrix containing 30 mg of dihydroxybenzoic acid in 1 ml 50% acetonitrile, 0.1% trifluoroacetic acid. Protein identifications were made using a Bruker Autoflex MALDI-TOF mass spectrometer with dihydroxybenzoic acid as the matrix, and data were analyzed using MASCOT software (www.matrixscience.com).

[b] In these cases, identification of the labeled peptide by mass spectrometry gave an unambiguous determination of the labeled Cys residue, except for GAPDH, which has two Cys residues on the MALDI-TOF-identified labeled peptide; based on data from other laboratories, Cys151 has been shown to form a sulfenic acid.

[c] Data present in literature showing sulfenic acid formation.

[d] Redox regulation known, but sulfenic acid not previously identified.

stimulated with 12-*O*-tetradecanoylphorbol-13-acetate (TPA). This peptide was identified by performing a tryptic digest, biotin-based affinity capture of the labeled peptides, and LC–MS/MS analysis (Fig. 4.6). Because this method is only expected to capture 1 or a few peptides per protein, the results will be heavily influenced by the choice of protease. For this reason, it may be desirable to use more than one protease for each sample in order to increase the number of peptides identified.

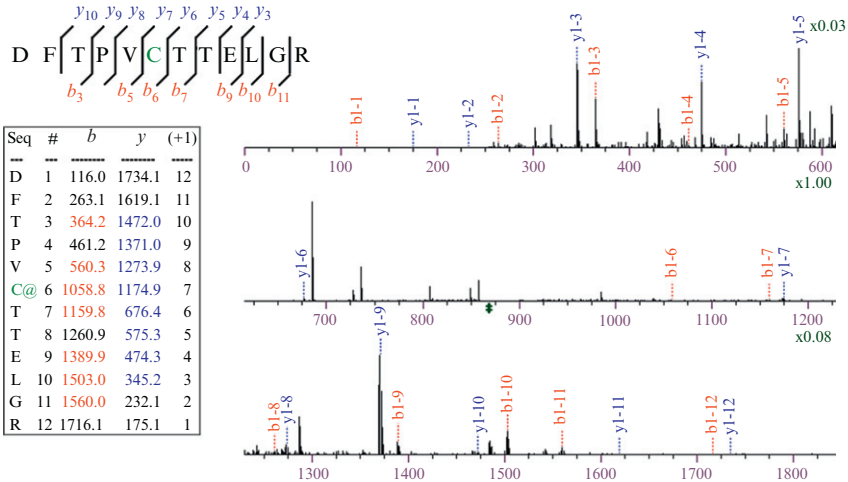

Figure 4.6 LC/MS/MS spectrum of a DCP-Bio1-labeled tryptic peptide from PrxVI labeled on the reactive Cys residue, Cys46. HEK293 cells were grown in DMEM media to 80% confluence, serum-starved for 20 h, and treated with 100 n*M* TPA for 1 min. Cells were scraped, then lysed in lysis buffer containing 5 m*M* DCP-Bio1 and 10 m*M* NEM and incubated at room temperature for 30 min; proteins in the sample were further treated under denaturing conditions by adding urea to 6*M* and incubating for 10 min with 10 m*M* DTT, then adding NEM to 20 m*M* for another 35 min incubation. To remove excess labeling agents and protease inhibitors, the sample was exchanged into digestion buffer (2 *M* urea, 100 m*M* ammonium bicarbonate) using a G-25 spin column. Trypsin was added (1:100, w/w) and incubated at 37 °C for 15 h. Excess trypsin and undigested protein was removed by passing peptides through a 5000 molecular weight cut-off Ultrafree-MC centrifugal filter (Millipore) following digestion. For biotin affinity capture, peptides were incubated with a preequilibrated monoavidin resin (from Pierce) at 4 °C overnight. The beads were washed several times with additional urea/bicarbonate buffer, followed by 10 m*M* ammonium bicarbonate, then water. Peptides were eluted with 30% acetonitrile containing 500 m*M* formic acid, then concentrated in a SpeedVac before analysis. Reverse phase chromatography on a C-18 column was used to resolve peptides, with a portion of the eluant injected directly into the LTQ mass spectrometer. As illustrated above, cleavage of the amide bond results in N-terminal fragments designated as "b" and C-terminal fragments designated as "y". The masses of both sets of ions are consistent with DCP-Bio1 linked covalently to Cys46 of human peroxiredoxin VI (PrxVI) (y7 − y6 = b6 − b5 = 498.5 *m/z*).

4. Summary

Reagents developed recently by us and others have provided a new set of tools to specifically trap the largely unstable protein sulfenic acid intermediate in cellular proteins. Using protocols optimized to minimize the presence of unlabeled proteins in our affinity-captured material, it is now possible to identify proteins and specific cysteine residues that are oxidized

in response to cellular stimulation and to monitor the conditions under which these oxidations occur. The protocols presented here are suitable for the large-scale identification of these modified proteins by high-throughput proteomics methods, yet can also be employed to investigate the oxidation of a particular protein or system by a lab with limited access to MS. Although the presence and location of an oxidized cysteine often does not directly indicate whether it modulates protein function, it is an important first step. Once the oxidized cysteine has been identified, future experiments can be designed that explore the role of these oxidations on protein function and cellular processes.

ACKNOWLEDGMENTS

This work was supported by NIH grants R21 CA112145 and R33 CA126659 to LBP and by an Established Investigator Grant to LBP from the American Heart Association. Support from a Ruth L. Kirschstein Individual Fellowship from the National Institutes of Health to KJN (F32 GM074537) and a grant from the NSF-NIGMS Program in Mathematical Biology to Jacquelyn S. Fetrow (RO1 GM075304) with LBP and LWD as coinvestigators is also acknowledged.

REFERENCES

Chen, C. H., Cheng, T. H., Lin, H., Shih, N. L., Chen, Y. L., Chen, Y. S., Cheng, C. F., Lian, W. S., Meng, T. C., Chiu, W. T., and Chen, J. J. (2006). Reactive oxygen species generation is involved in epidermal growth factor receptor transactivation through the transient oxidization of Src homology 2-containing tyrosine phosphatase in endothelin-1 signaling pathway in rat cardiac fibroblasts. *Mol. Pharmacol.* **69,** 1347–1355.

Claiborne, A., Yeh, J. I., Mallett, T. C., Luba, J., Crane, E. J. 3rd, Charrier, V., and Parsonage, D. (1999). Protein-sulfenic acids: Diverse roles for an unlikely player in enzyme catalysis and redox regulation. *Biochemistry* **38,** 15407–15416.

Cotgreave, I. A., Gerdes, R., Schuppe-Koistinen, I., and Lind, C. (2002). S-glutathionylation of glyceraldehyde-3-phosphate dehydrogenase: Role of thiol oxidation and catalysis by glutaredoxin. *Methods Enzymol.* **348,** 175–182.

Dennehy, M. K., Richards, K. A., Wernke, G. R., Shyr, Y., and Liebler, D. C. (2006). Cytosolic and nuclear protein targets of thiol-reactive electrophiles. *Chem. Res. Toxicol.* **19,** 20–29.

Fuangthong, M., and Helmann, J. D. (2002). The OhrR repressor senses organic hydroperoxides by reversible formation of a cysteine-sulfenic acid derivative. *Proc. Natl. Acad. Sci. USA* **99,** 6690–6695.

Hondorp, E. R., and Matthews, R. G. (2004). Oxidative stress inactivates cobalamin-independent methionine synthase (MetE) in *Escherichia coli*. *PLoS Biol.* **2,** e336.

Hong, M., Fuangthong, M., Helmann, J. D., and Brennan, R. G. (2005). Structure of an OhrR-ohrA operator complex reveals the DNA binding mechanism of the MarR family. *Mol. Cell* **20,** 131–141.

Hoppe, G., Chai, Y. C., Crabb, J. W., and Sears, J. (2004). Protein s-glutathionylation in retinal pigment epithelium converts heat shock protein 70 to an active chaperone. *Exp. Eye Res.* **78,** 1085–1092.

Jakob, U., Muse, W., Eser, M., and Bardwell, J. C. (1999). Chaperone activity with a redox switch. *Cell* **96,** 341–352.

Jones, D. P. (2006). Disruption of mitochondrial redox circuitry in oxidative stress. *Chem. Biol. Interact.* **163,** 38–53.

Kang, J. G., Paget, M. S., Seok, Y. J., Hahn, M. Y., Bae, J. B., Hahn, J. S., Kleanthous, C., Buttner, M. J., and Roe, J. H. (1999). RsrA, an anti-sigma factor regulated by redox change. *EMBO J.* **18,** 4292–4298.

Klomsiri, C., Nelson, K. J., Bechtold, E., Soito, L., Johnson, L. C., Todd Lowther, W., Seong-Eon Ryu, S., King, B., Furdui, C. M., and Poole, L. B. (2010). Use of dimedone-based chemical probes for sulfenic acid detection. Evaluation of conditions affecting probe incorporation into redox-sensitive proteins.. *Methods Enzymol.* **473,** 77–93.

Kuge, S., Arita, M., Murayama, A., Maeta, K., Izawa, S., Inoue, Y., and Nomoto, A. (2001). Regulation of the yeast Yap1p nuclear export signal is mediated by redox signal-induced reversible disulfide bond formation. *Mol. Cell Biol.* **21,** 6139–6150.

Kwon, J., Lee, S. R., Yang, K. S., Ahn, Y., Kim, Y. J., Stadtman, E. R., and Rhee, S. G. (2004). Reversible oxidation and inactivation of the tumor suppressor PTEN in cells stimulated with peptide growth factors. *Proc. Natl. Acad. Sci USA* **101,** 16419–16424.

Kwon, J., Qu, C. K., Maeng, J. S., Falahati, R., Lee, C., and Williams, M. S. (2005). Receptor-stimulated oxidation of SHP-2 promotes T-cell adhesion through SLP-76-ADAP. *EMBO J.* **24,** 2331–2341.

Lee, S. R., Yang, K. S., Kwon, J., Lee, C., Jeong, W., and Rhee, S. G. (2002). Reversible inactivation of the tumor suppressor PTEN by H2O2. *J. Biol. Chem.* **277,** 20336–20342.

Leonard, S. E., Reddie, K. G., and Carroll, K. S. (2009). Mining the thiol proteome for sulfenic acid modifications reveals new targets for oxidation in cells. *ACS Chem. Biol.* **4,** 783–799.

Meng, T. C., Fukada, T., and Tonks, N. K. (2002). Reversible oxidation and inactivation of protein tyrosine phosphatases in vivo. *Mol. Cell* **9,** 387–399.

Nelson, K. J., Parsonage, D., Hall, A., Karplus, P. A., and Poole, L. B. (2008). Cysteine pK_a values for the bacterial peroxiredoxin AhpC. *Biochemistry* **47,** 12860–12868.

Panmanee, W., Vattanaviboon, P., Poole, L. B., and Mongkolsuk, S. (2006). Novel organic hydroperoxide-sensing and responding mechanisms for OhrR, a major bacterial sensor and regulator of organic hydroperoxide stress. *J. Bacteriol.* **188,** 1389–1395.

Poole, L. B., and Ellis, H. R. (1996). Flavin-dependent alkyl hydroperoxide reductase from *Salmonella typhimurium*. 1. Purification and enzymatic activities of overexpressed AhpF and AhpC proteins. *Biochemistry* **35,** 56–64.

Poole, L. B., and Nelson, K. J. (2008). Discovering mechanisms of signaling-mediated cysteine oxidation. *Curr. Opin. Chem. Biol.* **12,** 18–24.

Poole, L. B., Karplus, P. A., and Claiborne, A. (2004). Protein sulfenic acids in redox signaling. *Annu. Rev. Pharmacol. Toxicol.* **44,** 325–347.

Poole, L. B., Klomsiri, C., Knaggs, S. A., Furdui, C. M., Nelson, K. J., Thomas, M. J., Fetrow, J. S., Daniel, L. W., and King, S. B. (2007). Fluorescent and affinity-based tools to detect cysteine sulfenic acid formation in proteins. *Bioconjug. Chem.* **18,** 2004–2017.

Rainwater, R., Parks, D., Anderson, M. E., Tegtmeyer, P., and Mann, K. (1995). Role of cysteine residues in regulation of p53 function. *Mol. Cell Biol.* **15,** 3892–3903.

Reddie, K. G., Seo, Y. H., Muse Iii, W. B., Leonard, S. E., and Carroll, K. S. (2008). A chemical approach for detecting sulfenic acid-modified proteins in living cells. *Mol. Biosyst.* **4,** 521–531.

Schmalhausen, E. V., Nagradova, N. K., Boschi-Muller, S., Branlant, G., and Muronetz, V. I. (1999). Mildly oxidized GAPDH: the coupling of the dehydrogenase and acyl phosphatase activities. *FEBS Lett.* **452,** 219–222.

Schneider, C., Pratt, D. A., Porter, N. A., and Brash, A. R. (2007). Control of oxygenation in lipoxygenase and cyclooxygenase catalysis. *Chem. Biol.* **14,** 473–488.

Shevchenko, A., Tomas, H., Havlis, J., Olsen, J. V., and Mann, M. (2006). In-gel digestion for mass spectrometric characterization of proteins and proteomes. *Nat. Protoc.* **1,** 2856–2860.

Shin, N. Y., Liu, Q., Stamer, S. L., and Liebler, D. C. (2007). Protein targets of reactive electrophiles in human liver microsomes. *Chem. Res. Toxicol.* **20,** 859–867.

Thomas, S. R., Witting, P. K., and Drummond, G. R. (2008). Redox control of endothelial function and dysfunction: molecular mechanisms and therapeutic opportunities. *Antioxid. Redox Signal.* **10,** 1713–1765.

Tonks, N. K. (2005). Redox redux: Revisiting PTPs and the control of cell signaling. *Cell* **121,** 667–670.

Zheng, M., Aslund, F., and Storz, G. (1998). Activation of the OxyR transcription factor by reversible disulfide bond formation. *Science* **279,** 1718–1721.

CHAPTER FIVE

Formation and Reactions of Sulfenic Acid in Human Serum Albumin

Beatriz Alvarez,[*,†] Sebastián Carballal,[*,†,‡] Lucía Turell,[*,†,§] *and* Rafael Radi[†,‡]

Contents

* Laboratorio de Enzimología, Facultad de Ciencias, Universidad de la República, Montevideo, Uruguay
† Center for Free Radical and Biomedical Research, Facultad de Medicina, Universidad de la República, Montevideo, Uruguay
‡ Departamento de Bioquímica, Facultad de Medicina, Universidad de la República, Montevideo, Uruguay
§ Laboratorio de Fisicoquímica Biológica, Facultad de Ciencias, Universidad de la República, Montevideo, Uruguay

Methods in Enzymology, Volume 473
ISSN 0076-6879, DOI: 10.1016/S0076-6879(10)73005-6

Abstract

Protein sulfenic acids (R–SOH) are receiving increased interest as intermediates in redox processes. Human serum albumin, the most abundant protein in plasma, possesses a single free thiol. We describe herein the different methodologies that we have employed to study the formation of sulfenic acid in this protein and characterize some of its properties, including reactions that lead to the formation of mixed disulfides and the sulfinic acid derivative. The thiol of albumin is oxidized by hydrogen peroxide and peroxynitrite to a relatively stable sulfenic acid, which can be detected through different strategies including reduction with sodium arsenite and reaction with glutathione. Dimedone trapping followed by mass spectrometry analysis confirmed the modification. The challenge of obtaining quantitative data regarding albumin sulfenic acid has been approached using the yellow thiol thionitrobenzoate. A careful analysis has led to the determination of the rate constants of the reactions of sulfenic acid with analytical probes and with possible biological targets such as plasma thiols, which lead to mixed disulfides, and hydrogen peroxide, which overoxidizes the sulfenic to sulfinic acid. Our results support the concept that sulfenic acid is a central intermediate in the formation of oxidized albumin species that are present in circulating albumin and increase under pathological conditions.

1. Introduction

Human serum albumin (HSA) is the predominant protein in the intravascular, extracellular space, constituting about 60% of total protein. It has a molecular mass of 66 kDa and ~19 negative charges at pH 7.4. Its single nonglycosylated polypeptidic chain, with 67% α-helixes and no β-sheets, contains three homologous domains, each containing two subdomains. Albumin is secreted from the liver into the bloodstream, but continuously travels into and out of the circulation, so that ~60% is distributed in extravascular tissues, particularly skin and muscle. After an average of 27 days, the molecule is degraded. The physiological functions of albumin include the maintenance of colloid osmotic pressure and the binding and transport of several ligands such as fatty acids, hormones, bilirubin, hemin, and drugs (Peters, 1996).

Albumin contains 35 cysteines. All but one form intraprotein disulfides, remaining only one free thiol, Cys34, located in a 9.5–10-Å crevice. This thiol can react with different targets. For example, it can react with plasma low molecular weight disulfides as well as the disulfide drug disulfiram forming a mixed albumin disulfide (HSA–SSR). It can also react with reactive oxygen and nitrogen species, giving rise to an antioxidant scavenging function. The reactivity of the albumin thiol is reflected in its heterogeneity. Indeed, in ~30% of circulating albumin, the Cys34 thiol is oxidized to

mixed disulfides or to higher oxidation states such as sulfinic (HSA–SO_2H) and sulfonic (HSA–SO_3H) acids, which cannot be reduced with thiol reagents. The heterogeneity of albumin can be revealed by mass spectrometry and chromatography among other techniques (for review see Turell *et al.*, 2009). The oxidized forms of albumin correlate with several conditions including renal diseases (Musante *et al.*, 2006, 2007; Terawaki *et al.*, 2004), liver failure (Oettl *et al.*, 2008), and aging (Era *et al.*, 1995; Giustarini *et al.*, 2006; Leto *et al.*, 1970), thus constituting potential markers of the scavenging activity of the albumin thiol (for review see Turell *et al.*, 2009).

A central intermediate in the oxidation of the albumin thiol is sulfenic acid (HSA–SOH). This elusive functional group is being identified in a growing list of proteins where it serves catalytic and signaling functions. In albumin, a relatively stable sulfenic acid is formed after exposure to oxidants such as hydrogen peroxide, and previous work from our group has led to its detection, quantification, and characterization (Alvarez *et al.*, 1999; Carballal *et al.*, 2003; Radi *et al.*, 1991a,b; Turell *et al.*, 2008). Working with the albumin protein has proved particularly challenging because of the possibility of binding of different reagents, because of allosterical changes and pH-dependent structural transitions, and because of the presence of 17 disulfide bridges in addition to the Cys34 thiol. In this chapter, we describe the methodology that we have used to study the properties of the sulfenic acid of HSA.

2. Preparation of Albumin Solutions

2.1. Source of albumin for biochemical studies

Pure human albumin suitable for laboratory work can be obtained from different commercial sources, including pharmaceutical preparations intended for clinical administration (Baxter Healthcare, Glendale, CA; ZLB Bioplasma, Switzerland or SIGMA, Fraction V). Alternatively, albumin can be freshly isolated from serum. The heterogeneity of albumin with regards to the Cys34 thiol is more pronounced in commercial preparations, which typically contain increased proportions of mixed disulfides and of nondithiothreitol reducible species (Turell *et al.*, 2009).

2.2. Albumin delipidation

Removal of fatty acids and other hydrophobic components from albumin is performed by charcoal treatment in acidic solution (Chen, 1967). Briefly, albumin (4 g) is dissolved in 40 mL of distilled water and the pH of the solution is lowered to 3.0 by the addition of 5 *M* HCl. Then, 2 g of activated charcoal are added. The choice of charcoal is critical; we use

SIGMA C4386 (washed with hydrochloric acid). After agitation for 1 h in an ice bath, charcoal is removed by centrifugation at 12,700×*g* for 30 min at 4 °C, followed by an additional centrifugation at 24,560×*g* for 30 min at 4 °C. The resulting supernatant is filtered through 0.8- and 0.22-μm membranes. Finally, the clarified albumin solution, typically 1.0–1.2 m*M*, is brought to pH 7.4 by the addition of 5 *M* NaOH.

2.3. Albumin thiol reduction

Since in commercial preparations the Cys34 thiol content is usually low, albumin has to be routinely reduced before working with it. Reducing the Cys34 thiol, which is mostly in the mixed disulfide state, while leaving the internal disulfide bridges intact, is challenging. No fixed recipe exists and procedures need to be adjusted for different albumin sources and batches. On our hands, the best results are obtained through incubation of delipidated albumin solutions (1.0–1.2 m*M*) with 10 m*M* 2-mercaptoethanol, overnight at 4 °C and pH 7.4, followed by gel filtration on Sephadex G-25 M (PD-10 columns, GE Healthcare) to remove excess reductant. This treatment typically yields albumin with ~0.7 SH/HSA ratios. Dithiothreitol should be used with caution because of the possibility of overreduction of the albumin molecule. We have obtained good results with overnight incubation at 4 °C with 5 m*M* dithiothreitol at pH 6.

2.4. Albumin quantification

The measurement of the concentration of albumin solutions is simple. In pure solutions, concentration can be determined from its absorbance at 279 nm ($\varepsilon = 0.531$ (g/L)$^{-1}$ cm^{-1}) for HSA; Peters, 1996), since it does not possess any cofactor. However, in biological fluids such as plasma or serum, where albumin is not pure, a specific method is needed. This is the case of the bromocresol purple (BCP) method. This dye presents a shift in its absorption maximum upon binding to albumin, providing an easy and specific way to measure albumin (Pinnell and Northam, 1978). In Fig. 5.1, the quantification of albumin in a fresh plasma sample is illustrated. A 500-fold dilution of plasma was mixed with BCP (40 μM in acetate buffer, 0.1 *M*, pH 5) and compared with a calibration curve using commercial HSA. Bromocresol green can also be used for albumin measurement. However, this dye yields overestimates because of nonspecific reactions with some globulins, specially acute phase reactants (Gustafsson, 1976).

2.5. Thiol quantification

Since the thiol content of albumin is variable, it is necessary to measure thiol concentration in albumin solutions immediately before using them. The Ellman method can be used for assaying thiols in HSA (Ellman and Lysko,

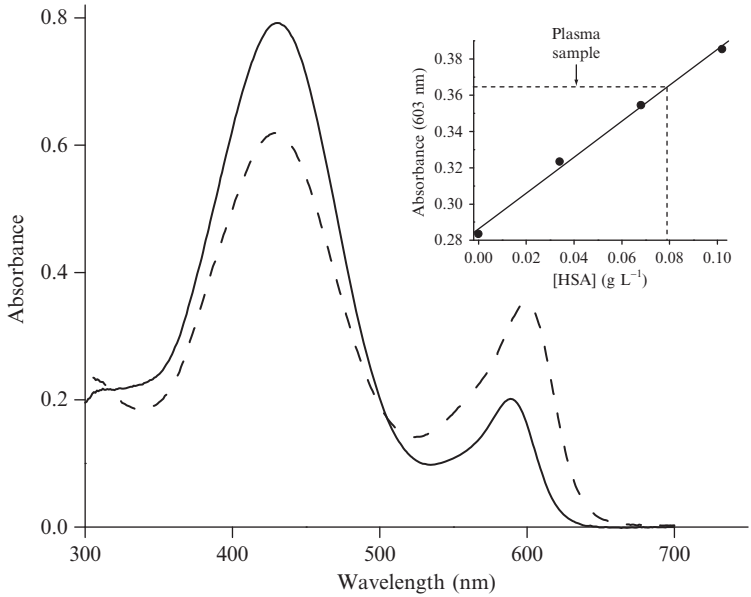

Figure 5.1 Quantification of human serum albumin using bromocresol purple (BCP). UV–vis spectra of BCP (40 μM, acetate buffer, 0.1 M, pH 5.2) in the absence (—) and in the presence (- - -) of HSA (0.066 g/L, 1 μM). *Inset*: Increasing volumes of commercial HSA (0–3 μL, 34.0 g/L) were mixed with BCP (40 μM, 1 mL). The absorbance was recorded at 603 nm and the data fitted the linear function: absorbance = 0.99[HSA] + 0.29. The absorbance of 2 μL of fresh plasma was 0.365, yielding an HSA concentration of 37.9 g/L in this sample.

1979). This method is based on the reaction of thiols with 5,5′-dithiobis (2-nitrobenzoic acid) (DTNB) with the formation of TNB (5-thio-2-nitrobenzoic acid), as in Eq. (5.1). A revised absorption coefficient at 412 nm of 14150 M^{-1} cm^{-1} is used to quantify the TNB formed (Riener *et al.*, 2002).

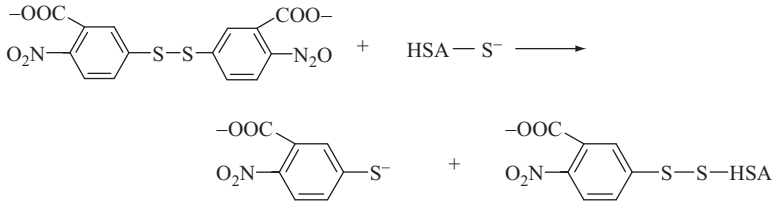

(5.1)

The reaction of DTNB with low molecular weight thiols like cysteine or glutathione is relatively fast and occurs within a few seconds. However, the reaction with the Cys34 thiol of albumin is slower. At pH 7.4, the reaction has a half-time of 3.9 min (room temperature, 0.2 mM DTNB,

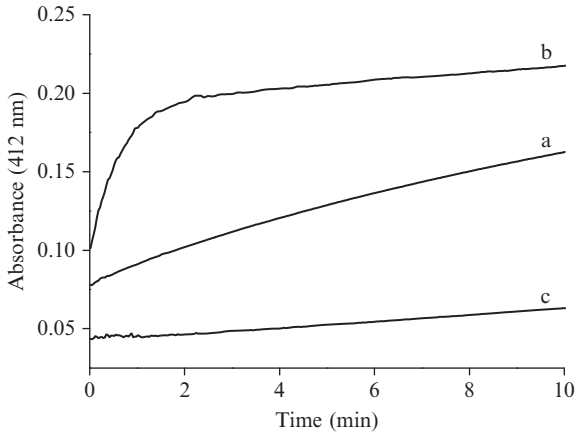

Figure 5.2 Quantification of the albumin thiol using 5,5′-dithiobis(2-nitrobenzoic acid) (DTNB). Reduced HSA (15 μM) was mixed with DTNB (0.2 mM) in phosphate buffer (0.1 M, pH 7.4) (trace a) or in pyrophosphate buffer (0.1 M, pH 9) (trace b) and the absorbance at 412 nm was recorded. A control without HSA in pyrophosphate buffer, pH 9, was included (trace c).

$\sim$20 μM HSA–SH). In order to make the reaction faster, albumin thiol quantification is performed at pH 9 (pyrophosphate buffer, 0.1 M), where the half-time is reduced to 0.85 min because of albumin thiol deprotonation and the reaction is driven to completion in a few minutes (Fig. 5.2). Protonation of TNB is not affected in this pH range (p$K_A \sim 4.4$). It is important to have a control without thiols to account for the alkaline dismutation of DTNB, which leads to increases in absorbance (Fig. 5.2).

Alternatively, titration with *p*-chloromercuribenzoate (*p*-CMB), Eq. (5.2), can be used to measure the albumin thiol (Boyer, 1954; Turell *et al.*, 2008). This reagent is instantaneously converted to *p*-hydroxymercuribenzoate in aqueous solution.

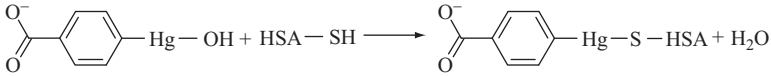

(5.2)

Briefly, HSA (30 μM) is titrated by adding aliquots of *p*-CMB in Tris buffer (0.1 M, pH 7.5) and the increase in absorbance at 250 nm is recorded (Fig. 5.3). Two inconveniences are that the procedure is time consuming and that the changes observed are relatively small.

Using both the methods, ratios ranging from 0.55 to 0.95 SH/HSA can be determined for reduced albumin, depending on the age of the solutions, on the source and batch of albumin and on the reduction procedure.

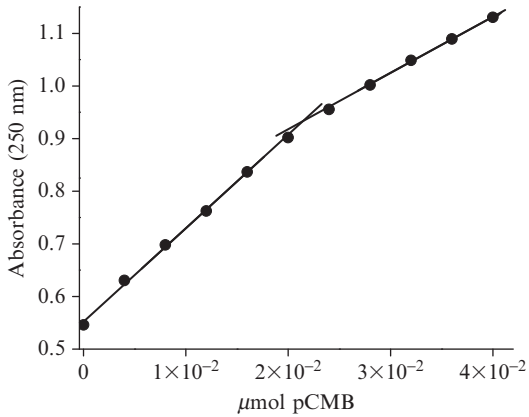

Figure 5.3 Quantification of the albumin thiol using *p*-chloromercuribenzoate (*p*-CMB). Titration of thiols in reduced HSA (30 μM) with 2 mM *p*-CMB in Tris buffer (0.1 M, pH 7.5).

2.6. Thiol blockage

The free thiol of albumin can be blocked by incubation of reduced HSA with a sevenfold excess of *N*-ethylmaleimide (NEM) under agitation for 30 min at 25 °C. Then, excess NEM is removed by gel filtration. Typically, this NEM treatment leaves no residual thiols. Alternatively, the thiol can be blocked by the addition of an equimolar amount of the chelator mercuric chloride ($HgCl_2$), but this treatment interferes with subsequent thiol additions or determinations with DTNB.

3. Preparation of Oxidized Albumin

Mild oxidation of the albumin thiol can be performed using hydrogen peroxide as oxidant. Previous work from our group has shown that HSA–SH reacts with hydrogen peroxide with approximately a one-to-one stoichiometry, as illustrated in Fig. 5.4. This stoichiometry is evidence that the product formed is distinct from disulfide, since two thiols would be oxidized per hydrogen peroxide if that was the case. Indeed, intermolecular albumin disulfides (HSA–SS–HSA) are not formed, probably because of steric restrictions. The reaction proceeds with a second-order rate constant of 2.3–2.7 $M^{-1}\,s^{-1}$ (Carballal *et al.*, 2003; Turell *et al.*, 2008), leading to the formation of HSA–SOH, Eq. (5.3). The two-electron oxidation mechanism implies the nucleophilic attack of the thiolate on the peroxidic oxygen.

$$\mathrm{HSA-S^- + H_2O_2 \rightarrow HSA-SOH + OH^-} \tag{5.3}$$

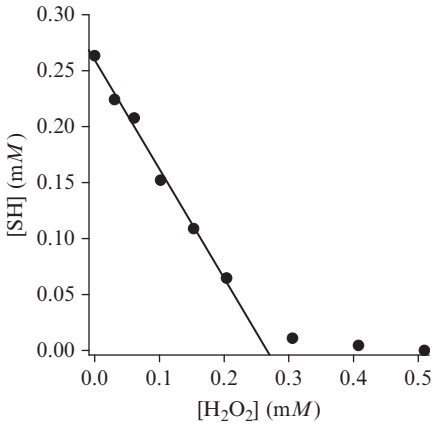

Figure 5.4 Stoichiometry of the reaction of the albumin thiol with hydrogen peroxide. Reduced HSA (0.5 m*M*) was mixed with hydrogen peroxide in phosphate buffer (0.05 *M*, pH 7.4, 0.1 m*M* dtpa). Samples were assayed for thiol content after 75 min at 37 °C. Reprinted with permission from Carballal *et al.* (2003). Copyright 2003 American Chemical Society.

Taking into account this rate constant, when the aim is to oxidize the thiol to sulfenic acid, albumin (0.5 m*M*) is incubated with 4 m*M* hydrogen peroxide for 4 min at 37 °C in phosphate buffer (0.1 *M*, pH 7.4, 0.1 m*M* diethylenetriaminepentaacetic acid, dtpa) (Turell *et al.*, 2008). Stock solutions of hydrogen peroxide are prepared from dilution of commercial sources in ultrapure water and quantified immediately before use from the absorbance at 240 nm, $\varepsilon = 43.6\ M^{-1}\ \text{cm}^{-1}$ (Claiborne, 1985). The reaction is stopped by the addition of enough catalase to consume 90% of the remaining hydrogen peroxide in ~3 s. In these conditions, a maximum ratio of 0.18 ± 0.02 HSA–SOH/HSA can be obtained, and the oxidized albumin solution is kept on ice and used the same day as prepared. When the aim is to overoxidize albumin, either the incubation time is increased to 30 min or the hydrogen peroxide concentration used is higher (15 m*M*) (Turell *et al.*, 2008).

Calculations involving catalase deserve special attention, since the kinetics do not obey the usual pattern (Aebi, 1984). For typical enzymes, standard units (μmol min^{-1}) are independent of substrate concentration because they are defined for saturating conditions. In contrast, for catalase the K_M is infinitely high and the decomposition of hydrogen peroxide always follows a first-order reaction. Catalase activity of stocks can be measured by the decrease in absorbance at 240 nm with 10 m*M* hydrogen peroxide during a short period of time (1–2 min), avoiding dioxygen bubbles and suicide inactivation. This allows to measure the initial rate of the reaction, v_0. Since standard units cannot be defined, the rate constant of the pseudo-first-order reaction (k', with $v_0 = k'[H_2O_2] = k[\text{catalase}][H_2O_2]$) is

recommended instead, as a measure of catalase concentration. Then, to calculate how much catalase should be added to a working solution to decompose a certain amount of hydrogen peroxide in a certain time, a new k' is calculated considering that $[H_2O_2] = [H_2O_2]_0 \exp(-k't)$, and the dilution related to the k' of the stock. For example, when 4 m*M* hydrogen peroxide is decomposed in 3 s, k' is 0.77 s^{-1}.

As an alternative to hydrogen peroxide, oxidation of the albumin thiol can be performed with peroxynitrite ($ONOO^-$), which reacts directly with HSA–SH with a second-order rate constant of $3.8 \times 10^3\ M^{-1}\ s^{-1}$ (pH 7.4, 37 °C) (Alvarez *et al.*, 1999; Radi *et al.*, 1991a). In addition, peroxynitrous acid can homolyze spontaneously with a rate constant of 0.9 s^{-1} (pH 7.4, 37 °C), yielding a ~30% free hydroxyl and nitrogen dioxide radicals. These radicals can also react with the albumin thiol in a one-electron oxidation process leading to thiyl radical, which can react with oxygen leading to a number of secondary radicals, finally yielding sulfenic and sulfinic acid (Bonini and Augusto, 2001; Carballal *et al.*, 2007; Quijano *et al.*, 1997). Due to reactions of the derived free radicals, in addition to thiol oxidation, nitration of tyrosine residues can occur with peroxynitrite (Alvarez *et al.*, 1999; Carballal *et al.*, 2003).

Peroxynitrite stock solutions in sodium hydroxide are synthesized from hydrogen peroxide and sodium nitrite (Saha *et al.*, 1998). Excess hydrogen peroxide is removed by treatment with manganese dioxide and peroxynitrite concentration is determined at 302 nm ($\varepsilon_{302} = 1670\ M^{-1}\ cm^{-1}$; Hughes and Nicklin, 1968) in 0.1 *M* sodium hydroxide immediately before use. Albumin oxidation is performed by incubating reduced HSA (0.5 m*M*) with peroxynitrite (1 m*M*) for 3 min at 37 °C in phosphate buffer (0.1 *M*, pH 7.4, 0.1 m*M* dtpa). To control the effects of potential peroxynitrite contaminants, reverse order of addition experiments must be performed by first decomposing peroxynitrite in the buffer (e.g., 2-min incubation) before mixing with albumin. It is critical to use phosphate buffer with peroxynitrite, since other buffers such as Tris and Hepes can interfere, reacting with peroxynitrite or its derived radicals. It is also important to prepare the phosphate buffer daily and to avoid the use of sodium hydroxide in order to minimize contamination with bicarbonate/carbon dioxide, which reacts with peroxynitrite. Also, because of the alkaline pH of peroxynitrite stock solutions, peroxynitrite additions should be <5% of total volume, in order to minimize changes in pH.

4. Detection of Albumin Sulfenic Acid

Since the sulfenic acid function does not possess distinguishing UV–vis absorbance or fluorescence features, different tools must be used to trap it and detect it. Herein, we analyze critically different strategies that we have used to detect the sulfenic acid of HSA.

4.1. Sodium arsenite

One of the first evidences for sulfenic acid formation in HSA was obtained from its reaction with sodium arsenite, since this reagent reduces sulfenic acid back to thiol but does not reduce disulfides (Radi *et al.*, 1991a,b). Indeed, incubation of oxidized HSA (4 m*M* H_2O_2, 4 min, 37 °C, pH 7.4) with 0.167 *M* sodium arsenite (10 min, 37 °C) led to an increase in the HSA–SH/HSA ratio by 0.051, which represents a 28% recovery with respect to the initial amount of HSA–SOH/HSA (0.18 ± 0.02). The low yield of recovery can be explained in terms of the spontaneous decay of HSA–SOH (1.7×10^{-3} s^{-1}) which competes with the reaction with arsenite (0.036 M^{-1} s^{-1}) (Turell *et al.*, 2008).

4.2. 7-chloro-4-nitrobenz-2-oxa-1,3-diazole (NBD-Cl)

The electrophilic reagent 7-chloro-4-nitrobenz-2-oxa-1,3-diazole (NBD-Cl) is widely used to detect protein sulfenic acids (Denu and Tanner, 1998; Ellis and Poole, 1997; Fuangthong and Helmann, 2002). This reagent reacts both with thiol and with sulfenic acid, leading to different products with distinct UV–vis absorbance characteristics, Eqs. (5.4) and (5.5). The sulfoxide product formed between sulfenic acid and NBD-Cl absorbs at ~350 nm, while the product with the thiol, a thioether, absorbs at ~420 nm.

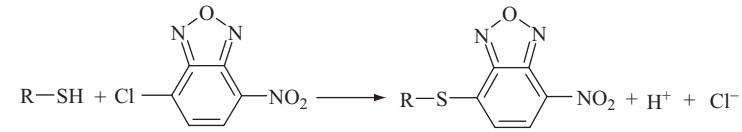

(5.4)

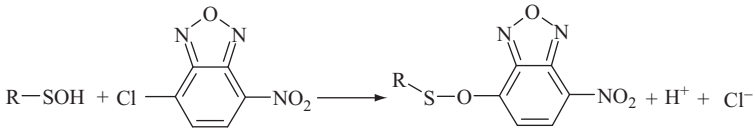

(5.5)

However, when reduced albumin (0.5 m*M*) was incubated with NBD-Cl (1 m*M*, 30 min, 37 °C, pH 7.4) followed by gel filtration to remove excess NBD-Cl, we observed a maximum at 400 nm which corresponds to the sum of the product with the thiol and the product with a tyrosine (~382 nm) (Aboderin, 1976; Turell *et al.*, 2008). In fact, when a stoichiometric NBD-Cl concentration was used, we observed a peak at 388 nm, indicating that NBD-Cl reacted preferentially with tyrosine. Furthermore, NBD-Cl binds noncovalently to HSA and absorbs at 343 nm, making it difficult to discriminate between noncovalently bound NBD-Cl and the product of the reaction with HSA–SOH. It is important to note that NBD-Cl binds tightly to HSA, since it cannot be removed by gel filtration. So, a large limitation of the use of NBD-Cl with albumin sulfenic acid is its

lack of specificity, making it an unsuitable reagent for spectrophotometric detection, although it may be used in mass spectrometry studies (Kratochwil *et al.*, 1999; Turell *et al.*, 2008).

4.3. Dimedone and mass spectrometry

Due to the electrophilic character of the sulfur atom of sulfenic acid, its reactivity toward nucleophilic reagents constitutes an important strategy for its detection, since other electrophilic groups are scarce in proteins (Allison, 1976; Poole *et al.*, 2007). Dimedone (5,5-dimethyl-1,3-cyclohexanedione) does not react with reduced thiol and reacts specifically with sulfenic acid, Eq. (5.6). The second-order rate constant with HSA–SOH was recently determined as 0.027 $M^{-1}\,s^{-1}$ (pH 7.4, 37 °C) (Turell *et al.*, 2008). This reaction leads to the formation of a stable thioether which can be identified by mass spectrometry. This approach provided the definite evidence for the formation of sulfenic acid in albumin samples oxidized with hydrogen peroxide and confirmed the formation of this derivative at the level of Cys34 (Carballal *et al.*, 2003).

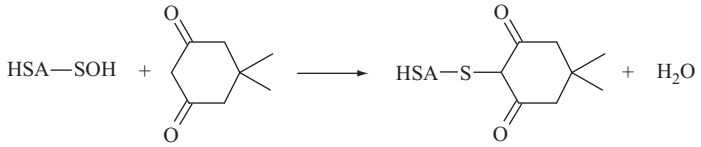

(5.6)

The mass spectrometry analysis of the tryptic map of albumin can be obscured by the presence of 35 cysteines that, after treatment with trypsin, undergo disulfide exchange reactions, immensely increasing the number of possible fragments. In fact, the tryptic fragment containing Cys34 in the reduced thiol state (residues 21–41, 2432.3 Da) usually cannot be directly observed. In order to detect the reduced thiol, reductive alkylation procedures that block thiols should be performed. For the detection of oxidized forms, reductive alkylation is not necessary.

To detect the dimedonylated tryptic fragment produced by reaction of HSA–SOH with dimedone, reduced HSA (0.5 m*M*) is first oxidized with hydrogen peroxide. Then, 2.5 m*M* dimedone (stock solution in 95% ethanol) is added and, after 30 min agitation at room temperature, the protein is passed through a water-equilibrated gel filtration column. For the reductive alkylation, samples (1 mg, ~30 μL) are mixed with 200 μL of Tris buffer (0.2 *M*, pH 8) containing 6 *M* guanidine, purged with argon and incubated for 2 h at 37 °C. Thiols are reduced overnight with 60 m*M* dithiothreitol, which represents an ~25-fold excess with respect to total protein cysteines, and then carboxymethylated with iodoacetic acid (216 m*M*) for 1 h in the dark at room temperature, followed by the addition of 2-mercaptoethanol (248 m*M*). The samples are washed and concentrated by ultrafiltration and resuspended in 200 μL of ammonium bicarbonate (0.1 *M*). Trypsin (10 μg) is added and left overnight at 37 °C. Peptide

Table 5.1 Oxidative modifications of the albumin cysteine observed through mass spectrometry

Cysteine modification	Condition	Monoisotopic theoretical mass (Da)[a]	Observed *m/z*	Observed mass (Da)[b]	Reference
R–SH thiol		2432.3	ND[c]	ND[c]	Carballal *et al.* (2003), Turell *et al.* (2008)
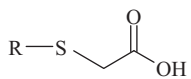 Carboxymethylcysteine	Reductive alkylation[d]	2490.3	831.4 (triply charged)[e]	2491.2	Carballal *et al.* (2003)
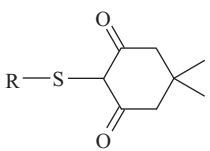 Dimedonylcysteine	+ H_2O_2 (1 m*M*, pH 7.4, 37 °C, 30 min) + dimedone (2.5 m*M*, 30 min) reductive alkylation[d]	2570.3	857.4 (triply charged)[e]	2569.2	Carballal *et al.* (2003)

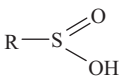 Sulfinic acid	$+H_2O_2$ (4 m*M*, pH 7.4, 37 °C, 30 min)	2464.3	1233.2 (doubly charged)[f]	2464.4	Turell *et al.* (2008)

[a] Expected mass of the tryptic fragment containing Cys34 (residues 21–41, ALVLIAFAQYLQQC_{34}PFEDHVK) and its modifications.
[b] Mass calculated from the *m/z* observed.
[c] ND, not detected.
[d] Reductive alkylation was performed by dithiothreitol reduction of disulfides in the presence of guanidine followed by treatment with iodoacetic acid as described in the text.
[e] Electrospray ionization (ESI) mass spectrometry (MS) analysis of peptides obtained after reductive alkylation with iodoacetic acid followed by tryptic digestion of albumin samples as described in the text. Peptide fragments were separated on a reverse-phase HPLC column (300 μM ID × 15 cm C18 PepMap) at a flow rate of 2 μL min^{-1} with a gradient from 20% to 100% acetonitrile/0.1% formic acid and analyzed in a Q-TOF III MS, Micromass, Manchester, UK. The location of the modification at Cys34 was confirmed through MS/MS analysis.
[f] Electrospray ionization (ESI) mass spectrometry (MS) analysis of peptides obtained after tryptic digestion of albumin samples (75 μM in ammonium bicarbonate, 50 m*M*, pH 8.2). Peptide mixtures were diluted 26-fold in 1% acetic acid/50% methanol, injected into a QTRAP 2000 mass spectrometer (Applied Biosystems/MDS Sciex) and analyzed directly in the enhanced resolution (ER) mode. The location of the modification at Cys34 was confirmed through MS/MS analysis.

fragments can be analyzed directly in the crude mixtures through matrix-assisted laser desorption ionization time-of-flight (MALDI-TOF) or electrospray ionization (ESI) mass spectrometry, or after separation through reverse phase high-performance liquid chromatography (HPLC). Table 5.1 illustrates the resulting analysis (Carballal *et al.*, 2003). In the control sample of reduced albumin, the tryptic fragment containing Cys34 was detected as the carboxymethylated derivative and MS/MS spectra of the triply charged ion confirmed the identity of the peptide. In the hydrogen peroxide-treated sample, a peptide with a mass increase of +138 Da could be detected, consistent with the reaction of dimedone with sulfenic acid. MS/MS spectra of the triply charged ion pinpointed the position of the dimedone modification at Cys34. Since reactions of dimedone with other groups such as aldehydes may be possible, mapping the alkylation to a specific cysteine residue is strongly recommended.

4.4. Glutathione

Evidence for sulfenic acid formation can also be obtained from its reaction with low molecular weight thiols. For glutathione, this reaction leads to the formation of mixed HSA–glutathione disulfide (HSA–SSG), which can also react with another glutathione, leading to the formation of glutathione disulfide (GSSG), Eqs. (5.7) and (5.8).

$$\mathrm{HSA-SOH + GSH \rightarrow HSA-SSG + H_2O} \tag{5.7}$$

$$\mathrm{HSA-SSG + GSH \rightarrow HSA-SH + GSSG} \tag{5.8}$$

Low molecular weight thiols do not react with reduced albumin thiol nor with higher oxidation states such as sulfinic acid. However, the potential reaction with disulfide, Eq. (5.8), should be taken into account. Thus, detection of sulfenic acid using low molecular weight thiols cannot be used with crude plasma samples that contain mixed albumin disulfides, but has proved very useful with laboratory samples that do not contain them (Carballal *et al.*, 2003).

To assess whether sulfenic acid formed from albumin reaction with hydrogen peroxide or peroxynitrite is able to oxidize glutathione, oxidized HSA (0.5 m*M*, prepared by incubation with hydrogen peroxide followed by catalase, or with peroxynitrite) is mixed with GSH (0.5 m*M*) and incubated for 30 min at 37 °C. Then, HSA is precipitated with perchloric acid (0.4 *M*) and centrifuged at 18,000×*g* for 10 min at 4 °C. Decreases in reduced GSH in the perchloric acid-soluble fraction can be determined by the DTNB assay. In turn, GSSG disulfide can be determined with NADPH and glutathione reductase (Sies and Akerboom, 1984) and mixed HSA–SSGs can be measured by reduction of disulfide bonds in the protein

fraction with sodium borohydride (5 m*M*) and quantification of glutathione. For example, oxidation of 0.14 m*M* GSH was detected (Carballal *et al.*, 2003), and recent results have revealed that the reaction of GSH with HSA–SOH is relatively slow, with a second-order rate constant of 2.9 M^{-1} s^{-1} (Turell *et al.*, 2008).

5. Quantification of Albumin Sulfenic Acid Using Thionitrobenzoate (TNB)

In contrast to glutathione, which does not have useful absorbance or fluorescence features and reacts relatively slowly with HSA–SOH, the yellow thiol thionitrobenzoate has become a valuable tool to characterize sulfenic acid. Its reactions with HSA–SOH, which occur within a few minutes, can be followed by the decrease in absorbance at 412 nm.

Thionitrobenzoate is not commercially available, so it must be synthesized in the laboratory. It is important to have solutions of TNB free of DTNB or other thiols. We developed a procedure based on the reduction of DTNB with 2-mercaptoethanol followed by ion exchange chromatography. A solution of DTNB (5 m*M*) is prepared in deionized water and alkalinized until complete dissolution. A 20-fold excess of 2-mercaptoethanol is added and the mixture is incubated for 30 min at room temperature. The amount of TNB formed (100% yield) is confirmed by the absorbance at 412 nm. Excess 2-mercaptoethanol is removed with a Q-Sepharose fast flow column previously equilibrated with Tris buffer (pH 7.5, 20 m*M*). After washing thoroughly with Tris buffer and water, TNB is eluted with HCl (50 m*M*). The acidic solutions are aliquoted and stored at −20 °C. In order to corroborate daily the absence of DTNB in the final TNB solution, an appropriate dilution of TNB is incubated with either reduced glutathione or 2-mercaptoethanol and no increases in the 412-nm absorbance should be observed.

Most procedures for detecting sulfenic acid, including mass spectrometry-based methods, yield qualitative data. The challenge of obtaining quantitative data was approached by our group by using TNB (Turell *et al.*, 2008). Although this reagent has been previously used for detecting sulfenic acid in other proteins by making endpoint measurements, these can be misleading in the case of albumin due to noncovalent binding of TNB and to the fact that the reaction is relatively complex. Thus, a careful analysis of the reaction and its kinetics is needed.

When oxidized HSA (50 μM) is mixed with TNB (80 μM, phosphate buffer, 0.1 *M*, pH 7.4, 25 °C), a biphasic decay of absorbance at 412 nm is observed. The first phase of the reaction (Fig. 5.5), lasting for ~15 min, fits an exponential plus straight line equation and is assigned to the reaction

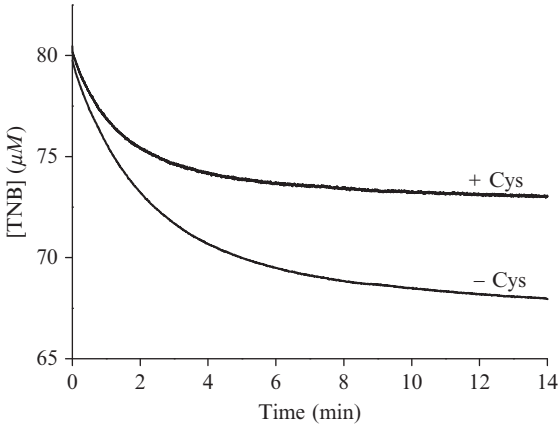

Figure 5.5 Reaction of albumin sulfenic acid with thionitrobenzoate (TNB) and competition with cysteine. HSA was oxidized with hydrogen peroxide (4 m*M*, 4 min, 37 °C) and the reaction was stopped with catalase. Aliquots (50 μM) were mixed with TNB (80 μM) at 25 °C in the absence or presence of cysteine (0.16 m*M*) using a stopped flow spectrophotometer at 412 nm.

between HSA–SOH and TNB to form the mixed disulfide HSA–STNB, Eq. (5.9), with a second-order rate constant of 105 M^{-1} s^{-1}.

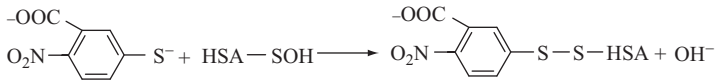

(5.9)

Accordingly, this phase of the reaction is first-order in TNB and oxidized HSA, and controls using reduced or NEM-blocked HSA showed no TNB consumption. Both the amplitude and the initial rate of the reaction can be used to quantify sulfenic acid. This approach yielded a HSA–SOH/HSA ratio of 0.18 ± 0.02. The relatively low yield of albumin sulfenic acid is puzzling and may involve conformational effects in addition to decay processes. It is critical to perform the reactions at 25 °C and ~80 μM TNB, since higher temperatures and concentrations led to increased consumption of TNB with a concomitant increase in the absorbance at 279 nm, probably due to partial denaturation of the protein.

6. Reactivity of Sulfenic Acid

The possibility of obtaining quantitative data using TNB enables to study the reactivity of HSA–SOH systematically. In order to do this, the reaction between HSA–SOH and TNB can be exploited in two ways.

First, a competition approach can be used. As illustrated in Fig. 5.5, the addition of a target other than TNB in the mixtures, such as cysteine, increases the observed rate constant (k_{obs}) of TNB decay (e.g., from 0.466 to 0.665 min^{-1} in the absence and presence of 0.16 m*M* cysteine, respectively) and decreases the amplitude. These parameters are obtained from the fit of the kinetic traces to an exponential plus straight line equation. The variation of k_{obs} with the concentration of target can be used to calculate second-order rate constants of HSA–SOH reactions. This approach was used to measure the rate constants of low molecular weight thiols present in plasma (Table 5.2) and ruled out reactions with amino groups of amino acids (Turell *et al.*, 2008).

Second, an initial rate approach can be used. Oxidized HSA is incubated in the absence or presence of possible targets. At increasing times, aliquots are mixed with TNB and the initial rate of TNB consumption, which is proportional to HSA–SOH concentration, is measured. This approach was used to determine the rate of spontaneous decay of sulfenic acid. Although relatively stable due to the absence of neighboring thiols and to its location in a crevice, HSA–SOH decays spontaneously with an apparent first-order rate constant of $1.7 \times 10^{-3}\ s^{-1}$. The decay does not involve the formation of sulfenamides, as has been proposed for other proteins (Salmeen *et al.*, 2003) and is currently under scrutiny. In addition, this approach ruled out reaction of HSA–SOH with the plasma reductants ascorbate and urate (Turell *et al.*, 2008).

Table 5.2 Rate constants of reactions of albumin sulfenic acid

Reagent	Rate constant ($M^{-1}\ s^{-1}$)[a]	Temperature (°C)	Procedure
Thionitrobenzoate	105 ± 11	25	
Dimedone	0.027 ± 0.009	37	Initial rate[b]
Sodium arsenite	0.036 ± 0.009	37	Initial rate[b]
Hydrogen peroxide	0.4 ± 0.2	37	Initial rate[b]
Cysteine	21.6 ± 0.2	25	Competition[c]
Glutathione	2.9 ± 0.5	25	Competition[c]
Homocysteine	9.3 ± 0.9	25	Competition[c]
Cysteinylglycine	55 ± 3	25	Competition[c]

[a] Rate constants are taken from Turell *et al.* (2008). The second-order rate constants of HSA–SOH reactions were determined at pH 7.4 using TNB.

[b] Initial rate approach where oxidized albumin was incubated at 37 °C in the presence of the reagents under study. At fixed time points, aliquots were removed, mixed with TNB and the initial rate of the decay of the absorbance at 412, which is proportional to the remaining HSA–SOH, was measured.

[c] Competition approach where both TNB and the reagent under study were mixed with oxidized albumin in a stopped flow spectrophotometer, following the increase in the exponential rate constant of the absorbance at 412 decay.

7. Detection of Albumin Sulfinic Acid

Once formed, one of the possible fates of albumin sulfenic acid is further reaction with hydrogen peroxide to form sulfinic acid. Through an initial rate approach, the second-order rate constant was determined as 0.4 M^{-1} s^{-1} (pH 7.4, 37 °C) (Turell *et al.*, 2008), Eq. (5.10).

$$\mathrm{HSA-SOH + H_2O_2 \rightarrow HSA-SO_2H + H_2O} \tag{5.10}$$

The formation of sulfinic acid was confirmed through mass spectrometric analysis of peptide mixtures obtained by overoxidation of albumin samples followed by trypsin digestion (Table 5.1). It is interesting to note that the analysis could be performed without reductive alkylation of cysteines and without HPLC separation of tryptic fragments (Turell *et al.*, 2008).

8. Conclusions

The experimental strategies described herein have allowed us to advance in the characterization of the sulfenic acid formed in HSA. Its particular environment, located in a cleft that prevents interprotein disulfide formation and with no thiols nearby to react with, is the basis of the kinetic stability that provides a valuable opportunity to assess the formation and decay processes of a protein sulfenic acid. The detailed analysis of the reactivity of albumin sulfenic acid with plasma components allows us to rationalize the possible fates of sulfenic acid formed in the circulation. Kinetic considerations of rate constant times concentration suggest that sulfenic acid is likely to react with free thiols forming mixed disulfides. Another possibility is further oxidation to sulfinic acid. The fact that mixed disulfides and higher oxidation states are present in circulating albumin and increase under pathological conditions (reviewed in Turell *et al.*, 2009) supports the concept that albumin sulfenic acid is a central intermediate in the oxidation of the albumin thiol.

ACKNOWLEDGMENTS

This work was supported by grants from Programa de Desarrollo Tecnológico-II (Ministry of Education and Culture, Uruguay), CSIC (Universidad de la República, Uruguay), Philip Morris USA Inc. and Philip Morris International, the International Centre of Genetic Engineering and Biotechnology, and the Howard Hughes Medical Institute. L.T. and S.C. acknowledge fellowships from PEDECIBA and ANII (Uruguay). R.R. is a Howard Hughes International Research Scholar.

REFERENCES

Aboderin, A. (1976). Reaction of chicken egg white lysozyme with 7-chloro-4-nitrobenz-2-oxa-1, 3-diazole. *Biochim.t Biophys. Acta* **420,** 177–186.

Aebi, H. (1984). Catalase in vitro. *Methods Enzymol.* **105,** 121–126.

Allison, W. (1976). Formation and reactions of sulfenic acids in proteins. *Acc. Chem. Res.* **9,** 293–299.

Alvarez, B., Ferrer-Sueta, G., Freeman, B. A., and Radi, R. (1999). Kinetics of peroxynitrite reaction with amino acids and human serum albumin. *J. Biol. Chem.* **274,** 842–848.

Bonini, M. G., and Augusto, O. (2001). Carbon dioxide stimulates the production of thiyl, sulfinyl, and disulfide radical anion from thiol oxidation by peroxynitrite. *J. Biol. Chem.* **276,** 9749–9754.

Boyer, P. D. (1954). Spectrophotometric study of the reaction of protein sulfhydryl groups with organic mercurials. *J. Am. Chem. Soc.* **76,** 4331–4337.

Carballal, S., Radi, R., Kirk, M. C., Barnes, S., Freeman, B. A., and Alvarez, B. (2003). Sulfenic acid formation in human serum albumin by hydrogen peroxide and peroxynitrite. *Biochemistry* **42,** 9906–9914.

Carballal, S., Alvarez, B., Turell, L., Botti, H., Freeman, B. A., and Radi, R. (2007). Sulfenic acid in human serum albumin. *Amino Acids* **32,** 543–551.

Chen, R. F. (1967). Removal of fatty acids from serum albumin by charcoal treatment. *J. Biol. Chem.* **242,** 173–181.

Claiborne, A. (1985). In Handbook of Methods for Oxygen Radical Research. CRC Press, Inc., Boca Raton, FL.

Denu, J. M., and Tanner, K. G. (1998). Specific and reversible inactivation of protein tyrosine phosphatases by hydrogen peroxide: Evidence for a sulfenic acid intermediate and implications for redox regulation. *Biochemistry* **37,** 5633–5642.

Ellis, H. R., and Poole, L. B. (1997). Novel application of 7-chloro-4-nitrobenzo-2-oxa-1, 3-diazole to identify cysteine sulfenic acid in the AhpC component of alkyl hydroperoxide reductase. *Biochemistry* **36,** 15013–15018.

Ellman, G., and Lysko, H. (1979). A precise method for the determination of whole blood and plasma sulfhydryl groups. *Anal. Biochem.* **93,** 98–102.

Era, S., Kuwata, K., Imai, H., Nakamura, K., Hayashi, T., and Sogami, M. (1995). Age-related change in redox state of human serum albumin. *Biochim. Biophys. Acta* **1247,** 12–16.

Fuangthong, M., and Helmann, J. D. (2002). The OhrR repressor senses organic hydroperoxides by reversible formation of a cysteine-sulfenic acid derivative. *Proc. Natl. Acad. Sci. USA* **99,** 6690–6695.

Giustarini, D., Dalle-Donne, I., Lorenzini, S., Milzani, A., and Rossi, R. (2006). Age-related influence on thiol, disulfide, and protein-mixed disulfide levels in human plasma. *J. Gerontol. A Biol. Sci. Med. Sci.* **61,** 1030–1038.

Gustafsson, J. E. (1976). Improved specificity of serum albumin determination and estimation of "acute phase reactants" by use of the bromcresol green reaction. *Clin. Chem.* **22,** 616–622.

Hughes, M. N., and Nicklin, H. G. (1968). The chemistry of pernitrites. Part I. Kietics of decomposition of pernitrous acid. *J. Chem. Soc. A* 450–452.

Kratochwil, N. A., Ivanov, A. I., Patriarca, M., Parkinson, J. A., Gouldsworthy, A. M., Murdoch, P., and Sadler, P. J. (1999). Surprising reactions of iodo Pt(IV) and Pt(II) complexes with human serum albumin: Detection of Cys34 sulfenic acid. *J. Am. Chem. Soc.* **121,** 8193–8203.

Leto, S., Yiengst, M. J., and Barrows, C. H. Jr. (1970). The effect of age and protein deprivation on the sulfhydryl content of serum albumin. *J. Gerontol.* **25,** 4–8.

Musante, L., Bruschi, M., Candiano, G., Petretto, A., Dimasi, N., Del Boccio, P., Urbani, A., Rialdi, G., and Ghiggeri, G. M. (2006). Characterization of oxidation end product of plasma albumin 'in vivo'. *Biochem. Biophys. Res. Commun.* **349,** 668–673.

Musante, L., Candiano, G., Petretto, A., Bruschi, M., Dimasi, N., Caridi, G., Pavone, B., Del Boccio, P., Galliano, M., Urbani, A., Scolari, F., Vincenti, F., and Ghiggeri, G. M. (2007). Active focal segmental glomerulosclerosis is associated with massive oxidation of plasma albumin. *J. Am. Soc. Nephrol.* **18,** 799–810.

Oettl, K., Stadlbauer, V., Petter, F., Greilberger, J., Putz-Bankuti, C., Hallstrom, S., Lackner, C., and Stauber, R. E. (2008). Oxidative damage of albumin in advanced liver disease. *Biochim. Biophys. Acta* **1782,** 469–473.

Peters, T. (1996). All About Albumin. Biochemistry, Genetics and Medical Applications. Academic Press, San Diego.

Pinnell, A. E., and Northam, B. E. (1978). New automated dye-binding method for serum albumin determination with bromcresol purple. *Clin. Chem.* **24,** 80–86.

Poole, L. B., Klomsiri, C., Knaggs, S. A., Furdui, C. M., Nelson, K. J., Thomas, M. J., Fetrow, J. S., Daniel, L. W., and King, S. B. (2007). Fluorescent and affinity-based tools to detect cysteine sulfenic acid formation in proteins. *Bioconjug. Chem.* **18,** 2004–2017.

Quijano, C., Alvarez, B., Gatti, R. M., Augusto, O., and Radi, R. (1997). Pathways of peroxynitrite oxidation of thiol groups. *Biochem. J.* **322**(Pt 1), 167–173.

Radi, R., Beckman, J. S., Bush, K. M., and Freeman, B. A. (1991a). Peroxynitrite oxidation of sulfhydryls. The cytotoxic potential of superoxide and nitric oxide. *J. Biol. Chem.* **266,** 4244–4250.

Radi, R., Bush, K. M., Cosgrove, T. P., and Freeman, B. A. (1991b). Reaction of xanthine oxidase-derived oxidants with lipid and protein of human plasma. *Arch. Biochem. Biophys.* **286,** 117–125.

Riener, C. K., Kada, G., and Gruber, H. J. (2002). Quick measurement of protein sulfhydryls with Ellman's reagent and with 4, 4′-dithiodipyridine. *Anal. Bioanal. Chem.* **373,** 266–276.

Saha, A., Goldstein, S., Cabelli, D., and Czapski, G. (1998). Determination of optimal conditions for synthesis of peroxynitrite by mixing acidified hydrogen peroxide with nitrite. *Free Radic. Biol. Med.* **24,** 653–659.

Salmeen, A., Andersen, J. N., Myers, M. P., Meng, T. C., Hinks, J. A., Tonks, N. K., and Barford, D. (2003). Redox regulation of protein tyrosine phosphatase 1B involves a sulphenyl-amide intermediate. *Nature* **423,** 769–773.

Sies, H., and Akerboom, T. P. (1984). Glutathione disulfide (GSSG) efflux from cells and tissues. *Methods Enzymol.* **105,** 445–451.

Terawaki, H., Yoshimura, K., Hasegawa, T., Matsuyama, Y., Negawa, T., Yamada, K., Matsushima, M., Nakayama, M., Hosoya, T., and Era, S. (2004). Oxidative stress is enhanced in correlation with renal dysfunction: Examination with the redox state of albumin. *Kidney Int.* **66,** 1988–1993.

Turell, L., Botti, H., Carballal, S., Ferrer-Sueta, G., Souza, J. M., Duran, R., Freeman, B. A., Radi, R., and Alvarez, B. (2008). Reactivity of sulfenic acid in human serum albumin. *Biochemistry* **47,** 358–367.

Turell, L., Botti, H., Carballal, S., Radi, R., and Alvarez, B. (2009). Sulfenic acid–a key intermediate in albumin thiol oxidation. *J. Chromatogr. B Analyt. Technol. Biomed. Life Sci.* **877,** 3384–3392.

CHAPTER SIX

Determination of GSH, GSSG, and GSNO Using HPLC with Electrochemical Detection

Li-Peng Yap,* Harsh Sancheti,* Maria D. Ybanez,† Jerome Garcia,* Enrique Cadenas,* *and* Derick Han†

Contents

Abstract

GSNO is an important intermediate in nitric oxide metabolism and mediates many ˙NO-mediated signaling pathways through the post-translational modification of redox-sensitive proteins. The detection of GSNO in biological samples has been hampered by a lack of sensitive and simple assays. In this work, we describe the utilization of HPLC with electrochemical detection for the identification and quantification of GSNO in biological samples. GSNO requires a high potential (>700 mV) for its electrochemical detection, similar to that of GSSG. A simple isocratic HPLC system can be used to separate and simultaneously detect GSH, GSSG, and GSNO electrochemically. This HPLC system can be utilized to measure the redox profile of biological samples and applied for the measurement of GSNO reductase activity in cells. Proper sample preparation is

* Department of Pharmacology and Pharmaceutical Sciences, School of Pharmacy, University of Southern California, Los Angeles, California, USA
† Research Center for Liver Diseases, Keck School of Medicine, University of Southern California, Los Angeles, California, USA

Methods in Enzymology, Volume 473
ISSN 0076-6879, DOI: 10.1016/S0076-6879(10)73006-8

essential in GSNO measurements, because artifactual formation of GSNO occurs in acidic conditions due to the reaction between GSH and nitrite. Treatment of samples with ammonium sulfamate or *N*-ethylmaleimide (NEM) can prevent the artifactual formation of GSNO and accurately detect GSNO in biological samples. Overall, the HPLC with electrochemical detection is a powerful tool to measure redox status in cells and tissues.

1. Introduction

The involvement of ˙NO as a pleiotropic signaling molecule in the regulation of numerous physiological processes, as well as its deleterious effects when generated in high amounts during pathophysiological diseases, such as during neuroinflammation, has spurred a significant amount of interest in ˙NO chemistry. Generated through the enzymatic oxidation of L-arginine to L-citrulline by nitric oxide synthases (NOS), the reactivity and consequences of ˙NO in biological systems is regulated by many complex and competing reactions; of which the reaction between ˙NO and thiols, to yield *S*-nitrosothiols, is extremely important in cell signaling (Davis *et al.*, 2001; Lamas *et al.*, 2007). Of relevance to cellular redox status and signaling—through protein post-translation modifications—is the formation of *S*-nitrosoglutathione (GSNO). The intracellular formation of GSNO is complex and postulated to occur through a series of mechanisms (see Martinez-Ruiz and Lamas, 2007). In the presence of O_2, ˙NO is oxidized to dinitrogen dioxide (N_2O_3), a nitrosating species (Martinez-Ruiz and Lamas, 2007; Eqs. (6.1) and (6.2)). This reaction is accelerated in membranes due to the partition coefficient of both ˙NO and O_2, and may enhance the yield of thiol nitrosation in membrane-rich environments such as mitochondria (Hogg, 2002).

$$2\dot{N}O + \tfrac{1}{2}O_2 \rightarrow N_2O_3 \tag{6.1}$$

$$N_2O_3 + RSH \rightarrow RSNO + H^+ + NO_2^- \tag{6.2}$$

The formation of GSNO can also occur through a transnitrosation reaction between two thiols; in this case, the reaction between a nitrosylated protein and GSH (Eq. (6.3)).

$$R - S - H + R' - S - NO \rightarrow R - S - NO + R' - SH \tag{6.3}$$

GSNO has been identified in a variety of tissues and is considered a biologically relevant metabolite of ˙NO due to its ability to modulate cellular signaling through the post-translational modifications of redox-sensitive proteins, that is, *S*-nitrosylation (Eq. (6.4)) and/or *S*-glutathionylation (Eq. (6.5)). This redox modulation of numerous proteins (see Dalle-Donne

et al., 2008; Martinez-Ruiz and Lamas, 2007; Stamler *et al.*, 2001) has been suggested to play a substantial role in ˙NO-regulated signaling, independent of guanylyl cyclase. Furthermore, increasing evidence points to a role for post-translationally modified proteins in disease pathology, such as in Alzheimer's disease (Dalle-Donne *et al.*, 2008).

$$\mathrm{GSNO} + \mathrm{Pr} - \mathrm{SH} \rightarrow \mathrm{Pr} - \mathrm{S} - \mathrm{NO} + \mathrm{GSH} \tag{6.4}$$

$$\mathrm{GSNO} + \mathrm{Pr} - \mathrm{SH} \rightarrow \mathrm{Pr} - \mathrm{S} - \mathrm{SG} + \mathrm{NO}^{-} \tag{6.5}$$

The intracellular stability of GSNO is governed by many factors, including chemically driven degradation reactions—thiol and metal-mediated decomposition—(Hogg, 2002; Singh *et al.*, 1996; Zeng *et al.*, 2001), and enzymatically driven reactions. The main enzymatic-dependent degradation described thus far is the reduction of GSNO to GSSG by glutathione-dependent formaldehyde dehydrogenase (or alcohol dehydrogenase III); later labeled by some groups as GSNO reductase (Hedberg *et al.*, 2003; Liu *et al.*, 2001; Eqs. (6.6)–(6.9)), due to its high specificity and affinity for GSNO and a reflection of the increasingly important role of GSNO in redox chemistry.

$$\mathrm{GSNO} + \mathrm{NADH} + \mathrm{H}^{+} \rightarrow \mathrm{GSNHOH} + \mathrm{NAD}^{+} \tag{6.6}$$

$$\mathrm{GSNHOH} + \mathrm{NADH} + \mathrm{H}^{+} \rightarrow \mathrm{GSNH_2} + \mathrm{NAD}^{+} + \mathrm{H_2O} \tag{6.7}$$

$$\mathrm{GSNH_2} + \mathrm{GSH} \rightarrow \mathrm{GSSG} + \mathrm{NH_3} \tag{6.8}$$

Because of the importance of GSNO in modulating ˙NO signaling processes, accurate and specific methods to measure GSNO in biological samples are needed. Traditionally, GSNO has been measured using HPLC with UV detection (~336 nm) (Steffen *et al.*, 2001; Tsikas *et al.*, 2001). However, this HPLC method suffers from both issues of specificity and sensitivity in measuring GSNO in biological samples. In this study, we adapted a HPLC coulometric electrochemical method for the detection of GSNO in biological samples. The coulometric HPLC method described in this work can simultaneously measure GSH, GSSG, and GSNO, thus providing a redox profile of biological samples.

2. Methods

2.1. High-performance liquid chromatography with electrochemical detection

GSH, GSNO, and GSSG were detected using HPLC with a coulometric electrochemical detector from ESA (Chelmsford, MA). Electrochemical detection has commonly been used to measure GSH and GSSG with

HPLC (Han *et al.*, 2006a; Harvey *et al.*, 1989; Rebrin *et al.*, 2007); however, its application for the measurement of GSNO has not been described. ESA offers CoulArray systems that utilize between 4 and 16 channels. We employed a 4-channel electrochemical array for the simultaneous detection of GSH, GSNO, and GSSG. The mobile phase for isocratic elution of the sulfhydryls was composed of 25 m*M* monobasic sodium phosphate, 0.5 m*M* 1-octane sulfonic acid (ion-pairing agents), and 2.5% acetonitrile, pH 2.7. All chemicals including GSH, GSSG, and GSNO were purchased from Sigma Chemicals (St. Louis, MO, USA). The pH for the mobile phase should be adjusted with 85% phosphoric acid. A flow rate of 1 mL/min was used with a C_{18} column (5 μM column, 4.6 × 250 mm). Acetonitrile is the key component in modulating the retention times of GSH, GSNO, and GSSG. With 2.5% of acetonitrile in the mobile phase, the retention times for GSH generally appears at ~5 min, GSNO ~16 min, and GSSG ~20 min (retention times also vary with the type of column used). Increasing acetonitrile levels in the mobile phase will decrease the elution time of the sulfhydryls, and conversely decreasing acetonitrile levels lengthen the retention time of all sulfhydryls, particularly GSNO and GSSG. It should also be noted that other sulfhydryls (i.e., methionine, cysteine, and cystine) can be simultaneously detected with this electrochemical system.

2.2. Hydrodynamic voltammogram of GSH, GSNO, and GSSG

GSNO, like GSSG, requires a high applied potential for detection. Figure 6.1 shows that the hydrodynamic voltammogram of GSNO is similar to GSSG, requiring a potential greater than +700 mV before a signal can be observed. The detection of GSH, on the other hand, occurs at low voltages and plateaus after +800 mV. Since both GSNO and GSSG are found at very low levels in biological samples, due to GSNO reductase and GSSG reductase activities, higher potentials (>+875 mV) are recommended for the detection of GSNO and GSSG in biological samples. In a coulochemical array, there are several possible configurations for the simultaneous detection of GSH, GSSG, and GSNO. A typical setting for a four-array electrode system used was 1 = +300, 2 = +450, 3 = +600, 4 = +900 mV. Electrodes 1 and 2 serve as screening electrodes to oxidize potentially interfering compounds. GSH is detected on electrodes 3 and 4, while GSSG and GSNO are monitored in electrode 4. Figure 6.2 shows a chromatogram of GSH, GSSG, and GSNO, detected with electrodes set at +600 and +900 mV. The peak of GSNO generally precedes GSSG by a couple of minutes (varying with the acetonitrile concentrations in the mobile phase). In a 2.5% acetonitrile concentration, the difference in the retention time between GSNO and GSSG is ~4 min. An alternative configuration for GSNO detection would be as follows: electrode 1 (+350 mV) to screen potentially interfering compounds with low

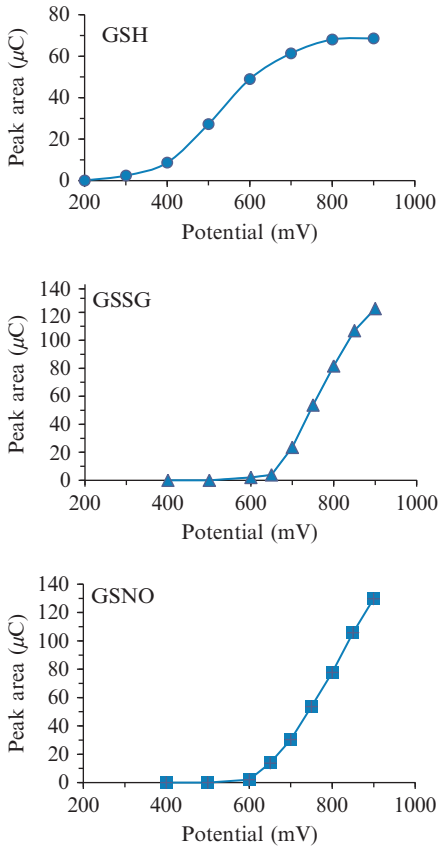

Figure 6.1 Hydrodynamic voltammogram of GSH, GSSG, and GSNO. The signal generated by GSH, GSSG, and GSNO standards at different voltages are shown.

potentials, electrode 2 (+500 mV) to detect GSH, electrode 3 (+700 mV) to screen potentially interfering compounds with high potentials, and electrode 4 (+900 mV) for GSNO and GSSG detection. This electrode configuration may be useful for samples where the presence of compounds that have high reduction potentials and retention times similar to GSNO that may potentially interfere with GSNO detection. However, it must be noted that the long-term use of high potentials (>+600 mV) causes the electrode to corrode quicker and burn out at a faster rate. Consequently, the high potential required to measure GSSG and GSNO shortens the lifetime of electrodes significantly. In addition, electrode drift is a frequent problem at the high potentials required to measure GSNO. Consequently, GSNO and other standards should be injected on a regular basis to monitor electrode drift during sample analysis.

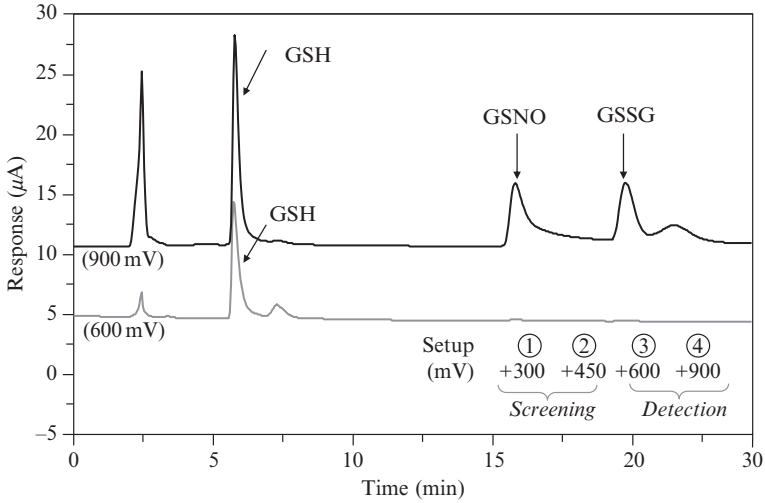

Figure 6.2 HPLC chromatogram of GSH, GSSG, and GSNO. The analysis shows GSH, GSSG, and GSNO signals at +600 and +900 mV. GSNO and GSSG cannot be generally detected until the potential reaches greater than +700 mV. Insert shows the electrode settings for all channels for optimal detection of GSH, GSNO, and GSSG.

2.3. GSNO detection in biological samples: Effect of sample preparation

The degradation of GSNO by GSNO reductase occurs at diffusion-controlled rates; hence, half-life of GSNO is short and rarely accumulates to high levels in cells. However, using the HPLC coulochemical array system, we were able to observe GSNO formation in neurons and astrocytes following $^{\cdot}$NO treatment (Yap *et al.*, 2010). For the measurement of GSNO, proper sample preparation is critical for accurate measurement. Although *S*-nitrosothiols are relatively stable, due to the slightly polar covalent bond between sulfur and nitrogen, the bond is susceptible to homolysis by strong, direct light (Hogg, 2002). Hence, during the measurement of GSNO, GSH, and GSSG, it is particularly important to use dark amber vials for all experiments, under minimal light exposure. In addition, GSNO can be artifactually generated during sample processing, particularly under acidic conditions.

For the measurement of GSH and GSSG in biological samples (i.e., cells, tissues, and plasma), acid treatment (i.e., 5% *o*-metaphosphoric acid and trichloroacetic acid) to prevent GSH autoxidation and to precipitate proteins, has been frequently used (Han *et al.*, 2006a; Rebrin *et al.*, 2007). Following acid treatment, samples are centrifuged (12,000 × *g* for 5 min) and the supernatant injected into the HPLC for GSH and GSSG

measurements. GSH is stable in acids, and the low pH prevents GSH from deprotonating and acting as a strong nucleophile to form glutathionylated proteins (Han *et al.*, 2006b). However, acid treatment for GSNO measurements creates a problem since nitrite and GSH react in acidic conditions to form GSNO (Eqs. (6.9)–(6.10)) (Tsikas, 2003). Because nitrite is a major oxidation product of ˙NO, it will be present in biological samples when ˙NO is produced. Consequently, the acidification of biological samples containing GSH and nitrite result in the artifactual formation of GSNO.

$$NO_2^- + H^+ \rightarrow HNO_2 \tag{6.9}$$

$$HNO_2 + GSH \rightarrow GSNO + H_2O \tag{6.10}$$

For GSNO measurements, nonacidic buffer must be utilized or additional steps must be taken to neutralize GSH or nitrite in samples. We investigated the utilization of ammonium sulfamate or *N*-ethylmaleimide (NEM) for the measurement of GSNO in neurons. Ammonium sulfamate neutralizes nitrite in biological samples under acidic conditions (Tsikas *et al.*, 2001). Conversely, NEM binds to the free thiol groups of GSH, preventing any possible reaction with nitrites under acidified conditions (Asensi *et al.*, 1994) to prevent any possible reaction with nitrites. The effect of sample preparation on GSNO measurements is illustrated in Table 6.1. The treatment of primary cultured neurons with the ˙NO donor, DETA-NO (20 μM), for 1 h causes GSNO formation in neurons, but the levels vary depending on sample preparation. The addition of only 5% *o*-metaphosphoric acid to neurons results in very high levels of GSNO. Clearly, the high GSNO levels in ˙NO-exposed neurons treated with

Table 6.1 Effect of sample preparation on GSNO levels in primary cultured neurons

	GSH	GSNO	GSSG
MPA treatment only			
Control	13.8 ± 5.1	0	0.041 ± 0.035
˙NO treatment	7.15 ± 5.8	2.81 ± 1.21	0.24 ± 0.19
AS plus MPA treatment			
Control	13.2 ± 6.1	0	0.038 ± 0.029
˙NO treatment	7.8 ± 6.0	0.21 ± 0.14	0.18 ± 0.15
NEM plus MPA treatment			
Control	–	0	0.049 ± 0.039
˙NO treatment	–	0.30 ± 0.23	0.23 ± 0.19

All values expressed as nmol per million cells. Primary cultured neurons were treated with a ˙NO donor, DETA-NO (20 μM) for 1 h. AS, ammonium sulfamate (25 m*M*); NEM, *N*-ethylmaleimide (20 m*M*); MPA, *o*-metaphosphoric acid (5%).

only *o*-metaphosphoric acid are partially due to artifactual formation since the treatment of neurons with ammonium sulfate (25 m*M*) dissolved in *o*-metaphosphoric acid resulted in significantly lower GSNO levels. Similarly, NEM treatment to neurons (20 m*M*), which chelates GSH, followed by *o*-metaphosphoric acid treatment, resulted in equally low levels of GSNO. Neither NEM or ammonium sulfamate resulted in the degradation of GSNO in standards or spiked biological samples. Sample preparation using NEM or ammonium sulfamate produced slightly varying GSNO values in neurons treated with DETA-NO, although the difference was not significant. An advantage of using ammonium sulfamate over NEM in sample preparation is the ability to simultaneously measure GSH, GSNO, and GSSG in the same sample, while NEM treatment only allows for GSNO and GSSG measurements. Consequently, we recommend ammonium sulfamate treatment for the measurement of GSNO in biological samples, although measurements with NEM pretreatment should also be done to ensure that the values obtained for GSNO and GSSG are correct. Overall, HPLC with electrochemical detection plus treatment with ammonia sulfamate allows for the simultaneous measurement of GSH, GSSG, and GSNO, thus providing an accurate measurement of the redox status in cells. In addition to increasing GSNO levels, $^{\cdot}$NO treatment to neurons caused an oxidation in the neuronal redox potential (increasing $\sim$42 mV) due to loss of GSH and increase in GSSG formation (Yap *et al.*, 2010).

2.4. Measurement of GSNO reductase activity using HPLC

Another application of the HPLC electrochemical system is the measurement of GSNO reductase activity in cells and tissues. For the measurement of GSNO reductase activity in primary cultured neurons, the following protocol was used. Neurons were washed with ice-cold PBS three times before lysis in reductase buffer (20 m*M* Tris–HCl, 0.5 m*M* EDTA, 0.1% NP-40, and 1 m*M* PMSF, pH 8). Lysate was sonicated three times (20 s, setting at 3.0, 100% pulse rate) at intervals with 1 min rest time on ice to disrupt cellular membranes and solubilize all proteins. To detect GSNO metabolizing activity, 1 mg/mL lysate was incubated with 100 μM of GSNO in the absence or presence of 200 μM NADH at room temperature (25°C). One hundred microliters of the lysate was removed at 5 min intervals and added into equal volumes of ice-cold 10% *o*-metaphosphoric acid. Samples were spun down at 10,000 $\times$ *g* for 10 min at 4°C to precipitate proteins and the supernatant was then collected and analyzed by HPLC for GSNO and GSSG formation. Figure 6.3 demonstrates that GSNO is only degraded by neuronal lysate when NADH is present. This suggests that GSNO degradation in neurons is mediated by the NADH-dependent GSNO reductase (Eqs. (6.6)–(6.8)). The decrease in GSNO in neuronal extracts was associated with the increase in the formation of GSSG that was

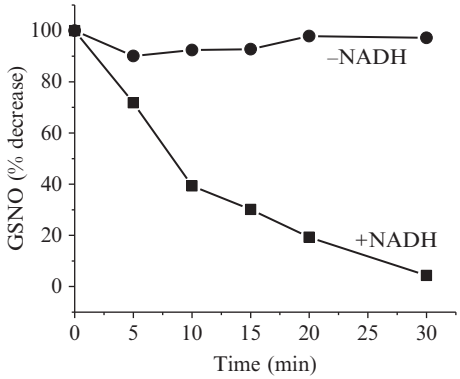

Figure 6.3 **Measurement of GSNO reductase in neurons activity using HPLC with electrochemical detection. GSNO (100 μM) is degraded by primary cultured neuronal lysates only in the presence of NADH (200 μM), suggesting that GSNO was being mediated by the NADH-dependent GSNO reductase. Values are expressed as percent of GSNO concentration at the start of the experiment.**

also observed by HPLC (data not shown). GSNO reductase activity has traditionally been measured by monitoring NADH levels, which is a substrate for many other enzymatic systems. HPLC with electrochemical detection is advantageous as a complementary approach for the measurement of GSNO reductase activity since GSNO levels can be directly measured.

3. Summary

HPLC with electrochemical detection is a simple (no derivatization required) and sensitive method for the simultaneous measurement of GSH, GSSG, and GSNO. This HPLC system can be utilized to measure the redox profile of biological samples and applied to the measurement of GSNO reductase activity in cells. The drawback of HPLC with electrochemical detection is that a high potential is required to measure GSNO and GSSG, which will shorten the lifetime of the electrode and cause electrode drift. Proper sample preparation is essential in GSNO measurements, since artifactual formation of GSNO will occur in acidic conditions due to a reaction between GSH and nitrite. Treatment of samples with ammonium sulfamate or NEM can prevent the artifactual generation of GSNO and accurately assesses GSNO levels in biological samples. Overall, the HPLC with electrochemical detection is a powerful tool to measure the redox status of cells and tissue.

ACKNOWLEDGMENTS

This work was supported by NIH Grant 2RO1 AG016718 and TRDRP grant 16RT-0186.

REFERENCES

Asensi, M., Sastre, J., Pallardo, F. V., Estrela, J. M., and Vina, J. (1994). Determination of oxidized glutathione in blood: High-performance liquid chromatography. *Methods Enzymol.* **234,** 367–371.

Dalle-Donne, I., Milzani, A., Gagliano, N., Colombo, R., Giustarini, D., and Rossi, R. (2008). Molecular mechanisms and potential clinical significance of *S*-glutathionylation. *Antioxid. Redox Signal.* **10,** 445–473.

Davis, K. L., Martin, E., Turko, I. V., and Murad, F. (2001). Novel effects of nitric oxide. *Annu. Rev. Pharmacol. Toxicol.* **41,** 203–236.

Han, D., Hanawa, N., Saberi, B., and Kaplowitz, N. (2006a). Hydrogen peroxide and redox modulation sensitize primary mouse hepatocytes to TNF-induced apoptosis. *Free Radic. Biol. Med.* **41,** 627–639.

Han, D., Hanawa, N., Saberi, B., and Kaplowitz, N. (2006b). Mechanisms of liver injury. III. Role of glutathione redox status in liver injury. *Am. J. Physiol. Gastrointest. Liver Physiol.* **291,** G1–G7.

Harvey, P. R., Ilson, R. G., and Strasberg, S. M. (1989). The simultaneous determination of oxidized and reduced glutathiones in liver tissue by ion pairing reverse phase high performance liquid chromatography with a coulometric electrochemical detector. *Clin. Chim. Acta* **180,** 203–212.

Hedberg, J. J., Griffiths, W. J., Nilsson, S. J., and Hoog, J. O. (2003). Reduction of *S*-nitrosoglutathione by human alcohol dehydrogenase 3 is an irreversible reaction as analysed by electrospray mass spectrometry. *Eur. J. Biochem.* **270,** 1249–1256.

Hogg, N. (2002). The biochemistry and physiology of *S*-nitrosothiols. *Annu. Rev. Pharmacol. Toxicol.* **42,** 585–600.

Lamas, S., Lowenstein, C. J., and Michel, T. (2007). Nitric oxide signaling comes of age: 20 years and thriving. *Cardiovasc. Res.* **75,** 207–209.

Liu, L., Hausladen, A., Zeng, M., Que, L., Heitman, J., and Stamler, J. S. (2001). A metabolic enzyme for *S*-nitrosothiol conserved from bacteria to humans. *Nature* **410,** 490–494.

Martinez-Ruiz, A., and Lamas, S. (2007). Signalling by NO-induced protein *S*-nitrosylation and *S*-glutathionylation: Convergences and divergences. *Cardiovasc. Res.* **75,** 220–228.

Rebrin, I., Forster, M. J., and Sohal, R. S. (2007). Effects of age and caloric intake on glutathione redox state in different brain regions of C57BL/6 and DBA/2 mice. *Brain Res.* **1127,** 10–18.

Singh, S. P., Wishnok, J. S., Keshive, M., Deen, W. M., and Tannenbaum, S. R. (1996). The chemistry of the *S*-nitrosoglutathione/glutathione system. *Proc. Natl. Acad. Sci. USA* **93,** 14428–14433.

Stamler, J. S., Lamas, S., and Fang, F. C. (2001). Nitrosylation. the prototypic redox-based signaling mechanism. *Cell* **106,** 675–683.

Steffen, M., Sarkela, T. M., Gybina, A. A., Steele, T. W., Trasseth, N. J., Kuehl, D., and Giulivi, C. (2001). Metabolism of *S*-nitrosoglutathione in intact mitochondria. *Biochem. J.* **356,** 395–402.

Tsikas, D. (2003). Measurement of physiological *S*-nitrosothiols: A problem child and a challenge. *Nitric Oxide* **9,** 53–55.

Tsikas, D., Denker, K., and Frolich, J. C. (2001). Artifactual-free analysis of *S*-nitrosoglutathione and *S*-nitroglutathione by neutral-pH, anion-pairing, high-performance liquid chromatography. Study on peroxynitrite-mediated S-nitration of glutathione to *S*-nitroglutathione under physiological conditions. *J. Chromatogr. A* **915,** 107–116.

Yap, L.-P., Garcia, J. V., Han, D., and Cadenas, E. (2010). Role of nitric oxide-mediated glutathionylation in neuronal function. Potential regulation of energy utilization. *Biochem. J.* **428,** 85–93.

Zeng, H., Spencer, N. Y., and Hogg, N. (2001). Metabolism of *S*-nitrosoglutathione by endothelial cells. *Am. J. Physiol. Heart Circ. Physiol.* **281,** H432–H439.

CHAPTER SEVEN

Measurement of Mixed Disulfides Including Glutathionylated Proteins

Raffaella Priora,* Lucia Coppo,* Sonia Salzano,† Paolo Di Simplicio,* *and* Pietro Ghezzi†

Contents

Abstract

Mixed disulfides between protein cysteines and low-molecular-weight thiol cysteine or glutathione lead to the formation of cysteinylated proteins or glutathionylated proteins. These types of posttranslational modification are of great importance in the so-called redox regulation, by which changes in the redox state of the cell regulate a number of biochemical processes.

We describe the methods for quantitatively measuring the various redox states of cellular thiols including protein cysteines and these mixed disulfides. These include spectrophotometric methods, which do not distinguish between protein-cysteine and protein-glutathione disulfides, and HPLC methods that make such distinction.

* Department of Neuroscience, Pharmacology Unit, University of Siena, Siena, Italy
† Brighton and Sussex Medical School, Falmer, Brighton, United Kingdom

Methods in Enzymology, Volume 473
ISSN 0076-6879, DOI: 10.1016/S0076-6879(10)73007-X

Finally, we report a method for labeling proteins susceptible to glutathionylation with biotin, to allow their visualization by Western blot after electrophoretic separation, which is used to identify proteins undergoing this posttranslational modification.

1. Introduction

Cysteine residues of proteins (PSH) are subjected to a variety of complex chemical modifications. They can be engaged in protein disulfides (PSSP) and in thiol-protein mixed disulfides between PSH and XSH (the latter could be GSH or cysteine) to form (PSSX), or be subjected to an irreversible attack by a great variety of electrophilic toxic agents forming PSX adducts, or to reversible/irreversible oxidative modifications at higher oxidation degrees (sulfenic acid, PSOH, reversible; sulfinic acid, PSO_2H, partially reversible; sulfonic acid, PSO_3H, irreversible).

There is a growing interest in the regulatory function of the formation of PSSX between protein cysteines and either glutathione (GSH; to produce PSSG) or free cysteine (CSH; to produce cysteinylated protein, PSSC). Protein glutathionylation has been described as a major form of protein *S*-thiolation by Brigelius and Sies (Brigelius *et al.*, 1982, 1983) and is now known to regulate the function of several proteins (Ghezzi, 2005; Ghezzi and Di Simplicio, 2007; Ghezzi *et al.*, 2005). Since the main intracellular thiol is GSH, glutathionylation is the most studied among the various forms of PSSX. However, as cysteine is extracellularly the main SH, protein cysteinylation is important for extracellular/secreted proteins (Watarai *et al.*, 2000).

Various mechanisms of PSSX formation mediated by oxidative or nitrosative events have been proposed (Martinez-Ruiz and Lamas, 2004). During oxidative stress, PSSG can be formed by different mechanisms, depending on the pK_a values, exposure of the PSH, and on the competition between GSH and PSH toward electrophilic agents:

(1) GS• + PS• → PSSG (radical reaction)
(2) PSH + oxidant → PSOH; PSOH + GSH → PSSG (When PSH is more susceptible to oxidation than GSH)
(3) GSH + oxidant → GSSG; GSSG + PSH → PSSG + GSH (When PSH is less susceptible to oxidation than GSH and PSH is well exposed to the protein surface)

Reduction of PSSG and PSSX (dethiolation) may occur enzymatically (via thioredoxins or glutaredoxins) or nonenzymatically, depending on the accessibility that PSSX have toward the SH engaged in the dethiolation processes (Priora *et al.*, 2010).

Chemical quantification of PSSG has classically relied on precipitating proteins with acid (disulfides are stabilized by acidic pH), followed by washing to remove free GSH, then reduction and measurement of the released GSH. There have been a number of modifications and variations to this approach. To further stabilize the mixed disulfides, addition of alkylating agents such as *N*-ethylmaleimide (NEM) is often used if samples need to undergo processing (e.g., electrophoresis). This will prevent loss of disulfide-bound glutathione due to exchange reactions with free thiols in the protein. On the other hand, exposing the protein precipitate to high pH has been used to release (by reduction) GSH from PSSG and to make it available for measurement. The same approach can be used to measure overall PSSX (by measuring the nonprotein SH released).

With the development of proteomics, appropriate techniques have been proposed to allow identification of proteins undergoing this type of post-translational modification (PTM) (Gianazza *et al.*, 2009). These techniques follow essentially two strategies. A first approach is to use labeled GSH (or GSSG) and identify proteins that have taken up the label, which can be radioactively labeled (35S) or biotinylated GSH (or its precursor, cysteine). A second approach relies on direct visualization of PSSG using anti-GSH antibodies. Both require running 1D or 2D gel electrophoresis under nonreducing conditions. Visualization of PSSX on gel electrophoresis is not clearly quantitative and is mainly used for identifying proteins susceptible to this PTM.

In this chapter, we describe one approach to quantitatively measuring PSSX and PSSG and one to labeling PSSG for visualization following electrophoretic separation.

2. Chemical Quantification of PSSX, PSSG, and PSSC

2.1. Principle

The method is derived from one that has been extensively used by the authors (Di Simplicio and Rossi, 1994; Rossi *et al.*, 1995) and is essentially based on precipitation of proteins with trichloroacetic acid (TCA) followed by alkaline pH-induced release of small-molecular-weight XSH (including GSH in the case of PSSG) and measurement of the XSH by DTNB. This method is here further improved by addition of dithiothreitol (DTT) to the sample after resuspension at neutral–basic pH, to prevent reformation of disulfides. Specifically, measuring released GSH by HPLC will provide a quantification of PSSG.

Here we present as an example the description of methods of PSSX determination by spectrophotometric (DTNB) and HPLC techniques in rat

tissue homogenates. In some experiments, homogenates were exposed *in vitro* to the thiol-specific oxidant, diamide (Kosower and Kosower, 1987), to enhance production of PSSX.

2.2. Reagents and solutions

1. Diamide (DIA), 20 m*M* in distilled H_2O
2. K_3EDTA solution: 100 m*M* in distilled H_2O
3. TCA, at various concentrations (range 1.5–60%) in water
4. Buffers:
   PB (0.1 or 0.2 *M*, as indicated): phosphate buffer pH 7.4
   PBE: 0.1 *M* phosphate buffer pH 7.0, with 2.5 m*M* K_3EDTA
5. NEM stock solutions 10 m*M*, 310 m*M* in 0.2 *M* PB
6. DTT, 5, 25, 50 m*M* in H_2O
7. Monobromobimane (mBrB), 40 m*M* in CH_3OH
8. 5,5′-Dithiobis(2-nitrobenzoic acid) (DTNB), 20 m*M* in PB 0.2 *M* ($\varepsilon_{410} = 13.64$ mM^{-1} cm^{-1})

2.3. Experimental procedure

2.3.1. Homogenate preparation

Tissue homogenates, typically from 0.2 g of tissue, were prepared in phosphate buffer (PBE) by an Ultra-Turrax homogenizer (~10 s) in ice-cooled plastic tubes containing 1.0 ml PBE, and at a weight:volume ratio of 1:5.

2.3.2. TCA precipitation

Homogenates (0.1 ml for liver; 0.2 ml for other tissues, e.g., kidney) were precipitated adding TCA to a final concentration of 6% (e.g., by adding 0.1 ml 12% TCA for liver or 0.1 ml TCA 18% for other tissues). After centrifugation at 7000×*g* for 4 min at room temperature, the supernatant (SN) and pellet (PT) were used for successive analysis.

2.3.3. XSH, XSSX, and XSSP assay by HPLC analysis

XSH, XSSX, and XSSP analysis was performed by HPLC after derivatization of XSH at basic pH with mBrB. The method was originally developed by Newton *et al.* (1981) and adapted to our purposes as follows.

2.3.3.1. XSH 0.030 ml of acid SN (or 0.030 ml PBE for blanks) was diluted with 0.200 ml H_2O; 0.030 ml of this solution was further diluted with 0.1 ml H_2O; and solid $NaHCO_3$ was added to the sample to saturation to have a pH near 8.0. Four microliters of 40 m*M* mBrB were then added and the samples were kept in the dark for 15 min. After centrifugation (7000×*g*, 2 min), 0.090 ml of SN was treated with 0.010 ml HCl 37% and

the acid sample (now pH = 2–3) was transferred to vials for HPLC analysis. 0.020 ml (typically containing 100–200 pmol of derivatized sample) was loaded onto HPLC column.

2.3.3.2. XSSX 0.100 ml of acid SN (or 0.100 ml PBE, blank) was treated with solid $NaHCO_3$ to saturation and 0.100 ml of 10 m*M* NEM was added to block soluble XSH. After 5 min, samples were centrifuged (7000×*g*, 2 min) and the NEM excess was removed from the SN by extraction with dichloromethane (at a ratio of 0.2 ml of the sample:3 ml dichloromethane). 0.100 ml of the sample was saturated with solid $NaHCO_3$ and treated with 5 μl of 5 m*M* DTT at room temperature for 15 min. Samples were then treated with 5 μl of 40 m*M* mBrB, kept in the dark for 15 min, and processed as described above for XSH (centrifugation and HCl treatment). 0.020 ml (typically containing 30–60 pmol of derivatized sample) was loaded onto HPLC column.

2.3.3.3. XSSP The remaining homogenate (see Section 2.3.1) was precipitated with TCA (6%, final concentration) and centrifuged (7000×*g*, 4 min), and PT was washed three times with 1.5% TCA and centrifuged, and resuspended with 1.0 ml of 0.2 *M* PB plus 0.012 ml of 100 m*M* K_3EDTA. 0.300 ml of resuspended homogenate was treated with 0.035 ml of 1 *N* NaOH (to bring pH to 8.2–8.4) and with 0.055 ml of 50 m*M* DTT (7.0 m*M* final concentration) for 20 min at room temperature under agitation. The sample was precipitated with TCA (0.045 ml 60% TCA, 6% final concentration) and centrifuged (7000×*g*, 2 min). 0.030 ml of SN was diluted with 0.070 ml H_2O, saturated with solid $NaHCO_3$, treated with 0.015 ml of 40 m*M* mBrB (15 min at dark), and processed as described above for XSH (centrifugation and HCl treatment). 0.020 ml (typically containing 50–150 pmol of derivatized sample) was loaded onto HPLC column.

PT deriving from DTT treatment was used to assay PSH (see Section 2.3.4.2).

2.3.4. PSSX and PSH assay by colorimetric method (DTNB)

2.3.4.1. PSSX PT from TCA-treated homogenate was washed with 1.5% TCA and centrifuged. The sample was resuspended with 1.0 ml of 0.2 *M* PB, then 0.012 ml of 100 m*M* K_3EDTA, plus 0.100 ml of 1 *N* NaOH (to bring pH to 8.2–8.4) were added. The sample was maintained for 30 min at room temperature under agitation and precipitated with TCA (6% final concentration). After centrifugation, 0.200 ml of SN (or 0.200 ml PB for blank) was put in a cuvette with 1.0 ml of 0.2 *M* PB and finally 0.010 ml of 20 m*M* DTNB was added. Readings at 410 nm were taken within 2–4 min of DTNB addition.

2.3.4.2. PSH PT (from Section 2.3.3.3) was washed twice with 0.8 ml 1.5% TCA, centrifuged (7000×*g*, 2 min), and resuspended in 0.120 ml of PB 0.2 *M*. Then 0.120 ml of 20 m*M* DTNB (to a final concentration of 10 m*M*) was added to the sample that was maintained for 10 min under agitation at dark at room temperature. After centrifugation (7000×*g*, 5 min), 0.025 ml of SN was added to the cuvette containing 1 ml of 0.1 *M* PB and the absorbance at 410 nm was measured. An appropriate blank was also included (1 ml PB 0.1 *M* + 0.025 ml DTNB 10 m*M*).

2.4. Results

In this section, we first give an example of results (Tables 7.1 and 7.2) and then explain the importance of a basic pH (Table 7.3) and of DTT (Table 7.4).

2.5. Typical data

Typical measurement of PSH and PSSX by the colorimetric method using DTNB is shown in Table 7.1.

Table 7.1 Quantification of PSSX and PSH from control or diamide-treated homogenates

	PSH	PSSX
Control	11.7 ± 0.7	0.13 ± 0.01
Diamide	8.7 ± 0.5	0.97 ± 0.14

Data are expressed as μmol/g protein; mean and SD on three different experiments. PSH and PSSX were assayed colorimetrically by DTNB in rat liver homogenates after TCA precipitation and resuspension at pH 8.2. When indicated, homogenates were treated with 1 m*M* diamide for 15 min at room temperature.

Table 7.2 Redox species of liver homogenates treated with 1 m*M* diamide for 15 min at room temperature

	GSH	GSSG	PSSG	CSH	CSSC	PSSC
Control	7235 ± 81	3.1 ± 0.2	85 ± 1	279 ± 32	3.7 ± 0.3	6.6 ± 0.3
Diamide	ND	ND	1302 ± 380	ND	ND	94 ± 22

Data are expressed as nmol/g tissue and represent the mean ± SD of three repeated analysis from different homogenate of the same liver using the HPLC assay. ND, not done.

Table 7.3 Influence of pH on GSH and CSH release from PSSX

	CSH	GSH	PSH
Control, pH 6.5	1.5	27.4	15.4
Control, pH 8.2	3.1	44.7	13.2
Diamide, pH 6.5	39.7	365	13.3
Diamide, pH 8.2	45.4	876	11.1

Values are expressed as nmol/g tissue.

Table 7.4 PSH and DTT concur to produce the maximum GSH and CSH release from PSSX at pH 8.2

	CSH	GSH	PSH
Control	2.4	50.8	13.2
Control + DTT	6.2	84.9	16.9
Control + NEM	0.8	1.6	1.8
Control + NEM + DTT	4.3	57	4.9
Diamide	70.1	1131	11.1
Diamide + DTT	94.2	1302	16.3
Diamide + NEM	4.3	57	1.2
Diamide + NEM + DTT	87.5	1203	7.4

Values are expressed as nmol/g tissue.

2.6. Importance of basic pH

To demonstrate the importance of a basic pH for PSSX and PSSG to release XSH and GSH (and thus to be measured), we performed the release of XSH from PSSX in TCA precipitates from liver homogenates (PSSX) at pH 8.2 or 6.5. Then we measured CSH and GSH by HPLC (see Section 2.3.3.3) and PSH by DTNB (see Section 2.3.4.2) (Table 7.3).

It can be seen that a basic pH is required for CSH and GSH to be efficiently released from PSSC and PSSG, thus allowing their quantitation.

2.7. Importance of DTT and PSH

To demonstrate the importance that DTT and endogenous PSH have to release XSH and GSH from PSSX and PSSG in the TCA precipitate (at pH 8.2) experiments were carried out measuring the XSH release from TCA precipitates in the presence and absence of DTT as well as with and without NEM pretreatment (to block endogenous PSH).

Results of a typical experiment repeated three times on different rats are shown in Table 7.4. When indicated, homogenates (either control or diamide-treated) were treated with 200 m*M* NEM for 15 min to block PSH in the sample. Then PSSX (PSSC and PSSG) were quantitated by measuring the release of CSH and GSH, respectively, with and without addition of DTT at the concentration described in the experimental procedures.

3. Visualization of PSSG by Western Blot

3.1. Principle

Biotinylated GSH ethyl ester is used to label the GSH pool. Then proteins that have incorporated biotinylated GSH will be visualized by Western blot after nonreducing electrophoresis. In the example provided, we used BioGEE to glutathionylate proteins in cell-free conditions (cell lysates). However, since the GSH ethyl ester is cell permeable (Puri and Meister, 1983; Wellner *et al.*, 1984) it can be used to label cells in culture (Sullivan *et al.*, 2000; Zimmermann *et al.*, 2007). Other means of biotinylating glutathionylated proteins imply the use of biotinyl GSH (Eaton *et al.*, 2002b), biotinyl GSSG (Brennan *et al.*, 2006), or, for studying protein cysteinylation, biotinylated cysteine (Eaton *et al.*, 2002a, 2003). A further advantage of the biotin tag is that proteins bearing this PTM can be enriched by streptavidin affinity chromatography.

It is important to note that electrophoresis must then be performed under nonreducing conditions. Furthermore, to prevent reduction of PSSG by other thiols in the sample or in reagents, such as BSA, NEM is used to alkylate free SH.

3.2. Methods and procedures

3.2.1. Preparation of cell extract

For the example provided, we used Raw 264.7 mouse macrophage cells cultured to confluence in 6-well tissue culture plates (cells are adherent). Cells are plated in 6-well tissue culture plates at a density of 2.4×10^6 in RPMI with 10% FCS. The next day, cells are washed with PBS, and then lysed by five cycles of freezing–thawing in a 150-μl/well of 50 m*M* Tris–HCl (pH 7.4), detached with the help of a cell scraper and centrifuged at $12{,}000\times g$ for 1 min in a refrigerated microcentrifuge. The SN is used as a source of cytosolic proteins. Protein concentration was measured by the DC protein assay kit Bio-Rad.

3.2.2. Labeling with BioGEE

A stock solution of BioGEE (Invitrogen, Carlsbad, CA) is prepared in dimethyl sulfoxide at a 12.5-m*M* concentration, immediately before use. One microliter of this solution (or nothing in the case of blank samples) was added to 50 μl of cytosol. Then, 1 μl of 2 *M* NEM is added to block free thiols.

3.2.3. Electrophoresis and Western blot

Boil samples (7 μl containing typically 15–20 μg of protein) for 5 min after adding 1/4 vol. of 4× Laemmli buffer (250 mmol/l Tris–HCl pH 6.8; 8% sodium dodecyl sulfate (SDS); 40% glycerol; 0.004% bromophenol blue) with or without 10% β-mercaptoethanol (2ME) to reduce disulfides.

Samples are electrophoresed on a 12% SDS–polyacrylamide gel in running buffer (3.03 g Tris base, 14.4 g glycine, 1 g SDS/1 l H_2O pH 8.3) for 1.5–2 h at 100 V. After electrophoresis, the proteins are transferred in transfer buffer (3.03 g Tris base, 14.4 g glycine, 20 ml methanol/1 l H_2O) from gel to membrane (nitrocellulose or PVDF), using an electroblotting apparatus for 1 h at 100 V.

Nonspecific binding sites are blocked by incubating the membrane for 1 h with 5% BSA in PBS-T (PBS with 0.1% Tween-20) containing 5 m*M* NEM to prevent reduction of disulfides. After three 10-min washes with PBS-T (PBS, 0.1% Tween-20), the membrane was incubated with a Streptavidin–POD conjugate Roche (dilution 1:25,000 in PBS-T) for 30 min at room temperature. After three additional washing, the proteins were visualized by ECL (kit ECL Western blotting analysis system, GE healthcare/Amersham).

3.3. Typical results

Figure 7.1 shows a typical Western blot. Lane 1 (left, nonreduced sample) shows a number of proteins labeled with biotin in the cytosol, indicating proteins susceptible to glutathionylation. When the same sample was reduced with 2ME (lane 2, right) most of the label was lost, indicating that it actually represented PSSG.

Other types of controls need to be made at last a couple of times during the set-up (e.g., without BioGEE as a number of proteins could react with streptavidin). However, we recommend that a reduced sample is always included to confirm that the biotin label is actually due to a disulfide bond (therefore a PSSG) and not to aspecific binding of biotin or streptavidin.

ACKNOWLEDGMENTS

This work was supported by the Brighton & Sussex Medical School and the RM Phillips Charitable Trust (P. G.).

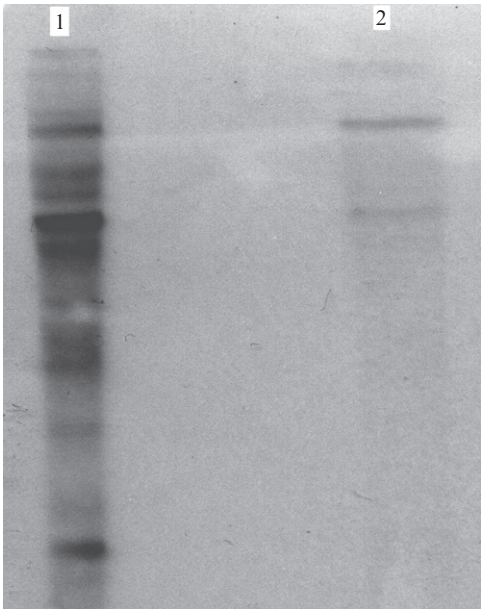

Figure 7.1 **A typical Western blot with anti-GSH antibodies to visualize glutathionylated proteins.**

REFERENCES

Brennan, J. P., *et al.* (2006). The utility of N, N-biotinyl glutathione disulfide in the study of protein S-glutathiolation. *Mol. Cell. Proteomics* **5,** 215–225.

Brigelius, R., *et al.* (1982). Increase in hepatic mixed disulphide and glutathione disulphide levels elicited by paraquat. *Biochem. Pharmacol.* **31,** 1637–1641.

Brigelius, R., *et al.* (1983). Identification and quantitation of glutathione in hepatic protein mixed disulfides and its relationship to glutathione disulfide. *Biochem. Pharmacol.* **32,** 2529–2534.

Di Simplicio, P., and Rossi, R. (1994). The time-course of mixed disulfide formation between GSH and proteins in rat blood after oxidative stress with tert-butyl hydroperoxide. *Biochim. Biophys. Acta* **1199,** 245–252.

Eaton, P., *et al.* (2002a). Detection, quantitation, purification, and identification of cardiac proteins S-thiolated during ischemia and reperfusion. *J. Biol. Chem.* **277,** 9806–9811.

Eaton, P., *et al.* (2002b). Glyceraldehyde phosphate dehydrogenase oxidation during cardiac ischemia and reperfusion. *J. Mol. Cell. Cardiol.* **34,** 1549–1560.

Eaton, P., *et al.* (2003). Reversible cysteine-targeted oxidation of proteins during renal oxidative stress. *J. Am. Soc. Nephrol.* **14,** S290–S296.

Ghezzi, P. (2005). Regulation of protein function by glutathionylation. *Free Radic. Res.* **39,** 573–580.

Ghezzi, P., and Di Simplicio, P. (2007). Glutathionylation pathways in drug response. *Curr. Opin. Pharmacol.* **7,** 398–403.

Ghezzi, P., *et al.* (2005). Thiol-disulfide balance: from the concept of oxidative stress to that of redox regulation. *Antioxid. Redox Signal.* **7,** 964–972.

Gianazza, E., *et al.* (2009). Detection of protein glutathionylation. *Methods Mol. Biol.* **519,** 397–415.

Kosower, N. S., and Kosower, E. M. (1987). Formation of disulfides with diamide. *Methods Enzymol.* **143,** 264–270.

Martinez-Ruiz, A., and Lamas, S. (2004). Detection and proteomic identification of S-nitrosylated proteins in endothelial cells. *Arch. Biochem. Biophys.* **423,** 192–199.

Newton, G. L., *et al.* (1981). Analysis of biological thiols: derivatization with monobromobimane and separation by reverse-phase high-performance liquid chromatography. *Anal. Biochem.* **114,** 383–387.

Priora, R., *et al.* (2010). The control of S-thiolation by cysteine via gamma-glutamyltranspeptidase and thiol exchanges in erythrocytes and plasma of diamide-treated rats. *Toxicol. Appl. Pharmacol.* **242,** 333–343.

Puri, R. N., and Meister, A. (1983). Transport of glutathione, as gamma-glutamylcysteinylglycyl ester, into liver and kidney. *Proc. Natl. Acad. Sci. USA* **80,** 5258–5260.

Rossi, R., *et al.* (1995). Thiol groups in proteins as endogenous reductants to determine glutathione-protein mixed disulphides in biological systems. *Biochim. Biophys. Acta* **1243,** 230–238.

Sullivan, D. M., *et al.* (2000). Identification of oxidant-sensitive proteins: TNF-alpha induces protein glutathiolation. *Biochemistry* **39,** 11121–11128.

Watarai, H., *et al.* (2000). Posttranslational modification of the glycosylation inhibiting factor (GIF) gene product generates bioactive GIF. *Proc. Natl. Acad. Sci. USA* **97,** 13251–13256.

Wellner, V. P., *et al.* (1984). Radioprotection by glutathione ester: transport of glutathione ester into human lymphoid cells and fibroblasts. *Proc. Natl. Acad. Sci. USA* **81,** 4732–4735.

Zimmermann, A. K., *et al.* (2007). Glutathione binding to the Bcl-2 homology-3 domain groove: A molecular basis for Bcl-2 antioxidant function at mitochondria. *J. Biol. Chem.* **282,** 29296–29304.

CHAPTER EIGHT

Detection and Quantification of Protein Disulfides in Biological Tissues: A Fluorescence-Based Proteomic Approach

Viviana I. Pérez,[*,§] Anson Pierce,[*,§,¶] Eric M. de Waal,[‡] Walter F. Ward,[†,§] Alex Bokov,[*,**] Asish Chaudhuri,[§,¶,#] *and* Arlan Richardson[*,†,§,¶]

Contents

* Department of Cellular & Structural Biology, The University of Texas Health Science Center at San Antonio, San Antonio, Texas, USA
† Department of Physiology, The University of Texas Health Science Center at San Antonio, San Antonio, Texas, USA
‡ Department of Biology, University of Texas at San Antonio, San Antonio, Texas, USA
§ Barshop Institute for Longevity and Aging Studies, The University of Texas Health Science Center at San Antonio, San Antonio, Texas, USA
¶ Geriatric Research Education and Clinical Center, South Texas Veterans Health Care System, San Antonio, Texas, USA
# Department of Biochemistry, The University of Texas Health Science Center at San Antonio, San Antonio, Texas, USA
** Department of Epidemiology & Biostatistics, The University of Texas Health Science Center at San Antonio, San Antonio, Texas, USA

Methods in Enzymology, Volume 473
ISSN 0076-6879, DOI: 10.1016/S0076-6879(10)73008-1

Abstract

While most of the amino acids in proteins are potential targets for oxidation, the thiol group in cysteine is one of the most reactive amino acid side chains. The thiol group can be oxidized to several states, including the disulfide bond. Despite the known sensitivity of cysteine to oxidation and the physiological importance of the thiol group to protein structure and function, little information is available on the oxidative modification of cysteine residues in proteins because of the lack of reproducible and sensitive assays to measure cysteine oxidation in the proteome. We have developed a fluorescence-based assay that allows one to quantify both the global level of protein disulfides in the cellular proteome as well as the disulfide content of individual proteins. This fluorescence-based assay is able to detect an increase in global protein disulfide levels after oxidative stress *in vitro* or *in vivo*. Using this assay, we show that the global protein disulfide levels increase significantly with age in liver cytosolic proteins, and we identified 11 proteins that show a more than twofold increase in disulfide content with age. Thus, the fluorescence-based assay we have developed allows one to quantify changes in the oxidation of cysteine residues to disulfides in the proteome of a cell or tissue.

Abbreviations

IAM	iodoacetamide
6-IAF	6-iodoacetamidofluorescein
NEM	*N*-ethylmaleimide
F-5M	fluorescein-5-maleimide
CHAPS	3-[3-(cholanaldopropyl)-dimethyl-ammonio]-1-propanesulphonate
EDTA	ethylenediaminetetraacetic acid
Asc. Ac.	ascorbic acid
$FeSO_4$	ferrous sulfate
HEPES	(*N*-[2-hydroxyethyl]piperazine-*N*′-[2-ethanesulfonic acid])
GAPDH	glyceraldehyde-3-phosphate dehydrogenase
IEF	isoelectric focusing
$MgCl_2$	magnesium chloride

MALDI-TOF/MS	matrix-assisted laser desorption ionization time-of-flight mass spectrometry
SDS-PAGE	sodium dodecyl sulfate-polyacrylamide gel electrophoresis
TCA	trichloroacetic acid
FU	fluorescent units

1. Introduction

Protein oxidation is thought to be involved in the etiology of many disease processes, including cardiovascular disease (Uchida *et al.*, 1994), diabetes (Olivares-Corichi *et al.*, 2005), and neurological disorders such as Alzheimer's and Parkinson's diseases (Butterfield and Kanski, 2001). In addition, protein oxidation is considered an important factor in the aging process (Bokov *et al.*, 2004). The evidence that protein oxidation may be involved in aging and disease processes is based primarily on measurements of one type of oxidative modification, carbonyl groups formed by the oxidation of lysine, arginine, proline, histidine, and cysteine residues in proteins. Although most of the amino acid side chains in proteins are sensitive to oxidative modifications, the thiol group in cysteine is extremely sensitive to oxidation (Berlett and Stadtman, 1997; Huggins *et al.*, 1993; Thomas and Mallis, 2001; Zhou and Gafni, 1991). Oxidative damage to cysteine residues in proteins is of particular physiological importance because cysteines are often found at the catalytic and regulatory sites of enzymes (Cumming *et al.*, 2004; Thomas and Mallis, 2001).

The thiol group in cysteine can be oxidized to several states, for example, reversible oxidation to disulfide bond (S–S), sulfenic acid (–SOH), and *S*-nitrosylation (–SNO) and irreversible oxidation to sulfonic (SO_2H) and sulfinic (SO_3H) acid, or modification of –SH by oxidized lipid adduct by Michael reaction (Eaton, 2006; Kim *et al.*, 2002; Thomas and Mallis, 2001). Among the various oxidation states of cysteine thiol, the disulfide bond (including mixed disulfide bond formed with glutathione) is of particular interest because (i) it inactivates the function of proteins, (ii) it can be involved in higher order protein aggregates, and (iii) it protects critical protein thiol(s) from irreversible oxidation.

Currently, despite the physiological significance of cysteine oxidation in protein structure and function, there is no assay available for the quantitative measurement of disulfides in the proteome of the cell or tissue. To date, the few studies that have studied the effect of oxidation of cysteine have

measured disulfide bonds in purified proteins (Chaudhuri *et al.*, 2001; Zeng *et al.*, 2001). Subsequently, we describe a fluorescence-based assay that allows one to quantify changes in the global levels of protein disulfide as well as to screen the proteome for changes in the disulfide content (nmole/nmole protein) of specific proteins using 2D gel electrophoresis and mass spectroscopy.

2. Material and Methods

2.1. Animals

Male C57BL/6 mice maintained in microisolator cages on a 12-h dark/light cycle were fed standard NIH-31 chow *ad libitum*. The ages of the young and old animals used for this study were 4–6 and 26–28 months, respectively. For the *in vivo* oxidative stress study, the animals were injected i.p. with diquat, 50 mg/kg, 6 h prior to sacrifice. For tissue collection, animals were euthanized by CO_2 inhalation, followed by cervical dislocation, and liver tissue was immediately excised and snaps frozen in liquid nitrogen. All procedures involving mice were approved by the Institutional Animal Care and Use Committee at the University of Texas Health Science Center at San Antonio and the subcommittee for Animal studies at Audie L. Murphy Memorial Veterans Hospital.

2.2. Gel electrophoresis-based protein disulfide assay

Cytosolic extracts were obtained from the liver by homogenization with 50 m*M* potassium phosphate buffer containing 0.5 m*M* $MgCl_2$, 1 m*M* EDTA, and a protease inhibitor cocktail (500 μM AEBSF, 150 n*M* aprotinin, 0.5 m*M* EDTA-disodium salt, and 1 μM leupeptin hemisulfate). To immediately block all free thiol groups in the proteins, an alkylating agent [200 m*M* *N*-ethylmaleimide (NEM), pH 7.0; or 200 m*M* iodoacetamide (IAM), pH 8.0)] was included in the homogenization buffer. The homogenates were centrifuged for 1 h at 100,000×*g* at 4 °C to obtain the cytosolic fraction, and the samples at 1 μg protein/μl, were further incubated for 1 h at 37 °C in homogenization containing 200 m*M* NEM or 200 m*M* IAM to ensure the blocking of free thiol in the sample. Free NEM or IAM was removed by protein precipitation with 10% trichloroacetic acid (TCA) and the pellet was washed three times with 100% ethanol/ethyl acetate (1:1). The precipitates were resuspended in 8 *M* urea and incubated with 1 m*M* dithiothreitol (DTT) for 30 min at 37 °C to reduce the disulfide bonds in the samples. The free thiol groups (–SH) arising from the reduced

disulfides were fluorescent-tagged with either 6-iodoacetamidofluorescein (6-IAF) 1 m*M* or fluorescein-5-maleimide (F-5M) 1 m*M*. The fluorescent-labeled protein (10 μg) was then subjected to 12% SDS-gel electrophoresis and the level of fluorescent-labeled protein in each lane was determined using a Typhoon 9400 (emission filter 526 nm) as a measure of disulfide content. After capturing the fluorescence image and importing it into the ImageQuant v5.0, the gel was fixed with 10% methanol and 7% acetic acid for 10 min, followed by staining overnight with the Sypro Ruby. The Sypro Ruby fluorescence in each lane was measured using a Typhoon 9400 (emission filter 620 nm) and used as a measure of protein, and the data were expressed as nmol of thiol/mg of protein using the standard curves described subsequently (Section 2.4).

2.3. Selection of the alkylating agents for measuring protein disulfide levels

Because the thiol group in cysteine is particularly sensitive to oxidation, the thiolate ion can form disulfide bonds rapidly during the preparation of samples by aerial oxidation. To prevent the nonspecific oxidation reaction of thiol groups during the handling of samples, it was essential to alkylate the free thiol groups using excess amounts of an efficient alkylating agent that can react quickly with free thiol groups immediately upon homogenization of the tissue. Two alkylating agents were compared, NEM and IAM, for example, the rate at which the agent can modify the free thiol groups and the extent of alkylation achieved. Liver tissue was homogenized as described in Section 2.2 in the presence of either NEM or IAM. Each cytosolic fraction was divided into two aliquots; one aliquot was treated with DTT (1 m*M*) to reduce the disulfide bonds, while in the other aliquot, the DTT was replaced with an equal volume of buffer. The exposure of thiol groups in the different aliquots, +DTT and −DTT, was followed by labeling of the NEM-treated samples with F-5M and the IAM-treated samples with 6-IAF. All samples were then subjected to SDS-gel electrophoresis to measure the fluorescence bound to protein. The data presented in Fig. 8.1 clearly show that IAM alkylates the free protein thiols more efficiently than NEM (Fig. 8.1 B; line 5 compared to Fig. 8.1 A; line 1). There was little incorporation of 6-IAF into protein observed in a nonreduced sample that was prealkylated with IAM, compared to the incorporation of F-5M in the nonreduced NEM-treated sample. The Sypro Ruby staining data show that the difference in the incorporation of 6-IAF or F-5M in DTT-untreated samples cannot be attributed to unequal loading of proteins (Fig. 8.1 A and B; lines 3–4 and 7–8). Therefore, IAM was used as the alkylating agent. We next examined the kinetics of the reaction between IAM and –SH groups. The data presented in Fig. 8.1 C demonstrate that IAM reacts very rapidly

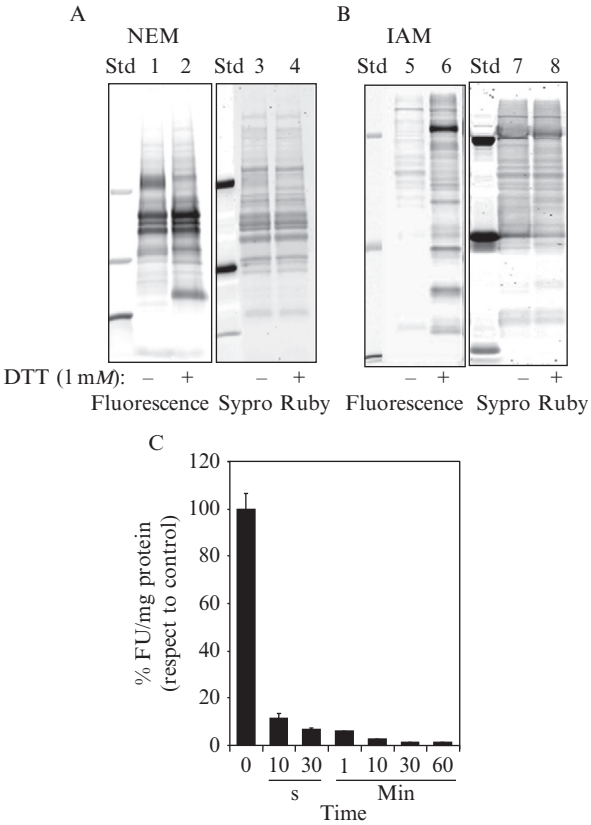

Figure 8.1 Validation of the gel-based fluorescent disulfide detection assay. Cytosolic proteins (1 mg/ml) isolated from young mice were alkylated with excess NEM (A) or IAM (B) and then treated with (lines 2 and 6) or without (lines 1 and 5) 1 m*M* DTT. The samples were then labeled with F-5M (for NEM-treated samples) or 6-IAF (for IAM-treated samples). Equal amounts of labeled protein (10 μg) were subjected to electrophoretic separation on a 12% SDS-polyacrylamide gel. Sypro-Ruby staining fluorescence of the same gels is shown in A (lines 3 and 4) and B (lines 7 and 8). The molecular weights of protein standards are shown. C demonstrates the reaction kinetic profile of the binding of IAM to the free thiol groups in cytosolic proteins. In brief, the cytosolic proteins were pretreated with or without IAM (200 m*M*) at different times (0, 10, 30 s and 1, 10, 30, and 60 min) followed by stopping the reaction by ethanol/ethyl acetate precipitation. The precipitates were dissolved in 100 m*M* phosphate buffer pH 8.0 containing 6 *M* urea, followed by labeling the unreacted free protein thiols in each of the sample aliquots with 6-IAF (0.1 m*M*). All of the samples (10 μg) were then subjected to 12% SDS-gel electrophoresis. The data are expressed as percentage of fluorescence of bound 6-IAF/mg of protein with respect to control.

with free thiols, for example, 90% of the thiols in the soluble proteome are alkylated by IAM within 10 s, and 99% of the thiol groups are alkylated within 30 min.

2.4. Transformation of fluorescence units to nmoles of protein disulfide

The 6-IAF fluorescence data obtained from ImageQuant analysis were converted to nmoles of protein thiol using a standard curve generated from the fluorescence intensity values of known substoichiometric concentrations of 6-IAF bound to three purified proteins (glyceraldehyde-3-phosphate dehydrogenase (GAPDH), enolase, and creatine kinase (CK)) as described in Fig. 8.2 A . Substoichiometric concentrations of 6-IAF were used to label the thiol groups in the proteins so that the fluorescence associated with the proteins after electrophoresis could be transformed to nmoles of IAF (Fig. 8.2 B). As shown in Fig. 8.2, the standard curves generated were the same for each of the three proteins. The calculation of microgram protein relative to the intensity of Sypro Ruby was obtained from a standard curve generated using different concentrations of the same three purified proteins (GAPDH, enolase, and CK) (Fig. 8.2 C and D). Using these standard curves (Fig. 8.2 B and D), we were able to express the disulfide levels as nmoles of thiol group (i.e., 6-IAF bound to protein/mg of protein).

2.5. 2D gel electrophoresis

Tissue from mice was homogenized as described earlier, and the 6-IAF-labeled cytosolic proteins were resolved using 2D PAGE as previously described (Chaudhuri *et al.*, 2006; Pierce *et al.*, 2006). The 6-IAF-labeled cytosolic proteins were separated in the first dimension by isoelectric focusing (IEF) using pH 3–10 Imobiline dry strips (GE Healthcare, Piscataway, NJ). The proteins were then separated in the second dimension using a 12% SDS-polyacrylamide gel (w/v). Following electrophoretic resolution of the proteins, the gels were scanned using a Typhoon 9400 with an excitation wavelength of 532 nm and an emission filter at 526 nm with a 40 nm bandpass to capture the fluorescence from the 6-IAF tagged protein. After capturing the fluorescence image and importing it into the ImageQuant v5.0, the gel was fixed with 10% methanol and 7% acetic acid for 10 min, followed by staining overnight with the Sypro Ruby. After washing the residual dye from the gel, the gel was placed in water and scanned using the Typhoon 9400 with a 610BP30 filter emission and 532 nm excitation wavelength to capture the fluorescence from each spot. The 6-IAF and Sypro Ruby fluorescent images were quantified from 16-bit grayscale images using ImageQuant v5.0., and the disulfide level in each spot is expressed as nmoles of thiol group (i.e., 6-IAF bound to protein) per mg of protein (Section 2.4).

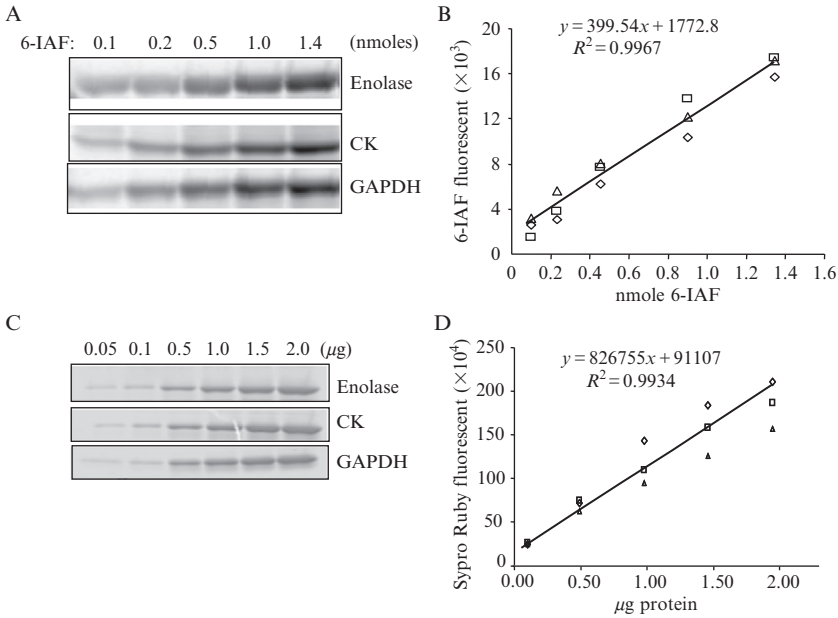

Figure 8.2 The transformation of fluorescence units to nmoles of protein disulfide. A stock solution of 6-IAF having a molar extinction coefficient (ε) of 82,000 M^{-1} cm^{-1} at 491 nm was prepared. A standard curve was generated by the reaction of various substoichiometric concentrations (3–40 pmoles) of 6-IAF with a constant concentration (200 μg) of each of three purified proteins [glyceraldehyde-3-phosphate dehydrogenase (GAPDH), enolase, and creatine kinase (CK)] dissolved in phosphate buffer, pH 8.0. Enolase, CK, and GAPDH (1 mg/ml) were labeled by treatment with different concentrations of 6-IAF (0.1, 0.2, 0.5, 1.0, 1.4 nmole of 6-IAF, respectively) and an equal amount of reaction mixture protein (7 μg) was then subjected to SDS-gel electrophoresis. The fluorescence intensity of the bound 6-IAF at each protein concentration was calculated using ImageQuant software. A shows the fluorescence-image of pure proteins (enolase, CK, and GAPDH) at different concentrations of 6-IAF. B shows the standard curve generated from the fluorescence intensities of different amounts of 6-IAF covalently bound to enolase (◊), CK (□), and GAPDH (Δ). The line was generated by using the data obtained by all three proteins. The calculation of microgram protein relative to the intensity of Sypro Ruby was obtained from a standard curve generated from the fluorescence intensities of Sypro Ruby associated with the varying concentrations of enolase (◊), CK (□), and GAPDH (Δ) (C). The line was generated by using the data obtained by all three proteins (D).

2.6. Identification of proteins by MALDI-TOF/MS

Spots containing the proteins of interest were excised from the 2D gels and digested *in situ* with modified trypsin. The peptides were concentrated and purified using a Montage in-gel digest kit. The resulting digests were analyzed by MALDI-TOF/MS using an Applied Biosystems Voyager

DE-STR or a Thermo Finnigan LCQ/MALDI-TOF. Mass spectra were generated by the summation of 100 laser shots. Mascot was utilized for the identification of the resolved proteins. Unmodified tryptic peptide profiles were generated and used, with carbamidomethyl and methionine oxidation as variable modifications, to search the peptide profile maintained by the NCBInr. The peptide tolerance was set at 75 ppm, and MOWSE scores greater than 60 were used to identify the proteins.

3. Results

3.1. Measurement of changes in protein disulfide levels in response to oxidative stress

To test the ability of our assay to measure the changes in cysteine oxidation, we measured the global levels of protein disulfides in response to oxidative stress. The changes in the disulfide content of cytosolic proteins was first measured in response to *in vitro* oxidative stress, for example, cytosolic liver protein samples were incubated with varying concentrations of ascorbic acid (Asc.) and ferrous sulfate to generate hydroxyl radicals (Chao *et al.*, 1997). Using SDS-gel electrophoresis as described in Section 2.2, we measured the global disulfide content of cytosolic proteins after various levels of oxidative stress. The data in Fig. 8.3 show that a significant increase in the incorporation of 6-IAF into protein was observed with increasing concentrations of ascorbate/ferrous sulfate.

To determine whether the disulfide detection assay was sensitive enough to detect changes in cysteine oxidation in response to an *in vivo* oxidative stress, mice were treated with diquat, which generates superoxide anions in liver and other tissues (Jones and Vale, 2000; Smith, 1985). Previously, we showed that diquat treatment induces oxidative damage to lipid and DNA in the livers of mice and that the increase in oxidative damage was maximum 6 h after diquat treatment (Han *et al.*, 2008). The data in Fig. 8.4 A show that the global disulfide content of cytosolic proteins from liver increased 30% after diquat treatment. These data demonstrated that our assay can detect changes in cysteine oxidation *in vivo*.

3.2. Measurement of changes in protein disulfide levels in young and old mice

Previous studies have shown that protein oxidation, as measured by carbonyl groups, increases with age (Chaudhuri *et al.*, 2006; Oliver *et al.*, 1987; Sohal *et al.*, 1993, 1995). Therefore, we measured the oxidation of cysteine to disulfides in cytosolic proteins isolated from young and old mice using

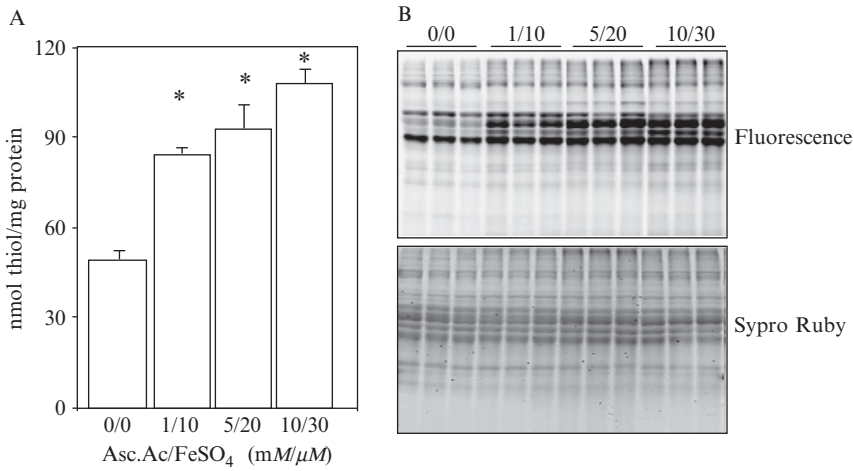

Figure 8.3 Changes in global disulfide bond content in liver cytosolic proteins induced by an oxidative stress *in vitro*. Graph A: Liver cytosolic proteins isolated from young mice were incubated at 37 °C for 60 min in dark with varying concentrations of Asc. (m*M*) and ferrous sulfate (μM) (0/0; 1/10; 5/20; 10/30 m$M/\mu M$). The samples were then labeled with 6-IAF, and equal amounts of protein (10 μg) were subjected to SDS-polyacrylamide gel electrophoresis (SDS-PAGE). The data were obtained by the average of the ratio of 6-IAF to Sypro Ruby per milligram of protein. The data are the mean ± SEM for three different animals and expressed as nmol of thiol/mg of protein. Representative fluorescence gels for 6-IAF and Sypro Ruby are shown in B. The asterisk (*) denotes values that are significantly ($p < 0.05$) different from control (0/0).

the assay we have developed. As shown in Fig. 8.4 B, the global protein disulfide levels increased 28% with age. We previously reported a 100% increase in the carbonyl content of liver cytosolic proteins with age (Chaudhuri *et al.*, 2006).

Previous studies also showed that oxidative damage to proteins as measured by carbonyl groups varies greatly from protein to protein (Chaudhuri *et al.*, 2006; Yoo and Regnier, 2004); therefore, we measured the disulfide levels in specific proteins from young and old mice using 2D gel electrophoresis. The disulfide content of individual proteins was quantified and expressed as a ratio of the fluorescent intensity of 6-IAF/Sypro Ruby of individual protein spots for cytosolic proteins from the livers of young and old mice. Fig. 8.5 A shows the 6-IAF fluorescence of a 2D gel from the liver extracts of an old mouse. We were able to compare the 6-IAF fluorescence of 86 spots from the four young and four old mice, and these data are presented in Fig. 8.5 B. For our analysis, we focused on those spots that showed a twofold increase in disulfide content with age and a coefficient of variation of 0.37 or less. Thirteen spots met these criteria, and the

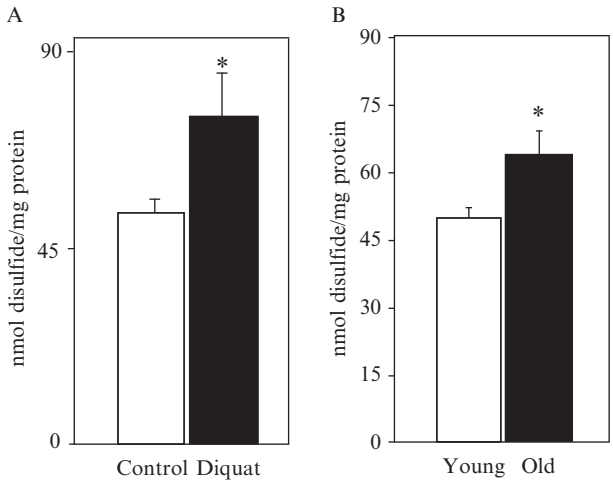

Figure 8.4 Changes in global disulfide bond content in liver cytosolic proteins induced by oxidative stress *in vivo*. Cytosolic proteins isolated from livers of young mice before and after diquat (50 mg/kg) treatment for 6 h (graph A) or liver cytosolic proteins obtained from young and old mice (Fig. 8.4 B) were labeled with 6-IAF and equal amounts of protein (10 μg) were then subjected to 12% SDS-gel electrophoresis. The data were obtained by the average of the ratio of 6-IAF to Sypro Ruby per milligram of protein and expressed as nmol thiol/mg of protein. The data are the mean ± SEM, $n = 4$. The asterisk (*) denotes values that are significantly ($p < 0.05$) different from control without diquat (A) or young mice (B).

identities of the 11 proteins in the 13 spots are given in Table 8.1. Our assay also allows us to calculate the disulfide content of specific proteins, that is, the mole of thiol/mole of protein using the molecular weights of the individual proteins. The data in Table 8.1 show that the average disulfide content of 11 proteins from old mice ranged from 0.06 to 3.0 mole of thiol/mole of protein.

3.3. Changes glyceraldehyde-3-phosphate dehydrogenase (GAPDH) activity in young and old mice

One of the proteins showing a twofold increase in disulfide content with age was GAPDH. Several studies have shown that oxidation of GAPDH leads to a loss in GAPDH activity (Pierce *et al.*, 2007; Schmalhausen *et al.*, 2003). To determine whether the age-related increase in disulfide content of GAPDH was correlated to a decrease in activity, we measured the activity of GAPDH in cytosolic extracts from the livers of young and old mice. As shown in Fig. 8.6, the activity of GAPDH was significantly lower (50%) in the livers of old mice. This decrease in GAPDH activity was

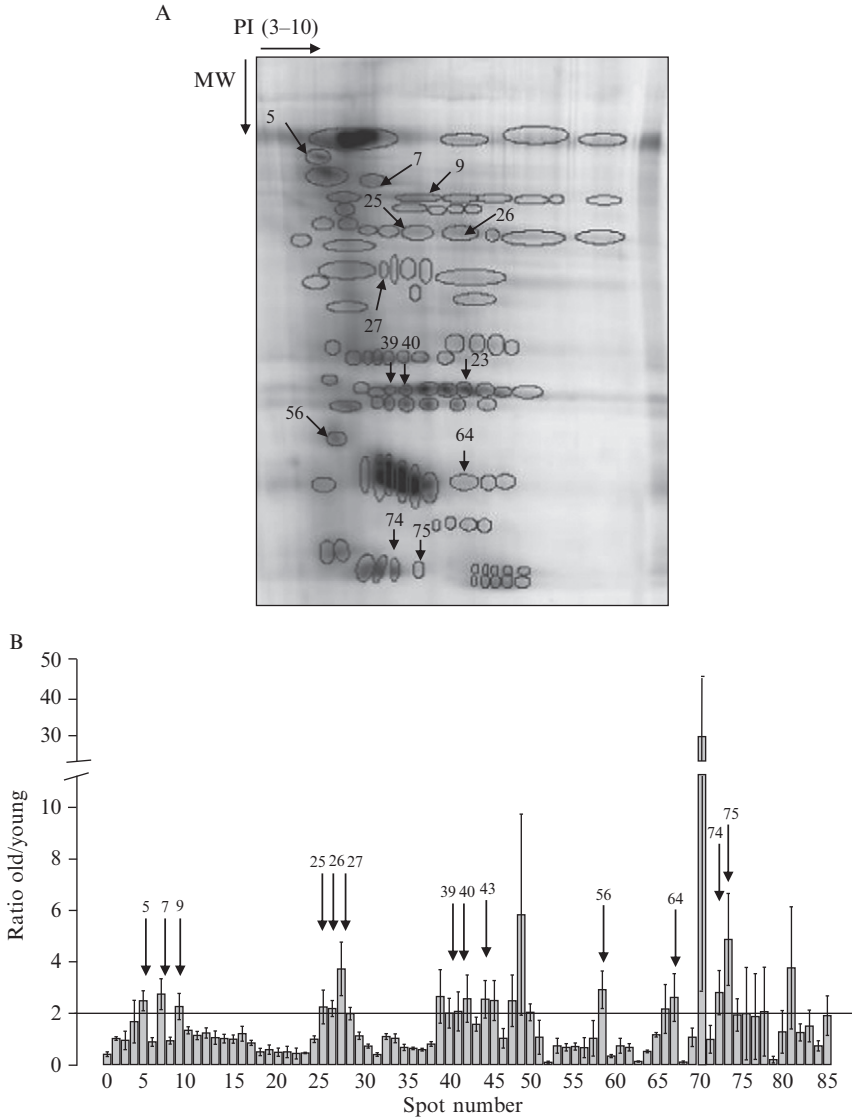

Figure 8.5 Quantitation of disulfide bond content in specific cytosolic proteins from the livers of young and old mice. Cytosolic extracts from 4 young and 4 old mice were labeled with 6-IAF and proteins were separated by 2D gel electrophoresis as we described in the Material and Methods (Section 2). To calculate the changes in disulfide content in individual proteins with age, we measured the intensity of 6-IAF and Sypro-Ruby fluorescence for each spot. An example of 6-IAF fluorescence of a 2D-gel of cytosol from old mice is shown. The circles show the location of 86 spots that were compared in young and old mice. The 6-IAF/Sypro Ruby ratio for each spot from each old mice ($n = 4$) was divided by the average of 6-IAF/Sypro Ruby ratio for the same spot from young mice ($n = 4$). The graph B shows the mean ± SEM ($n = 4$) for each of the 86 spots compared. The 13 spots analyzed by MOLDI/TOF MS are shown by arrows on the graph and 2D gel, and the identities of the proteins in these spots are given in Table 8.1.

Table 8.1 Identification of specific cytosolic proteins from the livers of old mice with twofold or greater age-related change in the level of disulfide content

Spot #	Protein	NCBInr #	Mass	Peptides matched	% coverage	MOWSE score	Fold changes O/Y (mol/mol)	Mole thiol/ mole protein in old mice
5	Phosphodiesterase 6A	Q8K0A8	90154	5	13	68	2.4	0.8
7	Organic cation Transporter	Q63089	61501	5	20	68	2.7	0.4
9	Serin/threonine-protein kinase ORS-1	Q6P9R2	58168	6	15	67	3.3	0.1
25	GAPDH	P16858	36008	7	22	58	2.2	0.2
26	Acyl-coenzyme A thioesterase	Q8VHK0	35980	3	16	55	2.2	0.06
27	Regucalcin	Q64374	33385	4	21	71	3.7	3.0
39	Peroxiredoxin 1	P35700	22162	24	35	155	2.0	0.4
40	Peroxiredoxin 1	P35700	22162	51	49	319	2.0	0.9
43	Peroxiredoxin 1	P35700	22162	66	49	434	2.5	1
56	Rab14 (Ras-related protein)	Q91V41	23751	3	31	71	2.5	0.8
64	Regulator of G-protein signaling-1(RGS1)	P97844	18823	5	35	58	2.6	1.1
74	D-dopachrome tautomerase	O35215	13125	12	23	61	2.8	1.2
75	Heat response protein	Q569N4	18462	17	32	337	4.8	2.4

To calculate the changes in disulfide content in individual target proteins (pmoles of disulfides/μg of proteins), the pixel intensity of 6-IAF bound to each spot was converted to pmoles of disulfide using the standard curve described in Fig. 8.2 B, followed by calculating the microgram of protein in each spot from the pixel intensity of Sypro Ruby associated with each spot using the composite standard curve generated from GAPDH, enolase, and CK as described in Fig. 8.2 D. The disulfide content in old protein samples was expressed as a mole of thiol/mole of protein using the molecular weights of the individual proteins.

not due to the reduced levels of GAPDH as shown by the Western blot in Fig. 8.6. To confirm that the loss in GAPDH activity was due to increased cysteine oxidation to disulfides, we added DTT to the samples. As shown in Fig. 8.6, the activity of GAPDH was increased after DTT treatment in both the young and old samples; however, there was no significant difference in GAPDH activities of the DTT-treated samples between young and old mice, suggesting that the increase in disulfide content (i.e., reversible cysteine oxidation) was responsible for the age-related decline in GAPDH activity.

4. Discussion

We have developed a fluorescence-based assay that allows investigators to study how cysteine oxidation changes in cells and tissues. One of the difficulties in measuring cysteine oxidation is the potential for nonspecific oxidation reaction of thiols during the handling of samples because of the extreme sensitivity of the thiol group to oxidation. To prevent the nonspecific oxidation of thiol groups in proteins, we immediately add an excess amount of an alkylating agent (IAM) to the homogenates to react with all

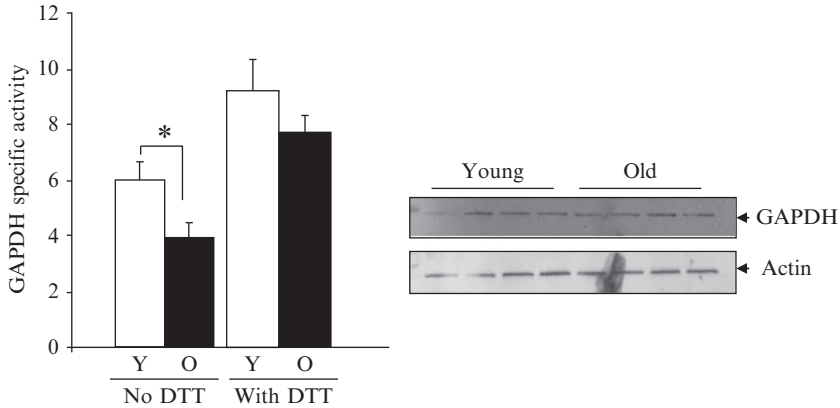

Figure 8.6 Effect of age on GAPDH activity. GAPDH activity was measured as previously described by Pierce *et al.* (2008) in liver cytosolic protein extracts in the presence or absence of 3.8 m*M* DTT. Enzyme units were expressed as the amount of enzyme required to convert 1 μmol of glyceraldehyde-3-phosphate to 1,3-bisphosphoglycerate/min. The data are presented as the mean ± SEM ($n = 4$), and the asterisk (*) denotes values that are significantly ($p < 0.05$) different from young mice. A representative Western blot for GAPDH protein levels in the cytosol from the livers of young and old mice is shown using a polyclonal rabbit antihuman GAPDH antibody (Alamo Laboratories, San Antonio, TX).

free thiol groups. We show that IAM rapidly blocks the free thiol groups in protein extracts, which allows one to measure the cysteine residues involved in disulfide bonds by the appearance of thiol groups after reduction by dithiothreitol (DTT). DTT generates thiol groups from disulfide bonds within or between proteins and glutathionylation as well as thiol groups generated from the reduction of sulfenic acid and *S*-nitrosyl groups. The thiol groups generated by DTT are then quantified by reacting them with 6-IAF and quantifying the amount of fluorescence bound to proteins.

The fluorescence-based assay is a relatively simple and rapid assay that can reproducibly detect changes in disulfide content (thiols generated by DTT reduction) of proteins in response to an oxidative stress *in vitro* and *in vivo*. Using this assay, we show that the disulfide content of cytosolic proteins from the liver increases with age, indicating that the oxidation ofcysteine residues in proteins increases with age. These data are consistent with previous studies showing an age-related increase in the global oxidative modification of proteins, for example, carbonyl groups (Chaudhuri *et al.*, 2006; Oliver *et al.*, 1987; Sohal *et al.*, 1993, 1995), nitrotyrosination (Kanski and Schoneich, 2005; Schoneich, 2006), *S*-nitrosylation (Raju *et al.*, 2005), and methionine sulfoxide (Cabreiro *et al.*, 2006; Stadtman *et al.*, 2005). Using 2D gel electrophoresis, we show that the fluorescence-based assay can be used to screen the proteome of a tissue for changes in the disulfide content of specific proteins. The disulfide content of specific proteins, that is, the mole of thiol/mole of protein, can also be calculated using our assay. We found that the disulfide content of 11 cytosolic proteins from the livers of old mice ranged from 0.06 to 3.0 mole of thiol/mole of protein. The age-related increase in disulfide content of one of the 11 proteins, GAPDH, was shown to be correlated to a decrease in enzyme activity, which arose from increased thiol oxidation.

ACKNOWLEDGMENTS

This work was supported by VA-VISN grant (A.R.C.), a VA Merit Review grant, an Ellison Medical Foundation grant, an NIH-NIA grant, R37HE26557 (A.R.), and an NIH-NIA grant, R01 AG025362 (W.F.W). We would like to thank Kevin Hakala and Orlando Valerino for their technical assistance.

REFERENCES

Berlett, B. S., and Stadtman, E. R. (1997). Protein oxidation in aging, disease, and oxidative stress. *J. Biol. Chem.* **272,** 20313–20316.

Bokov, A., Chaudhuri, A., and Richardson, A. (2004). The role of oxidative damage and stress in aging. *Mech. Ageing Dev.* **125,** 811–826.

Butterfield, D. A., and Kanski, J. (2001). Brain protein oxidation in age-related neurodegenerative disorders that are associated with aggregated proteins. *Mech. Ageing Dev.* **122,** 945–962.

Cabreiro, F., Picot, C. R., Friguet, B., and Petropoulos, I. (2006). Methionine sulfoxide reductases: Relevance to aging and protection against oxidative stress. *Ann. NY Acad. Sci.* **1067,** 37–44.

Chao, C. C., Ma, Y. S., and Stadtman, E. R. (1997). Modification of protein surface hydrophobicity and methionine oxidation by oxidative systems. *Proc. Natl. Acad. Sci. USA* **94,** 2969–2974.

Chaudhuri, A. R., Khan, I. A., and Luduena, R. F. (2001). Detection of disulfide bonds in bovine brain tubulin and their role in protein folding and microtubule assembly in vitro: A novel disulfide detection approach. *Biochemistry* **40,** 8834–8841.

Chaudhuri, A. R., de Waal, E. M., Pierce, A., Van Remmen, H., Ward, W. F., and Richardson, A. (2006). Detection of protein carbonyls in aging liver tissue: A fluorescence-based proteomic approach. *Mech. Ageing Dev.* **127,** 849–861.

Cumming, R. C., Andon, N. L., Haynes, P. A., Park, M., Fischer, W. H., and Schubert, D. (2004). Protein disulfide bond formation in the cytoplasm during oxidative stress. *J. Biol. Chem.* **279,** 21749–21758.

Eaton, P. (2006). Protein thiol oxidation in health and disease: Techniques for measuring disulfides and related modifications in complex protein mixtures. *Free Radic. Biol. Med.* **40,** 1889–1899.

Han, E. S., Muller, F. L., Perez, V. I., Qi, W., Liang, H., Xi, L., Fu, C., Doyle, E., Hickey, M., Cornell, J., Epstein, C. J., Roberts, L. J., Van Remmen, H., and Richardson, A. (2008). The in vivo gene expression signature of oxidative stress. *Physiol. Genomics* **34,** 112–126.

Huggins, T. G., Wells-Knecht, M. C., Detorie, N. A., Baynes, J. W., and Thorpe, S. R. (1993). Formation of o-tyrosine and dityrosine in proteins during radiolytic and metal-catalyzed oxidation. *J. Biol. Chem.* **268,** 12341–12347.

Jones, G. M., and Vale, J. A. (2000). Mechanisms of toxicity, clinical features, and management of diquat poisoning: A review. *J. Toxicol. Clin. Toxicol.* **38,** 123–128.

Kanski, J., and Schoneich, C. (2005). Protein nitration in biological aging: Proteomic and tandem mass spectrometric characterization of nitrated sites. *Methods Enzymol.* **396,** 160–171.

Kim, S. O., Merchant, K., Nudelman, R., Beyer, W. F., Jr., Keng, T., DeAngelo, J., Hausladen, A., and Stamler, J. S. (2002). OxyR: A molecular code for redox-related signaling. *Cell* **109,** 383–396.

Olivares-Corichi, I. M., Ceballos, G., Medina-Santillan, R., Medina-Navarro, R., Guzman-Grenfell, A. M., and Hicks, J. J. (2005). Oxidation by reactive oxygen species (ROS) alters the structure of human insulin and decreases the insulin-dependent D-glucose-C14 utilization by human adipose tissue. *Front. Biosci.* **10,** 3127–3131.

Oliver, C. N., Ahn, B. W., Moerman, E. J., Goldstein, S., and Stadtman, E. R. (1987). Age-related changes in oxidized proteins. *J. Biol. Chem.* **262,** 5488–5491.

Pierce, A., deWaal, E., Van Remmen, H., Richardson, A., and Chaudhuri, A. (2006). A novel approach for screening the proteome for changes in protein conformation. *Biochemistry* **45,** 3077–3085.

Pierce, A. P., de Waal, E., McManus, L. M., Shireman, P. K., and Chaudhuri, A. R. (2007). Oxidation and structural perturbation of redox-sensitive enzymes in injured skeletal muscle. *Free Radic. Biol. Med.* **43,** 1584–1593.

Pierce, A., Mirzaei, H., Muller, F., De Waal, E., Taylor, A. B., Leonard, S., Van Remmen, H., Regnier, F., Richardson, A., and Chaudhuri, A. (2008). GAPDH is conformationally and functionally altered in association with oxidative stress in mouse models of amyotrophic lateral sclerosis. *J. Mol. Biol.* **382,** 1195–1210.

Raju, S. V., Barouch, L. A., and Hare, J. M. (2005). Nitric oxide and oxidative stress in cardiovascular aging. *Sci. Aging Knowledge Environ.* **21,** re4.

Schmalhausen, E. V., Pleten, A. P., and Muronetz, V. I. (2003). Ascorbate-induced oxidation of glyceraldehyde 3-phosphate dehydrogenase. *Biochem. Biophys. Res. Commun.* **308,** 492–496.

Schoneich, C. (2006). Protein modification in aging: An update. *Exp. Gerontol.* **41,** 807–812.

Smith, L. L. (1985). Paraquat toxicity. *Philos. Trans. R. Soc. Lond. B Biol. Sci.* **311,** 647–657.

Sohal, R. S., Agarwal, S., Dubey, A., and Orr, W. C. (1993). Protein oxidative damage is associated with life expectancy of houseflies. *Proc. Natl. Acad. Sci. USA* **90,** 7255–7259.

Sohal, R. S., Sohal, B. H., and Orr, W. C. (1995). Mitochondrial superoxide and hydrogen peroxide generation, protein oxidative damage, and longevity in different species of flies. *Free Radic. Biol. Med.* **19,** 499–504.

Stadtman, E. R., Van Remmen, H., Richardson, A., Wehr, N. B., and Levine, R. L. (2005). Methionine oxidation and aging. *Biochim. Biophys. Acta* **1703,** 135–140.

Thomas, J. A., and Mallis, R. J. (2001). Aging and oxidation of reactive protein sulfhydryls. *Exp. Gerontol.* **36,** 1519–1526.

Uchida, K., Toyokuni, S., Nishikawa, K., Kawakishi, S., Oda, H., Hiai, H., and Stadtman, E. R. (1994). Michael addition-type 4-hydroxy-2-nonenal adducts in modified low-density lipoproteins: Markers for atherosclerosis. *Biochemistry* **33,** 12487–12494.

Yoo, B. S., and Regnier, F. E. (2004). Protoemic analysis of carbonylated proteins in two-dimensional gel electrophoresis using avidin-fluorescein affinity staining. *Electrophoresis* **25,** 1334–1341.

Zeng, R., Xu, Q., Shao, X. X., Wang, K. Y., and Xia, Q. C. (2001). Determination of the disulfide bond pattern of a novel C-type lectin from snake venom by mass spectrometry. *Rapid Commun. Mass Spectrom.* **15,** 2213–22120.

Zhou, J. Q., and Gafni, A. (1991). Exposure of rat muscle phosphoglycerate kinase to a nonenzymatic MFO system generates the old form of the enzyme. *J. Gerontol.* **46,** B217–B221.

CHAPTER NINE

Measurement and Identification of *S*-Glutathiolated Proteins

Bradford G. Hill,* Kota V. Ramana,† Jian Cai,‡ Aruni Bhatnagar,* *and* Satish K. Srivastava†

Contents

Abstract

Protein thiol modifications occur under both physiological and pathological conditions and can regulate protein function, redox signaling, and cell viability. The thiolation of proteins by glutathione (GSH) appears to be a particularly important mode of posttranslational modification that is increased under conditions of oxidative or nitrosative stress. Modification of proteins by glutathiolation has been shown to affect the structure and function of several susceptible proteins and protect them from subsequent oxidative injury. In many cases, the glutathiolated proteins are low in abundance, and dethiolation occurs readily. Therefore, sensitive, reliable, and reproducible methods are required for

* Diabetes and Obesity Center, University of Louisville, Louisville, Kentucky, USA
† The Department of Biochemistry and Molecular Biology, University of Texas Medical Branch, Galveston, Texas, USA
‡ Department of Pharmacology and Toxicology, University of Louisville, Louisville, Kentucky, USA

Methods in Enzymology, Volume 473
ISSN 0076-6879, DOI: 10.1016/S0076-6879(10)73009-3

measuring both the total levels of protein glutathiolation and for identifying glutathiolated proteins under given conditions. These methods necessitate the preservation or the controlled removal of the GSH adducts during sample preparation for the accurate measurement of total *S*-glutathiolation and for the identification of protein–GSH adducts. In this chapter, we briefly review and provide protocols for chemical, mass spectrometric, immunological, and radioactive tagging techniques, for measuring protein *S*-glutathiolation in cells and tissues.

1. Introduction

Glutathione (GSH) is a ubiquitous, cysteine-containing tripeptide (γ-Glu-Cys-Gly) that is abundant in most eukaryotic cells. The intracellular concentration of GSH varies between 0.1 and 10 m*M*. A complete lack of GSH is incompatible with long-term survival. Most of the functions of GSH depend upon its cysteine residue, which participates in several types of reactions, including displacement, nucleophilic addition, and thiol–disulfide exchange. GSH provides reducing equivalents to glutathione peroxidases, and the oxidized glutathione (GSSG) generated by these reactions is reduced by GSSG reductases. By participating in these reactions, GSH helps to maintain cellular sulfhydryl residues in a reduced state. GSH also reacts with free radicals generating glutathionyl radicals that can combine with each other to form GSSG. In addition, GSH reduces dehydroascorbic acid (generated by radical-induced oxidation) to ascorbic acid. Because of these properties, GSH is viewed as the first line of defense against oxidants and the ultimate radical sink. In addition to participating in redox reactions, GSH also forms conjugates with metals and endogenous or xenobiotic electrophiles by participating in reactions catalyzed by glutathione-*S*-transferases (GSTs). Recent studies indicate that GSH is also an important participant and a regulator of the biological activity of nitric oxide (NO). Although NO does not directly react with thiols, upon autoxidation by molecular oxygen, it can form nitrosothiols. These compounds have been detected *in vivo* and are thought to be important mediators of NO action and NO-induced protein glutathiolation (Klatt and Lamas, 2000).

The propensity of GSH to undergo thiol–disulfide exchange reactions favors ready reaction of the tripeptide with cysteinyl side chains of proteins. Proteins bound to GSH, previously called protein–GSH mixed-disulfides and now referred to as either glutathiolated or glutathionylated proteins, have been detected in several cells and tissues (Biswas *et al.*, 2006; Hill and Bhatnagar, 2007; Shackelford *et al.*, 2005). It was initially thought that glutathiolated proteins were mostly generated by the oxidation of protein cysteine residues by GSSG, where GSSG reacts with protein thiols via a thiol–disulfide

exchange. Specific transmembrane transporters that extrude GSSG from the cell (such as the multidrug resistance protein and RLIP) may therefore be important in regulating the level of glutathiolated proteins. Recent evidence, however, indicates that the adduction of GSH to protein cysteines is primarily facilitated by transnitrosation reactions or sulfenic acids (Hill and Bhatnagar, 2007; West *et al.*, 2006). As shown in Scheme 9.1, both NO and reactive oxygen species can promote the formation of *S*-glutathiolated proteins. The induction of protein *S*-glutathiolation by nitrosoglutathione (GSNO) was first demonstrated by us for aldose reductase (Chandra *et al.*, 1997). Incubation of the protein led to the stoichiometric adduction of a single GSH residue at the active site of the enzyme and resulted in complete inhibition of its catalytic activity. The enzyme was also found to be glutathiolated in vascular smooth muscle cells exposed to NO donors (Ramana *et al.*, 2003). Later studies have shown that peroxynitrite arising from NO donors or pathological stimuli triggers *S*-glutathiolation of proteins such as the sarco/endoplasmic reticulum calcium ATPase (SERCA) (Adachi *et al.*, 2004) and p21ras (Clavreul *et al.*, 2006). Significantly, these proteins are glutathiolated *in vivo* and the modification of their cysteine residues alters protein function, suggesting that posttranslational modification by glutathiolation may be a significant mechanism of redox regulation employed by NO. In this regard, it has been shown that an increase in endogenous NO synthesis either by the stimulation of endothelial NO synthase in aorta (West *et al.*, 2006), overexpression of inducible NO synthase in the heart (Reinartz *et al.*, 2008; West *et al.,* 2006), or L-arginine treatment (West *et al.,* 2008) increases protein *S*-glutathiolation, indicating that NO at physiological levels regulates protein function by inducing protein adduction to GSH. In addition, the oxidation products of GSNO (e.g., glutathione sulfonic acid, glutathione disulfide *S*-oxide, and glutathione disulfide-*S*-dioxide) as well as protein sulfenic acids generated by the reaction of protein thiols or GSH with hydrogen peroxide have been suggested to be significant intracellular glutathiolating agents (Bindoli *et al.*, 2008; Li *et al.*, 2001). The view that glutathiolation is a regulated mode of signal transduction is supported further by the recent discovery of enzymatic pathways for protein deglutathiolation. Several studies show that the deglutathiolation of proteins is catalyzed by glutaredoxin, thioredoxin, and protein disulfide isomerases. The role of glutathiolation in signal transduction and regulation of protein function have been extensively reviewed elsewhere (Biswas *et al.*, 2006; Hill and Bhatnagar, 2007; Shackelford *et al.*, 2005).

Although the physiological significance of protein glutathiolation has not been fully assessed, it is currently believed that the addition of GSH to protein sulfhydryls prevents excessive oxidation and thereby preserves protein integrity and function under conditions of oxidative stress. This is consistent with the increase in protein glutathiolation due to endogenously generated hydrogen peroxide (Adachi *et al.*, 2004) and peroxynitrite (Clavreul *et al.*, 2006), as well as exposure to oxidized LDL (Clavreul

et al., 2006), cigarette smoke (Muscat *et al.*, 2004), and hyperoxic conditions (Knickelbein *et al.*, 1996). Protein glutathiolation due to NO generation may reflect the fact that *S*-nitrosated proteins are readily glutathiolated (West *et al.*, 2006) and that glutathiolation may be an essential step in protein denitrosation (Baba *et al.*, 2009). Also, recent evidence suggests that the functions of several enzymes and structural proteins are regulated by *S*-glutathiolation (Hill and Bhatnagar, 2007). It is important, therefore, that specific, sensitive, and reliable methods are used to study *S*-thiolation reactions and the proteins modified by GSH. Most studies have exploited the use of techniques or combinations thereof that: (1) quantify or estimate global changes in glutathiolated proteins, (2) identify proteins modified by GSH and their specific sites of adduction, and (3) determine how GSH modifications regulate protein function and physiological and pathological responses. The following is a brief description of several methods used to measure global changes in protein glutathiolation and identify glutathiolated proteins and sites of modification. We also discuss some of the new approaches for identifying proteins that are glutathiolated in cells or in animals *in situ*.

2. Chemical Methods for the Measurement of Glutathiolated Proteins

Early methods for measuring glutathiolated proteins were developed to quantify the total amount of GSH bound to proteins. The overall aim of these approaches was to demonstrate that GSH (or cysteine) forms a covalent attachment with proteins and that the levels of glutathiolated proteins (or mixed disulfides) change with specific diseases or pathological conditions associated with oxidative stress. These approaches are still useful to measure the extent of protein glutathiolation, although they are of limited value in identifying specific proteins or residues modified by GSH.

To quantify the amount of GSH bound to proteins, Harding (1970) reduced proteins by sodium borohydride and then quantified the GSH released by colorimetric measurements using DTNB. The method is simple and straightforward, but requires large amounts of protein and is not specific for GSH, because protein-bound cysteine is also released and reported in colorimetric measurements. To identify GSH specifically, the thiol liberated by sodium borohydrate was measured either by HPLC or by the GSH reductase recycling assay. Nevertheless, the long procedures of reduction and subsequent HPLC analysis increased the likelihood of GSH autoxidation and the possibility of obtaining erroneous results, leading to an underestimation of the extent of intracellular protein glutathiolation. Moreover, reductants (either sodium borohydride or DTT) interfere with the

measurement of GSH in both the recycling and HPLC methods. Therefore, to expedite sample preparation and to avoid reduction, Lou *et al.* (1986) developed a new method for measuring protein glutathiolation in which protein-bound GSH was cleaved and oxidized by performic acid. This procedure results in the formation of free non-protein-bound glutathione-sulfonic acid (GSO_3H) which can be quantified by anion-exchange chromatography. The method minimizes the potential for GSH autoxidation, is reproducible and reliable, and results in the quantitative release of GSH from proteins. However, it is not very sensitive and requires large amounts of tissue. To improve sensitivity, Kumari *et al.* (1994) modified this method by introducing an additional step in which the glutathione-sulfonic acid is derivatized with phenylisothiocyanate. The phenylthiocarbamyl derivative can then be separated and quantified by reverse-phase HPLC. This modification resulted in reduction of the volume required for lyophilization from 100–300 ml to 2 ml. This method, described in detail below, is at least 20× more sensitive than the nonderivatized measurement of sulfonic acid.

2.1. Release of protein-bound GSH by oxidation

In this method, glutathiolated proteins are subjected to performic acid oxidation to cleave the S–S bond with simultaneous oxidation of GSH to glutathione-sulfonic acid. Excessive performic acid is removed by lyophilization and the solution is deproteinized by ultrafiltration. The recovery of GSSG and glutathione-sulfonic acid is >90%. Reagent glutathione-sulfonic acid is used as a standard.

2.1.1. Measurement of glutathione-sulfonic acid

2.1.1.1. Synthesis of reagent glutathione-sulfonic acid

1. Dissolve the appropriate amount of GSSG in 125 μl of performic acid in a prechilled test tube.
2. Vortex and allow the oxidation to continue for 2.5 h in an ice bath.
3. Add 2 ml deionized water and lyophilize the sample in a Speed Vac.
4. Add 100 μl of 2:2:1 methanol:water:triethylamine (TEA) and dry on a Speed Vac.
5. Add 80 μl of 7:1:1:1 methanol:water:TEA:phenylisothiocyanate (PITC). The solution should be made fresh immediately before use and stored at −20 °C under nitrogen.
6. Dry and resuspend the sample in 100–200 ml water. Filter through a 0.2 μm filter.

2.1.1.2. Measurement of glutathione-sulfonic acid liberated from glutathiolated proteins

1. Homogenize the tissue in an appropriate volume of potassium phosphate (10 m*M* K-phosphate, pH 7.0, containing protease inhibitors).
2. Add trichloroacetic acid (TCA) to a final concentration of 10% to precipitate the proteins and centrifuge at 13,000×*g* for 10 min.
3. Disrupt the pellet and wash 3× with 10% TCA, centrifuging after each wash.
4. Wash the pellet 1× with 1:1 methanol:ether, and dry the pellet at 40 °C under nitrogen.
5. Resuspend the pellet in 125 μl performic acid and vortex. Incubate on ice for 2.5 h and add 0.2 ml deionized water.
6. Lyophilize the sample in a Speed Vac and dissolve in 1.0 ml deionized water.
7. Add sulfosalicyclic acid to a final concentration of 15% and centrifuge at 13,000×*g* for 10 min.
8. Remove the supernatant and dry on Speed Vac. Reconstitute in 100 μl of 2:2:1 methanol:water:TEA and dry again on Speed Vac.
9. Add 80 ml of 7:1:1:1 methanol:water:TEA:PITC.
10. Vortex and incubate at room temperature for 20 min and dry on Speed Vac.
11. Resuspend the sample in 100–200 ml water and filter through a 0.2-μm filter.
12. For HPLC, 10–50 ml of sample are injected into an ODS column equilibrated with 0.14 *M* sodium acetate, containing 0.1% TFA and 6% acetonitrile, pH adjusted to 6.4 with acetic acid. Sulfonic acids are eluted with an isocratic gradient at a flow rate of 0.5 ml/min, and the absorbance is measured at 251 nm using an absorbance detector. Using these conditions, a linear increase in peak area is observed from 0.05 to 3 nmols of GSO_3H.

3. Detection of Glutathiolated Proteins by ESI/MS

Proteins adducted with GSH can be readily detected by a characteristic +305 Da shift in mass by electrospray mass spectrometry (ESI/MS). Because of its superior sensitivity and specificity, this technique has become the method of choice for measuring glutathiolation of purified proteins for structural or kinetic analysis. Although only small quantities of protein are required, best results are obtained with highly purified or homogenous protein solutions. Impurities decrease the signal-to-noise ratio and can interfere with accurate

mass estimation. Proteins are usually modified in ionic medium and therefore the protein has to be exchanged into nonionic medium for ESI/MS. This requires a rather high (0.2–1.0 mg/ml) initial concentration of pure protein for accurate mass determination. Nevertheless, ESI/MS is a soft-ionization technique which does not disrupt the protein-SSG bond.

3.1. Mass spectrometric analysis

Incubate 0.5–1.0 mg protein with 0.1 *M* DTT at 37 °C for 1 h in 100 m*M* phosphate buffer, pH 7.0. This is essential to reduce all disulfide bonds and sulfenic acids incurred during storage. Long-term storage in β-mercaptoethanol is not advisable. At 4 °C, the thiol has a half-life of 24 h and thus needs to be replenished constantly if the protein is to be stored for long periods. Storage with β-mercaptoethanol results in the formation of a mixed disulfide, which could significantly affect the protein structure or function. Storage in 1 m*M* DTT is preferable, but does not ensure that the protein remains in a fully reduced state. Hence, it is advisable to reduce the protein immediately before use.

1. For glutathiolation, the reduced protein is incubated with 1 m*M* GSSG or 1 m*M* GSNO at 25 °C for 1 h. Aliquots can be withdrawn at different times to measure changes in activity. With several proteins, we have found that GSNO is a better glutathiolating agent than GSSG. The disadvantage of using GSNO is that it could result in the formation of nitrosated proteins. Glutathiolation can be induced more specifically by GSSG; however, in some cases (for example, actin), it may be necessary to "activate" the cysteine residue. For this, incubate 25–50 μM protein with a 20-*M* excess of DTNB (20 m*M* in 1% $NaHCO_3$) and follow the reaction at 412 nm until 1 equivalent of TNB is released ($\varepsilon_{412} = 14.15$ mM^{-1} cm^{-1}). Excess reagent is removed by Sephadex G-25 filtration, and the eluted, activated protein sample is reacted with a 50-*M* excess of GSH under spectrophotometric control to quantify the extent of glutathiolation. This procedure results in stoichiometric induction of GSH adducts in protein samples and provide a sensitive measure of the extent of glutathiolation.
2. For desalting, load the protein on a Sephadex G-25 column equilibrated with N_2-saturated 10 m*M* ammonium acetate.
3. For ESI/MS analysis, dilute the desalted protein with the flow-injection solvent (acetonitrile:H_2O:formic acid 50:50:1, v/v/v). The mixture is infused into the spectrometer at a rate of 10 μl/min. For Micromass LCZ spectrometer, the following conditions are routinely used in our laboratory: capillary voltage, 3.1 kV; cone voltage, 27 V; extractor voltage, 4 V; source block temperature, 100 °C; desolvation temperature, 200 °C. Spectra can be acquired at 200 a.m.u./s over a 200–2000 a.m.u. range.

The instrument is calibrated with myoglobin. The spectra from each ion are then summed and deconvoluted with MaxEnt software (MaxEnt Solutions, Suffolk, UK).

An example demonstrating stoichiometric induction of a single GSH molecule in actin, using the procedure described earlier, is shown in Fig. 9.1A . An additional advantage of ESI/MS is that the site of modification can be readily identified following protease digestion. As shown in Fig. 9.1B, reduced and glutathiolated actin samples were digested with Glu-C. The digestion was stopped by the addition of formic acid, the peptides were cleaned with C18 ZipTip, and the peptide mixture was analyzed by ESI/MS. The peptides from actin, found to be glutathiolated following incubation of the intact protein with GSNO, are shown in Table 9.1.

4. Identification of *S*-Glutathiolated Proteins in Cells and Tissues

4.1. Western blot analysis

Western blot analysis has emerged as the technique of choice for the measurement of glutathiolated proteins. This approach is possible due to the availability of a specific IgG2a mouse monoclonal antibody that recognizes GSH–protein complexes (from ViroGen, Watertown, MA, USA). The protein A-purified antibody is used to detect glutathiolated proteins on Western blots under nonreducing conditions. Both one-dimensional (1D) and two-dimensional (2D) gel electrophoresis can be used to detect pure glutathiolated proteins or proteins glutathiolated in cells or tissues *in situ*. An additional variant of this technique is to purify glutathiolated proteins on a GSH-affinity column and then analyze the eluent by ESI/MS (Celli *et al.*, 2003). However, enrichment on the glutathiolated proteins by a GSH-affinity column may require large amounts of protein and is likely to generate a mixture of different proteins which could need to be separated further either by 1D or 2D gel electrophoresis before mass spectrometric analysis.

For measuring glutathiolated proteins in isolated proteins, *N*-ethylmaleimide (NEM; generally 5–25 m*M*) is added to the protein solution upon completion of, or to prevent further, protein thiolation reactions. For convenience, we add the proteins directly to Laemmli sample buffer containing 25 m*M* NEM prior to SDS-PAGE. For cells or tissues, NEM (25 m*M*) is added to both the lysis/homogenization buffer and the Laemmli sample buffer. It is also critical that NEM be present during the blocking step after transfer of the proteins to PVDF or nitrocellulose membranes; this step increases the detection of glutathiolated

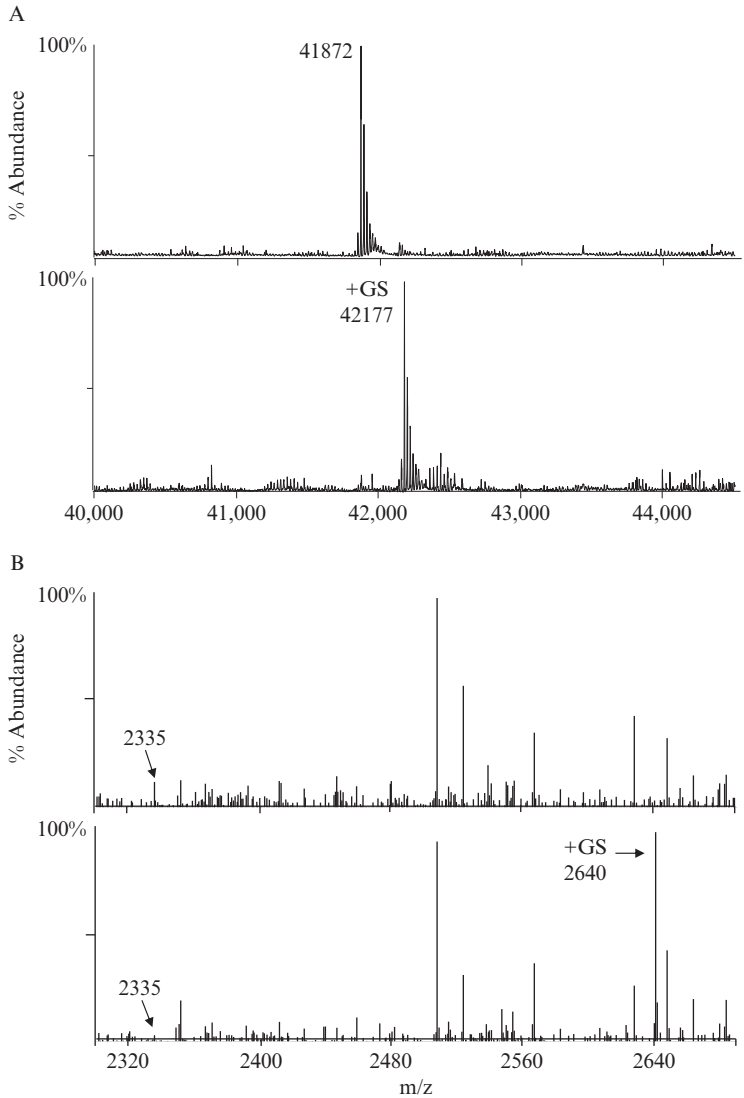

Figure 9.1 Analysis of reduced and glutathiolated actin by mass spectrometry. (A) Deconvoluted ESI$^+$/MS spectra of actin before (upper panel) and after (lower panel) modification by GSNO. The protein was first reduced by DTT and excess DTT was removed by Sephadex gel filtration. The reduced protein was then added to acetonitrile:water:acetic acid for spectrometric analysis (upper panel). The reduced protein was then incubated with 1 m*M* GSNO (in 20 m*M* Tris, pH 7.5) for 1 h. The protein was desalted and then analyzed by ESI/MS (lower panel). Note the +305 Da shift in the mass of the major ion, indicating the adduction of a single glutathione molecule to one molecule of actin. (B) ESI/MS spectra of native and GS-actin after hydrolysis with Glu-C. Two peaks (*m/z* 2640 and 3820) were observed only in the GS-actin spectrum and those corresponding to the addition of 305 Da to peaks from the sample of the native protein (*m/z* 2335 and 3515) were identified.

Table 9.1 Actin peptides found to be susceptible to GSNO-mediated glutathione modification *in vitro*

Treatment	Sequence	MW (expected)	MW (observed)	Delta	Modification
Control	TTALVCDNGSGLVKAGFAGDDAPR	2335.13	2335.13	0	−
GSNO	TTALV**C**DNGSGLVKAGFAGDDAPR	2335.13	2640.19	305.06	+
Control	TTALVCDNGSGLVKAGFAGDDAPRAVFPSIVGRPR	3514.82	3514.82	0	−
GSNO	TTALV**C**DNGSGLVKAGFAGDDAPRAVFPSIVGRPR	3514.82	3819.93	305.11	+

Actin samples were analyzed by ESI-MS before digestion. GSNO-treated actin was shown to be modified by one molecule of glutathione (Fig. 9.1). The actin samples (without or with modification) were dried by Speed Vac, dissolved in 50 m*M* NH_4HCO_3 containing 8 *M* urea, and digested with Glu-C (20 ng/5 μl in 50 m*M* NH_4HCO_3) at 30 °C for 6 h, and digestion was stopped by adding 30 μl 5% formic acid. Peptides from these samples were cleaned with C18 ZipTip and analyzed by ESI-MS.

proteins several-fold by preventing the reduction of GSH adducts by thiol-containing proteins in the milk or reactive thiols in albumin. For this, NEM (2.5 m*M* final concentration) is added to 5% blocking milk (or equivalent albumin blocking mixtures) and allowed to stir at room temperature for 30 min. After blocking for 2 h, the membranes are washed 3× with Tris-buffered saline containing 0.1% Tween-20 (TBS-Tween). The anti-protein–GSH monoclonal antibody is then diluted 1:1000 in TBS-Tween and incubated on a rocker for 2 h at room temperature or overnight at 4 °C. Secondary antibodies are also diluted in TBS-Tween. An example of glutathiolated protein detection using this method is shown in Fig. 9.2C. In this image, immunoreactivity was visualized by chemifluorescence using a Typhoon 9400 Imager (Amersham Biosciences), and the intensity of the resulting bands was analyzed with ImageQuantTL software (Amersham Biosciences).

For 2D gel analysis, cells or tissues can be lysed or homogenized in low salt buffer (e.g., 5 m*M* Tris, pH 7.0) containing nonionic detergents (e.g., 1% Triton X-100 or NP-40) and 25 m*M* NEM. The proteins can then be loaded on immobilized pH gradient strips and focused using typical protocols. As a general rule, one should load approximately 3× the amount of protein used in 1D gels; for example, if 10 μg protein is generally needed to detect glutathiolated proteins by 1D Western blotting, 30–40 μg protein should be loaded on the IPG strips. If the sample to be analyzed by 2D techniques contains too much salt, a "clean-up" step may be required. For this, the following protocol can be used:

1. Add trichloroacetic acid (TCA; 10%, v/v) to tissue homogenates or cell lysates and allow to incubate on ice for 10 min.
2. Centrifuge the sample for 5 min at 13,000×*g*.
3. Wash the precipitated protein pellet 3× with acetone to remove remaining TCA. This step can also help remove lipids that cause streaking.
4. Resuspend the protein pellet in 10 m*M* Tris, pH 6.8, containing 8 *M* urea, 1 m*M* EDTA, and 1 m*M* NEM. In some cases, it may be required to incubate the sample overnight at 4 °C for adequate resolubilization.
5. Measure protein by the Bradford method (Bradford, 1976). Make the BSA standard and assay dilutions in the same buffer as in Step 4.
6. Add the protein mixture (40 μg) to the appropriate amount of rehydration buffer (e.g., for 7 cm IPG strips from Biorad, a final volume of 125 μl is desirable) and focus the proteins on pH 3–10 or 5–8 IPG strips.

Prior to the second dimension, equilibrate the strips in base equilibration buffer containing 25 m*M* NEM. If overlay agarose solution is used, include NEM in this solution as well. To obtain peptides for matrix-assisted laser desorption ionization-time-of-flight mass spectrometry (MALDI-TOF/MS), excise protein spots that were immunoreactive with anti-PSSG antibodies form parallel Sypro Ruby-stained gels and digest with trypsin using a modified version of the method described by Jensen *et al.* (1999) and West

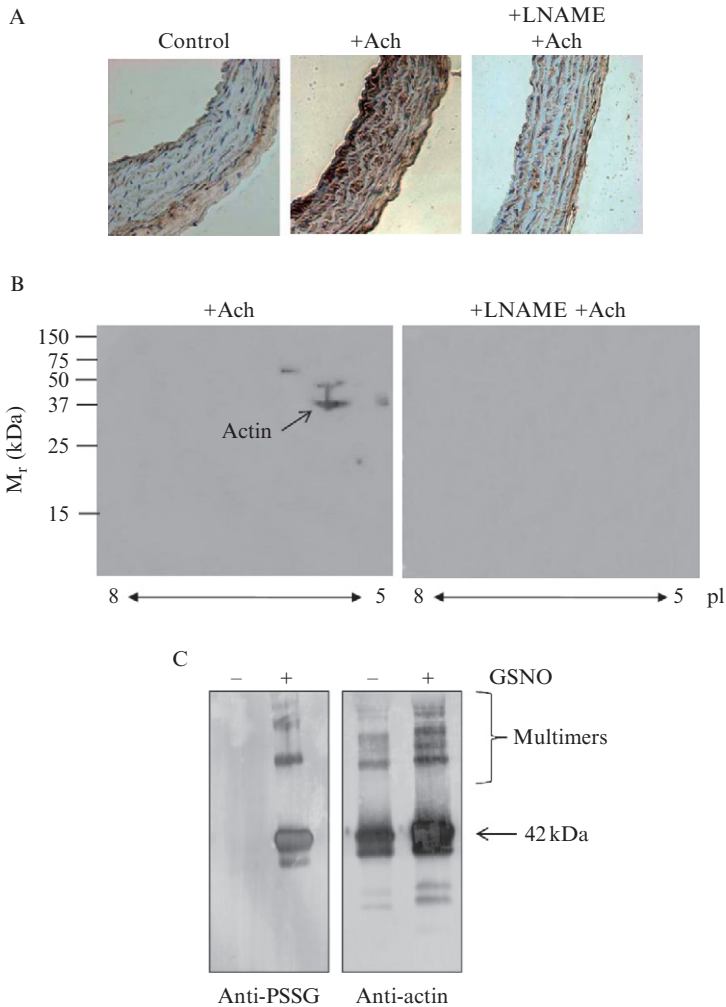

Figure 9.2 Immunological detection of glutathiolated proteins. (A) Photomicrographs of aortic rings stained with the antiglutathione antibody. Aortic rings were dissected from adult male rats, mounted *ex vivo* in a perfusion bath, and precontracted with 1 μM phenylephrine. The rings were either left untreated (control), stimulated with 1 μM acetylcholine (+Ach), or treated with acetylcholine in the presence of 100 μM L-NAME, a NO synthase inhibitor. Immediately after treatment, the rings were fixed and stained with the antiglutathione antibody (1:200 dilution). (B) Two-dimensional Western blots of aortic rings precontracted with phenylephrine and relaxed by acetylcholine in the absence or presence of L-NAME. Extracts of aortic rings were subjected to 2D Western blot analysis using the antiglutathione antibody. *Note*: The major immunopositive spot corresponds to actin (as indicated in the figure). (C) One-dimensional SDS-PAGE of rabbit skeletal muscle actin before (–) and after (+) treatment with 1 mM GSNO. The treated and untreated proteins were separated by SDS-PAGE, and Western blots were developed with the antiglutathione (anti-PSSG) and antiactin antibodies.

et al. (2006). The peptide masses obtained by MALDI-TOF/MS analysis can then be used in a database search (e.g., the National Center for Biotechnology Information) to identify the parent proteins. An example of 2D analysis of glutathiolated proteins using these methods is shown in Fig. 9.2B.

In some cases, it may be necessary to immunoprecipitate proteins prior to ESI/MS or MALDI-TOF/MS analysis. For this, we homogenize the tissue in 50 m*M* Tris, pH 7.4, containing 250 m*M* sucrose, 10 m*M* iodoacetic acid (IAA), and 1% protease inhibitor cocktail. The homogenates are then centrifuged at 14,000×*g* for 15 min at 4 °C, and the supernatant is incubated in the dark for 1 h at room temperature. The homogenate is then passed through a Sephadex G25 (PD-10) column to remove excess IAA, and the glutathiolated proteins are immunoprecipitated with the anti-PSSG Ab. Nonspecific mouse IgG is used as a control for the immunoprecipitations. The proteins are eluted by boiling the agarose beads in Laemmli buffer containing 25 m*M* NEM. The proteins are then separated by nonreducing SDS-PAGE and visualized by silver staining. The protein bands can then be excised for mass spectrometric analysis. Note that NEM or iodoacetamide (IAM) should be substituted for IAA if 2D analysis will be performed after the immunoprecipitation step; IAA imparts a negative charge that could cause proteins to focus to "false" isoelectric points.

4.2. Immunohistochemical staining

As shown in Fig. 9.2A, the anti-protein–GSH (PSSG) antibody can also be used to detect glutathiolated proteins in tissue sections using standard histology techniques (West *et al.*, 2006). For this:

1. For immunocytochemistry, fix cells in 100% acetone, wash with PBS, and then incubate in PBS containing 10% goat serum for 30 min. For immunohistochemical analysis, tissue sections (e.g., rat aortic rings) can be fixed in formalin and stored in 70% ethanol.
2. Incubate the sections with the anti-PSSG antibody overnight (1:200 dilution), wash with PBS, and then incubate with fluorescent secondary antibodies (e.g., Alexa-488, Molecular Probes) for 2 h at room temperature.
3. Rinse the slides with PBS and mount with a coverslip using Fluorsave reagent (Calbiochem).
4. Acquire fluorescent and phase contrast images using a water-immersion objective and a high-resolution, high-sensitivity camera (e.g., Spot Insight QE). The images can be quantified using Metamorph software.

4.3. Radioactive tagging

An additional approach for identifying glutathiolated protein in cells is to radiolabel the GSH pool in cells before treating with a glutathiolating agent. The main advantage of this technique is that it is sensitive and robust and can be used under a variety of conditions. The main disadvantage is that it does not permit discrimination between proteins modified by GSH and those ligated to cysteines. However, immunoprecipitation with the anti-PSSG antibody can be used to purify the glutathiolated protein for further analysis by ESI/MS or MALDI-TOF/MS, and incorporation of the radiolabel in the immunoprecipitate adds confidence that the protein is glutathiolated. For radiolabel tagging:

1. Grow cells to 80–90% confluency in 10 cm^3 dishes.
2. Remove the medium and wash twice with Kreb's Heinslet buffer (KH buffer; 118 m*M* NaCl, 4.7 m*M* KCl, 25 m*M* $MgCl_2$, 3 m*M* $CaCl_2$, 1.25 m*M* KH_2PO_4, 0.5 m*M* EDTA, 25 m*M* $NaHCO_3$, 10 m*M* glucose pH 7.4).
3. Add cycloheximide (2 μg/ml) in KH buffer to prevent direct incorporation of the label in the cellular proteins.
4. After 60 min of incubation at 37 °C in 5% CO_2, add 20 μmol/ml of L-[^{35}S]-cysteine to the cells and incubate for an additional 5 h to label the intracellular GSH pool.
5. To initiate glutathiolation, add either 100 μM H_2O_2, diamide (0.25 m*M*) or NO donors such as SNAP (1 m*M* prepared in 100% DMSO). Add the same volume of the vehicle to control cells. Diamide can be used as a general positive control and requires only ~10 min of incubation to induce >50% maximal glutathiolation.
6. Incubate cells at 37 °C for 1 h.
7. Remove KH buffer and wash with 5 ml of fresh KH buffer.
8. Lyse the cells in ice cold Tris–Triton buffer (1% Triton X-100, 0.5% NP-40, 150 m*M* NaCl, 10 m*M* Tris, pH 7.0, 1 m*M* EDTA, 1 m*M* EGTA, and protease and phosphatase inhibitor cocktails) containing 25 m*M* NEM.
9. Centrifuge at 10,000×*g* for 5 min at 4 °C. Save an aliquot of the supernatant to measure protein concentration. A detergent-compatible Lowry method (e.g., the DC Lowry assay, Biorad) works well for samples containing detergent and NEM.
10. If immunoprecipitation is required, remove excess NEM by gel filtration, and, to 500 μg of total lysate protein, add 2 volumes of immunoprecipitation buffer (2% Triton X-100, 300 m*M* NaCl, 20 m*M* Tris pH 7.4, 2 m*M* EDTA, 2 m*M* EGTA, 0.4 m*M* $Na_2O_2V_7$, 0.4 m*M* PMSF, 1.0% NP-40, and 20 μl of protease inhibitor cocktail). Add the required antibody and incubate the samples with rocking at room temperature for 2 h or overnight at 4 °C. After incubation, add

100 μl of protein-A agarose beads, followed by overnight incubation on a continuous shaker at 4 °C to precipitate free and bound IgG. After the incubation, centrifuge the samples at 10,000×*g* for 5 min and wash three to five times with immunoprecipitation buffer.

11. Resuspend the pellet in 50 μl of Laemmli sample buffer-containing NEM and centrifuge at 10,000×*g* for 5 min.
12. Separate proteins in the supernatant by SDS-PAGE.
13. Dry the gels and measure radioactivity by autoradiography.
14. To establish specificity, treat similarly prepared homogenates or lysates with 50 m*M* DTT. Repeat Steps 7–13. The difference in radioactivity associated with specific proteins bands from those samples treated without or with 50 m*M* DTT reflects the extent of specific *S*-thiolation.

For most cells, simply incubating the cells with [^{35}S]-cysteine is sufficient for adequate labeling of the thiol pool to induce detectable glutathiolation of the protein of interest. However, when the protein is only weakly glutathiolated, it may be necessary to radiolabel the thiol pool after depleting the intracellular thiols (Li *et al.*, 2001; Ward *et al.*, 2000). To deplete endogenous low-molecular weight thiols, replace the medium on 75% confluent cells with DMEM lacking sulfur-containing amino acids and containing 10% dialyzed serum for 16 h at 37 °C. Next, add the protein synthesis inhibitor cycloheximide and [^{35}S]-cysteine as described earlier.

4.4. Biotin labeling

In this method, cells or tissues are incubated with biotinylated GSSG. The derivatized GSSG reacts with susceptible protein thiols to form protein–SSG–biotin adducts. The adducts can be detected by Western blotting with streptavidin or by other avidin-based techniques. Biotinylated proteins can also be localized in cells by fluorescence microscopy (Brennan *et al.*, 2006). The extended spacer arm of biotin–SSG provides maximal accessibility of biotin for avidin conjugates. The biotin–SSG conjugate is membrane permeable and traverses the cell membrane to react with cytosolic proteins (Brennan *et al.*, 2006).

4.4.1. Biotinylation of oxidized glutathione

1. Add 111.4 mg sulfosuccinimidyl-6-(biotinamido)hexanoate (Merck Biosciences Ltd., Nottingham, UK) to 61.2 mg GSSG in 1.8 ml water and adjust the pH to 7.2 with NaOH.
2. Let the mixture sit for 1 h at room temperature.
3. Quench the reaction with 1 *M* Tris–HCl, pH 7.2 to a final volume of 2 ml.

4. Separate the mixture by HPLC using an ODS column. Monitor the absorbance (190–400 nm) with a diode array detector.
5. Verify the mass of the purified compound (biotin–GSSG) by ESI/MS or MALDI-TOF/MS. The derivative ion should conform to an m/z value of 1290.85.

4.4.2. Modification of cellular proteins

1. Incubate cells in serum-free medium with 5 m*M* biotin–SSG for at least 10 min.
2. After incubation, pellet cells by centrifugation and discard the supernatant.
3. Lyse cells in lysis buffer containing 25 m*M* NEM. Alternatively, use Laemmli sample buffer-containing NEM. Do not add reducing agents (DTT or 2-mercaptoethanol) to the medium.
4. For SDS-PAGE, separate the proteins on nonreducing 10% SDS-polyacrylamide gels. To establish specificity, run a separate gel with 10% 2-mercaptoethanol added to the lysis/Laemmli buffer.
5. Transfer the samples to PVDF membranes using standard Western blotting protocols.
6. To visualize biotinylated proteins, incubate the Western blots with streptavidin-HRP followed by the ECL reagent.

In addition, a cell-permeable, biotinylated GSH analog—biotinylated GSH ethyl ester (BioGEE; Invitrogen, Carlsbad, CA)—can be used to detect glutathiolated proteins under conditions of oxidative stress. Cells preincubated with BioGEE can be treated as desired and then either lysed for Western blot analysis or fixed and permeabilized for the detection of protein glutathiolation with streptavidin conjugates by either flow cytometry or fluorescence microscopy. As with biotinylated GSSG, BioGEE can be used to extract and analyze glutathiolated proteins by immunoprecipitation and mass spectrometry. The primary advantages of using BioGEE over biotinylated GSSG include its increased cell permeability and its use for detecting *S*-glutathiolation due not only to increased GSSG but also to increased *S*-oxidation and -nitrosation (see Scheme 9.1).

5. Conclusions

The choice of a specific method for detecting glutathiolated proteins depends upon the overall objective of the experiments. If changes in the total extent of protein glutathiolation are of interest, it is advisable to measure the free GSH liberated from the oxidation of protein-bound GSH by performic acid. The method is quantitative and reproducible and

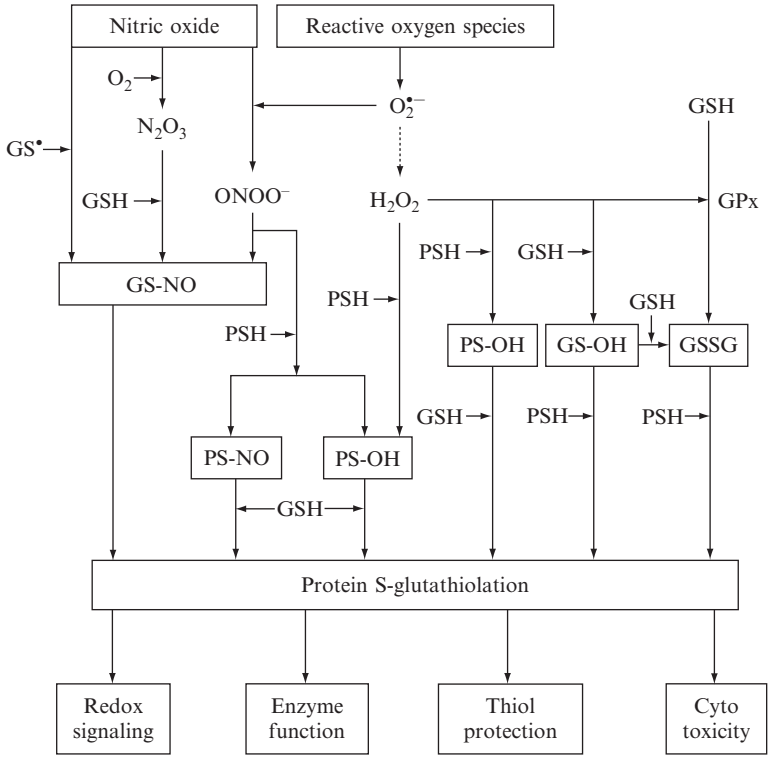

Scheme 9.1 Mechanisms of protein *S*-glutathiolation by nitric oxide and reactive oxygen species. In most cells, GSSG and nitrosoglutathione (GSNO) are likely to be the most significant glutathiolating agents. The cellular abundance of GSSG is regulated by processes that generate GSSG, such as the reduction of peroxides by glutathione peroxidases (GP). GSNO formed after direct reaction of NO with thiol radicals or after the reaction of glutathione with advanced nitrogen oxide species (e.g., N_2O_3) enters into transnitrosation reactions that also result in *S*-glutathiolated proteins. Peroxynitrite ($ONOO^-$), formed from the reaction of NO with superoxide, is able to mediate the formation of both S-nitrosated (PS-NO) and sulfenic acid-modified (PS-OH) proteins and glutathione; these "activated" thiols react readily to form protein–glutathione adducts. Hydrogen peroxide also promotes PS-OH/GS-OH formation that leads to protein glutathiolation. Protein glutathiolation can facilitate redox cell signaling, regulate enzyme function, protect protein thiols from advanced protein oxidation, and, in some cases, promote cell death.

provides an accurate estimate of global changes in protein glutathiolation. This information is difficult to extract from immunoblotting techniques. If, however, the objective is to identify specific proteins that are modified by glutathiolation, the use of the anti-protein–GSH antibody is recommended. It has been noted that the reactivity of the antibody depends upon the nature surrounding the epitope and that some glutathiolated proteins are

not recognized or only weakly recognized by the antibody (Brennan *et al.*, 2006). Nevertheless, the antibody technique allows the detection of glutathiolated proteins in cells and tissues under conditions of oxidative or nitrosative stress, without the addition of exogenous reagents at arbitrary concentrations. The biotinylation method also allows for the detection of *S*-glutathiolated proteins by Western blotting. This method is advantageous because it could be readily adapted to purify and identify the modified proteins using avidin-based procedures. However, it requires the exogenous addition of GSSG and thus is not suitable for measuring glutathiolated proteins generated in tissues during intrinsic oxidative stress or due to increases in NO production. Hence, the biotinylation technique cannot be used to screen for the presence of glutathiolated proteins in diseased tissue samples. Regardless of the specific procedure for sample preparation, the identification of glutathiolated proteins is greatly facilitated by the use of mass spectrometry. Glutathiolated proteins can be immunoprecipitated from cell lysates and then separated by SDS-PAGE or directly resolved on 2D gels and identified by either LC/MS or MALDI-TOF/MS. Further, MS/MS analysis can be employed to identify which specific sulfhydryl residues are modified by GSH. It is expected that the use of these sensitive methods will lead to a better recognition of the role of protein glutathiolation in cell signaling and function.

ACKNOWLEDGMENT

This work was partially supported by NIH grants GM71036, DK36118, HL-55477, HL-59378, HL-78825, and RR-024489.

REFERENCES

Adachi, T., Weisbrod, R. M., Pimentel, D. R., Ying, J., Sharov, V. S., Schoneich, C., and Cohen, R. A. (2004). S-Glutathiolation by peroxynitrite activates SERCA during arterial relaxation by nitric oxide. *Nat. Med.* **10,** 1200–1207.

Baba, S. P., Wetzelberger, K., Hoetker, J. D., and Bhatnagar, A. (2009). Posttranslational glutathiolation of aldose reductase (AKR1B1): A possible mechanism of protein recovery from S-nitrosylation. *Chem. Biol. Interact.* **178,** 250–258.

Bindoli, A., Fukuto, J. M., and Forman, H. J. (2008). Thiol chemistry in peroxidase catalysis and redox signaling. *Antioxid. Redox Signal.* **10,** 1549–1564.

Biswas, S., Chida, A. S., and Rahman, I. (2006). Redox modifications of protein-thiols: emerging roles in cell signaling. *Biochem. Pharmacol.* **71,** 551–564.

Bradford, M. M. (1976). A rapid and sensitive method for the quantitation of microgram quantities of protein utilizing the principle of protein-dye binding. *Anal. Biochem.* **72,** 248–254.

Brennan, J. P., Miller, J. I., Fuller, W., Wait, R., Begum, S., Dunn, M. J., and Eaton, P. (2006). The utility of N,N-biotinyl glutathione disulfide in the study of protein S-glutathiolation. *Mol. Cell. Proteomics* **5,** 215–225.

Celli, N., Motos-Gallardo, A., Tamburro, A., Favaloro, B., and Rotilio, D. (2003). Liquid chromatography-electrospray mass spectrometry study of cysteine-10 S-glutathiolation in recombinant glutathione S-transferase of Ochrobactrum anthropi. *J. Chromatogr. B Analyt. Technol. Biomed. Life Sci.* **787,** 405–413.

Chandra, A., Srivastava, S., Petrash, J. M., Bhatnagar, A., and Srivastava, S. K. (1997). Modification of aldose reductase by S-nitrosoglutathione. *Biochemistry* **36,** 15801–15809.

Clavreul, N., Adachi, T., Pimental, D. R., Ido, Y., Schoneich, C., and Cohen, R. A. (2006). S-glutathiolation by peroxynitrite of p21ras at cysteine-118 mediates its direct activation and downstream signaling in endothelial cells. *FASEB J.* **20,** 518–520.

Harding, J. J. (1970). Free and protein-bound glutathione in normal and cataractous human lenses. *Biochem. J.* **117,** 957–960.

Hill, B. G., and Bhatnagar, A. (2007). Role of glutathiolation in preservation, restoration and regulation of protein function. *IUBMB Life* **59,** 21–26.

Jensen, O. N., Wilm, M., Shevchenko, A., and Mann, M. (1999). Sample preparation methods for mass spectrometric peptide mapping directly from 2-DE gels. *Methods Mol. Biol.* **112,** 513–530.

Klatt, P., and Lamas, S. (2000). Regulation of protein function by S-glutathiolation in response to oxidative and nitrosative stress. *Eur. J. Biochem.* **267,** 4928–4944.

Knickelbein, R. G., Ingbar, D. H., Seres, T., Snow, K., Johnston, R. B., Jr., Fayemi, O., Gumkowski, F., Jamieson, J. D., and Warshaw, J. B. (1996). Hyperoxia enhances expression of gamma-glutamyl transpeptidase and increases protein S-glutathiolation in rat lung. *Am. J. Physiol.* **270,** L115–L122.

Kumari, K., Khanna, P., Ansari, N. H., and Srivastava, S. K. (1994). High-performance liquid chromatography method for the determination of protein–glutathione mixed disulfide. *Anal. Biochem.* **220,** 374–376.

Li, J., Huang, F. L., and Huang, K. P. (2001). Glutathiolation of proteins by glutathione disulfide S-oxide derived from S-nitrosoglutathione. Modifications of rat brain neurogranin/RC3 and neuromodulin/GAP-43. *J. Biol. Chem.* **276,** 3098–3105.

Lou, M. F., McKellar, R., and Chyan, O. (1986). Quantitation of lens protein mixed disulfides by ion-exchange chromatography. *Exp. Eye Res.* **42,** 607–616.

Muscat, J. E., Kleinman, W., Colosimo, S., Muir, A., Lazarus, P., Park, J., and Richie, J. P., Jr. (2004). Enhanced protein glutathiolation and oxidative stress in cigarette smokers. *Free Radic. Biol. Med.* **36,** 464–470.

Ramana, K. V., Chandra, D., Srivastava, S., Bhatnagar, A., and Srivastava, S. K. (2003). Nitric oxide regulates the polyol pathway of glucose metabolism in vascular smooth muscle cells. *FASEB J.* **17,** 417–425.

Reinartz, M., Ding, Z., Flogel, U., Godecke, A., and Schrader, J. (2008). Nitrosative stress leads to protein glutathiolation, increased s-nitrosation, and up-regulation of peroxiredoxins in the heart. *J. Biol. Chem.* **283,** 17440–17449.

Shackelford, R. E., Heinloth, A. N., Heard, S. C., and Paules, R. S. (2005). Cellular and molecular targets of protein S-glutathiolation. *Antioxid. Redox Signal.* **7,** 940–950.

Ward, N. E., Stewart, J. R., Ioannides, C. G., and O'Brian, C. A. (2000). Oxidant-induced S-glutathiolation inactivates protein kinase C-alpha (PKC-alpha): a potential mechanism of PKC isozyme regulation. *Biochemistry* **39,** 10319–10329.

West, M. B., Hill, B. G., Xuan, Y. T., and Bhatnagar, A. (2006). Protein glutathiolation by nitric oxide: an intracellular mechanism regulating redox protein modification. *FASEB J.* **20,** 1715–1717.

West, M. B., Ramana, K. V., Kaiserova, K., Srivastava, S. K., and Bhatnagar, A. (2008). L-arginine prevents metabolic effects of high glucose in diabetic mice. *FEBS Lett.* **582,** 2609–2614.

CHAPTER TEN

Proteome Screens for Cys Residues Oxidation: The Redoxome

Giovanni Chiappetta,* Sega Ndiaye,† Aeid Igbaria,* Chitranshu Kumar,* Joelle Vinh,† *and* Michel B. Toledano*

Contents

Abstract

The oxidation of the cysteine (Cys) residue to sulfenic (–S–OH), disulfide (–S–S–), or *S*-nitroso (S–NO) forms are thought to be a posttranslational modifications that regulate protein function. However, despite a few solid examples of its occurrence, thiol-redox regulation of protein function is still debated and often seen as an exotic phenomenon. A systematic and exhaustive characterization of all oxidized Cys residues, an experimental approach called redox proteomics or redoxome analysis, should help establish the physiological scope of Cys residue oxidation and give clues to its mechanisms. Redox proteomics still remains a technical challenge, mainly because of the labile nature of thiol-redox reactions and the lack of tools to directly detect the modified residues. Here we consider recent technical advances in redox proteomics, focusing on a gel-based fluorescent method and on the shotgun OxICAT technique.

* Laboratoire Stress Oxydants et Cancer, DSV, IBITECS, CEA-Saclay, Gif-sur-Yvette, France
† Biological Mass Spectrometry and Proteomics, USR CNRS/ESPCI ParisTech, Ecole Supérieure de Physique et de Chimie Industrielles, Paris Cedex, France

Methods in Enzymology, Volume 473
ISSN 0076-6879, DOI: 10.1016/S0076-6879(10)73010-X

1. Introduction

Until recently, cysteine (Cys) residue oxidation was thought to be confined to the endoplasmic-reticulum (ER), in which catalyzed disulfide bond formation contributes to the folding of proteins in their way to secretion (Ito and Inaba, 2008; Sevier and Kaiser, 2008), and to a few cytoplasmic enzymes that carry an oxidation–reduction step in their catalytic cycle, such as ribonucleotide reductase or the thiol- and selenothiol-based peroxiredoxins and glutathione peroxidases (Fourquet *et al.*, 2008; Toledano *et al.*, 2007). The paradigm concept of the ER as an oxidizing environment and the cytoplasm, and remaining compartments, as reducing ones has shifted as a result of an increasing number of observations indicating the occurrence of Cys residue oxidation as a posttranslational modification regulating the function of cytoplasmic and nuclear proteins (D'Autreaux and Toledano, 2007; Janssen-Heininger *et al.*, 2008; Linke and Jakob, 2003; Rhee *et al.*, 2005; Toledano *et al.*, 2004). Cys residue oxidation to the sulfenic (–S–OH), disulfide (–S–S–), or *S*-nitro (*S*-nitrosylation, S–NO) forms have been identified in several proteins, and are proposed to drive cell signaling by H_2O_2 and nitric oxide (NO) (Hess *et al.*, 2005). Further, import into the mitochondrial intermembrane space (IMS) of a protein subclass was recently shown to involve catalyzed disulfide formation that mediates folding of the polypeptide, thereby preventing its back-translocation to the cytoplasm (Mesecke *et al.*, 2005). Cys residue oxidation in the ER and IMS is mechanistically well understood, as being a catalyzed event for which the enzyme is identified. In contrast, the occurrence of Cys residue oxidation in the cytoplasm is not well understood, except for a few cases for which an oxidation mechanism has been described (D'Autreaux and Toledano, 2007). A systematic and exhaustive characterization of all oxidized Cys residues, an experimental approach called redox proteomics or redoxome analysis, should help establish the inventory of all thiol-redox-based phenomena and their physiological scope. In addition, inventory of the targets of the thiol reductases thioredoxins and glutaredoxins might be established through redoxome analyses of cells in which either of these activities has been shut down. Here we consider the main experimental methods that have been devised to characterize Cys residue oxidation at the proteome-wide level. We then focus on a two-dimensional electrophoresis gel (2DE)-based fluorescent method and on the novel shotgun proteomics OxICAT method developed by Jakob and colleagues (Leichert *et al.*, 2008), two approaches having complementary attributes (Fu *et al.*, 2008). These methods have already provided important advances in understanding thiol-redox metabolism. Nevertheless, redox proteomics still remains a technological challenge and needs further improvements.

2. General Considerations

2.1. Limits in the access to Cys-residues redox modifications

Proteomic analysis is a powerful tool to depict the posttranslational modifications of the proteome, but is still limited with regard to the characterization of the redox state of cysteine (Cys) residues. One major limit is the chemical labile nature of Cys residues redox modifications. Upon cell disruption, air-mediated Cys oxidation can occur and reciprocally disulfides can be reduced by cellular reductases, or they can reshuffle, thereby causing loss of information. Acidic quenching of thiol groups, which consists of breaking cells in the presence of trichloroacetic acid (TCA), circumvents this problem, also precipitating soluble proteins (Delaunay *et al.*, 2000; Le Moan *et al.*, 2009). Acidic quenching relies on the property of the thiol group to engage in redox reactions only when in the thiolate (deprotonated) form ($-S^-$), which occurs when the pH of the solution > p*K*a value of the Cys residue. Free cysteine has a p*K*a of 8.3, and Cys residues have p*K*a values from 4 to 10 depending on their amino acid environment. Thus, at pH < 1, all Cys residues are protonated and cannot undergo redox modifications. Alternatively, cell-permeable Cys-specific reagents, such as the alkylating agents iodoacetamide (IAM) or *N*-ethylmaleimide (NEM), can also trap Cys residues in their *in vivo* redox state and therefore can substitute for the TCA-based acidic quenching in specific protocols.

Lack of antibodies capable of recognizing oxidized Cys residues prevents the "*divide et impera*" strategy of immunoenrichment protocols or selective detection of proteins separated by 2D gels (Eaton, 2006).

Mass spectrometry (MS) detection of oxidized Cys residues has also limitations. Reducing agents, such as dithiothreitol (DTT) or tris(2-carboxyethyl) phosphine (TCEP), which are routinely used for improving protein solubility during cell extraction or for increasing the efficiency of polypeptide-enzymatic hydrolysis for MS-sample preparation, must be avoided or used with caution. Further, disulfide-linked peptides are more resistant to fragmentation under low-energy collision-induced-dissociation (CID) (Gorman *et al.*, 2002), and may undergo in-source reduction during UV MALDI experiments (337 nm) (Patterson and Katta, 1994).

2.2. Acid quenching and Cys differential labeling

TCA-based acidic quenching is common to and the first step of all methods described here. Upon solubilizing TCA-precipitated cell extracts by pH increase >6.8, reduced versus oxidized cysteine residues are differentially labeled—sequentially, before and after reduction with DTT—with Cys-specific reagents. Most of these reagents are derived from IAM or

NEM. Of note, one can increase the stringency of screens by targeting the Cys residue with low p*K*a, which make up a majority of redox-regulated residues. This can be achieved using low pH conditions during the oxidized-residues alkylation step (Boivin *et al.*, 2008). The Cys-redox forms accessible to analysis are essentially disulfide bonds, whether intra- or intermolecular, including *S*-glutathionylation. The sulfinic and sulfonic acid forms are not reducible, but can conceivably be accessed when comparing two conditions, with one carrying a large proportion of the Cys residue in these higher irreversibly oxidized forms. Cysteine residues in the sulfenic acid form are difficult to identify because of their unstable chemical nature, although this has been achieved by exclusive reduction of the sulfenic acid by sodium arsenite (Saurin *et al.*, 2004), or by its reaction with specific chemicals such as dimedone (Poole *et al.*, 2005).

3. Overview of the Different Methods

3.1. 2DE-based methods

Most 2DE separation-based methods use NEM or IAM coupled to a functional group that has analytical usefulness and/or can be visualized on the gel.

3.1.1. Radioactive ^{14}C-based labeling

Radioactive ^{14}C-IAM and ^{14}C-NEM have been used to selectively detect and quantify oxidized proteins on 2D gels (Leichert and Jakob, 2004; Le Moan *et al.*, 2006). Upon blocking reduced Cys residue with cold IAM or NEM, oxidized residues are reduced and labeled with the ^{14}C-labeled corresponding reagent. Proteins containing oxidized protein-thiols are then visualized by autoradiography or by storage phosphor technology after 2DE separation. Radioactive signals can be normalized to the amount of protein estimated by Coomassie staining (Leichert and Jakob, 2004), or to the signals of total Cys residues obtained by labeling all Cys residues after extract reduction (Le Moan *et al.*, 2006). This procedure has the advantage of not generating differences in protein 2DE migration since the same reagent is used for both reduced and oxidized Cys residues. Moreover, these reagents are commonly used for proteomic analysis, and are compatible with all analytical steps. The main limitation of this procedure is the signal-to-noise ratio, which is often very high and the need of manipulating radioactive compounds.

3.1.2. Single fluorescence-based labeling

The IAM-derivatives 5-iodoacetamidofluorescein (Baty *et al.*, 2002) and BODIPY FL C1-IA (Hochgrafe *et al.*, 2005), and monobromobimane (Yano, 2003), a Cys-specific reagent that fluoresces upon UV irradiation, have been used to

reveal the extent of Cys residue oxidation by 2D gels. Reduced Cys residues were blocked by alkylation with NEM or IAM, and oxidized residues were labeled with the fluorescent Cys-reagent. Labeled proteins were visualized on 2D gels using an infrared fluorescence imaging system. Estimates of spots intensity, normalized to the protein amount in one protocol (Hochgrafe *et al.*, 2005), were taken as indexes of protein-thiol oxidation.

3.1.3. The DIGE approach

An improvement of 2DE-based fluorescence analysis of the redoxome has been obtained by applying the differential in gel electrophoresis (DIGE) technique. This strategy uses a set of fluorophores of similar molecular weights and chemical structures that differ by their spectral features. Redox-DIGE has been performed using the NEM or IAM derivatives of Cyanine (Cy3, Cy5) (Bruschi *et al.*, 2009; Fu *et al.*, 2008; Hurd *et al.*, 2007) and DY-dyes (Riederer and Riederer, 2007). Upon blocking reduced thiols by alkylation, the oxidized thiols of two different cell extracts are labeled with two different fluorophores. Labeled cell extracts are then mixed and analyzed on the same 2DE. Differences in Cys residues oxidation between samples are quantified by the intensity of each fluorophore at each spot. Acquisition of fluorescence intensities is performed by the dual-channel imaging technique with a laser scan capable of recording different wavelengths (Bernhardt *et al.*, 1999). Such multiplexed analysis overcomes the lack of reproducibility of the 2DE separation procedure when comparing two conditions and limits the number of gels that have to be done. However, the major limitation of this procedure is that fluorescence intensity cannot be normalized to the protein amount when using two dyes. Coomassie staining cannot be adapted here for protein quantification because of the very low amounts of cell extracts used in the procedure, and staining by the Sypro or Flamingo dyes (Bio-Rad) can modify 2DE profiles (Dietz *et al.*, 2009). Due to this limitation, redox-DIGE has so far compared only cell extracts or subfractions (mitochondria) of it treated or not by H_2O_2. Hence, redox-DIGE cannot be used to compare different cell extracts, because changes in protein expression profiles will invalidate quantitative estimates.

3.1.4. Two-fluorescent dyes differential labeling

To circumvent the limitation of redox-DIGE in cell extracts comparisons, Le Moan *et al.* (2009) proposed a new gel-based approach. This procedure consists in differentially labeling both reduced and oxidized thiols (Fig. 10.1A) using two 2DE-compatible fluorescent dyes absorbing and emitting at different wavelengths of the infrared region (Dy680 and Dy780, Dynomics). After 2DE separation, the ratio of the intensity of each fluorophore at each spot reflects the Cys residue(s) redox state of the corresponding protein. As the value obtained is a ratio, it is independent of the protein amount, allowing comparison of cell extracts independently separated by 2DE. Although the multiplexed feature of

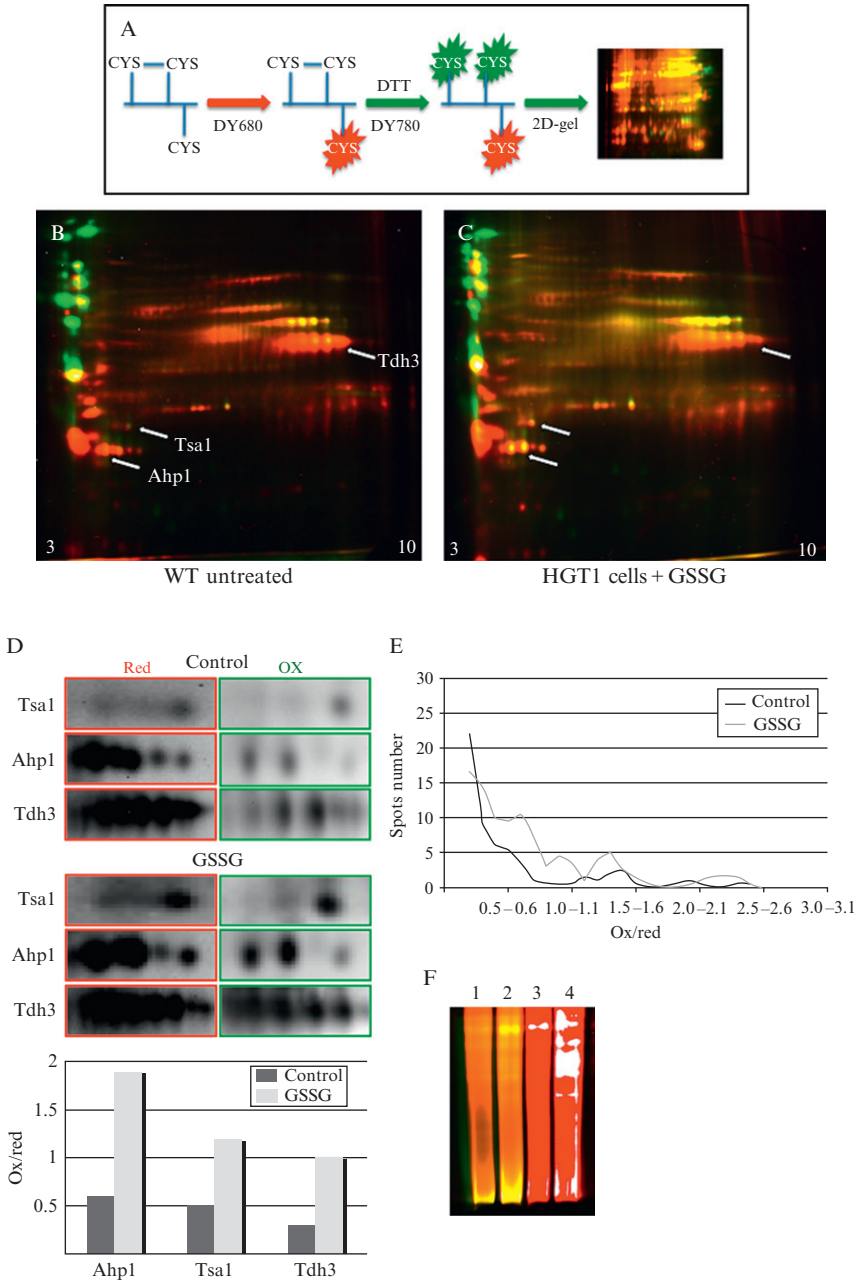

Figure 10.1 Use of the 2DE-based two-fluorescent dyes approach in *S. cerevisiae*. (A) Schematics of the procedure. Extracts of wild-type (WT) and of (B) HGT1 cells exposed to 50 μM GSSG during 30 min (C) were submitted to the two-fluorescent dyes

redox-DIGE is lost here, this approach provides a powerful means of comparing snapshots of the redoxome of cells grown under different conditions or having gene mutations. The two-fluorescent dyes differential labeling approach will be thoroughly detailed below.

3.1.5. The biotin-HPDP-based procedure decreases cell extracts complexities

As mentioned above, one limit of redox proteomics is the lack of proper tools for decreasing samples complexities. The thiol-reagent *N*-(6-(biotininamido) hexyl)-3′-(2′-pyridylthio)propionamide (biotin-HPDP) contains a biotin moiety and attaches to free thiols by means of a disulfide linkage. It can therefore be used to specifically enrich for the oxidized protein-thiol fraction of the proteome (Jaffrey and Snyder, 2001; Le Moan *et al.*, 2006). Upon blocking free thiols by NEM- or IAM-alkylation, oxidized Cys residues are reacted with biotin-HPDP. Labeled proteins are then adsorbed to a streptavidin column by virtue of their biotin moiety, eluted by reduction with DTT—which leave the biotin-HPDP label attached to the column—and separated by 2DE. 2DE of extracts from different cell cultures can be compared giving a rough estimate of differences in Cys residue oxidation, and spots can also be excised from gels for MS identification. Using this approach, about 60 oxidized protein-thiols were identified in yeast (Le Moan *et al.*, 2006). This labeling procedure can also serve as a labeling step for shotgun proteomic analysis (Wan *et al.*, 2007), and polypeptides could even be digested before affinity-purification, thus enriching for Cys-containing peptides.

3.2. Shotgun proteomic: The MS-based ICAT technology

The 2DE-based methods described above have many limits with regard to reproducibility, time-consumption of 2DE procedures, and the need of skilful operators. They also carry major drawbacks: the extent of oxidation

differential labeling protocol and separated by 2DE. Arrows indicate the spots of the peroxiredoxins Tsa1, Ahp1 and of glyceraldehyde-3-phosphate dehydrogenase (Tdh3). (D) The regions of the 2DE of panels B and C containing Tsa1, Ahp1, and Tdh3 were overblown, and the images corresponding to the DY780 (reduced Cys residues) and DY680 (Oxidized Cys residues) fluorescences are shown separately. Spot quantification of the oxidized to reduced Cys residues (Ox/Red) is represented below, as indicated. (E) Graphic representation of the Ox/Red ratios of the 150 larger spots of the 2DE of B and C, as indicated. (F) Reduced Cys residues saturation control analyzed by one-dimensional SDS–PAGE. Lanes 1 and 2 correspond to the experimental differentially labeled samples used in the 2DE of B and C, respectively. Here, both fluorescence colors can be seen as in the 2DE. Lanes 3 and 4 represent the saturation control of the same samples, respectively. Here, the reduced Cys residues labeled samples were submitted to the second dye without prior reduction of oxidized Cys residues. Reduced Cys residue saturation is optimal, as no green fluorescence is seen.

can only be roughly estimated and always corresponds to an average contribution of the Cys residues present in a polypeptide. Further, when applicable, protein identification must be performed by one spot at a time and the oxidized Cys residue cannot be identified. Another important limitation is that only the most abundant proteins are usually visualized on 2DE, denying all attempts of exhaustiveness.

Isotope coded affinity tag (ICAT) is a shotgun proteomic strategy based on the use of isotopic Cys-specific reagents that has been initially introduced for protein expression profiles measurements (Gygi *et al.*, 1999). ICAT has been adapted to redox proteomics coined OxICAT (Leichert *et al.*, 2008). OxICAT addresses all drawbacks of conventional 2DE-based procedures, potentially allowing exhaustive identification of all oxidized Cys residues in one single analysis, the precise identification of the oxidized Cys residues within polypeptides, and the rigorous estimate of the extent of oxidation at the level of each Cys residue. It therefore not only constitutes a screening procedure for identifying oxidized protein-thiols, but can also be used for comparative analysis between different cell cultures. The ICAT reagent consists of the IAM-moiety, a cleavable biotin tag, and a nine-carbon linker, which exists in an isotopically light ^{12}C- and heavy ^{13}C-form (Gygi *et al.*, 1999). After acidic quenching, oxidized versus reduced Cys residues are differentially labeled with the heavy and light ICAT reagents. Extracts are then submitted to enzymatic digestion and the ICAT-labeled peptides purified by streptavidin–biotin affinity chromatography. Purified peptides, and hence their oxidized Cys residues, are identified by LC–MS/MS, which also establishes the ratio of oxidized to reduced (heavy to light) Cys residues according to MS signal relative intensities. As the extent of oxidation is given as an Ox/Red ratio, absolute proteins amounts are not considered, therefore allowing cell extracts comparisons. Some limitations of OxICAT should be however underlined. When quantification relies on simple MS measurements, no discrimination is possible between different Cys residues within a given peptide. Furthermore, the yield of purification of some Cys-containing peptides can be low and therefore not detected by MS. The OxICAT method will be thoroughly detailed below.

4. Results and Discussion

4.1. Methods

4.1.1. Chemicals

TCA (Fluka), Urea (PlusOne, GE) CHAPS (PlusOne, GE), nondetergent sulfobetain 256 (NDSB) (Calbiochem), tris(hydroxymethyl)-aminomethane (Tris) (Fluka), IAM, Amberlite IRN-150L (PlusOne, GE), glass beads (Sigma-Aldrich), DY-680 and DY-780 dyes (Dynomics), 1,4-dithio-DL-

threitol (DTT) (Invitrogen), IPG buffer 3–10 (GE), microBCA kit (Pierce-Thermo), 18 cm immobiline dry gel-strip pH 3–10 nonlinear, (GE) glycerol (PlusOne, GE), sodium dodecyl sulfate (SDS) (Sigma-Aldrich), TCEP (Sigma-Aldrich), L-1-tosylamido-2-phenylethyl chloromethyl ketone (TPCK) treated trypsin (Sigma-Aldrich), α-cyano-4-hydroxycinnamic acid (CHCA) (Sigma-Aldrich), and ICAT kit (Applied Biosystems, ABI). Chemicals for casting SDS–PAGE gels are purchased from Bio-Rad. Highest purity solvents are purchased from Sigma-Aldrich.

4.1.2. Cell lysis procedures

For the OxICAT procedure, we used the human uterine cervix carcinoma cell line HeLa. Five hundred microliters of a TCA water solution (20%, w/v) was added to the pellet of centrifuged cells (5.0×10^6 cells). The sample was incubated on ice for 15 min, and then centrifuged (13 000×*g*, 4 °C for 15 min). For the fluorescence labeling procedure, 400 μl of the TCA solution (20%, w/v) was added to the pellet of *Saccharomyces cerevisiae* cells grown to the exponential-phase (1.0×10^7 cells), together with 200 μl of glass beads. The sample was iteratively agitated on a vortex for 1 min and left on ice for 1 min, and then centrifuged (13,000×*g*, 4 °C for 15 min). For both human and yeast cell samples, the TCA-precipitated pellet was washed three times with prechilled acetone.

4.1.3. Two-fluorescent dyes differential labeling

The labeling solution [urea (8 *M*), CHAPS (4% w/v), NDSB (1% w/v), Tris–HCl (25 m*M* pH 7.5), IAM (200 m*M*), DY-680 or DY-780 (0.1 m*M*)] was prepared extemporaneously. Urea (5.0 g) was dissolved in MilliQ water (6.0 ml) (final volume 10 ml) by agitation, at room temperature. The urea solution was treated with Amberlite (0.1 g) for 10 min under agitation at room temperature, and then filtered on a 0.45-μm filter. CHAPS (400 mg) and NDSB (100 mg) were then added to the urea solution. IAM and DTT stock solutions (1 *M* each) were prepared by adding 184.9 mg/ml IAM or 154.2 mg/ml DTT to 1 ml of the urea/CHAPS/NDSB solution. The labeling solution was made by adding 465 μl of the urea/CHAPS/NDSB solution, 120 μl of the 1 *M* IAM stock solution, 10 μl of Tris–HCl (1.5 *M*, pH 7.5), 5 μl of DY-680 (10 μg/μl in dimethylformamide).

4.1.3.1. Labeling reduced thiols TCA-precipitated cell extracts were solubilized in labeling solution (600 μl), and the pH of the sample checked and adjusted by adding a few microliters Tris–HCl solution (1.5 *M*, pH 7.5) (residual TCA often remains). The dye was then added and the labeling reaction carried out at 30 °C for 1 h on a stirring device (900 rpm) in the dark. Ten microliters of the labeled sample was taken for reduced-thiol alkylation saturation control. The reduced-thiols labeled sample was then

centrifuged (13,000×*g*, 4 °C for 5 min) and the supernatant recovered. The excess dye was removed by precipitation with 600 μl of the TCA solution (20%).

4.1.3.2. Labeling oxidized thiols Disulfide bonds were reduced by solubilizing the TCA-precipitated pellet in 600 μl of reducing solution [578 μl of the urea/CHAPS/NDSB solution, 12 μl of the 1 *M* DTT stock solution (20 m*M* final), 10 μl of Tris–HCl (1.5 *M* pH 7.5)]. The reaction was carried out at 37 °C for 30 min on a stirring device (900 rpm). The excess DTT was removed by TCA precipitation. To label oxidized thiols, the TCA-precipitated sample was solubilized in 600 μl of the labeling solution that contained dye DY-780 instead of DY-680. The sample pH was also checked here. The reaction was carried for 15 min at 4 °C under stirring, and the excess dye removed by TCA precipitation.

4.1.3.3. Control of reduced-thiol alkylation saturation To the 10 μl aliquot of the reduced sample kept for this purpose, 110 μl of labeling buffer and 1 μl of DY-780 were added. The reaction was carried out at 4 °C for 15 min. The sample was then TCA-precipitated. The TCA pellet solubilized in Laemli buffer was separated by SDS–PAGE.

4.1.3.4. Cell extracts quantities The number of cells used for each condition analyzed should be set up to obtain at least 100 μg of yeast cell extract at the end of the labeling procedure, to allow triplicate 2DE analyses.

4.1.4. 2DE analysis

The TCA pellet of labeled extracts was solubilized in 100 μl of freshly prepared loading buffer [urea (8 *M*), CHAPS (2%, w/v), NDSB (1%, w/v), IPG Buffer 3–10 (0.5%, v/v)]. Protein concentration was measured by bicinchoninic acid-based colorimetric detection (micro BCA Kit, Pierce). Twenty micrograms of extracts were used for analytical gels, and 600 μg of unlabeled extract for preparative gels. Samples were diluted in 350 μl loading buffer and loaded on an 18 cm Immobiline DryStrip, pH 3–10, nonlinear. Gel-strips were rehydrated with the Ettan IPGphor device for 12 h at 30 V, and submitted to isoelectric focusing (1 h 150 V constant, 2 h 500 V constant, 2 h 1000 V constant, 5 h 8000 V constant reaching ~43 kVh at the end of the run). The strips were first equilibrated for 15 min in 15 ml of the equilibration solution [urea (6 *M*), Tris–HCl (75 m*M* pH 8.8), glycerol (29.3%), SDS (2%, w/v), traces bromophenol blue] that contained DTT (10 mg/ml), then for 15 min in 15 ml of the equilibration solution containing IAM (25 mg/ml) in the dark. The second dimension was performed using the Ettan DALT six device, by overnight migration at 1.5 W/gel. Images of the analytical gels were recorded with the Odyssey scanner (LI-COR biosciences) at a resolution of 169 μm and

medium quality laser intensities. Image analyses used the Delta2D Decodon software. Preparative gels were stained with Coomassie brilliant blue or with Sypro following manufacturers' protocols. Gel spots were manually excised and submitted to *in situ* trypsin digestion followed by MALDI-MS/MS analysis.

4.1.5. The OxICAT procedure

OxICAT experiments were performed according to the procedure of Leichert *et al.* (2008). Briefly, 10^6 HeLa cells were used per sample. TCA-precipitated extracts' pellets were suspended in 80 μl of denaturing buffer [urea (6 *M*), SDS (0.5%, w/v), EDTA (10 m*M*), Tris–HCl (200 m*M*, pH 8.5)] to which was added one standard vial of light ICAT reagent dissolved in 20 μl of ACN. Free thiols were ICAT-labeled in the dark for 1 h at 37 °C on a stirring device (900 rpm). The reaction was stopped by TCA precipitation also removing excess reagents. The TCA-precipitated pellet was dissolved in 80 μl of denaturing buffer and 2 μl TCEP (50 m*M* stock solution) to which was added one standard vial of heavy ICAT reagent dissolved in 20 μl of ACN. Oxidized thiols were ICAT-labeled in the dark for 1 h at 37 °C on a stirring device (900 rpm). The reaction was stopped as above. Proteins were digested overnight at 37 °C by adding directly to the TCA-precipitated pellet 80 μl of digestion buffer [SDS (0.1%, w/v), Tris–HCl (pH 8.5, 50 m*M*)], 20 μl of ACN, and 100 μl of TPCK-treated trypsin solution (0.1 μg/μl). Peptide purification by SCX and avidin cartridges and biotin cleavage were performed according to the manufacturer's instructions.

4.1.6. MS analyses

Peptide mixtures obtained from *in situ* protein digestion were analyzed by MALDI-MS/MS using a 4800 MALDI-TOF/TOF (Applied Biosystems, ABI) mass spectrometer. Desalting of the samples (C18 Zip-Tip, Millipore) was performed if necessary. Proteolytic peptides solution (0.5 μl) and 1 μl of 5 μg/μl CHCA solution [ACN/water (7:3, v/v), TFA (0.1%, v/v)] were spotted onto a stainless steel MALDI plate. The samples were first analyzed in MS mode (constant laser intensity at 2100 (arbitrary units), just above the desorption threshold, 1200 shots averaged). The 15 most intense peaks (threshold of signal/noise ratio: 100) were selected as precursors for further MS/MS analyses (laser intensity at 3500, 2400 shots averaged, acceleration voltage 2 kV, CID mode OFF, and metastable suppressor mode ON).

4.1.7. LC/MALDI-MS/MS analyses

Nano-LC–MALDI-MS/MS experiments were performed on a 4800 TOF/TOF mass spectrometer (Applied Biosystems) coupled to an Ultimate3000 system (Dionex). Proteolytic peptide samples were loaded and desalted on a reversed-phase cartridge (C18 PepMap 100 Dionex, 15×1 mm, 5 μm) at

20 μl/min with solvent A (ACN/water 2:98, v/v, formic acid 0.1%, v/v), for 5 min before to be eluted on a reversed-phase column (C18 PepMap 100 Dionex, 150 mm×75 μm), at 220 nl/min with a linear gradient of solvent B (ACN/water 90:10, v/v, formic acid 0.1%, v/v) from 0% to 50% in 35 min. The eluate was continuously mixed online with a solution of CHCA [5 mg/ml in ACN/water (7:3, v/v), TFA (0.1%, v/v), 436 nl/min] with postcolumn a T junction. Two hundred and fourty spots were collected (one fraction/10 s) on a stainless steel MALDI plate and analyzed in MS and MS/MS modes. A first MS analysis of the spots generated a list of precursors that were further fragmented in the second MS/MS analysis. The protocol for MS acquisition was the same as above except that seven precursors instead of 15 were selected *per* spot for MS/MS analysis.

4.1.8. Protein identification

GPS software (Applied Biosystems) extracted peak lists from MS and MS/MS data for database search (*S/N* threshold: 50 for MS data and 30 for MS/MS data). The peak lists were submitted to MASCOT search engine (taxonomy *human* or *S. cerevisiae* according to the sample, Swiss Prot database, mass tolerance accuracy 50 ppm for MS and 0.3 Da for MS/MS, instrument type MALDI-TOF/TOF).

4.2. Results

4.2.1. The 2DE-based two-fluorescent dyes differential labeling approach

To circumvent the limit of redox-DIGE (see above), Le Moan *et al.* (2009) introduced a new gel-based approach consisting in differentially labeling both reduced and oxidized Cys resides with two-fluorescent Cys-specific reagents (Dy680 and Dy780, Dynomics) (Fig. 10.1A). We used this technique in *S. cerevisiae* to evaluate the effect of extremely high intracellular levels of glutathione (GSH) disulfide (GSSG) on the redox state of cytoplasmic protein-thiols. Such high GSSG levels are expected to cause widespread Cys residue oxidation. HGT1 is a glutathione-specific transporter (Srikanth *et al.*, 2005), and cells that overexpress it accumulate up to 100 m*M* GSH or GSSG, when grown in the presence of either of these compounds, respectively (Kumar *et al.*, unpublished data). We prepared extracts from exponentially growing wild-type (WT) cells and *HGT1*-expressing cells exposed to GSSG (50 μM) for 15 min, which are known to contain GSSG at concentrations of about 0.1–0.3 and 40 m*M*, respectively.

Differentially labeled and 2DE-separated proteins were detected as spots colored between the red and green tones (Fig. 10.1B and C). GSSG exposure caused some increase in the green over the red component for some spots, indicating increased oxidation of the corresponding proteins. We quantified

the green/red fluorescence ratio for three select proteins, the peroxiredoxins Tsa1 and Ahp1 and glyceraldehyde-3-phosphate dehydrogenase (Tdh3), which are all known to oxidize *in vivo* at Cys residues (Fig. 10.1D). All three were significantly more oxidized after GSSG treatment. We also quantified the green/red fluorescence intensities of the 150 more visible spots, enabling graphic representation and easy comparison of the redoxome of the two yeast samples (Fig. 10.1E). The increased oxidation caused by GSSG was not as important as expected, which might indicate that the GSSG/GSH couple has only a moderate effect on cytoplasmic thiol-redox control, in keeping with published results (Le Moan *et al.*, 2006).

Efficiency of protein extraction and the amount of Cys residues are highly dependent on the nature of the sample, which requires optimizing the procedure for each cell extract. It is also highly recommended that the reduced Cys residue saturation after the first labeling step be taken into account in order to avoid cross-reactions with the second dye. We indeed found that saturation could not be reached with fluorescent reagents, which led us to use the dye as a tracer by performing the first labeling step in the presence of a high concentration of IAM. Accordingly, saturation conditions have to be set up for each extracts by testing different concentrations of IAM, as shown in Fig. 10.1F. Proteins isoelectric focalization also requires optimization. Usually, 15–25 μg of cell extracts are sufficient for one 2DE. Sample dilution in loading buffer should avoid undesired high conductivity, but its occurrence, which limits the voltage that can be applied to the gel-strip, can be corrected by sample purification with the GE 2D Clean-up kit and/or by decreasing the concentration of IPG buffer.

In summary, 2DE-based two-fluorescent dyes differential labeling provides snapshots of the redoxome for easy and relatively fast comparisons of cellular conditions.

4.2.2. The shotgun OxICAT procedure

As already mentioned, the OxICAT procedure (Leichert *et al.*, 2008) identifies oxidized Cys residues within polypeptides, and rigorously quantifies their redox state as a ratio, thus allowing comparison of cell conditions. Further, as a high-throughput method, it theoretically considers all cellular Cys residues, most of which are inaccessible by the 2DE-based methods described above. We submitted untreated HeLa cells to the OxICAT procedure, and focused on the Parkinson disease (PD) protein 7 (DJ-1) within the MS data obtained. DJ-1 is a redox-responsive protein with neuroprotective functions, for which mutations have been linked to hereditary forms of PD (Kahle *et al.*, 2009). DJ-1 is also a biomarker for cancer and neurodegenerative diseases, particularly when in its oxidized form. Of its three Cys residues, DJ-1 Cys106 was shown to be oxidized to sulfinic, by crystallographic studies (Canet-Aviles *et al.*, 2004) and sulfonic by mass spectrometry analysis (Kinumi *et al.*, 2004). All Cys-containing proteolytic

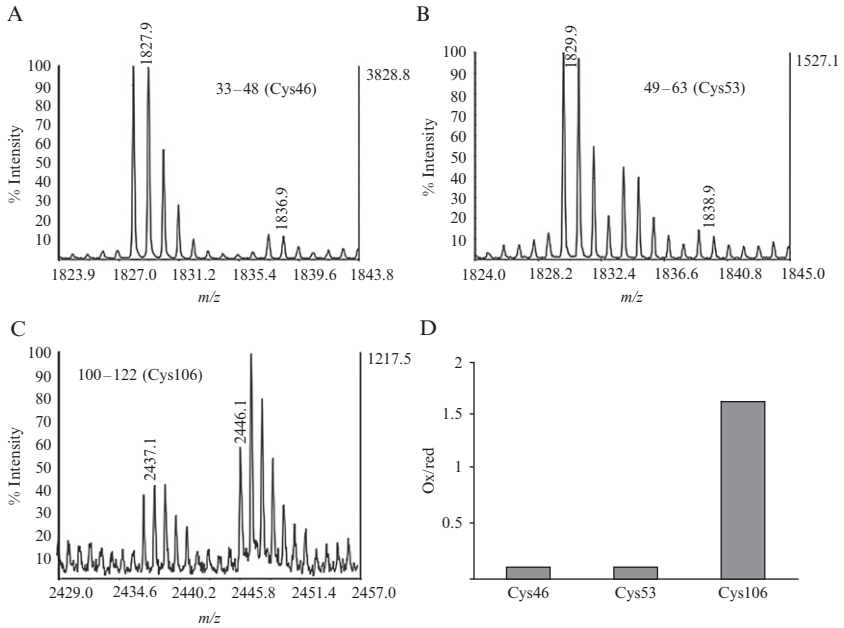

Figure 10.2 **The redox state of the DJ-1 three Cys residues (Cys46, Cys53, Cys106) as established by OxICAT. (A, B, and C) MALDI-MS spectra of the Cys residues-containing peptides, as indicated. (D) Quantification of the heavy to light (Ox/Red) ratio of the three Cys residues as indicated.**

peptides of DJ-1 were detected by MS analysis. Heavy-to-light ICAT ratio measurements showed that redox-sensitive Cys106 residue was indeed selectively and significantly oxidized (Fig. 10.2). The oxidized form of Cys106 identified here is either a disulfide, possibly formed with GSH or with another protein, but less likely a sulfenic acid, due to its instability. However, due to their nonreversibility, the Cys106 higher oxides identified by others, at least *in vivo*, are not accessible to the ICAT reagents.

The OxICAT strategy also requires optimizing reduced Cys residues ICAT reagent saturation as a crucial step, as suggested by Leichert *et al.* (2008). As a high-throughput method, OxICAT allows recording a huge amount of MS and MS/MS spectra, which have then to be processed. However, not all the information obtained is relevant, creating interferences with the LC–MS/MS detection of interesting peptides. Therefore, designing software tools helping establish peptides "inclusion lists" are important to consider according to one's own needs. LC–MALDI-MS/MS analysis is best suited for the OxICAT strategy, as LC-fractionated peptides are spotted onto the MALDI plate, subsequently allowing specific offline acquisitions using "inclusion lists," which can be performed iteratively without the need of preparing new samples and thus consuming the expensive ICAT reagents.

4.2.3. Complementarities of 2DE-based fluorescence and OxICAT methods

We confronted results obtained with HeLa cell extracts analyzed by the 2DE-based two-fluorescence labeling and OxICAT methods (Fig. 10.3). Vimentin, a protein of the intermediate filament family containing a single Cys residue (Cys328), and GRP78, a chaperone protein of the ER containing two Cys residues (Cys41 and Cys420), were both visible on the 2DE gel but were missing from the initial LC–MALDI-MS/MS analysis. We thus acquired additional MS/MS spectra from the same LC MALDI spots using an "inclusion list" specifying the theoretical masses of ICAT-labeled peptides corresponding to these proteins. We thereby identified MS spectra for the vimentin peptide 322-342 (Cys328) that indicated that this residue was fully reduced (Fig. 10.3A), in total concordance with the fluorescence data that also showed this residue fully reduced (Fig. 10.3C and D). We also identified MS spectra for GRP78 peptide 25–46 (Cys41) (Fig. 10.3B), but

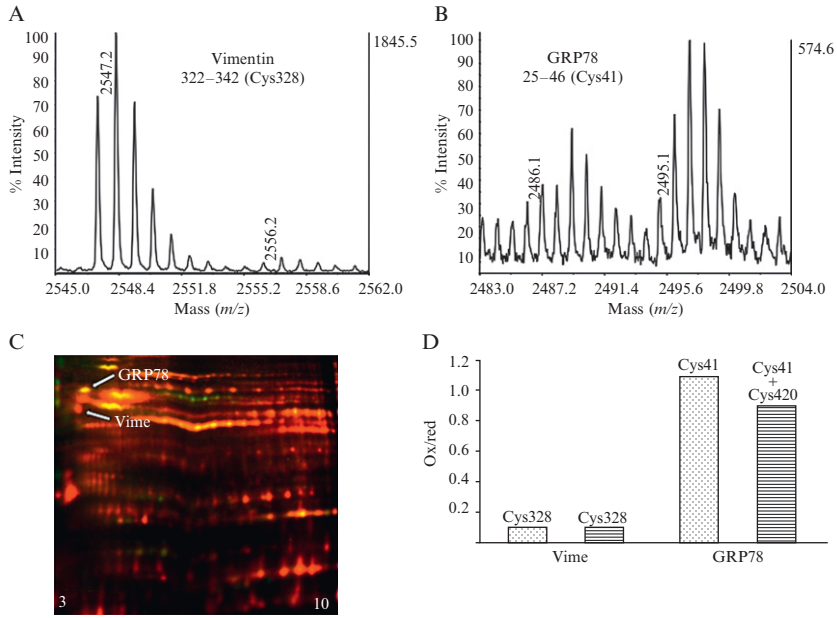

Figure 10.3 Confronting the results of the 2DE-based fluorescence and ICAT strategies. (A and B) HeLa cell extracts were submitted to OxICAT. Mass spectra of the vimentin peptide containing Cys328 (A) and the GRP78 peptide containing Cys41 (B) are represented, as indicated. (C) HeLa cell extracts were submitted to the 2DE-based fluorescence labeling procedure. The arrows indicate spots corresponding to vimentin and GRP78. (D) Oxidized to reduced ratios of vimentin GRP78 Cys residues established through the ICAT (spotted bars) and the 2DE-based fluorescence (stripped bars), as indicated.

not for the second GRP78 Cys-containing peptide (Cys420), which fell out of the experimental acquisition range, because of its large size ($m/z = 5069.6$). However, confronting the fluorescence data, which indicated that GRP78 is half-oxidized (Ox/Red ratio close to one) (Fig. 10.3C and D), and MS data, which indicated that GRP78 Cys41 is also half-oxidized (Fig. 10.3D), suggests that Cys420 is probably also oxidized, possibly to an intramolecular disulfide with Cys41. Indeed, Cys420 should also be half-oxidized to account for the half-oxidized state of GRP78 seen by fluorescence, a value reflecting the average redox state of both GRP78 Cys residues. This finding should be verified and the linearity between the fluorescence- and OxICAT-data validated by considering a larger number of proteins.

5. Conclusions

Redox proteomics is complex and remains an experimental challenge. OxICAT appears to be the most robust and reliable technique to identify and quantitatively assess the redox state of Cys residues. Further, its exhaustive nature will allow identification of proteins that are ignored by the other methods. Among the 2DE-based methods, the two-fluorescence differential labeling procedure appears to us the best method to obtain snapshots of the redoxome. This method should complement the OxICAT method when used as a screening procedure to select for the most informative cell conditions (growth, mutations, exogenous treatments, etc.), and also to select for interesting proteins that are then identified in the OxICAT MS data, as shown here. A systematic identification of the redoxome of mammalian cells should provide clues to understand Cys residues redox metabolism.

ACKNOWLEDGMENTS

We acknowledge the "DIM SEnT Région Ile-de-France" postdoctoral fellowship to GC. MBT is the recipient of a fund program "Equipe Labellisée Ligue 2009," from La Ligue Contre le Cancer (LCC).

REFERENCES

Baty, J. W., *et al.* (2002). Detection of oxidant sensitive thiol proteins by fluorescence labeling and two-electrophoresis. *Proteomics* **2,** 1261–1266.

Bernhardt, J., *et al.* (1999). Dual channel imaging of two-dimensional electropherograms in *Bacillus subtilis*. *Electrophoresis* **20,** 2225–2240.

Boivin, B., *et al.* (2008). A modified cysteinyl-labeling assay reveals reversible oxidation of protein tyrosine phosphatases in angiomyolipoma cells. *Proc. Natl. Acad. Sci. USA* **105,** 9959–9964.

Bruschi, M., *et al.* (2009). New iodo-acetamido cyanines for labeling cysteine thiol residues. A strategy for evaluating plasma proteins and their oxido-redox status. *Proteomics* **9,** 460–469.

Canet-Aviles, R. M., *et al.* (2004). The Parkinson's disease protein DJ-1 is neuroprotective due to cysteine-sulfinic acid-driven mitochondrial localization. *Proc. Natl. Acad. Sci. USA* **101,** 9103–9108.

D'Autreaux, B., and Toledano, M. B. (2007). ROS as signalling molecules: Mechanisms that generate specificity in ROS homeostasis. *Nat. Rev. Mol. Cell Biol.* **8,** 813–824.

Delaunay, A., *et al.* (2000). H2O2 sensing through oxidation of the Yap1 transcription factor. *EMBO J.* **19,** 5157–5166.

Dietz, L., *et al.* (2009). Quantitative DY-maleimide-based proteomic 2-DE-labeling strategies using human skin proteins. *Proteomics* **9,** 4298–4308.

Eaton, P. (2006). Protein thiol oxidation in health and disease: Techniques for measuring disulfides and related modifications in complex protein mixtures. *Free Radic. Biol. Med.* **40,** 1889–1899.

Fourquet, S., *et al.* (2008). The dual functions of thiol-based peroxidases in H_2O_2 scavenging and signaling. *Antioxid. Redox Signal.* **10,** 1565–1576.

Fu, C., *et al.* (2008). Quantitative analysis of redox-sensitive proteome with DIGE and ICAT. *J. Proteome Res.* **7,** 3789–3802.

Gorman, J. J., *et al.* (2002). Protein disulfide bond determination by mass spectrometry. *Mass Spectrom. Rev.* **21,** 183–216.

Gygi, S. P., *et al.* (1999). Protein analysis by mass spectrometry and sequence database searching: Tools for cancer research in the post-genomic era. *Electrophoresis* **20,** 310–319.

Hess, D. T., *et al.* (2005). Protein S-nitrosylation: Purview and parameters. *Nat. Rev. Mol. Cell Biol.* **6,** 150–166.

Hochgrafe, F., *et al.* (2005). Fluorescence thiol modification assay: Oxidatively modified proteins in *Bacillus subtilis*. *Mol. Microbiol.* **58,** 409–425.

Hurd, T. R., *et al.* (2007). Detection of reactive oxygen species-sensitive thiol proteins by redox difference gel electrophoresis: Implications for mitochondrial redox signaling. *J. Biol. Chem.* **282,** 22040–22051.

Ito, K., and Inaba, K. (2008). The disulfide bond formation (Dsb) system. *Curr. Opin. Struct. Biol.* **18,** 450–458.

Jaffrey, S. R., and Snyder, S. H. (2001). The biotin switch method for the detection of S-nitrosylated proteins. *Sci. STKE.* **86,** pl1.

Janssen-Heininger, Y. M., *et al.* (2008). Redox-based regulation of signal transduction: Principles, pitfalls, and promises. *Free Radic. Biol. Med.* **45,** 1–17.

Kahle, P. J., *et al.* (2009). DJ-1 and prevention of oxidative stress in Parkinson's disease and other age-related disorders. *Free Radic. Biol. Med.* **47,** 1354–1361.

Kinumi, T., *et al.* (2004). Cysteine-106 of DJ-1 is the most sensitive cysteine residue to hydrogen peroxide-mediated oxidation in vivo in human umbilical vein endothelial cells. *Biochem. Biophys. Res. Commun.* **317,** 722–728.

Le Moan, N., *et al.* (2006). The *Saccharomyces cerevisiae* proteome of oxidized protein thiols: Contrasted functions for the thioredoxin and glutathione pathways. *J. Biol. Chem.* **281,** 10420–10430.

Le Moan, N., *et al.* (2009). Protein-thiol oxidation, from single proteins to proteome-wide analyses. *Methods Mol. Biol.* **476,** 175–192.

Leichert, L. I., *et al.* (2008). Quantifying changes in the thiol redox proteome upon oxidative stress in vivo. *Proc. Natl. Acad. Sci. USA* **105,** 8197–8202.

Leichert, L. I., and Jakob, U. (2004). Protein thiol modifications visualized in vivo. *PLoS Biol.* **2,** e333.

Linke, K., and Jakob, U. (2003). Not every disulfide lasts forever: Disulfide bond formation as a redox switch. *Antioxid. Redox Signal.* **5,** 425–434.

Mesecke, N., *et al.* (2005). A disulfide relay system in the intermembrane space of mitochondria that mediates protein import. *Cell* **121,** 1059–1069.

Patterson, S. D., and Katta, V. (1994). Prompt fragmentation of disulfide-linked peptides during matrix-assisted laser desorption ionization mass spectrometry. *Anal. Chem.* **66,** 3727–3732.

Poole, L. B., *et al.* (2005). Synthesis of chemical probes to map sulfenic acid modifications on proteins. *Bioconjug. Chem.* **16,** 1624–1628.

Rhee, S. G., *et al.* (2005). Intracellular messenger function of hydrogen peroxide and its regulation by peroxiredoxins. *Curr. Opin. Cell Biol.* **17,** 183–189.

Riederer, I. M., and Riederer, B. M. (2007). Differential protein labeling with thiol-reactive infrared DY-680 and DY-780 maleimides and analysis by two-dimensional gel electrophoresis. *Proteomics* **7,** 1753–1756.

Saurin, A. T., *et al.* (2004). Widespread sulfenic acid formation in tissues in response to hydrogen peroxide. *Proc. Natl. Acad. Sci. USA* **101,** 17982–17987.

Sevier, C. S., and Kaiser, C. A. (2008). Ero1 and redox homeostasis in the endoplasmic reticulum. *Biochim. Biophys. Acta* **1783,** 549–556.

Srikanth, C. V., *et al.* (2005). Multiple cis-regulatory elements and the yeast sulphur regulatory network are required for the regulation of the yeast glutathione transporter, Hgt1p. *Curr. Genet.* **47,** 345–358.

Toledano, M. B., *et al.* (2004). Microbial H_2O_2 sensors as archetypical redox signaling modules. *Trends Biochem. Sci.* **29,** 351–357.

Toledano, M. B., *et al.* (2007). The system biology of thiol redox system in *Escherichia coli* and yeast: Differential functions in oxidative stress, iron metabolism and DNA synthesis. *FEBS Lett.* **581,** 3598–3607.

Wan, J., *et al.* (2007). Palmitoylated proteins: Purification and identification. *Nat. Protoc.* **2,** 1573–1584.

Yano, H. (2003). Fluorescent labeling of disulfide proteins on 2D gel for screening allergens: A preliminary study. *Anal. Chem.* **75,** 4682–4685.

CHAPTER ELEVEN

Identification by MS/MS of Disulfides Produced by a Functional Redox Transition

Pierluigi Mauri,* Stefano Toppo,† Antonella De Palma,* Louise Benazzi,* Matilde Maiorino,† *and* Fulvio Ursini†

Contents

Abstract

Among posttranslational modifications of proteins entailed with signal transduction, the redox transition is today brought to the focus as a major biochemical event accounting for the signaling functions of reactive oxygen species. Thermodynamic and kinetic criteria highlight hydroperoxides and protein disulfides as signaling and transducer elements, respectively, and growing biochemical evidence supports this notion. The protein Cys residue involved in this function must react fast and specifically with the oxidant and then with a second accessible Cys yielding the disulfide. These kinetic and structural constraints are shared with peroxidases and peroxiredoxins, which are competitors for the signaling hydroperoxide. In this chapter, a procedure based on MS/MS analysis for inter- and intrachain disulfide assignment in proteins undergoing

* Institute for Biomedical Technologies, National Research Council, Viale Fratelli Cervi, Segrate-Milano, Italy
† Department of Biological Chemistry, University of Padova, Viale G. Colombo, Padova, Italy

Methods in Enzymology, Volume 473
ISSN 0076-6879, DOI: 10.1016/S0076-6879(10)73011-1

redox-switch is presented. While the sensitivity of the modern MS/MS instruments permits the sequencing of double peptides linked by a disulfide bond, the major pitfall of the proteomic procedure is the thiol–disulfide scrambling taking place at the alkaline pH needed for the proteolytic reaction of trypsin. Instead, the use of pepsin at acidic pH prevents the disulfide scrambling, but the specificity of the proteolytic reaction is low and thus the complexity of fragmentation increases. We succeeded to limit this problem by heuristically assuming a conserved pepsin cleavage pattern of the protein both in the oxidized and the reduced form. Asymmetric cleavage of the disulfide by collisional fragmentation further corroborated the identification. In conclusion, the use of pepsin, integrated by a minimal computation, appears suitable for positively assigning inter- and intrachain disulfides generated by a functional redox-switch.

1. Introduction

The disulfide bond is the covalent link between two sulfur atoms (R–S–S–R) generated by the oxidation of two Cys residues. Chemically, this bond is related to that linking two oxygen or two selenium atoms that are more and less electronegative than sulfur in Group VIa, forming a peroxide (R–O–O–R) or a diselenide (R–Se–Se–R), respectively. This chemical proximity has a counterpart in biology where oxygen, sulfur, and selenium are pivotal players of the redox homeostasis of redox-prone Cys residues. In the redox flow, catalyzed by peroxidases, hydroperoxides are reduced forming disulfides through the formation of mixed disulfides or selenodisulfide (R–Se–S–R), intermediates of the catalytic cycle (Toppo *et al.*, 2009). There is no evidence, instead, for the biological function of diselenides so far identified only in SelL, a family of selenoproteins of aquatic organisms containing a thioredoxin motif where Sec replaces for Cys (Shchedrina *et al.*, 2007).

In biology, pathways for the formation of disulfides are: (a) free radical oxidation of the thiol, evolving to disulfide with a proximal thiol, through the formation of the intermediate disulfide anion radical (Mottley and Mason, 2001); (b) nucleophilic displacement reaction in the presence of a hydroperoxide producing a sulfenic acid residue (Barton *et al.*, 1973), eventually evolving to disulfide; (c) a thiol–disulfide exchange reaction (Maiorino *et al.*, 2007). While the formation of protein disulfides by mechanism (a) is possibly relevant as antioxidant mechanism, under conditions of a major flow of oxidizing free radicals, mechanisms (b) and (c) are involved in the formation and reshuffling of disulfides in proteins, respectively. The dissociation of the thiol for driving both these nucleophilic displacement reactions is a common feature of both these mechanisms. The pK_a value of the thiol is, therefore, a major constraint, although not sufficient per se, for a thiol–disulfide redox transition (Wang and Narayan, 2008).

The redox potential of a thiol–disulfide couple mirrors the conformational features of the covalent bond: the distance among atoms, the torsion angle of the bond, and the polarization. The thermodynamically driven oxidation of thiols to disulfides, encompassing enthalpic end entropic components, accounts for both the formation of structural disulfides and functional redox-switches (Wouters *et al.*, 2010). In general, when the low potential is the outcome of optimal distance, torsion angle, and minimal polarization of the bond, these disulfides, typically produced during the oxidative folding of proteins in the endoplasmic reticulum, have a structural role (Ito and Inaba, 2008).

In the cytosol, instead, the redox transition operates shifts between two conformations at rather close conformational energy (Wouters *et al.*, 2010). Not obeying the canonical rule prescribing a major drop of conformational energy following oxidation, these disulfides are predicted at relatively high potential in order to account for an easily reversible redox transition.

From these considerations, functional redox-switches emerge as similar to the intermediates of peroxidatic reactions where the active site is easily oxidized (Tosatto *et al.*, 2008) and transfers the oxidative potential toward a substrate or a specific protein. Therefore, the catalytic cycle of glutathione peroxidases—either containing selenium or sulfur—and peroxiredoxins, is representative of a reversible redox-switch.

While studying these mechanisms, we had to set up a simple procedure to settle the formation of specific disulfides and their evolution toward mixed disulfides with a small molecular weight thiol—such as GSH or mercaptoethanol—or with another protein such as thioredoxin.

This procedure was first set up to demonstrate that the catalytic selenium at the active site of GPx-4 binds, through a mixed selenodisulfide, a GSH molecule (Mauri *et al.*, 2003), thus providing the first direct evidence for this intermediate of the catalytic cycle. The procedure was adopted for the positive identification of peroxidatic and resolving Cys (C_p and C_r) of *Drosophila melanogaster* GPx (Maiorino *et al.*, 2007) and *Mycobacterium tuberculosis* peroxiredoxin (Trujillo *et al.*, 2006) and for identifying the intermediate disulfide formed between the peroxidase-specific redoxin and the C_r.

2. MS/MS Identification of Redox-Switches in Protein

In protein chemistry, structural disulfides are identified by comparing and resequencing peptides produced by different endoproteases under reducing and nonreducing conditions. These approaches (reviewed in Gorman *et al.*, 2002) are long and complex and today are progressively substituted by modern MS/MS-based technology.

When a protein containing a redox-switch is in its oxidized form, proteolysis produces either a fragment containing the disulfide or double fragments linked to each other by the disulfide. In both cases, the appearance of a new peptide with a mass 2 a.m.u. lower than the mass of either the reduced peptide or the sum of two peptides suggests an identification that will be validated by MS/MS sequencing.

The major drawback of the approach is the need of an alkaline pH for the activity of trypsin, the most specific and standardized endoprotease used in proteomics. In fact, when Cys are dissociated, a thiol–disulfide scrambling takes place by a nucleophilic attack of thiolate on the disulfide, as already pointed out by Sanger in 1953. This artifactual reshuffling deeply weakens the validity of the disulfide assignment (Gorman *et al.*, 2002).

Although this major pitfall is often overlooked in reports of disulfide identification, including glutathionylation, its occurrence, when trypsin is used and the protein contains free cysteines, is unavoidable. The use of alkylating agents to scavenge free Cys in our hands was not satisfactory since the possibility that a thiolate still reacts with a disulfide instead of reacting with the alkylating agent, cannot be fully ruled out.

The use of the endoprotease pepsin, which is active at acidic pH, prevents the thiol–disulfide scrambling, but this approach suffers from the low and unpredictable specificity of the proteolysis.

In our studies, this problem was worked out by heuristically assuming a constant proteolytic pattern in the oxidized and reduced protein. Candidate double peptides were identified according to the pattern of fragmentation observed under reducing conditions. MS/MS analysis of the double b-y series confirmed the correct identifications.

3. Analytical Procedure

3.1. Protein reduction and oxidation

The protein is reduced for 80 min at 37 °C with 50 m*M* DTT in 50 m*M* phosphate buffer, pH 7.5. The reductant is carefully removed by buffer exchange (gel-filtration on a Bio-Spin 6 column, twice repeated).

This reduced protein is oxidized by incubation with 20–50 μM hydrogen peroxide, for a maximum of 5 min. The neutral pH value and the short incubation time adopted, guarantee that only the labile Cys residues are oxidized.

When searching for the formation of an interchain disulfide, the oxidized protein is mixed with the second protein prepared as above in reduced form. Adjusting the sample to pH 2 by HCl stops the reaction.

3.2. Enzymatic digestions

Pepsin is added at an enzyme substrate ratio of 1:100 (w/w) in 100 m*M* ammonium acetate, pH 2.5. After 3 h incubation at room temperature, cooling on ice stops the reaction.

Ten microliters of the peptide mixtures is analyzed by means of liquid chromatography coupled to tandem mass spectrometry (LC–ESI-MS/MS).

3.3. LC–ESI-MS/MS

Analysis of peptides is performed by means of a Surveyor MS HPLC pump equipped with a MicroAS autosampler (20 μl loop) and coupled to an LTQ ion trap mass spectrometer by an electrospray interface (Thermo Electron, Milan, Italy). A reversed-phase C_{18} column (1 × 150 mm, 5 μm ACT, Aberdeen, Scotland) and an acetonitrile gradient are used (eluent A: 0.1% formic acid in water; eluent B: 0.1% formic acid in acetonitrile) at a flow rate of 50 μl/min. The gradient profile is 5% B for 4 min, followed by 5–50% B within 40 min.

For mass spectrometry, the heated capillary is held at 180 °C and voltage at 38 V. Spray voltage is 5.2 kV. Spectra are acquired in positive mode (in the range 400–2000 m/z) using dynamic exclusion for MS/MS analysis (relative collision energy of 35%, repeat count 3).

3.4. Data handling of mass spectra

Computer analysis of peptide MS/MS spectra is performed using Bioworks 3.3.1, based on SEQUEST algorithm (University of Washington, USA, licensed to Thermo Electron Corp.). For the peptic peptide mixture, the "no enzyme" option is used. As confidence of peptide identification, the minimum values of Xcorr were greater than 1.5, 2.0, and 2.5 for single, double, and triple charge ions, respectively. The minimum consecutive multicharge ions of a possible "double peptide" are 3.

3.5. Identification of the disulfide

From the analysis of the protein(s) in reduced form, a list of peptides covering the whole length of the protein is generated. Due to the limited specificity of pepsin, overlapping peptides are also observed. A new list is then generated by combining all the couples of Cys-containing peptides. This list is used to screen the MS spectrum. The SEQUEST algorithm, integrated by manual searching of the MS/MS data from peaks identified earlier, provides the final evidence of the double b-y series.

Identification is usually further confirmed by the evidence of fragments, produced by collisional breakdown of the peptide containing the disulfide,

where the cleavage of the C–S bond adjacent to the disulfide, leaves a Cys residue linked to a sulfur atom.

4. Discussion

Reversible formation of disulfides, leading to functionally relevant conformational shifts in proteins, emerges today as a novel relevant post-translational modification operating in cell signaling. The signaling hydroperoxide reacts with specific Cys residues of specific targets generating sulfenic acid derivatives that, in turn, react with a second Cys yielding a disulfide. Disulfides may also reshuffle, in the presence of a different oxidation-prone Cys residue, to new intra- or interchain disulfides eventually transducing the signal (Flohé, 2010; Forman *et al.*, 2010).

When the two Cys are not at a compatible distance, partial unfolding must take place before the disulfide is formed. In this case, besides the oxidative potential, it is also the new conformation that is expected to add biological properties to the protein as transducer of the signal. Examples of such functional redox-switches are proteins containing the thioredoxin redox motif, involved in redox homeostasis and oxidative folding (Wouters *et al.*, 2010) as well as nuclear factors responding to an oxidative signal (Choi *et al.*, 2001; Delaunay *et al.*, 2002).

A crucial determinant of the possibility for a Cys to play a role in oxidative signaling is the rate of the redox transition. Indeed, a fast rate for oxidation is required owing to the competition with enzymatic reactions that eliminate the hydroperoxide (Flohé, 2010; Forman *et al.*, 2010). In this respect, the structural and chemical determinants of kinetics of the redox transition of critical Cys in oxidation sensor/tranducers must be shared with hydroperoxide reducing enzymes.

An analytical approach set up for glutathione peroxidases and peroxiredoxins is, therefore, appropriate also for detecting the partners of the disulfide formation in oxidation sensors/transducers.

While the modern mass spectrometry technology has both sensitivity and specificity to provide a nonambiguous disulfide assignment, the limit of the analytical approach is the lack of specificity of pepsin, practically the sole endoprotease active at the acidic pH necessary to prevent any thiol disulfide exchange during proteolysis and/or unfolding.

The complexity of the series of possible double peptides linked by a disulfide depends on the total number of Cys residues in the protein. The solution is a typical example of combinations with repetition that can be easily solved as follows:

$$\binom{n+k-1}{k}$$

where, in this case, $k = 2$ as two Cys are necessary to form the S–S bond and n is the total number of Cys in the protein. This binomial coefficient takes into account the number of k-combinations (each of size two in this case) from a set S with n elements where repetition may occur. Repetition is intended when one Cys forms a disulfide bridge with itself or, in other words, two identical monomers are linked through an S–S bond between two homologous Cys. For example, when five Cys are available, the combinations of pairings are 15.

The result of this theoretical calculation is, apparently, encouraging, but the very limited specificity of pepsin contributes to a combinatorial explosion of possible forming dipeptides.

If we assume, for example, that dipeptides link proteolytic peptides from 6 up to 40 residues, the worst possible scenario, where five Cys are at stake, exceeds 1,300,000 of unique combinations. The calculated masses of all of these peptides may have isobaric solutions and, depending on the amino acid composition and Cys positions, the possible combinations can be surely lower. Indeed, the absolute number gives an idea of how complex the problem is.

A rigorous computational approach, based on the match of a database of theoretical peaks with the actual MS spectrum to detect the candidates for confirmation of the disulfide by MS/MS double sequencing, will provide a comprehensive computational and analytical solution for the assignment of a disulfide.

Nevertheless, our observation that the pepsin proteolytic cleavage sites are enough conserved in the reduced and oxidized protein, enormously simplified the analysis that was compatible with just a manual identification of new dipeptide fragments, the MW of which corresponded to the sum minus 2 a.m.u. of two fragments containing a Cys previously identified in the reduced protein.

Usual SEQUEST analysis, integrated by the manual inspection of spectra, is therefore sufficient to get information about the two b-y series of sequence. Furthermore, the frequent observation in MS/MS of a fragment containing a Cys linked to a sulfur atom, produced by the cleavage of the bond between carbon beta and sulfur in the Cys residue, provides the last piece of evidence for nonambiguous assignment of the disulfide.

As an example of the application of this procedure, we report (Fig. 11.1) a different spectrum confirming the published experiment where we demonstrated the formation of a disulfide between the C_r or *Dm*GPx and its specific thioredoxin, *Dm*Trx-2 (4).

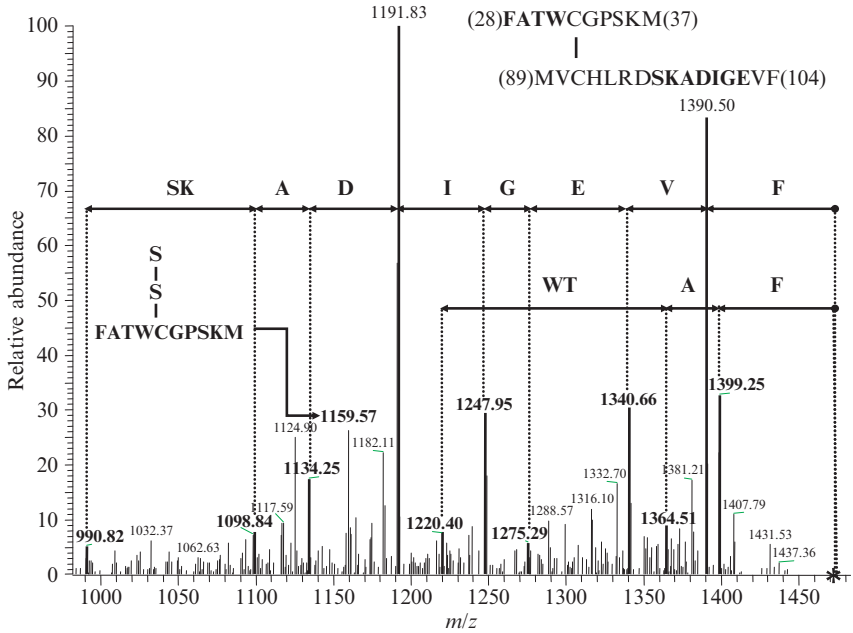

Figure 11.1 MS/MS spectrum (parent ion m/z 1473.6 = $[M+2H+]^{2+}$) of the fragment linking the peptides 89–104 of *Dm*GPx and 28-37 of *Dm*Trx-2$^{Cys35/Ser}$. A thioredoxin fragment with an S–S group resulting from asymmetric cleavage of the disulfide is indicated among identified residues providing diagnostic information about the double sequence. For this experiment, the C-terminal Cys of the CxxC motif of thioredoxin was mutated to serine to prevent the final rearrangement of the disulfide.

In conclusion, the use of pepsin, integrated by a minimal computation, appears suitable for positively assigning inter- and intrachain disulfides generated by a functional redox-switch.

REFERENCES

Barton, J. P., *et al.* (1973). Kinetics of the reaction of hydrogen peroxide with cysteine and cysteamine. *J. Chem. Soc., Perkin Trans.* **2**(11), 1547–1549.

Choi, H., *et al.* (2001). Structural basis of the redox switch in the OxyR transcription factor. *Cell* **105,** 103–113.

Delaunay, A., *et al.* (2002). A thiol peroxidase is an H2O2 receptor and redox-transducer in gene activation. *Cell* **111,** 471–481.

Flohé, L. (2010). Changing paradigma in thiology: From antioxidant defense towards redox regulation. *Methods Enzymol.* (this volume).

Forman, J. H., *et al.* (2010). Signaling functions of reactive oxygen species. *Biochemistry* **49**(5), 835–842.

Gorman, J. J., *et al.* (2002). Protein disulfide bond determination by mass spectrometry. *Mass Spectrom. Rev.* **21,** 183–216.

Ito, K., and Inaba, K. (2008). The disulfide bond formation (Dsb) system. *Curr. Opin. Struct. Biol.* **18,** 450–458.

Maiorino, M., *et al.* (2007). The thioredoxin specificity of *Drosophila* GPx: A paradigm for a peroxiredoxin-like mechanism of many glutathione peroxidases. *J. Mol. Biol.* **365,** 1033–1046.

Mauri, P., *et al.* (2003). Versatility of selenium catalysis in PHGPx unraveled by LC/ESI-MS/MS. *Biol. Chem.* **384,** 575–588.

Mottley, C., and Mason, R. P. (2001). Sulfur-centered radical formation from the antioxidant dihydrolipoic acid. *J. Biol. Chem.* **276,** 42677–42683.

Sanger, F. (1953). A disulphide interchange reaction. *Nature* **171,** 1025–1026.

Shchedrina, V. A., *et al.* (2007). Identification and characterization of a selenoprotein family containing a diselenide bond in a redox motif. *Proc. Natl. Acad. Sci. USA* **104,** 13919–13924.

Toppo, S., *et al.* (2009). Catalytic mechanisms and specificities of glutathione peroxidases: Variations of a basic scheme. *Biochim. Biophys. Acta* **1790,** 1486–1500.

Tosatto, S. C., *et al.* (2008). The catalytic site of glutathione peroxidases. *Antioxid. Redox Signal.* **10,** 1515–1526.

Trujillo, M., *et al.* (2006). The mycobacterial thioredoxin peroxidase can act as a one-cysteine peroxiredoxin. *J. Biol. Chem.* **281,** 20555–20566.

Wang, Y. H., and Narayan, M. (2008). pH dependence of the isomerase activity of protein disulfide isomerase: Insights into its functional relevance. *Protein J.* **27,** 181–185.

Wouters, M. A., *et al.* (2010). Disulfides as redox switches: From molecular mechanisms to functional significance. *Antioxid. Redox Signal.* **12,** 53–91.

CHAPTER TWELVE

Mass Spectrometry Approaches for the Redox Characterization of Protein Cysteine Residues: The Case of the Transcription Factor Pax-8

Andrea Scaloni* *and* Gianluca Tell†

Contents

Abstract

Regulation of protein structure and function by redox reactions has emerged as an exciting area of research study. The transduction of a redox signal into a biological response can be mediated in several ways, but a principal mechanism involves the modification of protein cysteine (Cys) residues. Several transcription factors, such as NF-κB, Egr-1, AP-1, and Pax, are regulated through redox-based mechanisms. Thus, redox regulation represents a key issue in specifically controlling gene expression. This study describes the combined use of MS

* Proteomics and Mass Spectrometry Laboratory, ISPAAM, National Research Council, Naples, Italy
† Department of Biomedical Sciences and Technologies, University of Udine, Udine, Italy

Methods in Enzymology, Volume 473
ISSN 0076-6879, DOI: 10.1016/S0076-6879(10)73012-3

procedures and protein-functional assays to investigate the redox state of a protein-regulating gene expression in thyroid, namely Pax-8, a member of the Pax family of transcription factors. Molecular characterization of the modified cysteine residues after various oxidative insults provided information on the mechanisms controlling protein-functional properties.

1. Introduction

In the ever-enlarging world of posttranslational modifications, the regulation of protein structure and function by reduction–oxidation (redox) reactions has emerged as an exciting area of research study. Reactive oxidative and nitrosative species (ROS and RNS), firstly believed as toxic by-products of inflammatory responses and xenobiotic exposure (Freeman and Crapo, 1982), are now also viewed as signaling mediators that are generated and inactivated in a controlled manner (Dröge, 2002; Hess *et al.*, 2005; Rhee 2006). Cellular redox reactions and their regulation rely on a broad array of proteins and metabolites that evolved to generate reactive species in a regulated mode as host defense and signaling intermediates, to scavenge catalytically or to inactivate reactive species, and to chemically sense the cellular environment by undergoing oxidation and reduction reactions (Dalle-Donne *et al.*, 2005, 2006).

The transduction of a redox signal into a biological response can be mediated in several ways, but a principal mechanism involves the modification of protein cysteine (Cys) residues (Hess *et al.*, 2005; Janssen-Heininger *et al.*, 2008). The thiol moiety of cysteine (Cys-SH) is particularly sensitive to redox reactions and is an established "redox sensor." Thus, secondary products of oxygen- and NO-dependent reactions, the downstream electrophilic products generated by ROS/RNS reaction with lipids, and glutathione (GSH) can transduce redox signaling by modifying protein Cys residues to sulfenic (Cys-SOH), sulfinic acid (Cys-SO_2H), sulfonic acid (Cys-SO_3H) (Dalle-Donne *et al.*, 2006; Janssen-Heininger *et al.*, 2008), *S*-electrophile adducts (Cys-*S*-E) (Liebler, 2008; Rudolph and Freeman, 2009), *S*-nitrosothiol (Cys-*S*-NO) (Hess *et al.*, 2005), and disulfide derivatives (Eaton, 2006; Ying *et al.*, 2007). Disulfides include cysteinylated proteins (Cys-*S*-SP), glutathionylated proteins (GS-SP) (Gallogly and Mieyal, 2007) as well as intramolecular protein disulfides and disulfide cross-links between different proteins (Dalle-Donne *et al.*, 2005; Ghezzi and Bonetto, 2003; Ying *et al.*, 2007). Protein thiol modifications can have different physiological effects, depending on its reversible or irreversible nature. It is a general opinion that reversible disulfide bond, sulfenic/sulfinic acid, and *S*-nitrosothiol formations are part of regulatory processes or protecting mechanisms affecting protein function, in which protein Cys

residues can cycle between the oxidized and reduced state. Conversely, irreversible modifications, such as oxidation to sulfonic acids (Cys-SO_3H) or adduct formation with some electrophilic by-products of membrane oxidation, cannot be counterbalanced by other metabolic processes, thus determining impaired protein function.

Not all the protein thiols are important as redox sensors, as most protein cysteines do not react with ROS and RNS in living organisms (Liebler, 2008). However, some thiols ionize to the thiolate anion state (i.e., those with a low pK_a) as a result of their surrounding three-dimensional amino acid environment. These Cys residues have enhanced reactivity for many ROS and RNS, and this provides a basis for specificity in thiol-mediated redox signaling (Janssen-Heininger *et al.*, 2008). Sometimes, reactive cysteines form short-lived catalytic intermediates in the reaction cycle of many enzymes (Hess *et al.*, 2005). This often means that the most important protein cysteines in terms of function are the very same as those susceptible to redox-dependent modifications. This allows ROS and RNS to alter the activity of some proteins by modifying the redox state of functionally essential cysteines, and serves as a simple signal transduction mechanism, which couples the protein redox state directly to functional activity. Thus, redox reactions can integrate more widely into cell signaling by directly modulating the activity (through Cys modification) of membrane receptors, ion channels, mitogen-activated protein kinases, Tyr and Ser/Thr phosphatases, chaperones, proteases, and transcription factors (Hess *et al.*, 2005; Janssen-Heininger *et al.*, 2008; Rudolph and Freeman, 2009).

With the introduction of matrix-assisted laser desorption/ionization (MALDI) and electrospray ionization (ESI) as soft ionization methods for mass spectrometry (MS) of biomolecules, cysteine redox reactions have been investigated directly at the protein level, assigning the nature and site (s) of modification (Dalle-Donne *et al.*, 2005, 2006). Direct protein mass measurement, peptide mass fingerprinting (PMF), and fragment fingerprinting upon collision-induced fragmentation (CID) experiments (MS/MS) have been widely used for this purpose. In the latter cases, high-sequence coverage is a prime prerequisite for the comprehensive assignment of cysteine modifications, generally obtained by direct MALDI-time-of-flight (TOF)-MS and/or liquid chromatography (LC)–ESI-MS/MS analysis of enzymatic digests. Recently, dedicated MS experiments based on (i) selective enrichment of redox-modified proteins by affinity techniques (Brennan *et al.*, 2006; Charles *et al.*, 2007; Codreanu *et al.*, 2009; Eaton, 2006; Grimsrud *et al.*, 2008; López-Sánchez *et al.*, 2009; Saurin *et al.*, 2004; Vila *et al.*, 2008), (ii) selective trapping of modified peptides by affinity techniques (Camerini *et al.*, 2007; Codreanu *et al.*, 2009; Dai *et al.*, 2005; Forrester *et al.*, 2009a; Greco *et al.*, 2006; Grimsrud *et al.*, 2008; Han and Chen, 2008; Hao *et al.*, 2006; Kim *et al.*, 2009; Liebler, 2008; Sethuraman *et al.*, 2004), and (iii) optimized CID and electron transfer dissociation (ETD) processes

(Hao and Gross, 2006; Mikesh *et al.*, 2006; Wang *et al.*, 2008; Wu *et al.*, 2009) have been introduced. These procedures resulted particularly important for the detection of unstable thiol modification products in modified proteins, such as Cys-SOH and Cys-SNO. Thus, this wide array of MS-based approaches have been used to elucidate the redox state of the cysteines present in isolated proteins modified *in vitro* by various reagents or resulting from biological tissues/fluids and modified *in vivo* as result of pathophysiological conditions (Hess *et al.*, 2005; Janssen-Heininger *et al.*, 2008; Liebler, 2008; Rudolph and Freeman, 2009).

This work illustrates how MS procedures and protein-functional assays can be used in combination to assess the redox state of a protein-regulating gene expression in thyroid, namely Pax-8, a member of the general family of Pax transcription factors (Fig. 12.1A) (Tell *et al.*, 1998a,b), here described as a paradigmatical example. Elucidation of the modified cysteine residues after various oxidative insults provided information on the mechanisms regulating protein-functional properties.

2. Materials and Methods

2.1. Protein expression and functional analysis

The Pax-8 Prd domain was expressed and purified as previously reported (Tell *et al.*, 1998a); it was dialyzed against water and stored in 1 m*M* DTT, at −80 °C, until used.

For functional studies, the DNA-binding activity of oxidized and reduced Pax-8 Prd domain was assayed by electrophoretic mobility shift assay (EMSA) analysis as previously reported (Tell *et al.*, 1998a). Briefly, the oxidized forms of the recombinant wild-type Prd domain of Pax-8 or the C37S mutant were obtained by prolonged air exposure. The reduced forms were obtained by treatment with 5 m*M* DTT for 5 min, at room temperature. At the end of the treatments, 90 ng of the wild-type-purified Pax-8 Prd domain or the C37S mutant samples were incubated with the 26-mer oligonucleotide C (0.1 pmol) resembling the Pax-8 binding site present on the thyroglobulin (Tg) promoter (Tell *et al.*, 1998a), for 20 min at room temperature, and loaded onto a native polyacrylamide gel for EMSA analysis. *In vivo* functional studies were performed through reporter assays on Tg promoter, by using HeLa cells as previously described (Tell *et al.*, 1998b), plasmids encoding for wild-type and redox-defective mutant C37S Pax-8 (Tell *et al.*, 1998a), and with wild-type and redox-defective mutant APE1/Ref-1 (Tell *et al.*, 2005).

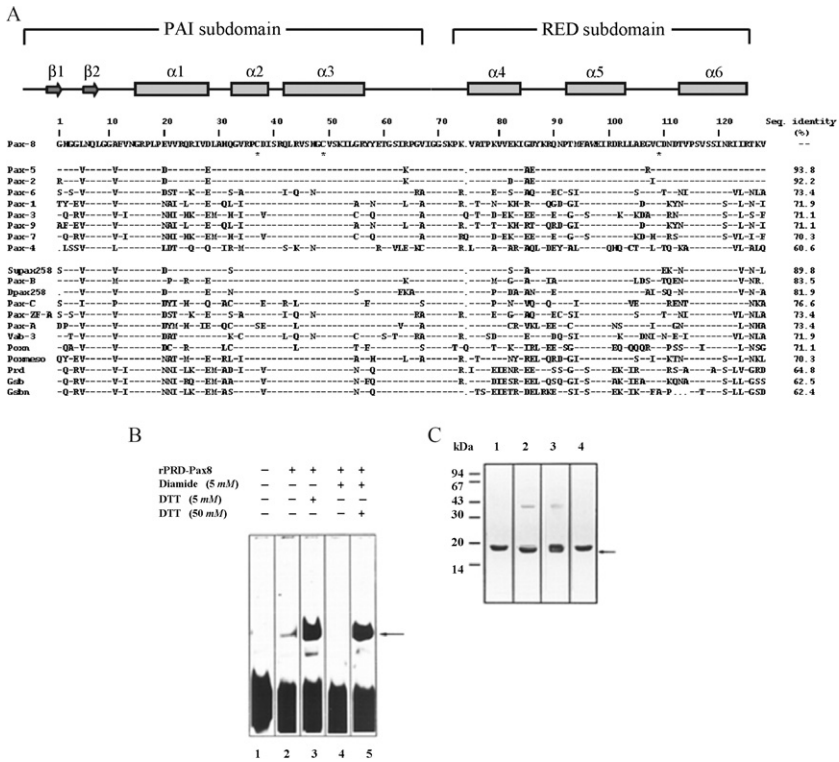

Figure 12.1 Redox potential controls the DNA-binding activity and the structure of the Pax-8 paired domain. Panel A, Sequence alignment of human Pax-8 Prd domain with homologous human proteins. The protein subdomain organization is reported as well as the conserved Cys residues (indicated with an asterisk). Panel B, EMSA of the oxidized and reduced forms of Pax-8 Prd domain incubated with the oligonucleotide C. The oxidized forms of the recombinant Pax-8 Prd domain were obtained by prolonged air exposure (lane 2) or by treatment with 2.5 m*M* diamide for 5 min, at 25 °C (lane 4). The reduced form was obtained by treatment with 5 m*M* DTT for 5 min, at 25 °C (lane 3). To test the reversibility of the oxidation process, samples obtained by oxidation with 2.5 m*M* diamide were subsequently treated with an excess of 50 m*M* DTT for 5 min, at 25 °C (lane 5). At the end of the treatments, 90 ng of purified Pax-8 were incubated with the oligonucleotide C (0.1 pmol), for 20 min, at 25 °C and loaded onto a native polyacrylamide gel for EMSA analysis. The arrow indicates the position of the protein–DNA complex. Panel C, Purified recombinant Prd domain Pax-8 (10 μg) was incubated with 5 m*M* DTT (lane 1), with 5 m*M* diamide (lane 2) for 5 min, at 25 °C, or oxidized by prolonged air exposure (lane 3). To test the reversibility of the oxidation process, samples obtained by oxidation with 2.5 m*M* diamide were subsequently treated with an excess of 50 m*M* DTT, for 5 min, at 25 °C (lane 4). Samples were then separated on a 15% SDS-PAGE; gel was stained with Coomassie Blue R-250. The arrow indicates the faster migrating form of the Pax-8 Prd domain.

2.2. Alkylation of protein samples with iodoacetamide and ESI-quadrupole-MS analysis

To assess cysteine oxidation status, protein samples were alkylated with 1.1 *M* iodoacetamide in 0.25 *M* Tris–HCl, 1.25 m*M* EDTA, containing 6 *M* guanidinium chloride pH 7.0, at 25 °C, for 1 min, in the dark. Proteins were freed from salt and reagent excess by passing the reaction mixture through an analytical Vydac C_4 column, as previously reported (Cecconi *et al.*, 2002; Vilardo *et al.*, 2001). Protein samples were manually collected and lyophilized. ESI mass spectra of intact protein species were recorded using a Platform-single quadrupole mass spectrometer (Micromass, UK). Multiply-charged data were accumulated over the range m/z 400–1800, and the spectra transformed onto a molecular-mass scale by using the Maximum Entropy (Micromass) technique. Mass calibration was performed by means of the multiply-charged ions from a separate injection of horse-heart myoglobin (molecular mass 16,951.5 Da). All masses are reported as average values.

2.3. Enzymatic digestion and MALDI-TOF peptide-mapping experiments

Samples of carboxamidomethylated proteins oxidized under various conditions (50 μg) were digested with trypsin in 50 m*M* NH_4HCO_3, pH 6.5, at 37 °C, overnight, using an enzyme/substrate ratio of 1:100 (w/w) and lyophilized. MALDI mass spectra were recorded using a Voyager DE-PRO MALDI-TOF mass spectrometer (Applied Biosystems, USA); peptide mixtures were loaded on the MALDI target, using the dried droplet technique and α-cyano-4-hydroxycinnamic acid as matrix. Internal mass calibration was performed with peptides derived from enzyme autoproteolysis. Spectra were acquired in linear and reflectron mode, elaborated using the DataExplorer 5.1 software (Applied Biosystems) and analyzed using the GPMAW 4.23 software (Lighthouse Data, Denmark), which generated a mass database output based on Pax-8 sequence, protease specificity, and the various dynamic modifications of Cys residues described in this work, including peptide cross-linking.

3. Results

3.1. Combined functional and MS analysis of the Pax-8 Prd domain under various redox conditions

The Prd domain of Pax-8 contains three Cys residues located at position 37 and 49 (PAI subdomain) and 109 (RED subdomain) (Fig. 12.1A). These residues are highly conserved within the whole family of Pax transcription

factors. To identify whether Pax-8 is sensitive to redox potential in the interaction with its respective DNA-binding site, the recombinant protein was treated with 50 m*M* DTT, the oxidizing agent diamide (2.5 m*M*), or was exposed to prolonged air conditions corresponding to an oxidative environment. The binding activity of the Pax-8 Prd domain to the oligonucleotide C (Tell *et al.*, 1998a) was examined by using EMSA. As shown in Fig. 12.1B (lane 2), the binding of the Pax-8 Prd domain, after prolonged air exposure oxidation, was greatly reduced when compared to that obtained with the same protein maintained under reducing conditions (Fig. 12.1B, lane 3). Diamide treatment abolished the interaction of the Prd domain with the oligonucleotide (Fig. 12.1B, lane 4); however, subsequent addition to this sample of a DTT excess completely restored its binding capability (Fig. 12.1B, lane 5), demonstrating that the effects elicited by oxidation were fully reversible and probably mediated by protein Cys residues.

Formation of intermolecular disulfides following oxidative/nitrosative insult generates macroscopic variation of protein molecular mass; on this basis, it has usually been detected by low-resolution techniques such as electrophoresis under nonreducing conditions (Eaton, 2006). To investigate whether the DNA-binding inhibition could be related to the oligomerization state of the Pax-8 Prd domain, we performed SDS-PAGE analysis of the samples used in the EMSA experiments. Pax-8 Prd domain was present as a single monomeric form under reducing conditions (5 m*M* DTT, Fig. 12.1C, lane 1). On the contrary, following a treatment with 2.5 m*M* diamide (Fig. 12.1C, lane 2) or after prolonged air exposure (Fig. 12.1C, lane 3), very slight amounts of dimeric species were also detected. The occurrence under oxidizing conditions of an additional faster migrating monomeric form (see the arrow in Fig. 12.1C) was interpreted as depending upon the presence of an intramolecular disulphide-bridged species with increased compactness (see below). The latter species were readily converted into the unique monomeric form observed under reducing conditions by the simple addition of a DTT excess to the oxidized samples (Fig. 12.1C, lane 4), confirming the reversibility of the phenomenon and thus underlining a possible regulatory role for the oxidation process.

The occurrence of mixed disulfides with low molecular weight compounds or intramolecular disulfides, determining limited variation in molecular mass of intact proteins, has been revealed by conventional MS procedures. In the case of *S*-glutathionylated, *S*-cysteinyl-glycinylated, *S*-cysteinylated, and *S*-sulfonated proteins, the occurrence of *S*-monoconjugated species has been ascertained by direct MS measurements of the intact proteins by detecting the corresponding adducts having a mass difference of +305, +176, +119, and +80 Da, respectively (Dalle-Donne *et al.*, 2005, 2006; Lim *et al.*, 2003), with respect to the reduced species; these adducts revert to the reduced protein after treatment with reducing agents. This approach has also been used

to evaluate the occurrence of Cys-NO, sulfinic, and sulfonic acids in proteins following oxidative/nitrosative insult or cysteines subjected to acrolein, 4-hydroxynonenal, 15-deoxy-Δ^{12-14}-prostaglandin J_2 and nitro-oleic acid addition, which present a mass difference of +29, +32, +48, +56, +156, +316, and +327 Da with respect to the reduced species, respectively (Batthyany *et al.*, 2006; Bennaars-Eiden *et al.*, 2002; Dalle-Donne *et al.*, 2005, 2006; Fang and Holmgren, 2006; Kaiserova *et al.*, 2006; Sehajpal *et al.*, 1999; Shibata *et al.*, 2003; Vunta *et al.*, 2007; Woo *et al.*, 2003; Zech *et al.*, 1999). In the case of intramolecular disulfides, the limited variation in the molecular mass of intact proteins compared with nonoxidized species ($\Delta m = -2$ Da for each S–S bond) determines the need for additional measurements. For this reason, a modification of the MS strategy conventionally used for the titration of free thiols in proteins has been applied to the detection of oxidized cysteines. By simply comparing the molecular-mass value of the intact protein in its native and stressed state, before and following extensive alkylation with iodoacetamide under denaturing nonreducing conditions, the number of the Cys residues involved in oxidative/nitrosative insult and the nature of the modification can be inferred (Cecconi *et al.*, 2002; Kim *et al.*, 2002; Vilardo *et al.*, 2001). In fact, cysteines involved in disulfides will not react with iodoacetamide, thus not generating the corresponding mass increase ($\Delta m = +57$ Da for each available SH), easily detectable by ESI measurements. Assuming a comparable ionization tendency for all the different species obtained following alkylation, this approach can be successfully applied to evaluate the relative amount of the various oxidatively/nitrosatively modified protein products.

Thus, this procedure has been used for the molecular characterization of the cysteine oxidation state in Pax-8 Prd domain samples subjected to various oxidative insults (Fig.12.2). In particular, ESI-Q-MS analysis of Pax-8 treated under reducing conditions revealed the presence of a single component having a molecular mass of 18,775.2 ± 1.1 Da (theor. value 18,774.9 Da). This sample, alkylated with iodoacetamide under denaturing nonreducing conditions, yielded a unique component with a mass value of 18,946.4 ± 1.5 Da (Fig.12.2A), which was ascribed to the introduction of three carboxamidomethyl (CAM) groups per protein molecule, thus demonstrating the fully reduced state of all cysteine residues present in Pax-8 sequence. Samples subjected to prolonged air exposure or treatment with 2.5 m*M* diamide showed a main protein component with a molecular mass of 18,773.6 ± 2.9 and 18,774.1 ± 3.4 Da, respectively. After alkylation with iodoacetamide under denaturing nonreducing conditions, these samples unveiled the occurrence of a mixture of two components with a mass value of 18,829.6 ± 1.3 and 18,947.1 ± 1.2 Da (air exposure) (Fig. 12.2B), and 18,830.2 ± 1.6 and 18,946.9 ± 1.8 Da (diamide) (Fig. 12.2C), present in different relative amounts. These components were associated to a Pax-8 form containing an intramolecular disulfide

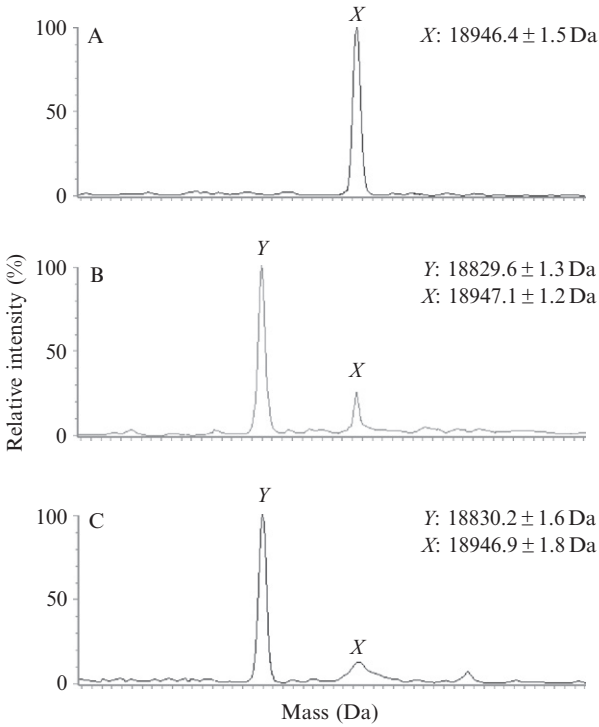

Figure 12.2 ESI-Q MS analysis of the Pax-8 Prd domain samples used in binding experiments following alkylation with iodoacetamide. Panel A, Mass spectrum of the reduced Pax-8 Prd sample after carboxamidomethylation under native nonreducing conditions. Panel B, Mass spectrum of the air-exposed Pax-8 Prd sample after carboxamidomethylation under native nonreducing conditions. Panel C, Mass spectrum of the diamide-treated Pax-8 Prd sample after carboxamidomethylation under native nonreducing conditions. The signals recorded in each spectrum were assigned to the corresponding protein species on the basis of their molecular-mass values.

and a reduced Cys residue and a Pax-8 form containing three reduced Cys residues, respectively. On the other hand, the occurrence of oxidation events leading to the conversion of Pax-8 Cys residues into sulfinic and sulfonic acids was excluded by the absence in the spectra of the alkylated samples of signals corresponding to protein forms containing an intramolecular disulfide and a sulfinic acid (theor. value 18,804.9 Da), an intramolecular disulfide and a sulfonic acid (theor. value 18,820.9 Da), two reduced Cys residues and a sulfinic acid (theor. value 18,920.9 Da), two reduced Cys residues and a sulfonic acid (theor. value 18,936.9 Da), a reduced Cys residue and two sulfinic acids (theor. value 18,895.9 Da), a reduced Cys residue and two sulfonic acids (theor. value 18,927.9 Da), three sulfinic acids (theor. value 18,870.9 Da), or three sulfonic acids (theor. value 18,918.9 Da).

3.2. MS assignment of modified Cys residues in Pax-8 Prd domain

Mixed disulfide assignment to specific Cys residues in protein can be obtained by mass mapping experiments on peptide mixtures generated from carboxamidomethylated species following alkylation under denaturing nonreducing conditions. A careful evaluation of experimental conditions suitable to avoid disulfide scrambling phenomena during protein hydrolysis is strongly recommended. Identification of the modified residues has been obtained by LC–ESI or MALDI-TOF peptide-mapping experiments, by detecting the peptides bearing a mass difference of +305 Da (*S*-glutathionylated), +176 Da (*S*-cysteinyl-glycinylated), +119 Da (*S*-cysteinylated), and +80 Da (*S*-sulfonated) with respect to the reduced species, and eventually confirmed by CID measurements (Barrett *et al.*, 1999; Cross and Templeton, 2004; Dalle-Donne *et al.*, 2005, 2006; Ghezzi *et al.*, 2006; Lim *et al.*, 2003). Similarly, cysteine pairing identification in species containing intramolecular disulfides as a result of oxidative/nitrosative insult has been derived from mass mapping and MS/MS experiments (Caselli *et al.*, 1998; Cecconi *et al.*, 2002; Chen *et al.*, 2009; Hashemy *et al.*, 2007; Kuge *et al.*, 2001; Sohn and Rudolph 2003; Song *et al.*, 2000; Song *et al.*, 2006; Tell *et al.*, 1998a; Vilardo *et al.*, 2001; Zheng *et al.*, 1998) conventionally used for the assignment of disulfides in native polypeptide species (Amiconi *et al.*, 2000; D'Innocenzo *et al.*, 2006; Hilvo *et al.*, 2008; Scaloni *et al.*, 1999). Analogously, assignment of cysteines that resulted *S*-nitrosylated, oxidized to sulfinic and sulfonic acids, or subjected to acrolein, 4-hydroxynonenal, 15-deoxy-Δ^{12-14}-prostaglandin J_2, and nitro-oleic acid addition has been obtained by MALDI or LC–ESI mass mapping experiments on protein digests, by revealing peptides bearing a mass difference of +29, +32, +48, +56/+38, +156/+138, +316, and +327 Da with respect to the reduced species, and confirmed by CID analysis (Batthyany *et al.*, 2006; Cesaratto *et al.*, 2005; Choi *et al.*, 2004; D'Elia *et al.*, 2003; Dalle-Donne *et al.*, 2005, 2006; Go *et al.*, 2007; Gu *et al.*, 2002; Kaiserova *et al.*, 2006; Kamata *et al.*, 2005; Lambert *et al.*, 2007; Martínez-Ruiz *et al.*, 2005; Oliva *et al.*, 2003; Pérez-Sala *et al.*, 2003; Rabilloud *et al.*, 2002; Romero-Puertas *et al.*, 2007; Salmeen *et al.*, 2003; Shibata *et al.*, 2003; Wagner *et al.*, 2002; Yang *et al.*, 2002). Generally, peptides containing cysteic acid have shown suppressed ionization, thus dedicated procedures have been developed for their analysis (Kinumi *et al.*, 2006). On the other hand, the reported instability of Cys-*S*-NO-containing peptides promoted the development of optimal MS conditions for their detection (Chen *et al.*, 2007; Hao and Gross, 2006; Mirza *et al.*, 1995; Wang *et al.*, 2008; Zhukova *et al.*, 2004) or its chemical modification before analysis (Camerini *et al.*, 2007; Forrester *et al.*, 2009b; Greco *et al.*, 2006; Han and Chen, 2008; Hao *et al.*, 2006).

MALDI-TOF peptide-mapping experiments were sufficient for the characterization of disulfide-containing Pax-8 species. In particular, Fig. 12.3 shows the mass spectra obtained for the tryptic digests of an air-exposed Prd domain sample of Pax-8 alkylated under native conditions, of an air-exposed sample of Pax-8 Prd domain, and of a reduced and alkylated Prd domain sample of Pax-8. Very similar results were obtained for air-exposed and diamide-treated samples of Pax-8 Prd domain (data not shown). In all cases, MALDI-TOF MS analysis allowed the verification of most of the protein primary structure and the determination of the redox state of the cysteine residues. The nature of the peptides containing a S–S bridge was confirmed by the reduction of the peptide mixtures with DTT followed by MALDI-TOF-MS detection of the two reduced fragments (data not shown). In the case of the air-exposed Prd domain sample of Pax-8 alkylated under native conditions (Fig. 12.2A), in addition to the signals at m/z 1836.7 and 2147.1, originated from the peptides (26–41) and (103–122) carboxamidomethylated at Cys37 and Cys109, respectively, two clear peaks at m/z 2593.8 and 2904.2 were present in the spectrum. These signals were assigned to the peptide pair (26–41) + (45–52) linked by a S–S bridge between Cys37 and Cys49 and to the peptide pair (45–52) + (103–122) linked by a S–S bridge between Cys49 and Cys109, respectively. Signals corresponding to other possible carboxamidomethylated or disulfide-bridged peptides were not present in the spectrum. In the case of the air-exposed Prd domain sample of Pax-8, the two signals corresponding to the peptides containing a disulphide bridge were still present in the spectrum at m/z 2594.2 and 2903.9, respectively (Fig. 12.2B). MALDI-TOF MS analysis also revealed peaks at m/z 1779.8 and 2090.1 associated to peptides (26–41) and (103–122) containing Cys37 and Cys109 in reduced form. On the contrary, the spectrum of the reduced and alkylated Prd domain sample of Pax-8 did not show the signals corresponding to the peptides containing the disulphide bridge (Fig. 12.2C). The signals at m/z 873.9, 1836.9, and 2147.3 clearly indicated that peptides (26–41), (45–52), and (103–122) presented fully carboxamidomethylated Cys37, Cys49, and Cys109.

These results demonstrated that the air-exposed and diamide-treated samples of Pax-8 Prd domain, having a reduced ability to bind DNA, were constituted of variable amounts of three molecular species. The first component presented Cys109 in a reduced form and a S–S bond between Cys37 and Cys49; the second one was characterized by the presence of a reduced Cys37 and the disulphide bridge between Cys49 and Cys109; the third one had all cysteines in a reduced state. The latter species was present in reduced amounts or practically absent in air-exposed and diamide-treated samples of Pax-8 Prd domain, respectively. In contrast, under conditions in which an effective DNA binding was detected, all the Cys residues of the protein were present in a completely reduced form.

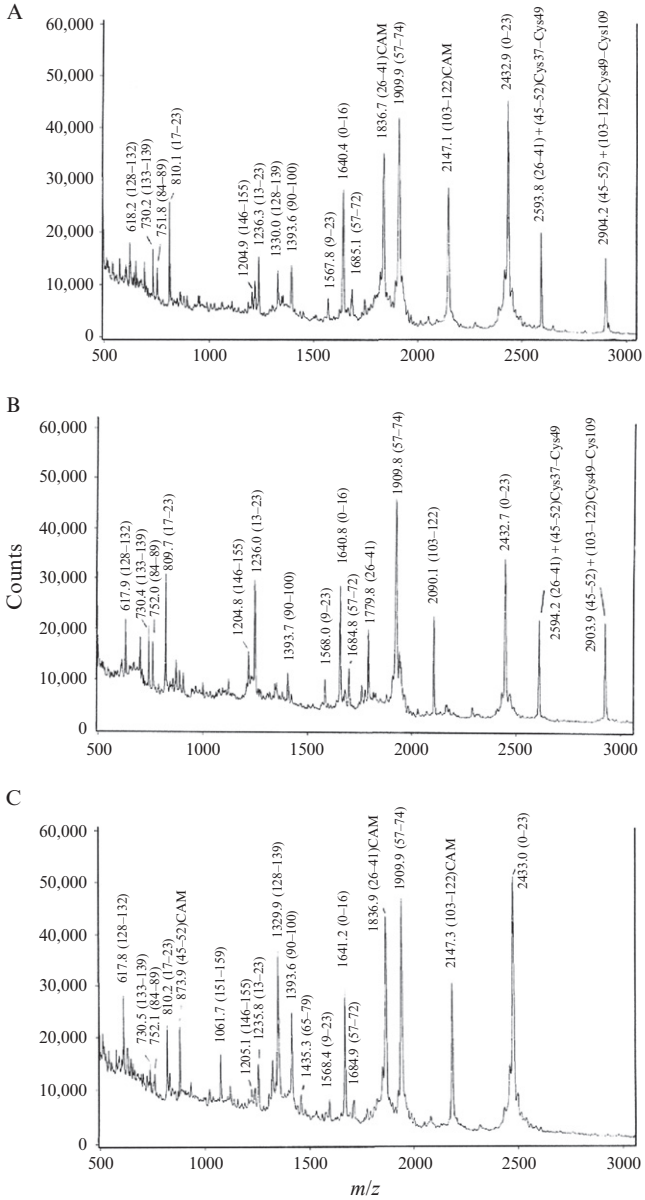

Figure 12.3 MALDI-TOF MS analysis of the Pax-8 Prd domain samples used in binding experiments following alkylation and digestion with trypsin. Panel A, Mass spectrum of the air-exposed Pax-8 Prd sample after carboxamidomethylation under native conditions. Panel B, Mass spectrum of the air-exposed Pax-8 Prd sample. Panel C, Mass spectrum of the reduced and carboxamidomethylated Pax-8 Prd sample. The signals recorded in each spectrum were assigned to the corresponding peptides

3.3. Functional role of the modified Cys residues on Pax-8 activity

Pax-8 DNA-binding activity has been found to depend on a redox reaction performed by the multifunctional endonuclease APE1/Ref-1 (Tell *et al.*, 2005, 2009, 2010) (Fig. 12.4). This protein ensures the reduction of two redox-sensitive cysteines in Pax-8 namely Cys37 and Cys49 (Tell *et al.*, 1998a,b), whose thiol moiety has been demonstrated to be essential for effective binding to DNA (see MS data reported earlier). Thus, thyrothropin (TSH)-dependent expression of thyroglobulin in thyroid cells was found to depend on ROS/cAMP-mediated activation of the redox functions of APE1/Ref-1 over Pax-8 transcriptional activity (Tell *et al.*, 2005). Site-directed mutagenesis experiments further demonstrated the essential role of APE1/Ref-1 in maintaining the reduced state of the redox-active Cys residues in Pax-8 Prd domain, thus allowing active DNA-binding over the Tg promoter sequence (Fig. 12.4). Interestingly, Pax-8 glutathionylation at Cys37 and Cys49, which occurs *in vivo*, has been proposed to prevent nucleotide binding by perturbing DNA–protein complex interface (Cao *et al.*, 2005). Importantly, such modifications require accessible and highly reactive thiol groups within the Prd domain. Indeed, Cys37 and Cys49 are highly accessible to the solvent, as demonstrated in the Pax-8 Prd domain structure recently determined in solution (Codutti *et al.*, 2008). pK_a calculations, performed on the Prd domains of Pax-5, Pax-6, homology-modeled Pax-8, and the 20 NMR structures available, showed confirmatory results. For all the Pax-8 models, a significant pK_a shift toward physiological pH values has been found for Cys37 (pK_a 7.9 $\pm$ 0.2) and Cys49 (pK_a 7.6 $\pm$ 0.3) thiol groups; conversely, Cys109 showed a slight shift toward alkaline pH values (pK_a 8.9 $\pm$ 0.7). Structurally, the anionic state of Cys37 and Cys49 seems to be stabilized by vicinal positively charged residues, such as Arg35, Arg41, and Lys52, conserved within the whole Pax family. Similar pK_a shifts have been found also for Pax-5 and Pax-6 homolog cysteines, showing that this feature is common to all proteins. Furthermore, the PAI subdomain cysteines were found to be accessible to the solvent (100% of the structures for Cys37 and 90% for Cys49), whereas Cys109 was more buried (accessible in 40% of the structures). Thus, as Cys37 and Cys49 are solvent exposed, it is unlikely that the DNA-binding inhibition due to glutathionylation is caused by a partial unfolding of the Prd domain, but rather by a masking effect on a large part of the DNA-binding interface. In conclusion,

within the protein sequence on the basis of their molecular mass. The signals of the disulfide-containing peptides are indicated with the corresponding peptide pairs, highlighting the cysteine involved in the S–S bridge. Peptides were numbered as previously reported for other Pax proteins (Tell *et al.*, 1998b).

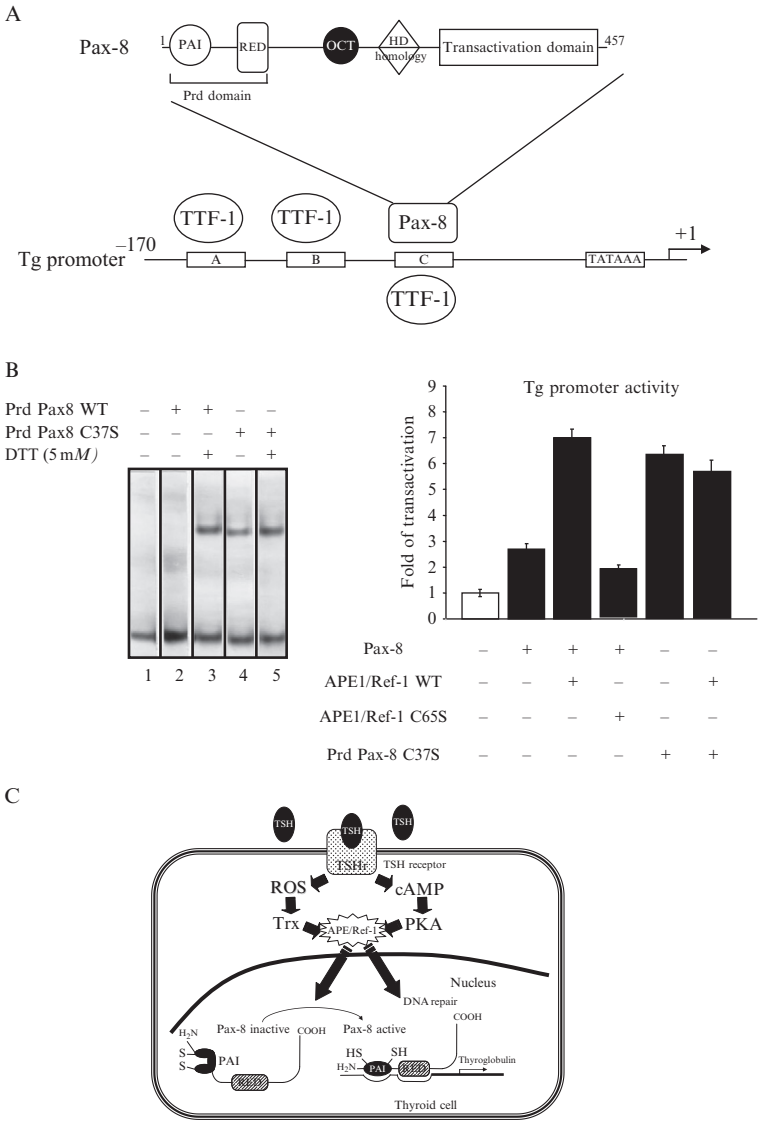

Figure 12.4 Functional relevance of the redox regulation of Pax-8 transcriptional activity. Panel A, Schematic representation of the domain organization of Pax-8 transcription factor. Prd represents the DNA-binding domain of Pax-8 and is organized in two independent H-T-H subdomains called PAI and RED (Tell *et al.*, 1999). OCT represents the octapeptide sequence, while HD represents the partial homeodomain sequence typical of the Pax-8 class of transcription factors (Tell *et al.*, 1997). Panel B, Redox status of Cys37 of Prd domain controls Pax-8 DNA-binding activity (left) and its transactivation properties on Thyroglobulin (Tg) promoter (right). *Left*: EMSA analysis of the oxidized and reduced forms of the wild-type Pax-8 Prd domain and of the Cys37

the intrinsic structure of the helix-turn-helix fold in the unbound Prd domain is responsible for the reactivity of the Cys37 and Cys49. Structural reasons can be also claimed to explain the reduced activity of Cys109, which results mostly buried and with a thiol pK_a shifted toward alkaline values. All these features are conserved also in Pax-5 and Pax-6 Prd domains, thus suggesting an important functional role for the conserved PAI cysteines.

4. Conclusions and Future Perspectives

Nowadays, redox-dependent posttranslational protein modifications have emerged as cell-signaling mechanisms linking cell machineries to various physiological and pathological/stressing status (Hess *et al.*, 2005; Janssen-Heininger *et al.*, 2008; Rhee, 2006; Rudolph and Freeman, 2009). The plethora of enzymes involved in the generation and degradation of ROS/RNS and in the recovery/degradation of oxidatively/nitrosatively modified proteins underline the importance of redox-related modification events for cellular function (Dalle-Donne *et al.*, 2006; Rhee, 2006). Specific Cys residues that are redox sensitive and functionally important have been identified in various proteins involved in downstream signaling events. In this contest, MS-based studies on isolated proteins allowed the recognition of redox-responsive thiols in (i) NF-kB (Lambert *et al.*, 2007; Matthews *et al.*, 1996, Vunta *et al.*, 2007), AP-1 (Pérez-Sala *et al.*, 2003), Nrf2/Keap-1 (Dinkova-Kostova *et al.*, 2002; Hong *et al.*, 2005; Wakabayashi *et al.*, 2004), c-Jun (Klatt *et al.*, 1999), OxyR (Kim *et al.*, 2002; Zheng *et al.*, 1998), Yap1p (Kuge *et al.*, 2001), and Pax-8 (Tell *et al.*, 1998a) transcription factors; (ii) matrix (Fu *et al.*, 2001; Gu *et al.*, 2002; Okamoto *et al.*, 2001), HIV-1 (Sehajpal *et al.*, 1999), and caspase (Zech *et al.*, 1999) proteases; (iii) cyclophilin A (Ghezzi *et al.*, 2006), HSP60 (Hamnell-Pamment *et al.*, 2005), and HSP90 (Carbone *et al.*, 2005; Martínez-Ruiz *et al.*, 2005) chaperones;

to Ser mutant (C37S) of Pax-8 Prd domain incubated with the C sequence. Cys to Ser mutation abolishes redox-sensitivity of the Prd DNA-binding activity. *Right*: Effect of APE1/Ref-1 on the activity on the Pax-8 transcriptional activity. Plasmids were transfected in HeLa cells at the concentration indicated in Section 2. Forty-eight hours after transfection, cells were harvested and CAT and Luc activities were measured. Mutation of the Cys37 to Ser in Pax-8 Prd domain abolished APE1/Ref-1 redox-mediated activation of Pax-8 transcriptional activity and conferred Pax-8 a "gain of function" phenotype. Note that the "redox-inactive" form of APE1/Ref-1 (Tell *et al.*, 2005) does not play any role in the Pax-8 mediated activation of the Tg promoter. Panel C, Biological model of the APE1/Ref-1 redox-mediated activation of Pax-8 transcriptional activity on thyroid-specific genes. Activation of the redox function of APE1/Ref-1 over Pax-8 Prd domain may be caused by increased ROS production and/or cAMP levels as a consequence of TSH stimulation of thyroid cells (Tell *et al.*, 2005, 2009, 2010).

(iv) GTPase members (Oliva *et al.*, 2003); (v) peroxisome proliferators-activated receptors (Elbrecht *et al.*, 1999; Lee *et al.*, 2002); (vi) transient receptor channels (Macpherson *et al.*, 2007); (vii) protein Tyr/Ser/Thr phosphatases (Barrett *et al.*, 1999; Caselli *et al.*, 1998; Chen *et al.*, 2007, 2009; Kamata *et al.*, 2005; Salmeen *et al.*, 2003; Sohn and Rudolph 2003); (viii) various metabolite and protein kinases (Cross and Templeton, 2004; Song *et al.*, 2000; Whalen *et al.*, 2007); and (ix) other important enzymes (Batthyany *et al.*, 2006; Bennaars-Eiden *et al.*, 2002; Casagrande *et al.*, 2002; Choi *et al.*, 2004; Fang and Holmgren, 2006; Go *et al.*, 2007; Haendeler *et al.*, 2002; Hao *et al.*, 2004; Hashemy *et al.*, 2007; Kaiserova *et al.*, 2006; Shibata *et al.*, 2003; Song *et al.*, 2006; Woo *et al.*, 2003; Yang *et al.*, 2002; Zhukova *et al.*, 2004). These highly conserved signaling pathways involving protein with sensitive thiols allow organisms to respond to oxidative insults, enhancing a capability for stress-related adaptive signaling reactions to oxidants and free radical mediators of inflammation and metabolic stress, and to electrophilic species that are present in the diet or generated as a consequence of toxin exposure. The availability of more incisive chemical and bioanalytical strategies for identifying and quantifying both the mediators and the molecular targets of these redox-signaling mechanisms is now propelling original discoveries in this area.

Recent studies have shown that there exist subproteomes that are targets of redox thiol-directed modifications. In fact, various proteomic techniques applied to the analysis of oxidatively/nitrosatively stressed biological tissues/fluids have unveiled specific groups of proteins that are modified in a parallel mode. These studies, whenever based on bidimensional electrophoresis (2-DE) analysis, have used protein labeling with modification-specific staining procedures (Bennaars-Eiden *et al.*, 2002; Brennan *et al.*, 2006; Charles *et al.*, 2007; Eaton, 2006; Ghezzi and Bonetto, 2003; Grimsrud *et al.*, 2008; Leonard *et al.*, 2009; Liebler, 2008; Pérez-Sala *et al.*, 2003) or have detected a variable availability of protein thiol groups to labeling with aspecific staining reagents (Bruschi *et al.*, 2009; Cuddihy *et al.*, 2009; Eaton, 2006; Forrester *et al.*, 2009b; Han *et al.*, 2008; Huang *et al.*, 2009; Saurin *et al.*, 2004; Tello *et al.*, 2009). In both cases, identification of the proteins containing redox-sensitive cysteines was obtained by spot digestion and LC–ESI-MS/MS or MALDI-TOF MS analysis.

Despite the contributions of 2-DE-based methods to the proteomic studies of thiol-modified proteins, 2-DE has a number of well-described limitations as a general platform for large-scale proteomic studies, including the analysis of membrane and low-abundance proteins. Therefore, "gel-free" proteomic approaches are now finding a more widespread diffusion, seeming particularly useful for the analysis of *in vivo* protein oxidation events, where a low degree of modification is generally observed. These methods are generally based on the digestion of whole-cell protein lysates, selective trapping of modified cysteine-containing peptides by affinity

techniques, and direct LC-ESI-MS/MS identification of the modified residues (Camerini *et al.*, 2007; Codreanu *et al.*, 2009; Forrester *et al.*, 2009a; Fu *et al.*, 2009; Greco *et al.*, 2006; Grimsrud *et al.*, 2008; Han and Chen, 2008; Hao *et al.*, 2006; Kim *et al.*, 2009; Leichert *et al.*, 2008; Liebler, 2008; Sethuraman *et al.*, 2004). Some of these applications will be discussed in detail in other chapters. These approaches are now unveiling subsets of proteins having cysteines susceptible to oxidative/nitrosative insult (Fu *et al.*, 2009; Leichert *et al.*, 2008; Sethuraman *et al.*, 2004) or, more incisively, disulfide-containing (Hains and Truscott, 2008), *S*-4-hydroxynonenal-addicted- (Codreanu *et al.*, 2009; Kim *et al.*, 2009; Sobecki *et al.*, 2009) and *S*-nitroso-proteomes (Camerini *et al.*, 2007; Forrester *et al.*, 2009a; Greco *et al.*, 2006; Han and Chen, 2008; Hao *et al.*, 2006) in various biological tissues/fluids. In some cases, quantitative methods based on the use of isobaric reagents have also been coupled to these investigations (Forrester *et al.*, 2009a; Fu *et al.*, 2009; Leichert *et al.*, 2008; Sethuraman *et al.*, 2004). Thus, novel protein targets of ROS and RNS are now being continuously discovered, elucidating unknown pathways that are activated or inactivated in a controlled manner.

ACKNOWLEDGMENTS

This work was partially supported by grants from the Italian National Research Council (RSTL 862) and Ministero dell'Istruzione, dell'Università e della Ricerca Scientifica (MIUR PRIN2008CCPKRP_002) to A. S. and from MIUR (FIRB RBRN07BMCT_008 and PRIN2008CCPKRP_003) and Regione Friuli-Venezia Giulia to G. T.

REFERENCES

Amiconi, G., Amoresano, A., Boumis, G., Brancaccio, A., De Cristofaro, R., De Pascalis, A., Di Girolamo, S., Maras, B., and Scaloni, A. (2000). A novel venombin B from *Agkistrodon contortrix contortrix*: Evidence for recognition properties in the surface around the primary specificity pocket different from thrombin. *Biochemistry* **39,** 10294–10308.

Barrett, W. C., DeGnore, J. P., König, S., Fales, H. M., Keng, Y. F., Zhang, Z. Y., Yim, M. B., and Chock, P. B. (1999). Regulation of PTP1B via glutathionylation of the active site Cys215. *Biochemistry* **38,** 6699–6705.

Batthyany, C., Schopfer, F. J., Baker, P. R., Durán, R., Baker, L. M., Huang, Y., Cerveñansky, C., Branchaud, B. P., and Freeman, B. A. (2006). Reversible post-translational modification of proteins by nitrated fatty acids in vivo. *J. Biol. Chem.* **281,** 20450–20463.

Bennaars-Eiden, A., Higgins, L., Hertzel, A. V., Kapphahn, R. J., Ferrington, D. A., and Bernlohr, D. A. (2002). Covalent modification of epithelial fatty acid-binding protein by 4-hydroxynonenal in vitro and in vivo. Evidence for a role in antioxidant biology. *J. Biol. Chem.* **277,** 50693–50702.

Brennan, J. P., Miller, J. I., Fuller, W., Wait, R., Begum, S., Dunn, M. J., and Eaton, P. (2006). The utility of N,N-biotinyl glutathione disulfide in the study of protein S-glutathiolation. *Mol. Cell. Proteomics* **5,** 215–225.

Bruschi, M., Grilli, S., Candiano, G., Fabbroni, S., Della Ciana, L., Petretto, A., Cantucci, L., Urbani, A., Gusmano, R., Scolari, F., and Ghiggeri, G. M. (2009). New iodo-acetamido cyanines for labeling cysteine thiol residues. A strategy for evaluating plasma proteins and their oxido-redox status. *Proteomics* **9,** 460–469.

Camerini, S., Polci, M. L., Restuccia, U., Usuelli, V., Malgaroli, A., and Bachi, A. (2007). A novel approach to identify proteins modified by nitric oxide: The HIS-TAG switch method. *J. Proteome Res.* **6,** 3224–3231.

Cao, X., Kambe, F., Lu, X., Kobayashi, N., Ohmori, S., and Seo, H. (2005). Glutathionylation of two cysteine residues in paired domain regulates DNA binding activity of Pax-8. *J. Biol. Chem.* **280,** 25901–25906.

Carbone, D. L., Doorn, J. A., Kiebler, Z., Ickes, B. R., and Petersen, D. R. (2005). Modification of heat shock protein 90 by 4-hydroxynonenal in a rat model of chronic alcoholic liver disease. *J. Pharmacol. Exp. Ther.* **315,** 8–15.

Casagrande, S., Bonetto, V., Fratelli, M., Gianazza, E., Eberini, I., Massignan, T., Salmona, M., Chang, G., Holmgren, A., and Ghezzi, P. (2002). Glutathionylation of human thioredoxin: A possible crosstalk between the glutathione and thioredoxin systems. *Proc. Natl. Acad. Sci. USA* **99,** 9745–9749.

Caselli, A., Marocchini, R., Camici, G., Manao, G., Moneti, G., Pieraccini, G., and Ramponi, G. (1998). The inactivation mechanism of low molecular weight phosphotyrosine-protein phosphatase by H_2O_2. *J. Biol. Chem.* **273,** 32554–32560.

Cecconi, I., Scaloni, A., Rastelli, G., Moroni, M., Vilardo, P. G., Costantino, L., Cappiello, M., Garland, D., Carper, D., Petrash, J. M., Del Corso, A., and Mura, U. (2002). Oxidative modification of aldose reductase induced by copper ion. Definition of the metal-protein interaction mechanism. *J. Biol. Chem.* **277,** 42017–42027.

Cesaratto, L., Vascotto, C., D'Ambrosio, C., Scaloni, A., Baccarani, U., Paron, I., Damante, G., Calligaris, S., Quadrifoglio, F., Tiribelli, C., and Tell, G. (2005). Over-oxidation of peroxiredoxins as an immediate and sensitive marker of oxidative stress in HepG2 cells and its application to the redox effects induced by ischemia/reperfusion in human liver. *Free Radic. Res.* **39,** 255–268.

Charles, R. L., Schröder, E., May, G., Free, P., Gaffney, P. R., Wait, R., Begum, S., Heads, R. J., and Eaton, P. (2007). Protein sulfenation as a redox sensor: Proteomics studies using a novel biotinylated dimedone analogue. *Mol. Cell. Proteomics* **6,** 1473–1484.

Chen, Y. Y., Huang, Y. F., Khoo, K. H., and Meng, T. C. (2007). Mass spectrometry-based analyses for identifying and characterizing S-nitrosylation of protein tyrosine phosphatases. *Methods* **42,** 243–249.

Chen, C. Y., Willard, D., and Rudolph, J. (2009). Redox regulation of SH2-domain-containing protein tyrosine phosphatases by two backdoor cysteines. *Biochemistry* **48,** 1399–1409.

Choi, J., Levey, A. I., Weintraub, S. T., Rees, H. D., Gearing, M., Chin, L., and Li, L. (2004). Oxidative modifications and don-regulation of ubiquitin C-terminal hydrolase L1 associated with idiopathic Parkinson's and Alzheimer's diseases. *J. Biol. Chem.* **279,** 13256–13264.

Codreanu, S. G., Zhang, B., Sobecki, S. M., Billheimer, D. D., and Liebler, D. C. (2009). Global analysis of protein damage by the lipid electrophile 4-hydroxy-2-nonenal. *Mol. Cell. Proteomics* **8,** 670–680.

Codutti, L., van Ingen, H., Vascotto, C., Fogolari, F., Corazza, A., Tell, G., Quadrifoglio, F., Viglino, P., Boelens, R., and Esposito, G. (2008). The solution structure of DNA-free Pax-8 paired box domain accounts for redox regulation of transcriptional activity in the Pax protein family. *J. Biol. Chem.* **283,** 33321–33328.

Cross, J. V., and Templeton, D. J. (2004). Oxidative stress inhibits MEKK1 by site-specific glutathionylation in the ATP-binding domain. *Biochem. J.* **381,** 675–683.

Cuddihy, S. L., Baty, J. W., Brown, K. K., Winterbourn, C. C., and Hampton, M. B. (2009). Proteomic detection of oxidized and reduced thiol proteins in cultured cells. *Methods Mol. Biol.* **519,** 363–375.

Dai, J., Wang, J., Zhang, Y., Lu, Z., Yang, B., Li, X., Cai, Y., and Qian, X. (2005). Enrichment and identification of cysteine-containing peptides from tryptic digests of performic oxidized proteins by strong cation exchange LC and MALDI-TOF/TOF MS. *Anal. Chem.* **77,** 7594–7604.

Dalle-Donne, I., Scaloni, A., Giustarini, D., Cavarra, E., Tell, G., Lungarella, G., Colombo, R., Rossi, R., and Milzani, A. (2005). Proteins as biomarkers of oxidative/nitrosative stress in diseases: The contribution of redox proteomics. *Mass Spectrom. Rev.* **24,** 55–99.

Dalle-Donne, I., Scaloni, A., and Butterfield, D. A. (2006). Redox Proteomics: From Protein Modifications to Cellular Dysfunction and Diseases. Wiley, pp. 1–944.

D'Elia, A., Paron, I., D'Ambrosio, C., Scaloni, A., D'Aurizio, F., Prescott, A., Damante, G., and Tell, G. (2003). A proteomic approach to identify early molecular targets of oxidative stress in human epithelial lens cells. *Biochem. J.* **378,** 929–937.

Dinkova-Kostova, A. T., Holtzclaw, W. D., Cole, R. N., Itoh, K., Wakabayashi, N., Katoh, Y., Yamamoto, M., and Talalay, P. (2002). Direct evidence that sulfhydryl groups of Keap1 are the sensors regulating induction of phase 2 enzymes that protect against carcinogens and oxidants. *Proc. Natl. Acad. Sci. USA* **99,** 11908–11913.

D'Innocenzo, B., Salzano, A. M., D'Ambrosio, C., Gazzano, A., Niccolini, A., Sorce, C., Dani, F. R., Scaloni, A., and Pelosi, P. (2006). Secretory proteins as potential semiochemical carriers in the horse. *Biochemistry* **45,** 13418–13428.

Dröge, W. (2002). Free radicals in the physiological control of cell function. *Physiol. Rev.* **82,** 47–95.

Eaton, P. (2006). Protein thiol oxidation in health and disease: Techniques for measuring disulfides and related modifications in complex protein mixtures. *Free Radic. Biol. Med.* **40,** 1889–1899.

Elbrecht, A., Chen, Y., Adams, A., Berger, J., Griffin, P., Klatt, T., Zhang, B., Menke, J., Zhou, G., Smith, R. G., and Moller, D. E. (1999). L-764406 is a partial agonist of human peroxisome proliferator-activated receptor gamma. The role of Cys313 in ligand binding. *J. Biol. Chem.* **274,** 7913–7922.

Fang, J., and Holmgren, A. (2006). Inhibition of thioredoxin and thioredoxin reductase by 4-hydroxy-2-nonenal in vitro and in vivo. *J. Am. Chem. Soc.* **128,** 1879–1885.

Forrester, M. T., Thompson, J. W., Foster, M. W., Nogueira, L., Moseley, M. A., and Stamler, J. S. (2009a). Proteomic analysis of S-nitrosylation and denitrosylation by resin-assisted capture. *Nat. Biotechnol.* **27,** 557–559.

Forrester, M. T., Foster, M. W., Benhar, M., and Stamler, J. S. (2009b). Detection of protein S-nitrosylation with the biotin-switch technique. *Free Radic. Biol. Med.* **46,** 119–126.

Freeman, B. A., and Crapo, J. D. (1982). Biology of disease: Free radicals and tissue injury. *Lab. Invest.* **47,** 412–426.

Fu, X., Kassim, S. Y., Parks, W. C., and Heinecke, J. W. (2001). Hypochlorous acid oxygenates the cysteine switch domain of pro-matrilysin (MMP-7). A mechanism for matrix metalloproteinase activation and atherosclerotic plaque rupture by myeloperoxidase. *J. Biol. Chem.* **276,** 41279–41287.

Fu, C., Wu, C., Liu, T., Ago, T., Zhai, P., Sadoshima, J., and Li, H. (2009). Elucidation of thioredoxin target protein networks in mouse. *Mol. Cell. Proteomics* **8,** 1674–1687.

Gallogly, M. M., and Mieyal, J. J. (2007). Mechanisms of reversible protein glutathionylation in redox signaling and oxidative stress. *Curr. Opin. Pharmacol.* **7,** 381–391.

Ghezzi, P., and Bonetto, V. (2003). Redox proteomics: Identification of oxidatively modified proteins. *Proteomics* **3,** 1145–1153.

Ghezzi, P., Casagrande, S., Massignan, T., Basso, M., Bellacchio, E., Mollica, L., Biasini, E., Tonelli, R., Eberini, I., Gianazza, E., Dai, W. W., Fratelli, M., *et al.* (2006). Redox regulation of cyclophilin A by glutathionylation. *Proteomics* **6,** 817–825.

Go, Y. M., Halvey, P. J., Hansen, J. M., Reed, M., Pohl, J., and Jones, D. P. (2007). Reactive aldehyde modification of thioredoxin-1 activates early steps of inflammation and cell adhesion. *Am. J. Pathol.* **171,** 1670–1681.

Greco, T. M., Hodara, R., Parastatidis, I., Heijnen, H. F., Dennehy, M. K., Liebler, D. C., and Ischiropoulos, H. (2006). Identification of S-nitrosylation motifs by site-specific mapping of the S-nitrosocysteine proteome in human vascular smooth muscle cells. *Proc. Natl. Acad. Sci. USA* **103,** 7420–7425.

Grimsrud, P. A., Xie, H., Griffin, T. J., and Bernlohr, D. A. (2008). Oxidative stress and covalent modification of protein with bioactive aldehydes. *J. Biol. Chem.* **283,** 21837–21841.

Gu, Z., Kaul, M., Yan, B., Kridel, S. J., Cui, J., Strongin, A., Smith, J. W., Liddington, R., and Lipton, S. A. (2002). S-nitrosylation of matrix metalloproteinases: Signaling pathway to neuronal cell death. *Science* **297,** 1186–1190.

Haendeler, J., Hoffmann, J., Tischler, V., Berk, B. C., Zeiher, A. M., and Dimmeler, S. (2002). Redox regulatory and antiapoptotic functions of thioredoxin depend on S-nitrosylation at Cys69. *Nat. Cell Biol.* **4,** 743–749.

Hains, P. G., and Truscott, R. J. (2008). Proteomic analysis of the oxidation of cysteine residues in human age-related nuclear cataract lenses. *Biochim. Biophys. Acta* **1784,** 1959–1964.

Hamnell-Pamment, Y., Lind, C., Palmberg, C., Bergman, T., and Cotgreave, I. A. (2005). Determination of sitespecificity of S-glutathionylated cellular proteins. *Biochem. Biophys. Res. Commun.* **332,** 362–369.

Han, P., and Chen, C. (2008). Detergent-free biotin switch combined with liquid chromatography/tandem mass spectrometry in the analysis of S-nitrosylated proteins. *Rapid Commun. Mass Spectrom.* **22,** 1137–1145.

Han, P., Zhou, X., Huang, B., Zhang, X., and Chen, C. (2008). On-gel fluorescent visualization and the site identification of S-nitrosylated proteins. *Anal. Biochem.* **377,** 150–155.

Hao, G., and Gross, S. S. (2006). Electrospray tandem mass spectrometry analysis of S- and N-nitrosopeptides: Facile loss of NO and radical-induced fragmentation. *J. Am. Soc. Mass Spectrom.* **17,** 1725–1730.

Hao, G., Xie, L., and Gross, S. S. (2004). Argininosuccinate synthetase is reversibly inactivated by S-nitrosylation in vitro and in vivo. *J. Biol. Chem.* **279,** 36192–36200.

Hao, G., Derakhshan, B., Shi, L., Campagne, F., and Gross, S. S. (2006). SNOSID, a proteomic method for identification of cysteine S-nitrosylation sites in complex protein mixtures. *Proc. Natl. Acad. Sci. USA* **103,** 1012–1017.

Hashemy, S. I., Johansson, C., Berndt, C., Lillig, C. H., and Holmgren, A. (2007). Oxidation and S-nitrosylation of cysteines in human cytosolic and mitochondrial glutaredoxins: Effects on structure and activity. *J. Biol. Chem.* **282,** 14428–14436.

Hess, D. T., Matsumoto, A., Kim, S., Marshall, H. E., and Stamler, J. S. (2005). Protein S-nitrosylation: Purview and parameters. *Nat. Rev. Mol. Cell. Biol.* **6,** 150–166.

Hilvo, M., Baranauskiene, L., Salzano, A. M., Scaloni, A., Matulis, D., Innocenti, A., Scozzafava, A., Monti, S. M., Di Fiore, A., De Simone, G., Lindfors, M., Jänis, J., *et al.* (2008). Biochemical characterization of CA IX, one of the most active carbonic anhydrase isozymes. *J. Biol. Chem.* **283,** 27799–27809.

Hong, F., Sekhar, K. R., Freeman, M. L., and Liebler, D. C. (2005). Specific patterns of electrophile adduction trigger Keap1 ubiquitination and Nrf2 activation. *J. Biol. Chem.* **280,** 31768–31775.

Huang, B., Liao, C. L., Lin, Y. P., Chen, S. C., and Wang, D. L. (2009). S-nitrosoproteome in endothelial cells revealed by a modified biotin switch approach coupled with Western blot-based two-dimensional gel electrophoresis. *J. Proteome Res.* **8,** 4835–4843.

Janssen-Heininger, Y. M., Mossman, B. T., Heintz, N. H., Forman, H. J., Kalyanaraman, B., Finkel, T., Stamler, J. S., Rhee, S. G., and van der Vliet, A. (2008). Redox-based regulation of signal transduction: Principles, pitfalls, and promises. *Free Radic. Biol. Med.* **45,** 1–17.

Kaiserova, K., Srivastava, S., Hoetker, J. D., Awe, S. O., Tang, X. L., Cai, J., and Bhatnagar, A. (2006). Redox activation of aldose reductase in the ischemic heart. *J. Biol. Chem.* **281,** 15110–15120.

Kamata, H., Honda, S., Maeda, S., Chang, L., Hirata, H., and Karin, M. (2005). Reactive oxygen species promote TNFalpha-induced death and sustained JNK activation by inhibiting MAP kinase phosphatases. *Cell* **120,** 649–661.

Kim, S. O., Merchant, K., Nudelman, R., Beyer, W. F. Jr., Keng, T., DeAngelo, J., Hausladen, A., and Stamler, J. S. (2002). OxyR: A molecular code for redox-related signaling. *Cell* **109,** 383–396.

Kim, H. Y., Tallman, K. A., Liebler, D. C., and Porter, N. A. (2009). An azido-biotin reagent for use in the isolation of protein adducts of lipid-derived electrophiles by streptavidin catch and photorelease. *Mol. Cell. Proteomics* **8,** 2080–2089.

Kinumi, T., Shimomae, Y., Arakawa, R., Tatsu, Y., Shigeri, Y., Yumoto, N., and Niki, E. (2006). Effective detection of peptides containing cysteine sulfonic acid using matrix-assisted laser desorption/ionization and laser desorption/ionization on porous silicon mass spectrometry. *J. Mass. Spectrom.* **41,** 103–112.

Klatt, P., Molina, E. P., De Lacoba, M. G., Padilla, C. A., Martinez-Galesteo, E., Barcena, J. A., and Lamas, S. (1999). Redox regulation of c-Jun DNA binding by reversible S-glutathiolation. *FASEB J.* **13,** 1481–1490.

Kuge, S., Arita, M., Murayama, A., Maeta, K., Izawa, S., Inoue, Y., and Nomoto, A. (2001). Regulation of the yeast Yap1p nuclear export signal is mediated by redox signal-induced reversible disulfide bond formation. *Mol. Cell. Biol.* **21,** 6139–6150.

Lambert, C., Li, J., Jonscher, K., Yang, T. C., Reigan, P., Quintana, M., Harvey, J., and Freed, B. M. (2007). Acrolein inhibits cytokine gene expression by alkylating cysteine and arginine residues in the NF-kappaB1 DNA binding domain. *J. Biol. Chem.* **282,** 19666–19675.

Lee, G., Elwood, F., McNally, J., Weiszmann, J., Lindstrom, M., Amaral, K., Nakamura, M., Miao, S., Cao, P., Learned, R. M., Chen, J. L., and Li, Y. (2002). T0070907, a selective ligand for peroxisome proliferator-activated receptor gamma, functions as an antagonist of biochemical and cellular activities. *J. Biol. Chem.* **277,** 19649–19657.

Leichert, L. I., Gehrke, F., Gudiseva, H. V., Blackwell, T., Ilbert, M., Walker, A. K., Strahler, J. R., Andrews, P. C., and Jakob, U. (2008). Quantifying changes in the thiol redox proteome upon oxidative stress in vivo. *Proc. Natl. Acad. Sci. USA* **105,** 8197–8202.

Leonard, S. E., Reddie, K. G., and Carroll, K. S. (2009). Mining the thiol proteome for sulfenic acid modifications reveals new targets for oxidation in cells. *ACS Chem. Biol.* **4,** 783–799.

Liebler, D. C. (2008). Protein damage by reactive electrophiles: Targets and consequences. *Chem. Res. Toxicol.* **21,** 117–128.

Lim, A., Prokaeva, T., McComb, M. E., Connors, L. H., Skinner, M., and Costello, C. E. (2003). Identification of S-sulfonation and S-thiolation of a novel transthyretin Phe33Cys variant from a patient diagnosed with familial transthyretin amyloidosis. *Protein Sci.* **12,** 1775–1785.

López-Sánchez, L. M., Muntané, J., de la Mata, M., and Rodríguez-Ariza, A. (2009). Unraveling the S-nitrosoproteome: Tools and strategies. *Proteomics* **9,** 808–818.

Macpherson, L. J., Dubin, A. E., Evans, M. J., Marr, F., Schultz, P. G., Cravatt, B. F., and Patapoutian, A. (2007). Noxious compounds activate TRPA1 ion channels through covalent modification of cysteines. *Nature* **445,** 541–545.

Martínez-Ruiz, A., Villanueva, L., González de Orduña, C., López-Ferrer, D., Higueras, M. A., Tarín, C., Rodríguez-Crespo, I., Vázquez, J., and Lamas, S. (2005). S-nitrosylation of Hsp90 promotes the inhibition of its ATPase and endothelial nitric oxide synthase regulatory activities. *Proc. Natl. Acad. Sci. USA* **102,** 8525–8530.

Matthews, J. R., Botting, C. H., Panico, M., Morris, H. R., and Hay, R. T. (1996). Inhibition of NF-kB DNA binding by nitric oxide. *Nucleic Acids Res.* **24,** 2236–2242.

Mikesh, L. M., Ueberheide, B., Chi, A., Coon, J. J., Syka, J. E., Shabanowitz, J., and Hunt, D. F. (2006). The utility of ETD mass spectrometry in proteomic analysis. *Biochim. Biophys. Acta* **1764,** 1811–1822.

Mirza, U., Chait, B., and Lander, H. M. (1995). Monitoring reactions of nitric oxide with peptides and proteins by electrospray ionization mass spectrometry. *J. Biol. Chem.* **270,** 17185–17188.

Okamoto, T., Akaike, T., Sawa, T., Miyamoto, Y., van der Vliet, A., and Maeda, H. (2001). Activation of matrix metalloproteinases by peroxynitrite-induced protein S-glutathiolation via disulfide S-oxide formation. *J. Biol. Chem.* **276,** 29596–29602.

Oliva, J. L., Pérez-Sala, D., Castrillo, A., Martínez, N., Cañada, F. J., Boscá, L., and Rojas, J. M. (2003). The cyclopentenone 15-deoxy-Δ12, 14-prostaglandin J2 binds to and activates H-Ras. *Proc. Natl. Acad. Sci. USA* **100,** 4772–4777.

Pérez-Sala, D., Cernuda-Morollón, E., and Cañada, F. J. (2003). Molecular basis for the direct inhibition of AP-1 DNA binding by 15-deoxy-Δ12, 14-prostaglandin J2. *J. Biol. Chem.* **278,** 51251–51260.

Rabilloud, T., Heller, M., Gasnier, F., Luche, S., Rey, C., Aebersold, R., Benahmed, M., Louisot, P., and Lunardi, J. (2002). Proteomics analysis of cellular response to oxidative stress. *J. Biol. Chem.* **277,** 19396–19401.

Rhee, S. G. (2006). Cell signaling. H_2O_2, a necessary evil for cell signaling. *Science* **312,** 1882–1883.

Romero-Puertas, M. C., Laxa, M., Mattè, A., Zaninotto, F., Finkemeier, I., Jones, A. M., Perazzolli, M., Vandelle, E., Dietz, K. J., and Delledonne, M. (2007). S-nitrosylation of peroxiredoxin II E promotes peroxynitrite-mediated tyrosine nitration. *Plant Cell* **19,** 4120–4130.

Rudolph, T. K., and Freeman, B. A. (2009). Transduction of redox signaling by electrophile-protein reactions. *Sci. Signal.* **2**(7), 1–13.

Salmeen, A., Andersen, J. N., Myers, M. P., Meng, T. C., Hinks, J. A., Tonks, N. K., and Barford, D. (2003). Redox regulation of protein tyrosine phosphatase 1B involves a sulphenyl-amide intermediate. *Nature* **423,** 769–773.

Saurin, A. T., Neubert, H., Brennan, J. P., and Eaton, P. (2004). Widespread sulfenic acid formation in tissues in response to hydrogen peroxide. *Proc. Natl. Acad. Sci. USA* **101,** 17982–17987.

Scaloni, A., Monti, M., Angeli, S., and Pelosi, P. (1999). Structural analysis and disulfide-bridge pairing of two odorant-binding proteins from *Bombyx mori*. *Biochem. Biophys. Res. Commun.* **266,** 386–391.

Sehajpal, P. K., Basu, A., Ogiste, J. S., and Lander, H. M. (1999). Reversible S-nitrosation and inhibition of HIV-1 protease. *Biochemistry* **38,** 13407–13413.

Sethuraman, M., McComb, M. E., Heibeck, T., Costello, C. E., and Cohen, R. A. (2004). ICAT approach to identify and quantify oxidant-sensitive protein thiols. *Mol. Cell. Proteomics* **3,** 273–278.

Shibata, T., Yamada, T., Ishii, T., Kumazawa, S., Nakamura, H., Masutani, H., Yodoi, J., and Uchida, K. (2003). Thioredoxin as a molecular target of cyclopentenone prostaglandins. *J. Biol. Chem.* **278,** 26046–26054.

Sobecki, S. M., Billheimer, D. D., and Liebler, D. C. (2009). Global analysis of protein damage by the lipid electrophile 4-hydroxy-2-nonenal. *Mol. Cell. Proteomics* **8,** 670–680.

Sohn, J., and Rudolph, J. (2003). Catalytic and chemical competence of regulation of Cdc25 phosphatase by oxidation/reduction. *Biochemistry* **42,** 10060–10070.

Song, E. J., Kim, Y. S., Chung, J. Y., Kim, E., Chae, S. K., and Lee, K. J. (2000). Oxidative modification of nucleoside diphosphate kinase and its identification by matrix-assisted laser desorption/ionization time-of-flight mass spectrometry. *Biochemistry* **39,** 10090–10097.

Song, H., Bao, S., Ramanadham, S., and Turk, J. (2006). Effects of biological oxidants on the catalytic activity and structure of group VIA phospholipase A2. *Biochemistry* **45,** 6392–6406.

Tell, G., Pellizzari, L., and Damante, G. (1997). Transcription factors and cancer. The example of Pax genes. *Adv. Clin. Pathol.* **1,** 243–255.

Tell, G., Scaloni, A., Pellizzari, L., Formisano, S., Pupillo, C., and Damante, G. (1998a). Redox potential controls the structure and DNA binding activity of the paired domain. *J. Biol. Chem.* **273,** 25062–25072.

Tell, G., Pellizzari, L., Cimarosti, D., Pucillo, C., and Damante, G. (1998b). Ref-1 controls pax-8 DNA-binding activity. *Biochem. Biophys. Res. Commun.* **252,** 178–183.

Tell, G., Pellizzari, L., and Damante, G. (1999). Co-operation between the PAI and RED subdomains of Pax-8 in the interaction with thyroglobulin promoter. *Biochem. J.* **337,** 253–262.

Tell, G., Damante, G., Caldwell, D., and Kelley, M. R. (2005). The intracellular localization of APE1/Ref-1: More than a passive phenomenon? *Antioxid. Redox Signal.* **7,** 367–384.

Tell, G., Quadrifoglio, F., Tiribelli, C., and Kelley, M. R. (2009). The many functions of APE1/Ref-1: Not only a DNA-repair enzyme. *Antioxid. Redox Signal.* **11,** 601–620.

Tell, G., Wilson, D. M. III, and Lee, C. H. (2010). Intrusion of a DNA-repair protein in the RNome world: Is this the beginning of a new era? *Mol. Cell. Biol.* **30**:366–371. PubMed PMID: 19901076.

Tello, D., Tarín, C., Ahicart, P., Bretón-Romero, R., Lamas, S., and Martínez-Ruiz, A. (2009). A "fluorescence switch" technique increases the sensitivity of proteomic detection and identification of S-nitrosylated proteins. *Proteomics* (in press).

Vila, A., Tallman, K. A., Jacobs, A. T., Liebler, D. C., Porter, N. A., and Marnett, L. J. (2008). Identification of protein targets of 4-hydroxynonenal using click chemistry for ex vivo biotinylation of azido and alkynyl derivatives. *Chem. Res. Toxicol.* **21,** 432–444.

Vilardo, P. G., Scaloni, A., Amodeo, P., Barsotti, C., Lecconi, I., Cappiello, M., Lopez Mendez, B., Rullo, R., Dal Monte, M., Del Corso, A., and Mura, U. (2001). Thiol/disulfide interconversion in bovine lens aldose reductase induced by intermediates of glutathione turnover. *Biochemistry* **40,** 11985–11994.

Vunta, H., Davis, F., Palempalli, U. D., Bhat, D., Arner, R. J., Thompson, J. T., Peterson, D. G., Reddy, C. C., and Prabhu, K. S. (2007). The anti-inflammatory effects of selenium are mediated through 15-deoxy-Δ12, 14-prostaglandin J2 in macrophages. *J. Biol. Chem.* **282,** 17964–17973.

Wagner, E., Luche, S., Penna, L., Chevallet, M., van Dorsselaer, A., Leize-Wagner, E., and Rabilloud, T. (2002). A method for detection of overoxidation of cysteines: Peroxiredoxins are oxidized in vivo at the active-site cysteine during oxidative stress. *Biochem. J.* **366,** 777–785.

Wakabayashi, N., Dinkova-Kostova, A. T., Holtzclaw, W. D., Kang, M. I., Kobayashi, A., Yamamoto, M., Kensler, T. W., and Talalay, P. (2004). Protection against electrophile

and oxidant stress by induction of the phase 2 response: Fate of cysteines of the Keap1 sensor modified by inducers. *Proc. Natl. Acad. Sci. USA* **101,** 2040–2045.

Wang, Y., Liu, T., Wu, C., and Li, H. (2008). A strategy for direct identification of protein S-nitrosylation sites by quadrupole time-of-flight mass spectrometry. *J. Am. Soc. Mass Spectrom.* **19,** 1353–1360.

Whalen, E. J., Foster, M. W., Matsumoto, A., Ozawa, K., Violin, J. D., Que, L. G., Nelson, C. D., Benhar, M., Keys, J. R., Rockman, H. A., Koch, W. J., Daaka, Y., *et al.* (2007). Regulation of beta-adrenergic receptor signaling by S-nitrosylation of G-protein-coupled receptor kinase 2. *Cell* **129,** 511–522.

Woo, H. A., Chae, H. Z., Hwang, S. C., Yang, K. S., Kang, S. W., Kim, K., and Rhee, S. G. (2003). Reversing the inactivation of peroxiredoxins caused by cysteine sulfinic acid formation. *Science* **300,** 653–656.

Wu, S. L., Jiang, H., Lu, Q., Dai, S., Hancock, W. S., and Karger, B. L. (2009). Mass spectrometric determination of disulfide linkages in recombinant therapeutic proteins using online LC-MS with electron-transfer dissociation. *Anal. Chem.* **81,** 112–122.

Yang, K. S., Kang, S. W., Woo, H. A., Hwang, S. C., Chae, H. Z., Kim, K., and Rhee, S. G. (2002). Inactivation of human peroxiredoxin I during catalysis as the result of the oxidation of the catalytic site cysteine to cysteine-sulfinic acid. *J. Biol. Chem.* **277,** 38029–38036.

Ying, J., Clavreul, N., Sethuraman, M., Adachi, T., and Cohen, R. A. (2007). Thiol oxidation in signaling and response to stress: Detection and quantification of physiological and pathophysiological thiol modifications. *Free Radic. Biol. Med.* **43,** 1099–1108.

Zech, B., Wilm, M., van Eldik, R., and Brune, B. (1999). Mass spectrometric analysis of nitric oxide-modified caspase-3. *J. Biol. Chem.* **274,** 20931–20936.

Zheng, M., Aslund, F., and Storz, G. (1998). Activation of the OxyR transcription factor by reversible disulfide bond formation. *Science* **279,** 1718–1721.

Zhukova, L., Zhukov, I., Bal, W., and Wyslouch-Cieszynska, A. (2004). Redox modifications of the C-terminal cysteine residue cause structural changes in S100A1 and S100B proteins. *Biochim. Biophys. Acta* **1742,** 191–201.

CHAPTER THIRTEEN

A Simple Method to Systematically Study Oxidatively Modified Proteins in Biological Samples and Its Applications

Byoung-Joon Song,* Soo-Kyung Suh,*,[1] *and* Kwan-Hoon Moon*

Contents

Abstract

Increased oxidative stress with elevated levels of reactive oxygen/nitrogen species (ROS/RNS) plays an important role in the pathophysiology of many disease states. Increased ROS/RNS can modulate the cellular macromolecules of DNA, lipids, and proteins, negatively affecting their normal functions. Numerous reports have described the properties and implications of oxidized DNA and lipids. However, oxidative modifications of proteins were not fully studied partially due to the requirement for specific reagents, the lack of methods to detect, purify, and identify oxidatively modified proteins, and the relatively late

* Laboratory of Membrane Biochemistry and Biophysics, National Institute on Alcohol Abuse and Alcoholism, Bethesda, Maryland, USA
[1] Current address: National Center for Toxicological Research, National Institute of Food and Drug Safety Evaluation, Korea Food and Drug Administration, Seoul, Korea

Methods in Enzymology, Volume 473
ISSN 0076-6879, DOI: 10.1016/S0076-6879(10)73013-5

development of highly sensitive analytical instruments. This chapter describes the detailed procedure for systematically identifying oxidative-modified proteins in biological samples. Applications and other suggestions to this method are also described to understand the functional roles of oxidatively modified proteins in promoting endoplasmic reticulum (ER) stress and mitochondrial dysfunction, which ultimately contribute to organ damage.

1. Introduction

It is generally accepted that increased oxidative/nitrosative stress plays an important role in promoting many disease states, including Alzheimer's disease, alcoholism-related organ damage, cancer, cardiovascular diseases, chronic inflammation, diabetes, eye diseases, Huntington's disease, kidney diseases, nonalcoholic liver diseases, Parkinson disease, sepsis, stroke, etc., although the etiological cause for each disease may be different. Exposure to potentially toxic chemicals, drugs, and environmental contaminants or agents, such as heavy metals, smoking, and UV/irradiation, can also produce increased levels of reactive oxygen/nitrogen species (ROS/RNS).

In most cases, disruption of the mitochondrial electron transport chain is known to produce large amounts of ROS (Lin and Beal, 2006). In addition to the ROS production through mitochondrial dysfunction, other enzymes are also known to produce ROS/RNS. These enzymes include: ethanol-inducible cytochrome P450 2E1 (CYP2E1), NADPH-oxidase, xanthine oxidase, and inducible nitric oxide synthase (iNOS) (Caro and Cederbaum, 2004; Kono *et al.*, 2000; Purohit *et al.*, 2009; Song *et al.*, 1996). Increased ROS/RNS interact with cellular macromolecules, such as DNA, lipid, and proteins, to produce oxidized DNAs, lipid peroxides, and oxidized proteins, respectively, and usually negatively affect their physiological functions.

In the past, numerous investigators have reported the increased production of oxidized DNA and lipid peroxides in many pathological states (see reviews by Esterbauer *et al.*, 1991; Minko *et al.*, 2009; Rubbo and Radi, 2008; Wells *et al.*, 2009). However, only a small number of reports systematically described the oxidized proteins under increased oxidative stress in many disease states. Part of the reason could be due to the requirement for specific reagents, the lack of suitable methods to systematically detect, purify, and identify oxidized proteins, and the relatively late development of highly sensitive mass spectral instruments.

Several amino acids are known to be oxidized under increased oxidative/nitrosative stress. For instance, it is known that cysteine (Cys), glutamine (Glu), histidine (His), lysine (Lys), methionine (Met), tyrosine (Tyr), tryptophane (Trp), etc. are oxidatively modified and their physiological functions altered under oxidative/nitrosative stress (Berlett and Stadtman, 1997;

Stadtman *et al.*, 2003). Oxidation of these amino acids in many enzymes usually leads to the formation of carbonylated proteins (with His, Arg, Lys, Pro, Thr, etc.) with concomitant irreversible inactivation of their catalytic activities (Hensley *et al.*, 1995). In contrast, some oxidized cysteines (i.e., sulfenic acid and disulfides) and methionine-sulfoxides are known to be reversibly reduced to cysteine and methionine, respectively, under proper conditions (Stadtman *et al.*, 2003) to regain their normal functions. Despite the possibilities of oxidative modifications of many other amino acids under increased oxidative/nitrosative stress, oxidation of Cys residues in various proteins was evaluated through redox-related Cys-targeted proteomics approaches (Baty *et al.*, 2002; Kim *et al.*, 2000; Sethuraman *et al.*, 2004; Venkatraman *et al.*, 2004), partly because of the availability of relatively specific agents (e.g., *N*-ethylmaleimide (NEM), iodoacetamide, or acid-cleavable isotope-coded affinity tag (ICAT) reagent) toward Cys residues and biotin-conjugated *N*-maleimide (biotin-NM) or biotin-iodoacetamide (BIAM).

Although a few Cys-targeted proteomics approaches have been reported (Kim *et al.*, 2000; Sethuraman *et al.*, 2004; Venkatraman *et al.*, 2004), these methods using BIAM, 4-iodobutyl-triphenylphosphonium, or ICAT reagent may have disadvantages (or limitations) in detecting subtle increments in the amounts of oxidatively modified proteins, primarily because the levels of oxidized proteins labeled with these reagents (e.g., BIAM, 4-iodobutyl-triphenylphosphonium, or ICAT) are inversely related to the increased levels of oxidative stress. To overcome these technical limitations (inconvenience), we have developed a simple, sensitive Cys-targeted biotin-switch method of using biotin-NM as a specific probe to systematically identify the oxidatively modified protein thiols. The levels of the oxidized proteins were positively correlated with increased oxidative stress in alcohol-exposed E47 HepG2 hepatoma cells with overexpressed human CYP2E1 (Suh *et al.*, 2004) and rodent tissues (Kim *et al.*, 2006a; Moon *et al.*, 2006).

As illustrated in Fig. 13.1, we initially labeled the free Cys thiols with NEM. After removing excess NEM by spinning through mini-spin Sephadex G25 columns (Amersham Biosciences-GE Healthcare), we reduced the oxidized cysteines (sulfenic acid, disulfides, mixed disulfides with glutathione, *S*-nitrosylated Cys, etc.) to free Cys thiols with dithiothreitol (DTT). The newly reduced sulfhydryl groups were then labeled with biotin-NM. After removing excess biotin-NM with the second Sephadex G25 mini-spin columns, we detected or affinity-purified biotin-labeled oxidized proteins with either streptavidin-agarose or monoclonal antibody to biotin-conjugated agarose. After washing the nonspecifically bound proteins, agarose-bound biotin-NM-labeled oxidized proteins were dissolved and analyzed by 1D SDS–polyacrylamide gel electrophoresis (PAGE) or 2D PAGE for protein display and identification by mass spectrometric analysis

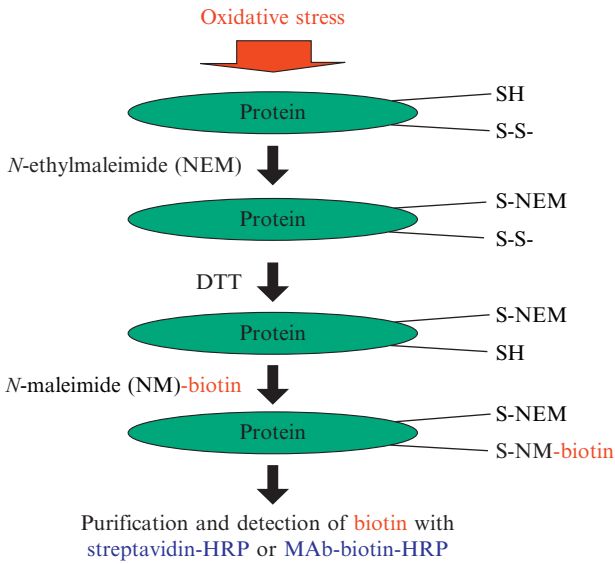

Figure 13.1 Schematic diagram to positively identify oxidized proteins by using a Cys-targeted biotin-switch method.

(Suh *et al.*, 2004). We believe that this Cys-targeted proteomics method for positively detecting oxidized proteins has a significant advantage over the previously described methods (Kim *et al.*, 2000; Sethuraman *et al.*, 2004; Venkatraman *et al.*, 2004) in detecting small increments in oxidized proteins under increased oxidative stress.

2. Materials

2.1. Chemicals and other materials

NEM, biotin-NM, DTT, CHAPS, and agarose-bound monoclonal antibody to biotin were obtained from Sigma Chemical (St Louis, MO) in highest purity. Horse radish peroxidase (HRP)-conjugated streptavidin, streptavidin-agarose, and monoclonal antibody against biotin (MAb-biotin) were purchased from Molecular Probe (Eugene, OR). Protease-inhibitor cocktail and phosphatase-inhibitor cocktail were purchased from Calbiochem (San Diego, CA). Sephadex G25 mini-spin columns and immobilized pH gradient IEF gel strips (usually pH 3–10) were obtained from Amersham Biosciences (Immobiline DryStrip from GE-Healthcare, Piscataway, NJ). Mass spectrometry-compatible silver stain was obtained from BioRad

(Silver Stain Plus, Hercules, CA). Porcine sequencing grade-modified trypsin was purchased from Promega (Madison, WI). Other reagents not mentioned here were the same as described (Kim *et al.*, 2006a; Moon *et al.*, 2006, 2008a,b; Suh *et al.*, 2004).

3. Methods

Actual procedures for identifying oxidatively modified Cys residues with biotin-NM

(1) Prepare proper buffer solutions freshly preequilibrated with nitrogen or argon gas for at least 30 min to remove oxygen dissolved in the extraction buffer. For isolating mitochondria, 250 m*M* sucrose should be included in the homogenizing buffer. However, no reducing agent such as DTT should be contained in the extraction buffer since it will interfere with the following biotin-switch method.
(2) After removing the culture media, briefly rinse E47 HepG2 hepatoma cells with oxygen-free PBS buffer for 10 min three times before cell harvest by spinning for 5 min at 1500×*g* at 4 °C.
(3) Homogenize the cells or tissue samples with cold STE buffer (250 m*M* sucrose, 50 m*M* Tris–Cl, pH 7.4, and 1 m*M* EDTA) with protease-inhibitor cocktail and phosphatase-inhibitor cocktail for 40 strokes with a glass–plastic homogenizer.
(4) Spin whole cell extracts from control and ethanol-treated E47 HepG2 hepatoma cells or tissue homogenates from ethanol-exposed rodent livers for 10 min at 500×*g* at 4 °C to collect plasma membrane, cell debris, and nuclear fractions as pellets. Transfer the soluble fractions and spin at 9000×*g* for 15 min at 4 °C to prepare crude mitochondrial fractions (pellets) or cytoplasm (supernatant).
(5) Transfer the soluble fractions into clean tubes and use them as cytosolic fraction (cytoplasm).
(6) Rinse the crude nuclear fraction (#4) and mitochondrial fraction (#4) with at least three times with fresh STE buffer and then spin again at 13,000×*g* for 10 min to remove any contaminating cytosolic proteins.
(7) Incubate the nuclear and mitochondrial proteins with the buffer (40 m*M* Hepes, 50 m*M* NaCl, 1% CHAPS, 1 m*M* EDTA, 1 m*M* EGTA, protease, and phosphatase inhibitor cocktails) for 15 min and then spin for 13,000×*g* to obtain the soluble proteins from the nuclear and mitochondrial fractions, respectively, as described (Kim *et al.*, 2006b). Determine the protein concentration for each sample group.
(8) For the biotin-switch labeling procedure, treat the same amounts of solubilized mitochondrial proteins (from each sample group) with 30 m*M* NEM for 20 min to block reduced thiols.

(9) Gently spin NEM-treated protein samples (e.g., cytosolic or solubilized mitochondrial proteins from each group) through Sephadex G25 mini-spin columns preequilibrated with the 1% CHAPS containing buffer. Sephadex G25 mini-spin columns are prespun at 300×*g* for 20 s to remove the equilibrium buffer. After removing the equilibrium buffer from the mini-spin columns, load the NEM-treated protein samples carefully onto the center of the Sephadex G25 beads (try to avoid loading proteins onto the side of the Sephadex beads in the mini-spin columns). Then, spin the Sephadex G25 mini-spin columns with protein samples at 1000×*g* for 1 min to efficiently collect the proteins as column eluates without NEM, which should be retained on the Sephadex G25 beads.

(10) Determine the protein concentration of the eluted proteins from the first Sephadex G25 mini-spin columns. Treat the same amount of eluted cytosolic or solubilized mitochondrial proteins with 5 m*M* DTT for 10 min to reduce any oxidized Cys residues (including sulfenic acid, disulfides, and mixed disulfides with glutathione or nitrosylated thiols) to reduced thiols.

(11) Incubate the protein samples with 7 m*M* biotin-NM for another 20 min to label freshly reduced Cys residues with biotin-NM.

(12) Purify the same amount of biotin-NM-labeled proteins (from each sample group) through the second Sephadex G25 mini-spin columns to remove excess amounts of biotin-NM, as carefully as described earlier (#9).

(13) For quick analysis, separate the biotin-NM-labeled oxidized proteins on 1D SDS–PAGE and subject them to immunoblot analysis with the specific monoclonal antibody against biotin or streptavidin-conjugated with HRP.

(14) To further characterize the identities of oxidatively modified proteins, purify the biotin-NM-labeled oxidized proteins with streptavidin-agarose beads (or agarose-bound monoclonal antibody to biotin). Wash the agarose-bound biotin-NM-labeled proteins with the elution buffer at least twice to remove nonspecifically bound proteins. Then, dissolve biotin-NM-labeled oxidized proteins in 2D PAGE buffer (8 *M* urea, 20 m*M* DTT, 2% CHAPS, 0.5% IPG buffer, and pH 3–10) for 30 min before isoelectrofocusing analysis on dry IPG strips for 24 h at 50,000 V h, as recommended by the manufacturer. Stain the oxidized proteins resolved on 2D gels with mass spectrometry-compatible Coomassie-blue or silver.

(15) Pick the Coomassie-blue-stained protein spots with new razor blades and analyze the protein identities by in-gel trypsin digestion followed by mass spectral analysis, as described (Blonder *et al.*, 2004; Suh *et al.*, 2004).

(16) Confirm the presence of oxidized proteins with immunoblot analysis and activity measurements (Moon *et al.*, 2005, 2007; Suh *et al.*, 2004).

4. Discussion

By using the redox-related, Cys-targeted proteomics method, we expect to detect a greater number and intensity of biotin-NM-labeled oxidized proteins under increased oxidative stress compared to those found in control tissues, as exemplified in alcohol-exposed cells/tissues (Fig. 13.2). This prediction was actually confirmed by data in ethanol-treated CYP2E1-containing E47 HepG2 hepatoma cells and rodent tissues (Suh *et al.*, 2004). In fact, significant increases in the number and intensity of oxidatively modified proteins were detected in the cytoplasm and mitochondria from ethanol-exposed mice or rats compared to that detected in pair-fed control rodents (Kim *et al.*, 2006a; Moon *et al.*, 2006; Song *et al.*, 2008).

Furthermore, the increased number and intensity of oxidatively modified proteins were also observed in nonalcohol-induced liver damage such as ischemia–reperfusion hepatic injury (Moon *et al.*, 2008a) or following exposure to 3,4-methylenedioxymethamphetamine (MDMA, ecstasy) (Moon *et al.*, 2008b). We would thus expect to detect increased levels of oxidized proteins in many other tissues such as brain (Moon *et al.*, unpublished observation) in various disease states.

4.1. Advantages of the simple redox-based Cys-targeted proteomics method

The redox-based, Cys-targeted approach exhibits multiple advantages over other existing methods.

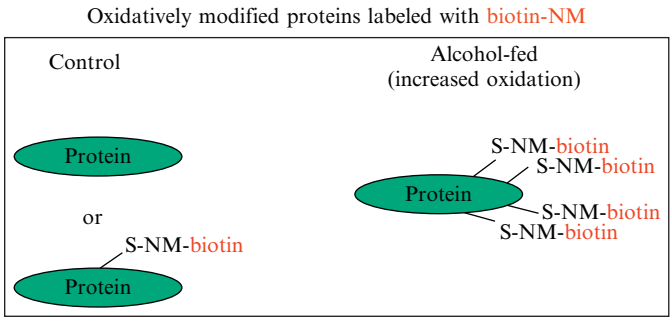

Figure 13.2 Comparison of biotin-NM-labeled oxidatively modified proteins in biological samples. The increased number of biotin-NM-labeled oxidized proteins under elevated oxidative stress (in alcohol-exposed cells/tissues than control cells/tissues).

4.1.1. Positive correlation between the levels of oxidized proteins and increased oxidative stress

It is known that oxidized Cys residues do not react with the sulfhydryl reagents such as BIAM and ICAT. Therefore, decreased efficiencies of labeling oxidized proteins with these methods would be expected. Unlike the other methods reported (Kim *et al.*, 2000; Sethuraman *et al.*, 2004; Venkatraman *et al.*, 2004), where the number of oxidized proteins was inversely related to increased oxidative stress, the current redox-based proteomics method allows the positive identification of oxidized proteins. In fact, we observed a positive correlation between the increased number of the oxidatively modified proteins and increased oxidative stress (Kim *et al.*, 2006a; Moon *et al.*, 2006, 2008a; Suh *et al.*, 2004).

4.1.2. No requirements for special reagents

Instead of requiring a specific antibody to 4-iodobutyltriphenyl-phosphonium (Venkatraman *et al.*, 2004) or a cysteine-specific ICAT reagent (Sethuraman *et al.*, 2004), this biotin-switch method described here does not need special reagents. All reagents used in this method are available commercially and easy to obtain (Suh *et al.*, 2004).

4.1.3. Functional proteomics analysis

The main objective of many proteomics approaches, including 2D Fluorescence Difference Gel Electrophoresis (2D DIGE) system, is to detect alterations in the expressed levels of many proteins in two different samples (e.g., treated and untreated controls). However, many proteins can be inhibited without significant quantitative differences, suggesting posttranslational modifications, including oxidative modifications of Cys residues (Kim *et al.*, 2006a; Moon *et al.*, 2006, 2008a). Identification of the oxidatively modified proteins detected with the Cys-targeted redox-proteomics approach allows us to predict functional implications (e.g., inhibition) of the oxidized proteins/enzymes even in the absence of any changes in protein contents. We can simply search for Cys residues in the active site(s) of each oxidized protein in the literature. For instance, mitochondrial 3-ketoacyl-CoA thiolase, the last enzyme in the mitochondrial β-oxidation pathway of fatty acids, contains two Cys residues and one His residue in its active site (Zeng and Li, 2004). Although its protein level was unchanged, we expected its inactivation through oxidative modifications of catalytic Cys residues under increased oxidative stress in alcohol-exposed animals (Moon *et al.*, 2006; Song *et al.*, 2008) and nonalcoholic liver injury models (Moon *et al.*, 2008a,b). In fact, the inhibition of 3-ketoacyl-CoA thiolase activity was correlated with fat accumulation measured by the biochemical measurement of triglyceride levels (Moon *et al.*, 2008a,b; Song *et al.*, 2008) and histological fat staining with oil red O dye (Moon *et al.*, 2006). The conservation of the active site Cys and

His residues between mitochondrial and peroxisomal 3-ketoacyl-CoA thiolases can be used in predicting the inhibition of the peroxisomal enzyme under increased oxidative stress. Similarly, we also expect inhibition of the oxidatively modified aldehyde dehydrogenase (ALDH) isozymes, such as ALDH5 and ALDH7, although expressed in low levels, since all ALDH isozymes contain a highly conserved Cys residue in their active sites (as discussed in Moon *et al.*, 2007).

4.1.4. Proteomics analysis for different sub-organelles

By using this simple biotin-switch method, we can systematically identify oxidatively modified proteins in different subcellular organelles (e.g., cytoplasm, mitochondria, endoplasmic reticulum (ER), and nuclear fractions) to theoretically study the underlying mechanisms of redox-related cellular metabolism, ER stress, mitochondrial dysfunction, and modulation of transcription factors, respectively. By studying the time-dependent oxidative modifications of various proteins and cell/tissue damage, we can generate many interesting hypotheses toward tissue damage. For instance, oxidative modifications and inactivation of ER-resident chaperone proteins, including protein disulfide isomerase (PDI), may lead to unfolded client proteins of PDI, leading to unfolded protein responses, and ER stress (Kim *et al.*, 2006a). In addition, by studying the time-dependent oxidation of mitochondrial proteins during ischemia–reperfusion liver injury, we reported that oxidative modifications of many mitochondrial proteins take place at much earlier than the actual tissue damage observed later (Moon *et al.*, 2008a). These results suggest that mitochondrial dysfunction through the oxidative inactivation of many mitochondrial proteins contributes to tissue damage.

4.1.5. Proteomics analysis for different tissues

In addition, we can identify oxidatively modified proteins in different organs/tissues (e.g., liver, brain, kidney, heart, intestine, etc.), depending on the target organs of interest (Moon *et al.*, 2008b and unpublished data). By comparing the patterns of oxidative protein modifications in different tissues, we can estimate the role of specific proteins in each organ.

4.1.6. Proteomics analysis for different disease states

Oxidatively modified proteins in different disease states (e.g., ischemia–reperfusion hepatic injury, diabetes, etc.) or following exposure to potentially toxic drugs/chemicals (e.g., MDMA-exposed rat liver or brain tissues) or environmental contaminants where increased oxidative stress plays a major role in cellular toxicity (Moon *et al.*, 2008a,b), can be studied.

4.1.7. Proteomics analysis for detecting mixed disulfides

Increased production of peroxynitrate (PN) in the presence of ROS/RNS can actively react with free Cys residues to form nitrosothiols as well as nitrate Tyr residues (3-nitroTyr) of many proteins and affect their functions (Lane *et al.*, 2001; Ottesen *et al.*, 2001). By using mild reducing agents such as ascorbate (Asc) or glutathione (GSH) (Jaffrey and Snyder, 2001; Kashiba-Iwatsuki *et al.*, 1997) instead of DTT in the second step in Fig. 13.1, proteins with mixed disulfides (e.g., glutathionylation, succinylation, or *S*-nitrosylation) can be identified, as reported (Moon *et al.*, 2006, 2008a).

4.1.8. Application in translational research

Finally, this method can be employed in translational studies by evaluating the effectiveness or progress of treatment with a certain beneficial agent (e.g., antioxidants or cell-protective agents). This can be accomplished by monitoring the levels of oxidatively modified proteins in the biological specimens before, during, and after treatment with a beneficial agent. For instance, a polyunsaturated fatty acid diet containing physiological levels of arachidonic and docosahexaenoic acids effectively prevented protein oxidation, mitochondrial dysfunction, and ultimately alcoholic fatty liver (Song *et al.*, 2008). Based on our data, it is expected that the beneficial effects of other antioxidants against many disease states will be demonstrated in future studies.

4.2. Limitations of the redox-based Cys-targeted proteomics and alternative approaches

4.2.1. Detection of oxidized proteins expressed in low levels

Despite many advantages, this Cys-targeted proteomics approach also has some limitations. One of the major disadvantages of this method is that it depends on the amount of target proteins expressed in a given cell/tissue. Common to all proteomics methods, the Cys-targeted redox-proteomics approach only allows the detection of oxidatively modified proteins expressed in abundance, as we originally described (Suh *et al.*, 2004). For instance, it is unlikely that this systematic approach could be successfully used in directly detecting the oxidation of many DNA repair enzymes, including O^6-methylguanine-DNA-methyltransferase, which contains Cys in its active site and can be inhibited via *S*-nitrosylation (Laval and Wink, 1994). Although the oxidation of O^6-methylguanine-DNA-methyltransferase or other DNA repair enzymes such as OGG1 was not observed in our studies (Kim *et al.*, 2006a; Moon *et al.*, 2006; Suh *et al.*, 2004), the failure to detect these proteins could be due to low expression levels of these proteins relative to other proteins in the liver.

A few other enzymes, that were not detected by our systematic Cys-targeted redox-proteomics approaches (Kim *et al.*, 2006a; Moon *et al.*, 2006) but confirmed for oxidative modifications of active site Cys residues, may include: Rpn2, which is a subunit of the 26S proteasome complex system (Zmijewski *et al.*, 2009), methionine adenosyltransferase (Avila *et al.*, 1997; Ruiz *et al.*, 1998), mitogen-activated protein kinase phosphatases (Heneberg and Dráber, 2005; Kim *et al.*, 2003), and tumor-suppressor protein PTEN (Lee *et al.*, 2002). Oxidative modifications of these proteins may not be easily detected by the Cys-targeted redox-proteomics approach described here due to low-expression levels of these proteins. However, it is possible to successfully demonstrate oxidative modifications of these or other key enzymes/proteins (including some transcription factors) by immunoprecipitation with a specific antibody against each target protein and then immunoblot analysis with a specific antibody against Cys-S-NO, 3-nitrotyrosine, or glutathione. This alternative approach should be correlated with the activity measurement to further confirm the functional implication of the oxidative modifications of the critical Cys or other amino-acid residues.

4.2.2. Detection of covalent modifications of Cys residues

Another point for consideration is that Cys residues can undergo many different covalent modifications such as conjugation with carbonyl compounds, such as acetaldehyde, acrolein, croton aldehyde, malondialdehyde, and 4-hydroxynonenal (4-HNE), all of which can be produced through lipid peroxidation under oxidative stress (Catalá, 2009; Esterbauer *et al.*, 1991). For instance, the Cys residues of mitochondrial ALDH2 are known to be modified by direct interaction with 4-HNE (Doorn *et al.*, 2006) as well as conjugation with the metabolites disulfiram, daunorubicin, and acetaminophen (discussed in Moon *et al.*, 2009) with concomitant ALDH2 inactivation. The ALDH2 activity is also decreased in many pathological conditions such as alcoholic fatty liver, hepatic cancer, aging, and hepatic ischemia–reperfusion injury (as discussed in Moon *et al.*, 2010). In most cases, the ALDH2 protein levels might not be altered, suggesting that the catalytic and other critical Cys residues of ALDH2 are likely oxidatively modified and/or conjugated with 4-HNE or other reactive metabolites such as acetaminophen and disulfiram. The covalent modifications of Cys residues by the latter cases can be demonstrated by measuring the enzyme activity after incubation with a strong reducing agent DTT, which cannot reverse the cysteine–carbonyl conjugates or drug-conjugation adducts. If the suppressed enzyme activities are recovered by the addition of DTT, the target proteins are likely to be oxidatively modified to sulfenic acid, *S*-nitrosylation, or disulfides (including mixed disulfides with glutathione). If the activities are not restored even after incubation with DTT, this likely represents the irreversible, covalent modifications (i.e., conjugation adducts) or hyper-oxidation of Cys residues to

sulfinic/sulfonic acids. Alternatively, other amino-acid residues of the target proteins may also be oxidatively modified and thus contribute to irreversible inactivation of the target protein (Moon *et al.*, 2010). Therefore, it is advised to consider many possible routes of oxidative modifications during interpretation of the data.

ACKNOWLEDGMENT

This research was supported by the intramural Program fund at the National Institute on Alcohol Abuse and Alcoholism. Part of this research was also supported by a grant for the Chronic Liver Disease Project (to B.J. Song) from the Center for Biological Modulators in South Korea. The authors are grateful to Drs. Sue-Goo Rhee and Klaus Gawrisch for their advice and support.

REFERENCES

Avila, M. A., Mingorance, J., Martínez-Chantar, M. L., Casado, M., Martin-Sanz, P., Boscá, L., and Mato, J. M. (1997). Regulation of rat liver S-adenosylmethionine synthetase during septic shock: Role of nitric oxide. *Hepatology* **25,** 391–396.

Baty, J. W., Hampton, M. B., and Winterbourn, C. C. (2002). Detection of oxidant sensitive thiol proteins by fluorescence labeling and two-dimensional electrophoresis. *Proteomics* **2,** 1261–1266.

Berlett, B. S., and Stadtman, E. R. (1997). Protein oxidation in aging, disease, and oxidative stress. *J. Biol. Chem.* **272,** 20313–20316.

Blonder, J., Conrads, T. P., Yu, L. R., Terunuma, A., Janini, G. M., Issaq, H. J., Vogel, J. C., and Veenstra, T. D. (2004). A detergent- and cyanogen bromide-free method for integral membrane proteomics: Application to Halobacterium purple membranes and the human epidermal membrane proteome. *Proteomics* **4,** 31–45.

Caro, A. A., and Cederbaum, A. I. (2004). Oxidative stress, toxicology, and pharmacology of CYP2E1. *Annu. Rev. Pharmacol. Toxicol.* **44,** 27–42.

Catalá, A. (2009). Lipid peroxidation of membrane phospholipids generates hydroxy-alkenals and oxidized phospholipids active in physiological and/or pathological conditions. *Chem. Phys. Lipids* **157,** 1–11.

Doorn, J. A., Hurley, T. D., and Petersen, D. R. (2006). Inhibition of human mitochondrial aldehyde dehydrogenase by 4-hydroxynon-2-enal and 4-oxonon-2-enal. *Chem. Res. Toxicol.* **19,** 102–110.

Esterbauer, H., Schaur, R. J., and Zollner, H. (1991). Chemistry and biochemistry of 4-hydroxynonenal, malonaldehyde and related aldehydes. *Free Radic. Biol. Med.* **11,** 81–128.

Heneberg, P., and Dráber, P. (2005). Regulation of cys-based protein tyrosine phosphatases via reactive oxygen and nitrogen species in mast cells and basophils. *Curr. Med. Chem.* **12,** 1859–1871.

Hensley, K., Hall, N., Subramaniam, R., Cole, P., Harris, M., Aksenov, M., Aksenova, M., Gabbita, S. P., Wu, J. F., Carney, J. M., Lovell, M., Markesbery, W. R., *et al.* (1995). Brain regional correspondence between Alzheimer's disease histopathology and biomarkers of protein oxidation. *J. Neurochem.* **65,** 2146–2156.

Jaffrey, S. R., and Snyder, S. H. (2001). The biotin switch method for the detection of S-nitrosylated proteins. *Sci. STKE* **2006,** pL1.

Kashiba-Iwatsuki, M., Kitoh, K., Kasahara, E., Yu, H., Nisikawa, M., Matsuo, M., and Inoue, M. (1997). Ascorbic acid and reducing agents regulate the fates and functions of S-nitrosothiols. *J. Biochem. (Tokyo)* **122,** 1208–1214.

Kim, J. R., Yoon, H. W., Kwon, K. S., Lee, S. R., and Rhee, S. G. (2000). Identification of proteins containing cysteine residues that are sensitive to oxidation by hydrogen peroxide at neutral pH. *Anal. Biochem.* **283,** 214–221.

Kim, H. S., Song, M. C., Kwak, I. H., Park, T. J., and Lim, I. K. (2003). Constitutive induction of p-Erk1/2 accompanied by reduced activities of protein phosphatases 1 and 2A and MKP3 due to reactive oxygen species during cellular senescence. *J. Biol. Chem.* **278,** 37497–37510.

Kim, B. J., Hood, B. L., Aragon, R. A., Hardwick, J. P., Conrads, T. P., Veenstra, T. D., and Song, B. J. (2006a). Increased oxidation and degradation of cytosolic proteins in alcohol-exposed mouse liver and hepatoma cells. *Proteomics* **6,** 1250–1260.

Kim, B. J., Ryu, S. W., and Song, B. J. (2006b). JNK- and p38 kinase mediated phosphorylation of Bax leads to its activation, mitochondrial translocation and apoptosis of human hepatoma HepG2 cells. *J. Biol. Chem.* **281,** 21256–21265.

Kono, H., Rusyn, I., Yin, M., Gabele, E., Yamashina, S., Dikalova, A., Kadiiska, M. B., Connor, H. D., Mason, R. P., Segal, B. H., Bradford, B. U., Holland, S. M., *et al.* (2000). NADPH oxidase-derived free radicals are key oxidants in alcohol-induced liver disease. *J. Clin. Invest.* **106,** 867–872.

Lane, P., Hao, G., and Gross, S. S. (2001). *S*-nitrosylation is emerging as a specific and fundamental posttranslational protein modification: Head-to-head comparison with O-phosphorylation. *Sci. STKE* **2006,** RE1.

Laval, F., and Wink, D. A. (1994). Inhibition by nitric oxide of the repair protein, O^6-methylguanine-DNA-methyltransferase. *Carcinogenesis* **15,** 443–447.

Lee, S. R., Yang, K. S., Kwon, J., Lee, C., Jeong, W., and Rhee, S. G. (2002). Reversible inactivation of the tumor suppressor PTEN by H_2O_2. *J. Biol. Chem.* **277,** 20336–20342.

Lin, M. T., and Beal, M. F. (2006). Mitochondrial dysfunction and oxidative stress in neurodegenerative diseases. *Nature* **443,** 787–795.

Minko, I. G., Kozekov, I. D., Harris, T. M., Rizzo, C. J., Lloyd, R. S., and Stone, M. P. (2009). Chemistry and biology of DNA containing 1, N(2)-deoxyguanosine adducts of the alpha, beta-unsaturated aldehydes acrolein, crotonaldehyde, and 4-hydroxynonenal. *Chem. Res. Toxicol.* **22,** 759–778.

Moon, K. H., Kim, B. J., and Song, B. J. (2005). Inhibition of mitochondrial aldehyde dehydrogenase by nitric oxide-mediated S-nitrosylation. *[FEBS Lett].* **579,** 6115–6120.

Moon, K. H., Hood, B. L., Kim, B. J., Hardwick, J. P., Conrads, T. P., Veenstra, T. D., and Song, B. J. (2006). Inactivation of oxidized and S-nitrosylated mitochondrial proteins in alcoholic fatty liver of rats. *Hepatology* **44,** 1218–1230.

Moon, K. H., Abdelmegeed, M. A., and Song, B. J. (2007). Inactivation of cytosolic aldehyde dehydrogenase via S-nitrosylation in ethanol-exposed rat liver. *FEBS Lett.* **581,** 3967–3972.

Moon, K. H., Hood, B. L., Mukhopadhyay, P., Rajesh, M., Abdelmegeed, M. A., Kwon, Y. I., Conrads, T. P., Veenstra, T. D., Song, B. J., and Pacher, P. (2008a). Oxidative inactivation of key mitochondrial proteins leads to dysfunction and injury in hepatic ischemia reperfusion. *Gastroenterology* **135,** 1344–1357.

Moon, K. H., Upreti, V. V., Yu, L. R., Lee, I. J., Ye, X., Eddington, N. D., Veenstra, T. D., and Song, B. J. (2008b). Mechanism of 3, 4-methylenedioxymethamphetamine (MDMA, ecstasy)-mediated mitochondrial dysfunction in rat liver. *Proteomics* **8,** 3906–3918.

Moon, K. H., Lee, Y. M., and Song, B. J. (2010). Inhibition of hepatic mitochondrial aldehyde dehydrogenase by carbon tetrachloride through JNK-mediated phosphorylation. *Free Radic. Biol. Med.* **48,** 391–398.

Ottesen, L. H., Harry, D., Frost, M., Davies, S., Khan, K., Halliwell, B., and Moore, K. (2001). Increased formation of S-nitrothiols and nitrotyrosine in cirrhotic rats during endotoxemia. *Free Radic. Biol. Med.* **31,** 790–798.

Purohit, V., Gao, B., and Song, B. J. (2009). Molecular mechanisms of alcoholic fatty liver. *Alcohol. Clin. Exp. Res.* **33,** 191–205.

Rubbo, H., and Radi, R. (2008). Protein and lipid nitration: Role in redox signaling and injury. *Biochim. Biophys. Acta* **1780,** 1318–1824.

Ruiz, F., Corrales, F. J., Miqued, C., and Mato, J. M. (1998). Nitric oxide inactivates rat hepatic methionine adenosyltransferase in vivo by S-nitrosylation. *Hepatology* **28,** 1051–1057.

Sethuraman, M., McComb, M. E., Heibeck, T., Costello, C. E., and Cohen, R. A. (2004). Isotope-coded affinity tag approach to identify and quantify oxidant-sensitive protein thiols. *Mol. Cell. Proteomics* **3,** 273–278.

Song, B. J., Koop, D. R., Ingelman-Sundberg, M., Nanji, A., and Cederbaum, A. I. (1996). Ethanol-inducible cytochrome P450 2E1: Biochemistry, molecular biology, and clinical relevance: 1996 update. *Alcohol. Clin. Exp. Res.* **20,** 138A–146A.

Song, B. J., Moon, K. H., Olsson, N. U., and Salem, N., Jr. (2008). Prevention of alcoholic fatty liver and mitochondrial dysfunction in the rat by long-chain polyunsaturated fatty acids. *J. Hepatol.* **49,** 262–273.

Stadtman, E. R., Moskovitz, J., and Levine, R. L. (2003). Oxidation of methionine residues of proteins: Biological consequences. *Antioxid. Redox Signal.* **5,** 577–582.

Suh, S. K., Hood, B. L., Kim, B. J., Conrad, T. P., Veenstra, T. D., and Song, B. J. (2004). Identification of oxidized mitochondrial proteins in alcohol-exposed human hepatoma cells and mouse liver. *Proteomics* **4,** 3401–3412.

Venkatraman, A., Landar, A., Davis, A. J., Ulasova, E., Page, G., Murphy, M. P., Darley-Usmar, V., and Bailey, S. M. (2004). Oxidative modification of hepatic mitochondria protein thiols: Effect of chronic alcohol consumption. *Am. J. Physiol. Gastrointest. Liver Physiol.* **286,** G521–G527.

Wells, P. G., McCallum, G. P., Chen, C. S., Henderson, J. T., Lee, C. J., Perstin, J., Preston, T. J., Wiley, M. J., and Wong, A. W. (2009). Oxidative stress in developmental origins of disease: Teratogenesis, neurodevelopmental deficits, and cancer. *Toxicol. Sci.* **108,** 4–18.

Zeng, J., and Li, D. (2004). Expression and purification of his-tagged rat mitochondrial 3-ketoacyl-CoA thiolase wild type and His352 mutant proteins. *Protein Expr. Purif.* **35,** 320–326.

Zmijewski, J., Banerjee, S., and Abraham, E. (2009). S-Glutathionylation of the Rpn2 regulatory subunit inhibits 26S proteosomal function. *J. Biol. Chem.* **284,** 22213–22221.

CHAPTER FOURTEEN

Direct and Indirect Detection Methods for the Analysis of *S*-Nitrosylated Peptides and Proteins

Federico Torta,* Lisa Elviri,† *and* Angela Bachi*

Contents

Abstract

Covalent binding of nitric oxide to specific cysteine residues in proteins is a key event in cellular redox signal transduction. This modification influences both physiological and pathological processes, such as cardiovascular, neurological, and cancer-associated events. Even though, since its introduction, the biotin switch technique is the most used indirect method for the study of *S*-nitrosylation both *in vivo* and *in vitro*, during the last years modifications of this method have emerged, allowing more efficient sample enrichment and the precise identification of the modified aminoacidic sites. At the same time, to bypass the difficulties generated by the multiple chemical reaction steps required by these labeling methods, the direct identification of the SNO groups by mass spectrometry is emerging as a useful tool in this field, although, until now, it has been limited to the study of synthetic or purified recombinant proteins. Here we present two different techniques, developed in our laboratories, for detection of *S*-nitrosylation: the first is based on a modification of the biotin switch technique and is called His-tag switch, and the second is a direct mass spectrometry-based method used to detect *in vivo* generated SNO groups.

* Biomolecular Mass Spectrometry Unit, Division of Genetics and Cell Biology, San Raffaele Scientific Institute, Milano, Italy
† Dipartimento di Chimica Generale ed Inorganica, Chimica Analitica, Chimica Fisica, Università di Parma, Parma, Italy

Methods in Enzymology, Volume 473
ISSN 0076-6879, DOI: 10.1016/S0076-6879(10)73014-7

1. Introduction

Nitric oxide (NO) is a gaseous free radical synthesized, in mammals, from L-arginine by enzymes known as nitric oxide synthases (NOS) (Gaston *et al.*, 2003). NO and NOS have been identified in many organs, including liver, vascular tissue, smooth and skeletal muscle, and the nervous system (Oess *et al.*, 2006). There are three isoforms of NOS: neuronal NOS (nNOS or NOS1), inducible NOS (iNOS or NOS2), and endothelial NOS (eNOS or NOS3), expressed in different cell types and under different conditions (Alderton *et al.*, 2001). The existence of a mitochondrial NOS (mtNOS) has also been suggested (Giulivi, 2003; Tatoyan and Giulivi, 1998).

NO is involved in physiological functions as blood vessel relaxation (Allen and Piantadosi, 2006), neurotransmission (Vincent, 2009), and immune cell response (Davies and Dow, 2009).

NO can react with and modify proteins, leading to *S*-nitrosylation and nitrotyrosination, which are two important posttranslational modifications that play a role in physiological and pathophysiological processes. In particular, *S*-nitrosylation is the reversible reaction of NO with the amino acid cysteine to form nitrosothiols (Stamler *et al.*, 1992). This modification has recently emerged as an important posttranslational modification that regulates a large variety of cellular functions and signaling events. For example, *S*-nitrosylation of NMDA (*N*-methyl-D-aspartate) glutamate receptors in neurons increases neuronal survival by preventing excitotoxicity (Lipton *et al.*, 2002). NO also inhibits caspases, cysteine proteases that play a critical role in apoptosis (Mannick *et al.*, 1999).

S-Nitrosylation has also been implicated in many pathological conditions. Indeed, NO has been reported to be a key molecule in common neurodegenerative diseases including stroke, multiple sclerosis, Parkinson's, and Alzheimer's disease (Cho *et al.*, 2009; Khan *et al.*, 2006; Prasad *et al.*, 2007; Yao *et al.*, 2004).

Growing evidence suggests that NO is a central molecule in several physiological functions also in plants, ranging from development to chloroplasts and mitochondria function, from stress to defense responses (Wendehenne *et al.*, 2004).

The level of *S*-nitrosylated species in biological samples is usually monitored after the induced release of NO from the originally modified thiol groups and the released NO can be quantified by different techniques as chemiluminescence, fluorescence, or electrochemistry (Cook *et al.*, 1996; Hausladen *et al.*, 2007; Palmer and Gaston, 2008). However, for the detection and the identification of *S*-nitrosylated peptides and proteins, mass spectrometry (MS)-based methods are required. Due to the low concentration of *S*-nitrosylated proteins *in vivo* and to the lability of this

type of modification, the enrichment of *S*-nitrosylated proteins and their direct detection by MS is still quite problematic (Jorge *et al.*, 2007). Despite the improvement of instruments, in terms of sensitivity and resolution, to the best of our knowledge, evidence of *S*-nitrosylated proteins identified out of protein crude extracts cannot be found in literature. This is the reason why the identification of *S*-nitrosylated cysteine sites have been mostly obtained by using indirect strategies, with the biotin switch technique (BST) being the method of choice. This experimental protocol was introduced by Jaffrey and Snyder (2001) and essentially consists in the conversion of the nitrosylated cysteines into biotinylated ones. In the first experimental step proteins are treated with a thiol blocking agent, such as mono-methyl thiosulphonate (MMTS), to chemically block all free thiols. Following the blocking step, the S–NO bond is specifically reduced to a free thiol, usually with millimolar concentrations of ascorbate. Free thiols are then reacted with a thiol-specific biotinylating agent, which results in a disulfide-linked label that can be used for Western blot analysis or affinity enrichment of the tagged proteins or peptides. Modifications of this protocol and the use of different labeling molecules have favored the evolution of the biotin switch into several new methods that improved the detection of the specific modified residues (Camerini *et al.*, 2007; Greco *et al.*, 2006; Hao *et al.*, 2006). In particular, our group introduced the use of a different technique (Camerini *et al.*, 2007) in which the biotin-tag is substituted by a digestion sensitive His-tag (see following paragraph). More recently, a methodology called "fluorescence switch" (Tello *et al.*, 2009) has improved the sensitivity of the classic BST when coupled to two-dimensional gel electrophoresis (2-DE). This method is quite similar to BST, but the *S*-nitrosylated groups are labeled by a fluorophore instead of biotin. In this case, in the absence of a pull-down enrichment step, which is substituted by a 2-DE separation, the total amount of the fluorescent protein is available for the mass spectrometric identification, enabling the use of a lower amount of starting material. However, as stated by the authors, this technique show some limitations as in the false positive identification of nonmodified protein fractions (that co-migrate with modified ones) and in the fact that the modified cysteine residue is not easily identified. This last bias is shared with the BST and has been solved after the introduction of the peptide-based methods (Hao *et al.*, 2006), where, before the pull-down step, the total protein mixture is digested with trypsin. In this way, only the modified peptides are then enriched and eluted for the following identification by MS: this is a fundamental improvement because only the localization of the modified residue can confer high confidence to the results.

Another newly introduced method called SNO-RAC (resin-assisted capture) uses a thiol-reactive resin instead of biotin, combining the labeling and pull-down steps of the BST (Forrester *et al.*, 2009b). After reduction with ascorbate of the SNO-sites, the proteins bind to the resin. At this stage,

the sample can be tryspinized on-resin and the resulting peptides labeled for quantitative proteomics measurements.

Thus, the increasing interest that *S*-nitrosylation is generating in the scientific community has raised a number of new techniques for isolation and identification of the proteins involved. This chapter describes two original methods developed in our laboratories to allow sensitive detection of nitrosothiols in biological samples, using both indirect and direct detection and based on MS.

2. Indirect Detection of *S*-Nitrosylated Proteins: His-tag Switch

Even if the biotin switch is nowadays the most extensively adopted technique to identify *S*-nitrosylated proteins in several biological contexts, the original protocol does not allow the identification of the nitrosylated residues because the biotin-tag is lost during the elution stage after the affinity enrichment. As the unambiguous recognition of the modified cysteine is essential to improve the quality of the analysis and to help the functional characterization of the identified proteins, novel methods have been developed in this direction.

With this aim, we modified the scheme of the biotin switch trying to improve the efficiency and the specificity of the method (Fig. 14.1). The fundamental difference from the commonly used procedure consists in the use of a tagging molecule that binds irreversibly to the free cysteine residues

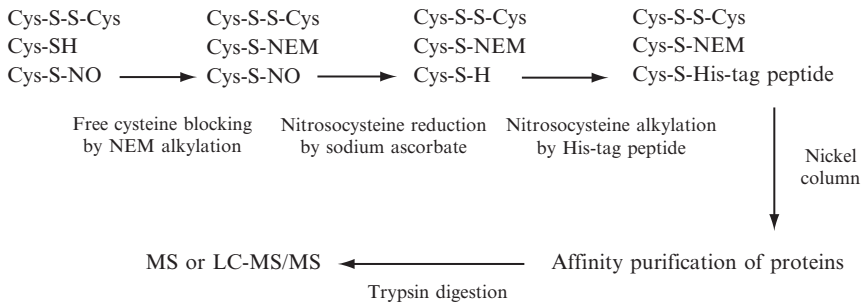

Figure 14.1 **Schematic representation of the procedure used for the His-tag switch. In the first step the free Cysteines are blocked by NEM alkylation. Afterwards the NO group is specifically removed by ascorbate and the newly generated thiols are alkylated with the His-tag peptide. His-tagged proteins can be detected directly, or after affinity purification on a Nickel column, by western blot with an anti-His-tag antibody. Specific gel bands can be cut and digested with trypsin and analyzed by mass spectrometry.**

and contains a His-tag instead of a biotin-tag. This approach was named His-tag switch because of the replacement of the NO moiety with the His-tag group at the end of the procedure.

2.1. Protocol for the analysis of *S*-nitrosylation using the His-tag switch

1. Isolate the tissue of interest (in our case rat cerebral cortex) and homogenize it in Potter tubes, on ice and in a buffer containing 20 m*M* Tris–HCl pH 7.4, 260 m*M* sucrose and proteases inhibitor cocktail. If the endogenous *S*-nitrosylation levels have to be measured, before the labeling step all the procedures reported here must be performed in the dark and in the presence of 1 m*M* EDTA and 0.1 m*M* neocuproine to minimize SNO groups degradation. Clarify the solution at 1200×*g* for 10 min at 4 °C; centrifuge the supernatant at 12,500×*g* for 20 min at 4 °C. Solubilize the obtained pellet in 5 m*M* Hepes, 320 m*M* sucrose in the presence of proteases inhibitor cocktail, and centrifuge at 10,000×*g* for 15 min.
2. Cell lysis: solubilize the pellet in a lysis buffer containing 150 m*M* NaCl, 100 m*M* Hepes pH 8, 1 m*M* EDTA, 0.1 m*M* neocuproine, 1% NP-40, 0.2% deoxycholate, proteases inhibitor cocktail, and incubate at 4 °C in the dark for 45 min with continuous mixing. EDTA and neocuproine are added to chelate divalent metals and Cu(I), thus protecting nitrosothiols from denitrosylation.
3. Isolation of the protein fraction: centrifuge at 13,000×*g* for 10 min, collect the supernatant containing the neuronal cytosolic proteins and evaluate the protein content with the Bradford assay.
4. *In vitro* nitrosylation: bring the total protein concentration to a maximum of 1 mg/ml (otherwise the nitrosylation and blocking reactions could be incomplete) with HEN buffer (Hepes 100 m*M* pH 8, EDTA 1 m*M*, neocuproine 0.1 m*M*). Incubate this solution with 500 μM *S*-nitrosoglutathione (GSNO) at 25 °C for 1 h. To identify the *S*-nitrosatable proteome of the brain cortex, GSNO was chosen as NO donor for its endogenous nature. As negative controls, part of the sample should be incubated in the same conditions with 500 μM GSH, to show that the nitrosylation is effective, and 10 m*M* dithiothreitol (DTT) to test the blocking reaction efficiency.
5. Blocking: block the unmodified cysteine residues with 100 m*M* *N*-ethylmaleimide (NEM) in HEN buffer, SDS 2.5%, at 40 °C for 1 h with continuous vortexing. These residues have to be blocked to avoid unspecific labeling in the next step while SDS and heat are necessary to allow a complete accessibility to all the thiols. NEM is preferred to other blocking agents because it binds irreversibly to the

free Cys residues and is compatible with the following in-gel digestion of protein bands. Dialyze NEM against the lysis buffer at 4 °C overnight.

6. Labeling: add 10 m*M* sodium ascorbate (Fluka) to reduce the SNO groups and 0.2 m*M* I-CH_2-CO-Gly-Arg-Ala-His_6 to perform the labeling of the SNO groups. Ascorbate is an SNO-specific reducing agent, which does not affect the other redox modifications on cysteines. The specificity of this reaction has been discussed by several authors (Forrester *et al.*, 2007; Giustarini *et al.*, 2008; Huang and Chen, 2006; Landino *et al.*, 2006), but recently, a complete analysis on how to proceed for a correct biotin switch experimental design has been published (Forrester *et al.*, 2009a), explaining how to avoid the potential pitfalls of this technique. Another control should be included at this point. The sample should also be treated in the absence of ascorbate to confirm the specificity of the labeling reaction. To synthesize the labeling molecule, *N*-succinimidyl iodoacetate (SIA) (Pierce, Rockford, IL) was incubated with a synthetic peptide containing the sequence Gly-Arg-Ala-His_6 in the molar ratio 7:1 in PBS for 1 h at 25 °C in the dark. The product was purified on Nickel column (Qiagen, GmbH, Hilden, Germany). This molecule has been designed to be sensitive to trypsin digestion such that the label can be detected as a mass shift of only 271.12 Da, which simplifies the mass spectrometric analysis. In addition, this novel tag offers the advantage of producing a reporter ion ($MH^+ = 912.40$ Da), related to the released sequence Ala-His_6, which is also detectable in the matrix-assisted laser desorption ionization-time-of-flight (MALDI-TOF) spectra.
7. Dialyze the solution containing His-tag-labeled proteins to eliminate the I-CH_2-CO-Gly-Arg-Ala-His_6 in excess.
8. Purify the tagged proteins by affinity chromatography, incubating the protein solution with a Nickel column for 30 min at 4 °C. After three washing steps with 50 m*M* imidazole, elute the labeled proteins by adding 500 m*M* imidazole.
9. Separate the purified proteins by reducing SDS-PAGE and perform detection by Coomassie staining and by Western blot with the anti-His antibody (Santa Cruz Biotechnology, diluted 1:1000) (Fig. 14.2).
10. In-gel digestion: cut the detectable bands, reduce, alkylate, and digest overnight with bovine trypsin following previously published procedures (Shevchenko *et al.*, 2006) and analyze the digest by MALDI-TOF MS or nano-liquid chromatography–electrospray ionization (nanoLC–ESI)-MS/MS.
11. MS analysis: use 1 μl of the supernatant of the digestion for MALDI-TOF MS analysis and mix it with the same amount of α-cyano-4-hydroxycinnamic acid as matrix, operating in reflector mode. Measure peptides in the mass range from 750 to 4000 Da. For the nanoLC–ESI-MS/MS analysis, the tryptic peptide mixtures should be acidified up to 5% formic acid and injected into a capillary chromatographic system.

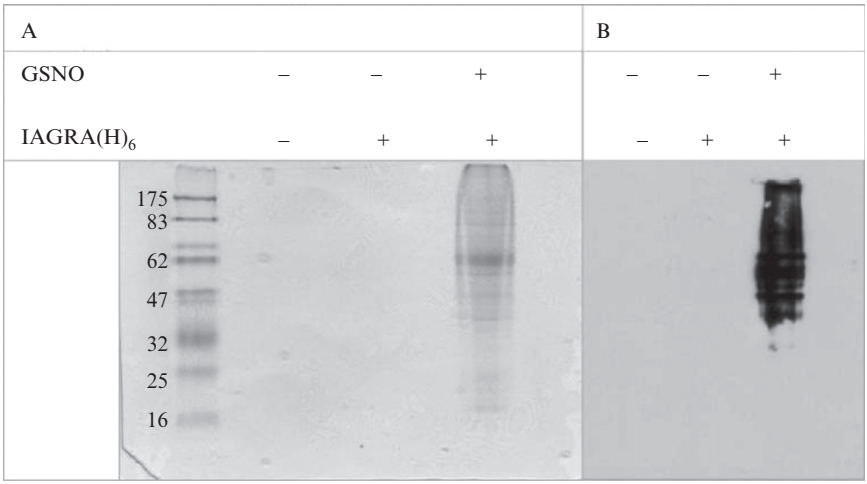

Figure 14.2 Enrichment of *S*-nitrosylated neuronal proteins from rat cerebral cortex. Proteins extracted from rat brain were in part treated with 10 m*M* GSNO as a positive control, blocked with NEM, reacted with the His-tag peptide (here indicated as IAGRA $(H)_6$) after reduction with ascorbate and purified on Nickel column. Eluates, containing His-tagged proteins, were then separated by 10% SDS–PAGE (A) and blotted with an anti-His-tag antibody (B). Bands cut from Coomassie stained gel in (A) were then digested and analyzed by mass spectrometry. Identified *S*-nitrosylated proteins are reported in the table.

Fractionate peptides on a reverse phase (RP) nanocolumn packed with C18 material. A gradient of eluents A (H_2O with 2% (v/v) ACN, 0.1% (v/v) formic acid) and B (ACN with 2% (v/v) H_2O with 0.1% (v/v) formic acid) is used to achieve separation, from 8% B (at 0 min 0.2 μl/min flow rate) to 48% B (at 60 min, 0.2 μl/min flow rate). Analyses are performed in positive ion mode. MS/MS spectra data files from each chromatographic run are first converted and then searched into databases using the following parameters: two missed cleavages, variable cysteine alkylation by NEM or I-CH_2-CO-Gly-Arg-Ala-His_6, and variable oxidation of methionine residue.

By using this method, after the analysis of neuronal cytosolic proteins extracted from cerebral cortex, many putative *S*-nitrosylated proteins were found (see Table 14.1). Twenty-eight peptides containing modified cysteines, corresponding to 19 proteins, were identified either by MALDI-TOF or nanoLC–MS/MS. Some of these proteins were already shown to be *S*-nitrosylated in the literature, but novel sites were also revealed. In addition, several other proteins were found (241 proteins identified with probability $>99\%$) for which the modified residues could not be identified.

Table 14.1 *S*-Nitrosylated proteins extracted from rat cerebral cortex and identified by the His-tag switch method

	Protein name	IPI code	Modified peptide	MS detection	
1	Heat shock protein 86	IPI00208256	DY**C**TR	MALDI	
2	Heat shock cognate 71 kDa protein	IPI00208205	V**C**NPIITK	MALDI	
			CNEIISWLDKNQTAEK	MALDI	
3	Dihydropyrimidinase-related protein 2	IPI00192034	GLYDGPV**C**EVSVTPK	MALDI	
			SITIANQTN**C**PLYVTK	MALDI	
4	Pyruvate kinase, isozymes M1/M2	IPI00231929	GIFPVL**C**K		nLCMS/MS
			NTGII**C**TIGPASR		nLC-MS/MS
			CLAAALIVLTESGR		nLC-MS/MS
5	Rab GDP dissociation inhibitor alpha	IPI00324986	NTNDANS**C**QIIIPQNQVNR	MALDI	
6	Tubulin alpha-1 chain	IPI00189795	YMA**CC**LLYRGDVVPK	MALDI	
			AV**C**MLSNTTAIAEAWAR	MALDI	
7	Phosphoglycerate kinase 1	IPI00231426	AAVPSIKF**C**LDNGAK	MALDI	
8	Fructose-bisphosphate aldolase A	IPI00231734	R**C**QYVTEK	MALDI	
9	L-lactate dehydrogenase A chain	IPI00197711	VIGSG**C**NLDSAR		nLC-MS/MS
10	Malate dehydrogenase, cytosolic	IPI00198717	ENFS**C**LTR		nLC-MS/MS
			VIVVGNPANTN**C**LTASK		nLC-MS/MS

11	Glyceraldehyde-3-phosphate dehydrogenase	IPI00212647	AAFS**C**DK VPTPNVSVVDLT**C**R	MALDI MALDI	nLC-MS/MS
12	14-3-3 protein epsilon (14-3-3E)	IPI00325135	A**C**RLAK	MALDI	
13	Pgam1 protein	IPI00421428	DAGYEFDI**C**FTSVQK	MALDI	
14	14-3-3 protein eta	IPI00231677	N**C**NDFQYESK	MALDI	
15	14-3-3 protein zeta/delta	IPI00324893	DI**C**NDVLSLLEK LAEQAERYDDMAA**C**MK	MALDI MALDI	nLC-MS/MS
16	Ckb Creatine kinase B-type	IPI00470288	F**C**TGLTQIETLFK		nLC-MS/MS
17	Ldhb L-lactate dehydrogenase B chain	IPI00231783	VIGSG**C**NLDSAR		nLC-MS/MS
18	Tuba4 Tubulin, alpha 4	IPI00362927	SIQFVDW**C**PTGFK		nLC-MS/MS
19	Peptidylprolyl isomerase A	IPI00387771	ITISD**C**GQL		nLC-MS/MS

Adapted from Camerini *et al.* (2007).

3. Direct Analysis of *S*-Nitrosylation by MS

The labile nature of the SNO group represents an obstacle against the progress of the study of *S*-nitrosylation by direct mass spectrometric detection. For example, when using MALDI-TOF MS, the laser energy required for peptide ionization also elicits the loss of NO from the Cysteine residue. However, under gentler conditions as in ESI-MS, *S*-nitrosylated peptides can be observed with a +29 Da difference respect to the unmodified ions (Lee *et al.*, 2007). In this case, fine tuning of instrument parameters enables the determination of *S*-nitrosylated sites directly, avoiding derivatization steps that could produce false positive identifications, due to the difficulty to control the multiple reactions present in protocols like the biotin switch. Up to now this kind of analysis has been used with synthetic peptides or purified recombinant proteins (Hao and Gross, 2006; Mirza *et al.*, 1995; Wang *et al.*, 2008). We present here a protocol that has been successfully applied in the study of *in vivo S*-nitrosylated phytochelatins (PCs), isolated from cadmium-stressed *Arabidopsis thaliana* cells (Elviri *et al.*, 2010). PCs are Cysteine-rich metal-binding peptides synthesized in plants from glutathione (GSH) to counteract the toxic effects of heavy metal ions (Rauser, 1999). They are $(\gamma\text{-Glu-Cys})_n$-X peptides, in which n usually ranges from 2 to 5 and X is commonly a Gly. The presence of *S*-nitrosylated PCs was reported for the first time by De Michele *et al.* (2009) and a regulation of content/function of PCs by NO, influencing cell viability, was postulated.

3.1. Protocol for the direct analysis of *S*-nitrosylated peptides

1. Collect about 400 mg of *A. thaliana* cells pellet, previously treated with $CdCl_2$, and homogenize them in a mortar in ice-cold 5% (w/v) 5-sulphosalicylic acid, containing 6.3 m*M* diethylenetriaminepentaacetic acid according to De Knecht *et al.* (1994) in 20 m*M* Tris–HCl pH 7.6 and 0.1 m*M* EDTA. After centrifugation at 10,000×*g* for 10 min at 4 °C, keep and filter the supernatants through Minisart 0.45-μm filters (Sartorius) before LC-MS assay. The extract can be stored up to 2 months at −20 °C before analysis. To block free Cysteines, carbamidomethylation can be performed by treating the final extract with iodoacetamide (final concentration 80 m*M*) for 20 min in the dark.
2. To include a positive control, treat a standard sample containing PC_x with GSNO as a NO donor. PC_x standard compounds (AnaSpec, San Jose, CA, USA) can be dissolved in 20 m*M* Tris–HCl pH 7.6 and 100 μM EDTA to a final concentration of 1 mg ml^{-1}. GSNO (50 μl of a 0.5 m*M* solution, final concentration 25 μM) is added to the PC_x solutions and the reaction mixtures incubated for 1 h at 37 °C in the dark.

3. Analyze the sample injecting it (injection volume 10 μl) into a liquid chromatography system equipped with a C18 column and using a gradient solvent system [(A) aqueous formic acid 0.1% (v/v)/(B) 0.05% (v/v) formic acid in acetonitrile] as follows: 5% solvent B for 2 min, then a linear gradient from 5% to 50% B in 21 min at a flow rate of 200 μl min^{-1}. Maintain solvent B at 50% for 5 min to clean the column before re-equilibration (10 min).
4. Analysis can be performed with different types of ESI mass spectrometers. In our analysis we used a LTQ XL linear ion trap instrument (Thermo Electron Corporation) and a triple quadrupole Quattro LC mass spectrometer (Micromass, Manchester, UK), thus we can suggest instrumental parameters to be used when optimizing performances for direct *S*-nitrosylation detection when using these machines. Optimized conditions of the interface for the LTQ XL linear ion trap are as follows: ESI voltage 3.5 kV, capillary voltage 20 V, capillary temperature 200 °C, range m/z 400–1300. Perform MS/MS collision-induced dissociation (CID) experiments under product-ion mode with a collision gas pressure of 2.3×10^{-3} mbar in the collision cell and varying the collision energy (CE) from 5 to 25 eV. Optimized conditions of the interface for the triple quadrupole Quattro LC are: ESI voltage 3.0 kV, cone voltage 30 V, rf lens 0.5 V, source temperature 130 °C, desolvation temperature 250 °C. Acquire continuum mode full-scan mass spectra over the m/z 400–1300 range using an acquisition time of 1 s and an interscan delay of 0.1 s. When operating under CID mode, the CE can be varied from 10 to 35 eV and the m/z range as a function of PC molecular mass. On the triple quadrupole analyzer, the neutral-loss scan acquisition can be used to monitor the loss of the HSNO (or SNOH) molecule (63 Da).

By analyzing cadmium-stressed *A. thaliana* cells, the presence of PC_2, PC_3, and PC_4 and the corresponding *in vivo S*-nitrosylated derivatives was demonstrated under mild interface conditions, needed to avoid the loss of NO directly in the source. Under the operating conditions used, no di- or tri-nitrosylated forms were detected in the sample. Based upon the LC separation, it can be observed that NO-PC_2, NO-PC_3, and NO-PC_4 give rise to only one chromatographic peak indicating the presence of an *in vivo S*-nitrosylated specific site, located on the first Cys residue starting from the N-terminal (Fig. 14.3). Despite the simmetry of PCs sequence, not all the Cysteines resulted equally susceptible to *S*-nitrosylation *in vivo*. Thus, one of the interesting general conclusions emerged from this direct study is the difference in the pattern between the *in vitro* and *in vivo* nitrosylated PCs. *In vitro*, after the use of a small concentration of GSNO as a donor, the PCs result to be either multinitrosylated or mononitrosylated unspecifically on different Cys residues. This finding opens the discussion

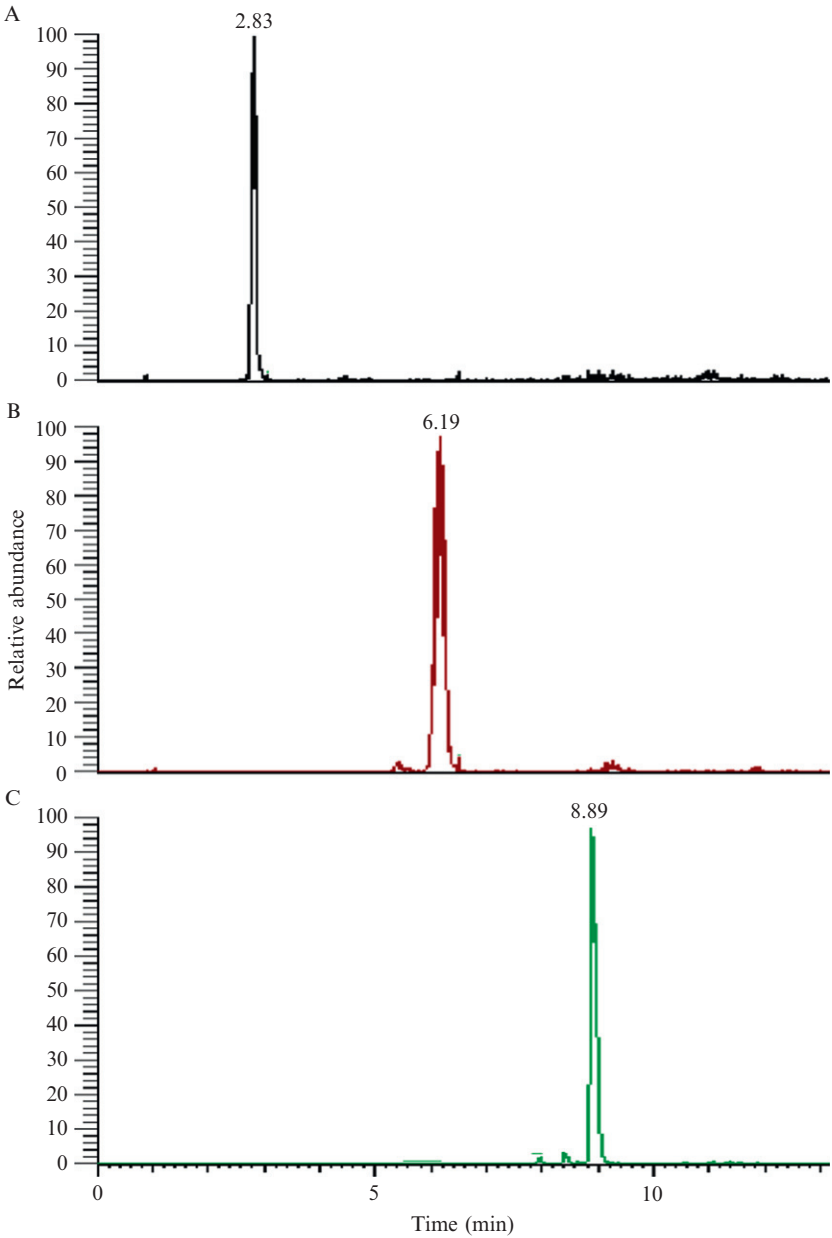

Figure 14.3 LC-LIT-MS profile of (A) PC_2-NO, (B) PC_3-NO, and (C) PC_4-NO characterized in cadmium-stressed *A. thaliana* cells. Experimental conditions: Gemini C18 column (100 × 2.0 mm, 3 μm particles), gradient elution with a [(A) aqueous formic acid 0.1% (v/v)/(B) 0.05% (v/v) formic acid in acetonitrile] mobile phase as reported in the experimental. Injection volume: 10 μl.

about how reliable is the study of a "nitrosable" proteome when using an external NO donor at high concentration, that could overnitrosylate unspecifically the available cysteines (Foster *et al.*, 2009).

The other finding that can be highlighted only by this kind of direct studies is the different stability of the SNO groups depending on the length of the aminoacidic chain that is modified. The stability of the NO moiety on the PCs identified in the sample was investigated by recording the product-ion mass spectra at different CE values. At the lowest CE value, in short chain PC_2 the nitro group is lost as NO, whereas in the case of PC_3 and PC_4 the loss of NO group is more favorable as neutral molecule (HSNO or SNOH) (Fig. 14.4). These results could implement the discussion on the influence of the amino acid sequence composition on the formation and the stability of the SNO groups. In this respect, several authors analyzed the three-dimensional structure of several proteins containing NO-reactive Cys residues and demonstrated that their nitrosylation and denitrosylation processes depend on the Cys atomic structural microenvironment rather than on a sequence consensus motif surrounding the modified residue (Ascenzi *et al.*, 2000; Hess *et al.*, 2001; Marino and Gladyshev, 2010).

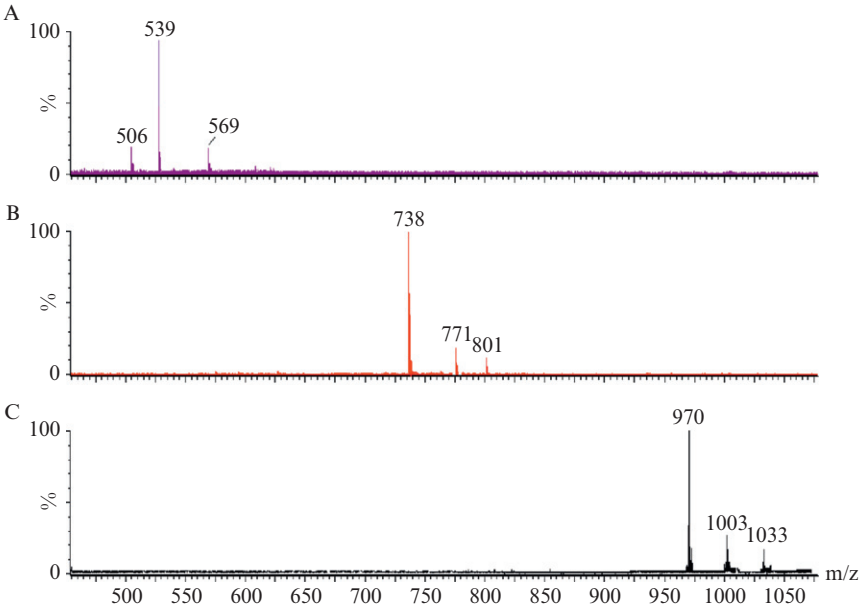

Figure 14.4 LC–ESI-LIT-MS/MS product ion mass spectra of (A) PC_2-NO ($[M+H]^+$ m/z 569), (B) PC_3-NO ($[M+H]^+$ m/z 801), and (C) PC_4-NO ($[M+H]^+$ m/z 1033) recorded at a collision energy of 15 eV.

4. Conclusions

This chapter describes two protocols developed by us for both the indirect and direct detection of *S*-nitrosylated peptides. The His-tag switch method allows a specific and efficient detection of SNO sites in proteins coming from complex mixtures, while the direct MS method was applied successfully to the analysis of *in vivo* nitrosylated peptides, showing the difference between the specificity of the *S*-nitrosylation process induced *in vivo* or *in vitro* by one of the most used NO donors, GSNO. These new methods should provide an additional procedure to shed light on the complexity of *S*-nitrosylation as a fine tuned signaling mechanism, in which most of the SNO groups are present only transiently in the reducing cellular environment and are regulated by the presence of enzymatic systems that have recently become of interest in this kind of studies (Benhar *et al.*, 2008, 2009; Paige *et al.*, 2008).

REFERENCES

Alderton, W. K., Cooper, C. E., and Knowles, R. G. (2001). Nitric oxide synthases: Structure, function and inhibition. *Biochem. J.* **357,** 593–615.

Allen, B. W., and Piantadosi, C. A. (2006). How do red blood cells cause hypoxic vasodilation? The SNO-hemoglobin paradigm. *Am. J. Physiol. Heart Circ. Physiol.* **291,** H1507–H1512.

Ascenzi, P., Colasanti, M., Persichini, T., Muolo, M., Polticelli, F., Venturini, G., Bordo, D., and Bolognesi, M. (2000). Re-evaluation of amino acid sequence and structural consensus rules for cysteine-nitric oxide reactivity. *Biol. Chem.* **381,** 623–627.

Benhar, M., Forrester, M. T., Hess, D. T., and Stamler, J. S. (2008). Regulated protein denitrosylation by cytosolic and mitochondrial thioredoxins. *Science* **320,** 1050–1054.

Benhar, M., Forrester, M. T., and Stamler, J. S. (2009). Protein denitrosylation: Enzymatic mechanisms and cellular functions. *Nat. Rev. Mol. Cell Biol.* **10,** 721–732.

Camerini, S., Polci, M. L., Restuccia, U., Usuelli, V., Malgaroli, A., and Bachi, A. (2007). A novel approach to identify proteins modified by nitric oxide: The HIS-TAG switch method. *J. Proteome Res.* **6,** 3224–3231.

Cho, D. H., Nakamura, T., Fang, J., Cieplak, P., Godzik, A., Gu, Z., and Lipton, S. A. (2009). S-nitrosylation of Drp1 mediates beta-amyloid-related mitochondrial fission and neuronal injury. *Science* **324,** 102–105.

Cook, J. A., Kim, S. Y., Teague, D., Krishna, M. C., Pacelli, R., Mitchell, J. B., Vodovotz, Y., Nims, R. W., Christodoulou, D., Miles, A. M., Grisham, M. B., and Wink, D. A. (1996). Convenient colorimetric and fluorometric assays for S-nitrosothiols. *Anal. Biochem.* **238,** 150–158.

Davies, S. A., and Dow, J. A. (2009). Modulation of epithelial innate immunity by autocrine production of nitric oxide. *Gen. Comp. Endocrinol.* **162,** 113–121.

De Knecht, J. A., Van Dillen, M., Koevoets, P., Schat, H., Verkleij, J., and Ernst, W. (1994). Phytochelatins in cadmium-sensitive and cadmium-Tolerant silene vulgaris (chain length distribution and sulfide incorporation). *Plant Physiol.* **104,** 255–261.

De Michele, R., Vurro, E., Rigo, C., Costa, A., Elviri, L., Di Valentin, M., Careri, M., Zottini, M., Sanita di Toppi, L., and Lo Schiavo, F. (2009). Nitric oxide is involved in cadmium-induced programmed cell death in Arabidopsis suspension cultures. *Plant Physiol.* **150,** 217–228.

Elviri, L., Speroni, F., Careri, M., Mangia, A., di Toppi, L.S., and Zottini, M. (2010). Identification of in vivo nitrosylated phytochelatins in Arabidopsis thaliana cells by liquid chromatography-direct electrospray-linear ion trap-mass spectrometry. *J. Chromatogr. A.* (in press).

Forrester, M. T., Foster, M. W., and Stamler, J. S. (2007). Assessment and application of the biotin switch technique for examining protein S-nitrosylation under conditions of pharmacologically induced oxidative stress. *J. Biol. Chem.* **282,** 13977–13983.

Forrester, M. T., Foster, M. W., Benhar, M., and Stamler, J. S. (2009a). Detection of protein S-nitrosylation with the biotin-switch technique. *Free Radic. Biol. Med.* **46,** 119–126.

Forrester, M. T., Thompson, J. W., Foster, M. W., Nogueira, L., Moseley, M. A., and Stamler, J. S. (2009b). Proteomic analysis of S-nitrosylation and denitrosylation by resin-assisted capture. *Nat. Biotechnol.* **27,** 557–559.

Foster, M. W., Forrester, M. T., and Stamler, J. S. (2009). A protein microarray-based analysis of S-nitrosylation. *Proc. Natl. Acad. Sci. USA* **106,** 18948–18953.

Gaston, B. M., Carver, J., Doctor, A., and Palmer, L. A. (2003). S-nitrosylation signaling in cell biology. *Mol. Interv.* **3,** 253–263.

Giulivi, C. (2003). Characterization and function of mitochondrial nitric-oxide synthase. *Free Radic. Biol. Med.* **34,** 397–408.

Giustarini, D., Dalle-Donne, I., Colombo, R., Milzani, A., and Rossi, R. (2008). Is ascorbate able to reduce disulfide bridges? A cautionary note. *Nitric Oxide* **19,** 252–258.

Greco, T. M., Hodara, R., Parastatidis, I., Heijnen, H. F., Dennehy, M. K., Liebler, D. C., and Ischiropoulos, H. (2006). Identification of S-nitrosylation motifs by site-specific mapping of the S-nitrosocysteine proteome in human vascular smooth muscle cells. *Proc. Natl. Acad. Sci. USA* **103,** 7420–7425.

Hao, G., and Gross, S. S. (2006). Electrospray tandem mass spectrometry analysis of S- and N-nitrosopeptides: Facile loss of NO and radical-induced fragmentation. *J. Am. Soc. Mass Spectrom.* **17,** 1725–1730.

Hao, G., Derakhshan, B., Shi, L., Campagne, F., and Gross, S. S. (2006). SNOSID, a proteomic method for identification of cysteine S-nitrosylation sites in complex protein mixtures. *Proc. Natl. Acad. Sci. USA* **103,** 1012–1017.

Hausladen, A., Rafikov, R., Angelo, M., Singel, D. J., Nudler, E., and Stamler, J. S. (2007). Assessment of nitric oxide signals by triiodide chemiluminescence. *Proc. Natl. Acad. Sci. USA* **104,** 2157–2162.

Hess, D. T., Matsumoto, A., Nudelman, R., and Stamler, J. S. (2001). S-nitrosylation: Spectrum and specificity. *Nat. Cell Biol.* **3,** E46–E49.

Huang, B., and Chen, C. (2006). An ascorbate-dependent artifact that interferes with the interpretation of the biotin switch assay. *Free Radic. Biol. Med.* **41,** 562–567.

Jaffrey, S. R., and Snyder, S. H. (2001). The biotin switch method for the detection of S-nitrosylated proteins. *Sci. STKE* **86,** PL1.

Jorge, I., Casas, E. M., Villar, M., Ortega-Perez, I., Lopez-Ferrer, D., Martinez-Ruiz, A., Carrera, M., Marina, A., Martinez, P., Serrano, H., Canas, B., Were, F., *et al.* (2007). High-sensitivity analysis of specific peptides in complex samples by selected MS/MS ion monitoring and linear ion trap mass spectrometry: Application to biological studies. *J. Mass Spectrom.* **42,** 1391–1403.

Khan, M., Jatana, M., Elango, C., Paintlia, A. S., Singh, A. K., and Singh, I. (2006). Cerebrovascular protection by various nitric oxide donors in rats after experimental stroke. *Nitric Oxide* **15,** 114–124.

Landino, L. M., Koumas, M. T., Mason, C. E., and Alston, J. A. (2006). Ascorbic acid reduction of microtubule protein disulfides and its relevance to protein S-nitrosylation assays. *Biochem. Biophys. Res. Commun.* **340,** 347–352.

Lee, S. J., Lee, J. R., Kim, Y. H., Park, Y. S., Park, S. I., Park, H. S., and Kim, K. P. (2007). Investigation of tyrosine nitration and nitrosylation of angiotensin II and bovine serum albumin with electrospray ionization mass spectrometry. *Rapid Commun. Mass Spectrom.* **21,** 2797–2804.

Lipton, S. A., Choi, Y. B., Takahashi, H., Zhang, D., Li, W., Godzik, A., and Bankston, L. A. (2002). Cysteine regulation of protein function—as exemplified by NMDA-receptor modulation. *Trends Neurosci.* **25,** 474–480.

Mannick, J. B., Hausladen, A., Liu, L., Hess, D. T., Zeng, M., Miao, Q. X., Kane, L. S., Gow, A. J., and Stamler, J. S. (1999). Fas-induced caspase denitrosylation. *Science* **284,** 651–654.

Marino, S. M., and Gladyshev, V. N. (2010). Structural analysis of cysteine S-nitrosylation: A modified acid-based motif and the emerging role of trans-nitrosylation. *J. Mol. Biol.* **395,** 844–859.

Mirza, U. A., Chait, B. T., and Lander, H. M. (1995). Monitoring reactions of nitric oxide with peptides and proteins by electrospray ionization-mass spectrometry. *J. Biol. Chem.* **270,** 17185–17188.

Oess, S., Icking, A., Fulton, D., Govers, R., and Muller-Esterl, W. (2006). Subcellular targeting and trafficking of nitric oxide synthases. *Biochem. J.* **396,** 401–409.

Paige, J. S., Xu, G., Stancevic, B., and Jaffrey, S. R. (2008). Nitrosothiol reactivity profiling identifies S-nitrosylated proteins with unexpected stability. *Chem. Biol.* **15,** 1307–1316.

Palmer, L. A., and Gaston, B. (2008). S-nitrosothiol assays that avoid the use of iodine. *Methods Enzymol.* **440,** 157–176.

Prasad, R., Giri, S., Nath, N., Singh, I., and Singh, A. K. (2007). GSNO attenuates EAE disease by S-nitrosylation-mediated modulation of endothelial-monocyte interactions. *Glia* **55,** 65–77.

Rauser, W. E. (1999). Structure and function of metal chelators produced by plants: The case for organic acids, amino acids, phytin, and metallothioneins. *Cell Biochem. Biophys.* **31,** 19–48.

Shevchenko, A., Tomas, H., Havlis, J., Olsen, J. V., and Mann, M. (2006). In-gel digestion for mass spectrometric characterization of proteins and proteomes. *Nat. Protoc.* **1,** 2856–2860.

Stamler, J. S., Simon, D. I., Osborne, J. A., Mullins, M. E., Jaraki, O., Michel, T., Singel, D. J., and Loscalzo, J. (1992). S-nitrosylation of proteins with nitric oxide: Synthesis and characterization of biologically active compounds. *Proc. Natl. Acad. Sci. USA* **89,** 444–448.

Tatoyan, A., and Giulivi, C. (1998). Purification and characterization of a nitric-oxide synthase from rat liver mitochondria. *J. Biol. Chem.* **273,** 11044–11048.

Tello, D., Tarin, C., Ahicart, P., Breton-Romero, R., Lamas, S., and Martinez-Ruiz, A. (2009). A "fluorescence switch" technique increases the sensitivity of proteomic detection and identification of S-nitrosylated proteins. *Proteomics* **23,** 5359–5370.

Vincent, S. R. (2009). Nitric oxide neurons and neurotransmission. *Prog. Neurobiol.* **90,** 246–255.

Wang, Y., Liu, T., Wu, C., and Li, H. (2008). A strategy for direct identification of protein S-nitrosylation sites by quadrupole time-of-flight mass spectrometry. *J. Am. Soc. Mass Spectrom.* **19,** 1353–1360.

Wendehenne, D., Durner, J., and Klessig, D. F. (2004). Nitric oxide: A new player in plant signalling and defence responses. *Curr. Opin. Plant Biol.* **7,** 449–455.

Yao, D., Gu, Z., Nakamura, T., Shi, Z. Q., Ma, Y., Gaston, B., Palmer, L. A., Rockenstein, E. M., Zhang, Z., Masliah, E., Uehara, T., and Lipton, S. A. (2004). Nitrosative stress linked to sporadic Parkinson's disease: S-nitrosylation of parkin regulates its E3 ubiquitin ligase activity. *Proc. Natl. Acad. Sci. USA* **101,** 10810–10814.

CHAPTER FIFTEEN

A Rapid Approach for the Detection, Quantification, and Discovery of Novel Sulfenic Acid or *S*-Nitrosothiol Modified Proteins Using a Biotin-Switch Method

Joseph R. Burgoyne *and* Philip Eaton

Contents

Abstract

The recent development of robust methods for the detection of proteins susceptible to *S*-nitrosylation (RSNO) and sulfenation (RSOH) has provided greater insight into the role of these oxidative modifications in cell signaling. These techniques, which have been termed "biotin-switch" methods, essentially use selective chemical reduction to swap an oxidative modification for a stable easily detectable biotin-tag. This allows for the rapid purification and subsequent detection of modified proteins using mass spectrometry. This chapter provides an overview of these biotin-switch methods, and explores its impact on the field of redox biology, including recent advances as well as limitations associated with this technique.

Cardiovascular Division, Department of Cardiology, King's College London, The Rayne Institute, St Thomas' Hospital, London, United Kingdom

Methods in Enzymology, Volume 473
ISSN 0076-6879, DOI: 10.1016/S0076-6879(10)73015-9

1. Introduction

For many years, it has been widely accepted by both the scientific and public community that oxidants are deleterious to health. This has led to the simple concept that antioxidants are a panacea, resulting in many clinical trials assessing the potential benefits of supplementation against most types of disease. Furthermore, many companies have commercialized various antioxidant health foods to profit from the simplistic view that they will maintain health or combat established disease. However, the failure of several high profile antioxidant trails has brought into question the true role oxidants actually play in physiological homeostasis and development (Heart Protection Study Collaborative Group, 2002; Miller *et al.*, 2005; Vainio, 2000). The failure of antioxidant therapy trials is consistent with a growing recognition that proteins and signaling pathways are extensively redox regulated (the "redoxome"). Antioxidant therapies may interfere with redox mechanisms that participate in healthy cell homeostasis or their responses that enable adaptation to stress or disease. In this scenario, antioxidants may be injurious, which is exactly what many trials have shown. Overall, this highlights the importance of physiological amounts of oxidants in signaling of healthy cells. The expanding library of identified redox sensor proteins that are regulated by oxidation has resulted largely from improved methods for their detection (Burgoyne *et al.*, 2007; Eaton, 2006; Savitsky and Finkel, 2002; Veal *et al.*, 2007).

Both nitrosylated thiols (RSNO) and sulfenated thiols (RSOH) are reversible oxidative modifications that can participate in redox signaling by directly modulating the functional activity of a number of proteins (specific examples are provided below). RSNO and RSOH are also common intermediates leading to several different oxidized states, including sulfination (RSO_2H), sulfonation (RSO_3H), formation of various types of disulfide, and sulfenylamidation (Salmeen *et al.*, 2003). Until relatively recently, proteins that were susceptible to RSNO and RSOH modifications were difficult to identify due to the lack of an effective method for their detection, which is made difficult due to the instability of these oxidation states. However, the development of the biotin-switch method by Jeffrey and Snyder to detect protein *S*-nitrosylation overcomes this problem by exchanging the labile RSNO modification for a readily detectable biotin-tag (Jaffrey and Snyder, 2001). The crucial step in this method being the selective reduction of cysteine *S*-nitrosothiols by ascorbate. By utilizing a similar method except using arsenite selective reduction of RSOH modified cysteines, we were able to selectively label proteins with this oxidative modification (Saurin *et al.*, 2004). The basic principal of these biotin-switch methods are summarized in Fig. 15.1.

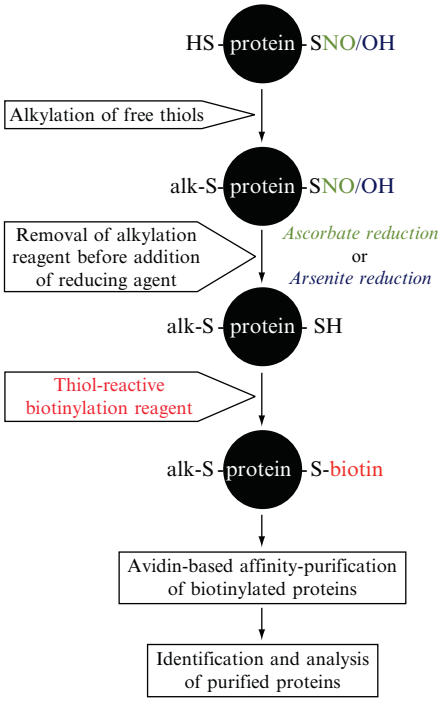

Figure 15.1 Diagram outlining the biotin-switch method. This procedure either utilizes the ascorbate reduction of the SNO bond or the arsenite reduction of SOH-modified cysteines. This is carried out under SDS-denaturing conditions, with subsequent protein labeling using a thiol-reactive biotinylation reagent. Proteins can then be purified using a streptavidin matrix and identified using mass spectrometry.

1.1. Nitrosative protein oxidation

The oxidative posttranslational modification *S*-nitrosylation is the covalent adduction of a nitric oxide (NO) moiety to a cysteine thiol. This is a modification that primarily occurs at cysteine thiols within an "acid–base" motif of the following consensus sequence: (Asp/Glu)Cys(Lys/Arg/His) (Stamler *et al.*, 1997). However, proximity of residues in the three-dimensional structure can also enable the correct environment for *S*-nitrosylation to occur (Ascenzi *et al.*, 2000; Perez-Mato *et al.*, 1999; Williams *et al.*, 2003). As well as inducing *S*-nitrosylation, NO can also bind to the metal iron centers of proteins including the heme center of guanylate cyclase. This activates the cyclase to generate 3′,5′-cyclic guanosine monophosphate (cGMP) (Kots *et al.*, 2009; Surks, 2007), a second messenger which activates the cGMP-dependent protein kinase, also known as protein kinase G (PKG). This enzyme is a major regulator of vasotone and its activation causes blood vessel dilation (vasorelaxation). Another mechanism of NO-mediated

signaling, which is independent of *S*-nitrosylation, is its ability to inhibit fibrinogen, which has no free cysteines. It does this by binding to electron-rich areas of the protein inducing a conformational change (Akhter *et al.*, 2002). Furthermore, the reaction between superoxide (O_2^-) and NO can give rise to the hybrid species peroxynitrite ($ONOO^-$). $ONOO^-$ has a different reactivity to that of NO, such that it can cause protein nitration at tyrosine residues (Beckman, 1996; Kuo and Kocis, 2002), and seems to prime proteins for *S*-glutathiolation (Adachi *et al.*, 2004; Viner *et al.*, 1999). O_2^- also functions to lower the bioavailability of NO, which potentially attenuates NO-dependent functions (Price *et al.*, 2000).

S-nitrosylation is a readily reversible modification with the recent identification of two enzyme systems that can denitrosylate proteins. The first identified denitrosylase is the enzyme *S*-nitrosoglutathione reductase (GSNOR), which was discovered using *in vivo* studies to denitrosylate GSNO (Liu *et al.*, 2001). Furthermore, a deficiency in GSNOR increased protein *S*-nitrosylation in activated cells expressing iNOS. This highlights a complex relationship between *S*-nitrosylation of low molecular weight compounds and protein thiols, whereby NO is mobile between these two populations. The second identified denitrosylase is thioredoxin which was discovered using the biotin-switch method, where it was shown that this enzyme can decrease cytosolic caspase-3 *S*-nitrosylation (Benhar *et al.*, 2008). Several proteins have also been identified using the biotin-switch method that are resistant to denitrosylation and are stably *S*-nitrosylated under basal conditions (Paige *et al.*, 2008). In addition, these proteins unlike other nitrosothiols were not denitrosylated when NO synthesis was inhibited.

Since the development of the ascorbate-dependent biotin-switch method, there has been a dramatic increase in the identification of proteins susceptible to *S*-nitrosylation. This has implicated this redox modification in a diverse array of cell signaling pathways including modulation of protein phosphorylation pathways (Brennan *et al.*, 2006; Burgoyne and Eaton, 2009; Chen *et al.*, 2008), myofilament regulation (Dalle-Donne *et al.*, 2000; Nogueira *et al.*, 2009), ion channel function (Gomez *et al.*, 2009; Gonzalez *et al.*, 2009; Xu *et al.*, 1998), G protein-coupled receptor signaling (Aronstam *et al.*, 1995; Kokkola *et al.*, 2005), regulation of apoptosis (An *et al.*, 2006; Azad *et al.*, 2006; Benhar and Stamler, 2005), endothelial cell migration (Pi *et al.*, 2009), neurotransmission (Kawano *et al.*, 2009; Kaye *et al.*, 2000; Wolosker *et al.*, 1996), metabolism (Eaton *et al.*, 2002b), protein degradation (Cordes *et al.*, 2009; Kapadia *et al.*, 2009), exocytosis (Matsushita *et al.*, 2003; Palmer *et al.*, 2008; Sossa *et al.*, 2007), cell adhesion (Forsythe and Befus, 2003; Thom *et al.*, 2008), and cell proliferation and control of mitochondria (Cai *et al.*, 2006; Cho *et al.*, 2009; Hammoud *et al.*, 2007; Moon *et al.*, 2005; Zhang *et al.*, 2005a). Furthermore, *S*-nitrosothiol modification of proteins has been shown to be an important mediator in

several disease states including tumor formation and growth (Azad *et al.*, 2009; Chanvorachote *et al.*, 2009), age-related muscle dysfunction (Wu *et al.*, 2009), several neurodegenerative disorders (Chung *et al.*, 2004; Tsang *et al.*, 2009; Uehara *et al.*, 2006), ischemia reperfusion injury (Lima *et al.*, 2009; Sun *et al.*, 2007), diabetes (Cordes *et al.*, 2009; Wadham *et al.*, 2007), nitrate tolerance (Sayed *et al.*, 2008), and inflammation and disorders of the skeletal muscle (Bellinger *et al.*, 2009; Lim *et al.*, 2008).

A prerequisite for *S*-nitrosylation is the formation of reactive nitrogen species (RNS), as authentic NO has a low reactivity with protein thiols. RNS with *S*-nitrosylation activity include the nitrosonium ion (NO^+) and dinitrogen trioxide (N_2O_3). It is likely that changes in the formation of these RNS occur when the balance between NO and reactive oxygen species (ROS) formation is altered. Little is known about the exact biochemical reactions that actually lead to the formation of these *S*-nitrosylating RNS. However, it has been suggested that the transition metals, copper (Cu^{2+}) and iron (Fe^{2+}), may be able to catalyze the transfer of NO group from GSNO or nitrite to reactive cysteine thiols, a mechanism termed transnitrosylation (Luchsinger *et al.*, 2003; Romeo *et al.*, 2002; Stubauer *et al.*, 1999; Tao and English, 2003). Recent work supports an additional mechanism in which low radical fluxes representative of the cellular environment were studied *in vitro*. Formation of NO^+ and N_2O_3 was found to be likely dependent on the reaction between the intermediate peroxynitrous acid and excess NO. With a ratio of 3:1 of NO to superoxide (O_2^-) being optimal for increased protein *S*-nitrosylation (Daiber *et al.*, 2009).

While using the biotin-switch assay to identify potential candidate substrates for *S*-nitrosylation, cells or tissue are normally treated with a NO donor. Common NO donors that were originally used in conjunction with the biotin-switch assay are SNAP and GSNO. However, it has been shown that both of these NO donors are unable to directly enter cells without being first converted in the presence of cysteine (or cystine in the case of GSNO) to form CysNO. The CysNO generated can then be transported into cells by an L-amino acid transport system (Zhang and Hogg, 2005). Using chemiluminescence, the SNO content in a mouse macrophage cell line (RAW264.7) was measured using a range of NO donors, each at a concentration of 500 μM. SNAP generated 34.3 $\pm$ 4.4 pmol/mg of *S*-nitrosylated proteins, GSNO created 58.4 $\pm$ 5.0 pmol/mg whereas CysNO produced a much larger robust increase in SNO with 12,750 $\pm$ 370 pmol/mg of protein being modified. The addition of L-cysteine to GSNO dramatically increased SNO content to 4180 $\pm$ 182 pmol/mg (Zhang and Hogg, 2004). As SNAP and GSNO are poor nitrosylating agents without the presence of cysteine, it has become common to use CysNO with the biotin-switch assay, as it generates a large robust detectable increase in protein *S*-nitrosylation. However, the (patho)physiological relevance of this transnitrosylating form of NO is not well defined.

NO is biosynthesized from the oxidation of L-arginine by the enzyme nitric oxide synthase (NOS), generating L-citrulline as a by-product. Three different isoforms of NOS have been identified and are termed neuronal NOS (nNOS or NOS1), inducible NOS (iNOS or NOS2), and endothelial NOS (eNOS or NOS3) (Forstermann *et al.*, 1991; Hare and Stamler, 1999). nNOS and eNOS are constitutively expressed and are involved in the regulation of normal cellular function and are activated by calcium and calmodulin, producing low levels of NO. iNOS is expressed in response to an array of stimuli (e.g., cytokines, stress, bacterial infection), and this isoform produces high levels of NO independent of calcium (Taylor and Geller, 2000). eNOS is localized within membrane caveolae in close proximity to the L-type calcium channel, whereas nNOS is localized to the sarcoplasmic reticulum in a complex with the ryanodine receptor in muscle cells (Barouch *et al.*, 2002), and to the cytoplasm in others cell types. The compartmentalization of synthesis means NO is confined to the proximity of its targets allowing efficient and controlled signal transduction (Fig. 15.2). Indeed, many of the targets of protein *S*-nitrosylation are colocalized with NOS enzymes, and some substrates physically interact with the synthase, such as procaspase-3 (Matsumoto *et al.*, 2003).

Some physiological scenarios during which marked changes in protein *S*-nitrosylation occur have been identified. For example, during endothelial cell hypoxia there is an imbalance in NO and O_2^- formation, enhancing RNS generation and protein *S*-nitrosylation (Matsumoto *et al.*, 2003). The same occurs during cardiac ischemic preconditioning, where increased protein *S*-nitrosylation was observed (Sun *et al.*, 2007). Analysis of this protected cardiac tissue using the biotin-switch method showed many of the *S*-nitrosylated proteins are regulators of mitochondrial energetics and calcium transport; perhaps consistent with a central role of this organelle in limiting injury during ischemia and reperfusion.

The biotin-switch method relies on an indirect approach for detecting *S*-nitrosylated proteins by substituting modified SNOs with a detectable biotin-tag. However, one major query relates to the specificity of ascorbate for SNO reduction. Some researchers have suggested ascorbate lacks specificity, and may reduce sulfenic acids or "soft" disulfides (Giustarini *et al.*, 2008; Monteiro *et al.*, 2007). Evidence from one publication has shown that ascorbic acid can reduce the $ONOO^-$ anion-induced disulfides in the microtubule-associated protein-2, tubulin, and tau. This could potentially lead to the generation of false-positives when using the biotin-switch method (Landino *et al.*, 2006). Another study has shown that ascorbate can generate misleading results during the biotin-labeling step. This was demonstrated by pretreating BSA with 20 m*M* 2-mercaptoethanol so that only approximately 0.5–1% was *S*-nitrosylated. This then underwent biotin-switch analysis and generated a detectable signal comparable to that of

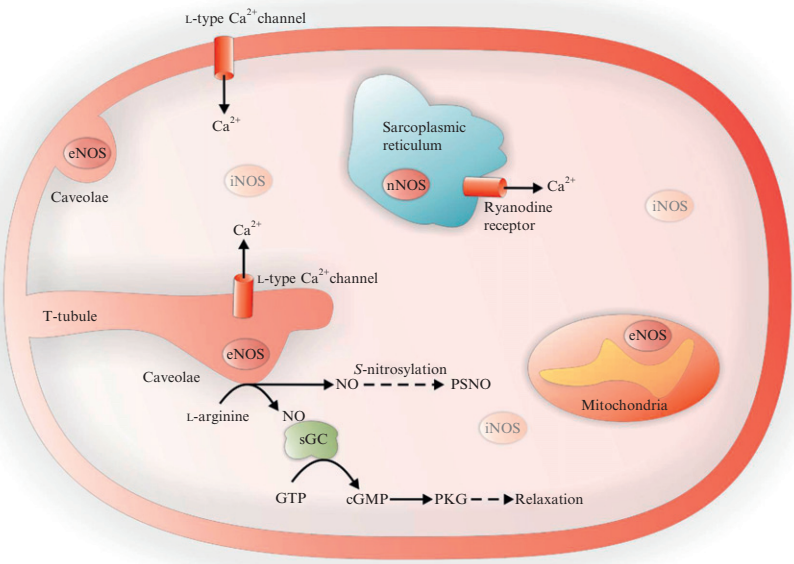

Figure 15.2 Sub-cellular localization of NOS isoforms. eNOS is localized within membrane caveolae in close proximity to the L-type calcium channel, and nNOS is localized to the sarcoplasmic reticulum in a complex with the ryanodine receptor. iNOS is localized to the cytosol and is expressed at low levels under basal conditions, becoming elevated in response to an appropriate stimuli. Nitric oxide generated from arginine can regulate cell signaling by increasing protein *S*-nitrosylation or by enhancing the activity of guanylate cyclase.

nonreduced BSA, which contained a higher SNO content. These findings were the result of ascorbate increasing the rate of protein biotinylation; highlighting another complexity of the biotin-switch method (Huang and Chen, 2006). A recent publication has suggested using sinapinic acid instead of ascorbate for the reduction of *S*-nitrosothiols. The reason being that sinapinic acid is more selective for SNOs as it does not reduce disulfides (Kallakunta *et al.*, 2009). A thorough assessment of the biotin-switch method has however shown that H_2O_2, which induces both protein sulfenic acid and disulfide bond formation, did not increase labeling by the biotin-switch method (Forrester *et al.*, 2007).

It is now clear that the predominant issue with the ascorbate-dependent biotin-switch assay is not the selectivity of ascorbate for *S*-nitrosothiols, but rather the sensitivity of this technique for modified proteins. The sensitivity of the ascorbate-dependent biotin-switch method has been compared with that of the highly sensitive tri-iodide chemiluminescence measurement of SNO levels. The biotin-switch method was relatively insensitive, only

detecting relatively high levels of SNOs (in the nmol/mg protein range) in cells exposed to CysNO. It was also unable to detect low levels generated during physiological NO generation (Zhang *et al.*, 2005b). Recently the sensitivity of the biotin-switch method was enhanced by the addition of copper to ascorbate during the reduction and labeling step of the method (Wang *et al.*, 2008). Treatment of normal human bronchial epithelial cells with 10 μM CysNO generated no detectable difference in labeling between ascorbate and nonascorbate-treated samples, and *S*-nitrosylation appeared the same as in untreated controls. However, by including 10 μM copper(II) sulfate in the reductive labeling step in the absence of metal chelators there was a substantial increase in ascorbate-induced labeling. This provides evidence that copper is required for efficient ascorbate reduction of SNOs and leads to a considerable enhancement of the sensitivity of the biotin-switch method. However, the use of copper to enhance sensitivity could be at the expense of selective reduction of SNO. This reinforces the need to investigate in detail putative *S*-nitrosylated proteins identified; examining new candidates on a case-by-case basis to firmly corroborate regulation in this way. It is also important to remember that treatment of tissues or cells with an exogenous *S*-nitrosylating agent will lead to global *S*-nitrosylation that is unlikely to reflect true physiological signaling, which likely involves discretely localized NO and RNS formation.

1.2. Sulfenic acid formation

The oxidant hydrogen peroxide (H_2O_2) is continually generated intracellularly through dismutation of superoxide (O_2^-) (Liochev and Fridovich, 2007), which can either be spontaneous or is enzymatically mediated by superoxide dismutase. A number of lipid peroxides can also be generated which have related oxidation chemistry to H_2O_2 (Niki *et al.*, 2005). Peroxides function as signaling molecules by principally oxidizing protein cysteine thiols to form a sulfenic acid (RSOH) modification (Burgoyne *et al.*, 2007; Savitsky and Finkel, 2002; Schroder and Eaton, 2008; Veal *et al.*, 2007). Cysteines that are sensitive to this form of oxidation are generally stabilized in the more reactive deprotonated thiolate (RS^-) form. This anionic state usually involves close proximity to the basic amino acids lysine or arginine, which deprotonate the thiol to achieve a "reactive cysteine." With only a small proportion of cysteines having the correct structure to undergo transition to a sulfenic acid, this provides a basis for specificity in thiol-mediated redox signaling. Protein sulfenates are generally short-lived due to their high reactivity with reducing equivalents, especially abundant species such as thiols which react to form disulfides (O'Brian and Chu, 2005). This lability makes protein sulfenic acids difficult to detect as the modification can be easily lost during sample preparation due to reduction or conversion to another oxidized state. However, the use

of a biotin-switch method that utilizes the selective arsenite reduction of the RSOH bond has proved effective in the detection, purification, and identification of protein sulfenic acids (Saurin *et al.*, 2004). This analysis included an alkylating agent during cell lysis or tissue homogenization, which stabilizes any RSOH modifications by preventing its reduction by other thiols in the system. The alkylating agent may also limit artifacts by derivatizing protein thiols which may otherwise react with molecular oxygen to form false-positive sulfenates.

The cellular prerequisite for protein sulfenic acid formation is the generation of oxidant molecules, especially peroxides such as H_2O_2. H_2O_2 results from the reduction of O_2^-, which itself is produced by many sources including xanthine oxidase, NADPH oxidase (NOX), lipoxygenase, cyclooxygenase, uncoupled NOS, and leakage from the electron transport chain by cytochrome *c* oxidase. For most of these enzymes, O_2^- is a by-product of catalysis, with only the NOX enzymes generating O_2^- as a primary outcome. NOX enzymes generate large amounts of O_2^- by transferring the electrons from NADPH to molecular oxygen leading to its one-electron reduction and the formation of O_2^- ($2O_2 + NADPH \rightarrow 2O_2^- + H^+ + NADP^+$). This enzyme has been found to be abundant in the cardiovascular system and consists of five different isoforms with varying levels of expression of each depending on the tissue type. In the endothelium, NOX2 and NOX4 are expressed, whereas vascular smooth muscle contains NOX1, NOX2 and NOX4, and cardiomyocytes, NOX2 and NOX4 (Cave *et al.*, 2006). Under physiological conditions NOX4 and the constitutively active NOX2 generate low controlled amounts of O_2^-. The formation of this oxidant is tightly regulated allowing it to act as a controlled mediator in normal cellular redox signaling. During vascular disease NOX1 is upregulated in vascular smooth muscle cells and NOX2 expression is increased in endothelial cells and invading phagocytic cells (Sorescu *et al.*, 2002; Wingler *et al.*, 2001). Both of these isoforms generate large quantities of O_2^- which overwhelm the antioxidant system leading to aberrant protein oxidation and cellular dysfunction. Several stimuli are known to increase O_2^- formation in a NOX-dependent manner. These include growth factors (platelet derived growth factor (PDGF), endothelial growth factor (EGF), vascular endothelial growth factor (VEGF)), insulin, cyclic strain, tumor necrosis factor-α (TNF-α), and angiotensin II (Bedard and Krause, 2007; Brandes and Kreuzer, 2005).

H_2O_2 generates a diverse range of biological effects that vary dramatically depending on its concentration. Under basal conditions, transient increases in H_2O_2 are believed to be important in homeostatic signaling (see Fig. 15.3). With beneficial implications linked to cell survival (Dong *et al.*, 2005), cardioprotection (Costa *et al.*, 2006; Hegstad *et al.*, 1997), regulation of vascular tone (Shimokawa and Morikawa, 2005), tissue growth and repair, and the regulation of inflammation (Mantovani *et al.*,

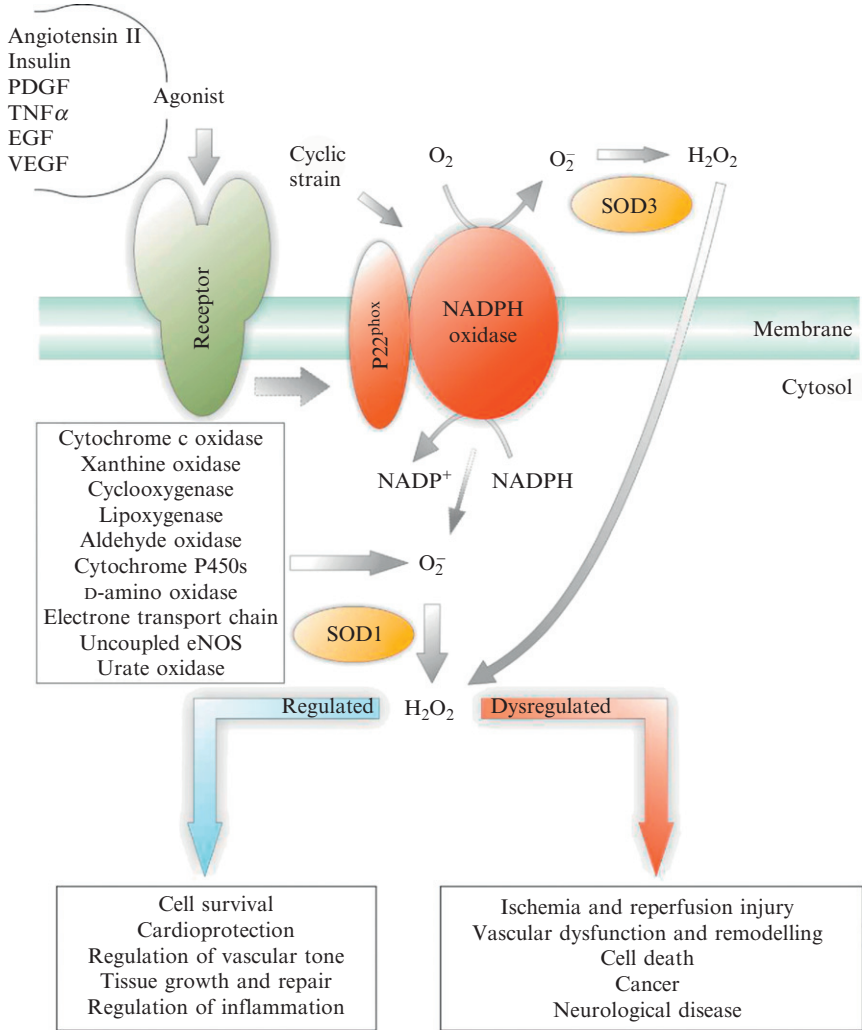

Figure 15.3 Summary of the formation and the physiological and pathophysiological effects of H_2O_2.

2007; Roy *et al.*, 2006; Zanetti *et al.*, 2002). H_2O_2 can act as a second messenger, being produced in a regulated manner in response to precise triggers, such as receptor stimulation. H_2O_2 may selectively oxidize specific reactive cysteine residues on target proteins, which in some cases alters their function. H_2O_2 does not unselectively oxidize all manner of cellular thiols, simply because the vast majority of cellular thiols are not charged at physiological pH and so react too slowly to achieve stochiometric oxidation.

Proteins known to be susceptible to and regulated by H_2O_2-mediated oxidation include kinases (c-Jun NH_2-terminal kinase, Sty1, cAMP dependent kinase, cGMP-dependent kinase, MEK kinase 1, IκB kinase-β, and Src tyrosine kinase), phosphatases (phosphatidylinositol-3,4,5-trisphosphate 3-phosphatase, low-molecular-weight protein tyrosine phosphatases, M-phase inducer phosphatase 3, protein tyrosine phosphatase 1B, and cdc25), transcription factors (OxyR, OhrR, c-Jun/c-Fos, heat shock factor 1, BRCA1-associated C-terminal helicase, and Nrf-2/Keap-1), ion channels (K(ATP) channels and the ryanodine receptor), metabolic enzymes (glyceraldehyde 3-phosphate dehydrogenase), RNA binding proteins (RNase H1), *N*-acetyl transferases (serotonin *N*-acetyl transferase), and stress proteins (Burgoyne *et al.*, 2007; Eaton *et al.*, 2002a; Savitsky and Finkel, 2002; Veal *et al.*, 2007). In several of these proteins, sulfenic acid formation is an intermediate prior to transition to an alternate, generally more stable oxidized state. A sulfenic acid can be resolved by a reactive thiol that is in close proximity leading to disulfide bond formation. Alternatively, reduced GSH might resolve the sulfenate leading to protein glutathiolation. It is also possible that other thiol-reactive oxidant sensor proteins actually serve to capture the oxidant and form an activated intermediate state, which then reacts with a target protein, so transferring the oxidation. Such oxidant sensors might include thioredoxin or peroxiredoxin, which have both been shown to behave in this way (Veal *et al.*, 2007).

H_2O_2 beyond certain amounts (which will be specific to an individual cellular scenario) can lead to aberrant protein oxidation states, which are likely dependent on an initial formation of a sulfenic acid (Charles *et al.*, 2007). H_2O_2 can drive sulfenic acids to higher irreversible oxidized states; first to the sulfinic and then to sulfonic acid form (Burgoyne *et al.*, 2007; Savitsky and Finkel, 2002; Schroder *et al.*, 2008; Veal *et al.*, 2007). Reversal of the protein sulfinic acids back to the reduced thiol state has been demonstrated for 2-Cys peroxiredoxin proteins, and is catalyzed enzymatically by sulfiredoxin (Biteau *et al.*, 2003). This sulfiredoxin repair reaction appears to be selective for this single class of proteins, and may have evolved to recover the cellular reducing system after a large oxidative onslaught. Therefore, the global accumulation of proteins that are sulfinated or sulfonated is often associated with cellular dysfunction. The detrimental role of dysregulated H_2O_2 in several disease states has been well documented, including injury during ischemia and reperfusion (Wolkart *et al.*, 2006), vascular dysfunction and remodeling (Cai, 2005; Xu and Touyz, 2006), cell death (Hampton *et al.*, 1998; Slater *et al.*, 1995), neurological disease and cancer (Lopez-Lazaro, 2007; Miller *et al.*, 2009; Moreira *et al.*, 2005).

The biotin-switch method for detecting protein sulfenic acids has not been as extensively used or characterized as that for *S*-nitrosylation. However, the same considerations should be taken into account with the identification of any modified proteins after exogenous oxidant treatment.

A full characterization needs to be carried out to determine if a protein sulfenation event couples to a functional response; and is not simply a nonstoichiometric, background oxidation, or an artifact of using biologically irrelevant amounts of H_2O_2.

2. Overview of Analytical Strategy

The biotin-switch protocol used in this laboratory utilizes maleimide as an alkylating agent to block free thiols rather than methyl methanethiosulfonate (MMTS), which was originally used. MMTS disulfide exchanges to block free protein thiols, a reaction that generates a free thiol form of MMTS. This reduced form of MMTS may complicate the biotin-switch assay by possibly reducing nitrosothiols in the system causing a loss in detection. There is also a risk that it may reduce protein disulfides, making these cysteines susceptible to artifactual *S*-nitrosylation and false-positive identifications. The use of lightproof Eppendorf tubes throughout the protocol when analyzing protein *S*-nitrosylation is crucial to minimize light-dependent protein denitrosylation. Furthermore, the use of small protein spin desalting columns (Pierce, product #89849) or larger disposable PD-10 columns (GE Healthcare Life Sciences) to remove alkylating agent rather than acetone precipitation saves time and increases labeling efficiency. This improves the sensitivity of detecting protein *S*-nitrosylation, as this is a labile modification which is lost progressively with handling time. During the labeling step 10 μM copper (II) sulfate can be added to the biotin-HPDP containing buffer without DTPA and neocuproine, to potentially enhance detection of *S*-nitrosylated proteins. However, the use of copper(II) sulfate in the biotin-switch assay has not been extensively characterized and therefore is absent from the protocol outlined below. The advantage of using *N*-[6-(Biotinamido) hexyl]-3′-(2′-pyridyldithio)propionamide (biotin-HPDP) is that unlike other biotin-alkylating agents it forms a reversible disulfide bond with reduced thiols. This disulfide allows labeled proteins to be selectively eluted from the streptavidin–agarose using 2-mecaptoethanol. This dramatically reduces elution of proteins nonspecifically bound to streptavidin–agarose, which can occur if SDS sample buffer is used to elute instead of a disulfide reducing agent. To generate a positive control or identify potential candidates for *S*-nitrosylation the compound *S*-nitrosocysteine (CysNO) can be used as it induces a high robust increase in this modification. A protocol for generating CysNO is shown below. However, any proteins identified using the biotin-switch method after treatment of tissue or cells with exogenous oxidant should be further characterized to determine if this is a true biological modification. This can be done by carrying out the biotin-switch method and comparing untreated controls to a physiological or pathological intervention.

It is possible that the treatment alters the *S*-nitrosylation state of a protein; albeit this is not evident from examination of the whole lysate staining intensity profile following the biotin-switch assay. This may occur if a low abundance protein is *S*-nitrosylated, and thus is below the level of detection. To address this, avidin-based affinity capture of modified proteins followed by immunostaining for candidate protein of interest can help. The presence of relatively more of such a protein in a sample following an intervention indicates comparably greater amount of *S*-nitrosylation. However, a major limitation is the *S*-nitrosylated target proteins have to already be established. Ultimately, the biological importance of an *S*-nitrosylation event can be substantiated by replacing wild-type protein with a mutant in which the redox active cysteine is converted to a charge conserved serine.

2.1. Generating *S*-nitrosocysteine

CysNO is generated by mixing 100 m*M* L-cysteine, 100 m*M* sodium nitrite, and 100 m*M* hydrochloric acid in the dark for 10 min. This is followed by the addition of 100 m*M* sodium hydroxide to neutralize the reaction. The concentration of CysNO is determined using a spectrophotometer, measuring absorbance at 334 nm and using the extinction coefficient of 900 M^{-1} cm^{-1}. The CysNO should then be diluted to a suitable concentration in 100 m*M* Tris–HCl buffer pH 7.4 with the pH being verified using a pH meter or pH strips. CysNO should also be made up fresh just before the start of each experiment.

2.2. Tissue preparation

When analyzing cultured cells they should be washed in medium free of fetal bovine serum before treatment with oxidative stimuli. When inducing *S*-nitrosylation cells should be kept in the dark during incubation due to the instability of this modification when exposed to light. After the incubation of cells with appropriate oxidative stimuli they should be washed in phosphate buffered solution (or suitable buffer depending on cell type) before being scraped directly into blocking buffer. When using the biotin-switch method to detect protein *S*-nitrosylation the blocking buffer should contain 2% SDS, 100 m*M* maleimide, 0.2 m*M* neocuproine, and 1 m*M* DTPA in 100 m*M* Tris–HCl buffer pH 7.4. The use of maleimide will prevent artificial oxidation of proteins by exposure to air, and will also stabilize protein oxidation by preventing reduction and exchange reactions. The metal chelating agents, neocuproine and DTPA, are crucial as they prevent metal ion-dependent reduction of *S*-nitrosothiol modifications. When using the biotin-switch method to detect protein sulfenation the same blocking buffer should be used except neocuproine and DTPA; which were not investigated in the initial development of this method.

However, these chelating agents are anticipated to be compatible with the arsenite-dependent biotin-switch method.

For preparation of organs for biotin-switch analysis, the organ of interest should be swiftly rinsed in a suitable buffer rapidly after excision to remove as much blood as possible. After rinsing the organ, it should be snap-frozen or immediately homogenized using a tissue grinder. Homogenization is in a buffer containing 2% SDS and 100 m*M* maleimide in 100 m*M* Tris–HCl buffer pH 7.4, with 0.2 m*M* neocuproine and 1 m*M* DTPA also being added if samples are to be used for protein *S*-nitrosylation analysis.

2.3. Detection of modified proteins using the biotin-switch method

Homogenized tissue or cell lysate should be incubated at 50 °C for 25 min in an Eppendorf tube shaker (Eppendorf, Thermomixer Compact) to allow protein denaturation and efficient thiol alkylation. This is then followed by centrifugation at 25,000 rpm for 5 min to pellet any insoluble material, after which the maleimide is removed by applying 120 μl of supernantent for each sample to separate desalting spin columns (Pierce, product #89849). The eluates are then divided so that 50 μl is added to 50 μl of labeling buffer A (0.2 m*M* biotin-HPDP and 1% SDS in Tris–HCl buffer pH 7.4, with 0.4 m*M* neocuproine and 2 m*M* DTPA if analyzing *S*-nitrosylation). Another 50 μl should be added to 50 μl of labeling buffer B (0.2 m*M* biotin-HPDP, 60 m*M* ascorbate, 1% SDS, 0.4 m*M* neocuproine and 2 m*M* DTPA in Tris–HCl buffer pH 7.4 for *S*-nitrosylation, or 0.2 m*M* biotin-HPDP, 40 m*M* sodium arsenite, and 2% SDS in Tris–HCl buffer pH 7.4 for sulfenation). The mixtures are then incubated for 1 h at room temperature. For analysis of *S*-nitrosylation samples should be kept in the dark during this incubation period. After incubation the addition of 100 m*M* maleimide to each tube helps quench the labeling reactions, followed by the addition of SDS sample buffer. Samples should be run on nonreducing SDS–PAGE gels, Western blotted and probed using streptavidin–HRP to determine levels of *S*-nitrosylation or protein sulfenation in each sample. Figure 15.4 provides an example of detection of protein *S*-nitrosylation in rat aortic smooth muscle cells (A10 cells) after exposure to CysNO.

2.4. Detection and purification of modified proteins after the biotin-switch method

To purify adequate amounts of *S*-nitrosylated or sulfenated proteins for proteomic identification studies, a large scale preparation of protein prepared by the biotin-switch has to be undertaken. Samples should be prepared as described above and blocked at 50 °C for 25 min. However (as these samples are larger), maleimide is removed from samples by applying 2.5 ml of sample

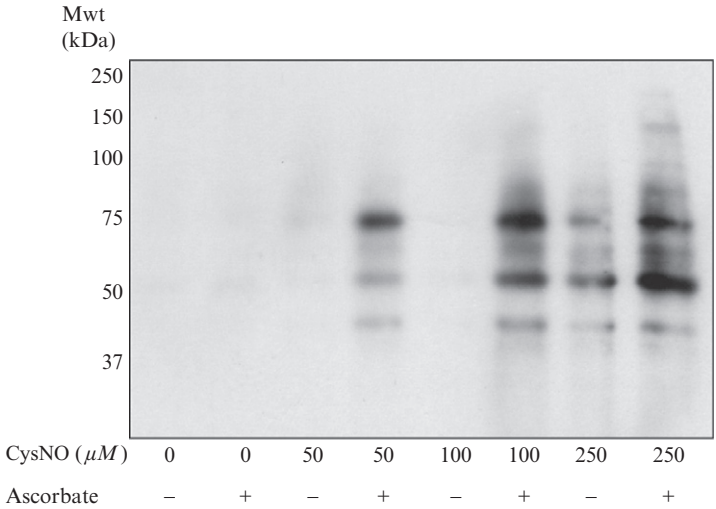

Figure 15.4 **Assessing the ascorbate-dependent biotin-switch assay using rat aortic smooth muscle (A10) cells treated with the NO-donor CysNO. *S*-nitrosylation was detected in A10 cell lysate using the ascorbate-dependent biotin-switch method. Proteins were separated by SDS–PAGE, transferred to PVDF membranes and probed with streptavidin–HRP to detect *S*-nitrosylated proteins. Treatment of A10 cells for 30 min with CysNO generated a dose-dependent increase in ascorbate-reliant protein labeling.**

onto individual PD-10 desalting columns (GE Healthcare Life Sciences). After samples have passed through the column by gravity flow they are then eluted using 3 ml of elution buffer (1% SDS and 100 m*M* maleimide in Tris–HCl buffer pH 7.4, also with 0.2 m*M* neocuproine and 1 m*M* DTPA when analyzing *S*-nitrosylation). The eluate is then divided so that 0.1 ml of each is combined with 0.1 ml of labeling buffer A (0.2 m*M* biotin-HPDP and 1% SDS in Tris–HCl buffer pH 7.4, with 0.4 m*M* neocuproine and 2 m*M* DTPA if analyzing protein *S*-nitrosylation). This reaction is not used for affinity purification but instead is Western blotted to determine if there has been complete sample alkylation during the blocking step. When preparing the sample for affinity purification in preparation for proteomic analysis, 2.7 ml of each eluate is added to 2.7 ml of labeling buffer B (0.2 m*M* biotin-HPDP, 60 m*M* ascorbate, 1% SDS, 0.4 m*M* neocuproine and 2 m*M* DTPA in Tris–HCl buffer pH 7.4 for *S*-nitrosylation, and 0.2 m*M* biotin-HPDP, 40 m*M* sodium arsenite and 1% SDS in Tris–HCl buffer pH 7.4 for sulfenation). These mixtures are then incubated at room temperature for 1 h (in the dark if analyzing *S*-nitrosylation). After incubation, samples should be filtered through PD-10 desalting columns to remove free biotin-HPDP and excess, free SDS. The addition of 100 m*M* maleimide to the eluate ensures labeling is fully quenched. A small aliquot of each sample can be added to

sample buffer and run on a nonreducing SDS–PAGE gel. Gels are then Western blotted to PVDF membrane and probed using streptavidin–HRP to determine levels of *S*-nitrosylated or sulfenated proteins in each sample, to check if the procedure has worked before subsequent affinity capture experiments.

To affinity purify biotinylated proteins after the biotin-switch method, samples that had undergone the labeling protocol are each individually incubated with streptavidin–agarose (prewashed in 1% Triton X-100 in 100 m*M* Tris buffer pH 7.4) and rotated for 3 h at 4 °C in the presence of protease inhibitors (Roche Complete EDTA-free, product #11873580001) and 1% Triton X-100 in 100 m*M* Tris buffer pH 7.4. After incubation, streptavidin–agarose beads are spin-washed twice in wash buffer containing 100 m*M* Tris pH 7.4 and 1% Triton X-100 (15 min incubation at 4 °C each time). Streptavidin–agarose beads are then placed into empty spin columns (Sigma, product #SC1000) and washed a further three times with 0.4 ml of wash buffer. Biotinylated proteins are eluted from streptavidin–agarose by adding 50 μl of 100 m*M* Tris pH 7.4 containing 100 m*M* 2-mercaptoethanol and 0.2% Triton X-100. The 2-mercaptoehanol breaks the disulfide bond between the protein and biotin-tag, releasing the protein from the matrix. The eluates are added to 50 μl of reducing SDS sample buffer and resolved by SDS–PAGE, which is then stained with colloidal Coomassie Blue. Unique bands are excised using a clean scalpel blade and analyzed by mass spectrometry to identify the proteins, and possibly also the site of modification.

3. Conclusions

The development of the biotin-switch method has allowed us to greatly extend the known library of proteins subject to *S*-nitrosylation and sulfenation. This helps enhance our understanding of the role of redox biology in both health and disease. It is likely that the biotin-switch method will continue to be utilized for the identification of *S*-nitrosylated proteins as this is perhaps the best overall technology currently available and is an effective way to identify potentially novel targets. Each of the increasing number of proteins identified as potential *S*-nitrosylation or sulfenation targets needs to be ultimately assessed on a case-by-case basis to determine if the modification occurs under physiological or pathophysiological conditions and whether it has a functional correlate. It may also be worth considering that the use of SDS-denaturing conditions in this analysis of *S*-nitrosylated or sulfenated proteins is anticipated to destabilize these oxidative modification in many proteins. Consequently, these methods may not be suitable for studying all proteins regulated in this way, and that the prevalence of these modifications is being greatly underestimated.

ACKNOWLEDGMENTS

This work was supported by a Sir Henry Wellcome postdoctoral fellowship from The Wellcome Trust (Sponsor Reference 085483/Z/08/Z; to J. R. B.) and the Medical Research Council (Sponsor Reference G0700320).

REFERENCES

Adachi, T., Weisbrod, R. M., Pimentel, D. R., Ying, J., Sharov, V. S., Schoneich, C., and Cohen, R. A. (2004). S-Glutathiolation by peroxynitrite activates SERCA during arterial relaxation by nitric oxide. *Nat. Med.* **10,** 1200–1207.

Akhter, S., Vignini, A., Wen, Z., English, A., Wang, P. G., and Mutus, B. (2002). Evidence for S-nitrosothiol-dependent changes in fibrinogen that do not involve transnitrosation or thiolation. *Proc. Natl. Acad. Sci. USA* **99,** 9172–9177.

An, H. J., Maeng, O., Kang, K. H., Lee, J. O., Kim, Y. S., Paik, S. G., and Lee, H. (2006). Activation of Ras up-regulates pro-apoptotic BNIP3 in nitric oxide-induced cell death. *J. Biol. Chem.* **281,** 33939–33948.

Aronstam, R. S., Martin, D. C., Dennison, R. L., and Cooley, H. G. (1995). S-nitrosylation of m2 muscarinic receptor thiols disrupts receptor-G-protein coupling. *Ann. NY Acad. Sci.* **757,** 215–217.

Ascenzi, P., Colasanti, M., Persichini, T., Muolo, M., Polticelli, F., Venturini, G., Bordo, D., and Bolognesi, M. (2000). Re-evaluation of amino acid sequence and structural consensus rules for cysteine-nitric oxide reactivity. *Biol. Chem.* **381,** 623–627.

Azad, N., Vallyathan, V., Wang, L., Tantishaiyakul, V., Stehlik, C., Leonard, S. S., and Rojanasakul, Y. (2006). S-nitrosylation of Bcl-2 inhibits its ubiquitin-proteasomal degradation. A novel antiapoptotic mechanism that suppresses apoptosis. *J. Biol. Chem.* **281,** 34124–34134.

Azad, N., Iyer, A. K., Wang, L., Lu, Y., Medan, D., Castranova, V., and Rojanasakul, Y. (2009). Nitric oxide-mediated Bcl-2 stabilization potentiates malignant transformation of human lung epithelial cells. *Am. J. Respir. Cell Mol. Biol.* 2009-0094OC.

Barouch, L. A., Harrison, R. W., Skaf, M. W., Rosas, G. O., Cappola, T. P., Kobeissi, Z. A., Hobai, I. A., Lemmon, C. A., Burnett, A. L., O'Rourke, B., Rodriguez, E. R., Huang, P. L., *et al.* (2002). Nitric oxide regulates the heart by spatial confinement of nitric oxide synthase isoforms. *Nature* **416,** 337–339.

Beckman, J. S. (1996). Oxidative damage and tyrosine nitration from peroxynitrite. *Chem. Res. Toxicol.* **9,** 836–844.

Bedard, K., and Krause, K. H. (2007). The NOX family of ROS-generating NADPH oxidases: Physiology and pathophysiology. *Physiol. Rev.* **87,** 245–313.

Bellinger, A. M., Reiken, S., Carlson, C., Mongillo, M., Liu, X., Rothman, L., Matecki, S., Lacampagne, A., and Marks, A. R. (2009). Hypernitrosylated ryanodine receptor calcium release channels are leaky in dystrophic muscle. *Nat. Med.* **15,** 325–330.

Benhar, M., and Stamler, J. S. (2005). A central role for S-nitrosylation in apoptosis. *Nat. Cell Biol.* **7,** 645–646.

Benhar, M., Forrester, M. T., Hess, D. T., and Stamler, J. S. (2008). Regulated protein denitrosylation by cytosolic and mitochondrial thioredoxins. *Science* **320,** 1050–1054.

Biteau, B., Labarre, J., and Toledano, M. B. (2003). ATP-dependent reduction of cysteine-sulphinic acid by S. cerevisiae sulphiredoxin. *Nature* **425,** 980–984.

Brandes, R. P., and Kreuzer, J. (2005). Vascular NADPH oxidases: Molecular mechanisms of activation. *Cardiovasc. Res.* **65,** 16–27.

Brennan, J. P., Bardswell, S. C., Burgoyne, J. R., Fuller, W., Schroder, E., Wait, R., Begum, S., Kentish, J. C., and Eaton, P. (2006). Oxidant-induced activation of type I protein kinase A is mediated by RI subunit interprotein disulfide bond formation. *J. Biol. Chem.* **281,** 21827–21836.

Burgoyne, J. R., and Eaton, P. (2009). Transnitrosylating nitric oxide species directly activate type I protein kinase A, providing a novel adenylate cyclase-independent cross-talk to beta-adrenergic-like signaling. *J. Biol. Chem.* **284,** 29260–29268.

Burgoyne, J. R., Madhani, M., Cuello, F., Charles, R. L., Brennan, J. P., Schroder, E., Browning, D. D., and Eaton, P. (2007). Cysteine redox sensor in PKGIa enables oxidant-induced activation. *Science* **317,** 1393–1397.

Cai, H. (2005). Hydrogen peroxide regulation of endothelial function: Origins, mechanisms, and consequences. *Cardiovasc. Res.* **68,** 26–36.

Cai, J., Jiang, W. G., Ahmed, A., and Boulton, M. (2006). Vascular endothelial growth factor-induced endothelial cell proliferation is regulated by interaction between VEGFR-2, SH-PTP1 and eNOS. *Microvasc. Res.* **71,** 20–31.

Cave, A. C., Brewer, A. C., Narayanapanicker, A., Ray, R., Grieve, D. J., Walker, S., and Shah, A. M. (2006). NADPH oxidases in cardiovascular health and disease. *Antioxid. Redox Signal.* **8,** 691–728.

Chanvorachote, P., Nimmannit, U., Lu, Y., Talbott, S., Jiang, B. H., and Rojanasakul, Y. (2009). Nitric oxide regulates lung carcinoma cell anoikis through inhibition of ubiquitin-proteasomal degradation of caveolin-1. *J. Biol. Chem.* **284,** 28476–28484.

Charles, R. L., Schroder, E., May, G., Free, P., Gaffney, P. R., Wait, R., Begum, S., Heads, R. J., and Eaton, P. (2007). Protein sulfenation as a redox sensor: Proteomics studies using a novel biotinylated dimedone analogue. *Mol. Cell. Proteomics* **6,** 1473–1484.

Chen, Y. Y., Chu, H. M., Pan, K. T., Teng, C. H., Wang, D. L., Wang, A. H., Khoo, K. H., and Meng, T. C. (2008). Cysteine S-nitrosylation protects protein-tyrosine phosphatase 1B against oxidation-induced permanent inactivation. *J. Biol. Chem.* **283,** 35265–35272.

Cho, D. H., Nakamura, T., Fang, J., Cieplak, P., Godzik, A., Gu, Z., and Lipton, S. A. (2009). S-nitrosylation of Drp1 mediates beta-amyloid-related mitochondrial fission and neuronal injury. *Science* **324,** 102–105.

Chung, K. K., Thomas, B., Li, X., Pletnikova, O., Troncoso, J. C., Marsh, L., Dawson, V. L., and Dawson, T. M. (2004). S-nitrosylation of parkin regulates ubiquitination and compromises parkin's protective function. *Science* **304,** 1328–1331.

Cordes, C. M., Bennett, R. G., Siford, G. L., and Hamel, F. G. (2009). Nitric oxide inhibits insulin-degrading enzyme activity and function through S-nitrosylation. *Biochem. Pharmacol.* **77,** 1064–1073.

Costa, A. D., Jakob, R., Costa, C. L., Andrukhiv, K., West, I. C., and Garlid, K. D. (2006). The mechanism by which the mitochondrial ATP-sensitive K+ channel opening and H_2O_2 inhibit the mitochondrial permeability transition. *J. Biol. Chem.* **281,** 20801–20808.

Daiber, A., Schildknecht, S., Muller, J., Kamuf, J., Bachschmid, M. M., and Ullrich, V. (2009). Chemical model systems for cellular nitros(yl)ation reactions. *Free Radic. Biol. Med.* **47,** 458–467.

Dalle-Donne, I., Milzani, A., Giustarini, D., Di Simplicio, P., Colombo, R., and Rossi, R. (2000). S-NO-actin: S-nitrosylation kinetics and the effect on isolated vascular smooth muscle. *J. Muscle Res. Cell Motil.* **21,** 171–181.

Dong, F., Zhang, X., Wold, L. E., Ren, Q., Zhang, Z., and Ren, J. (2005). Endothelin-1 enhances oxidative stress, cell proliferation and reduces apoptosis in human umbilical vein endothelial cells: Role of ETB receptor, NADPH oxidase and caveolin-1. *Br. J. Pharmacol.* **145,** 323–333.

Eaton, P. (2006). Protein thiol oxidation in health and disease: Techniques for measuring disulfides and related modifications in complex protein mixtures. *Free Radic. Biol. Med.* **40,** 1889–1899.

Eaton, P., Fuller, W., and Shattock, M. J. (2002a). S-thiolation of HSP27 regulates its multimeric aggregate size independently of phosphorylation. *J. Biol. Chem.* **277,** 21189–21196.

Eaton, P., Wright, N., Hearse, D. J., and Shattock, M. J. (2002b). Glyceraldehyde phosphate dehydrogenase oxidation during cardiac ischemia and reperfusion. *J. Mol. Cell. Cardiol.* **34,** 1549–1560.

Forrester, M. T., Foster, M. W., and Stamler, J. S. (2007). Assessment and application of the biotin switch technique for examining protein S-nitrosylation under conditions of pharmacologically induced oxidative stress. *J. Biol. Chem.* **282,** 13977–13983.

Forstermann, U., Schmidt, H. H., Pollock, J. S., Sheng, H., Mitchell, J. A., Warner, T. D., Nakane, M., and Murad, F. (1991). Isoforms of nitric oxide synthase. Characterization and purification from different cell types. *Biochem. Pharmacol.* **42,** 1849–1857.

Forsythe, P., and Befus, A. D. (2003). Inhibition of calpain is a component of nitric oxide-induced down-regulation of human mast cell adhesion. *J. Immunol.* **170,** 287–293.

Giustarini, D., Dalle-Donne, I., Colombo, R., Milzani, A., and Rossi, R. (2008). Is ascorbate able to reduce disulfide bridges? A cautionary note. *Nitric Oxide* **19,** 252–258.

Gomez, R., Caballero, R., Barana, A., Amoros, I., Calvo, E., Lopez, J. A., Klein, H., Vaquero, M., Osuna, L., Atienza, F., Almendral, J., Pinto, A., *et al.* (2009). Nitric oxide increases cardiac IK1 by nitrosylation of cysteine 76 of Kir2.1 channels. *Circ. Res.* **105,** 383–392.

Gonzalez, D. R., AT, M. S., Sun, Q. A., Stamler, J. S., and Hare, J. M. (2009). S-nitrosylation of cardiac ion channels. *J. Cardiovasc. Pharmacol.* **54,** 188–195.

Hammoud, L., Xiang, F., Lu, X., Brunner, F., Leco, K., and Feng, Q. (2007). Endothelial nitric oxide synthase promotes neonatal cardiomyocyte proliferation by inhibiting tissue inhibitor of metalloproteinase-3 expression. *Cardiovasc. Res.* **75,** 359–368.

Hampton, M. B., Fadeel, B., and Orrenius, S. (1998). Redox regulation of the caspases during apoptosis. *Ann. NY Acad. Sci.* **854,** 328–335.

Hare, J. M., and Stamler, J. S. (1999). NOS: Modulator, not mediator of cardiac performance. *Nat. Med.* **5,** 273–274.

Heart Protection Study Collaborative Group (2002). MRC/BHF Heart Protection Study of antioxidant vitamin supplementation in 20,536 high-risk individuals: A randomised placebo-controlled trial. *Lancet* **360,** 23–33.

Hegstad, A. C., Antonsen, O. H., and Ytrehus, K. (1997). Low concentrations of hydrogen peroxide improve post-ischaemic metabolic and functional recovery in isolated perfused rat hearts. *J. Mol. Cell. Cardiol.* **29,** 2779–2787.

Huang, B., and Chen, C. (2006). An ascorbate-dependent artifact that interferes with the interpretation of the biotin switch assay. *Free Radic. Biol. Med.* **41,** 562–567.

Jaffrey, S. R., and Snyder, S. H. (2001). The biotin switch method for the detection of S-nitrosylated proteins. *Sci. STKE* **2001,** p11.

Kallakunta, V. M., Staruch, A., and Mutus, B. (2009). Sinapinic acid can replace ascorbate in the biotin switch assay. *Biochim. Biophys. Acta* **1800,** 23–30.

Kapadia, M. R., Eng, J. W., Jiang, Q., Stoyanovsky, D. A., and Kibbe, M. R. (2009). Nitric oxide regulates the 26S proteasome in vascular smooth muscle cells. *Nitric Oxide* **20,** 279–288.

Kawano, T., Zoga, V., Kimura, M., Liang, M. Y., Wu, H. E., Gemes, G., McCallum, J. B., Kwok, W. M., Hogan, Q. H., and Sarantopoulos, C. D. (2009). Nitric oxide activates ATP-sensitive potassium channels in mammalian sensory neurons: Action by direct S-nitrosylation. *Mol. Pain* **5,** 12.

Kaye, D. M., Gruskin, S., Smith, A. I., and Esler, M. D. (2000). Nitric oxide mediated modulation of norepinephrine transport: Identification of a potential target for S-nitrosylation. *Br. J. Pharmacol.* **130,** 1060–1064.

Kokkola, T., Savinainen, J. R., Monkkonen, K. S., Retamal, M. D., and Laitinen, J. T. (2005). S-nitrosothiols modulate G protein-coupled receptor signaling in a reversible and highly receptor-specific manner. *BMC Cell Biol.* **6,** 21.

Kots, A. Y., Martin, E., Sharina, I. G., and Murad, F. (2009). A short history of cGMP, guanylyl cyclases, and cGMP-dependent protein kinases. *Handb. Exp. Pharmacol.* 1–14.

Kuo, W. N., and Kocis, J. M. (2002). Nitration/S-nitrosation of proteins by peroxynitrite-treatment and subsequent modification by glutathione S-transferase and glutathione peroxidase. *Mol. Cell. Biochem.* **233,** 57–63.

Landino, L. M., Koumas, M. T., Mason, C. E., and Alston, J. A. (2006). Ascorbic acid reduction of microtubule protein disulfides and its relevance to protein S-nitrosylation assays. *Biochem. Biophys. Res. Commun.* **340,** 347–352.

Lim, S. Y., Raftery, M., Cai, H., Hsu, K., Yan, W. X., Hseih, H. L., Watts, R. N., Richardson, D., Thomas, S., Perry, M., and Geczy, C. L. (2008). S-nitrosylated S100A8: Novel anti-inflammatory properties. *J. Immunol.* **181,** 5627–5636.

Lima, B., Lam, G. K., Xie, L., Diesen, D. L., Villamizar, N., Nienaber, J., Messina, E., Bowles, D., Kontos, C. D., Hare, J. M., Stamler, J. S., and Rockman, H. A. (2009). Endogenous S-nitrosothiols protect against myocardial injury. *Proc. Natl. Acad. Sci. USA* **106,** 6297–6302.

Liochev, S. I., and Fridovich, I. (2007). The effects of superoxide dismutase on H_2O_2 formation. *Free Radic. Biol. Med.* **42,** 1465–1469.

Liu, L., Hausladen, A., Zeng, M., Que, L., Heitman, J., and Stamler, J. S. (2001). A metabolic enzyme for S-nitrosothiol conserved from bacteria to humans. *Nature* **410,** 490–494.

Lopez-Lazaro, M. (2007). Dual role of hydrogen peroxide in cancer: Possible relevance to cancer chemoprevention and therapy. *Cancer Lett.* **252,** 1–8.

Luchsinger, B. P., Rich, E. N., Gow, A. J., Williams, E. M., Stamler, J. S., and Singel, D. J. (2003). Routes to S-nitroso-hemoglobin formation with heme redox and preferential reactivity in the beta subunits. *Proc. Natl. Acad. Sci. USA* **100,** 461–466.

Mantovani, A., Garlanda, C., Locati, M., Rodriguez, T. V., Feo, S. G., Savino, B., and Vecchi, A. (2007). Regulatory pathways in inflammation. *Autoimmun. Rev.* **7,** 8–11.

Matsumoto, A., Comatas, K. E., Liu, L., and Stamler, J. S. (2003). Screening for nitric oxide-dependent protein-protein interactions. *Science* **301,** 657–661.

Matsushita, K., Morrell, C. N., Cambien, B., Yang, S. X., Yamakuchi, M., Bao, C., Hara, M. R., Quick, R. A., Cao, W., O'Rourke, B., Lowenstein, J. M., Pevsner, J., *et al.* (2003). Nitric oxide regulates exocytosis by S-nitrosylation of N-ethylmaleimide-sensitive factor. *Cell* **115,** 139–150.

Miller, E. R. III, Pastor-Barriuso, R., Dalal, D., Riemersma, R. A., Appel, L. J., and Guallar, E. (2005). Meta-analysis: High-dosage vitamin E supplementation may increase all-cause mortality. *Ann. Intern. Med.* **142,** 37–46.

Miller, T. W., Isenberg, J. S., and Roberts, D. D. (2009). Molecular regulation of tumor angiogenesis and perfusion via redox signaling. *Chem. Rev.* **109,** 3099–3124.

Monteiro, G., Horta, B. B., Pimenta, D. C., Augusto, O., and Netto, L. E. (2007). Reduction of 1-Cys peroxiredoxins by ascorbate changes the thiol-specific antioxidant paradigm, revealing another function of vitamin C. *Proc. Natl. Acad. Sci. USA* **104,** 4886–4891.

Moon, K. H., Kim, B. J., and Song, B. J. (2005). Inhibition of mitochondrial aldehyde dehydrogenase by nitric oxide-mediated S-nitrosylation. *FEBS Lett.* **579,** 6115–6120.

Moreira, P. I., Honda, K., Liu, Q., Santos, M. S., Oliveira, C. R., Aliev, G., Nunomura, A., Zhu, X., Smith, M. A., and Perry, G. (2005). Oxidative stress: The old enemy in Alzheimer's disease pathophysiology. *Curr. Alzheimer Res.* **2,** 403–408.

Niki, E., Yoshida, Y., Saito, Y., and Noguchi, N. (2005). Lipid peroxidation: Mechanisms, inhibition, and biological effects. *Biochem. Biophys. Res. Commun.* **338,** 668–676.

Nogueira, L., Figueiredo-Freitas, C., Casimiro-Lopes, G., Magdesian, M. H., Assreuy, J., and Sorenson, M. M. (2009). Myosin is reversibly inhibited by S-nitrosylation. *Biochem. J.* **424,** 221–231.

O'Brian, C. A., and Chu, F. (2005). Post-translational disulfide modifications in cell signaling—Role of inter-protein, intra-protein, S-glutathionyl, and S-cysteaminyl disulfide modifications in signal transmission. *Free Radic. Res.* **39,** 471–480.

Paige, J. S., Xu, G., Stancevic, B., and Jaffrey, S. R. (2008). Nitrosothiol reactivity profiling identifies S-nitrosylated proteins with unexpected stability. *Chem. Biol.* **15,** 1307–1316.

Palmer, Z. J., Duncan, R. R., Johnson, J. R., Lian, L. Y., Mello, L. V., Booth, D., Barclay, J. W., Graham, M. E., Burgoyne, R. D., Prior, I. A., and Morgan, A. (2008). S-nitrosylation of syntaxin 1 at Cys(145) is a regulatory switch controlling Munc18-1 binding. *Biochem. J.* **413,** 479–491.

Perez-Mato, I., Castro, C., Ruiz, F. A., Corrales, F. J., and Mato, J. M. (1999). Methionine adenosyltransferase S-nitrosylation is regulated by the basic and acidic amino acids surrounding the target thiol. *J. Biol. Chem.* **274,** 17075–17079.

Pi, X., Wu, Y., Ferguson, J. E. III, Portbury, A. L., and Patterson, C. (2009). SDF-1alpha stimulates JNK3 activity via eNOS-dependent nitrosylation of MKP7 to enhance endothelial migration. *Proc. Natl. Acad. Sci. USA* **106,** 5675–5680.

Price, D. T., Vita, J. A., and Keaney, J. F. Jr. (2000). Redox control of vascular nitric oxide bioavailability. *Antioxid. Redox Signal.* **2,** 919–935.

Romeo, A. A., Capobianco, J. A., and English, A. M. (2002). Heme nitrosylation of deoxyhemoglobin by s-nitrosoglutathione requires copper. *J. Biol. Chem.* **277,** 24135–24141.

Roy, S., Khanna, S., Nallu, K., Hunt, T. K., and Sen, C. K. (2006). Dermal wound healing is subject to redox control. *Mol. Ther.* **13,** 211–220.

Salmeen, A., Andersen, J. N., Myers, M. P., Meng, T. C., Hinks, J. A., Tonks, N. K., and Barford, D. (2003). Redox regulation of protein tyrosine phosphatase 1B involves a sulphenyl-amide intermediate. *Nature* **423,** 769–773.

Saurin, A. T., Neubert, H., Brennan, J. P., and Eaton, P. (2004). Widespread sulfenic acid formation in tissues in response to hydrogen peroxide. *Proc. Natl. Acad. Sci. USA* **101,** 17982–17987.

Savitsky, P. A., and Finkel, T. (2002). Redox regulation of Cdc25C. *J. Biol. Chem.* **277,** 20535–20540.

Sayed, N., Kim, D. D., Fioramonti, X., Iwahashi, T., Duran, W. N., and Beuve, A. (2008). Nitroglycerin-induced S-nitrosylation and desensitization of soluble guanylyl cyclase contribute to nitrate tolerance. *Circ. Res.* **103,** 606–614.

Schroder, E., and Eaton, P. (2008). Hydrogen peroxide as an endogenous mediator and exogenous tool in cardiovascular research: Issues and considerations. *Curr. Opin. Pharmacol.* **8,** 153–159.

Schroder, E., Brennan, J. P., and Eaton, P. (2008). Cardiac peroxiredoxins undergo complex modifications during cardiac oxidant stress. *Am. J. Physiol. Heart Circ. Physiol.* **295,** H425–H433.

Shimokawa, H., and Morikawa, K. (2005). Hydrogen peroxide is an endothelium-derived hyperpolarizing factor in animals and humans. *J. Mol. Cell. Cardiol.* **39,** 725–732.

Slater, A. F., Stefan, C., Nobel, I., van den Dobbelsteen, D. J., and Orrenius, S. (1995). Signalling mechanisms and oxidative stress in apoptosis. *Toxicol. Lett.* **82–83,** 149–153.

Sorescu, D., Weiss, D., Lassegue, B., Clempus, R. E., Szocs, K., Sorescu, G. P., Valppu, L., Quinn, M. T., Lambeth, J. D., Vega, J. D., Taylor, W. R., and Griendling, K. K. (2002). Superoxide production and expression of nox family proteins in human atherosclerosis. *Circulation* **105,** 1429–1435.

Sossa, K. G., Beattie, J. B., and Carroll, R. C. (2007). AMPAR exocytosis through NO modulation of PICK1. *Neuropharmacology* **53,** 92–100.

Stamler, J. S., Toone, E. J., Lipton, S. A., and Sucher, N. J. (1997). (S)NO signals: Translocation, regulation, and a consensus motif. *Neuron* **18,** 691–696.

Stubauer, G., Giuffre, A., and Sarti, P. (1999). Mechanism of S-nitrosothiol formation and degradation mediated by copper ions. *J. Biol. Chem.* **274,** 28128–28133.

Sun, J., Morgan, M., Shen, R. F., Steenbergen, C., and Murphy, E. (2007). Preconditioning results in S-nitrosylation of proteins involved in regulation of mitochondrial energetics and calcium transport. *Circ. Res.* **101,** 1155–1163.

Surks, H. K. (2007). cGMP-dependent protein kinase I and smooth muscle relaxation: A tale of two isoforms. *Circ. Res.* **101,** 1078–1080.

Tao, L., and English, A. M. (2003). Mechanism of S-nitrosation of recombinant human brain calbindin D28K. *Biochemistry* **42,** 3326–3334.

Taylor, B. S., and Geller, D. A. (2000). Molecular regulation of the human inducible nitric oxide synthase (iNOS) gene. *Shock* **13,** 413–424.

Thom, S. R., Bhopale, V. M., Mancini, D. J., and Milovanova, T. N. (2008). Actin S-nitrosylation inhibits neutrophil beta2 integrin function. *J. Biol. Chem.* **283,** 10822–10834.

Tsang, A. H., Lee, Y. I., Ko, H. S., Savitt, J. M., Pletnikova, O., Troncoso, J. C., Dawson, V. L., Dawson, T. M., and Chung, K. K. (2009). S-nitrosylation of XIAP compromises neuronal survival in Parkinson's disease. *Proc. Natl. Acad. Sci. USA* **106,** 4900–4905.

Uehara, T., Nakamura, T., Yao, D., Shi, Z. Q., Gu, Z., Ma, Y., Masliah, E., Nomura, Y., and Lipton, S. A. (2006). S-nitrosylated protein-disulphide isomerase links protein misfolding to neurodegeneration. *Nature* **441,** 513–517.

Vainio, H. (2000). Chemoprevention of cancer: Lessons to be learned from beta-carotene trials. *Toxicol. Lett.* **112–113,** 513–517.

Veal, E. A., Day, A. M., and Morgan, B. A. (2007). Hydrogen peroxide sensing and signaling. *Mol. Cell* **26,** 1–14.

Viner, R. I., Williams, T. D., and Schoneich, C. (1999). Peroxynitrite modification of protein thiols: Oxidation, nitrosylation, and S-glutathiolation of functionally important cysteine residue(s) in the sarcoplasmic reticulum Ca-ATPase. *Biochemistry* **38,** 12408–12415.

Wadham, C., Parker, A., Wang, L., and Xia, P. (2007). High glucose attenuates protein S-nitrosylation in endothelial cells: Role of oxidative stress. *Diabetes* **56,** 2715–2721.

Wang, X., Kettenhofen, N. J., Shiva, S., Hogg, N., and Gladwin, M. T. (2008). Copper dependence of the biotin switch assay: Modified assay for measuring cellular and blood nitrosated proteins. *Free Radic. Biol. Med.* **44,** 1362–1372.

Williams, J. G., Pappu, K., and Campbell, S. L. (2003). Structural and biochemical studies of p21Ras S-nitrosylation and nitric oxide-mediated guanine nucleotide exchange. *Proc. Natl. Acad. Sci. USA* **100,** 6376–6381.

Wingler, K., Wunsch, S., Kreutz, R., Rothermund, L., Paul, M., and Schmidt, H. H. (2001). Upregulation of the vascular NAD(P)H-oxidase isoforms Nox1 and Nox4 by the renin-angiotensin system in vitro and in vivo. *Free Radic. Biol. Med.* **31,** 1456–1464.

Wolkart, G., Kaber, G., Kojda, G., and Brunner, F. (2006). Role of endogenous hydrogen peroxide in cardiovascular ischaemia/reperfusion function: Studies in mouse hearts with catalase-overexpression in the vascular endothelium. *Pharmacol. Res.* **54,** 50–56.

Wolosker, H., Reis, M., Assreuy, J., and de Meis, L. (1996). Inhibition of glutamate uptake and proton pumping in synaptic vesicles by S-nitrosylation. *J. Neurochem.* **66,** 1943–1948.

Wu, M., Katta, A., Gadde, M. K., Liu, H., Kakarla, S. K., Fannin, J., Paturi, S., Arvapalli, R. K., Rice, K. M., Wang, Y., and Blough, E. R. (2009). Aging-associated dysfunction of Akt/protein kinase B: S-nitrosylation and acetaminophen intervention. *PLoS One* **4,** e6430.

Xu, S., and Touyz, R. M. (2006). Reactive oxygen species and vascular remodelling in hypertension: Still alive. *Can. J. Cardiol.* **22,** 947–951.

Xu, L., Eu, J. P., Meissner, G., and Stamler, J. S. (1998). Activation of the cardiac calcium release channel (ryanodine receptor) by poly-S-nitrosylation. *Science* **279,** 234–237.

Zanetti, M., Katusic, Z. S., and O'Brien, T. (2002). Adenoviral-mediated overexpression of catalase inhibits endothelial cell proliferation. *Am. J. Physiol. Heart Circ. Physiol.* **283,** H2620–H2626.

Zhang, Y., and Hogg, N. (2004). The mechanism of transmembrane S-nitrosothiol transport. *Proc. Natl. Acad. Sci. USA* **101,** 7891–7896.

Zhang, Y., and Hogg, N. (2005). S-Nitrosothiols: Cellular formation and transport. *Free Radic. Biol. Med.* **38,** 831–838.

Zhang, J., Jin, B., Li, L., Block, E. R., and Patel, J. M. (2005a). Nitric oxide-induced persistent inhibition and nitrosylation of active site cysteine residues of mitochondrial cytochrome-c oxidase in lung endothelial cells. *Am. J. Physiol. Cell Physiol.* **288,** C840–C849.

Zhang, Y., Keszler, A., Broniowska, K. A., and Hogg, N. (2005b). Characterization and application of the biotin-switch assay for the identification of S-nitrosated proteins. *Free Radic. Biol. Med.* **38,** 874–881.

CHAPTER SIXTEEN

Protein Adducts of Aldehydic Lipid Peroxidation Products: Identification and Characterization of Protein Adducts Using an Aldehyde/Keto-Reactive Probe in Combination with Mass Spectrometry

Claudia S. Maier, Juan Chavez, Jing Wang, *and* Jianyong Wu

Contents

Department of Chemistry, Oregon State University, Corvallis, Oregon, USA

Methods in Enzymology, Volume 473
ISSN 0076-6879, DOI: 10.1016/S0076-6879(10)73016-0

Abstract

This chapter describes a mass spectrometry-based strategy that facilitates the unambiguous identification and characterization of proteins modified by lipid peroxidation-derived 2-alkenals. The approach employs a biotinylated hydroxyl amine derivative as an aldehyde/keto-reactive probe in conjunction with selective enrichment and tandem mass spectrometric analysis. Methodological details are given for model studies involving a distinct protein and 4-hydroxy-2-nonenal (HNE). The method was also evaluated for an exposure study of a cell culture system with HNE that yielded the major protein targets of HNE in human monocytic THP-1 cells. The application of the approach to complex biological systems is demonstrated for the identification and characterization of endogenous protein targets of aldehydic lipid peroxidation products present in cardiac mitochondria.

1. Introduction

Reactive oxygen species (ROS) are constantly generated within cells, for instance, by environmental insults (e.g., UV light), metal-catalyzed reactions, as products of the inflammatory response in neutrophils and macrophages and as by-products of oxidative phosphorylation. The production of ROS and derived secondary products are largely counteracted by an intricate antioxidant system. The extent of imbalance between ROS production and removal by cellular antioxidant defenses determines the degree of oxidative stress (Beckman and Ames, 1998; Finkel and Holbrook, 2000).

Nonenzymatic peroxidation of polyunsaturated fatty acids (PUFA) present in membranes and lipoproteins results in the formation of reactive aldehydes (Esterbauer *et al.*, 1991). For example, radical-mediated hydrogen abstraction and oxidation of the prototypic ω-6 PUFA linoleic acid results in the formation of a set of unsaturated hydroperoxides: 13-hydroperoxy-octadecadienoic acid (13-HPODE) and 9-hydroperoxy-octadecadienoic acid (9-HPODE). Subsequent oxidative cleavage results in the formation of 2-alkenals that contain the ω-tail of the PUFA or retain the carboxyl terminus (Esterbauer *et al.*, 1991; Sayre *et al.*, 2006). Examples of α,β-unsaturated aldehydic lipoxidation products derived from linoleic acid are (a) 4-oxo-2-nonenal (ONE) and 4-hydroxy-2-nonenal (HNE) and (b) the carboxy terminating aldehydes 9,12-dioxo-10-dodecenoic acid (DODE) and 9-hydroxy-12-oxo-10-dodecenoic acid (HODA) (Sayre *et al.*, 2006;

Spiteller *et al.*, 2001). The latter carboxylated alkenals usually remain esterified to the phospholipid, but can be liberated by lipases (Spiteller, 2001).

Oxidative decomposition of ω-3 PUFAs leads to formation of 4-hydroxy-2(*E*)-hexenal (Catalá, 2009). Acrolein, 2-propenal, is commonly considered as a lipid peroxidation (LPO) product, but can also be formed by diverse metabolic routes, for example, polyamine oxidation and myeloperoxidase-mediated oxidation of threonine. Acrolein is also a by-product of cigarette smoking and burning of fossil fuels (Stevens and Maier, 2008). Other α,β-unsaturated carbonylic lipoxidation products include the cyclopentenone-containing isoprostanes. Radical-induced oxidation of arachidonic acid gives rise to cyclopentenone-A_2- and J_2-isoprostanes (Chen *et al.*, 1999), while eicosapentaenoic acid (EPA) yields cyclopentenone-A_3/J_3-isoprostanes (Brooks *et al.*, 2008).

There is increasing interest in the characterization of protein modifications caused by electrophilic lipid peroxidation products. Elevated levels of oxidatively modified proteins have been linked to diverse cardiovascular diseases (Uchida, 2000), liver inflammation (Poli *et al.*, 2008), renal failure (Helga *et al.*, 2004), and neurodegenerative disorders (Butterfield and Sultana, 2008), as well as aging (Beckman and Ames, 1998; Montine *et al.*, 2002). Because lipid peroxidation-derived aldehydes are electrophiles, one possible route in which LPO-derived aldehydes exerts their impact on cellular functions and cytotoxicity is the direct modification of proteins. An overview of the many possible structures of LPO-derived protein side-chain adducts is given in a recent review by Sayre *et al.* (2006). Modification of proteins by reactive oxylipids has been linked to protein misfolding (Bieschke *et al.*, 2006; Qin *et al.*, 2007), protein dysfunction (Stewart *et al.*, 2007), aberrant protein processing and degradation (Carbone *et al.*, 2004; Farout *et al.*, 2006; Powell *et al.*, 2005), and modulation of diverse intracellular signaling pathways (Lee *et al.*, 2009; West and Marnett, 2006).

This chapter describes a chemical labeling approach in combination with mass spectrometry to facilitate the unambiguous identification and characterization of proteins modified by lipid peroxidation-derived 2-alkenals. The approach is based on selective labeling of aldehyde/keto groups present in oxidatively modified proteins and the subsequent targeted analysis of the modified proteins by liquid chromatography-tandem mass spectrometry (LC-MS/MS).

2. Modification of Proteins by Aldehydic Lipid Peroxidation Products

Protein adduct formation is predominately caused by 1,4-Michael-type addition of α,β-unsaturated aldehydes to nucleophilic side chains, for example, the cysteine thiol, the histidine imidazole moiety, and the ε-amino

group of lysine residues (Berlett and Stadtman, 1997; Sayre *et al.*, 2006). Representative Michael-type adducts of 4-hydroxy-2-alkenals are given in Fig. 16.1A. In addition, *in vitro* studies with arginine-containing peptides have demonstrated that ONE can form adducts with the guanidinyl side chain (Doorn and Petersen, 2003; Oe *et al.*, 2003b). Model studies at the amino acid level indicated that the Michael adduct reactivity of HNE and ONE declines in the following order: Cys ≫ His > Lys (> Arg for ONE) (Sayre *et al.*, 2006). Uchida *et al.* reported that the modification of lysine residues by 2-enals resulted in the formation of N^{ε}-(3-formyl-3,4-dehydropiperidino)lysine (FDP-lysine) derivatives (Furuhata *et al.*, 2002; Ichihashi *et al.*, 2001) (Fig. 16.1B). FDP-lysine functions as electrophile in the reaction with glutathione (Furuhata *et al.*, 2002) and retains a free aldehyde group which should make the FDP-lysine-containing protein amenable to the described chemical labeling approach. The Sayre group reported that the long-lived ONE-derived adduct of lysine residues is actually a 4-ketoamide adduct rather a Michael adduct (Zhu and Sayre, 2007). Because DODE and ONE share the same 4-oxo-2-enal functional element, adduct formation of DODE with the ε-amino group of lysine may also yield ketoamide adducts (Fig. 16.1C). Ketoamide adducts retain the keto functionality and, therefore, our strategy to chemically tag the aldehyde/keto group in oxidatively modified proteins by utilizing an aldehyde/keto reactive hydroxylamine-functionalized biotin derivative should be applicable to these long-lived protein modifications. LPO-derived 4-hydroxy- and 4-oxo-2-alkenals Michael protein adducts can also further engage in protein cross-linking, resulting in the loss of the carbonyl functionality (Stewart *et al.*, 2007; Zhang *et al.*, 2003).

3. Redox Proteomics of Protein Targets of Reactive Lipid Peroxidation Products

Many studies have been reported that use a gel-based redox proteomics approach to identify protein targets using a combination of 2D gel electrophoresis, immunostaining, or oxyblots, image analysis, in-gel digestion followed by mass spectrometry-based protein identifications in cultured cells, organelles, and tissues (Butterfield and Sultana, 2008; Chung *et al.*, 2009; Reed *et al.*, 2009; Sultana *et al.*, 2009). Although these studies commonly provide only putative protein identifications, they provide good starting points for in-depth studies of distinct proteins in order to determine the site and the functional consequences of an aldehydic modification (Carbone *et al.*, 2005; Eliuk *et al.*, 2007; Roede *et al.*, 2008).

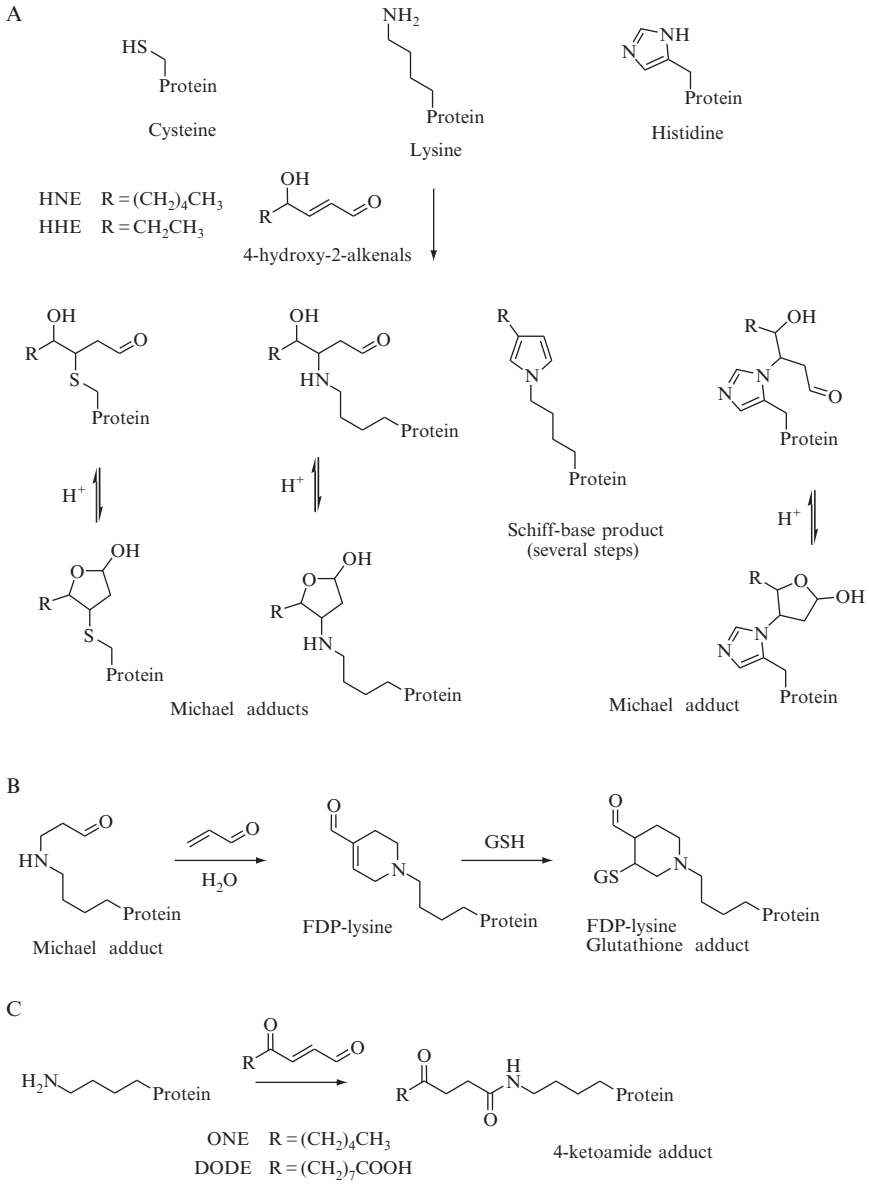

Figure 16.1 Possible modifications of proteins by aldehydic lipid peroxidation products. (A) Michael-type addition and Schiff's base formation of 2-alkenals involving nuclephilic side chains commonly found in proteins. (B) Proposed formation and structure of FDP-lysine adducts. The Michael adduct of lysine reacts further with an second 2-enal (e.g., acrolein) molecule via Michael addition followed by an aldol condensation yielding the FDP-lysine adduct. FDP-lysine is an electrophile due to its 2-enal moiety and can readily react with nucleophiles, such as glutathione. (C) 4-Ketoamide lysine adduct formation involving the ε-amino group of lysine and lipids with a 4-oxo-2-enal reactive moiety.

4. Mass Spectrometry-Based Approaches for the Identification and Characterization of Protein Adducts of Aldehydic Lipid Peroxidation Products

Gel-free mass spectrometry-based proteomics studies have emerged that attempt to characterize protein targets of aldehydic modifications in complex biological systems. These strategies focus on covalently tagging oxidatively modified proteins and their subsequent targeted analysis by tandem mass spectrometry (Table 16.1) (Chavez *et al.*, 2006; Codreanu *et al.*, 2009; Danni *et al.*, 2007; Han *et al.*, 2007). Alternative approaches utilize solid phase capture of protein–HNE adducts in conjunction with LC-MS/MS analyses for obtaining protein and modification site identifications (Roe *et al.*, 2007). In addition, reactive HNE surrogate probes have been developed that allow biotin/streptavidin catch and photorelease of protein–HNE adducts employing *ex vivo* click chemistry (Kim *et al.*, 2009; Vila *et al.*, 2008).

Table 16.1 Chemical probes (in alphabetical order) used for MS/MS-based analyses of protein adducts of LPO-derived enals in complex biological systems

Probe	Application	Refs.
ARP[a]	Mitochondrial protein targets of LPO-derived alkenals	Chavez *et al.* (2006)
	Protein targets of HNE in THP-1 cells	Chavez *et al.* (2010)
Biotin hydrazide[a]	Protein carbonyls in skeletal muscle mitochondria[d]	Danni *et al.* (2007)
Biotin-LC-hydrazide[a]	Protein targets of HNE exposure in RKO cells	Codreanu *et al.* (2009)
HICAT[b]	Mitochondrial protein targets of HNE exposure; endogenous protein adducts	Han *et al.* (2007)
Hydrazide-functionalized beads[c]	Protein targets of HNE in yeast whole cell lysate after treatment with HNE	Roe *et al.* (2007)
	Model peptide–HNE adducts in mouse brain tryptic digest	Rauniyar *et al.* (2008)

ARP, aldehyde reactive probe (*N′*-aminooxymethylcarbonylhydrazino-D-biotin); Biotin-LC-hydrazide, biotinamidohexanoic acid hydrazide; HICAT, hydrazide-functionalized isotope-coded affinity tag.
[a] Commercially available.
[b] Synthesis described by Han *et al.* (2007).
[c] Preparation described by Roe *et al.* (2007).
[d] No specific carbonylation sites were reported.

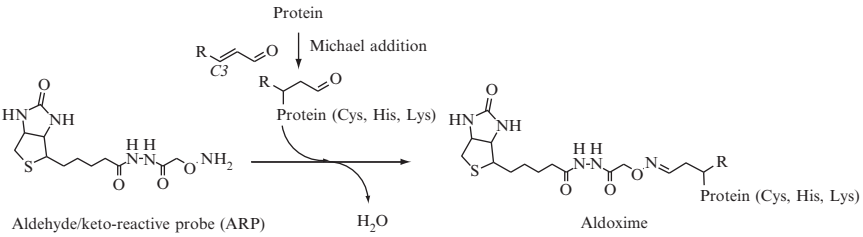

Figure 16.2 **Reaction of aldehyde/keto-containing peptide and protein adducts of lipoxidation products with *N′*-aminooxymethylcarbonylhydrazino-D-biotin as an aldehyde/keto-reactive probe (ARP).**

Our laboratory emphasizes chemical approaches that allow specific tagging of oxidatively modified proteins and their subsequent analysis by mass spectrometry techniques to obtain high content information on the target molecule and posttranslational modification chemistry. In this context, we have explored the use of hydrazide-functionalized isotope-coded affinity probes (HICATs) (Han *et al.*, 2007) and a biotinylated hydroxylamine derivative, *N′*-aminooxymethylcarbonylhydrazino-D-biotin (aldehyde reactive probe, ARP) for the derivatization, enrichment, and mass spectrometric characterization of oxylipid-modified proteins (Chavez *et al.*, 2006). The hydroxyl amine group of ARP forms with the aldehyde/keto groups present in lipoxidation-derived protein adducts aldoxime/ketoxime derivatives which are sufficiently stable for the subsequent analysis by LC-MS/MS (Fig. 16.2). This contribution details a gel-free mass spectrometry-based strategy to unambiguously identify and characterize protein adducts of α,β-unsaturated aldehydes based on our recently introduced ARP-labeling strategy (Fig. 16.3). We demonstrate the utility of this method to determine mechanisms of oxidative protein insult at the molecular level in proteins, cellular, and tissue samples.

5. Experimental Strategy of Using an Aldehyde/Keto-Reactive Probe for the Targeted Analysis of Protein Adducts of Aldehydic Lipid Peroxidation Products

Only tandem mass spectrometric approaches allow for unambiguous assignments of protein adducts because these techniques enable the localization of the modification to a specific residue and provide mass assignments for the modifying entity. The targeted tandem mass spectrometry-based analysis of aldehydic protein adducts using an aldehyde/keto-specific probe involves four steps: (I) chemical tagging of proteins that contain the aldehydic modification using the aldehyde/keto-reactive probe, (II) proteolysis, (III) an enrichment step that involves capture of the chemically tagged aldehydic oxylipid adduct

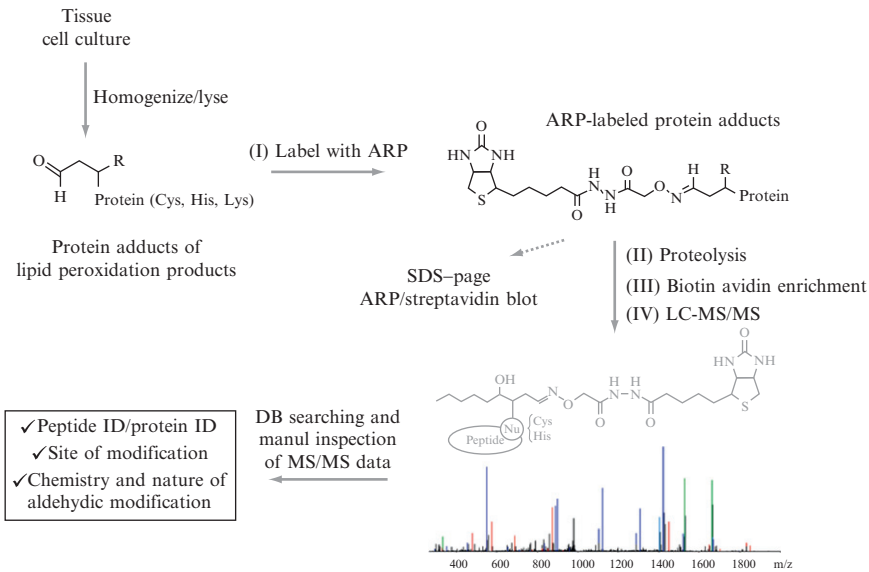

Figure 16.3 **The ARP-labeling strategy in conjunction with mass spectrometry-based identification and characterization of protein adducts of lipid peroxidation-derived aldehydes.**

and subsequent release of the tagged peptide adduct, and (IV) LC-MS/MS analysis of the peptide adduct (Fig. 16.3). This strategy allows the unambiguous assignment of the modified peptide including mass information on the nature of the α,β-unsaturated aldehyde and the localization of the aldehydic modification to a partial sequence, in many cases, to a distinct residue. Figure 16.4 outlines the experimental workflow for the ARP-labeling strategy. The ARP-labeling strategy is applicable to distinct protein systems, cellular systems as well as to complex biological matrices to identify and characterize low-abundance protein adducts of lipoxidation-derived aldehydes. The targeted nature of the analyses should allow obtaining more complete data on the distribution of oxidative protein modifications caused by LPO-derived aldehydes in biological samples, a prerequisite for the successful conduction of proteome-wide studies for investigating and accessing protein–oxylipid adducts under condition of oxidative stress associated with certain diseases and aging.

5.1. ARP-labeling of aldehydic protein adducts of 2-alkenals and tryptic proteolysis

The ARP-labeling reaction of Michael-type protein adducts of 2-alkenals is carried out by using a final ARP (Dojindo Laboratories, Kumamoto, Japan) concentration of 2.5–5 m*M* in 10 m*M* sodium phosphate buffer, pH 7.4, for

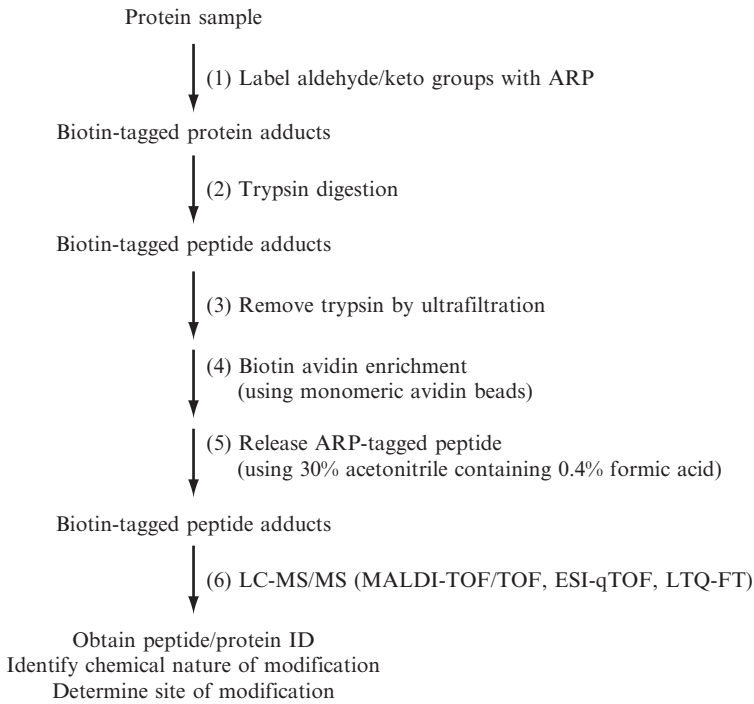

Figure 16.4 **Experimental flowchart for the ARP-labeling strategy and subsequent mass spectrometry-based identification of aldehydic protein adducts.**

1–2 h at room temperature. Unreacted ARP is removed by using centrifugal ultrafiltration units (Biomax (Millipore) or Microcon (Amicon) units, both with 10-kDa MWCO) or gel filtration columns (Zeba desalting spin column, 7-kDa MWCO, Thermo/Pierce). In the case of protein model studies, ARP-labeled aldehydic protein adducts can be chromatographically isolated and subjected to mass analysis. To determine the site of modification, protein samples are subjected to digestion with trypsin (E:S 1:50, modified trypsin, Promega) overnight at 37 °C.

5.2. Enrichment of ARP-labeled peptide adducts using biotin avidin affinity chromatography

Peptides containing the ARP label are captured on monomeric avidin affinity columns (Ultralink monomeric avidin, Thermo/Pierce) as described (Chavez *et al.*, 2006). Briefly, monomeric avidin beads are packed into a 0.5-ml Handee mini-spin column (Thermo/Pierce) and prepared for the capture/release protocol according to the manufacture's instruction. Peptide digests are passed over the avidin beads whereby the ARP-labeled

peptides are captured. Nonspecific and nonlabeled peptides are removed by extensive washing with PBS (20 m*M* NaH_2PO_4, 300 m*M* NaCl). ARP-labeled peptides are eluted from the affinity column by using 30% aqueous acetonitrile containing 0.4% formic acid and the resulting fractions are concentrated by vacuum centrifugation.

5.3. Tandem mass spectrometry for peptide identification and determining the site of adduction

For determining the peptide IDs and site of modifications of ARP-labeled adducts, reversed-phase (C_{18}) chromatography in combination with tandem mass spectrometry (LC-MS/MS) is used. So far, three different mass spectrometry systems were employed and evaluated for the identification and characterization of ARP-labeled peptide adducts: (a) nanoLC separation of ARP-labeled peptides and subsequent tandem mass spectral (MS/MS) analysis using a MALDI time-of-flight/time-of-flight (TOF/TOF) instrument (4700 Proteomics Analyzer, Applied Biosystems); (b) an Electrospray Ionization (ESI) quadrupole TOF (qTOF) mass spectrometer (Micromass/Waters) coupled to nanoAcquity UPLC system (Waters); and (c) a capillary LC (Waters) coupled to a hybrid linear ion trap-FT-ICR (7-Tesla) mass spectrometer (LTQ-FT Ultra, Thermo Finnigan). Because the different instruments utilize different ionization types and collision-induced fragmentation techniques, tandem mass spectra of peptide adducts obtained on different LC-MS/MS systems are provided. Distinct mass spectral features are discussed in the respective figure legends. It is recommended that the LC-MS/MS analyses and data interpretation are performed in close collaboration with mass spectrometry professionals.

4700 Proteomics Analyzer: This TOF/TOF instrument is equipped with a MALDI source utilizing a 200-Hz frequency-tripled Nd:YAG laser operating at a wavelength of 355 nm. Protein mass spectra are acquired in the linear mode, whereas peptide mass spectra are obtained in the reflector mode. For both modes, the accelerating voltage is set to 20 kV. For all peptide MS/MS analyses described in this chapter, the following instrument settings were used. The precursor ion was selected by operating the timed gate with an approximately 3–10 Da width. A collision energy of 1 kV was used and the gas pressure (air) in the collision cell was set to 6×10^{-7} Torr. Fragment ions were accelerated with 15 kV into the reflector.

To prepare the fraction containing the ARP-labeled peptides for MALDI-MS/MS analysis, the peptides were loaded onto a trap cartridge, back-flushed onto a PepMap C_{18} column (150 mm $\times$ 75 μm inner diameter), chromatographically separated, and spotted to stainless steel MALDI target plate using a Dionex/LC Packings Ultimate nanoLC system coupled to a Probot^{TM} target spotter. Gradient elutions have to be tailored to the respective peptide sample. For most peptide separations, a binary gradient

system can be used that consists of solvent A, 0.1% aqueous trifluoroacetic acid (TFA) containing 5% acetonitrile, and solvent B, 80% aqueous acetonitrile containing 0.1% TFA. Peptides are eluted using a linear gradient with a slope of 0.8%/min over 60 min. The eluate is continuously mixed with the MALDI matrix solution (2 mg/ml α-cyano-4-hydroxycinnamic acid in 50% aqueous acetonitrile containing 0.1% TFA) and spotted onto a 144-spot MALDI target. The spotting time is typically set to 20 s but depends on the complexity of the peptide sample.

ESI-qTOF Instrument: For the described peptide LC-MS/MS analyses, the electrospray source is operated in the positive mode with a spray voltage of 3.5 kV. The mass spectrometer is operated in data-dependent acquisition mode: a 0.6 s survey scan is followed by a 2.4-s period in which MS/MS analyses on the three most abundant precursor ions detected in the survey scan are acquired. A 60-s dynamic exclusion of previously selected ions is used. The collision energy for MS/MS (25–65 eV) is dynamically selected based on the charge state of the ion selected by the quadrupole analyzer. To obtain optimal mass measurement accuracy, lock spray mass correction is performed on the doubly charged ion of Glu^1-fibrinopeptide ($[M+2H]^{2+}$ 785.8426 Th) every 30 s.

For nanoLC-MS/MS analyses of peptides, the ESI-qTOF instrument is connected to a nanoAcquity UPLC system (Waters Milford, MA). Typically, ARP-labeled peptide adducts are fractionated on a BEH C_{18} column (100 μm i.d. × 200 mm, 1.7 μm; Waters, Milford, MA) using a linear 60-min gradient of a binary solvent system consisting of solvent A (2% acetonitrile/0.1% formic acid) and solvent B (acetonitrile containing 0.1% formic acid). The solvent composition is changed at a rate of 0.8%/min.

LTQ-FT Ultra: For the described analyses, the instrument was equipped with a Michrom ADVANCE ESI source and coupled to a capillary HPLC (CapLC, Waters). Peptide mixtures are separated on C_{18} column (Agilent Zorbax 300SB-C_{18}, 250 × 0.3 mm, 5 μm) using a flow rate of 4 μl/min with a binary solvent system consisting of solvent A, 0.1% formic acid, and solvent B, 0.1% formic acid in acetonitrile.

The ESI source voltage is set to 1.8 kV. The LTQ-FT mass spectrometer is operated in a data-dependent MS/MS acquisition mode. Full scan mass spectral data from 400 to 1800 m/z with the resolving power set to 100,000 at m/z 400 is obtained by using the ICR cell (AGC target 1×10^6 ions; maximum ion accumulation time, 1000 ms). MS/MS data of the five most abundant doubly or triply charged ions detected in the full scan survey MS experiment is acquired by using the linear ion trap. For precursor ion selection an isolation width of ±2 Th is used. An AGC target value of 3×10^5 ions and a maximum ion accumulation time of 50 ms are used for MS/MS scans in the ion trap. The normalized collision energy is set to 35%, and three microscans are acquired per spectrum. Previously selected ions are excluded from further sequencing for 60 s.

5.4. Searching of MS/MS data against protein sequence databases for the identification of peptide sequences and peptide adducts

There are numerous software tools available to aid the interpretation of fragment ion spectra to obtain peptide identifications. Depending on the instrument with which the fragment ion mass spectral data have been acquired, software tools will facilitate the transformation of the instrument-specific data files in peaklist files that are suitable for processing using the different bioinformatic software packages available.

The mass spectral data discussed in this contribution were processed using MASCOT (Matrix Sciences, Inc.) (David *et al.*, 1999). Instrumentation-independent search parameters include choice of database (e.g., for the discussed data, Swiss-Prot database limited to human or Rodentia) and proteolytic processing (e.g., Trypsin/P was selected as the digesting enzyme allowing for the possibility of one missed cleavage site). The instrument-dependent search parameters include instrument type and the respective mass tolerances. For MALDI-TOF/TOF and ESI-qTOF MS/MS data the following settings were used: precursor ion tolerance ± 100 ppm and fragment ion tolerance ± 0.1 Da. For data acquired on the LTQ-FT instrument, the precursor ion mass tolerance was set to 10 ppm, and the fragment ion tolerance to 0.5 Da. Mascot allows inclusion of two types of peptide modifications: fixed modification and variable modifications. For the peptide adduct analyses discussed, the following variable modifications are critical: Met oxidation (147.04 Da, monoisotopic residue mass), ARP-acrolein-modified Cys, His, and Lys (monoisotopic residue masses 472.16, 506.21, and 497.24 Da, respectively), and ARP-HNE-modified Cys, His, and Lys (monoisotopic residue masses 572.25, 606.29, and 597.2 Da, respectively).

6. Applications of the ARP-Labeling Strategy

Figure 16.5 summarizes the typical analytical stages of the ARP method illustrated on the modification of a model protein by HNE and the subsequent characterization of the resulting product (Chavez *et al.*, 2006). In Fig. 16.5A, the MALDI mass spectrum of the model protein after modification with HNE is shown. The mass difference (Δm 156 Da) between the molecular ion of the protein and the protein adduct indicates Michael adduction by HNE. Mass spectral analysis of the reaction mixture after incubation with ARP reveals that the protein–HNE adduct was tagged by the aldehyde/keto-specific biotinylation probe, ARP. Aldoxime formation between the Michael addition product of HNE and ARP results in a

mass difference of 313.1 Da between the HNE-modified protein and the ARP-labeled protein adduct (Fig. 16.5B). Figure 16.5C depicts the MALDI mass fingerprint of the respective tryptic digest; the ARP-HNE-modified peptide T2 (*m/z* 2201.1) is shifted by 469.2 Da compared to the unmodified peptide T2 (*m/z* 1731.9). Subsequent tandem mass spectral analysis of the ARP-labeled T2 HNE–peptide adduct reveals modification of the His residue at position 3 of T2 based on the *m/z* difference of 606.3 Da between the y_{12}- and y_{13}-ion (monoisotopic residue mass for His-HNE-ARP 606.29 Da ($C_{27}H_{42}N_8O_6S$)) (Fig. 16.5D).

We recently reported the unambiguous identification of the major protein targets of HNE exposure in human monocytic THP-1 cells.

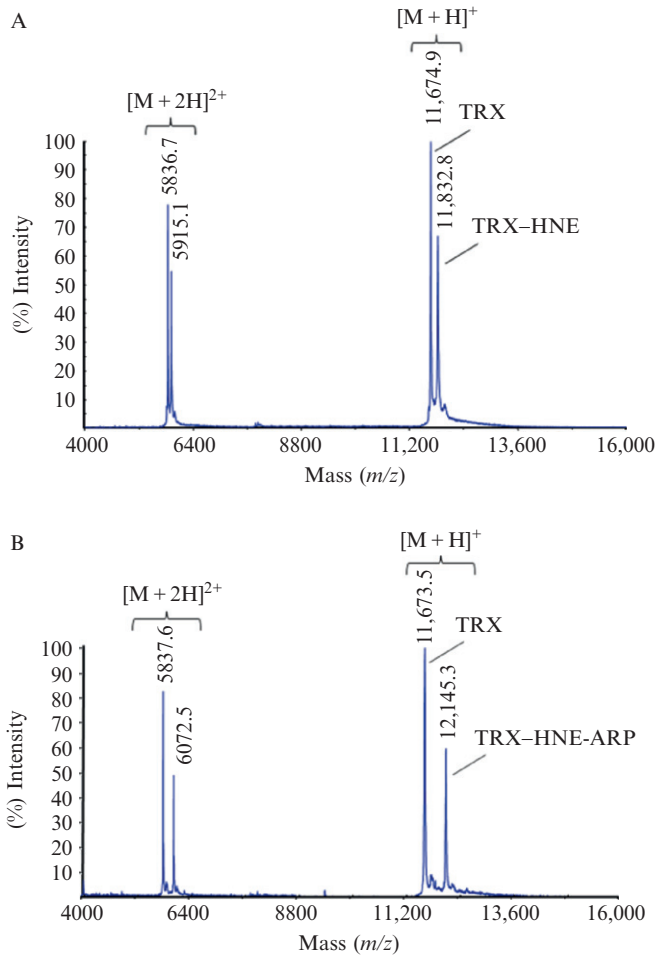

Figure 16.5 (Continued)

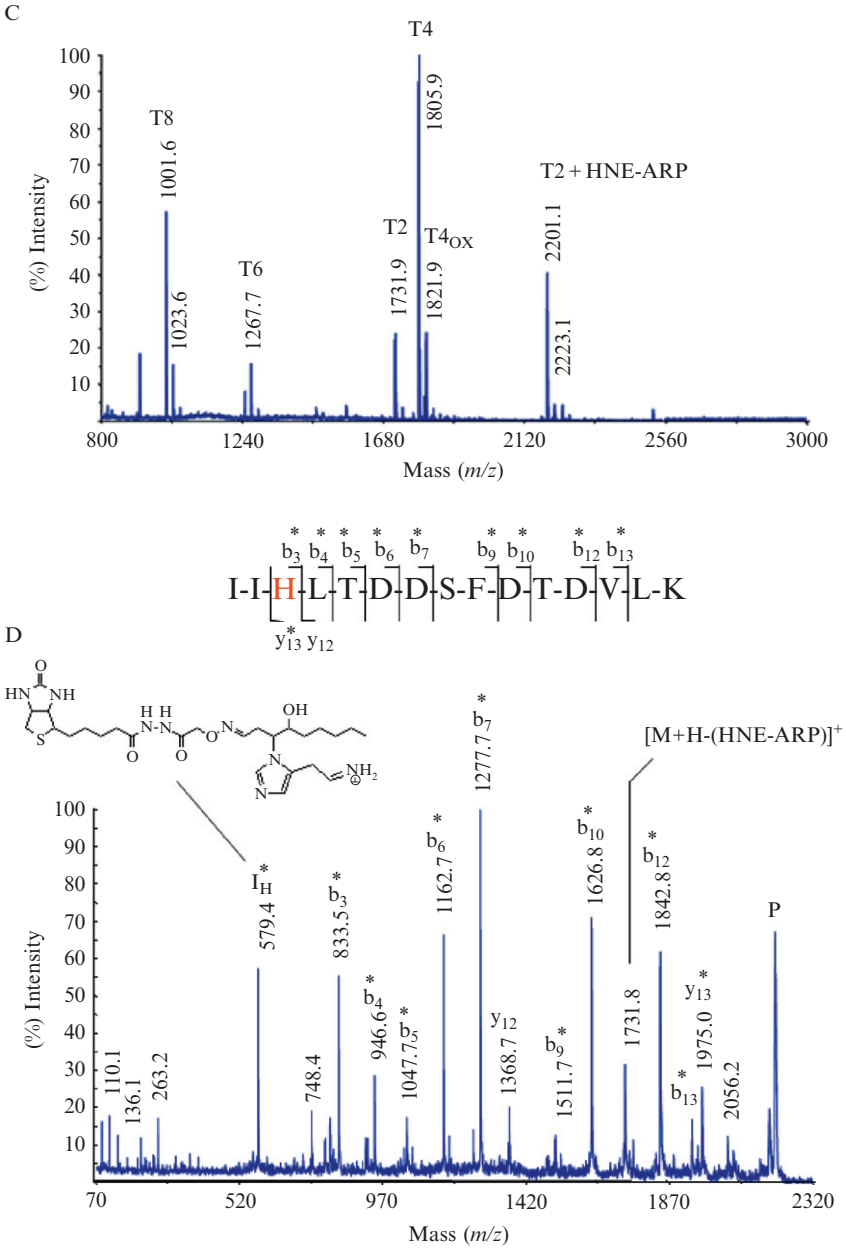

Figure 16.5 Identification and characterization of a Michael-type protein adduct of HNE. (A) MALDI mass spectrum of the model protein thioredoxin after modification with HNE. (B) MALDI mass spectrum of the HNE-modified thioredoxin after labeling with ARP. The mass difference of ~472 Da between the molecular ion at *m/z* 11,673.5

Employing the ARP-labeling strategy, 18 peptides were identified with ARP-HNE modification to distinct cysteine or histidine residues. The majority of the identified protein targets of HNE were cytoskeletal proteins, proteins involved in glycolysis, metabolic processes and RNA binding, and regulation of translation (Chavez *et al.*, 2010). The use of high resolution mass spectrometers that provide high mass accuracy for the characterization of complex peptide mixture becomes increasingly popular. The confidence in the identification of a peptide is increased by accurately measuring the mass of a peptide. This is of particular relevance for the ARP-labeling strategy because identification is based on the correct assignment of a single peptide adduct. Figure 16.6 features the type of data that are obtained using a hybrid linear quadrupole ion trap/FT-ICR (LTQ-FT) mass spectrometer for the identification of HNE-modified peptides. Accurate determination of peptide masses was achieved using the FT-ICR MS, whereas MS/MS data were acquired using the linear ion trap.

For instance, Fig. 16.6 depicts the mass spectral data that led to the assignment of Cys-347 as one of the adduction sites of HNE in the tubulin-α 1 protein. The tandem mass spectrum provides peptide assignment and localization of the HNE adduction site (Fig. 16.6A). The unambiguous assignment of the adduction site is predominately derived from the *m/z*-difference between the b_n-ions at *m/z* 876.2 9 (b_7) and 1448.5 (b_8) ion (monoisotopic residue mass for Cys-HNE-ARP 572.25 Da ($C_{24}H_{40}N_6O_6S_2$)). In addition, the observation of a diagnostic ion at *m/z* 1527.5, indicating loss of the ARP-HNE moiety from the precursor ion, supports the assignment of the peptide adduct. A possible caveat of the ARP approach is that peptide assignments are usually based on single peptide identification. Therefore, it is desirable to

and 12,145.3 is indicative for the presence of the HNE-ARP oxime moiety (theoretical mass shift: Δ*m* 469 Da). Michael adduct formation results in a mass increase of 156 Da and the subsequent derivatization with ARP under aldoxime formation yields an additional mass shift of 313 Da. (C) Mass spectrum of the tryptic digest of mixture of TRX and ARP-labeled TRX–HNE adduct. The ARP-labeled HNE-modified peptide T2 is observed at *m/z* 2201.1 i.e., 469 Da higher compared to the unmodified peptide T2 at *m/z* 1731.9. (D) Tandem mass spectrum of the ARP-labeled HNE-modified peptide of thioredoxin encompassing the residue 4–18. The b-type fragment ions (b_3–b_7, b_9, b_{10}, b_{12}, and b_{13}) are shifted by 469 Da to higher *m/z* values compared to the theoretical *m/z* values that would be expected for the unmodified peptide. The coherent mass shift of the b_n-ions indicates that the ARP-HNE moiety is present near the N-terminus of this peptide. The mass difference of 606.3 Da between the fragment ions y_{12} and y_{13} localize the APR-HNE moiety to the His residue at position 3 in this peptide. In addition, the intense ARP-HNE-modified His immonium ion at *m/z* 579.4 supports the assignment of the His residue as the site of modification by HNE. Mass spectral analyses were performed on a MALDI-TOF/TOF instrument (4700 Applied Biosystems Proteome Analyzer) using α-cyano-4-hydroxycinnamic acid as matrix. Fragment ions marked with an asterisk (*) retained the ARP-HNE moiety during collision-induced fragmentation.

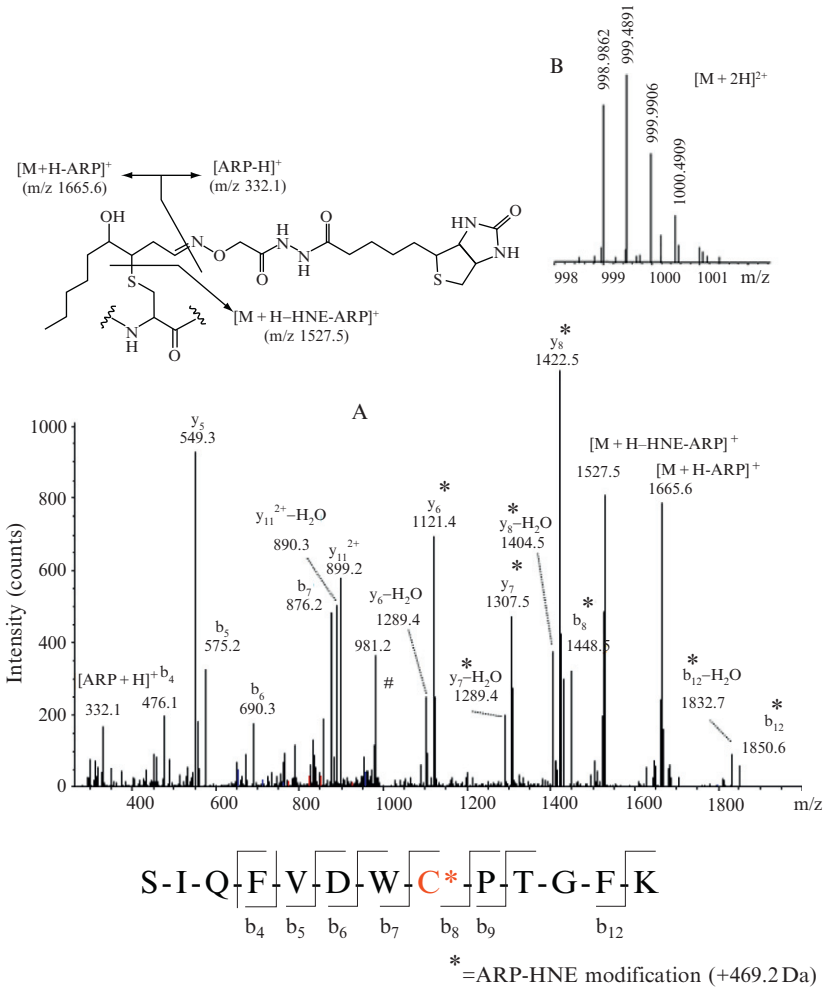

Figure 16.6 Mass spectral analysis of the ARP-labeled HNE-modified peptide SIQFVDWC*PTGFK from tubulin-α1B using a LTQ-FT mass spectrometer. (A) Tandem mass spectrum of the doubly protonated precursor ion which was used for collision-induced fragmentation in the linear ion trap of an LTQ-FT mass spectrometer. Fragment ions marked with an asterisk (*) retained the ARP-HNE moiety during collision-induced fragmentation and allowed the unambiguous assignment of the Cys residue as site of HNE adduction. (B) FT-ICR full scan mass spectrum showing the doubly protonated $[M+2H]^{2+}$ ion cluster region. Exact mass determination using the ICR cell of the instrument yielded for the monoisotopic ion a m/z value of 998.9862 Th which reflects a mass accuracy of -0.4 ppm (calculated m/z 998.9866). Having both analytical information, sequencing data and exact mass, enables the identification of the peptide as the partial sequence 340–352 of tubulin-α1B chain (TBA1B_Human; Swiss-Prot P68363) with Cys-347 modified by HNE with high confidence.

conduct peptide mass measurements with the highest possible accuracy to enhance the confidence in the peptide assignment. The FT-ICR full scan spectrum of the doubly protonated ion, $[M+2H]^{2+}$, of the ARP-labeled HNE-modified peptide SIQFVDWC★PTGFK from tubulin-α1B is depicted in Fig. 16.6B. The monoisotopic $[M+2H]^{2+}$ ion at m/z 998.9862 was determined with an accuracy of −0.4 ppm (monoisotopic m/z_{calc} 998.9866 Th) ascertaining high confidence in the peptide assignment.

The applicability of the ARP-labeling strategy to complex biological mixtures is illustrated on the identification of *in vivo* Michael-type protein adducts of LPO-derived aldehydes in mitochondria isolated from rat heart. Our studies repeatedly identified as target site of HNE the Cys-166 residue in long-chain-specific acyl-CoA dehydrogenase (ACADL-RAT; Swiss-Prot P15650) (Chavez *et al.*, 2006). Several distinct adduction sites to constituents of the respiratory complexes were identified and characterized by tandem mass spectrometry. For example, the MALDI mass spectra depicted in Fig. 16.7 provided the basis for the identification of a modification "hot spot" of Complex III subunit 2 of the electron transport chain (UQCR2_RAT; Swiss-Prot P32551). Note, in this example, the peptide derived from the core 2 protein of Complex III was found to be susceptible to modification by different α,β-unsaturated aldehydes on the Cys-191 residue. This level of information describing site-specific protein modifications by endogenous lipid peroxidation products is exclusively achievable by tandem mass spectrometry-based strategies.

Darley-Usmar and colleagues demonstrated that the cyclopentenone-containing electrophile 15-deoxy-$\Delta^{12,14}$-prostaglandin J_2 (15d-PGJ_2) modulates cell death pathways and induces apoptosis in liver cells (Landar *et al.*, 2006). Using a biotinylated 15d-PGJ_2 derivative they were able to identify several putative mitochondrial targets of 15d-PGJ_2, of which two seem to be relevant to triggering the permeability transition pore (PTP) and leading to apoptosis: the adenine nucleotide translocase (ANT) and ATP-synthase. ANT shuffles ATP from the mitochondrial matrix to the cytosol and functions as one of the modulators of the pore opening process in which ANT thiols are proposed to serve as redox-sensitive sensors (Crompton, 1999; Crompton *et al.*, 1999). We reported recently that ANT is a major target of acrolein adduction and identified the cysteine residue in position 256 as site of modification (Han *et al.*, 2007). It seems plausible that cysteine modification by electrophilic lipids promotes activation of ANT (Dmitriev, 2007). Electrophile stress potentiates opening of the mitochondrial PTP under conditions of elevated Ca^{2+} levels in the mitochondrial matrix (Brookes *et al.*, 2004). Elevated Ca^{2+} levels result in upregulation of the oxidative phosphorylation machinery including the ATP-synthase to meet the increased demands of ATP during apoptosis (Nicotera *et al.*, 1998). Enhanced respiratory chain activity may lead to increased levels of ROS production and, concomitantly, lipid peroxidation. We identified several

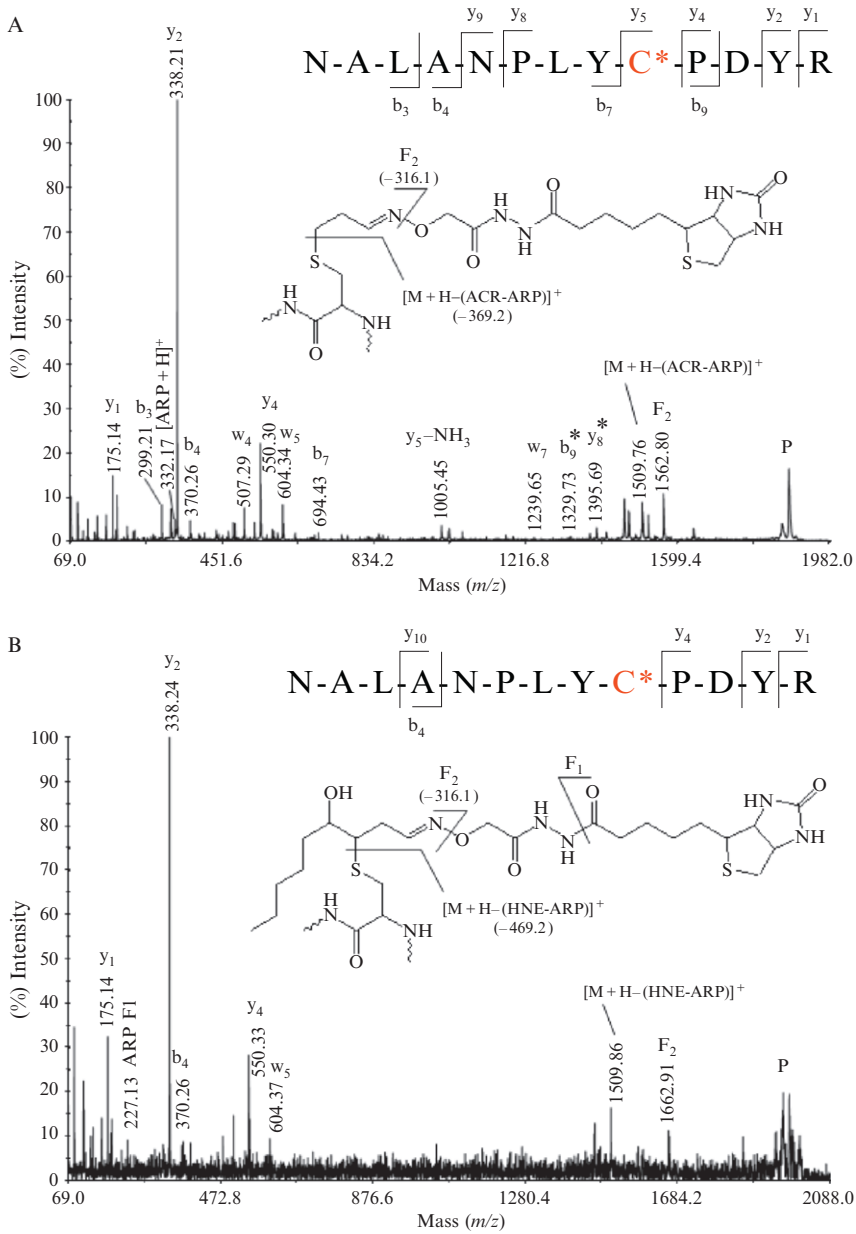

Figure 16.7 Tandem mass spectral identification and characterization of endogenous peptide adducts of lipid peroxidation products after applying the ARP derivatization and enrichment strategy to determine the protein targets of aldehydic lipid peroxidation products in rat cardiac mitochondria. (A) MALDI-MS/MS spectrum of the ARP-labeled acrolein-modified peptide of the core protein 2 of the ubiquinol–cytochrome *c*

sites in subunits of ATP-synthase that were modified by acrolein: Cys-294 in ATPase α-chain, Cys-78 in ATP-synthase γ-chain, Cys-239 in ATP B-chain, Cys-41 in ATP-synthase O subunit (OSCP) and Cys-100 in ATP-synthase D chain. It seems possible that modifications of ATPase and ANT by α,β-unsaturated aldehydes may interfere with apoptotic cell death pathways. Further work is needed to determine the mechanisms by which α,β-unsaturated aldehydes and other electrophiles modulate mitochondrial processes and function.

7. Interpretation of MS/MS Spectra of Protein Adducts and the Use of Diagnostic Marker Ions

Mass spectrometric studies of protein and peptide adducts of aldehydic lipid aldehydes have been conducted using many different instrument types. Mass spectral analyses of proteins modified by diverse LPO-derived aldehydes indicate that Michael adducts of 4-hydroxy-2-alkenals on Cys and His seem to be sufficiently stable to a wide range of experimental conditions and can be readily observed without reductive stabilization or other derivatizations (Rauniyar *et al.*, 2008; Roe *et al.*, 2007; Roede *et al.*, 2008; Shonsey *et al.*, 2008; Williams *et al.*, 2007). In contrast, the Michael adduct of HNE on Lys residue has been observed exclusively after reductive stabilization using sodium borohydride ($NaBH_4$) (Lin *et al.*, 2005). Studies of model proteins modified *in vitro* by α,β-unsaturated aldehydes indicate the potential of using proteolytic analyses in conjunction with mass spectrometry to identify and characterize cross-links caused by LPO-derived aldehydes (Liu *et al.*, 2003; Oe *et al.*, 2003a).

Besides facilitating avidin affinity-based enrichment, the derivatization of protein adducts of LPO-derived aldehydes by an aldehyde/keto-specific probe has as additional advantage the introduction of an extra layer of confidence based on the specificity of the hydroxylamine chemistry for aldehyde/keto groups. ARP-derivatized protein and peptides adducts are

reductase complex (UQCR2_RAT; Swiss-Prot P32551) encompassing the residue 183–195 and (B) the respective peptide with Cys-191 modified by HNE. Mitochondrial protein samples were treated with 5 m*M* ARP for 1 h at room temperature. Subsequent to the removal of unreacted ARP using desalting spin column the protein sample was digested with trypsin. ARP-labeled peptides were enriched using a monomeric avidin column. The enriched peptide samples were subjected to reversed-phase (C_{18}) nanoLC, automatically mixed with MALDI matrix, spotted onto a target plate, and subjected to MALDI-MS/MS analyses (using a 4700 Applied Biosystems' Proteomics Analyzer). Fragment ions marked with an asterisk (*) retained the ARP-HNE moiety during collision-induced fragmentation.

well amenable to mass spectral measurements and the oxime bond is sufficiently stable for retaining the ARP-aldehyde moiety on the peptide fragment ions allowing the use of automated database search software for aiding in the analysis of tandem mass spectral data (Fig. 16.5–16.7).

Collision-induced dissociation of ARP-labeled peptide adducts yielded, beside the usual peptide-specific fragment ions of the b_n and y_n types, frequently nonpeptide fragment ions that originated from the ARP tag, including the ions observed at m/z 227.1 (F1) and m/z 332.2 ($[ARP+H]^+$). Additionally, in the ESI-MS/MS spectrum depicted in Figure 16.6 intense ion peaks at m/z 1665.6 and 1527.5 are visible indicating that $[ARP-H]^+$ is expelled and the resulting ion, $[M+H-ARP]^+$, undergoes loss of dehydrated HNE (−138 Da) resulting in an ion that appears at m/z 1527.5 ($[M+H–(HNE-ARP)]^+$, i.e., charge reduction and a total loss of −470.5 Da is observed upon CID of the doubly protonated precursor ion (m/z 998.99). In contrast, fragment ions that indicate neutral loss of the ARP-lipid moiety from singly protonated precursor ions are visible in the MALDI MS/MS spectra (Fig. 16.5D and 16.7). Ions that relate to fragmentations involving the ARP-lipid aldehyde moiety may therefore serve as diagnostic marker ions in the interpretation of tandem mass spectra of peptide adducts of lipid aldehyde.

Noteworthy, Prokai and coworkers explore the high propensity of aldehydic protein adducts to undergo neutral loss fragmentation via retro Michael addition reaction for neutral-loss-dependent MS^3 strategies to facilitate large-scale analyses of these protein modifications (Rauniyar *et al.*, 2008).

8. Conclusion

This chapter summarizes our ongoing efforts to develop and apply chemical labeling approaches in combination with tandem mass spectrometry to determine protein targets of *in vivo* oxidative stress. Here, an experimental approach is described that enables the unambiguous identification and characterization of proteins modified by lipid peroxidation-derived 2-alkenals. This approach employs a biotinylated hydroxylamine derivate as aldehyde/keto-reactive probe in conjunction with selective enrichment and tandem mass spectrometric analysis. Model studies allow studying the chemistry of LPO-derived aldehydes and properties of the resulting peptide and protein adducts in mass spectrometry-based sequencing studies. Methodological details are given for an exposure study of a cell culture system with HNE that yielded the major protein targets of HNE in human monocytic THP-1 cells. The utility of the ARP-labeling approach is also demonstrated for the identification and characterization of endogenous mitochondrial protein targets of aldehydic lipid peroxidation products. The diverse applications indicate that the described method can possibly

be equally well applied to the targeted analysis of other aldehydic addition products, such FDP-lysine and 4-ketoamide lysine residues.

Which factors direct the modification of proteins by LPO-derived aldehydes under physiological conditions? A few reports have appeared that started the discussion to what extent do protein structural parameters govern the sensitivity of distinct sites toward modification by LPO-derived aldehydes and other electrophiles. A scenario is emerging in which the dielectric constant, surface accessibility and the modulation of the nucleophilicity and basicity of a certain residue by its microenvironment may govern the propensity of a distinct site to modifications by electrophiles (Roe *et al.*, 2007; Sayre *et al.*, 2006). In this context, various alkylating reagents have been employed to determine preferred target sites of modifications (Marley *et al.*, 2005; Shin *et al.*, 2007; Wong and Liebler, 2008). We explored the use of a sterically demanding butyltriphenylphosphonium group as a chemical tool for the identification of mitochondrial protein thiols that exhibit a large degree of surface accessibility (Marley *et al.*, 2005). In this study, Cys-385 of aconitase was readily alkylated by (4-iodo)butyltriphenylphosphonium iodide (IBTP). The same cysteine residue was also found to be susceptible to modification by another alkylation reagent and has been identified to be modified by acrolein in rat cardiac mitochondria (Fig. 16.8). The same cysteine residue was also described as being susceptible to oxidative modification by peroxynitrite (Han *et al.*, 2005). The compilation of reactivity parameters for distinct sites that show high reactivity toward electrophilic agents may provide the foundation for future attempts to predict protein susceptibility to these modifications.

To conclude, the ARP-labeling method is a versatile analytical strategy for the identification and characterization of carbonyl-containing protein adducts of lipid peroxidation products. We further anticipate that our approach may also find some applicability in the area of oxidative stress insults by metal-catalyzed oxidations (Maisonneuve *et al.*, 2009; Mirzaei and Regnier, 2005, 2007).

Additional experimental methods (not related to ARP derivatization of aldehydic protein adducts):

Derivatization of protein thiols using iodobutyl triphenylphosphonium (IBTP): Frozen mitochondria (isolated according to Suh *et al.* (2003)) were suspended in 10 m*M* potassium phosphate buffer (pH 8.2) containing 250 m*M* sucrose. Surface accessible protein thiols were alkylated with 1 m*M* IBTP for 30 min at 37 °C. For this purpose, a 33 m*M* stock solution of IBTP prepared in 50 m*M* potassium phosphate buffer containing 30% acetonitrile was prepared. The final IBTP concentration in the reaction mixture was approximately 1 m*M*. After several freeze–thaw cycles to disrupt mitochondrial membranes, the soluble mitochondrial proteins were recovered after centrifugal removal of the insoluble membrane fraction. Tryptic digests were submitted to LC-ESI MS/MS analysis using Micromass/Water qToF instrument.

Labeling of protein thiols using a cleavable ICAT probe: Soluble protein lysate was prepared by shaking isolated rat cardiac mitochondria in the presence of 1% Triton X-100 (v/v) for 1 h on ice. ICAT labeling of protein thiols was performed under nondenaturing conditions but otherwise following the procedure outlined in Applied Biosystems' cICAT labeling kit. Briefly, cICAT labeling was performed for 2 h at 37 °C in the dark. The protein sample was incubated overnight at 37 °C with trypsin (E:S ratio 1:40).

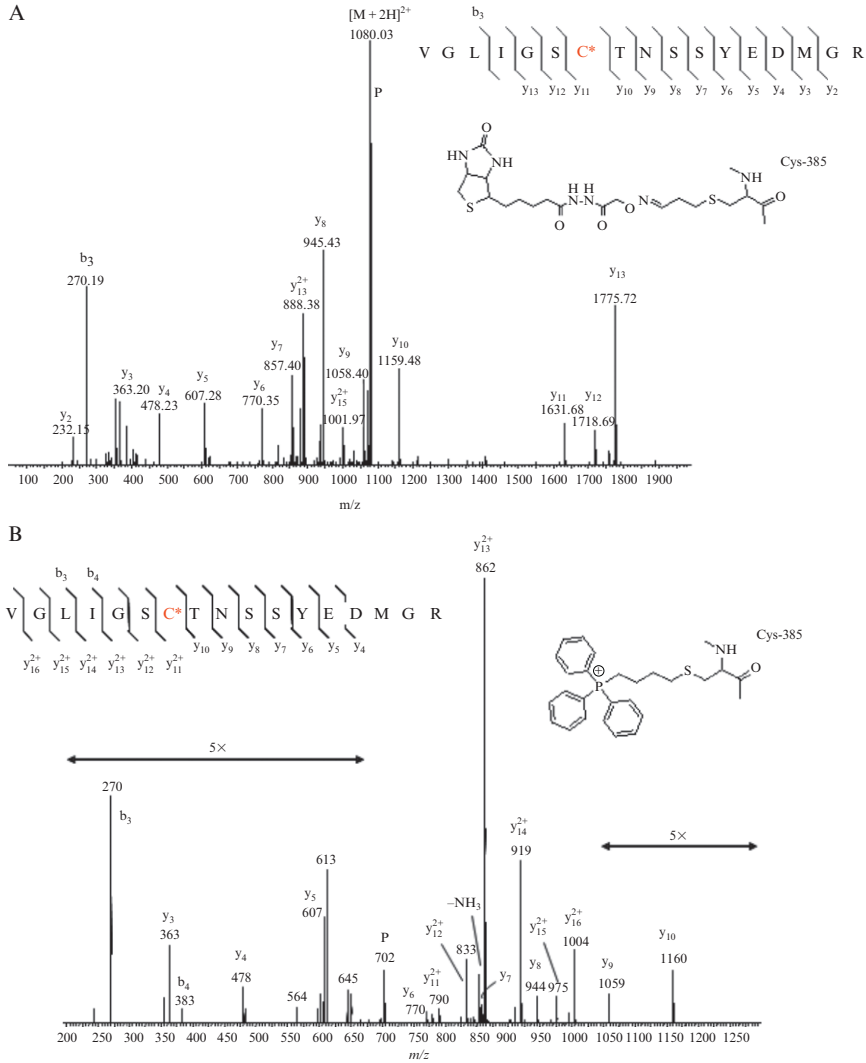

Figure 16.8 (Continued)

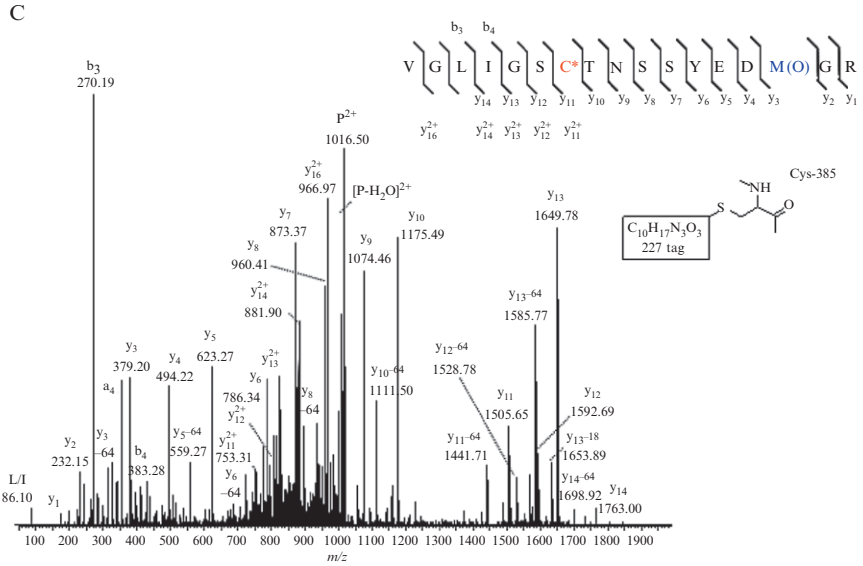

Figure 16.8 ESI-MS/MS spectral analysis of (A) the ARP-labeled acrolein-modified peptide of aconitase ($[M+2H]^{2+}$, *m/z* 1079.47); (B) the respective peptide with Cys-385 alkylated with a sterically demanding triphenylphosphonium group ($[M+2H]^{3+}$, *m/z* 702.3); and (C) tagged with the thiol-specific cleavable ICAT probe ($[M+2H]^{2+}$, *m/z* 1016.50). Peptide identification and characterization of the respective modification was achieved by nanoLC-ESI-MS/MS analysis using a Waters/Micromass Global quadrupole time-of-flight instrument operated in the data-dependent acquisition mode. P, denotes precursor ion.

Proteolytic digests were cleaned up using a strong cation-exchange (SCX) spin column. cICAT-labeled peptides were enriched using ultraLink-immobilized monomeric avidin column. After release of cICAT-labeled peptides using 30% aqueous acetonitrile containing 0.4% formic acid, the eluate was lyophilized and the biotin moiety was removed by using cleaving reagent A and B from the Applied Biosystems kit. Prior to LC-ESI-qTOF MS/MS analysis the lyophilized sample was dissolved in 0.1% aqueous TFA containing 1% acetonitrile.

ACKNOWLEDGMENT

We are grateful to Brian Arbogast and Michael Hare for technical assistance. This work was supported by grants from the NIH (AG025372, HL081721, ES00210) and the Oregon Medical Research Foundation. The Mass Spectrometry Facility of the Environmental Health Sciences Center at Oregon State University is supported in part by NIH/NIEHS grant P30ES00210.

REFERENCES

Beckman, K. B., and Ames, B. N. (1998). The free radical theory of aging matures. *Physiol. Rev.* **78,** 547–581.

Berlett, B. S., and Stadtman, E. R. (1997). Protein oxidation in aging, disease, and oxidative stress. *J. Biol. Chem.* **272,** 20313–20316.

Bieschke, J., *et al.* (2006). Small molecule oxidation products trigger disease-associated protein misfolding. *Acc. Chem. Res.* **39,** 611–619.

Brookes, P. S., *et al.* (2004). Calcium, ATP, and ROS: A mitochondrial love-hate triangle. *Am. J. Physiol. Cell Physiol.* **287,** C817–C833.

Brooks, J. D., *et al.* (2008). Formation of highly reactive cyclopentenone isoprostane compounds (A3/J3-isoprostanes) in vivo from eicosapentaenoic acid. *J. Biol. Chem.* **283,** 12043–12055.

Butterfield, D. A., and Sultana, R. (2008). Redox proteomics: Understanding oxidative stress in the progression of age-related neurodegenerative disorders. *Expert Rev. Proteomics* **5,** 157–160.

Carbone, D. L., *et al.* (2004). 4-Hydroxynonenal regulates 26S proteasomal degradation of alcohol dehydrogenase. *Free Radic. Biol. Med.* **37,** 1430–1439.

Carbone, D. L., *et al.* (2005). Cysteine modification by lipid peroxidation products inhibits protein disulfide isomerase. *Chem. Res. Toxicol.* **18,** 1324–1331.

Catalá, A. (2009). Lipid peroxidation of membrane phospholipids generates hydroxy-alkenals and oxidized phospholipids active in physiological and/or pathological conditions. *Chem. Phys. Lipids* **157,** 1–11.

Chavez, J., *et al.* (2006). New role for an old probe: Affinity labeling of oxylipid protein conjugates by N'-aminooxymethylcarbonylhydrazino D-biotin. *Anal. Chem.* **78,** 6847–6854.

Chavez, J., *et al.* (2010). Site-specific protein adducts of 4-hydroxy-2(E)-nonenal in human THP-1 monocytic cells: Protein carbonylation is dimished by ascorbic acid. *Chem. Res. Toxicol.* **23,** 37–47.

Chen, Y., *et al.* (1999). Formation of reactive cyclopentenone compounds in vivo as products of the isoprostane pathway. *J. Biol. Chem.* **274,** 10863–10868.

Chung, W.-G., *et al.* (2009). Hop proanthocyanidins induce apoptosis, protein carbonylation, and cytoskeleton disorganization in human colorectal adenocarcinoma cells via reactive oxygen species. *Food Chem. Toxicol.* **47,** 827–836.

Codreanu, S. G., *et al.* (2009). Global analysis of protein damage by the lipid electrophile 4-hydroxy-2-nonenal. *Mol. Cell. Proteomics* **8,** 670–680.

Crompton, M. (1999). The mitochondrial permeability transition pore and its role in cell death. *Biochem. J.* **341**(Pt 2), 233–249.

Crompton, M., *et al.* (1999). The mitochondrial permeability transition pore. *Biochem. Soc. Symp.* **66,** 167–179.

Danni, L. M., *et al.* (2007). Identification of carbonylated proteins from enriched rat skeletal muscle mitochondria using affinity chromatography-stable isotope labeling and tandem mass spectrometry. *Proteomics* **7,** 1150–1163.

David, N. P., *et al.* (1999). Probability-based protein identification by searching sequence databases using mass spectrometry data. *Electrophoresis* **20,** 3551–3567.

Dmitriev, L. F. (2007). The involvement of lipid radical cycles and the adenine nucleotide translocator in neurodegenerative diseases. *J. Alzheimers Dis.* **11,** 183–190.

Doorn, J. A., and Petersen, D. R. (2003). Covalent adduction of nucleophilic amino acids by 4-hydroxynonenal and 4-oxononenal. *Chem. Biol. Interact.* **143–144,** 93–100.

Eliuk, S. M., *et al.* (2007). Active site modifications of the brain isoform of creatine kinase by 4-hydroxy-2-nonenal correlate with reduced enzyme activity: Mapping of modified sites

by fourier transform-ion cyclotron resonance mass spectrometry. *Chem. Res. Toxicol.* **20,** 1260–1268.

Esterbauer, H., *et al.* (1991). Chemistry and biochemistry of 4-hydroxynonenal, malonaldehyde and related aldehydes. *Free Radic. Biol. Med.* **11,** 81–128.

Farout, L., *et al.* (2006). Inactivation of the proteasome by 4-hydroxy-2-nonenal is site specific and dependant on 20S proteasome subtypes. *Arch. Biochem. Biophys.* **453,** 135–142.

Finkel, T., and Holbrook, N. J. (2000). Oxidants, oxidative stress and the biology of ageing. *Nature* **408,** 239–247.

Furuhata, A., *et al.* (2002). Thiolation of protein-bound carcinogenic aldehyde. *J. Biol. Chem.* **277,** 27919–27926.

Han, D., *et al.* (2005). Sites and mechanisms of aconitase inactivation by peroxynitrite: Modulation by citrate and glutathione. *Biochemistry* **44,** 11986–11996.

Han, B., *et al.* (2007). Design, synthesis, and application of a hydrazide-functionalized isotope-coded affinity tag for the quantification of oxylipid-protein conjugates. *Anal. Chem.* **79,** 3342–3354.

Helga, S., *et al.* (2004). Genomic damage in end-stage renal failure: Potential involvement of advanced glycation end products and carbonyl stress. *Semin. Nephrol.* **24,** 474–478.

Ichihashi, K., *et al.* (2001). Endogenous formation of protein adducts with carcinogenic aldehydes. *J. Biol. Chem.* **276,** 23903–23913.

Kim, H.-Y. H., *et al.* (2009). An azido-biotin reagent for use in the isolation of protein adducts of lipid-derived electrophiles by streptavidin catch and photorelease. *Mol. Cell. Proteomics* **8,** 2080–2089.

Landar, A., *et al.* (2006). Interaction of electrophilic lipid oxidation products with mitochondria in endothelial cells and formation of reactive oxygen species. *Am. J. Physiol. Heart Circ. Physiol.* **290,** H1777–H1787.

Lee, H. P., *et al.* (2009). The essential role of ERK in 4-oxo-2-nonenal-mediated cytotoxicity in SH-SY5Y human neuroblastoma cells. *J. Neurochem.* **108,** 1434–1441.

Lin, D., *et al.* (2005). 4-Oxo-2-nonenal is both more neurotoxic and more protein reactive than 4-Hydroxy-2-nonenal. *Chem. Res. Toxicol.* **18,** 1219–1231.

Liu, Z., *et al.* (2003). Mass spectroscopic characterization of protein modification by 4-Hydroxy-2-(E)-nonenal and 4-Oxo-2-(E)-nonenal. *Chem. Res. Toxicol.* **16,** 901–911.

Maisonneuve, E., *et al.* (2009). Rules governing selective protein carbonylation. *PLoS One* **4,** e7269.

Marley, K., *et al.* (2005). Mass tagging approach for mitochondrial thiol proteins. *J. Proteome Res.* **4,** 1403–1412.

Mirzaei, H., and Regnier, F. (2005). Enrichment of carbonylated peptides using Girard P reagent and strong cation exchange chromatography. *Anal. Chem.* **78,** 770–778.

Mirzaei, H., and Regnier, F. (2007). Identification of yeast oxidized proteins: Chromatographic top-down approach for identification of carbonylated, fragmented and cross-linked proteins in yeast. *J. Chromatogr. A* **1141,** 22–31.

Montine, T. J., *et al.* (2002). Lipid peroxidation in aging brain and Alzheimer's disease. *Free Radic. Biol. Med.* **33,** 620–626.

Nicotera, P., *et al.* (1998). Intracellular ATP, a switch in the decision between apoptosis and necrosis. *Toxicol. Lett.* **102–103,** 139–142.

Oe, T., *et al.* (2003a). A novel lipid hydroperoxide-derived cyclic covalent modification to histone H4. *J. Biol. Chem.* **278,** 42098–42105.

Oe, T., *et al.* (2003b). A novel lipid hydroperoxide-derived modification to arginine. *Chem. Res. Toxicol.* **16,** 1598–1605.

Poli, G., *et al.* (2008). 4-Hydroxynonenal-protein adducts: A reliable biomarker of lipid oxidation in liver diseases. *Mol. Aspects Med.* **29,** 67–71.

Powell, S. R., *et al.* (2005). Aggregates of oxidized proteins (lipofuscin) induce apoptosis through proteasome inhibition and dysregulation of proapoptotic proteins. *Free Radic. Biol. Med.* **38,** 1093–1101.

Qin, Z., *et al.* (2007). Effect of 4-hydroxy-2-nonenal modification on α-synuclein aggregation. *J. Biol. Chem.* **282,** 5862–5870.

Rauniyar, N., *et al.* (2008). Characterization of 4-hydroxy-2-nonenal-modified peptides by liquid chromatography-tandem mass spectrometry using data-dependent acquisition: Neutral loss-driven MS3 versus neutral loss-driven electron capture dissociation. *Anal. Chem.* **81,** 782–789.

Reed, T. T., *et al.* (2009). Proteomic identification of HNE-bound proteins in early Alzheimer disease: Insights into the role of lipid peroxidation in the progression of AD. *Brain Res.* **1274,** 66–76.

Roe, M. R., *et al.* (2007). Proteomic mapping of 4-hydroxynonenal protein modification sites by solid-phase hydrazide chemistry and mass spectrometry. *Anal. Chem.* **79,** 3747–3756.

Roede, J. R., *et al.* (2008). In vitro and in silico characterization of peroxiredoxin-6 modified by 4-hydroxynonenal and 4-oxononenal. *Chem. Res. Toxicol.* **21,** 2289–2299.

Sayre, L. M., *et al.* (2006). Protein adducts generated from products of lipid oxidation: Focus on HNE and one. *Drug Metab. Rev.* **38,** 651–675.

Shin, N.-Y., *et al.* (2007). Protein targets of reactive electrophiles in human liver microsomes. *Chem. Res. Toxicol.* **20,** 859–867.

Shonsey, E. M., *et al.* (2008). Inactivation of human liver bile acid CoA:amino acid N-acyltransferase by the electrophilic lipid, 4-hydroxynonenal. *J. Lipid Res.* **49,** 282–294.

Spiteller, G. (2001). Lipid peroxidation in aging and age-dependent diseases. *Exp. Gerontol.* **36,** 1425–1457.

Spiteller, P., *et al.* (2001). Aldehydic lipid peroxidation products derived from linoleic acid. *Biochim. Biophys. Acta* **1531,** 188–208.

Stevens, J. F., and Maier, C. S. (2008). Acrolein: Sources, metabolism, and biomolecular interactions relevant to human health and disease. *Mol. Nutr. Food Res.* **52,** 7–25.

Stewart, B. J., *et al.* (2007). Residue-specific adduction of tubulin by 4-hydroxynonenal and 4-oxononenal causes cross-linking and inhibits polymerization. *Chem. Res. Toxicol.* **20,** 1111–1119.

Suh, J. H., *et al.* (2003). Two subpopulations of mitochondria in the aging rat heart display heterogenous levels of oxidative stress. *Free Radic. Biol. Med.* **35,** 1064–1072.

Sultana, R., *et al.* (2009). Proteomics identification of oxidatively modified proteins in brain. *Proteomics* 291–301.

Uchida, K. (2000). Role of reactive aldehyde in cardiovascular diseases. *Free Radic. Biol. Med.* **28,** 1685–1696.

Vila, A., *et al.* (2008). Identification of protein targets of 4-hydroxynonenal using click chemistry for ex vivo biotinylation of azido and alkynyl derivatives. *Chem. Res. Toxicol.* **21,** 432–444.

West, J. D., and Marnett, L. J. (2006). Endogenous reactive intermediates as modulators of cell signaling and cell death. *Chem. Res. Toxicol.* **19,** 173–194.

Williams, M. V., *et al.* (2007). Covalent adducts arising from the decomposition products of lipid hydroperoxides in the presence of cytochrome c. *Chem. Res. Toxicol.* **20,** 767–775.

Wong, H. L., and Liebler, D. C. (2008). Mitochondrial protein targets of thiol-reactive electrophiles. *Chem. Res. Toxicol.* **21,** 796–804.

Zhang, W.-H., *et al.* (2003). Model studies on protein side chain modification by 4-Oxo-2-nonenal. *Chem. Res. Toxicol.* **16,** 512–523.

Zhu, X., and Sayre, L. M. (2007). Long-lived 4-oxo-2-enal-derived apparent lysine Michael adducts are actually the isomeric 4-ketoamides. *Chem. Res. Toxicol.* **20,** 165–170.

Author Index

C

D

E

H

M

S

T

X

Y

Subject Index

Q

T

W